QUALITY OF ORNAMENTAL CROPS: EFFECT OF GENOTYPE, PREHARVEST, AND IMPROVED PRODUCTION CHAINS ON QUALITY ATTRIBUTES OF ORNAMENTAL CROPS

EDITED BY: Patricia Duarte De Oliveira Paiva, Julian C. Verdonk, Antonio Ferrante, Margherita Irene Beruto, Rob Eduard Schouten, Peter J. Batt and Renato Paiva

PUBLISHED IN: Frontiers in Plant Science

frontiers Research Topics

ISSN 1664-8714
ISBN 978-2-88974-678-1
DOI 10.3389/978-2-88974-678-1

About Frontiers

Frontiers is more than just an open-access publisher of scholarly articles: it is a pioneering approach to the world of academia, radically improving the way scholarly research is managed. The grand vision of Frontiers is a world where all people have an equal opportunity to seek, share and generate knowledge. Frontiers provides immediate and permanent online open access to all its publications, but this alone is not enough to realize our grand goals.

Frontiers Journal Series

The Frontiers Journal Series is a multi-tier and interdisciplinary set of open-access, online journals, promising a paradigm shift from the current review, selection and dissemination processes in academic publishing. All Frontiers journals are driven by researchers for researchers; therefore, they constitute a service to the scholarly community. At the same time, the Frontiers Journal Series operates on a revolutionary invention, the tiered publishing system, initially addressing specific communities of scholars, and gradually climbing up to broader public understanding, thus serving the interests of the lay society, too.

Dedication to Quality

Each Frontiers article is a landmark of the highest quality, thanks to genuinely collaborative interactions between authors and review editors, who include some of the world's best academicians. Research must be certified by peers before entering a stream of knowledge that may eventually reach the public - and shape society; therefore, Frontiers only applies the most rigorous and unbiased reviews.
Frontiers revolutionizes research publishing by freely delivering the most outstanding research, evaluated with no bias from both the academic and social point of view. By applying the most advanced information technologies, Frontiers is catapulting scholarly publishing into a new generation.

What are Frontiers Research Topics?

Frontiers Research Topics are very popular trademarks of the Frontiers Journals Series: they are collections of at least ten articles, all centered on a particular subject. With their unique mix of varied contributions from Original Research to Review Articles, Frontiers Research Topics unify the most influential researchers, the latest key findings and historical advances in a hot research area! Find out more on how to host your own Frontiers Research Topic or contribute to one as an author by contacting the Frontiers Editorial Office: frontiersin.org/about/contact

QUALITY OF ORNAMENTAL CROPS: EFFECT OF GENOTYPE, PREHARVEST, AND IMPROVED PRODUCTION CHAINS ON QUALITY ATTRIBUTES OF ORNAMENTAL CROPS

Topic Editors:
Patricia Duarte De Oliveira Paiva, Federal University of Lavras, Brazil
Julian C. Verdonk, Wageningen University and Research, Netherlands
Antonio Ferrante, University of Milan, Italy
Margherita Irene Beruto, Istituto Regionale per la Floricoltura (IRF), Italy
Rob Eduard Schouten, Wageningen University and Research, Netherlands
Peter J. Batt, Curtin University, Australia
Renato Paiva, Universidade Federal de Lavras, Brazil

Citation: De Oliveira Paiva, P. D., Verdonk, J. C., Ferrante, A., Beruto, M. I., Schouten, R. E., Batt, P. J., Paiva, R., eds. (2022). Quality of Ornamental Crops: Effect of Genotype, Preharvest, and Improved Production Chains on Quality Attributes of Ornamental Crops. Lausanne: Frontiers Media SA.
doi: 10.3389/978-2-88974-678-1

Table of Contents

frontiers | Frontiers in Plant Science

TYPE Editorial
PUBLISHED 03 August 2022
DOI 10.3389/fpls.2022.918864

OPEN ACCESS

EDITED BY
Youssef Rouphael,
University of Naples Federico II, Italy

REVIEWED BY
Chiara Cirillo,
University of Naples Federico II, Italy

*CORRESPONDENCE
Patricia Duarte de Oliveira Paiva
patriciapaiva@ufla.br

SPECIALTY SECTION
This article was submitted to Crop and Product Physiology, a section of the journal Frontiers in Plant Science

RECEIVED 12 April 2022
ACCEPTED 14 July 2022
PUBLISHED 03 August 2022

CITATION
Verdonk JC, Ferrante A, Beruto MI, Batt P, Paiva R, Schouten RE and Paiva PDO (2022) Editorial: Quality of Ornamental Crops: Effect of Genotype, Preharvest, and Improved Production Chains on Quality Attributes of Ornamental Crops. *Front. Plant Sci.* 13:918864. doi: 10.3389/fpls.2022.918864

Editorial: Quality of Ornamental Crops: Effect of Genotype, Preharvest, and Improved Production Chains on Quality Attributes of Ornamental Crops

Julian C. Verdonk[1], Antonio Ferrante[2], Margherita Irene Beruto[3], Peter Batt[4], Renato Paiva[5], Rob E. Schouten[6] and Patricia Duarte de Oliveira Paiva[7]*

[1]Horticulture and Product Physiology, Plant Science Group, Wageningen University and Research, Wageningen, Netherlands, [2]University of Milan, Milan, Italy, [3]Istituto Regionale per la Floricoltura, Sanremo, Italy, [4]Curtin University, Perth, WA, Australia, [5]Departamento de Biologia, Instituto de Ciências Biológicas, Universidade Federal de Lavras, Lavras, Brazil, [6]Food and Bio Based Research, Wageningen University and Research, Wageningen, Netherlands, [7]Departamento de Agricultura, Escola de Ciências Agrárias, Universidade Federal de Lavras, Lavras, Brazil

KEYWORDS

ornamental plant, postharvest, biotechnology, plant physiology, floriculture

Editorial on the Research Topic
Quality of Ornamental Crops: Effect of Genotype, Preharvest, and Improved Production Chains on Quality Attributes of Ornamental Crops

Acceptance of ornamental crops depends on the aesthetic value, the combination of flower number, shape, and size, as well as on the color, fragrance, and uniformity of blooming of these flowers. Plant shape, color, and patterning also are important. Vase life and keeping quality are often dependent on these features remaining at certain values, and the absence of pests and diseases. Reasons for quality loss are numerous. The quality of ornamental crops is realized in field or greenhouse by selecting the best genotype of the species of interest and the best cultivation conditions. Environmental conditions during preharvest such as temperature, relative humidity, light intensity, quality, and periodicity, are essential for crop physiology and influence quality and yield. The combination genotype and environment can be used to optimize to grow the best quality possible.

After harvest, the quality cannot be improved but only preserved. Postharvest storage conditions and treatments can be optimized to preserve quality; long vase life of cut flowers, and post-production life of potted plants at the consumer. This Research Topic collects reviews and research papers that cover quality, production, and distribution chain of ornamental crops. It is aimed to bring together research on innovation, technology, and sustainability of ornamental plant production, in order to stimulate the development of ornamental crop research, particularly focused on cut and potted flowers

and foliage. In the 20 articles published, both reviews and experimental, the most recent advances on ornamental plants as biotechnology, physiology, nutrition, propagation, and pre- and postharvest treatments are highlighted.

Quality aspects of ornamental crops

The aesthetic value of ornamental crops, combined with expected postharvest life defines the acceptance on the market. The first, is largely depended on shape, color, fragrance, and uniformity of blooming. Some of the articles are studies on the improvement of quality. Because humans cannot distinguish colors equally, a new digital image methodology—FloCIA (Flower Color Image Analysis) software, was developed for color evaluation in sunflower ray floret. The main advantage is the high accuracy of color category matching and the concise information that may be applied for color evaluation, mainly by breeders and traders (Zoric et al.). Fragrance emission was shown to be influenced by light and temperature during postharvest conditions. The quality of the scent is affected by light and temperature, indicating the importance of adequate pre-harvest conditions. For narcissus, 15°-5°C thermoperiod and a 12:12 Light Dark photoperiod provide the richest scent profile production. This information can be used to optimize or manipulate fragrance, which is good for consumers, and could also be interesting for the perfume industry (Terry et al.).

Genotype and molecular biology strategies

Although the acceptance of transgenic crops is not widespread, the acceptance in ornamental crops is considered higher (Chandler and Sanchez, 2012). The unintentional release of GM petunia which could produce an orange color not previously seen in the genus demonstrates the possibilities, as well as the absence of long-term consequences (Bashandy and Teeri, 2017; Boutigny et al., 2020). A biotechnological study of genes related to a compact phenotype was carried out in *Kalanchoe blossfeldiana*. The over expression of the genes collectively responsible for hairy root or Ri phenotype resulted in a desired more compact plant morphology, and reduced ethylene sensitivity, resulting in increased postharvest longevity (Trevenzoli et al.). Another interesting approach is the use of interspecies hybrids to create new sources for breeding targets. The results obtained for Pelargonium may consist in a start point to study the genetics of organelle management and expression, concerning in an evolutionary context and/or genes involved in these processes studies (Breman et al.).

The processes of divergence and speciation, associated with the role of geography and climate changes, can be visualized with evolutionary research. Understanding these processes allows for estimating the genetic structure and demographic history of closely related species. A study with *Rhododendron dauricum* and *R. mucronulatum* was performed and showed the genetic differentiation and a clustered monophyletic group when SLAF data was used but not in cpDNA. The evolutionary process of these species was a consequence of an interspecific gene flow, and the divergence was maintained by natural selection (Yang et al.).

In woody plants native to temperate and boreal regions, bud dormancy and cold acclimation are strictly regulated induced by shortening daylength and low temperature. Dehydration is essential to decrease free water that could lead to mechanical stress caused by extracellular ice formation. Dehydrins are a subset of cold induced genes, involved with the plant protection against freezing. They also interact with carbohydrates, which are associated with cold hardiness. Together they may help the plant improve cold hardiness. During cold acclimation of roses cultivars, a *Dehydrin* (*RhDHN5*) was upregulated, but the stem water content remained stable. Differences in carbohydrate metabolism and related genes, could not be attributed to cold hardiness, indicating different cold adaptation strategies (Ouyang et al.).

Preharvest

Proper cultivation is essential for yield and quality. Many (ornamental) plants are produced from stock plants by planting shoot tip cuttings that form adventitious roots. The review article from Druege summarizes the main processes involved in vegetative propagation by rooting of shoot tip cuttings, used for many ornamental plant species. Besides the influence of environmental factors and plant genotype, the author emphasizes the bottlenecks, the role of auxins and cytokinins, C, and N surplus and utilization, strigolactones, wound-induced accumulation of ethylene, and jasmonic acid, and the relation with the vitality of cuttings or insufficient adventitious root formation.

The author proposes a targeted approach to analyse and group plant species and cultivars according to potential bottlenecks, and proposes to combine this with the machine learning inspired concept of the "plant perceptron" (Scheres and van der Putten, 2017). Knowing these factors and roles may allow for improving propagation protocols, maximizing the plant genetic endogenous potential, and contributing to demand for sustainability (Druege).

Concerning advances in plant *in vitro* propagation, a methodology for direct somatic embryogenesis and organogenesis of clematis cultivars is presented, studying the effect of plant growth regulators by using several concentrations. In the study performed, the process was affected by the light intensity and temperature, besides it was observed that some cultivars presented a higher frequency of secondary somatic

embryogenesis. Surprisingly, the response from different cultivars was quite similar. In other species, often large differences in shoot formation exist between genotypes. The results show an important advance, since it is the first time that the studied clematis cultivars have been shown to possess high morphogenic capacity due to a combination of methods applied during micropropagation (Mitrofanova et al.).

For plant production stages, beneficial bacteria may play an important role by acting as biostimulant for avoiding water-deficit stress in ornamental plants cultivated in the greenhouse. Bacteria were isolated from the rhizosphere of water stressed greenhouse ornamentals: coleus, petunia, geranium, vinca, and zinnia. Ten isolates were tested on petunia and geranium during discontinued irrigation. The combination of *in vitro* and greenhouse experiments led to the identification of Pseudomonas strains that can increase tolerance to and recovery from water stress (Nordstedt et al.).

In another approach, animal-based protein hydrolysate (PH) was tested for biostimulant properties. When applied as a foliar spray in petunia, contributed to achieve extra-grade plants, by improved net photosynthesis and stomatal conductance. This is a promising result since improving the metabolism, may turn nutrients absorption more efficient, leading to sustainable production practices (Cristiano and De Lucia).

During potted roses production, pinching is a technique that is used to stimulate branching. However, it can lead to leaves to turn yellow and abscise. The same problem occurs in plants under low light conditions, as in home and offices. To prevent this, the application of the cytokinin thidiazuron (TDZ) may be used, resulting in plants with shorter and thicker stems. The study performed by Çelikel et al. indicates the antagonistic effect of TDZ (cytokinin) and GA3 in potted rose in the control of stem maturation and elongation. It was demonstrated that TDZ regulates shoot elongation and stem enlargement through the modulation of bioactive GA biosynthesis. The application of both, Ga3 and TDZ resulted in normal elongation growth, maintaining the compactness, and being an alternative for plant height control.

Postharvest light has shown promise for the preservation of quality in postharvest, the practical application of light during postharvest is challenging because packing material (boxes etc.), as well as the plant products themselves potentially (partially) blocks the light to reach all plant tissues. An interesting approach discussed the effectiveness of external light stimuli on pre and postharvest, for improving the quality of cut flowers. Also, it is highlighted future research focus, considering the understanding of how light stimuli affect several features of cut flowers and investigating the reaction among species and cultivars (Horibe). Recent work has indicated that by applying specific treatments during the cultivation, quality can be improved (Affandi et al., 2020, 2022; Min et al., 2021). The results of the study by Terfa et al. show that increased blue light during preharvest improved stomatal function under high RH conditions. Ornamentals grown under high RH often suffer from stomatal malfunction leading to reduced vase life (Arve et al., 2013; Aliniaeifard and van Meeteren, 2014; Schouten et al., 2018). This was shown to be connected to increased [ABA]. The degradation of ABA-GE by β-glucosidase steers the diurnal ABA pool turnover, and this activity was shown to be induced by Blue LED light. The B-light during the day led to increased β-glucosidase activity during the night that led to ABA release. This preharvest B-light could be used to improve postharvest water balance of roses.

Improved production chains

Quality can be preserved during the distribution chain by controlling the post-production conditions (Manfredini et al., 2017; Sales et al., 2021). Cut flowers quality can be preserved after harvest by lowering the metabolism. Immediately after harvest the temperature must be lowered for reducing respiration, ethylene production, and water loss. Recently, it has been reported the importance of light quality during the storage of cut flowers. In chilling sensitive Anthurium, it was shown that the light spectrum could reduce chilling injury symptoms. Cut anthurium flowers showed the longest vase life if stored under red light and the shortest vase life was observed in cut spathes exposed to blue light (Aliniaeifard et al.). On the contrary, for carnation cut flowers, blue light exposure improves vase life, by inducing the antioxidant defense system in petals (Aalifar et al.).

In cut flower conservation after harvest, the use of auxins is not very common. There are not many studies that explore the use. In Red Cestrum, pulse treatments of auxin demonstrated that addition of auxin can reduce floret bud abscission, and that the efficacy was improved by raising the solution pH since this condition contributes to the auxins acropetally transport (Abebie et al.).

The use of putrescine was investigated as a new strategy for cut foliage conservation after harvest, showing to be effective to alleviate senescence. Spraying putrescine on foliage may prevent membrane impairment and injury, besides affecting plant metabolism, and delaying senescence (Qu et al.). A promising nutrient for postharvest is selenium and its role on the longevity of ethylene-sensitive flowers was discussed in a review indicating a positive alternative, commercially viable and environmentally friendly (Costa et al.).

Future and outlook

The potential new products may be found by observations of the efficacy in other species, as well as in animals and humans. For example, in the study developed by Li et al., they found that Magnesium hydride (MgH_2) which is a solid-state hydrogen source with high storage capacity (7.6 wt%), is a potential product for postharvest. Initially evaluated in medicine, the

effectiveness was also observed in plants, analyzing cur carnation flowers. The results showed that MgH_2-supplying H_2 could prolong the vase life *via* H_2S signaling. Also, this indicates that future studies may consider a possible application of hydrogen-releasing not only for postharvest but also for production (Li et al.).

The use of mathematics, machine learning information-processing system, connecting with some recent concepts as plant perceptron were presented by Druege as application approaches for plant studies. This may be in connection with early plant responses, as it was demonstrated for cutting root formation concerning the role of plant hormones JA, ET or IAA and the Aux/IAA-ARF modules (Druege).

The mechanisms and key factors in the plant-microorganism-abiotic environment are indicated as future subject for research on plant propagation (Druege).

A relatively new topic is to use the light spectrum, intensity, and perhaps period to improve quality. This can be done during pre and postharvest as discussed above. Although there are many studies in all phases of plant life, the effects of different light spectra on post-harvest performance of cut flowers are largely unknown. To advance in this knowledge, the use of light emitting diodes (LEDs), allows studying the main light spectra Red (R) and blue (B) wavelengths on plants. The low energy use and lower temperature released by LED modules have improved possibilities to apply them, as well as the reduced costs. In post-harvest phase, an enhanced of the activity of antioxidant systems may occur in consequence of the light spectra, affecting the longevity, but some detailed studies are still required. In this way, these results show important contributions for flower post-harvest.

In the end, all the publications of this Research Topic contributed with outstanding information for the ornamental plant area.

Author contributions

All authors listed, have made substantial, direct, and intellectual contributions to the topic, and approved it for publication.

Acknowledgments

The Editors would like to thank all authors that participated in this Research Topic by submitting the articles resulting from their research and with the support of the funders. Special acknowledgment goes to the reviewers, both from editorial board and external, who have contributed with very important comments and suggestions, and realized fundamental support for this publication.

Conflict of interest

The authors declare that the research was conducted in the absence of any commercial or financial relationships that could be construed as a potential conflict of interest.

Publisher's note

References

Affandi, F. Y., Prayoga, T., Ouzounis, T., Giday, H., Verdonk, J. C., Woltering, E. J., et al. (2022). Additional blue LED during cultivation induces cold tolerance in tomato fruit but only to an optimum. *Biology* 11, 101. doi: 10.3390/biology11010101

Affandi, F. Y., Verdonk, J. C., Ouzounis, T., Ji, Y., Woltering, E. J., and Schouten, R. E. (2020). Far-red light during cultivation induces postharvest cold tolerance in tomato fruit. *Postharvest Biol. Technol.* 159, 111019. doi: 10.1016/j.postharvbio.2019.111019

Aliniaeifard, S., and van Meeteren, U. (2014). Natural variation in stomatal response to closing stimuli among *Arabidopsis thaliana* accessions after exposure to low VPD as a tool to recognize the mechanism of disturbed stomatal functioning. *J. Exp. Bot.* 65, 6529–6542. doi: 10.1093/jxb/eru370

Arve, L. E., Terfa, M. T., Gislerød, H. R., Olsen, J. E., and Torre, S. (2013). High relative air humidity and continuous light reduce stomata functionality by affecting the ABA regulation in rose leaves. *Plant Cell Environ.* 36, 382–392. doi: 10.1111/j.1365-3040.2012.02580.x

Bashandy, H., and Teeri, T. H. (2017). Genetically engineered orange petunias on the market. *Planta* 246, 277–280. doi: 10.1007/s00425-017-2722-8

Boutigny, A.-L., Dohin, N., Pornin, D., and Rolland, M. (2020). Overview and detectability of the genetic modifications in ornamental plants. *Hortic. Res.* 7, 1–12. doi: 10.1038/s41438-019-0232-5

Chandler, S. F., and Sanchez, C. (2012). Genetic modification; the development of transgenic ornamental plant varieties. *Plant Biotechnol. J.* 10, 891–903. doi: 10.1111/j.1467-7652.2012.00693.x

Manfredini, G. M., Paiva, P. D. O., Almeida, E. F. A., Reis, M. V., and Maia, M. O. (2017). Storage and methyl jasmonate in postharvest conservation of roses cv. Avalanche. *Ornam. Hortic.* 23, 207–211. doi: 10.14295/oh.v23i2.992

Min, Q., Marcelis, L. F. M., Nicole, C. C. S., and Woltering, E. J. (2021). High light intensity applied shortly before harvest improves lettuce nutritional quality and extends the shelf life. *Front. Plant Sci.* 12, 615355. doi: 10.3389/fpls.2021.615355

Sales, T. S.,Paiva, P. D. O., Manfredini, G. M., Nascimento, A. M. P., and Reis, M. V. (2021). Water relations in cut calla lily flowers maintained under different postharvest solutions. *Ornam. Hortic.* 27, 126–136. doi: 10.1590/2447-536X.v27i2.2235

Scheres, B., and van der Putten, W. H. (2017). The plant perceptron connects environment to development. *Nature* 543, 337–345. doi: 10.1038/nature22010

Schouten, R. E., van Dien, L., Shahin, A., Heimovaara, S., van Meeteren, U., and Verdonk, J. C. (2018). Combined preharvest and postharvest treatments affect rapid leaf wilting in Bouvardia cut flowers. *Sci. Hortic.* 227, 75–78. doi: 10.1016/j.scienta.2017.09.014

frontiers in Plant Science

ORIGINAL RESEARCH
published: 28 January 2020
doi: 10.3389/fpls.2019.01754

Identification of *Pseudomonas* Spp. That Increase Ornamental Crop Quality During Abiotic Stress

Nathan P. Nordstedt[1], *Laura J. Chapin*[1], *Christopher G. Taylor*[2] *and Michelle L. Jones*[1*]

[1] *Department of Horticulture and Crop Science, Ohio Agricultural Research and Development Center, The Ohio State University, Wooster, OH, United States,* [2] *Department of Plant Pathology, Ohio Agricultural Research and Development Center, The Ohio State University, Wooster, OH, United States*

OPEN ACCESS

Edited by:
Julian C. Verdonk, Wageningen University and Research, Netherlands

Reviewed by:
Kazuo Nakashima, Japan International Research Center for Agricultural Sciences, Japan
Adeyemi Oladapo Aremu, North-West University, South Africa

****Correspondence:***
Michelle L. Jones
jones.1968@osu.edu

Specialty section:
This article was submitted to Crop and Product Physiology, a section of the journal Frontiers in Plant Science

Received: *16 October 2019*
Accepted: *13 December 2019*
Published: *28 January 2020*

Citation:
Nordstedt NP, Chapin LJ, Taylor CG and Jones ML (2020) Identification of Pseudomonas Spp. That Increase Ornamental Crop Quality During Abiotic Stress. Front. Plant Sci. 10:1754. doi: 10.3389/fpls.2019.01754

The sustainability of ornamental crop production is of increasing concern to both producers and consumers. As resources become more limited, it is important for greenhouse growers to reduce production inputs such as water and chemical fertilizers, without sacrificing crop quality. Plant growth promoting rhizobacteria (PGPR) can stimulate plant growth under resource-limiting conditions by enhancing tolerance to abiotic stress and increasing nutrient availability, uptake, and assimilation. PGPR are beneficial bacteria that colonize the rhizosphere, the narrow zone of soil in the vicinity of the roots that is influenced by root exudates. In this study, *in vitro* experiments were utilized to screen a collection of 44 *Pseudomonas* strains for their ability to withstand osmotic stress. A high-throughput greenhouse experiment was then utilized to evaluate selected strains for their ability to stimulate plant growth under resource-limiting conditions when applied to ornamental crop production systems. The development of a high-throughput greenhouse trial identified two pseudomonads, *P. poae* 29G9 and *P. fluorescens* 90F12-2, that increased petunia flower number and plant biomass under drought and low-nutrient conditions. These two strains were validated in a production-scale experiment to evaluate the effects on growth promotion of three economically important crops: *Petunia* × *hybrida*, *Impatiens walleriana*, and *Viola* × *wittrockiana*. Plants treated with the two bacteria strains had greater shoot biomass than untreated control plants when grown under low-nutrient conditions and after recovery from drought stress. Bacteria treatment resulted in increased flower numbers in drought-stressed *P. hybrida* and *I. walleriana*. In addition, bacteria-treated plants grown under low-nutrient conditions had higher leaf nutrient content compared to the untreated plants. Collectively, these results show that the combination of *in vitro* and greenhouse experiments can efficiently identify beneficial *Pseudomonas* strains that increase the quality of ornamental crops grown under resource-limiting conditions.

Keywords: drought, floriculture, greenhouse production, high-throughput, horticulture, low nutrient, plant growth promoting rhizobacteria, plant-microbe interaction

INTRODUCTION

Greenhouse-grown ornamentals are largely produced in containers using soilless growing mixes (Ball, 1998). Until recently, little attention has been given to the development of beneficial microbial communities within these containerized growing systems and to determining how these plant-bacteria associations can be used to improve ornamental crop quality. The rising costs of fertilizing and irrigating greenhouse crops have increased the interest in beneficial bacteria that can improve water and nutrient-use efficiency while reducing leaching and potential environmental contamination (Adesemoye et al., 2009). Plant growth promoting rhizobacteria (PGPR) can positively impact plant growth and resilience, resulting in a higher quality crop that is also more tolerant of drought and nutrient deficient conditions that might be encountered during shipping and retailing (i.e. postproduction abiotic stresses) (Waterland et al., 2010; Ruzzi and Aroca, 2015).

Plant growth promoting rhizobacteria (PGPR) comprise many taxonomic groups with diverse plant hosts (Kloepper et al., 1989). These bacteria colonize the rhizosphere, a narrow zone of soil that is associated with the roots and influenced by root exudates. In these beneficial plant-microbe interactions, the host plant secretes compounds into the rhizosphere that are used as a food source by the bacteria, which in turn stimulate plant growth and mediate stress responses through multiple mechanisms (Lugtenberg and Kamilova, 2009). PGPR can directly promote plant growth and abiotic stress tolerance by facilitating the acquisition of essential nutrients or by modulating the production of plant hormones (Goswami et al., 2016).

The application of bacteria that modify phytohormone concentrations such as gibberellins, abscisic acid, and auxin have been shown to increase osmotic stress tolerance and yield of soybean (Kang et al., 2014), reduce water loss in grape (Salomon et al., 2014), and increase rooting of kiwi (Erturk et al., 2010), respectively. Bacterial production of the enzyme ACC deaminase reduces production of the stress hormone ethylene in plants under drought (Glick, 2005), resulting in increased growth of tomato and pepper (Mayak et al., 2004), pea (Zahir et al., 2008), and maize (Zafar-ul-Hye et al., 2014) plants grown under water-limiting conditions. In addition, there is evidence that bacteria that withstand osmotic stress *in vitro* can confer this stress tolerance to plants (Asghar et al., 2015; Habib et al., 2016). The ability for bacteria to withstand osmotic stress is often attributed to their ability to form biofilms of exopolysaccharides (EPS), preventing desiccation under conditions of osmotic stress. Colonization of plant roots by EPS-producing bacteria increases tolerance to drought stress and increases shoot biomass of wheat (Hussain et al., 2014a) and root and shoot length of maize (Hussain et al., 2014b).

PGPR can improve plant nutrition by increasing nutrient availability, uptake, and assimilation. *Rhizobium* have been documented extensively for their ability to fix atmospheric nitrogen in symbiotic relationship with leguminous plants (Sessitsch et al., 2002). However, free-living nitrogen-fixing bacteria increase yield in corn (Garcia De Salamone et al., 1996; Kuan et al., 2016), plant size and nitrogen content of wheat (Sabry et al., 1997), and nitrogen uptake in tomato (Adesemoye et al., 2010). Phosphate solubilizing bacteria stimulate growth of many crops, resulting in increased yield and nutrient content of lettuce (Lai et al., 2008), improved germination and plant size of rice (Ashrafuzzaman et al., 2009), and increased berry production of raspberry (Orhan et al., 2006). PGPR that produce siderophores can chelate iron and make it more bioavailable to plants. Inoculation with these PGPR have been shown to increase iron content in plants (Zhou et al., 2018). The application of PGPR with the ability to enhance nutrient bioavailability have been used as a tool to reduce chemical fertilizer inputs without sacrificing crop quality (Adesemoye et al., 2009).

The genus *Pseudomonas* has been well studied for its ability to stimulate plant growth under drought and low-nutrient conditions (Jha and Saraf, 2015). Inoculation with *Pseudomonas* spp. results in an increase of root and shoot length and total plant biomass in sunflower, finger millet, and peas when subjected to drought conditions (Zahir et al., 2008; Sandhya et al., 2009; Chandra et al., 2018). Aspen seedlings grown under nutrient-limiting conditions and treated with *Pseudomonas fluorescens* strains Pf0-1, SBW25, and WH6 and *P. protegens* Pf-5 have increased nutrient uptake and root length and biomass (Shinde et al., 2017). The *Pseudomonas putida* strain UW4 has served as a model system for studying the molecular and transcriptional properties of the enzyme ACC deaminase (Hontzeas et al., 2004; Cheng et al., 2008). The genus is also considered a model root colonizer, making it an optimal system to use in studying beneficial plant-microbe interactions (Lugtenberg et al., 2001).

Although there is growth in the area of PGPR research, much of this work has been conducted *in vitro* or focused on agronomic crops with little emphasis on ornamental crops (Paulitz and Richard, 2001; Vejan et al., 2016). There is evidence to suggest that PGPR tested *in vitro* often do not have the same growth-promoting effects when applied *in planta* (Ryu et al., 2005). In addition, many of these microorganisms originate from the soils of agronomic fields, and it is to be expected that changes in environment and abiotic factors would influence the efficacy of these organisms (Naylor and Coleman-Derr, 2018). Therefore, the inability to translate results from *in vitro* or field soil studies to greenhouse production of ornamental crops is of concern. The aim of this study was to identify *Pseudomonas* strains that stimulated growth and improved the quality of greenhouse-grown ornamentals under both drought and low-nutrient conditions.

MATERIALS AND METHODS

Selection of Osmoadaptive Bacteria

An *in vitro* osmoadaptability bioassay was adapted from Asghar et al. (2015) for the selection of osmotic stress tolerant bacteria within a collection of 44 *Pseudomonas* strains originating from a variety of natural sources including water, soil, and plants (Mavrodi et al., 2012; Subedi et al., 2019). Briefly, single bacteria colonies were inoculated into separate wells of a 96-well microtiter

plate pre-filled with 200 µL LB. Bacteria were incubated at 28°C with shaking at 120 rpm for 18 h. The optical density at 595 nm (OD_{595}) was measured using a spectrophotometer (DTX880, Beckman Coulter, Brea, CA) and adjusted to OD_{595} of 0.8 with LB. Ten microliters of the bacteria cultures were transferred to a microtiter plate prefilled with tryptic soy broth (TSB) or yeast extract mannitol broth (YEM), each amended with 30% PEG_{8000} (w/v). Each bacteria strain was assayed on three separate microtiter plates for each media type (n = 3). Plates were incubated at 28°C with shaking at 120 rpm. After 96 h, the OD_{595} was measured to quantify the growth in PEG.

In Planta Evaluation of Bacteria

Experiment 1: High-Throughput Greenhouse Evaluation of Plant Responses to Treatment With Osmoadaptive Bacteria Strains

Petunia × *hybrida* 'Picobella Blue' seeds (Syngenta Flowers, Gilroy, CA) were sown in Pro-Mix PGX media (Premier Tech Horticulture, Quakertown, PA) and fertilized at each watering with 50 mg L^{-1} N from 15N–2.2P–12.5K–2.9Ca–1.2Mg water soluble fertilizer (JR Peters Inc., Allentown, PA) until transplant. Plants were grown in a greenhouse with temperatures set at 24/18°C (day/night) and a 16-h photoperiod. Supplemental lighting was supplied by high pressure sodium and metal halide lights (GLX/GLS e-systems GROW lights, PARSource, Petaluma, CA, USA) to maintain light levels above 250 µmol m^{-2} s^{-1}. Seedlings were transplanted four weeks after sowing to 6.35 cm pots containing a 1:1 mix by volume of sand and turface (Profile Products LLC, Buffalo Grove, IL). Plants were arranged in a randomized complete block design (RCBD) with four blocks, and four single-plant replicates per block (n = 16).

To prepare bacteria inoculum, liquid LB media was inoculated with individual bacteria cultures selected from the *in vitro* osmoadaptability bioassay (**Table 1**) and incubated at 28°C for 9 h with shaking at 250 rpm. After incubation, cultures were adjusted to OD_{595} = 0.8 with LB. Final bacteria inoculum for treating the plants was prepared by diluting each culture 1:100 in reverse osmosis (RO) water. Uninoculated LB media diluted 1:100 with RO water was used as a negative control.

TABLE 1 | *Pseudomonas* strains selected for their ability to withstand PEG-mediated osmotic stress *in vitro*.

Strain	Species	Source	Evaluated in multi-species greenhouse trial
14B11	*P. chlororaphis*	Missouri River	
14D6	*P. chlororaphis*	Mississippi River	
29G9	*P. poae*	Herbarium Sample	x
36B3	*P. fluorescens*	Wyoming Soil	
37D10	*P. brassicacearum*	Wyoming Soil	
48B8	*P. chlororaphis*	Wisconsin Soil	
48G9	*P. chlororaphis*	Wisconsin Soil	
89F1	*P. fluorescens*	Missouri Soil	
90F12-2	*P. fluorescens*	Missouri Soil	x
94G2	*P. frederiksbergensis*	Missouri Soil	

Selected strains were also evaluated in planta *in a high-throughput greenhouse trial. Pseudomonas strains shown to increase plant growth in the high-throughput greenhouse trial were then evaluated in a multi-species greenhouse trial.*

Experiment 1a: Drought Stress

A greenhouse trial was developed to determine if bacteria application can enhance growth and recovery of petunia plants following drought stress. Following transplant, plants were fertilized at each irrigation with 50 mg L^{-1} N from 15N–2.2P–12.5K–2.9Ca–1.2Mg water soluble fertilizer (JR Peters Inc.). Plants were treated weekly with 40 mL bacteria inoculum or negative control LB solution, beginning the day after transplant. This volume saturated the growing media without resulting in leaching. Drought treatment began three weeks post-transplant by discontinuing weekly bacteria treatments and irrigation until all plants showed visible loss of turgidity across the plant. Plants were initially rewatered with RO water and regular irrigation with fertilizer and weekly bacteria treatments were then resumed. Plant performance was evaluated six weeks post-transplant. Flower numbers (including both open flowers and flower buds showing color) were counted and shoots (including stems, leaves, and flowers) were harvested. Tissue was dried in a forced-air oven at 49°C for at least 96 h and then weighed to measure shoot dry weight.

Experiment 1b: Low-Nutrient Stress

A second greenhouse trial was developed to evaluate the effect of bacteria application on petunia plant growth under low-nutrient conditions. After transplanting, plants were maintained with 25 mg L^{-1} N from 15N–2.2P–12.5K–2.9Ca–1.2Mg water soluble fertilizer (JR Peters Inc.) at every irrigation to induce low-nutrient stress (Ball, 1998). Plants were also treated weekly with 40 mL bacteria inoculum as described previously. Uninoculated LB media was used as the negative control. Plant performance was evaluated as described for Experiment 1a.

Experiment 2: Multi-Species Greenhouse Validation of Two *Pseudomonas* Strains

Petunia × *hybrida* 'Picobella Blue' (Syngenta Flowers), *Impatiens walleriana* 'Super Elfin Ruby' (PanAmerican Seed, West Chicago, IL), and *Viola* × *wittrockiana* 'Delta Pure Red' (Syngenta Flowers) seeds were sown and grown similar to Experiment 1. Seedlings were transplanted to 11.4 cm diameter pots containing Pro-Mix PGX (Premier Tech Horticulture) three weeks after sowing. Plants for each species were arranged in a RCBD with one plant per block. Due to variation in seed germination rates, there were 13, 14, and 18 blocks for *P. hybrida*, *V. wittrockiana*, and *I. walleriana*, respectively. Each species was blocked and analyzed independently. Bacteria inoculum was prepared according to the protocol in Experiment 1.

Experiment 2a: Drought Stress

A greenhouse trial was developed to validate the effect of bacteria application on plant growth and performance after recovery from drought stress. The greenhouse trial was conducted similarly to Experiment 1a with modifications due to pot size. Each plant was treated weekly with 120 mL of bacteria inoculum or negative control LB solution to saturate the growing media without resulting in leaching. Drought treatment began five weeks post-transplant and plant performance was evaluated as described for Experiment 1 at nine weeks post-transplant. In

addition, adhering media was washed from the roots, root tissue was dried in a forced-air oven at 49°C for at least 96 h, and root dry weight was used to calculate the root:shoot.

Experiment 2b: Low-Nutrient Stress

A second greenhouse trial was developed to validate the effect of bacteria application on plant growth under low-nutrient conditions. The greenhouse trial was conducted similarly to Experiment 1b, and each plant was treated weekly with 120 mL of bacteria inoculum. Plant performance was determined by flower number and shoot biomass as described for Experiment 1, and root dry weight was determined as described in Experiment 2a to calculate the root:shoot. Plants were harvested at 8 weeks post-transplant. In addition, dried leaf and stem tissue was pooled for tissue nutrient analysis. At least three plants per treatment of each species were pooled per sample. Dried tissue was ground to pass through a 2-mm sieve. All nutrient analyses were conducted at the Service Testing and Research Laboratory (STAR Lab, The Ohio State University/OARDC, Wooster, OH). Total nitrogen analysis was conducted on a 100 mg sample using the Dumas combustion method (Vario Max combustion analyzer, Elementar America, Inc., Germany) (Sweeney, 1989). Following tissue digestion using a microwave system (Discover SP-D, CEM Corporation) and nitric acid digestion, a 250 mg sample was analyzed for P, K, Ca, Mg, and S using an inductively coupled plasma spectrometer (ICP)(model PS3000, Leeman Labs Inc., Hudson, NH) (Isaac and Johnson, 1985).

Statistical Analysis

Statistical analyses were conducted in R Studio version 3.5.2 using an analysis of variance (ANOVA) with the model: $Y = \mu + \text{treatment} + \text{block}$. Factors that had a significant p-value ($p < 0.05$) were analyzed using Tukey's Honest Significant Difference.

RESULTS

In Vitro Selection of Osmoadaptive Bacteria

A total of 44 *Pseudomonas* strains were screened for their ability to withstand osmotic stress *in vitro* by growing independently in Yeast Extract Mannitol (YEM) or Tryptic Soy Broth (TSB) media, both containing 30% polyethylene glycol (PEG). When grown in PEG-amended YEM, over 75% of the strains had an OD less than 0.1, and ten strains had at least 4-fold higher OD readings (**Figure 1**). These ten strains were selected for further evaluation based on their high level of osmoadaptability in the PEG-amended YEM (**Table 1**). No additional strains were selected in the TSB media containing PEG (data not shown).

Development of a High-Throughput Greenhouse Trial to Evaluate the Efficacy of *In Vitro*-Selected Bacteria to Increase Plant Growth

The ten *Pseudomonas* strains selected from the *in vitro* osmoadaptability bioassay were evaluated independently in drought and low-nutrient greenhouse trials for their ability to improve plant growth under abiotic stress as compared to the negative control. Although results were not statistically significant, there was a general increase in both shoot biomass and flower number in plants treated with bacteria. For petunia plants subjected to drought conditions, application of strains 90F12-2, 89F1, 29G9, 14D6, 48B8, and 37D10 increased the average flower number (**Figure 2A**) and strains 90F12-2, 89F1, 14D6, 29G9, 14B11, and 48B8 increased the average shoot biomass (**Figure 2B**), compared to untreated control plants. Of those strains, five bacteria increased both the average flower

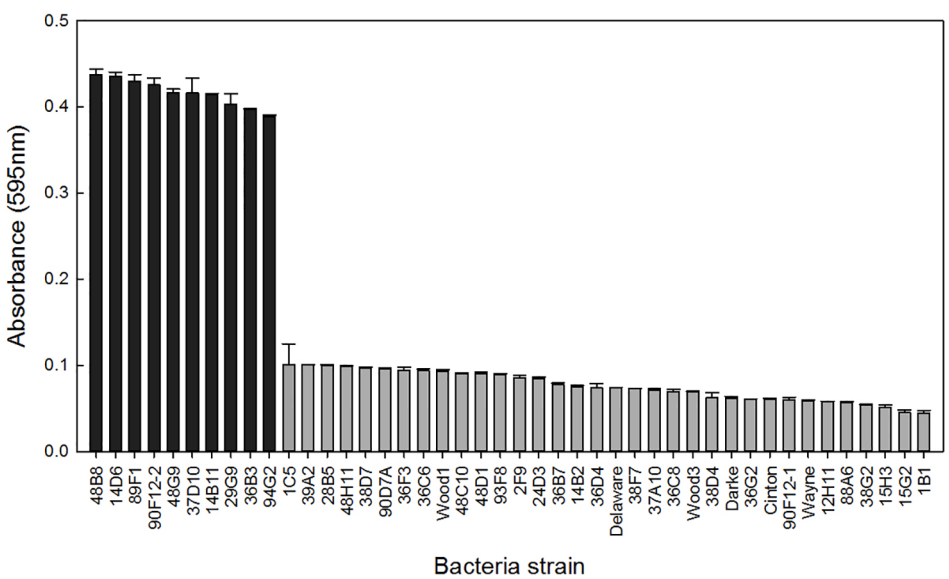

FIGURE 1 | Bacteria strains were grown in YEM media containing 30% polyethylene glycol to induce osmotic stress. Bars represent the mean (± SE) optical density (595nm) of the strains after 96 h incubation at 28°C (n = 3). Strains with an absorbance greater than 0.3 (black) were selected for further evaluation.

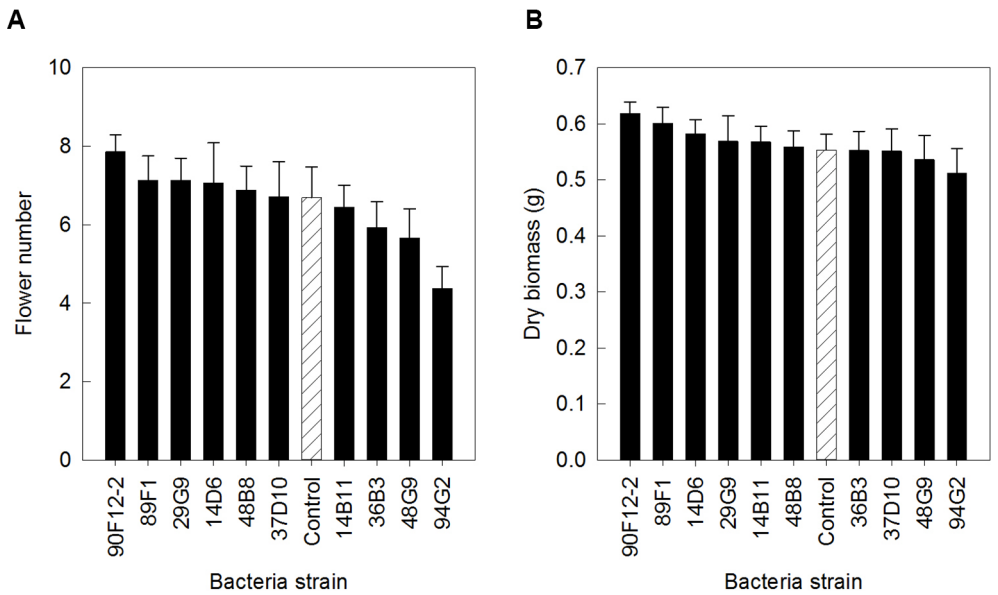

FIGURE 2 | Plant growth performance parameters for *Petunia* 'Picobella Blue' plants subjected to drought stress three weeks after transplant (n = 16). Plants were treated with bacteria inoculum weekly after transplant (black) and compared to the uninoculated control (white with lines). Total number of flowers **(A)** and total shoot biomass (dry weight) **(B)** was measured two weeks after rewatering following drought stress. Due to the high-throughput nature of the trial, results were not statistically significant. Trends in plant growth promotion were used for selection. Bars represent mean (± SE).

number and shoot biomass: 90F12-2, 29G9, 89F1, 14D6, and 48B8. Under low-nutrient conditions, application of strains 29G9, 36B3, 90F12-2, 37D10, and 94G2 increased the average flower number (**Figure 3A**) and strains 36B3, 90F12-2, 94G2, 37D10, 14D6, 29G9, and 89F1 increased the average shoot biomass (**Figure 3B**) of petunia plants. Of those strains, five strains increased the average of both flower number and shoot biomass: 29G9, 36B3, 90F12-2, 37D10, and 94G2. Due to the high-throughput nature of these trials, the trends in plant growth improvement were used to select for strains suitable for further

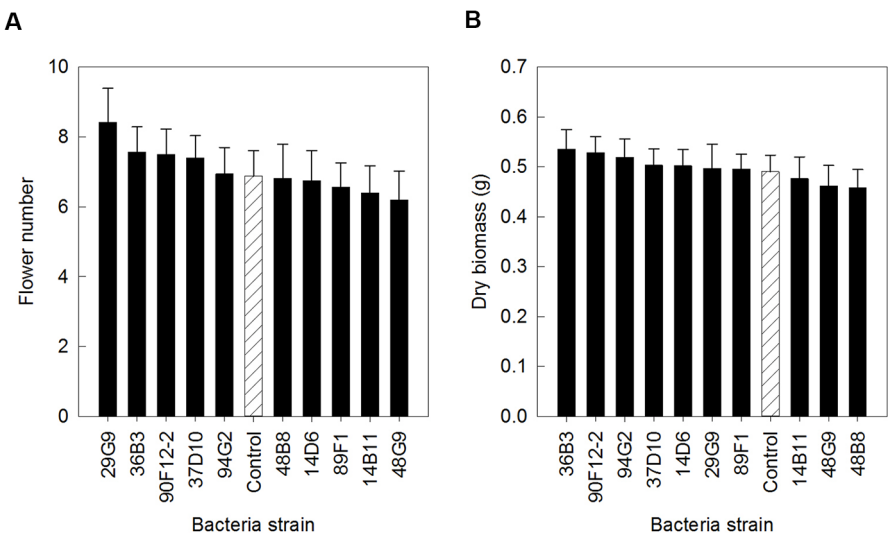

FIGURE 3 | Plant growth performance parameters for *Petunia* 'Picobella Blue' plants grown with 25 mg L^{-1} N from 15N–2.2P–12.5K–2.9Ca–1.2Mg water soluble fertilizer at every irrigation to induce low-nutrient stress (n = 16). Plants were treated with bacteria inoculum weekly after transplant (black) and compared to the uninoculated control (white with lines). Total number of flowers **(A)** and total shoot biomass (dry weight) **(B)** was measured six weeks after transplant. Due to the high-throughput nature of the trial, results were not statistically significant. Trends in plant growth promotion were used for selection. Bars represent mean (± SE).

evaluation. *Pseudomonas* strains 29G9 and 90F12-2 increased both average flower number and shoot biomass in petunias grown under both drought and low-nutrient conditions (**Figures 2** and **3**).

Evaluation of Two *Pseudomonas* Strains to Increase Plant Growth and Stress Tolerance in Ornamental Crops

The two *Pseudomonas* strains identified in the high-throughput trial were evaluated for their ability to increase plant size and flower number in *P. hybrida*, *I. walleriana*, and *V. wittrockiana* subjected to drought and low-nutrient conditions. Overall, plants subjected to low-nutrient conditions and treated with each of the strains were visibly healthier, larger, and of higher quality compared to the uninoculated control plants. Control plants showed visible leaf yellowing, which was not observed in plants treated with bacteria (**Figure 4**). Application of the two bacteria strains significantly increased flower number and shoot biomass of *P. hybrida* subjected to drought stress by an average of 27% and 51%, respectively (**Figures 5A, B**). Under low nutrient conditions, application of each of the strains also increased *P. hybrida* shoot biomass by an average of 38% (**Figure 6B**). The root:shoot ratio of *P. hybrida* subjected to drought and low-nutrient stress was significantly lower for plants treated with each of the strains compared to the uninoculated control (**Figures 5C** and **6C**). For *I. walleriana* subjected to drought stress, the application of both strains increased flower number by an average of 55%, a 1.5-fold increase (**Figure 5A**). In addition, both strains increased shoot biomass of *I. walleriana* subjected to drought conditions by an average of 31% (**Figure 5B**). Strain 29G9 increased flower number by an average of 47% (**Figure 6A**), and both strains increased shoot biomass by an average of 39% (**Figure 6B**) for *I. walleriana* grown under low-nutrient conditions. There was no significant difference in root:shoot ratio of *I. walleriana* plants subjected to drought or low-nutrient conditions (**Figures 5C** and **6C**). In addition, there was no significant difference in flower number of *V. wittrockiana* plants treated with *Pseudomonas* and subjected to drought (**Figure 5A**) or low-nutrient conditions (**Figure 6A**) as compared to the uninoculated control. However, application of both strains increased shoot biomass of *V. wittrockiana* subjected to drought conditions by an average of 33% (**Figure 5B**) and increased the average shoot biomass of *V. wittrockiana* grown under low-nutrient conditions by 48%, a 1.5-fold increase (**Figure 6B**). Finally, there was a significant decrease in root: shoot ratio in *V. wittrockiana* plants subjected to drought and low-nutrient conditions and treated with both of the strains compared to the uninoculated control (**Figures 5C** and **6C**).

Nutrient Content of Plant Leaf Tissue When Treated With Plant Growth-Promoting Rhizobacteria

All plants were grown under low-nutrient regimes, which resulted in lower than optimum tissue nutrient content (Dole and Wilkins, 1999). On average, the application of bacteria resulted in higher shoot macronutrient content than plants that were not treated with bacteria (negative control). The application of each bacteria strain increased the nitrogen

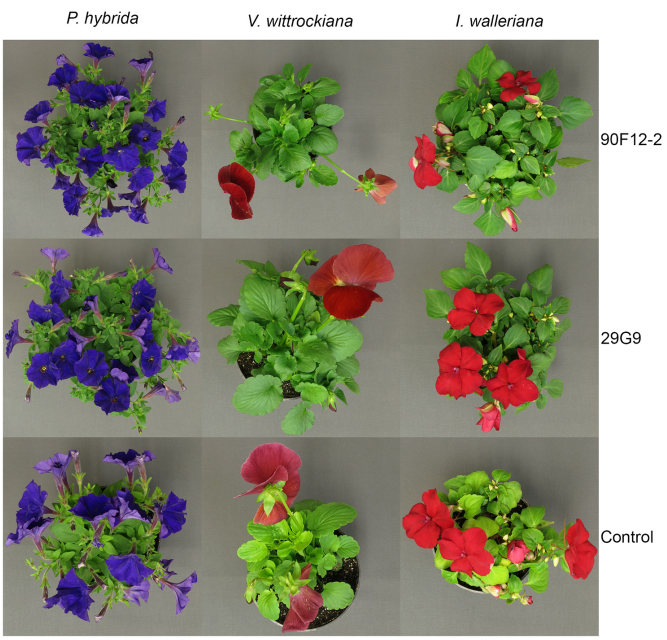

FIGURE 4 | Visual crop quality of *Petunia* × *hybrida*, *Impatiens walleriana*, and *Viola* × *wittrockiana* plants eight weeks after transplant. Plants were grown with 25 mg L^{-1} N from 15N–2.2P–12.5K–2.9Ca–1.2Mg water soluble fertilizer at every irrigation to induce low-nutrient stress and treated weekly with *Pseudomonas* strains 90F12-2, 29G9, or uninoculated LB (control).

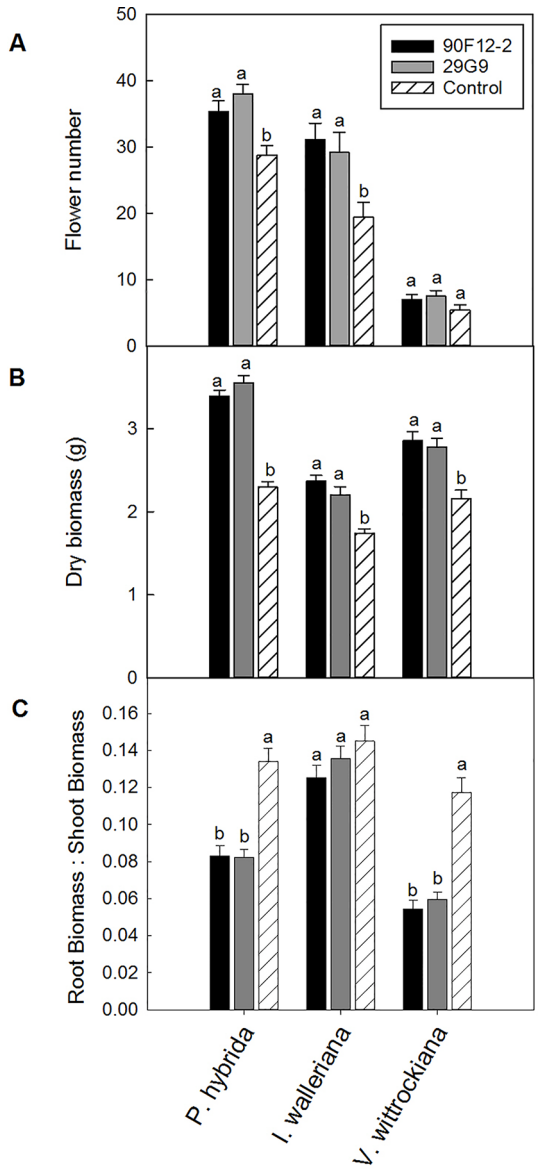

FIGURE 5 | Plant growth performance parameters for *Petunia* × *hybrida*, *Impatiens walleriana*, and *Viola* × *wittrockiana* plants subjected to drought stress five weeks after transplant (n = 13, 18, 14). Plants were treated with bacteria inoculum weekly after transplant. Plants treated with strains 90F12-2 (black) and 29G9 (light gray) were compared to the uninoculated control (white with lines). Total number of flowers **(A)** and total shoot biomass (dry weight) **(B)** was measured two weeks after rewatering following drought stress. Root:shoot **(C)** was calculated with root and shoot dry weights. Bars represent the mean (± SE) with different letters representing significant difference ($p < 0.05$).

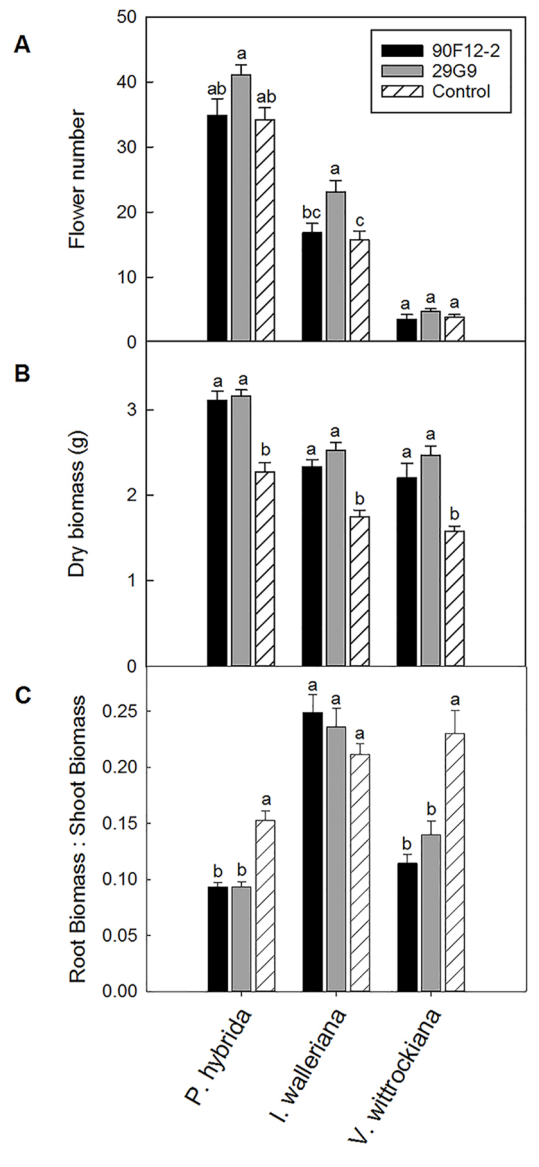

FIGURE 6 | Plant growth performance parameters for *Petunia* × *hybrida*, *Impatiens walleriana*, and *Viola* × *wittrockiana* plants grown with 25 mg L^{-1} N from 15N–2.2P–12.5K–2.9Ca–1.2Mg water soluble fertilizer at every irrigation to induce low-nutrient stress (n = 13, 18, 14). Plants were treated with bacteria inoculum weekly after transplant. Plants treated with strains 90F12-2 (black) and 29G9 (light gray) were compared to the uninoculated control (white with lines). Total number of flowers **(A)** and total shoot biomass (dry weight) **(B)** was measured eight weeks after transplant. Root:shoot **(C)** was calculated with root and shoot dry weights. Bars represent the mean (± SE) with different letters representing significant difference ($p < 0.05$).

content of *P. hybrida* by at least 41% in plant leaf tissue compared to the uninoculated control (**Figure 7A**). There was no difference in the content of other nutrients in petunia leaf tissue. Similar to *P. hybrida*, both pseudomonads increased the nitrogen content of *I. walleriana* leaves by at least 78%. In addition, both strains increased the phosphorus, potassium, calcium, magnesium, and sulfur content of *I. walleriana* in plant leaf tissue by at least 9, 19, 21, 30, and 17%, respectively, compared to the negative control (**Figure 7**). The application of both strains increased the nitrogen content of *V. wittrockiana* leaf tissue by at least 78%. Both strains also increased phosphorus, potassium, calcium, and sulfur content of *V. wittrockiana* in plant leaf tissue by at least 23, 31, 30, and 62%, respectively, compared to the uninoculated control

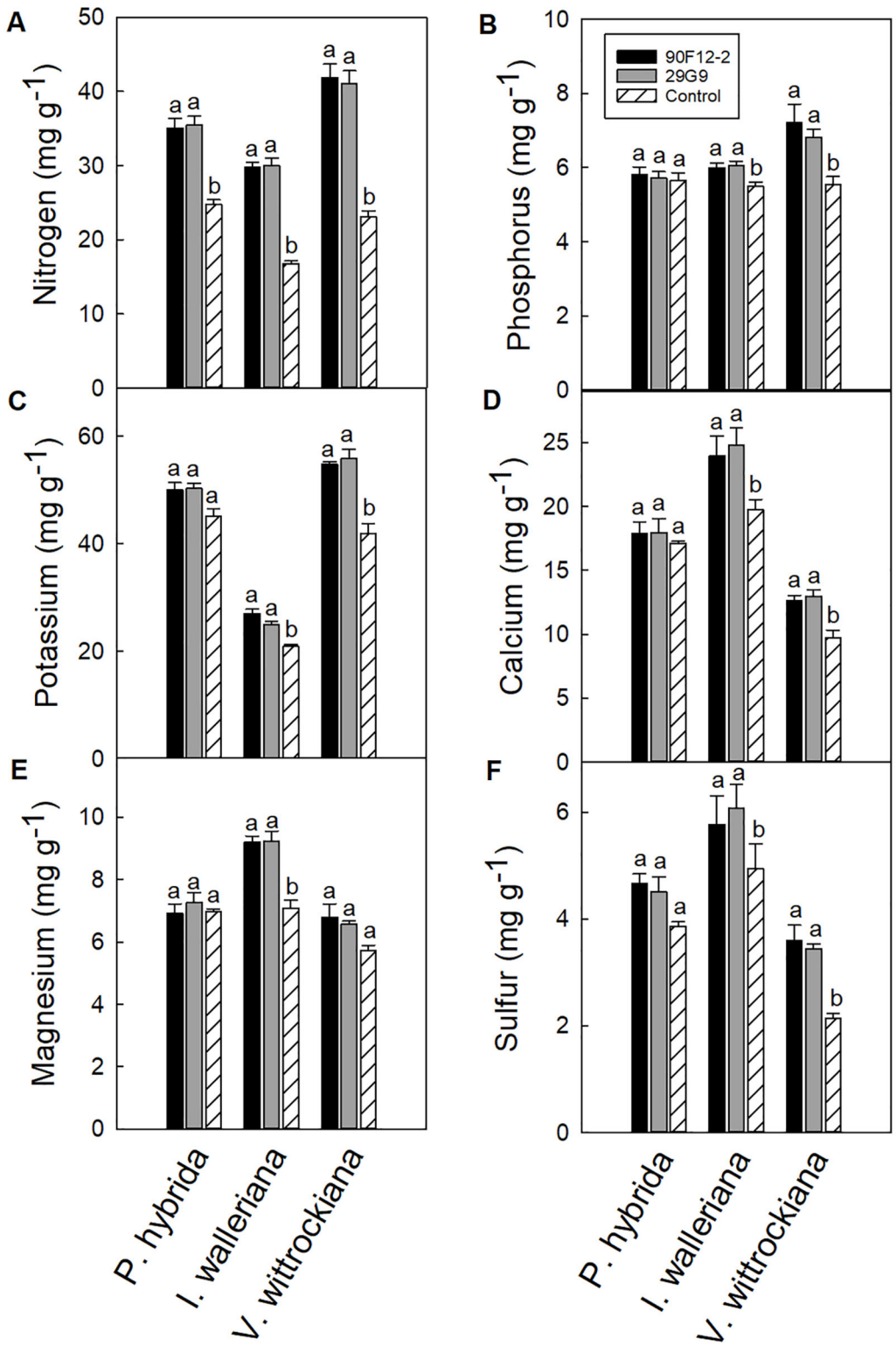

FIGURE 7 | Leaf tissue nutrient content of *Petunia* × *hybrida*, *Impatiens walleriana*, and *Viola* × *wittrockiana* plants grown under low-nutrient conditions: nitrogen **(A)**, phosphorus **(B)**, potassium **(C)**, calcium **(D)**, magnesium **(E)**, and sulfur **(F)**. Plants were treated with bacteria inoculum weekly after transplant and tissue was harvested eight weeks after transplant. Plants treated with strains 90F12-2 (black) and 29G9 (light gray) were compared to the uninoculated control (white with lines). Bars represent the mean (± SE) with different letters representing significant difference ($p < 0.05$).

(**Figures 7A–D, F**). There was no difference in magnesium foliar nutrient content in *V. wittrockiana* leaf tissue between bacteria treatments and the negative control (**Figure 7E**).

DISCUSSION

Here, we established high-throughput *in vitro* and *in planta* assays to selected *Pseudomonas* strains that stimulate ornamental plant growth under water and nutrient deficient conditions. The use of PEG to select osmotic stress tolerant bacteria and the effect of these bacteria on plant tolerance to drought stress is well documented (Forchetti et al., 2007; Vardharajula et al., 2011; Hussain et al., 2014a; Asghar et al., 2015). Our study utilized a similar approach, validating the utility of this bioassay to screen larger collections of bacteria for their osmoadaptive properties. Similar to these previous studies, we found YEM growing media to be the most effective for selecting osmoadaptive bacteria. We utilized the PEG selection to narrow the collection of 44 Pseudomonads to ten osmotic stress tolerant strains (**Figure 1**). Our high-throughput greenhouse trial successfully confirmed that the bacteria could enhance plant stress tolerance and identified two strains that increased shoot biomass and flower number under both abiotic stress conditions (**Figures 2** and **3**). Studies have shown that application of osmotic stress tolerant bacteria originating from the rhizosphere and endosphere can stimulate plant growth under varied levels of drought stress. Bacteria able to grow *in vitro* in media supplemented with varying levels of PEG and subsequently evaluated *in planta* increase maize biomass and relative water content (Vardharajula et al., 2011), root length, and shoot biomass of wheat (Chakraborty et al., 2013; Asghar et al., 2015).

In addition to osmoadaptive properties, many PGPR exhibit other growth-promoting characteristics such as siderophore production, phosphate solubilization, and hormone regulation (Vardharajula et al., 2011; Chakraborty et al., 2013; Asghar et al., 2015). To further investigate the application of the *Pseudomonas* strains, we developed a multi-species greenhouse trial. Host specificity in plant-microbe interactions has been well-studied in both agronomic and horticulture crops, showing varied effects on plant growth depending on bacteria and plant genotype (Moutia et al., 2010; Pedraza et al., 2010). Due to species diversity in ornamental crop production systems, it is necessary to identify beneficial bacteria that can stimulate plant growth across a broad host range. Both *Pseudomonas* strains did not exhibit host specificity as they stimulated shoot growth of *P. hybrida, I. walleriana,* and *V. wittrockiana* under both drought and low-nutrient conditions. These results further demonstrate the broad utility of these bacteria in greenhouse production systems with a wide range of plant species that could encounter both drought and low-nutrient conditions. In addition, we found that the two *Pseudomonas* strains were able to colonize the rhizosphere of *P. hybrida* plants at least 8 weeks post-treatment (data not shown), supporting their ability to form a mutualistic relationship with the plants to stimulate plant growth. Our results support previous work that has shown general plant growth promotion of *Pelargonium peltatum, Chrysanthemum* sp., and *Dahlia variabilis* plants inoculated with *Pseudomonas* sp. (Göre and Altin, 2006).

Facilitating the uptake of nutrients by plants is one of the most common mechanisms that bacteria employ to stimulate plant growth. Some PGPR can fix atmospheric nitrogen, produce siderophores to provide iron to plant roots, solubilize mineral phosphate into a bioavailable form to plants, and synthesize different phytohormones and enzymes that can modulate plant development and lead to an increase in nutrient uptake (Glick, 1995). While positive growth responses were seen across all three plant species in our study, leaf nutrient content was more consistently increased in *I. walleriana* and *V. wittrockiana* plants treated with bacteria. Similarly, the visual symptoms of leaf yellowing in control plants compared to bacteria treated plants were more severe in *I. walleriana* and *V. wittrockiana* than *P. hybrida* (**Figure 4**). Previous studies evaluating the influence of bacteria inoculation on plants grown under low-nutrient conditions demonstrate a similar increase in foliar N and P content (Eid et al., 2009; Hoda and Mona, 2014), whereas strawberry plants treated with PGPR strains had an increase in N, P, K, Ca, Fe, Cu, and Mn foliar nutrient content (Ipek et al., 2014), and wheat plants grown under reduced fertility had an increase in N, P, K, Fe, Cu, Mn, and Zn when treated with different PGPR strains (Rana et al., 2012). Our study expands on this literature by documenting a similar plant response in a peat-based greenhouse media. Although our results varied depending on the bacteria treatment and plant species, increases in foliar N, P, K, Ca, Mg, and S content were observed (**Figure 7**). In addition, the significant decrease in the root:shoot ratio of inoculated *P. hybrida* and *V. wittrockiana* plants shows that plants treated with bacteria are able to sustain more shoot biomass with fewer roots compared to inoculated plants. This provides evidence that the bacteria are increasing bioavailability of nutrients or increasing nutrient use efficiency in plants, reducing the energy that plants have to expend to produce roots in search of adequate nutrients and likely contributing to the increase in overall crop quality (**Figure 4**).

Although many plant-PGPR studies are conducted in controlled environment greenhouses, these results can be difficult to translate to ornamental crop production due to the use of agronomic crop species and non-traditional soil-based growing media in these studies. PGPR strains have been evaluated as a tool to increase the quality of different ornamentals, demonstrating the ability of these bacteria to increase crop quality under varying conditions. As flower number is a major contributor to ornamental crop value, PGPR that increase flower number are of interest to the horticulture industry. *Bacillus subtilis* and *Glomus* sp. increase total flower number of *Tagetes erecta* plants when cultivated in a sandy loam soil (Flores et al., 2007), and inoculation with *Pseudomonas putida* and *P. fluorescens* strains increases plant size and flower number of *Pelargonium peltatum, Chrysanthemum* sp., and *Dahlia variabilis* plants cultivated under greenhouse conditions (Göre and Altin, 2006). In addition, application of the nitrogen-fixing *Azospirillum lipoferum* and the phosphate-solubilizing *Bacillus polymxa* increases the flower number of *Petunia* × *hybrida plants* grown

under field conditions with different levels of fertility (Hoda and Mona, 2014). *Azotobacter chroococcum* and *Bacillus megaterium* have also been shown to increase plant growth and nutrient content of *Matthiola incana* plants when cultivated in soil under reduced and optimal fertility levels (Eid et al., 2009). Although our results varied across treatment, plant species, and stress, flower number was significantly increased in some scenarios. Application of both strains significantly increased flower number of *P. hybrida* subjected to drought stress, whereas application of strain 29G9 showed the most consistent positive effect across experiments, increasing flower number of *P. hybrida and I. walleriana* plants subjected to drought stress, and *I. walleriana* plants grown under low-nutrient conditions. No significant difference in flower number was observed between experiments with *V. wittrockiana*, which might be explained by the species' habit of producing fewer flowers than other species. Our study expands on the current literature by evaluating the effect of bacterial application on economically-important ornamental species, grown in a peat-based growing media, and subjected to multiple abiotic stress conditions. Utilizing cultural inputs similar to those that would be used in commercial greenhouse facilities further validates the potential for these bacteria to be used across a wide range of growing conditions and abiotic stresses that can negatively impact crop quality.

P. poae strains increase plant growth of millet under drought conditions (Ranveer et al., 2016) and are capable of producing siderophores (Tian et al., 2009) and solubilizing phosphate (Woo et al., 2010; Ahmed et al., 2014), mechanisms typically associated with plant growth promotion. *P. fluorescens* strains also produce siderophores and solubilize phosphate (Goswami et al., 2016), in addition to stimulating growth of rice seedlings (Goswami et al., 2016) and acting as a biocontrol agent (Bhattacharyya and Jha, 2012).

This data will directly impact the scientific community studying beneficial plant-microbe interactions by providing efficient methods to translate *in vitro* selection to *in planta* observations. In addition, this information will benefit the horticulture industry by providing evidence that PGPR can be used as an effective tool to reduce fertilizer inputs without reducing crop quality. In conclusion, *in vitro* bioassays are effective at selecting candidate PGPR; however, their ability to stimulate plant growth should also be validated *in planta*. Our research has developed two greenhouse trials that can be used for the *in planta* validation of PGPR-mediated plant growth promotion under drought and nutrient-limiting conditions and in multiple plant species. Future research should focus on optimizing the application parameters such as application timing, concentration of bacteria inoculum, and incubation time of the bacteria culture.

DATA AVAILABILITY STATEMENT

The datasets generated for this study will not be made publicly available. All datasets generated for this study are included in the article/supplementary material.

AUTHOR CONTRIBUTIONS

NN, LC, and MJ conceived the experimental design. NN and LC collected the data. NN performed all analyses and led the writing of the manuscript. LC, CT, and MJ edited the manuscript. CT provided bacteria strains.

FUNDING

Salaries and research support were provided in part by State and Federal funds appropriated to the OARDC, The Ohio State University. Journal Article Number HCS 19-12. This work was financially supported by the American Floral Endowment and the OSU D.C. Kiplinger Floriculture Endowment. Support was also provided by The Ohio State University Distinguished Fellowship and the OARDC Director's Graduate Associateship.

ACKNOWLEDGMENTS

We thank Ball Horticultural Company (West Chicago, IL) and Syngenta Flowers (Gilroy, CA) for providing seeds.

REFERENCES

Adesemoye, A. O., Torbert, H. A., and Kloepper, J. W. (2009). Plant growth-promoting rhizobacteria allow reduced application rates of chemical fertilizers. *Microb. Ecol.* 58, 921–929. doi: 10.1007/s00248-009-9531-y

Adesemoye, A. O., Torbert, H. A., and Kloepper, J. W. (2010). Increased plant uptake of nitrogen from 15N-depleted fertilizer using plant growth-promoting rhizobacteria. *Appl. Soil Ecol.* 46, 54–58. doi: 10.1016/j.apsoil.2010.06.010

Ahmed, E. A., Hassan, E. A., Tobgy, K. M. K. E., and Ramadan, E. M. (2014). Evaluation of rhizobacteria of some medicinal plants for plant growth promotion and biological control. *Ann. Agric. Sci.* 59, 273–280. doi: 10.1016/j.aoas.2014.11.016

Asghar, H. N., Zahir, Z. A., Akram, M. A., Ahmad, H. T., and Hussain, M. B. (2015). Isolation and screening of beneficial bacteria to ameliorate drought stress in wheat. *Soil Environ.* 34, 100–110.

Ashrafuzzaman, M., Hossen, F. A., Razi Ismail, M., Hoque, A., Islam, M. Z., Shahidullah, S. M., et al. (2009). Efficiency of plant growth promoting rhizobacteria (PGPR) for the enhancement of rice growth. *Afr. J. Biotechnol.* 8, 12471252.

Ball, V. (1998). *Ball redbook. 16th ed.,*. Ed. V. Ball Batavia (IL: Ball Publishing).

Bhattacharyya, P. N., and Jha, D. K. (2012). Plant growth-promoting rhizobacteria (PGPR): emergence in agriculture. *World J. Microbiol. Biotechnol.* 28, 1327–1350. doi: 10.1007/s11274-011-0979-9

Chakraborty, U., Chakraborty, B. N., Chakraborty, A. P., and Dey, P. L. (2013). Water stress amelioration and plant growth promotion in wheat plants by osmotic stress tolerant bacteria. *World J. Microbiol. Biotechnol.* 29, 789–803. doi: 10.1007/s11274-012-1234-8

Chandra, D., Srivastava, R., Glick, B. R., and Sharma, A. K. (2018). Drought-tolerant Pseudomonas spp. improve the growth performance of finger millet (Eleusine coracana (L.) Gaertn.) under non-stressed and drought-stressed conditions. *Pedosphere* 28, 227–240. doi: 10.1016/S1002-0160(18)60013-X

Cheng, Z., Duncker, B. P., McConkey, B. J., and Glick, B. R. (2008). Transcriptional regulation of ACC deaminase gene expression in

Pseudomonas putida UW4. *Can. J. Microbiol.* 54, 128–136. doi: 10.1139/W07-128

Dole, J. M., and Wilkins, H. F. (1999). *Floriculture priciples and species* (Upper Saddle River, New Jersey: Prentice-Hall, Inc.).

Eid, A. R., Awad, M. N., and Hamouda, H. A. (2009). Evaluate effectiveness of bio and mineral fertilization on the growth parameters and marketable cut flowers of Matthiola incana L. *Am. J. Agric. Environ. Sci.* 5, 509–518.

Erturk, Y., Ercisli, S., Haznedar, A., and Cakmakci, R. (2010). Effects of plant growth promoting rhizobacteria (PGPR) on rooting and root growth of kiwifruit. *Biol. Res.* 43, 91–98. doi: 10.4067/S0716-97602010000100011

Flores, A. C., Luna, A. A. E., and Portugal, V. O. (2007). Yield and quality enhancement of marigold flowers by inoculation with Bacillus subtilis and Glomus fasciculatum. *J. Sustain. Agric.* 31, 21–31. doi: 10.1300/J064v31n01

Forchetti, G., Masciarelli, O., Alemano, S., Alvarez, D., and Abdala, G. (2007). Endophytic bacteria in sunflower (Helianthus annuus L.): isolation, characterization, and production of jasmonates and abscisic acid in culture medium. *Appl. Microbiol. Biotechnol.* 76, 1145–1152. doi: 10.1007/s00253-007-1077-7

Göre, M. E., and Altin, N. (2006). Growth promoting of some ornamental plants by root treatment with specific fluorescent pseudomonads. *J. Biol. Sci.* 6, 610–615.

Garcia De Salamone, I. E., Döbereiner, J., Urquiaga, S., and Boddey, R. M. (1996). Biological nitrogen fixation in Azospirillum strain-maize genotype associations as evaluated by the 15N isotope dilution technique. *Biol. Fertil. Soils* 23, 249–256. doi: 10.1007/BF00335952

Glick, B. R. (1995). The enhancement of plant growth by free-living bacteria. *Can. J. Microbiol.* 41, 109–117. doi: 10.1139/m95-015

Glick, B. R. (2005). Modulation of plant ethylene levels by the bacterial enzyme ACC deaminase. *FEMS Microbiol. Lett.* 251, 1–7. doi: 10.1016/j.femsle.2005.07.030

Goswami, D., Thakker, J. N., and Dhandhukia, P. C. (2016). Portraying mechanics of plant growth promoting rhizobacteria (PGPR): A review. *Cogent Food Agric.* 2, 1–19. doi: 10.1080/23311932.2015.1127500

Habib, S. H., Kausar, H., Saud, H. M., Ismail, M. R., and Othman, R. (2016). Molecular characterization of stress tolerant plant growth promoting rhizobacteria (PGPR) for growth enhancement of rice. *Int. J. Agric. Biol.* 18, 184–191. doi: 10.17957/IJAB/15.0094

Hoda, E. E.-M., and Mona, S. (2014). Effect of bio and chemical fertilizers on growth and flowering of Petunia hybrida plants. *Am. J. Plant Physiol.* 9, 68–77. doi: 10.3923/ajpp.2014.68.77

Hontzeas, N., Zoidakis, J., Glick, B. R., and Abu-Omar, M. M. (2004). Expression and characterization of 1-aminocyclopropane-1-carboxylate deaminase from the rhizobacterium Pseudomonas putida UW4: A key enzyme in bacterial plant growth promotion. *Biochim. Biophys. Acta - Proteins Proteomics* 1703, 11–19. doi: 10.1016/j.bbapap.2004.09.015

Hussain, M. B., Zahir, Z. A., Asghar, H. N., and Asgher, M. (2014a). Can catalase and exopolysaccharides producing rhizobia ameliorate drought stress in wheat? *Int. J. Agric. Biol.* 16, 3–13.

Hussain, M. B., Zahir, Z. A., Asghar, H. N., and Mahmood, S. (2014b). Scrutinizing rhizobia to rescue maize growth under reduced water conditions. *Soil Sci. Soc Am. J.* 78, 538. doi: 10.2136/sssaj2013.07.0315

Ipek, M., Pirlak, L., Esitken, A., Figen Dönmez, M., Turan, M., and Sahin, F. (2014). Plant growth-promoting rhizobacteria (PGPR) increase yield, growth and nutrition of strawberry under high-calcareous soil conditions. *J. Plant Nutr.* 37, 990–1001. doi: 10.1080/01904167.2014.881857

Isaac, R. A., and Johnson, W. C. (1985). Elemental analysis of plant tissue by plasma emission spectroscopy: collaborative study. *Assoc. Off. Anal. Chem.* 68, 499–505.

Jha, C. K., and Saraf, M. (2015). Plant growth promoting rhizobacteria (PGPR): a review. *J. Agric. Res. Dev.* 5, 108–119. doi: 10.13140/RG.2.1.5171.2164

Kang, S. M., Radhakrishnan, R., Khan, A. L., Kim, M. J., Park, J. M., Kim, B. R., et al. (2014). Gibberellin secreting rhizobacterium, Pseudomonas putida H-2-3 modulates the hormonal and stress physiology of soybean to improve the plant growth under saline and drought conditions. *Plant Physiol. Biochem.* 84, 115–124. doi: 10.1016/j.plaphy.2014.09.001

Kloepper, J. W., Lifshitz, R., and Zablotovicz, R. M. (1989). Free-living bacteria inocula for enhancing crop productivity. *Trends Biotechnol.* 7, 39–44. doi: 10.1016/0167-7799(89)90057-7

Kuan, K. B., Othman, R., Rahim, K. A., and Shamsuddin, Z. H. (2016). Plant growth-promoting rhizobacteria inoculation to enhance vegetative growth, nitrogen fixation and nitrogen remobilisation of maize under greenhouse conditions. *PloS One* 11, 1–19. doi: 10.1371/journal.pone.0152478

Lai, W. A., Rekha, P. D., Arun, A. B., and Young, C. C. (2008). Effect of mineral fertilizer, pig manure, and Azospirillum rugosum on growth and nutrient contents of Lactuca sativa L. *Biol. Fertil. Soils* 45, 155–164. doi: 10.1007/s00374-008-0313-3

Lugtenberg, B., and Kamilova, F. (2009). Plant-growth-promoting rhizobacteria. *Annu. Rev. Microbiol.* 63, 541–556. doi: 10.1016/B978-0-12-374984-0.01169-4

Lugtenberg, B. J. J., Dekkers, L., and Bloemberg, G. V. (2001). Molecular determinants of rhizosphere colonization by Pseudomonas. *Annu. Rev. Phytopathol.* 39, 461–490. doi: 10.1146/annurev.phyto.39.1.461

Mavrodi, O. V., Walter, N., Elateek, S., Taylor, C. G., and Okubara, P. A. (2012). Suppression of Rhizoctonia and Pythium root rot of wheat by new strains of Pseudomonas. *Biol. Control* 62, 93–102. doi: 10.1016/j.biocontrol.2012.03.013

Mayak, S., Tirosh, T., and Glick, B. R. (2004). Plant growth-promoting bacteria that confer resistance to water stress in tomatoes and peppers. *Plant Sci.* 166, 525–530. doi: 10.1016/j.plantsci.2003.10.025

Moutia, J.-F. Y., Saumtally, S., Spaepen, S., and Vanderleyden, J. (2010). Plant growth promotion by Azospirillum sp. in sugarcane is influenced by genotype and drought stress. *Plant Soil* 337, 233–242. doi: 10.1007/s11104-010-0519-7

Naylor, D., and Coleman-Derr, D. (2018). Drought stress and root-associated bacterial communities. *Front. Plant Sci.* 8, 1–16. doi: 10.3389/fpls.2017.02223

Orhan, E., Esitken, A., Ercisli, S., Turan, M., and Sahin, F. (2006). Effects of plant growth promoting rhizobacteria (PGPR) on yield, growth and nutrient contents in organically growing raspberry. *Sci. Hortic. (Amsterdam).* 111, 38–43. doi: 10.1016/j.scienta.2006.09.002

Paulitz, T. C., and Richard, R. B. (2001). Biological control in greenhouse systems. *Annu. Rev. Phytopathol.* 39, 103–133. doi: 10.1146/annurev.phyto.39.1.103

Pedraza, R. O., Motok, J., Salazar, S. M., Ragout, A. L., Mentel, M. I., Tortora, M. L., et al. (2010). Growth-promotion of strawberry plants inoculated with Azospirillum brasilense. *World J. Microbiol. Biotechnol.* 26, 265–272. doi: 10.1007/s11274-009-0169-1

Rana, A., Saharan, B., Nain, L., Prasanna, R., and Shivay, Y. S. (2012). Enhancing micronutrient uptake and yield of wheat through bacterial PGPR consortia. *Soil Sci. Plant Nutr.* 58, 573–582. doi: 10.1080/00380768.2012.716750

Ranveer, K., Yogendra, S. G., Ishwar, P. S., Suvigya, S., and Amit, K. S. (2016). Impact of arbuscular mycorrhizal fungus, Glomus intraradices, Streptomyces and Pseudomonas spp. strain on finger millet (Eleusine coracana L.) cv Korchara under water deficit condition. *Afr. J. Biotechnol.* 14, 3219–3227. doi: 10.5897/ajb2015.14479

Ruzzi, M., and Aroca, R. (2015). Plant growth-promoting rhizobacteria act as biostimulants in horticulture. *Sci. Hortic. (Amsterdam).* 196, 124–134. doi: 10.1016/j.scienta.2015.08.042

Ryu, C.-M., Hu, C.-H., Locy, R. D., and Kloepper, J. W. (2005). Study of mechanisms for plant growth promotion elicited by rhizobacteria in Arabidopsis thaliana. *Plant Soil* 268, 285–292. doi: 10.1007/s11104-004-0301-9

Sabry, S. R. S., Saleh, S. A., Batchelor, C. A., Jones, J., Jotham, J., Webster, G., et al. (1997). Endophytic establishment of Azorhizobium caulinodans in wheat. *Proc. R. Soc* 264, 341–346.

Salomon, M. V., Bottini, R., de Souza Filho, G. A., Cohen, A. C., Moreno, D., Gil, M., et al. (2014). Bacteria isolated from roots and rhizosphere of Vitis vinifera retard water losses, induce abscisic acid accumulation and synthesis of defense-related terpenes in in vitro cultured grapevine. *Physiol. Plant* 151, 359–374. doi: 10.1111/ppl.12117

Sandhya, V., Ali, S. K. Z., Grover, M., Reddy, G., and Venkateswarlu, B. (2009). Alleviation of drought stress effects in sunflower seedlings by the exopolysaccharides producing Pseudomonas putida strain GAP-p45. *Biol. Fertil. Soils* 46, 17–26. doi: 10.1007/s00374-009-0401-z

Sessitsch, A., Howieson, J. G., Perret, X., Antoun, H., and Martínez-Romero, E. (2002). Advances in rhizobium research. *CRC. Crit. Rev. Plant Sci.* 21, 323–378. doi: 10.1080/0735-260291044278

Shinde, S., Cumming, J. R., Collart, F. R., Noirot, P. H., and Larsen, P. E. (2017). Pseudomonas fluorescens transportome ts linked to strain-specific plant

growth promotion in aspen seedlings under nutrient stress. *Front. Plant Sci.* 8, 1–13. doi: 10.3389/fpls.2017.00348

Subedi, N., Taylor, C. G., Paul, P. A., and Miller, S. A. (2019). Combining partial host resistance with bacterial biocontrol agents improves outcomes for tomatoes infected with Ralstonia pseudosolanacearum. *Crop Prot.* In press. doi: 10.1016/j.cropro.2019.03.024

Sweeney, R. (1989). Generic combustion method for determination of crude protein in feeds: collaborative study. *Assoc. Off. Anal. Chem.* 72, 770–774.

Tian, F., Ding, Y., Zhu, H., Yao, L., and Du, B. (2009). Genetic diversity of siderophore-producing bacteria of tobacco rhizosphere. *Braz. J. Microbiol.* 40, 276–284. doi: 10.1590/s1517-83822009000200013

Vardharajula, S., Ali, S. Z., Grover, M., Reddy, G., and Bandi, V. (2011). Drought-tolerant plant growth promoting Bacillus spp.: Effect on growth, osmolytes, and antioxidant status of maize under drought stress. *J. Plant Interact.* 6, 1–14. doi: 10.1080/17429145.2010.535178

Vejan, P., Abdullah, R., Khadiran, T., Ismail, S., and Nasrulhaq Boyce, A. (2016). Role of plant growth promoting rhizobacteria in agricultural sustainability-a review. *Molecules* 21, 1–17. doi: 10.3390/molecules21050573

Waterland, N. L., Campbell, C. A., Finer, J. J., and Jones, M. L. (2010). Abscisic acid application enhances drought stress tolerance in bedding plants. *HortScience* 45, 409–413. doi: 10.21273/HORTSCI.45.3.409

Woo, S.-M., Lee, M., Hong, I., Poonguzhali, S., and Sa, T. (2010). Isolation and characterization of phosphate solubilizing bacteria from Chinese cabbage, in: *19th World Congress of Soil Science, Soil Solutions for a Changing World Conference Proceedings.* pp. 56–59.

Zafar-ul-Hye, M., Farooq, H. M., Zahir, Z. A., Hussain, M., and Hussain, A. (2014). Application of ACC-deaminase containing rhizobacteria with fertilizer improves maize production under drought and salinity stress application of ACC-deaminase containing rhizobacteria with fertilizer improves maize production under drought and salinity St. *Int. J. Agric. Biol.* 16, 591–596.

Zahir, Z. A., Munir, A., Asghar, H. N., Shaharoona, B., and Arshad, M. (2008). Effectiveness of rhizobacteria containing ACC deaminase for growth promotion of peas (Pisum sativum) under drought conditions. *J. Microbiol. Biotechnol.* 18, 958–963.

Zhou, C., Zhu, L., Ma, Z., and Wang, J. (2018). Improved iron acquisition of Astragalus sinicus under low iron-availability conditions by soil-borne bacteria Burkholderia cepacia. *J. Plant Interact.* 13, 9–20. doi: 10.1080/17429145.2017.1407000

Conflict of Interest: The authors declare that the research was conducted in the absence of any commercial or financial relationships that could be construed as a potential conflict of interest.

frontiers in Plant Science

ORIGINAL RESEARCH
published: 24 March 2020
doi: 10.3389/fpls.2020.00327

Cold Acclimation and Deacclimation of Two Garden Rose Cultivars Under Controlled Daylength and Temperature

Lin Ouyang[1,2], Leen Leus[3], Ellen De Keyser[3] and Marie-Christine Van Labeke[2]**

[1] Institute of Urban Agriculture, Chinese Academy of Agricultural Sciences, Chengdu, China, [2] Department of Plants and Crops, Ghent University, Ghent, Belgium, [3] Plant Sciences Unit, Flanders Research Institute for Agriculture, Fisheries and Food (ILVO), Melle, Belgium

Low temperature stress is an important abiotic stress for garden roses in northern regions. Two garden rose cultivars ('Dagmar Hastrup' and 'Chandos Beauty') were selected to study the role of dehydrin and of carbohydrate metabolism during cold acclimation and deacclimation under the controlled daylength and temperature. The presence of bud dormancy was also observed as this could prevent budburst during warm spells. Both cultivars showed a similar changing pattern of cold acclimation and deacclimation and did not differ in their lowest LT_{50} values. *Dehydrin* (*RhDHN5*) was up-regulated by low temperatures and not by dehydration stress as the stem water content remained stable during the treatments. Total soluble sugars accumulated with a transient up-regulation of *RhBAM3* (a key gene in starch hydrolysis) for 'Dagmar Hastrup' at 2°C and a strong expression under both 2 and −3°C for 'Chandos Beauty'. At 2 and −3°C, raffinose and stachyose strongly accumulated though the up-regulation of *RhRS6* and *RhGK* differed in the cultivars. Although similar cold hardiness levels were reached, carbohydrate metabolism in response to cold stress is different in the two cultivars. Increasing the temperature after a cold period resulted in fast deacclimation as found by the downregulation of *RhDHN5* and *RhBAM3*, the decrease of raffinose and stachyose. Bud endodormancy was hardly present in both cultivars.

Keywords: cold stress, LT_{50}, stem water content, bud dormancy, dehydrins, carbohydrate metabolism, gene expression

OPEN ACCESS

Edited by:
Antonio Ferrante, University of Milan, Italy

Reviewed by:
Sofia Valenzuela, University of Concepción, Chile
Marta A. Fernandez Reyes, University of Concepción, Chile

****Correspondence:***
Lin Ouyang
linouyang1101@outlook.com
Marie-Christine Van Labeke
mariechristine.vanlabeke@ugent.be

Specialty section:
This article was submitted to Crop and Product Physiology, a section of the journal Frontiers in Plant Science

Received: *10 November 2019*
Accepted: *05 March 2020*
Published: *24 March 2020*

Citation:
Ouyang L, Leus L, De Keyser E and Van Labeke M-C (2020) Cold Acclimation and Deacclimation of Two Garden Rose Cultivars Under Controlled Daylength and Temperature. Front. Plant Sci. 11:327. doi: 10.3389/fpls.2020.00327

INTRODUCTION

In order to withstand freezing temperatures in mid-winter, woody perennials will develop low temperature tolerance during autumn, also called cold acclimation. Cold acclimation is strongly influenced by environmental triggers and is mainly induced by short days and/or lower temperatures. After reaching maximum levels of cold hardiness in winter also called mid-winter

Abbreviations: BAM/BMY, β-amylase; DHN, dehydrin; DPE2, disproportionating enzyme 2; EL, Electrolyte leakage; FRK, fructokinase; GK, galactokinase; HXK, hexokinase; INV, invertase; I_t, index of injury; LT_{50}, the temperature causing 50% of index of injury; MIPS, myo-inositol-phosphate synthase; PPFD, photosynthetic photon flux density; RFOs, raffinose family oligosaccharides; Rh, Rosa × hybrida; RS, raffinose synthase; SPS, sucrose phosphate synthase; SUS, sucrose synthase; USDA, the United States Department of Agriculture.

hardiness, increasing temperatures toward spring induce the deacclimation process leading to a reduction or loss of cold hardiness. Most woody plants also develop physiological bud dormancy or endodormancy in autumn, a state of temporal growth suspension within the meristem (Rohde and Bhalerao, 2007). However, low temperatures can induce cold acclimation without inducing dormancy (Kalberer et al., 2006). In woody plants native to temperate and boreal zones, bud dormancy and cold acclimation are governed through a complex but precise regulation of genes (Welling and Palva, 2006; Ruttink et al., 2007; Wisniewski et al., 2015). These two processes can be induced by low, non-freezing temperatures and/or short daylength although these environmental triggers are species dependent (Li et al., 2003; Heide, 2008; Wisniewski et al., 2014). The presence of endodormancy prevents regrowth and concomitant deacclimation during warm spells in winter (Kalberer et al., 2006; Wisniewski et al., 2018).

Cold acclimation and deacclimation are related to changes in cellular water status (Pagter and Arora, 2013). During cold acclimation, tissue dehydration has been detected in many woody plants as the decrease of free water resulting in higher tolerance to mechanical stress caused by extracellular ice formation (Li et al., 2002; Améglio et al., 2003). In contrast, deacclimation is associated with increasing tissue water content in perennials (Pagter et al., 2011a).

Recently, Wisniewski et al. (2018) reviewed the molecular control of cold tolerance in trees. Cold acclimation involves a transcriptomic reprogramming where the C-repeat/DREB binding factor (*CBF*) dependent pathway plays a central role (Shi et al., 2018). This has been largely investigated in *Arabidopsis thaliana* and is also identified in poplar, blueberry, apple and peach (Wisniewski et al., 2014). A large set of cold responsive (*COR*) genes can be induced via the *CBF*-dependent pathway and regulates the accumulation of cryoprotective proteins and soluble sugars, thus protecting membranes and reducing cellular dehydration (Chinnusamy et al., 2007).

Dehydrins are the D-11 subgroup of late embryogenesis abundant proteins (LEA) which are encoded by *COR*. The protein sequence is highly hydrophilic and they are involved in the plants' protective reactions to cellular dehydration and they have antifreeze and/or cryoprotective properties (Close, 1997; Wisniewski et al., 1999; Hanin et al., 2011). The accumulation of dehydrins is frequently observed in woody plants during cold acclimation (Wisniewski et al., 1996; Close, 1997). Seasonal patterns of dehydrin proteins and transcripts are present in woody plants and a decline in both protein quantification and gene expression in spring has been associated with deacclimation (Artlip et al., 1997; Kontunen-Soppela et al., 2000; Arora et al., 2004). *RhDHN5* and *RhDHN6* are isolated based on the dehydrin (*ppdhn1*) in peach (*Prunus persica*) which has higher transcript levels in the bark tissue of both evergreen and deciduous peach during autumn and early winter (Artlip et al., 1997). *RhDHN5* and *RhDHN6* also present a seasonal expression pattern showing an up-regulation in November–January and down-regulation from February to April (Ouyang et al., 2019a).

It is assumed that dehydrins interact with sucrose by forming stable glasses (Wolkers et al., 2001) and are regulated by sucrose during cold acclimation (Rekarte-Cowie et al., 2008). The accumulation of soluble carbohydrates together with the accumulation of dehydrins may help the plants to develop their maximum levels of cold hardiness (Trischuk et al., 2014). Soluble carbohydrates act as compatible solutes (osmoregulators/osmolytes) to stabilize cellular osmotic potential to lower the freezing point and prevent the formation of intracellular ice crystals (Guy, 1990; Xin and Browse, 2000; Li et al., 2004). Their accumulation under low temperature has also a role in scavenging of reactive oxygen species and they act as signaling molecules (Welling and Palva, 2006; Theocharis et al., 2012). Degradation of starch and accumulation of soluble sugars especially sucrose and raffinose family of oligosaccharides (RFOs) are frequently reported during cold acclimation in *Arabidopsis* and several woody plants (Palonen, 1999; Palonen and Junttila, 1999; Guy et al., 2008; Pagter et al., 2008). Re-synthesis of starch at regrowth during spring accompanied by loss of soluble sugars was observed in woody plants during deacclimation (Morin et al., 2007; Pagter and Arora, 2013). Genes encoding galactinol synthase and BAM (a key enzyme in starch degradation) are up-regulated by the CBF regulon during cold acclimation, resulting in higher soluble sugar levels (Fowler and Thomashow, 2002; Wisniewski et al., 2014). Likewise, genes encoding SPS and INV in sucrose metabolism and raffinose synthase (RS) in RFOs biosynthesis change in abundance during cold acclimation (Usadel et al., 2008; Yue et al., 2015).

Despite the economic importance of roses in gardens and landscaping, and breeding efforts to develop roses with improved hardiness, hardly any reports on bud dormancy or factors affecting cold acclimation can be found. Observations under field conditions showed that dehydrins and carbohydrate metabolism are associated with cold hardiness in garden roses (Ouyang et al., 2019a). However, seasonal observations are subject to fluctuating temperatures, which result in acclimation/deacclimation/reacclimation events, making it difficult to distinguish the molecular/metabolic changes associated with cold acclimation. Furthermore, hardly any literature reports on whether the dormant state of garden roses during winter is linked to environmental parameters (ecodormancy) or if a true endodormancy is established.

In the present study, we aimed to characterize basic differences of cold acclimation in two cultivars with distinct genetic background and different mid-winter hardiness. 'Dagmar Hastrup' (diploid, Hybrid Rugosa), introduced in 1914, is closely related to the species *Rosa rugosa*. In contrast, 'Chandos Beauty' (tetraploid, Hybrid Tea), introduced in 2005, has a complicated genetic background (including ±10 rose species) reflecting the development of modern rose cultivars. In a 3-year field study including 17 different cultivars/species, 'Dagmar Hastrup' belonged to the most cold-hardy group while 'Chandos Beauty' belonged to the most cold-susceptible group (Ouyang et al., 2019b). Furthermore 'Dagmar Hastrup' developed a higher level of mid-winter hardiness (determined by LT_{50}) than 'Chandos Beauty' in a field study (Ouyang et al., 2019a).

This contrast in acquiring cold hardiness predicts different strategies to face up to the challenges imposed by freezing temperatures. To test this hypothesis, we simulated the progression of cold acclimation in natural conditions and analyzed dehydration and carbohydrate dynamics under a controlled drop in temperature and photoperiod (acclimation) followed by a subsequent increase (deacclimation) using gene expression and metabolite analysis. Further, we investigated the presence of bud dormancy as this might also influence the process of cold acclimation and may be different in both cultivars. Through this approach, we aim to further clarify the role of dehydrins and carbohydrate metabolism in cold hardiness in garden roses.

MATERIALS AND METHODS

Plant Material

Two garden roses, 'Dagmar Hastrup' (diploid, Hybrid Rugosa, more cold-hardy; coldest USDA zone 3b) and 'Chandos Beauty' (tetraploid, Hybrid Tea, less cold-hardy, coldest USDA zone 6b), were selected for this study. Plants of each cultivar were clonally propagated and obtained from Pheno Geno Roses BV (Eindhoven, Netherlands).

For the bud dormancy experiment (2017–2018), current year stems of field-grown roses (51° 0′ N, 3° 48′ E, Melle, Belgium) were used. Roses were planted in a double row, with 30 plants per cultivar per row. Plants had been established 3 years before sampling.

For the controlled acclimation and deacclimation experiment, 1-year-old container-grown plants (2 L pots, 60 plants/cultivar), still actively growing, were obtained at the end of October 2016. Upon arrival, plants were kept in the greenhouse to maintain active growth until the start of the experiment (minimum air temperatures 5°C). During the daytime plants were supplemented with 100 μmol m^{-2} s^{-1} PPFD at canopy when the outdoor light intensity was lower than 75 W m^{-2} (600 W SON-T lamps, Philips, Eindhoven, Netherlands).

Experiments

Experiment 1: Bud Dormancy

From the field grown plants, a randomly chosen set of 30 current-year stems was collected from both cultivars on September 18, 2017, October 20, 2017, November 15, 2017, December 20, 2017, January 18, 2018, and February 17, 2018, respectively. Bud dormancy was measured by a single node cutting test (Arias and Crabbé, 1975). Nodes from the second and third apical position of the chosen 30 stems of each cultivar were cut in single-node cuttings (±1-cm stem sections) (n = 60). The sections were inserted into a peat substrate in trays and were placed in a growth chamber at 20 ± 2°C, relative humidity ± 70%, daylength 16 h and light intensity 100 μmol m^{-1} s^{-1} (Plasma lamps, Gavita International, Aalsmeer, Netherlands). Bud break (BBCH scale 07 when scale tips dispersed along the bud axis) (Meier et al., 2009) was recorded three times per week. The percentage of bud dormancy was calculated after 30 days of observation. Buds that failed to break were assigned a time of 30 days. The mean time (days) to bud break (MTB) was calculated based on the formula below.

$$MTB = \frac{\sum \{(number\ of\ new\ breaking\ buds) \times day\} + number\ of\ non\ breaking\ buds \times 30}{total\ number\ of\ tested\ buds}$$

Experiment 2: Controlled Acclimation and Deacclimation

The experimental design was a controlled acclimation and deacclimation protocol using 60 potted multi-branched roses for each cultivar (**Supplementary Figure S1**). This protocol is based on Palonen et al. (2000) and modified with respect to the results of our previous field study (Ouyang et al., 2019a). The branches per pot were selected randomly and used for a one-date sampling during the whole acclimation-deacclimation treatment. The experiment started on December 19, 2016 and ended February 27, 2017. A temperature of 20/18°C (day/night) and photoperiod of 16 h (SON-T high pressure lamps, 100 μmol·m^{-2}·s^{-1} PPFD at plant level) was provided for the plants under greenhouse conditions for 3 weeks until 19 December, followed by a decrease of temperature (13/6°C) and daylength (8 h) for 4 weeks (20 December to 16 January). Besides the sampled pots, other plants were placed in a climate chamber for 2 weeks at 2°C (17 January to 30 January) followed by 2 weeks at sub-zero temperatures (−3°C) (31 January to 13 February). The photoperiod remained at 8 h but the light intensity was reduced to 5–10 μmol·m^{-2}·s^{-1} as provided by fluorescent lamps (Philip Master TL-D 36W/830 Reflux, Philips, Eindhoven, Netherlands). Finally, a deacclimation phase was simulated in a greenhouse at 100 μmol·m^{-2}·s^{-1} PPFD with the remaining plants 1 week at 20/18°C with a photoperiod of 8 h (14 February to 20 February) followed by 1 week at 20/18°C with a photoperiod extended to 14 h (21 February to 27 February).

Current-year stems were sampled for the determination of cold hardiness, stem water content, and carbohydrate content (four biological replicates per cultivar per analysis) on 19 December, 2 January, 16 January, 23 January, 30 January, 6 February, 13 February, 20 February, and 27 February (9 time points). For the gene expression analysis, stem tissue was sampled (three biological replicates per cultivar) on 19 December, 20 December, 2 January, 16 January, 17 January, 23 January, 30 January, 31 January, 6 February, 13 February, 14 February, 20 February, and 27 February (13 time points). Four extra sampling time points (20 December, 17 January, 31 January, and 14 February) were included for gene expression analysis, as a transient expression may happen when environmental conditions change. For both gene expression and carbohydrate analysis, each replicate was a balanced mix of the apical, middle, and basal part of one individual stem. For the determination of cold hardiness and water content, samples were kept on ice and immediately transferred to the laboratory for analysis. Samples for carbohydrate analysis and gene expression were flash frozen in liquid nitrogen and stored at −80°C until analysis.

Determination of Cold Hardiness

Cold hardiness levels were determined by means of LT_{50} (the temperature causing 50% of index of injury) in a controlled freezing test for each cultivar (n = 4). Internodal stem segments (0.5-cm-long) were taken from the middle part of the current-year stem, then rinsed under distilled water for 10 s and placed in 2 mL Eppendorf microcentrifuge tubes (Eppendorf, Hamburg, Germany) with 0.5 mL distilled water and a few grains of sand (VWR International, Leuven, Belgium). Within each repetition, one stem segment was maintained at a reference temperature of 4°C as control. Stem segments were placed in a cryostat of Polystat 37 (Fisher Scientific, Merelbeke, Belgium) from 0°C to seven target temperatures (−5, −10, −15, −20, −25, −30, and −35°C) at a cooling rate of 6°C h^{-1} (0.1°C min^{-1}). Meanwhile, one segment was placed at −80°C for 5 h. After thawing overnight at 4°C, all the segments were incubated in 10 mL of 10 mM boric acid (H_3BO_3) and 0.002% Triton-X at room temperature for 20 h. EL was measured before and after autoclaving at 120°C for 30 min using WTW Inolab conductivity meter Level 1 (WTW GmbH & Co. KG, Weinheim, Germany) with a TetraCon 325 conductivity cell. Index of Injury (I_t) based on EL values was calculated according to Flint et al. (1967) and transformed into the adjusted I_t value taking into account the I_t at −80°C (100% injury value) (Lim et al., 1998). The LT_{50} was calculated from the injury versus temperature plot by means of logistic regression.

Stem Water Content

Fresh weight (FW) of 5–6 cm segments of each cultivar from the median part of the stem was determined, followed by drying at 80°C for 48 h to determine the dry weight (DW) (n = 4). Stem water content (g H_2O g^{-1} DW) was calculated on a dry weight basis as [(FW-DW)/DW].

Analysis of Carbohydrates

Tissue samples of stems were ground in liquid nitrogen with a mill (IKA® A11 Basic Analytical Mill, Staufen, Germany). Soluble carbohydrates were analyzed as described by Ouyang et al. (2019a) for each cultivar (n = 4). In short, soluble carbohydrates were extracted in 80% ethanol and quantified by high performance anion-exchange chromatography with pulsed amperometric detection (ACQUITY UPLC H-Class, Waters, Milford, MA, United States). Starch, expressed as glucose equivalents after acid hydrolysis, was determined spectrophotometrically at 340 nm by the enzymatic reduction of $NADP^+$ (UV-VIS, Biotek Uvikon XL, Bad Friedrichshall, Germany) with a HXK/glucose-6-phosphate dehydrogenase assay.

RNA Extraction and Reverse Transcription

Tissue samples of stems were ground in liquid nitrogen using a mortar and pestle. RNA was extracted from 100 mg of ground tissue sample using a CTAB protocol for each cultivar (n = 3). RNA quality was assessed with the NanoDrop (ND-1000) spectrophotometer (Isogen Life Science, Utrecht, Netherlands) (**Supplementary Table S1**). RNA integrity was determined by the Experion Automated Electrophoresis System and RNA StdSens Chips (Bio-Rad Laboratories N.V., Temse, Belgium) on a random selection of over 10% of the total sample numbers across both cultivars and all sampling points (**Supplementary Figures S2, S3**). RNA samples were converted to single-stranded cDNA using the iScript cDNA Synthesis Kit (Bio-Rad Laboratories N.V., Temse, Belgium) starting from 600 ng of RNA. Detailed protocols were as described in Luypaert et al. (2017).

Gene Isolation

Coding sequences of *RhSPS1* (involved in sucrose metabolism), and *RhHXK1* and *RhFRK4* (involved in hexose catabolism) were newly obtained (**Supplementary Table S2**) and the method is as described in Ouyang et al. (2019a). BLASTx (Altschul et al., 1997) was used to confirm fragment identity (**Supplementary Table S3**). In addition to these four sequences, eight sequences obtained previously in Ouyang et al. (2019a) were also studied here: seven key genes associated in carbohydrate metabolism (*RhBAM3* and *RhDPE2* in starch catabolism, *RhSUS* and *RhINV2* in sucrose metabolism; *RhMIPS* in myo-inositol synthesis pathway, and *RhGK* and *RhRS6* in the raffinose synthesis pathway) and *RhDHN5* (dehydrin gene) (**Supplementary Table S2**). Given the similar up-regulation pattern of *RhDHN5* and *RhDHN6* and their link to cold hardiness (Ouyang et al., 2019a), we limited further research to *RhDHN5*.

Gene Expression

RT-qPCR primers for *RhSPS1*, *RhHXK1*, and *RhFRK4* were designed using Primer3Plus software (Untergasser et al., 2007) (**Supplementary Table S4**). RT-qPCR primers for all the other genes (including two reference genes) were designed by Ouyang et al. (2019a) (**Supplementary Table S4**). Gene specific amplification efficiencies were determined by LinRegPCR (Ruijter et al., 2009) (**Supplementary Table S4**). RT-qPCR analysis was performed as described in Ouyang et al. (2019a) using cDNA synthesized from RNA samples of stem tissues. A normalization factor based on two validated reference genes (*PGK and RPS18c*; M-value = 0.391; CV-value = 0.137) was used for calculation of calibrated normalized relative quantities (CNRQ) using qbase+ software (Biogazelle, Ghent, Belgium) (Hellemans et al., 2007). CNRQ values were exported to Microsoft Excel. Biological replicates were averaged geometrically.

Statistical Analysis

Homoscedasticity of all the data was checked by Levene's test ($P \geq 0.01$). If homoscedasticity of data was fulfilled, data were analyzed using ANOVA with Scheffé's *post hoc* test (P = 0.05). If homoscedasticity of data failed the Levene's test, data were analyzed using one-way ANOVA with Games–Howell's *post hoc* test for physiological data (LT_{50}, stem water content and carbohydrate concentration) and using Kruskal–Wallis test (P = 0.05) with Bonferroni correction for multiple tests for gene expression data. Calibrated normalized relative quantity (CNRQ) values of gene expression data were log-transformed. Correlations between LT_{50} and physiological data were analyzed

by Pearson's two-tailed test ($P = 0.05$), while correlations between LT_{50} and gene expression were analyzed by Spearman's two-tailed test ($P = 0.05$) excluding the data of the transcript levels on climate changing points (20 December, 17 January, 31 January, and 14 February). If $P > 0.05$, there is no significant correlation; if $P < 0.05$, there is a significant correlation; if $P < 0.01$, there is a moderately strong correlation; and if $P < 0.001$, there is a very strong correlation. Statistical analyses were performed in SPSS Statistics (version 24) and all figures were made in SigmaPlot (version 13.0). Gene expression graphs are based on non-log transformed data.

RESULTS

Seasonal Changes in Bud Dormancy

Bud dormancy followed a similar seasonal dynamic for both cultivars, although a deeper dormancy level was found for 'Dagmar Hastrup' (**Figure 1**). For 'Dagmar Hastrup', most buds were dormant on 18 September (96.1%) (**Figure 1A**). However, cold requirements were low, only 39.8% of buds were dormant on 20 October when the average temperature was still above 10°C (**Figures 1A,C**). Bud dormancy decreased further to 15% on 15 November when average temperature dropped below 10°C for 21 days and even below 7°C for 10 days and daylength decreased below 10 h (**Figures 1A,C**). For 'Chandos Beauty', only 54% of the buds were dormant on 18 September, and dormancy released in 80% of the buds from October on. The mean time to bud break was highest in September and reached 29 days for 'Dagmar Hastrup' and 20 days for 'Chandos Beauty.' From October till February, the mean time to bud break decreased sharply for both cultivars (**Figure 1B**). From February on, the average temperature decreased below 5°C and even freezing temperatures occurred while the daylength increased from 9 to 10 h, bud break took only 3 days for 'Chandos Beauty' and 5 days for 'Dagmar Hastrup' on 17 February (**Figure 1B**).

Change of Cold Hardiness and Stem Water Content Under Controlled Conditions

Both cultivars showed a similar changing pattern of cold hardiness levels during acclimation (weeks 0–8) and deacclimation (weeks 8–10) (**Figure 2A**). The LT_{50} of non-acclimated plants ranged from −8.9°C for 'Dagmar Hastrup'

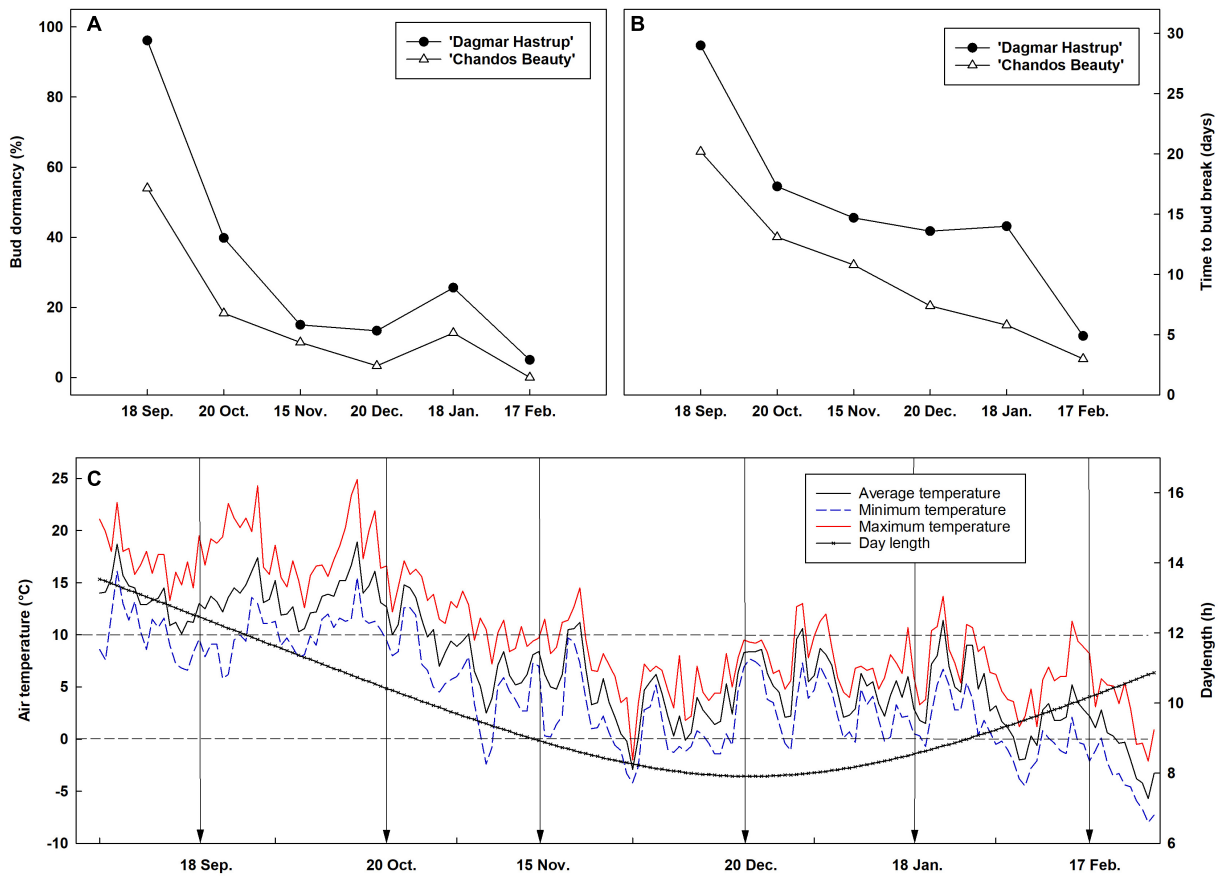

FIGURE 1 | Seasonal evolution of bud dormancy **(A)** and mean time to bud break **(B)** from 60 single-node cuttings in the apical zone of 'Chandos Beauty' and 'Dagmar Hastrup' from September 2017 to February 2018 with the corresponding air temperature and daylength conditions **(C)** in the field. The arrow in **(C)** indicates the sampling time points.

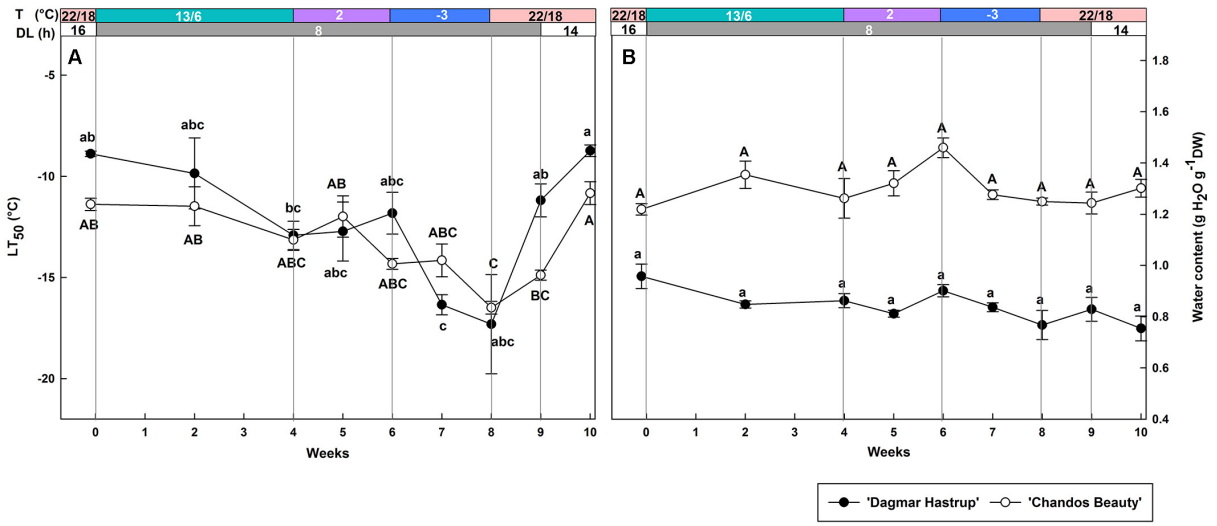

FIGURE 2 | Changes in LT_{50} **(A)** and stem water content **(B)** for 'Dagmar Hastrup' and 'Chandos Beauty.' The strips above the figure indicate the provided temperature (T) and daylength (DL). Data of LT_{50} for 'Dagmar Hastrup' were analyzed using one-way ANOVA with Games–Howell's *post hoc* test ($P = 0.05$). Data of LT_{50} for 'Chandos Beauty' and water content was analyzed using ANOVA with Scheffé's *post hoc* test ($P = 0.05$). Different letters indicate significant differences between sampling dates for each cultivar. Value per cultivar per sampling date is mean ± SE ($n = 4$).

to −11.4°C for 'Chandos Beauty.' Decreasing the photoperiod to 8 h and lowering the temperature to 13/6°C reduced LT_{50} for both cultivars; decrease of the temperature to 2°C did not significantly decrease the LT_{50}. A change to freezing temperatures at −3°C for 2 weeks (weeks 6–8) further decreased LT_{50} to significantly lower values of −16.5°C for both cultivars compared to week 0 (**Figure 2A**). Both cultivars reacted quickly to deacclimation temperatures of 22/18°C. 'Dagmar Hastrup' lost its cold hardiness after 1 week (week 9) under short daylength (8 h) while 'Chandos Beauty' was fully deacclimated after 2 weeks (week 10) when long days (14 h) were provided.

No significant variation in stem water content was found for both cultivars under changing temperatures and daylength (**Figure 2B**). 'Chandos Beauty' had, however, a higher stem water content ranging from 1.22 at the start to 1.46 g H_2O g^{-1} DW after 10 weeks compared to 'Dagmar Hastrup' (0.96 g H_2O g^{-1} DW at the start to 0.75 g H_2O g^{-1} DW after 10 weeks).

Carbohydrate Metabolism

Overall, starch content was significantly lower for 'Dagmar Hastrup' than for 'Chandos Beauty' ($P = 0.001$, **Figure 3A**). For 'Dagmar Hastrup,' starch increased slightly reaching 4.0 mg g^{-1} DW after 1 week at 2°C (week 5), but dropped significantly at sub-zero temperatures by 45% to 2.2 mg g^{-1} DW (week 9) and remained low under deacclimation. In contrast starch levels remained relatively stable (10.9–13.0 mg g^{-1} DW) during cold acclimation and deacclimation in 'Chandos Beauty.'

Total soluble sugars were significantly influenced by cold acclimation and deacclimation for both cultivars (**Figure 3B**). For 'Dagmar Hastrup', the content increased significantly by 54.4% from 6.5 to 10.0 mg g^{-1} DW during weeks 0–4 (13/6°C, 8 h) and remained stable at 2 and −3°C. The sugar content of 'Dagmar Hastrup' decreased by 72.6% during deacclimation (weeks 8–10, 22/18°C). For 'Chandos Beauty,' sugars decreased by 20.1% during weeks 0–4 (13/6°C, 8 h) and increased significantly by 33.5% during 2 and −3°C treatments reaching maximum of 47.1 mg g^{-1} DW at week 8 (−3°C, 8 h). During deacclimation (weeks 8–10; 22/18°C), sugar content decreased prominently by 54.5% for 'Chandos Beauty' to 21.4 mg g^{-1} DW.

Sucrose, hexoses (glucose + fructose), raffinose and stachyose were analyzed during acclimation and deacclimation, respectively (**Figures 3C–F**). Sucrose and hexose levels were significantly higher at the start for 'Chandos Beauty' than for 'Dagmar Hastrup' and remained higher during the experiment (**Figures 3C,D**). For 'Dagmar Hastrup,' sucrose hardly changed during the experiment (**Figure 3C**). Hexoses increased by 65.7% during weeks 0–4 (13/6°C, 8 h) and remained stable (between 3.4 and 5.5 mg g^{-1} DW) during 2 and −3°C treatments. Deacclimation resulted in decreasing hexose levels of 'Dagmar Hastrup' by 69.9% to 1.0 mg g^{-1} DW (**Figure 3D**). For 'Chandos Beauty,' the temperature drop to 13/6°C resulted in a decreasing of sucrose and hexoses by 17.5 and 31.7%, respectively (weeks 0–4). Further decrease of the temperature resulted in a non-significant increase by 27.5% for sucrose and fluctuating levels of hexose between 9.3 and 13.3 mg g^{-1} DW (weeks 4–8). Deacclimation temperatures (22/18°C) led to a significant decrease of both sucrose and hexoses of 'Chandos Beauty' by 50.0 and 49.1%, respectively (**Figures 3C,D**).

Both raffinose and stachyose content was strongly influenced by ambient temperatures for both cultivars (**Figures 3E,F**). A decrease to 2°C resulted in an increase of raffinose; this increase was further enhanced by sub-zero temperatures. For stachyose, no change was noted until 2 weeks at 2°C with the content of 0.06 mg g^{-1}

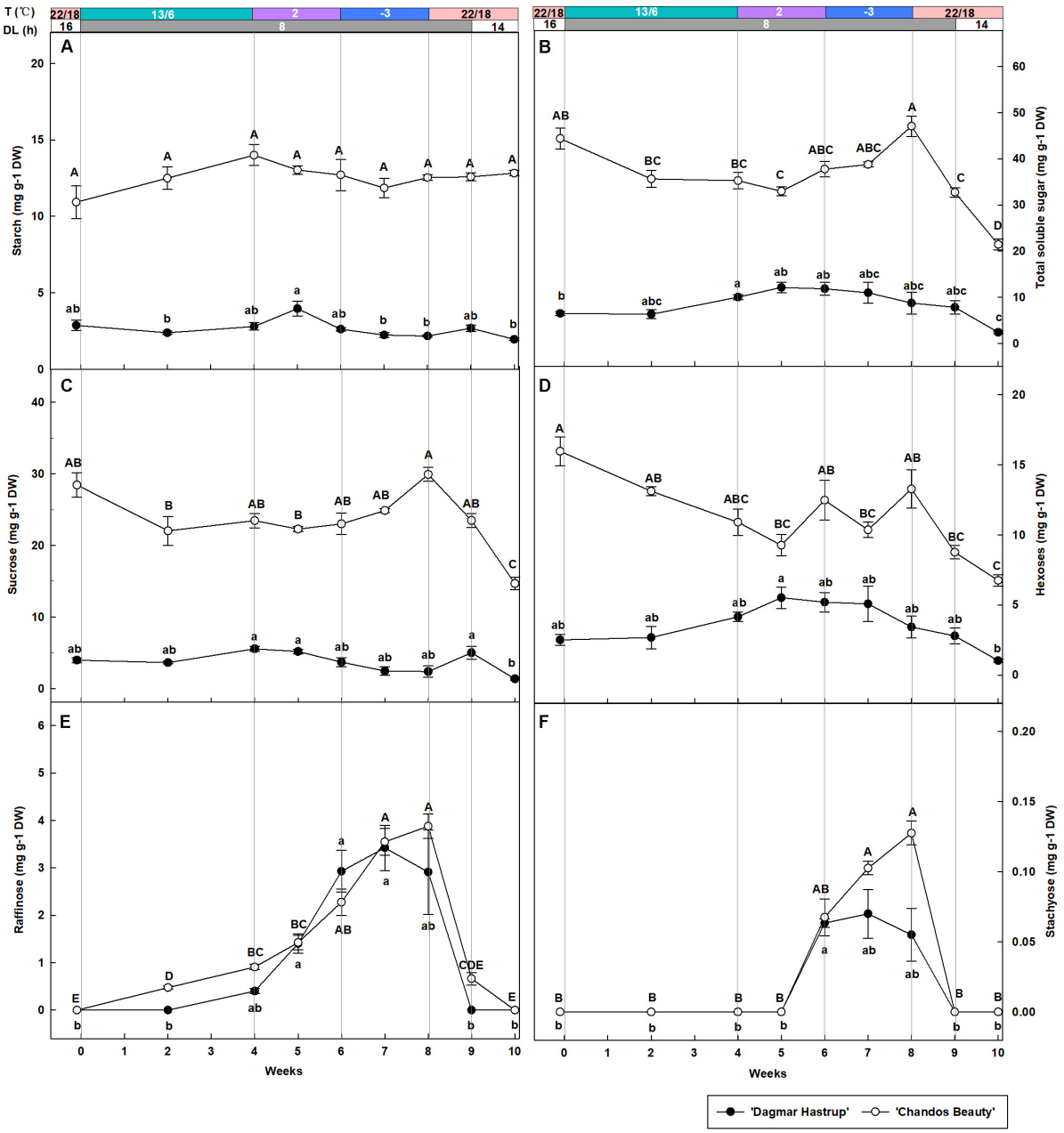

FIGURE 3 | Changes in the content of starch **(A)**, total soluble sugars **(B)** sucrose **(C)**, hexoses (glucose + fructose) **(D)**, raffinose **(E)**, and stachyose **(F)** of 'Dagmar Hastrup' and 'Chandos Beauty' under controlled climate condition. The stripes above the figure indicate the provided temperature (T) and daylength (DL). Data of total soluble sugar: starch, raffinose, and stachyose were analyzed using one-way ANOVA with Games–Howell's *post hoc* test ($P = 0.05$). Data of starch, sucrose and hexoses were analyzed using ANOVA with Scheffé's *post hoc* test ($P = 0.05$). Different letters indicate significant differences between sampling dates for each cultivar. Value per cultivar per sampling date is mean ± SE ($n = 4$).

DW for both cultivars. Here again, sub-zero temperatures further enhanced stachyose content for 'Chandos Beauty' but not for 'Dagmar Hastrup' (**Figures 3E,F**). For 'Dagmar Hastrup,' the raffinose and stachyose peaked at the end of week 7 at 3.4 and 0.07 mg g^{-1} DW, respectively. For 'Chandos Beauty,' the largest amount of raffinose (3.5 mg g^{-1} DW) and stachyose (0.13 mg g^{-1} DW) were found at the end of week 8.

Additionally, raffinose and stachyose correlated negatively ($P < 0.01$) with LT_{50} for both cultivars. For 'Chandos Beauty,' total soluble sugars and sucrose were negatively correlated with LT_{50}. No correlations were found for hexoses (**Table 1**).

Expression Analysis of *RhDHN5*

The up-regulation of *RhDHN5* during acclimation was very similar for 'Dagmar Hastrup' and 'Chandos Beauty' (**Figure 4**).

TABLE 1 | Pearson's correlation coefficients between LT_{50} and carbohydrate concentration, and Spearman's correlation coefficients between LT_{50} and gene expression for 'Dagmar Hastrup' and 'Chandos Beauty,' $^{*}P < 0.05$, $^{**}P < 0.01$; ns, not significant.

Test items	LT_{50} of 'Chandos Beauty'	LT_{50} of 'Dagmar Hastrup'
Total soluble sugars	-0.44*	ns
Sucrose	−0.48**	ns
Raffinose	−0.67**	−0.56**
Stachyose	−0.63**	−0.53**
RhDHN5	−0.58**	−0.66**
RhBAM3	−0.53**	−0.55**
RhDPE2	ns	−0.64**
RhSUS	ns	0.62**
RhFRK4	ns	0.67**
RhHXK1	ns	0.53**
RhMIPS	ns	0.52**

Decreasing the temperature to 13/6°C under short daylength gradually increased transcript levels. *RhDHN5* transcripts further accumulated by decreasing the temperature to 2°C and sub-zero temperatures. The highest expression levels (CNRQs around 6) were reached after 2 weeks at −3°C which induced a 25- and 76-fold change, respectively, compared to non-acclimated plants (22/18°C, 16 h, 19 December). Deacclimation (22/18°C with short days) leads to a strong and immediate decrease (after 24 h) in transcript levels with CNRQs below 1. Two weeks after the start of the deacclimation, transcript levels were similar to those of non-acclimated plants (19 December).

Expression Analysis of Starch Metabolism-Related Genes

The expression of *RhBAM3* and *RhDPE2*, two genes involved in the starch catabolic pathway, are given (**Figures 5A–C**). A remarkable induction of *RhBAM3* was present in both cultivars when temperatures decreased to 2°C. As there is an important difference in the range of CNRQs levels of the two cultivars, results are presented separately (**Figures 5A,B**). For 'Dagmar Hastrup,' a transient higher expression was observed in *RhBAM3* 24 h after the ambient temperature dropped to 2°C. One week later, *RhBAM3* transcripts had decreased and remained relatively stable when temperatures further dropped below zero. During deacclimation (22/14°C), *RhBAM3* transcripts dropped significantly to nearly undetectable levels. For 'Chandos Beauty,' *RhBAM3* was transiently up-regulated 24 h after a change to 2°C and then decreased; the transcript levels increased again by a shift to −3°C and accumulated to their highest level in the following 2 weeks (**Figure 5B**). The expression of *RhDPE2* was not linked to *RhBAM3* (**Figure 5C**). For 'Dagmar Hastrup,' a higher transcript abundance of *RhDPE2* was seen when temperature was low (2 and −3°C, 17 January to 13 February). However, for 'Chandos Beauty,' low temperature did not induce expression of *RhDPE2* and higher transcript levels were present for non-acclimated plants (19 December) and after 1 week of deacclimation (22/14°C, 20 February).

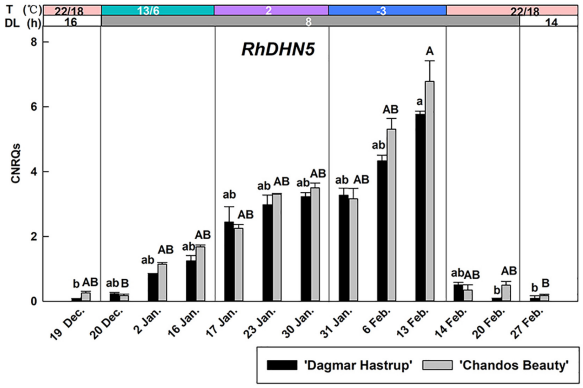

FIGURE 4 | Expression of *RhDHN5* for 'Dagmar Hastrup' and 'Chandos Beauty' under a controlled climate. The stripes above the figure indicate provided temperature (T) and daylength (DL). Data were assessed by the Kruskal–Wallis test ($P = 0.05$). CNRQ (calibrated normalized relative quantity) per cultivar per sampling date is presented as geometric mean ± SE ($n = 3$). Different letters indicate significant differences between sampling dates for each cultivar.

Expression Analysis of Sugar Metabolism Related Genes

The expression of *RhSPS1* decreased slightly from 1.05 to 0.67 under conditions of cold acclimation for 'Dagmar Hastrup,' while deacclimation enhanced its expression for both cultivars (**Figure 5D**).

For 'Dagmar Hastrup'. *RhINV2* transcripts increased after 2 weeks at −3°C, while deacclimation downregulated the expression. For 'Chandos Beauty,' low temperatures (both 2 and −3°C) did not influence the expression levels of *RhINV2*, although 2 weeks of deacclimation increased fourfold of the expression compared to the expression at the end of −3°C treatment (**Figure 5F**).

The expression of *RhSUS*, *RhHXK1*, and *RhFRK4* was very similar for both cultivars (**Figures 5E,G,H**). Acclimation treatments resulted in low transcript levels while non-acclimated plants (start of the experiment) and deacclimated plants (end of the experiment) had higher transcript levels.

RhMIPS is involved in the biosynthesis of myo-inositol (**Figure 5I**). For both cultivars, the transcript levels of *RhMIPS* decreased during low temperature treatment from 13/6°C to −3°C. During deacclimation, when temperature raised to 20/18°C, transcript levels increased significantly for both cultivars after 1 week and were strongly induced for 'Chandos Beauty' when light provision shifted from short days to long days.

RhGK and *RhRS6* are involved in the biosynthesis of RFOs (**Figures 5J,K**). Shortening the photoperiod from 16 to 8 h at 13/6°C decreased the expression of *RhGK* from 2.15 to 0.75 for 'Dagmar Hastrup.' Lowering the temperature further to 2°C enhanced transcript levels, while further transcript accumulation was found after 2 weeks at −3°C (**Figure 5J**). For 'Chandos Beauty,' the transcript levels of *RhGK* were suppressed during cold acclimation and gradually increased during deacclimation (**Figure 5J**).

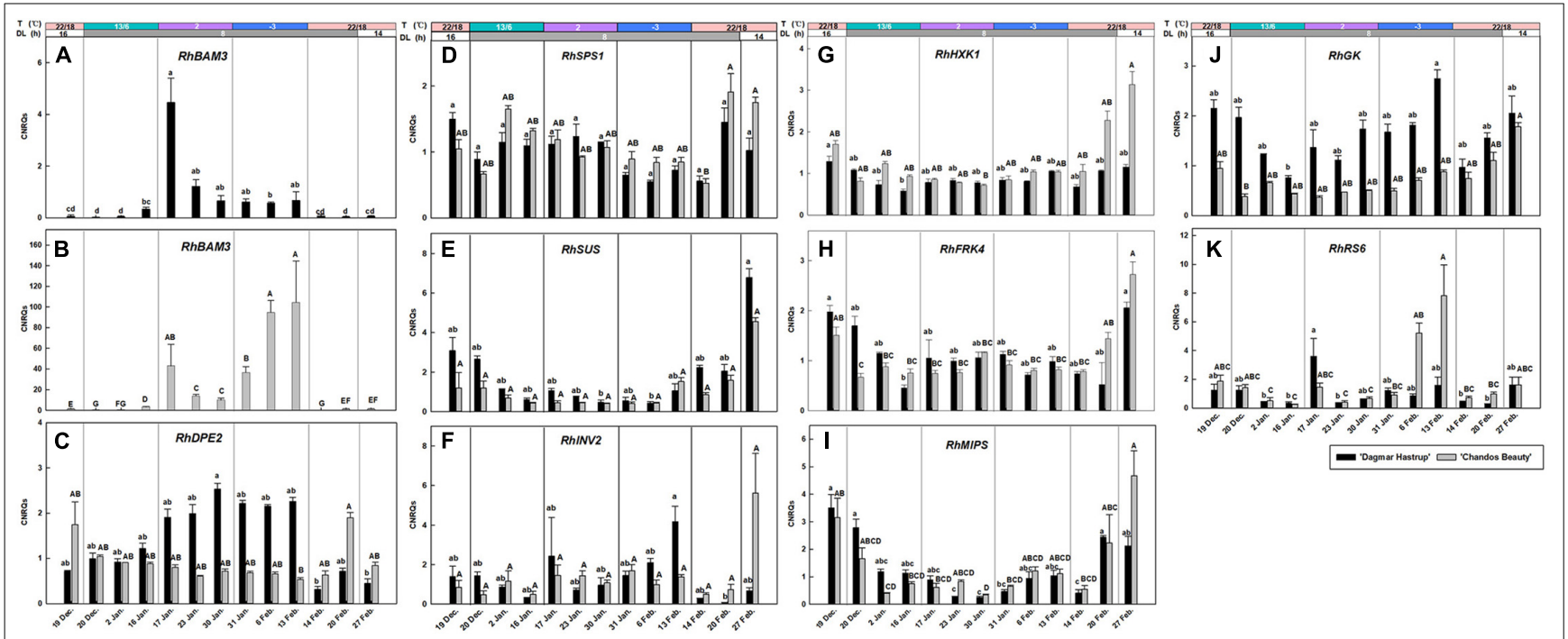

FIGURE 5 | Expression of *RhBAM3* and *RhDPE2* associated with starch catabolism **(A–C)**, *RhSPS1*, *RhSUS*, and *RhINV2* in sucrose metabolism **(D–F)**, *RhHXK1* and *RhFRK4* in hexose catabolism **(G,H)**, *RhMIPS* in myo-inositol synthesis **(I)** and *RhGK* and *RhRS6* in RFOs synthesis **(J,K)**. The stripes above the figure indicate the temperature (T) and daylength (DL). Data of *RhBAM3*, *RhMIPS* and *RhRS6* were assessed by one-way ANOVA with Scheffé's *post hoc* test ($P = 0.05$). Others were assessed by Kruskal–Wallis test ($P = 0.05$). CNRQ (calibrated normalized relative quantity) per cultivar per sampling date is presented as geometric mean ± SE ($n = 3$).

The up-regulation of *RhRS6* was cultivar dependent. For 'Dagmar Hastrup,' a transient increase was found 24 h after the temperature dropped from 13/6 to 2°C. A decrease to −3°C did not further affect the transcription of this gene (**Figure 5K**). For 'Chandos Beauty,' temperatures of 2°C did not influence transcript levels but freezing temperatures of −3°C resulted in an up-regulation after 1 week, with this up-regulation remaining high during the 2nd week at −3°C. A fast response to the deacclimation treatment (20/18°C) of *RhRS6* was found as the transcript levels reduced 24 h after the start of the treatment at 22/18°C (**Figure 5K**).

The correlation analyses between LT_{50} values and gene expression levels are given in **Table 1**. *RhDHN5* transcripts strongly correlated with LT_{50} for both cultivars ($P < 0.01$). In addition, for 'Dagmar Hastrup,' the expression of *RhDPE2* and *RhBAM3* (starch degradation) was negatively correlated with LT_{50}. However, the transcript level of *RhSUS* (sucrose metabolism), *RhFRK* and *RhHXK* (hexoses catabolism), and *RhMIPS* (myo-inositol synthesis) are positively correlated with LT_{50}. For 'Chandos Beauty,' only a negative correlation between LT_{50} and *RhBAM3* was present.

DISCUSSION

In an earlier field study we reported that 'Dagmar Hastrup' had a higher cold hardiness levels compared to 'Chandos Beauty' during the period November–January (Ouyang et al., 2019a). However, the understanding of environmental control on acclimation is hampered by the fluctuating environmental parameters in field studies. Also, it is not known if roses develop endodormancy, a process that might develop simultaneously with cold acclimation.

Our single node cutting experiment shows that endodormancy is present in the axillary buds of apical zones for both cultivars in September but less than 50% of the buds remain dormant in October. This indicates that roses have a low chilling demand, which is even lower for the less cold-hardy 'Chandos Beauty' as revealed also by a lower MTB (**Figure 1**). Rose buds are thus dominantly ecodormant (caused by environmental factors) during winter but differences in MTB indicate that cultivar differences in reaction to warm spells clearly exist till January. As both rose cultivars hardly showed bud endodormancy, warm spells may result in a fast bud break.

In this study, a controlled acclimation process did not result in a different level of cold acclimation between the cultivars (LT_{50} around −15°C, 8 weeks after the start of the cold acclimation treatment) although the more cold-hardy 'Dagmar Hastrup' reacts more strongly to the −3°C treatment (**Figure 2A**). The similar cold hardiness levels detected in these two cultivars may be due to a relative short period of low temperature treatment (2 weeks) and that therefore the 'Dagmar Hastrup' did not develop its maximum hardiness levels yet. Deacclimation occurred very rapidly and occurred sooner in 'Dagmar Hastrup.' A faster deacclimation than acclimation has also been observed in other woody plants and herbs (Gay and Eagles, 1991; Arora et al., 1992). Kalberer et al. (2007) found that the hardier *Rhododendron canadense* deacclimated faster than the less cold-hardy *Rhododendron prunifolium*. Likewise, it is found that the deacclimation level was greater in the hardier *Hydrangea* genotypes suggested that the deacclimation resistance is not correlated to the cold hardiness levels in mid-winter (Pagter et al., 2011b). Although a faster deacclimation may make the cultivar more susceptible to spring frost, the reacclimation capacity may also influence the resistance to these frost events. A rapid reacclimation was found in dehardened buds of three azalea genotypes within 1 day of exposure to a reacclimation regime (Kalberer et al., 2007) and the reacclimation capacity did not significantly associate with deacclimation resistance (Arora and Rowland, 2011). Therefore, reacclimation ability is also an important trait when coping with warm spells and needs to be further studied in roses.

Despite a similar level of cold acclimation between these rose cultivars, differences in physiological parameters and molecular patterns were found. Similar to our field results (Ouyang et al., 2019a), the more cold-hardy 'Dagmar Hastrup' had a stable and lower stem water content. A low tissue water content combined with a high amount of solutes (sugars and antifreeze proteins) slows down the speed of ice formation and migration of intracellular water to extracellular water (Gusta et al., 2004). Several field studies show that the stem water content of woody plants decreased during acclimation (Ashworth et al., 1993; Pagter et al., 2011b) which was also observed for 'Chandos Beauty' (Ouyang et al., 2019a). However, in this study, controlled acclimation did not lead to any decrease of the stem water content of 'Chandos Beauty' (**Figure 2B**) which may be attributed to the relative short cold treatment. Dehydrins are correlated to both dehydration and cold hardiness (Hanin et al., 2011). Both rose cultivars had a stable stem water content, thus changes in the expression of *RhDHN5* must be induced by a temperature response.

RhDHN5 gradually increased during the different steps of cold acclimation and strongly correlates with cold hardiness levels for both cultivars (**Figure 4** and **Table 1**). This is consistent with the results of seasonal acclimation in roses (Ouyang et al., 2019a) and of bark tissues in both evergreen and deciduous peach genotypes (Arora and Wisniewski, 1996; Wisniewski et al., 1996; Artlip et al., 1997). As our first cold acclimation step also includes a transition to short days, we cannot exclude a photoperiodic response as well. However, in hybrid aspen and silver birch, transcript levels of dehydrin showed only a limited response to photoperiod but increased strongly under decreasing temperature (Welling et al., 2002; Puhakainen, 2004). Also in peach bark, *ppdhn1* did not respond to 3 weeks of short days at 20°C (Gusta et al., 2005). The abrupt decrease of *RhDHN5* transcript levels after 1 day of deacclimation (22/18°C, 8 h) suggests that *RhDHN5* may be linked to freezing avoidance by promoting supercooling. A similar sharp decrease in protein abundance of a 105-kD dehydrin was observed within 1 day of deacclimation in *Rhododendron viscosum* var. serrulatum and was assumed to be associated with the freezing avoidance strategy (supercooling) (Kalberer et al., 2007). It is noteworthy

that our stem samples are including both bark tissues and xylem tissues. The dehydrin protein PCA60 (encoded by *ppdh1*, homolog of *RhDHN5*) in peach was freely located in cytoplasm, plastids, and nucleus of bark cells and xylem ray parenchyma cells (Wisniewski et al., 1999). Under cold stress, PCA60 was assumed to bind to ice to prevent water to migrate to ice crystals and therefore the proteins that accumulated within xylem ray parenchyma may inhibit intracellular ice nucleation and promote supercooling in the cells (Wisniewski et al., 1999). Supercooling in xylem tissue may also be a strategy to prevent the damage of cellular dehydration observed in several woody-plant species (Gusta et al., 1983). Freezing tolerance and freezing avoidance (supercooling) are not mutually exclusive and may both contribute to the development of cold hardiness of woody plants (Wisniewski and Ashworth, 1986; Wisniewski et al., 2018).

A high number of solutes is another acclimation strategy in cold tolerance. Starch-to-sugar interconversion is commonly observed in woody plants during cold acclimation and deacclimation (Sauter, 1988). In this study total soluble sugars increased during cold acclimation, especially for 'Chandos Beauty' where they also strongly correlated to LT_{50}. Low temperature and corresponding low respiration rates as well as translocation of sugars from senescing leaves might explain this net carbon gain in the stems (Levitt, 1980; Kalberer et al., 2006). Enzymes of the starch catabolic pathway responded to cold acclimation. *RhBAM3* was induced by low temperatures, as is also reported for other species (Elle and Sauter, 2000; Kaplan et al., 2006). For 'Dagmar Hastrup,' a decrease to 2°C induced a transient up-regulation of *RhBAM3* but no further obvious increase was found at sub-zero temperatures (**Figure 5A**). In contrast, temperatures of 2°C induced *RhBAM3* expression for 'Chandos Beauty,' which increased further at −3°C (**Figure 5B**). The up-regulation of *RhBAM3* during cold acclimation was not clearly present in the field study (Ouyang et al., 2019a). Here we identified a transient expression pattern induced by low temperature which makes it difficult to detect in the longer time-span samples. *RhBAM3* (Acc No. MH249079, **Supplementary Table S4**), was extracted according to *VcBMY* of blueberry (*Vaccinium corymbosum* L.) (**Supplementary Table S2**). *VcBMY* was reported to be associated with cold hardiness and its closest homolog in *Arabidopsis* is *AtBAM3* (identity 71%). In *Arabidopsis*, several *BAM* gene family members were isolated but *BAM3* (also called *BMY8*) is the only cold shock induced amylase gene (Maruyama et al., 2009). *AtBAM3* or its homolog in other plants was reported as playing a dominant role in hydrolyzing starch (Scheidig et al., 2002; Kaplan and Guy, 2005). *PtrBAM1*, a close homolog of *AtBAM3* isolated from trifoliate orange (*Poncirus trifoliata*), can be directly regulated by CBF and contributes to cold hardiness by regulating sugar content (Peng et al., 2014). In our study, the up-regulation of *RhBAM3* may also directly regulate the accumulation of soluble sugars (**Figures 3B**, **5A,B**). Maltose is the direct breakdown product of starch by chloroplast-localized BAM which is then converted into glucose in the cytosol by DPE2 (disproportionating enzyme 2) (Kaplan et al., 2006). Only for 'Dagmar Hastrup', this conversion was found as *RhDPE2* was upregulated by both 2 and −3°C (**Figure 5C**) and this was also shown during seasonal acclimation (Ouyang et al., 2019a). This is also visible at metabolic level, with increasing hexose levels observed under cold acclimation. For 'Chandos Beauty', an accumulation of maltose levels might be expected, which by itself can protect membranes and proteins in the stroma (Kaplan et al., 2006).

Glucose and fructose are converted into Glc-6-P and Fru-6-P, which are precursors of sucrose biosynthesis by HXK and FRK. In *Arabidopsis*, the transcript levels of *HXK* and *FRK* were abundant during cold acclimation, thus contributing to the early increase of Glc-6-P and Fru-6-P (Kaplan et al., 2007). In tea plant (*Camellia sinensis*), *CsHXK3* is up-regulated during cold acclimation and is related to sugar-signaling (Yue et al., 2015). However, although our *RhHXK1* (MH249074, **Supplementary Table S4**) is the homolog sequence of *CsHXK3* (KJ489422, **Supplementary Table S2**), the transcript levels were rather suppressed. Similarly, the expression of *RhFRK4* was also down-regulated.

The conversion of hexoses to sucrose enhanced sucrose levels at −3°C for 'Chandos Beauty' (**Figures 3C,D**). In contrast, the overall sucrose levels of 'Dagmar Hastrup' were lower and decreased at low temperature (**Figure 3C**). SPS is the key enzyme in sucrose synthesis in both photosynthetic and non-photosynthetic tissues (Dali et al., 1992; Gutiorrez-Miceli et al., 2002). In both rose cultivars, however, *RhSPS1* transcripts decreased under cold acclimation (**Figure 5D**). Changes in soluble sugars do not strongly correlate with the transcript abundances during cold acclimation. This may be due to the posttranslational modifications that changes the stability of the related enzymes (Toroser and Huber, 1997). The function of SUS is more for sucrose degradation than sucrose synthesis and its activity correlates positively to starch synthesis (Dochlert, 1990; Dali et al., 1992). In both rose cultivars, *RhSUS* transcript levels were down-regulated when temperature decreased (**Figure 5E**) which is also reported in a previous field study during November–January (Ouyang et al., 2019a). Furthermore, invertase activity can result in cleavage of sucrose into glucose and fructose. No up-regulation of *RhINV2* under cold acclimation is present for 'Chandos Beauty.'

It is well-established that high sugar amounts and especially RFOs are correlated to cold hardiness in different organs (shoots, leaf, and buds) of woody species (Hinesley et al., 1992; Ögren, 1997; Imanishi et al., 1998; Palonen et al., 2000; Pagter et al., 2008; Van Labeke and Volckaert, 2010; Trischuk et al., 2014). Raffinose and stachyose accumulate prominently for both cultivars during acclimation and the levels correlated with LT_{50} values, indicating their importance in cold acclimation (**Table 1**). RFOs, although present in smaller amounts at cellular level, are the most effective inhibitors to prevent crystallization of sucrose (Koster and Leopold, 1988). Raffinose biosynthesis was faster for the less cold-hardy 'Chandos Beauty,' where moderate temperatures (13/6°C) with short days already induced biosynthesis, although accumulation was strongly induced by low temperatures (2°C) and sub-zero temperatures (−3°C) (**Figure 3E**). Stachyose reached higher levels for 'Chandos Beauty' at −3°C, but overall stachyose levels of both cultivars were low (**Figure 3F**). RFOs (raffinose and stachyose) accumulation was also clearly observed in the seasonal study (Ouyang et al., 2019a).

Biosynthesis of RFOs starts from galactinol, which is synthesized from UDP-galactose and myo-inositol through galactinol synthase. Myo-inositol is produced from Glc6P by myo-inositol phosphate synthase (MIPS) and UDP-galactose is formed from D-galactoside by GK. Despite the increase of RFOs in roses under cold stress, *RhMIPS* was clearly downregulated by both moderate (13/6°C) and lower temperatures (2 and −3°C) (**Figure 5I**) confirming earlier field observations (Ouyang et al., 2019a).

In 'Dagmar Hastrup' only, *RhGK* was induced by both 2 and −3°C. The increasing UDP-galactose levels thus correlate with the accumulation of raffinose (**Figure 5J**). *Raffinose synthase* (*RS*) encodes the enzyme of the rate-limiting step in raffinose biosynthesis and its regulation precedes the biosynthesis of raffinose (Kaplan et al., 2007). The expression of *RhRS6* was induced early for 'Dagmar Hastrup' when temperatures decreased from 13/6 to 2°C, corresponding to the rapid increase of raffinose and stachyose during this period (**Figures 3E,F**, **5K**). For 'Chandos Beauty' significant up-regulation started later and was strongly induced by sub-zero temperatures (**Figure 5K**). *RS* up-regulation under low temperature was also reported in *Arabidopsis*, grape and tea plant (Kaplan et al., 2007; Yue et al., 2015; Chai et al., 2019). *RhGK* and *RhRS6* showed a clearer up-regulation pattern under low temperatures in the controlled-climate study compared to the field study (Ouyang et al., 2019a).

The reversibility of the cold response during deacclimation on the gene expression level was strongly present in the cold associated genes (*RhDPE2* for 'Dagmar Hastrup,' *RhBAM3* and *RhDHN5* for both cultivars). While gene expression data during deacclimation have rarely been reported in stems/bark of woody plants, the decrease of dehydrins and metabolites such as RFOs has been reported in several studies (Kalberer et al., 2006; Pagter et al., 2011b; Shin et al., 2015).

This reversibility of the cold response was also found in the up-regulation of *RhSUS*, *RhSPS1*, *RhHXK1*, *RhFRK4*, *RhINV2*, and *RhMIPS* for 'Chandos Beauty' and *RhSUS*, *RhSPS1*, *RhFRK4*, and *RhMIPS* for 'Dagmar Hastrup' at 1 and/or 2 weeks after the start of the deacclimation, which is related to bud burst and shooting as more carbon in the sink organs is needed (**Figures 5D–H**). Most transcripts were more strongly enhanced during deacclimation for the moderately cold-hardy 'Chandos Beauty' than for the more cold-hardy 'Dagmar Hastrup.' This response is also found in to the mean time to bud break (MTB) observed for both cultivars: bud break and shooting in 'Chandos Beauty' was earlier than in 'Dagmar Hastrup' (**Figure 1**).

CONCLUSION

Dehydrin (*RhDHN5*) and carbohydrate metabolism were both associated with the development of cold hardiness. The up regulation of *RhDHN5* during acclimation is mainly triggered by low temperatures as stem water content remained stable. Soluble sugars accumulated with up-regulated of *RhBAM3* during cold acclimation. Raffinose and stachyose accumulated greatly during cold acclimation, but the associated genes (*RhRS6* and *RhGK*) of their biosynthesis showed genotype specific up-regulation. Although similar cold hardiness levels were reached in both rose genotypes, differences in carbohydrate metabolism and related gene expression were present. The different regulation may be linked to their distinct genetic background and indicates different cold adaptation strategies in rose genotypes. Deacclimation was fast in both genotypes. The lack of endodormancy in both cultivars may increase the risk for shoot damage in these new deacclimated shoots when temperature drops again.

DATA AVAILABILITY STATEMENT

All datasets generated for this study are included in the article/**Supplementary Material**.

AUTHOR CONTRIBUTIONS

LO and M-CV planned the experiments. LO conducted the experiments and analyzed all the data. LO, ED and M-CV interpreted the data. LO wrote the manuscript. M-CV and LL critically revised the manuscript. All authors read and approved the manuscript.

FUNDING

This work was supported by China Scholarship Council (CSC) and Fundamental Research Funds for Institute of Urban Agriculture, Chinese Academy of Agricultural Sciences (No. S2020002).

ACKNOWLEDGMENTS

We thank Pheno Geno Roses, BV (Netherlands) for providing the rose material and PCS Ornamental Plant Research (Destelbergen, Belgium) for providing the cold chamber rooms. We also appreciated Dieter Van De Putte for assistance during bud dormancy experiment; Magali Losschaert for assistance during RT-qPCR analysis; Annelies Christiaens for the help in the experiments in PCS; Christophe Petit for technical assistance and Miriam Levenson for English-language editing.

SUPPLEMENTARY MATERIAL

The Supplementary Material for this article can be found online at: https://www.frontiersin.org/articles/10.3389/fpls.2020.00327/full#supplementary-material

REFERENCES

Altschul, S. F., Madden, T. L., Schäffer, A. A., Zhang, J., Zhang, Z., Miller, W., et al. (1997). Gapped BLAST and PSI-BLAST:a new generation of protein database search programs. *Nucleic Acids Res.* 25, 3389–3402. doi: 10.1093/nar/25.17.3389

Améglio, T., Pigeon, D., Archilla, O., Frizot, N., Saint-Joanis, B., Reynoird, J. P., et al. (2003). Adaptation to cold temperature and response to freezing in roses. *Acta Hortic.* 618, 515–520. doi: 10.17660/ActaHortic.2003.618.60

Arias, O., and Crabbé, J. (1975). Altérations de l'état de dormance ultérieur des bourgeons obtenues par diverses modalités de décapitations estivale, réalisées sur de jeunes plants de *Prunus avium* L. *CR Acad. Sci.* 280, 2449–2452.

Arora, R., and Rowland, L. J. (2011). Physiological research on winter-hardiness?: deacclimation resistance, reacclimation ability, photoprotection strategies, and a cold acclimation protocol design. *HortScience* 46, 1070–1078. doi: 10.21273/hortsci.46.8.1070

Arora, R., Rowland, L. J., Ogden, E. L., Dhanaraj, A. L., Marian, C. O., Ehlenfeldt, M. K., et al. (2004). Dehardening kinetics, bud development, and dehydrin metabolism in blueberry cultivars during deacclimation at constant, warm temperatures. *J. Am. Soc. Hort. Sci.* 129, 667–674. doi: 10.21273/jashs.129.5.0667

Arora, R., and Wisniewski, M. (1996). Accumulation of a 60-kD dehydrin protein in peach xylem tissues and its relationship to cold acclimation. *HortScience* 31, 923–925. doi: 10.21273/hortsci.31.6.923

Arora, R., Wisniewski, M. E., and Scorza, R. (1992). Cold acclimation in genetically related (sibling) deciduous and evergreen peach (*Prunus persica* [L.] *Batsch)*: I. seasonal changes in cold hardiness and polypeptides of bark and xylem tissues. *Plant Physiol.* 99, 1562–1568. doi: 10.1104/pp.99.4.1562

Artlip, T. S., Callahan, A. M., Bassett, C. L., and Wisniewski, M. E. (1997). Seasonal expression of a dehydrin gene in sibling deciduous and evergreen genotypes of peach (*Prunus persica* [L.] *Batsch)*. *Plant Mol. Biol.* 33, 61–70. doi: 10.1023/A:1005787909506

Ashworth, E. N., Malone, S. R., and Ristic, Z. (1993). Response of woody plant cells to dehydrative stress. *Int. J. Plant Sci.* 154, 90–99. doi: 10.1086/297094

Chai, F., Liu, W., Xiang, Y., Meng, X., Sun, X., Cheng, C., et al. (2019). Comparative metabolic profiling of *Vitis amurensis* and *Vitis vinifera* during cold acclimation. *Hortic. Res.* 6:8. doi: 10.1038/s41438-018-0083-5

Chinnusamy, V., Zhu, J., and Zhu, J. K. (2007). Cold stress regulation of gene expression in plants. *Trends Plant Sci.* 12, 444–451. doi: 10.1016/j.tplants.2007.07.002

Close, T. J. (1997). Dehydrins: a commonalty in the response of plants to dehydration and low temperature. *Physiol. Plant.* 100, 291–296. doi: 10.1034/j.1399-3054.1997.1000210.x

Dali, N., Michaud, D., and Yelle, S. (1992). Evidence for the involvement of sucrose phosphate synthase in the pathway of sugar accumulation in sucrose-accumulating tomato fruits. *Plant Physiol.* 99, 434–438. doi: 10.1104/pp.99.2.434

Dochlert, D. C. (1990). Distribution of enzyme activities within the developing maize (*Zea mays*) kernel in relation to starch, oil and protein accumulation. *Physiol. Plant.* 78, 560–567. doi: 10.1111/j.1399-3054.1990.tb05242.x

Elle, D., and Sauter, J. J. (2000). Seasonal changes of activity of a starch granule bound endoamylase and of a swtarch phosphorylase in poplar wood (*Populus* × *canadensis* Moench ‹robusta›) and their possible regulation by temperature and phytohormones. *J. Plant Physiol.* 156, 731–740. doi: 10.1016/s0176-1617(00)80239-4

Flint, H. L., Boyce, B. R., and Beattie, D. J. (1967). Index of injury—a useful expression of freezing injury to plant tissues as determined by the electrolytic method. *Can. J. Plant Sci.* 47, 229–230. doi: 10.4141/cjps67-043

Fowler, S., and Thomashow, M. F. (2002). Arabidopsis transcriptome profiling indicates that multiple regulatory pathways are activated during cold acclimation in addition to the CBF cold response pathway. *Plant Cell* 14, 1675–1690. doi: 10.1105/tpc.003483.Toward

Gay, A. P., and Eagles, C. F. (1991). Quantitative analysis of cold hardening and dehardening in Lolium. *Ann. Bot.* 67, 339–345. doi: 10.1093/oxfordjournals.aob.a088144

Gusta, L. V., Trischuk, R., and Weiser, C. J. (2005). Plant cold acclimation: The role of abscisic acid. *J. Plant Growth Regul.* 24, 308–318. doi: 10.1007/s00344-005-0079-x

Gusta, L. V., Tyler, N. J., and Chen, T. H. (1983). Deep undercooling in woody taxa growing north of the -40 °C isotherm. *Plant Physiol.* 72, 122–128. doi: 10.1104/pp.72.1.122

Gusta, L. V., Wisniewski, M., Nesbitt, N. T., and Gusta, M. L. (2004). The effect of water, sugars, and proteins on the pattern of ice nucleation and propagation in acclimated and nonacclimated canola leaves. *Plant Physiol.* 135, 1642–1653. doi: 10.1104/pp.103.028308

Gutiorrez-Miceli, F. A., Rodriguez-Mendiola, M. A., Ochoa-Alejo, N., Méndez-Salas, R., Dendooven, L., and Arias-Castro, C. (2002). Relationship between sucrose accumulation and activities of sucrose-phosphatase, sucrose synthase, neutral invertase and soluble acid invertase in micropropagated sugarcane plants. *Acta Physiol. Plant.* 24, 441–446. doi: 10.1007/s11738-002-0041-5

Guy, C., Kaplan, F., Kopka, J., Selbig, J., and Hincha, D. K. (2008). Metabolomics of temperature stress. *Physiol. Plant.* 132, 220–235. doi: 10.1111/j.1399-3054.2007.00999.x

Guy, C. L. (1990). Cold acclimation and freezing stress tolerance: role of protein metabolism. *Annu. Rev. Plant Physiol. Plant Mol. Biol.* 41, 187–223. doi: 10.1146/annurev.pp.41.060190.001155

Hanin, M., Brini, F., Ebel, C., Toda, Y., Takeda, S., and Masmoudi, K. (2011). Plant dehydrins and stress tolerance: versatile proteins for complex mechanisms. *Plant Signal. Behav.* 6, 1503–1509. doi: 10.4161/psb.6.10.17088

Heide, O. M. (2008). Interaction of photoperiod and temperature in the control of growth and dormancy of *Prunus* species. *Sci. Hortic. (Amsterdam).* 115, 309–314. doi: 10.1016/j.scienta.2007.10.005

Hellemans, J., Mortier, G., De Paepe, A., Speleman, F., and Vandesompele, J. (2007). qBase relative quantification framework and software for management and automated analysis of real-time quantitative PCR data. *Genome Biol.* 8:R19. doi: 10.1186/gb-2007-8-2-r19

Hinesley, L., Pharr, D., Snelling, L., and Funderburk, S. (1992). Foliar raffinose and sucrose in four conifer species: relationship to seasonal temperature. *J. Am. Soc. Hortic. Sci.* 117, 852–855. doi: 10.21273/jashs.117.5.852

Imanishi, H. T., Suzuki, T., Masuda, K., and Harada, T. (1998). Accumulation of raffinose and stachyose in shoot apices of *Lonicera caerulea* L. during cold acclimation. *Sci. Hortic. (Amsterdam).* 72, 255–263. doi: 10.1016/S0304-4238(97)00129-5

Kalberer, S. R., Leyva-Estrada, N., Krebs, S. L., and Arora, R. (2007). Frost dehardening and rehardening of floral buds of deciduous azaleas are influenced by genotypic biogeography. *Environ. Exp. Bot.* 59, 264–275. doi: 10.1016/j.envexpbot.2006.02.001

Kalberer, S. R., Wisniewski, M., and Arora, R. (2006). Deacclimation and reacclimation of cold-hardy plants: current understanding and emerging concepts. *Plant Sci.* 171, 3–16. doi: 10.1016/j.plantsci.2006.02.013

Kaplan, F., and Guy, C. L. (2005). RNA interference of *Arabidopsis* beta-amylase8 prevents maltose accumulation upon cold shock and increases sensitivity of PSII photochemical efficiency to freezing stress. *Plant J.* 44, 730–743. doi: 10.1111/j.1365-313X.2005.02565.x

Kaplan, F., Kopka, J., Sung, D. Y., Zhao, W., Popp, M., Porat, R., et al. (2007). Transcript and metabolite profiling during cold acclimation of *Arabidopsis* reveals an intricate relationship of cold-regulated gene expression with modifications in metabolite content. *Plant J.* 50, 967–981. doi: 10.1111/j.1365-313X.2007.03100.x

Kaplan, F., Sung, D. Y., and Guy, C. L. (2006). Roles of β-amylase and starch breakdown during temperatures stress. *Physiol. Plant.* 126, 120–128. doi: 10.1111/j.1399-3054.2006.00604.x

Kontunen-Soppela, S., Taulavuori, K., Taulavuori, E., Lähdesmäki, P., and Laine, K. (2000). Soluble proteins and dehydrins in nitrogen-fertilized Scots pine seedlings during deacclimation and the onset of growth. *Physiol. Plant.* 109, 404–409. doi: 10.1034/j.1399-3054.2000.100406.x

Koster, K. L., and Leopold, A. C. (1988). Sugars and desiccation tolerance in seeds. *Plant Physiol.* 88, 829–832. doi: 10.1104/pp.88.3.829

Levitt, J. (1980). *Responses of Plants to Environmental Stresses: Chilling, Freezing and High Temperature Stresses*, 2nd Edn, Vol. 1. New York, NY: Academic Press, doi: 10.1016/0160-9327(81)90046-6

Li, C., Junttila, O., Ernstsen, A., Heino, P., and Palva, E. T. (2003). Photoperiodic control of growth, cold acclimation and dormancy development in silver birch (*Betula pendula*) ecotypes. *Physiol. Plant.* 117, 206–212. doi: 10.1034/j.1399-3054.2003.00002.x

Li, C., Junttila, O., and Palva, E. T. (2004). Environmental regulation and physiological basis of freezing tolerance in woody plants. *Acta Physiol. Plant.* 26, 213–222. doi: 10.1007/s11738-004-0010-2

Li, C., Puhakainen, T., Welling, A., Viherä-Aarnio, A., Ernstsen, A., Junttila, O., et al. (2002). Cold acclimation in silver birch (*Betula pendula*). Development of freezing tolerance in different tissues and climatic ecotypes. *Physiol. Plant.* 116, 478–488. doi: 10.1034/j.1399-3054.2002.1160406.x

Lim, C. C., Arora, R., and Townsend, E. C. (1998). Comparing gompertz and richards functions to estimate freezing injury in *Rhododendron* using electrolyte leakage. *J. Am. Soc. Hortic. Sci.* 123, 246–252. doi: 10.21273/jashs.123.2.246

Luypaert, G., Witters, J., Van Huylenbroeck, J., De Clercq, P., De Riek, J., and De Keyser, E. (2017). Induced expression of selected plant defence related genes in pot azalea, *Rhododendron simsii* hybrid. *Euphytica* 213:227. doi: 10.1007/s10681-017-2010-5

Maruyama, K., Takeda, M., Kidokoro, S., Yamada, K., Sakuma, Y., Urano, K., et al. (2009). Metabolic pathways involved in cold acclimation identified by integrated analysis of metabolites and transcripts regulated by DREB1A and DREB2A. *Plant Physiol.* 150, 1972–1980. doi: 10.1104/pp.109.135327

Meier, U., Bleiholder, H., Brumme, H., Bruns, E., Mehring, B., Proll, T., et al. (2009). Phenological growth stages of roses (Rosa sp.): Codification and description according to the BBCH scale. *Ann. Appl. Biol.* 154, 231–238. doi: 10.1111/j.1744-7348.2008.00287.x

Morin, X., Améglio, T., Ahas, R., Kurz-Besson, C., Lanta, V., Lebourgeois, F., et al. (2007). Variation in cold hardiness and carbohydrate concentration from dormancy induction to bud burst among provenances of three European oak species. *Tree Physiol.* 27, 817–825. doi: 10.1093/treephys/27.6.817

Ögren, E. (1997). Relationship between temperature, respiratory loss of sugar and premature dehardening in dormant Scots pine seedlings. *Tree Physiol.* 17, 47–51. doi: 10.1093/treephys/17.1.47

Ouyang, L., Leus, L., De Keyser, E., and Van Labeke, M.-C. (2019a). Seasonal changes in cold hardiness and carbohydrate metabolism in four garden rose cultivars. *J. Plant Physiol.* 232, 188–199. doi: 10.1016/j.jplph.2018.12.001

Ouyang, L., Leus, L., and Van Labeke, M.-C. (2019b). Three-year screening for cold hardiness of garden roses. *Sci. Hortic. (Amsterdam)* 245, 12–18. doi: 10.1016/j.scienta.2018.10.003

Pagter, M., and Arora, R. (2013). Winter survival and deacclimation of perennials under warming climate: physiological perspectives. *Physiol. Plant.* 147, 75–87. doi: 10.1111/j.1399-3054.2012.01650.x

Pagter, M., Hausman, J. F., and Arora, R. (2011a). Deacclimation kinetics and carbohydrate changes in stem tissues of *Hydrangea* in response to an experimental warm spell. *Plant Sci.* 180, 140–148. doi: 10.1016/j.plantsci.2010.07.009

Pagter, M., Lefèvre, I., Arora, R., and Hausman, J. F. (2011b). Quantitative and qualitative changes in carbohydrates associated with spring deacclimation in contrasting *Hydrangea* species. *Environ. Exp. Bot.* 72, 358–367. doi: 10.1016/j.envexpbot.2011.02.019

Pagter, M., Jensen, C. R., Petersen, K. K., Liu, F., and Arora, R. (2008). Changes in carbohydrates, ABA and bark proteins during seasonal cold acclimation and deacclimation in *Hydrangea* species differing in cold hardiness. *Physiol. Plant.* 134, 473–485. doi: 10.1111/j.1399-3054.2008.01154.x

Palonen, P. (1999). Relationship of seasonal changes in carbohydrates and cold hardiness in canes and buds of three red raspberry cultivars. *J. Am. Soc. Hortic. Sci.* 124, 507–513. doi: 10.21273/jashs.124.5.507

Palonen, P., Buszard, D., and Donnelly, D. (2000). Changes in carbohydrates and freezing tolerance during cold acclimation of red raspberry cultivars grown in vitro and in vivo. *Physiol. Plant.* 110, 393–401. doi: 10.1111/j.1399-3054.2000.1100314.x

Palonen, P., and Junttila, O. (1999). Cold hardening of raspberry plants in vitro is enhanced by increasing sucrose in the culture medium. *Physiol. Plant.* 106, 386–392. doi: 10.1034/j.1399-3054.1999.106405.x

Peng, T., Zhu, X., Duan, N., and Liu, J. H. (2014). *PtrBAM1*, a β-amylase-coding gene of Poncirus trifoliata, is a CBF regulon member with function in cold tolerance by modulating soluble sugar levels. *Plant Cell Environ.* 37, 2754–2767. doi: 10.1111/pce.12384

Puhakainen, T. (2004). Short-day potentiation of low temperature-induced gene expression of a C-repeat-binding factor-controlled gene during cold acclimation in silver birch. *Plant Physiol.* 136, 4299–4307. doi: 10.1104/pp.104.047258

Rekarte-Cowie, I., Ebshish, O. S., Mohamed, K. S., and Pearce, R. S. (2008). Sucrose helps regulate cold acclimation of *Arabidopsis thaliana*. *J. Exp. Bot.* 59, 4205–4217. doi: 10.1093/jxb/ern262

Rohde, A., and Bhalerao, R. P. (2007). Plant dormancy in the perennial context. *Trends Plant Sci.* 12, 217–223. doi: 10.1016/j.tplants.2007.03.012

Ruijter, J. M., Ramakers, C., Hoogaars, W. M. H., Karlen, Y., Bakker, O., Van den hoff, M. J. B., et al. (2009). Amplification efficiency: linking baseline and bias in the analysis of quantitative PCR data. *Nucleic Acids Res.* 37:e45. doi: 10.1093/nar/gkp045

Ruttink, T., Arend, M., Morreel, K., Storme, V., Rombauts, S., Fromm, J., et al. (2007). A molecular timetable for apical bud formation and dormancy induction in poplar. *Plant Cell* 19, 2370–2390. doi: 10.1105/tpc.107.052811

Sauter, J. J. (1988). Temperature-induced changes in starch and sugars in the stem of *Populus x canadensis* «?robusta?». *J. Plant Physiol.* 132, 608–612. doi: 10.1016/S0176-1617(88)80263-3

Scheidig, A., Fröhlich, A., Schulze, S., Lloyd, J. R., and Kossmann, J. (2002). Downregulation of a chloroplast-targeted β-amylase leads to a starch-excess phenotype in leaves. *Plant J.* 30, 581–591. doi: 10.1046/j.1365-313X.2002.01317.x

Shi, Y., Ding, Y., and Yang, S. (2018). Molecular regulation of CBF signaling in cold acclimation. *Trends Plant Sci.* 23, 623–637. doi: 10.1016/j.tplants.2018.04.002

Shin, H., Kim, K., Oh, Y., Yun, S. K., Oh, S.-I., Sung, J., et al. (2015). Carbohydrate changes in peach shoot tissues and their relationship to cold acclimation and deacclimation. *Hortic. J.* 84, 21–29. doi: 10.2503/hortj.MI-013

Theocharis, A., Clément, C., and Barka, E. A. (2012). Physiological and molecular changes in plants grown at low temperatures. *Planta* 235, 1091–1105. doi: 10.1007/s00425-012-1641-y

Toroser, D., and Huber, S. C. (1997). Protein phosphorylation as a mechanism for osmotic-stress activation of sucrose-phosphate synthase in spinach leaves. *Plant Physiol.* 114, 947–955. doi: 10.1104/pp.114.3.947

Trischuk, R. G., Schilling, B. S., Low, N. H., Gray, G. R., and Gusta, L. V. (2014). Cold acclimation, de-acclimation and re-acclimation of spring canola, winter canola and winter wheat: The role of carbohydrates, cold-induced stress proteins and vernalization. *Environ. Exp. Bot.* 106, 156–163. doi: 10.1016/j.envexpbot.2014.02.013

Untergasser, A., Nijveen, H., Rao, X., Bisseling, T., Geurts, R., and Leunissen, J. A. M. (2007). Primer3Plus, an enhanced web interface to Primer3. *Nucleic Acids Res.* 35, 71–74. doi: 10.1093/nar/gkm306

Usadel, B., Bläsing, O. E., Gibon, Y., Poree, F., Höhne, M., Günter, M., et al. (2008). Multilevel genomic analysis of the response of transcripts, enzyme activities and metabolites in *Arabidopsis* rosettes to a progressive decrease of temperature in the non-freezing range. *Plant Cell Environ.* 31, 518–547. doi: 10.1111/j.1365-3040.2007.01763.x

Van Labeke, M. C., and Volckaert, E. (2010). Evaluation of electrolyte leakage for detecting cold acclimatization in six deciduous tree species. *Acta Hortic.* 885, 403–410. doi: 10.17660/actahortic.2010.885.56

Welling, A., Moritz, T., Palva, E. T., and Junttila, O. (2002). Independent activation of cold acclimation by low temperature and short photoperiod in hybrid aspen. *Plant Physiol.* 129, 1633–1641. doi: 10.1104/pp.003814

Welling, A., and Palva, E. T. (2006). Molecular control of cold acclimation in trees. *Physiol. Plant.* 127, 167–181. doi: 10.1111/j.1399-3054.2006.00672.x

Wisniewski, M., and Ashworth, E. N. (1986). A comparison of seasonal ultrastructural changes in stem tissues of peach (*Prunus persica*) that exhibit contrasting mechanisms of cold hardiness. *Bot. Gaz.* 147, 407–417. doi: 10.1086/337608

Wisniewski, M., Close, T. J., Artlip, T., and Arora, R. (1996). Seasonal patterns of dehydrins and 70-kDa heat-shock proteins in bark tissues of eight species of woody plants. *Physiol. Plant.* 96, 496–505. doi: 10.1111/j.1399-3054.1996.tb00464.x

Wisniewski, M., Nassuth, A., and Arora, R. (2018). Cold hardiness in trees: a mini-review. *Front. Plant Sci.* 9:1394. doi: 10.3389/fpls.2018.01394

Wisniewski, M., Nassuth, A., Teulières, C., Marque, C., Rowland, J., Cao, P. B., et al. (2014). Genomics of cold hardiness in woody plants. *CRC. Crit. Rev. Plant Sci.* 33, 92–124. doi: 10.1080/07352689.2014.870408

Wisniewski, M., Norelli, J., and Artlip, T. (2015). Overexpression of a peach CBF gene in apple: a model for understanding the integration of growth, dormancy, and cold hardiness in woody plants. *Front. Plant Sci.* 6:85. doi: 10.3389/fpls.2015.00085

Wisniewski, M., Webb, R., Balsamo, R., Close, T. J., Yu, X.-M., and Griffith, M. (1999). Purification, immunolocalization, cryoprotective, and antifreeze activity of PCA60: A dehydrin from peach (*Prunus persica*). *Physiol. Plant.* 105, 600–608. doi: 10.1034/j.1399-3054.1999.105402.x

Wolkers, W. F., McCready, S., Brandt, W. F., Lindsey, G. G., and Hoekstra, F. A. (2001). Isolation and characterization of a D-7 LEA protein from pollen that stabilizes glasses in vitro. *Biochim. Biophys. Acta – Protein Struct. Mol. Enzymol.* 1544, 196–206. doi: 10.1016/S0167-4838(00)00220-X

Xin, Z., and Browse, J. (2000). Cold comfort farm: The acclimation of plants to freezing temperatures. *Plant Cell Environ.* 23, 893–902. doi: 10.1046/j.1365-3040.2000.00611.x

Yue, C., Cao, H. L., Wang, L., Zhou, Y. H., Huang, Y. T., Hao, X. Y., et al. (2015). Effects of cold acclimation on sugar metabolism and sugar-related gene expression in tea plant during the winter season. *Plant Mol. Biol.* 88, 591–608. doi: 10.1007/s11103-015-0345-7

Conflict of Interest: The authors declare that the research was conducted in the absence of any commercial or financial relationships that could be construed as a potential conflict of interest.

frontiers in Plant Science

ORIGINAL RESEARCH
published: 26 May 2020
doi: 10.3389/fpls.2020.00511

Blue Light Improves Vase Life of Carnation Cut Flowers Through Its Effect on the Antioxidant Defense System

Mostafa Aalifar[1], Sasan Aliniaeifard[1], Mostafa Arab[1], Mahboobeh Zare Mehrjerdi[1], Shirin Dianati Daylami[1], Margrethe Serek[2], Ernst Woltering[3,4] and Tao Li[5]**

[1] Photosynthesis Laboratory, Department of Horticulture, Aburaihan Campus, University of Tehran, Tehran, Iran, [2] Faculty of Natural Sciences, Institute of Horticultural Production Systems, Floriculture, Leibniz University Hannover, Hannover, Germany, [3] Wageningen Food & Biobased Research, Wageningen, Netherlands, [4] Horticulture and Product Physiology, Wageningen University & Research, Wageningen, Netherlands, [5] Institute of Environment and Sustainable Development in Agriculture, Chinese Academy of Agricultural Sciences, Beijing, China

OPEN ACCESS

Edited by:
Patrícia Duarte De Oliveira Paiva, Federal University of Lavras, Brazil

Reviewed by:
Chao Ma, China Agricultural University, China
Roberta Paradiso, University of Naples Federico II, Italy

***Correspondence:**
Sasan Aliniaeifard
aliniaeifard@ut.ac.ir
Tao Li
litao06@caas.cn

Specialty section:
This article was submitted to Crop and Product Physiology, a section of the journal Frontiers in Plant Science

Received: *18 December 2019*
Accepted: *06 April 2020*
Published: *26 May 2020*

Citation:
Aalifar M, Aliniaeifard S, Arab M, Zare Mehrjerdi M, Dianati Daylami S, Serek M, Woltering E and Li T (2020) Blue Light Improves Vase Life of Carnation Cut Flowers Through Its Effect on the Antioxidant Defense System. Front. Plant Sci. 11:511. doi: 10.3389/fpls.2020.00511

Improving marketability and extension of vase life of cut flowers has practical significance for the development of the cut flower industry. Although considerable efforts have been made over many years to improve the vase life of cut flowers through controlling the immediate environment and through post-harvest use of floral preservatives, the impact of lighting environment on vase life has been largely overlooked. In the current study, the effect of three LED light spectra [white (400–730 nm), blue (peak at 460 nm), and red (peak at 660 nm)] at 150 μmol m^{-2} s^{-1} on vase life and on physiological and biochemical characteristics of carnation cut flowers was investigated. Exposure to blue light (BL) considerably delayed senescence and improved vase life over that of flowers exposed to red light (RL) and white light (WL). H_2O_2 and malondialdehyde (MDA) contents in petals gradually increased during vase life; the increase was lowest in BL-exposed flowers. As a consequence, BL-exposed flowers maintained a higher membrane stability index (MSI) compared to RL- and WL-exposed flowers. A higher activity of antioxidant enzymes [superoxide dismutase (SOD), peroxidase (POD), catalase (CAT), and ascorbate peroxidase (APX)] was detected in petals of BL-exposed flowers, compared to their activities in RL- and WL-exposed flowers. In BL-exposed flowers, the decline in petal carotenoid contents was delayed in comparison to RL- and WL-exposed flowers. Maximum quantum efficiency of photosystem II (Fv/Fm) and a higher percentage of open stomata were observed in leaves of BL-exposed flowers. Sucrose and glucose contents accumulated in petals during vase life; sugar concentrations were higher in BL-exposed flowers than in RL- and WL-exposed flowers. It is concluded that BL exposure improves the vase life of carnation cut flowers through its effect on the antioxidant defense system in petals and on photosynthetic performance in the leaves.

Keywords: antioxidant enzymes, carnation, light spectrum, oxidative stress, radiation, vase life

INTRODUCTION

Ornamental plant production is an expanding industry worldwide and has great potential for continued future growth in international markets (Jerzy et al., 2011). However, cut flowers generally have a short vase life depending on genetic and environmental factors, and this often limits development of the industry (Kumar et al., 2014; Van Meeteren and Aliniaeifard, 2016). Carnation (*Dianthus caryophyllus* L.) is one of the most popular and important of cut flowers for the ornamental industry, also useful as an ornamental model plant, for which the genome has been sequenced (Karami et al., 2008; Yagi et al., 2013). Normally carnations have a short vase life of around 5–10 days depending on the cultivar.

Post-harvest senescence of cut flowers is an active process involving physiological and biochemical changes (Buchanan-Wollaston and Morris, 2000; Rubinstein, 2000; Battelli et al., 2011), and is regulated by a cell death program (Arora and Singh, 2006; Van Doorn and Woltering, 2008; Wagstaff et al., 2009; Van Doorn, 2011). Physiological and biochemical aspects of carnation senescence have previously been described (Sugawara et al., 2002; Shibuya and Ichimura, 2010; Satoh, 2011), and conditions during growth of mother plants, storage and handling, environment, and phyto-hormones all play roles in senescence regulation (Karimi et al., 2012; Asil et al., 2013; Hotta et al., 2016). Particularly since it is a model flower, the mechanisms involved in vase life determination have attracted much interest (Sugawara et al., 2002; Tanase et al., 2008; Satoh, 2011; Tanase et al., 2015).

In recent years considerable efforts have been made to improve vase life of cut flowers through controlling the post-harvest environment; however, the influence of lighting environment on vase life has largely been overlooked. Light is one of the most influential and versatile of environmental stimuli controlling plant life from seed germination to plant senescence (Rodrigues et al., 2014). Some studies have shown that light delays senescence during post-harvest storage of some horticultural products such as basil (Costa et al., 2013), broccoli (Zhan et al., 2012), spinach (Lester et al., 2010), mushrooms (Oms-Oliu et al., 2010), and cabbage (Perrin, 1982). However, both negative and positive effects of different light spectra on the post-harvest longevity of horticultural products such as tomato, asparagus, strawberry, broccoli, peach, lettuce, and pot *Chrysanthemum* have been reported (Jerzy et al., 2011; Dhakal and Baek, 2014; Woltering and Seifu, 2014; Xu et al., 2014; Gong et al., 2015; Hasperué et al., 2016a,b; Mastropasqua et al., 2016). To date, the effects of light spectra on post-harvest performance of cut flowers have not been studied in detail and the mechanisms underlying the responses to different spectra remain largely unknown.

Photosynthesis is the main process providing energy input for growth and development. Previous studies have reported that plants grown under blue light (BL) are characterized by higher photosynthetic electron transport and chlorophyll a/b ratios than plants grown under red light (RL) (Eskins et al., 1991). Zheng and Van Labeke (2017a,b), demonstrated that BL resulted in the highest maximum quantum efficiency (Φ_{PSII}) and quantum yield (F_v/F_m) in *Cordyline australis*, *Ficus benjamina*, *Sinningia speciosa,* and *Chrysanthemum morifolium*. However, knowledge about the effects of the lighting environment on photosynthesis of leaves of cut flowers and the subsequent importance of photosynthetic performance on vase life is largely unknown.

Oxidative stress plays a key role in cut flower senescence. Several reports have shown that different light spectra strongly affect the activity of antioxidant systems in different plant species such as *Solanum lycopersicum* (Kim et al., 2013), *Kalanchoe pinnata* (Nascimento et al., 2013), *Fragaria ananassa* (Xu et al., 2014), *Brassica oleracea* (Deng et al., 2017), and *Camptotheca acuminata* (Yu et al., 2017). These studies revealed that an enhanced antioxidant system improves post-harvest longevity of these products (Xu et al., 2014; Deng et al., 2017). Therefore, studying the antioxidant defense system during post-harvest assessment of horticultural products will help advance our knowledge of the regulatory role of environmental cues on the vase life of cut flowers.

Only one report, Jerzy et al. (2011), studied the effects of different light spectra on post-harvest longevity of pot *Chrysanthemum,* and the literature concerning the effect of light spectra on cut flower vase life, and the underlying response mechanisms, are scarce. Therefore, the purpose of this study was to explore the effects of light spectra on the vase life of carnation flowers and to investigate the underlying mechanisms determining their vase life.

MATERIALS AND METHODS

Plant Materials and Growth Conditions

Cut flowers of a standard type of carnation (*Dianthus caryophyllus* cv. 'Moon light') (40–45 cm in length) were obtained from a commercial greenhouse in the early morning. Healthy flowers were harvested at the commercial stage of flower development, described as 'fully open,' when the outer petals were reflected at right angles to the pedicel and the inner ones were relatively small and immature (Nichols and Ho, 1975). The stems were placed in tap water and the end of each stem was re-cut under water to 30 cm to allow for water uptake by the vessel elements of the stem. Thereafter, 12 replicates per treatment were randomly allocated to three spectral light treatments. Air temperature of the test room was set at 21 ± 2°C and flowers received a photoperiod of 12/12 h light/dark cycles.

Light Treatments

For applying light treatments, LED modules (Iran grow light, Tehran, Iran) were placed in the top of chambers (120 cm × 90 cm × 80 cm). Three light spectra consisting of red (R; peak at 660 nm), blue (B; peak at 460 nm), and white (W; 400–730 nm) were used in the chambers without any other illumination sources. Light intensity at the flower level was set at 150 μmol m^{-2} s^{-1} by adjusting the distance of the light source. Light spectral distribution was measured using a Sekonic C7000 SpectroMaster spectrometer (Sekonic, Corp., Tokyo, Japan) in the range of 300–800 nm (**Figure 1**) and uniformity was verified by measuring the light intensity at five points of each light treatment at the flower level.

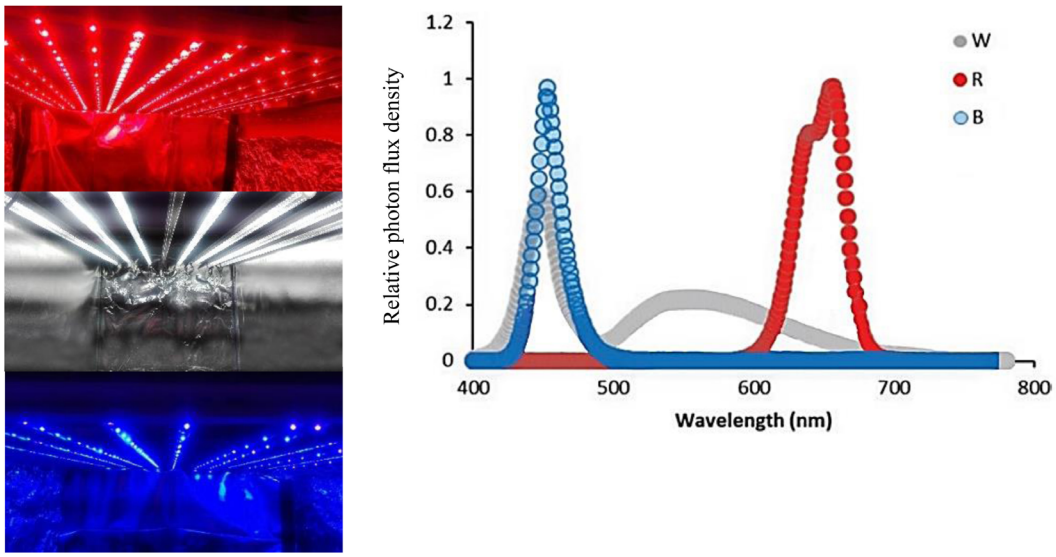

FIGURE 1 | Light spectra of the white (W), red (R), and blue (B) lighting environments measured at the flower level in the cabinets.

Vase Life

The degree of flower wilting and vase life of flowers was determined according to the morphological stages (Paulin et al., 1986) and appearance of symptoms such as shrinkage, brown edges, wilting stems, and yellow/brown foliage (VBN, 2005). The petals were judged to have senesced when they wilted or became necrotic at the edges (Mor et al., 1980). Vase life of individual flowers was defined by the duration from the starting time to the occurrence of flower wilting (Yamamoto et al., 1992).

Relative Fresh Weight (RFW) and Water Uptake

Flower stems were daily weighed and the following formula was used to measure relative fresh weight:

$$\mathrm{RFW}(\%) = \frac{(\text{Fresh weight of flower during vase stage} - \text{Fresh weight of flower at day 0})}{\text{Fresh weight of flower at day 0}} \times 100 \quad (1)$$

Flower weight was determined at time 0 and at 2, 4, 6, 8, 10, 12, and 15 days following onset of the trial (Zeng et al., 2011). Flowers were placed in 300 mL of tap water. At the different time points, the amount of water (mL) taken up was measured and thereafter the level was brought back up again to 300 mL. At the end of the trial, cumulative water uptake was calculated.

Malondialdehyde (MDA) and Hydrogen Peroxide (H_2O_2) Contents

Malondialdehyde (MDA) and H_2O_2 were measured as indices of lipid peroxidation and oxidative stress. The petals of flowers were collected and ground in liquid nitrogen and then homogenized in 4% ice-cold trichloroacetic acid (TCA). The homogeneous samples were then centrifuged at 13,000 *g* for 15 min at 5°C. The supernatants were used for the measurement of MDA (Heath and Parker, 1968) and H_2O_2 (Guo et al., 2006) contents. Absorbance was spectrophotometrically (Lambda 25 UV/VIS) measured at 532 and 500 nm for H_2O_2 and MDA, respectively. The MDA and H_2O_2 were expressed as μmol g^{-1} on a fresh weight basis.

Petal Membrane Stability Index (MSI)

For determining petal membrane stability, two samples of plant material (15 disks of petals) were prepared and dipped in 10 mL double distilled water. One of them was kept at 40°C for 30 min and its electrical conductivity (EC) was measured (EC1). The second sample was kept in a boiling water bath (100°C) for 10 min, cooled to room temperature, and EC also recorded (EC2). MSI was determined according to Sairam et al. (1997) based on the following equation:

$$\mathrm{MSI}(\%) = \left[1 - \left(\frac{\mathrm{EC1}}{\mathrm{EC2}}\right)\right] \times 100$$

Measurement of Carbohydrate Levels

Samples from petals were collected during the vase life of flowers (0, 8, 10, and 15 days following start of the trial) and immediately frozen in liquid nitrogen then stored at −80°C. Sugars (sucrose and glucose) and starch were determined by enzymatic assays according to Trethewey et al. (1998) and Hajirezaei et al. (2000). Concentrations of sucrose and glucose were determined in microplates via NADH-specific extinction at 340 nm. The results were expressed as μmol g^{-1} on a fresh weight basis.

Pigment Analysis

Carotenoids were determined by extraction in 80% acetone as described by Lichtenthaler and Buschmann (2001). Their absorbance was recorded at 470 nm with a spectrophotometer (Lambda 25 UV/VIS) according to Lichtenthaler and Buschmann

(2001). The entire process was conducted in low light conditions and placing the samples on ice, and the results expressed as mg g^{-1} on a fresh weight basis.

Determination of Antioxidant Enzyme Activity

Frozen petal samples (0.2 g for each replicate) were ground in 5 mL of 50 mM sodium phosphate-buffer (pH 7.8) at 4°C. Samples were centrifuged at 13,000 *g* for 20 min and the supernatant was used to measure the activity of antioxidant enzymes. The 3-mL reaction solution for SOD contained 63 μM ρ-nitro blue tetrazolium chloride, 1.3 μM riboflavin, 13 μM methionine, 50 mM phosphate buffer (pH 7.8), and enzyme extract. Absorbance was measured at 560 nm with a spectrophotometer (Lambda 25 UV/VIS). The 3-mL reaction solution for CAT contained 50 mM phosphate buffer (pH 7.0), 15 mM H_2O_2, and 50 μl of enzyme extract. The reaction was initiated by adding enzyme extract. The decrease of absorbance of H_2O_2 over 1 min at 240 nm was recorded. The 3-mL reaction solution for APX contained 0.5 mM AsA, 0.1 mM H_2O_2, 50 mM phosphate buffer (pH 7.0) and 0.1 mL enzyme extract. APX activity was evaluated by following the decrease in absorbance of AsA over 1 min at 290 nm. The 3-mL reaction solution for POX contained 0.2% (w/v) *o*-dianisidine, 0.1M potassium phosphate buffer (pH 7.8) and the enzyme extract. Absorbance was measured at 470 nm (Han et al., 2008; Chen et al., 2009). The results were expressed as μmol min^{-1} mg^{-1} of total protein for CAT, APX and POD and U mg^{-1} for SOD.

Stomatal Opening and Polyphasic Chlorophyll a Florescence (OJIP)

On the 8th day of vase life at 2 h after exposure to different light treatments, stomatal opening was determined using a nail polish replica method on the lower epidermis of the second lateral leaflets from the apex (abaxial side) as described by Aliniaeifard and Van Meeteren (2016). The nail polish layer was separated with a strip of transparent sticky tape and pasted on a glass slide and observed using a light microscope (BH-323, Olympus, Tokyo, Japan). Pore aperture of more than 6 μm was considered as open stomata, less than 3 μm as closed, and between 3 and 6 μm as semi-closed. The polyphasic chlorophyll a fluorescence (OJIP) transients were determined using a Fluorpen FP 100-MAX (Photon Systems Instruments, Drásov, Czechia) on young fully expanded carnation leaves after 20 min dark adaptation (Strasser , and Strasser, 1995) according to the JIP test (Strasser et al., 2000) at 1, 4, 8, and 12 days following onset of the trial. The measurement of transient fluorescence was induced by a saturating light of 3000 μmol m^{-2} s^{-1} PPFD. Three leaves of each cut carnation stem were used for each replicate. The parameters obtained from this protocol were calculated according to Kalhor et al. (2018).

Statistical Analysis

The data were statistically evaluated by the 'completely randomized design' method using SAS software (Statistical Analysis System, version 9). Means were separated using the Duncan Multiple Range test at a significance level of 0.01. Three (for all measurements traits except vase life) or nine (vase life) replicates were considered for each treatment. A pooled sample of outer and inner petals from each cut carnation flowers was used for measurements of biochemical traits for each replicate. In **Figures 3–8**, the measurements were conducted up until the end of vase life.

RESULTS

Blue Light Improves the Vase Life of Carnation Cut Flowers

The vase life of flowers was significantly ($P > 0.01$) prolonged by exposure to B spectral light. The vase life of BL-exposed flowers was 5 days longer than the vase life of WL-exposed flowers (**Figures 2**, **3**). Exposure to RL shortened the vase life of flowers in comparison with WL exposure (**Figures 2**, **3**). Exposure to BL approximately doubled the vase life compared

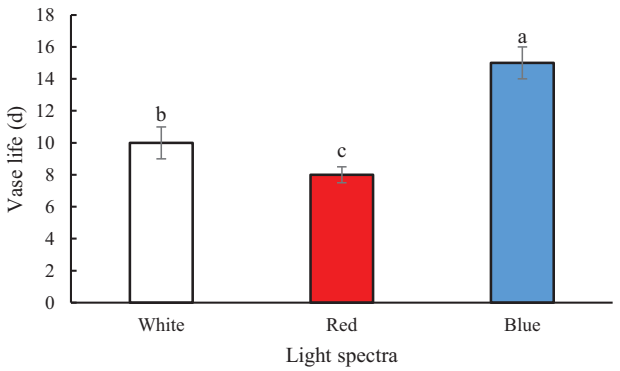

FIGURE 2 | Effects of light spectra on the vase life of carnation cut flowers. Averages ± SEM ($n = 9$) are shown. Cut flowers were placed in cabinets (120 cm × 90 cm × 80 cm) with different light spectra (white, red, or blue light). Light intensity at the flower level was set at 150 μmol m^{-2} s^{-1}. Air temperature of the test room was set at 21 ± 2°C and flowers received a photoperiod of 12/12 h light/dark cycles. Different letters indicate that values are significantly different at $P < 0.01$ according to Duncan's multiple range tests.

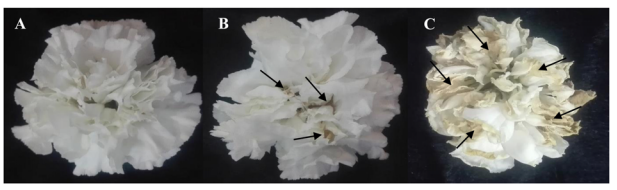

FIGURE 3 | Effects of light spectra (**A**; blue light, **B**; white light, and **C**; red light) on vase life of carnation cut flowers on the 10th day of vase life. Cut flowers were placed in cabinets (120 cm × 90 cm × 80 cm) with different light spectra (white, red, or blue light). Light intensity at the flower level was set at 150 μmol m^{-2} s^{-1}. Air temperature of the test room was set at 21 ± 2°C and flowers received a photoperiod of 12/12 h light/dark cycles. The arrows indicate areas that are turning yellow and brown.

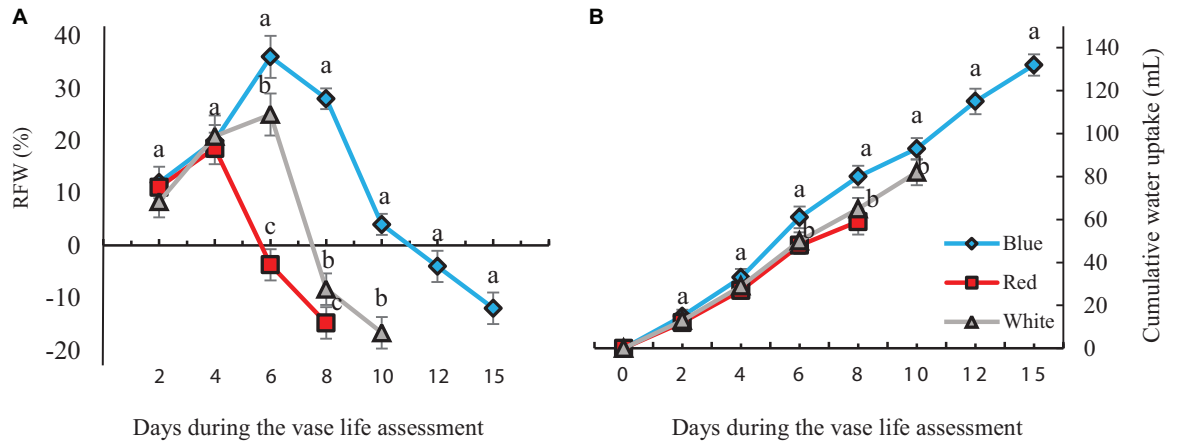

FIGURE 4 | Effects of different light spectra (blue, red, and white) on the relative fresh weight [RFW, **(A)**] and cumulative water uptake **(B)** of carnation cut flowers during storage. Cut flowers were placed in cabinets (120 cm × 90 cm × 80 cm) with different light spectra (white, red, or blue light). Light intensity at the flower level was set at 150 μmol m^{-2} s^{-1}. Air temperature of the test room was set at 21 ± 2°C and flowers received a photoperiod of 12/12 h light/dark cycles. Averages ± SEM (n = 3) are presented. Different letters indicate that values are significantly different at $P < 0.01$ according to Duncan's multiple range tests.

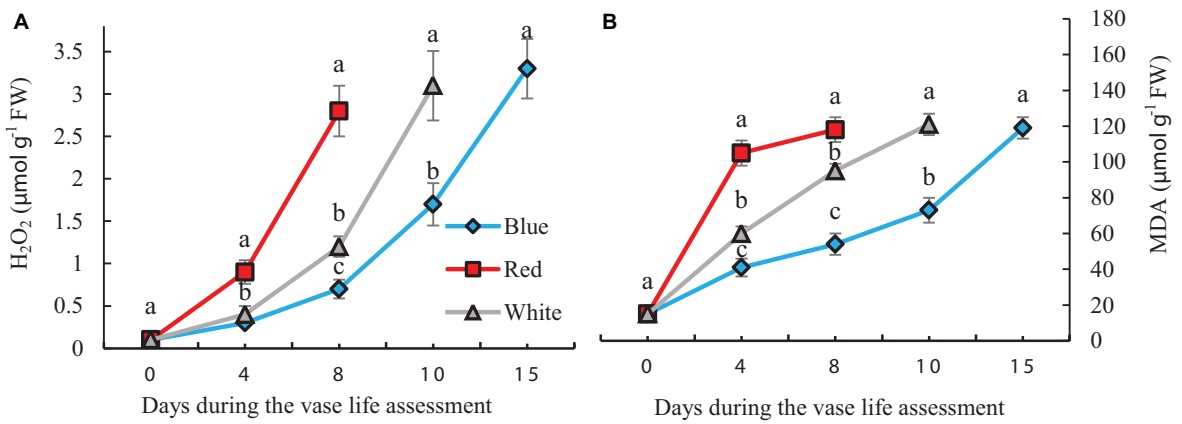

FIGURE 5 | Effects of different light spectra on H_2O_2 **(A)** and Malondialdehyde (MDA) **(B)** contents in the petals of carnation cut flowers during vase life. Cut flowers were placed in cabinets (120 cm × 90 cm × 80 cm) with different light spectra (white, red, or blue light). Light intensity at the flower level was set at 150 μmol m^{-2} s^{-1}. Air temperature of the test room was set at 21 ± 2°CC and flowers received a photoperiod of 12/12 h light/dark cycles. Means ± SEM are presented (n = 3). Different letters indicate that values are significantly different at $P < 0.01$ according to Duncan's multiple range tests.

to RL exposure (**Figures 2**, **3**). These results are indicative of positive effects of B wavelength on the post-harvest performance of carnation flowers.

Relative Fresh Weight (RFW) and Water Uptake of Cut Flowers

The RFW of flowers increased till day 4 of vase life in RL-exposed flowers and till day 6 of BL- and WL-exposed flowers, and decreased thereafter (**Figure 4**). There was no distinct difference in RFW among the light treatments during the first 4 days. On the 6th day of vase life, the RFW of RL-exposed flowers was three and four times lower than that of WL- and BL-exposed flowers. Following day 6 till the end of vase life assessment, RFW of BL-exposed flowers was significantly higher than the RFW of flowers exposed to other light spectra (**Figure 4**).

The highest and lowest water uptake was found in BL- and RL-exposed flowers, respectively. At the end of these measurements, the cumulative water uptake of BL-exposed flowers was 30 and 18% more than that of RL- and WL-exposed flowers. These results indicate that exposure to BL significantly improves water uptake and postpones weight loss of flowers during their vase life.

Blue Light Delays and Reduces Severity of Oxidative Damage to Carnation Petals

H_2O_2 and MDA contents were measured to assess the oxidative damage to the petals. H_2O_2 gradually accumulated in the carnation petals during vase life. BL significantly reduced the concentration of H_2O_2 by 35, 25, and 42% on days 4, 8, and 10, respectively, compared to the concentration of H_2O_2 in WL-exposed flowers (**Figure 5A**). In petals of

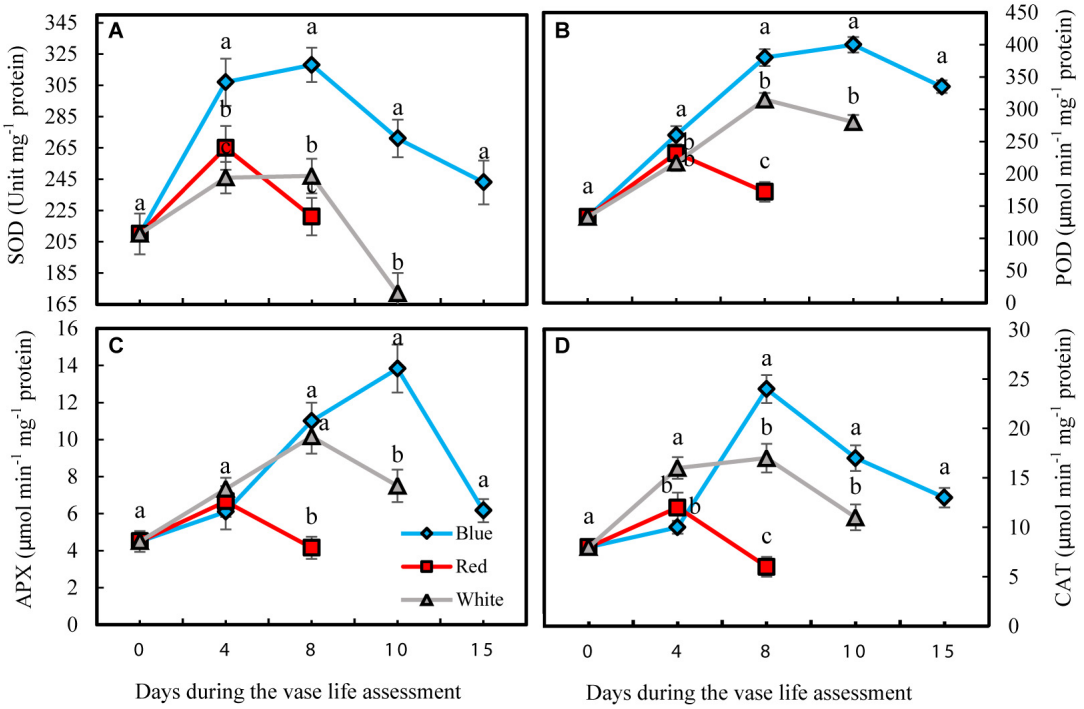

FIGURE 6 | Effects of light spectra on the antioxidant enzymes activity during vase life in cut carnation flower petals. Cut flowers were placed in cabinets (120 cm × 90 cm × 80 cm) with different light spectra (white, red, or blue light). Light intensity at the flower level was set at 150 µmol m^{-2} s^{-1}. Air temperature of the test room was set at 21 ± 2°C and flowers received a photoperiod of 12/12 h light/dark cycles. **(A)** Superoxide dismutase (SOD); **(B)** Peroxidase (POD); **(C)** Ascorbate peroxidase (APX), and **(D)** Catalase (CAT). Means ± SEM are presented (n = 3). Different letters indicate that values are significantly different at $P < 0.01$ according to Duncan's multiple range tests.

RL-exposed flowers, concentrations of H_2O_2 showed an earlier increase than with the other light spectra. On the 8th day of vase life, H_2O_2 content in RL-exposed flowers was four times higher than in BL-exposed flowers. Similar to H_2O_2, MDA content also gradually accumulated in the carnation petals during vase life. Exposure to BL caused reductions in MDA contents during the whole vase life assessment period compared to the MDA content of RL- and WL-exposed flowers. MDA content in RL-exposed flowers was approximately doubled in comparison with BL-exposed flowers during vase life (**Figure 5B**). These results indicate that post-harvest application of BL can decrease the severity of oxidative damage to carnation petals.

Blue Light Enhances Antioxidant Enzyme Activities in the Petals of Carnation Cut Flowers

Antioxidant enzyme activities in petals were significantly influenced by light spectra during vase life. Activity of antioxidant enzymes was divided into two phases for all the flowers that were exposed to different light spectra; in the first phase there was an induction in the activity of antioxidant enzymes, and in the second phase their activities declined (**Figure 6**). For the RL-exposed flowers, activities of antioxidant enzymes reached their maximum levels at an earlier time than the BL- and WL-exposed flowers. The magnitude of increase in antioxidant enzyme activities in BL-exposed flowers was significantly greater than the amplification of enzyme activity in RL- and WL-exposed flowers. In the case of SOD, its activity in BL-exposed flowers was always higher than its activity in RL- and WL-exposed flowers following the start of vase life (**Figure 6A**). After 4 days, POD activity in BL-exposed flowers was higher than in RL- and WL-exposed flowers (**Figure 6B**). APX and CAT activities in RL-exposed flowers at the last day of vase life were lower than initial activities, while the activity of these enzymes were more than doubled or tripled in their maximum activities in WL- and BL-exposed flowers, respectively (**Figures 6C,D**). These results indicate that BL is an environmental signal that results in augmentation of petal antioxidant enzyme activities.

Blue Light Maintains Membrane Stability Index (MSI) During Vase Life of Carnation

On the 8th day of vase life assessment, BL- and WL-exposed flowers had significantly ($P < 0.01$) higher petal MSI than in the petals of RL-exposed flowers (**Figure 7**). On the 10th day, the highest MSI (87%) was detected in BL-exposed flowers, significantly higher than the MSI of WL-exposed flowers (58%). On the 15th day when petals of RL- and WL-exposed flowers were wilted, BL-exposed flowers retained 61%

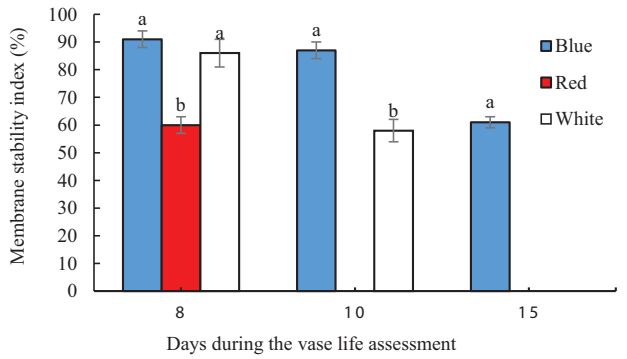

FIGURE 7 | Effects of light spectra on petal membrane stability index (MSI) of carnation cut flowers during vase life. Cut flowers were placed in cabinets (120 cm × 90 cm × 80 cm) with different light spectra (white, red, or blue light). Light intensity at the flower level was set at 150 μmol m^{-2} s^{-1}. Air temperature of the test room was set at 21 ± 2°C and flowers received a photoperiod of 12/12 h light/dark cycles. Means ± SEM are presented (n = 3). Different letters indicate that values are significantly different at $P < 0.01$ according to Duncan's multiple range tests.

MSI in their petals (**Figure 7**). These results indicate that BL maintains the stability of the petals during storage and delays senescence.

Blue Light and Duration of Storage Increase Petal Carbohydrate Content

Carbohydrate status of the petals was largely influenced by exposure of flowers to different light spectra. Concentrations of sucrose and glucose and starch were determined during the vase life in the petals of cut carnation flowers under different light spectra. The starch level in the petals invariably remained below the detection limit of 0.5 μmol g^{-1} FW (data not shown).

Petals had lower sucrose levels compared to glucose under all different light spectra (**Figure 8**). Concentrations of both glucose and sucrose increased over the whole vase life period in flowers under all light spectra (**Figures 8A,B**). Concentrations of both glucose and sucrose were higher in the petals of BL-exposed flowers in comparison with their concentrations in WL and RL-exposed flowers during all stages of vase life (**Figures 8A,B**). At day 15, sugar levels in petals of BL-exposed flowers were 2.5 times more than their initial levels and were doubled compared to their levels in RL-exposed flowers on the last day of their vase life (8 and 10 days from onset of experiment).

Effect of Light Spectra on the Concentration of Carotenoids in Flowers

Significant differences were observed in concentrations of carotenoids during the vase life of flowers exposed to different light spectra. The concentrations gradually decreased during the vase life in all treatments; however the extent of this decline was highest in RL-exposed flowers (**Figure 9**). Under exposure to BL and WL, the decreases in carotenoid contents were less pronounced compared to their contents under RL (**Figure 9**). These results showed the negative role of RL in maintaining carotenoids of carnation petals.

Stomatal Status and Photosynthetic Biophysical Analysis in Leaves

Stomatal status in the leaves of carnation cut flowers was affected by light spectra (**Table 1**). A higher percentage of fully open stomata was observed on the leaves of BL-exposed flowers (95%) than in the RL-exposed flowers (0%) (**Table 1**). WL-exposed flowers showed a high percentage of semi-closed stomata (80%) (**Table 1**).

At the 1st day of the vase life, there was no difference among Fv/Fm in leaves of flowers under different light spectra

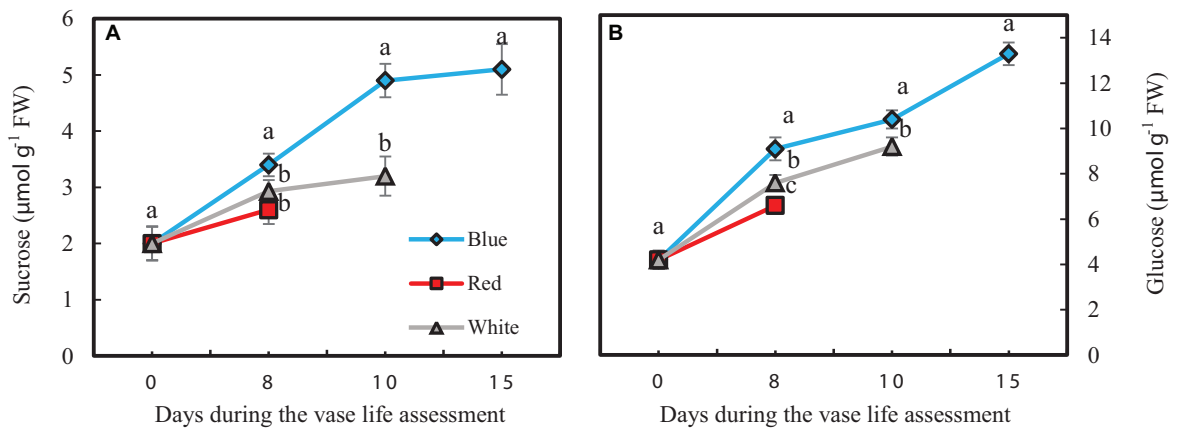

FIGURE 8 | Effects of different light spectra on the content of sucrose **(A)** and glucose **(B)** in the petals of carnation cut flowers during vase life. Cut flowers were placed in cabinets (120 cm × 90 cm × 80 cm) with different light spectra (white, red, or blue light). Light intensity at the flower level was set at 150 μmol m^{-2} s^{-1}. Air temperature of the test room was set at 21 ± 2°C and flowers received a photoperiod of 12/12 h light/dark cycles. Means ± SEM are presented (n = 3). Different letters indicate that values are significantly different at $P < 0.01$ according to Duncan's multiple range tests.

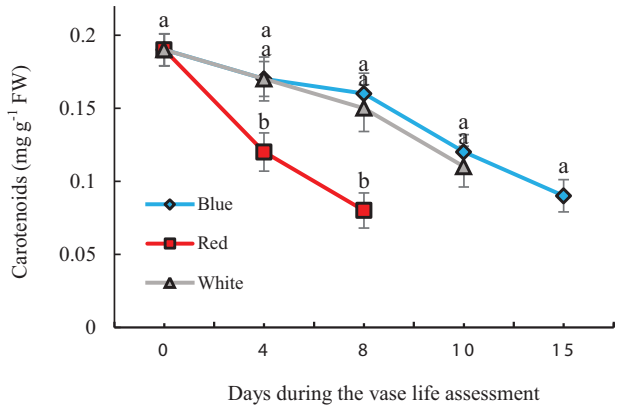

FIGURE 9 | Effects of different light spectra on the content of carotenoids in cut carnation flower. Cut flowers were placed in cabinets (120 cm × 90 cm × 80 cm) with different light spectra (white, red, or blue light). Light intensity at the flower level was set at 150 μmol m^{-2} s^{-1}. Air temperature of the test room was set at 21 ± 2°C and flowers received a photoperiod of 12/12 h light/dark cycles. Means ± SEM are presented (n = 3). Different letters indicate that values are significantly different at $P < 0.01$ according to Duncan's multiple range tests.

TABLE 1 | Percentage of open, closed, and semi-closed stomata in the leaves of carnation cut flowers following 8 days of exposure to different light spectra.

Light spectra	Stomatal status		
	Open	Closed	Semi-closed
Blue	95^{a}	0^{c}	5^{b}
White	5^{b}	15^{b}	80^{a}
Red	0^{c}	100^{a}	0^{c}

Pore aperture more than 6 μm was considered as open stomata, less than 3 μm as closed, and between 3 and 6 μm as semi-closed. Twenty stomata (n = 20) from three leaves were considered for each replicate. Sampling was done at 2 h after exposure to different light treatments. Letters indicate that values significantly different at P < 0.01 according to Duncan's multiple range tests.

(**Figure 10A**). Fv/Fm of RL-exposed flowers significantly decreased during vase life, while no significant difference was observed for Fv/Fm of BL- and WL-exposed flowers. At day 12 of vase life, the highest and lowest F_v/F_m was detected in BL- and RL-exposed flowers, respectively (**Figure 10A**). The specific energy fluxes per reaction center (RC) for energy absorption (ABS/RC), dissipated energy flux (DI_0/RC) and trapped energy flux (TR_0/RC) increased but performance index on the absorption basis (PI/ABS) and electron transport flux (ET_0/RC) decreased during vase life for flowers under all light spectra (**Figure 10**). At day 12, highest ABS/RC, DI_0/RC and TR_0/RC and lowest PI/ABS and ET_0/RC were detected in RL-exposed flowers, while no significant difference was detected for these parameters between BL- and WL-exposed flowers (**Figure 10**). These results are indicative of the negative impact of RL on the photosynthetic performance of carnation leaves.

DISCUSSION

Petal senescence is a major physiological process that influences quality attributes and limits vase life of cut flowers (Kumar et al., 2014). Post-harvest application of light spectra on vegetable and fruit has attracted much attention in recent times (Dhakal and Baek, 2014; Gong et al., 2015; Hasperué et al., 2016a,b), with some studies showing beneficial effects of light on vase life of hyacinth (Krzymińska and Karasiewicz, 2017) and pot chrysanthemums (Jerzy et al., 2011). Information regarding the role of different light spectra on vase life of cut flowers is scarce however. In the present study, we exposed carnation cut flowers during vase life to 150 μmol m^{-2} s^{-1} of white, blue or red light derived from LEDs for 12 h per day. BL significantly delayed flower senescence and therefore extended vase life.

Senescence of petals in cut flowers is related to a series of highly regulated biochemical and physiological processes. The maintenance of water relations and good water uptake are among the most important factors for the vase life of a variety of cut flowers (Slootwet, 1995; Van Meeteren and Aliniaeifard, 2016). Adverse water relations can lead to problems in flower opening, premature petal wilting and bending of the pedicel, all resulting in shortened vase life (Yamada et al., 2007; Aliniaeifard and Van Meeteren, 2016). It is well-recognized that light spectra are involved in stomatal movement and that BL stimulates stomatal opening (Noichinda et al., 2007). Therefore BL might increase water transport efficiency by increasing transpiration rate and water uptake. Unlike vegetables and fruit (Xu et al., 2014; Hasperué et al., 2016b; Van Meeteren and Aliniaeifard, 2016), elevated water uptake, higher transpiration rates and water loss are beneficial for cut flowers placed in water (Elibox and Umaharan, 2010; Lu et al., 2010). Findings of the present study confirmed that the openness of stomata in the BL treatment coincided with an improved vase life of flowers, increased water uptake, transpiration rate and fresh weight.

Blue light improved carbohydrate levels in the petals during vase life (**Figure 6**). Sugars are the major source of energy and their deficiency results in senescence of cut flowers (Liao et al., 2000; Singh et al., 2008). Sucrose and glucose are involved in diverse plant processes including antioxidant metabolism, anthocyanin biosynthesis and storage and cell wall biosynthesis. It has been reported that higher amount of sugars in petals is associated with a delay in the senescence of cut flowers (Solfanelli et al., 2006; Agulló-Antón et al., 2011). The starch content in the carnation petals was very low (below the detection limit of 0.5 μmol g^{-1} FW); similar results have been obtained for the amount of starch in carnation by Agulló-Antón et al. (2011). Change in sugar levels as a result of exposure to different light spectra has been previously reported (Ohashi-Kaneko et al., 2007; Mastropasqua et al., 2016). Light is the driving force of photosynthesis for production of carbohydrates. Influence of light spectrum on the photosynthetic performance of flowers such as roses during cultivation has been recently reported (Bayat et al., 2018). Consistent with our results, Miao et al. (2019) reported that application of BL induced better photosynthetic performance

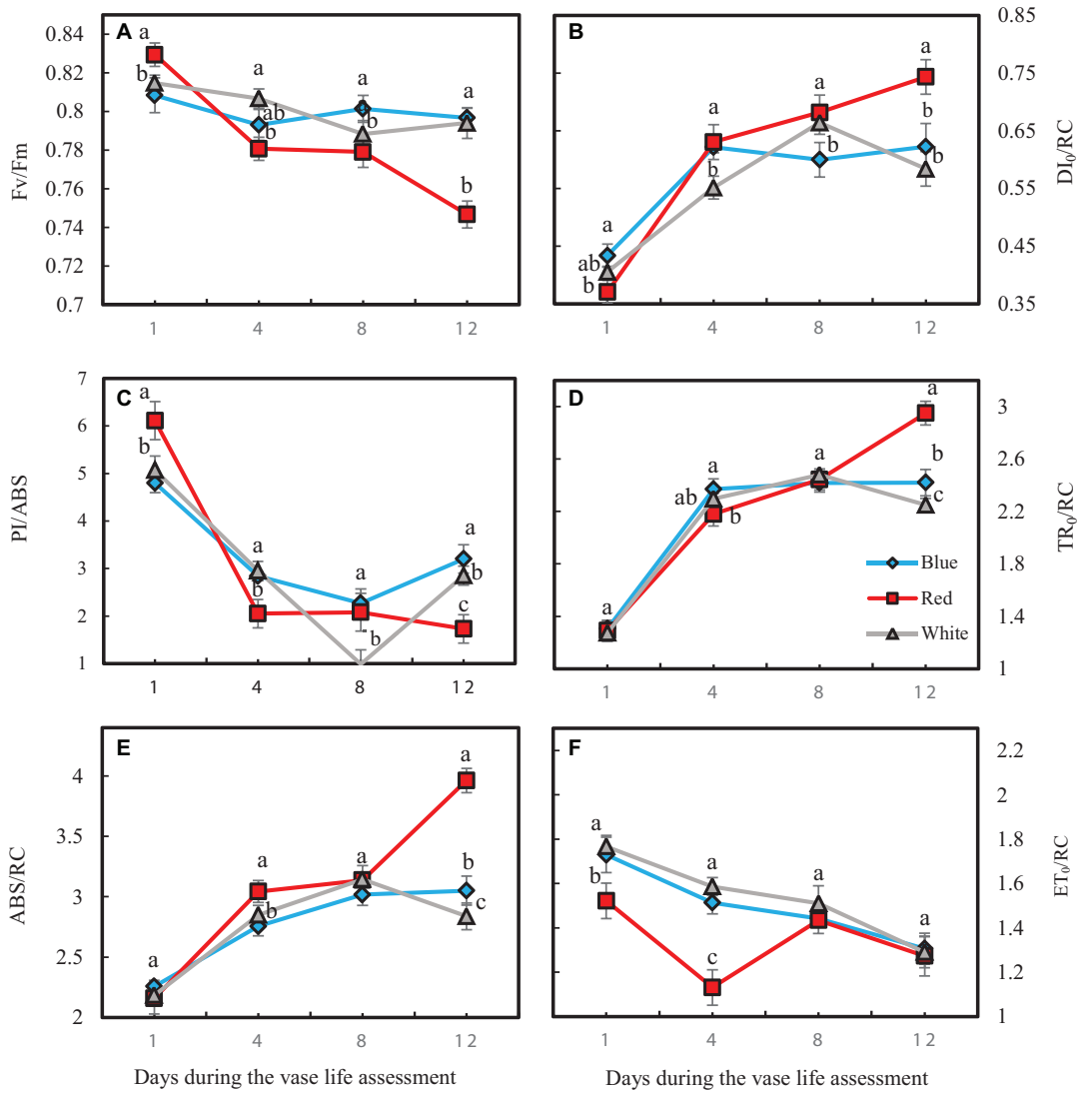

FIGURE 10 | Parameters related to OJIP test including Fv/Fm **(A)**, DI_0/RC **(B)**, PI/ABS **(C)**, TR_0/RC **(D)**, ABS/RC **(E)**, and ET_0/RC **(F)** obtained from the transient florescence exhibited by leaves of carnation. Cut flowers were placed in cabinets (120 cm × 90 cm × 80 cm) with different light spectra (white, red, or blue light). Light intensity at the flower level was set at 150 μmol m^{-2} s^{-1}. Air temperature of the test room was set at 21 ± 2°C and flowers received a photoperiod of 12/12 h light/dark cycles. Means ± SEM are presented (n = 3). Different letters indicate that values are significantly different at $P < 0.01$ according to Duncan's multiple range tests.

than RL in cucumber plants during cultivation. Similar results were also reported for *Chrysanthemum*, *Cordyline australis*, *Ficus benjamina*, and *Sinningia speciosa* during cultivation (Zheng and Van Labeke, 2017a,b). In the current study in carnation, BL (and also WL) maintained a high performance of photosynthesis through limiting energy dissipation and elevating electron transport in the electron transport chain of the photosynthetic apparatus. This consequently resulted in an increase in sugar content from harvest to senescence. Application of ^{14}C-sucrose showed that carnation petals act as a strong sink for absorption of sucrose (Ho and Nichols, 1975; Nichols and Ho, 1975). The significant increase in the sugar content in petals under BL might be correlated with the preserved photosynthetic ability in the leaves (Hogewoning et al., 2010; Muneer et al., 2014; Zheng and Van Labeke, 2017a,b) and translocation of sugars from the leaves toward the petals (Ho and Nichols, 1975), where a significant increase in the two sugars occurred. Nichols and Ho (1975) showed that the sucrose levels decrease during flower senescence in carnation. Decrease in soluble carbohydrate levels is related to lack of a carbohydrate source for cut flowers (Van Geest et al., 2016). It has been reported that carbohydrate levels decrease during vase life of different genotypes of chrysanthemum. However, when the flowers are fed by sucrose the levels of glucose and fructose increase during vase life (Van Geest et al., 2016). In the present experiment, due to presence of light

intensities above the light compensation point, photosynthesis in leaves and calyx may have provided sugars for the flowers (as the main sink of carbohydrates). As a result it led to elevation in glucose and fructose levels during the vase life. The decrease in carbohydrate content in carnation reported by Ho and Nichols (1975) was probably due to light levels below the light compensation point during the vase life study. This indicates that the performance of the photosynthesis system plays an important role in extending vase life of carnation flowers. However, whether photosynthesis-derived carbohydrates directly influence the vase life of cut flowers is a matter for further research.

Oxidative stress was decreased and the antioxidant defense system was augmented in petals as a result of exposure to BL (**Figures 4–6**). The carotenoids are among the most important pigments that take part in antioxidative defense in higher plants (Yu et al., 2017). In the present study, the concentration of carotenoids decreased in flowers under all light spectra, but BL maintained higher carotenoids during vase life (**Figure 9**). Similar results, where application of BL increased the concentration of carotenoids, have been found in lettuce, pepper and broccoli (Li and Kubota, 2009; Gangadhar et al., 2012; Kopsell and Sams, 2013; Hasperué et al., 2016a). These results are similar to those reported by Hasperué et al. (2016a,b); who reported elevated carotenoid levels as a result of BL application as a post-harvest treatment on brussels sprouts and broccoli. It seems that stability and presence of appropriate levels of carotenoids is important to maintain the integrity of membranes, ROS detoxification and other associated physiological processes. Damage to membranes and H_2O_2 accumulation are considered as oxidative damage during senescence processes (Dhindsa et al., 1981; Bayat et al., 2018), and previous studies have shown that ROS accumulation is coincident with flower senescence (Rogers, 2013). Antioxidant enzymes such as SOD, CAT, APX and POD are the most important defense enzymes for detoxification of ROS in plant tissues (Ye et al., 2017). Increase in antioxidant enzymes activity usually helps neutralize the potential harmful effects of photo-oxidative damage to tissues (Lee et al., 2016; Hasan et al., 2017). Elevated antioxidant enzyme activity, and as a consequence, decrease in lipid peroxidation and H_2O_2 content, have been reported in response to BL in vegetables such as lettuce (Johkan et al., 2010), tomato (Kim et al., 2013), Chinese cabbage and kale (Lee et al., 2016). In the present study, SOD and CAT activities were elevated as a result of exposure to BL. Ye et al. (2017) reported higher activity of SOD and CAT in *Anoectochilus roxburghii* leaves with exposure to BL than with exposure to RL. Similar results were also reported for *Rehmannia glutinosa* (Manivannan et al., 2015) and tomato plants (Kim et al., 2013). APX and CAT in the AsA-GSH cycle and also POD enzyme are responsible for the degradation of H_2O_2 generated by SOD in plant cells. We showed that the activity of CAT, APX, and POD had similar patterns of change to that observed for SOD activity in BL-exposed flowers, with higher APX, SOD, POD, and CAT activities during vase life; as a result, they contained lower H_2O_2 in their petals in comparison with RL and WL treatments. This is in line with the findings of Manivannan et al. (2015) and Simlat et al. (2016) who also showed that BL induces activation of the antioxidant defense system in *Rehmannia glutinosa* and *Stevia rebaudiana*. These findings suggest that CAT, APX and POD work in a coordinated manner to scavenge H_2O_2 and that BL might induce their activities. MDA is the product of membrane lipid peroxidation, which is indicative of compromised integrity and structure of the membranes. In line with the other ameliorative effects of BL on oxidative damage, it delayed MDA accumulation in the petals and improved MSI compared to MDA and MSI under other light spectra. This resulted in a decrease in lipid degradation and peroxidation of cell membranes. These results are in accordance with those reported by Xu et al. (2014), who found a postponing effect of BL on MDA content of strawberry fruit during storage.

Of the parameters that were influenced by the light treatments the greatest difference was observed between BL and RL, WL being intermediate or similar to BL. This may be related to the relatively high proportion of B spectrum (41% in the range of 400–500 nm and 18% in the range of 600–700 nm) in the white LEDs. The observed beneficial effects of BL and to a lesser extent WL on, for example, vase life and the antioxidant enzymes, presumably are related to the percentage of BL. However, one could also argue that the lower proportion of RL caused the observed effects.

Carnation vase life is under the influence of ethylene. The longer vase life observed in our experiments under BL may have been due to lower ethylene production, although this was not measured. Light levels and quality can influence ethylene production, but the exact mechanism is still poorly understood. In addition, depending on the tissue under study and the other environmental conditions, light and different wavelengths may either stimulate or reduce ethylene production. There is currently no information available on the effect of light on ethylene production and its signaling pathway in cut flowers, and this would be an interesting topic for further experiments.

CONCLUSION

The most important finding of the present study is that BL has a positive effect on the post-harvest life of carnation at physiological and biochemical levels. Our report on physiological and biochemical changes during vase life of flowers under different light spectra provides valuable information regarding the mechanism underlying the beneficial effects of BL on the determination of vase life. Therefore, management of lighting during post-harvest storage is important for improving vase life of cut carnation flowers. Based on the obtained results, BL boosted the antioxidant defense system in carnation cut flowers. In our experiments, cut flowers were exposed during their vase life to light levels that are well above the levels applied in the consumer's home. Therefore, application of the results would not likely be with the consumer. This intensity of light, however, can be applied during storage and in retail facilities. As well as lower temperatures, a novel display design including LED light of suitable wavelengths and intensity may significantly prolong

the storage or display life of the flowers and may serve as an non-chemical flower preservative.

DATA AVAILABILITY STATEMENT

The datasets generated for this study are available on request to the corresponding author.

AUTHOR CONTRIBUTIONS

MAa, SA, MAr, and MM planned and designed the research, performed the experiments, analyzed the data, and wrote the final version of the manuscript. MS, SD, and EW critically revised the manuscript and edited it to present form. TL helped in providing the materials and critically revised the manuscript. All authors read and approved the final manuscript.

FUNDING

We would like to thank The National Natural Science Foundation of China (No. 31501808), Iran National Science Foundation (INSF) (grant number 96006991) and University of Tehran for their supports.

ACKNOWLEDGMENTS

The authors would like to thank Dr. Ian Ferguson for linguistic editing of the manuscript.

REFERENCES

Agulló-Antón, M. Á., Sánchez-Bravo, J., Acosta, M., and Druege, U. (2011). Auxins or sugars: what makes the difference in the adventitious rooting of stored carnation cuttings? *J. Plant Growth Regul.* 30, 100–113. doi: 10.1007/s00344-010-9174-8

Aliniaeifard, S., and Van Meeteren, U. (2016). Stomatal characteristics and desiccation response of leaves of cut chrysanthemum (*Chrysanthemum morifolium*) flowers grown at high air humidity. *Sci. Hortic.* 205, 84–89. doi: 10.1016/j.scienta.2016.04.025

Arora, A., and Singh, V. P. (2006). Polyols regulate the flower senescence by delaying programmed cell death in Gladiolus. *J. Plant Biochem. Biotechnol.* 15, 139–142. doi: 10.1007/bf03321918

Asil, M. H., Karimi, M., and Zakizadeh, H. (2013). 1-MCP improves the postharvest quality of cut spray carnation (*Dianthus caryophyllus* L.)'Optima'flowers. *Hortic. Environ. Biotechnol.* 54, 58–62. doi: 10.1007/s13580-013-0044-8

Battelli, R., Lomardi, L., Rogers, H. J., Picciarelli, P., Lorenzi, R., and Ceccarelli, N. (2011). Changes in the ultrastructure, protease and caspase-like activities during flower senescence in *Lilium longiflorum*. *Plant Sci.* 180, 716–725. doi: 10.1016/j.plantsci.2011.01.024

Bayat, L., Arab, M., Aliniaeifard, S., Seif, M., Lastochkina, O., and Li, T. (2018). Effects of growth under different light spectra on the subsequent high light tolerance in rose plants. *AoB Plants.* 10:ly052. doi: 10.1093/aobpla/ply052

Buchanan-Wollaston, V., and Morris, K. (2000). "Senescence and cell death in *Brassica napus* and *Arabidopsis*," in *Programmed Cell Death in Animals and Plants*, eds J. A. Bryant, S. G. Hughes, and J. M. Garland (Oxford: Bios Scientific Publishers Ltd), 163–174.

Chen, C., Lu, S., Chen, Y., Wang, Z., Niu, Y., and Guo, Z. (2009). A gamma-ray induced dwarf mutant from seeded Bermuda grass and its physiological responses to drought stress. *HortScience* 134, 22–30. doi: 10.21273/jashs.134.1.22

Costa, L., Montano, Y. M., Carrión, C., Rolny, N., and Guiamet, J. J. (2013). Application of low intensity light pulses to delay postharvest senescence of *Ocimum basilicum* leaves. *Postharvest Biol. Technol.* 86, 181–191. doi: 10.1016/j.postharvbio.2013.06.017

Deng, M., Qian, H., Chen, L., Sun, B., Chang, J., Miao, H., et al. (2017). Influence of pre-harvest red light irradiation on main phytochemicals and antioxidant activity of Chinese kale sprouts. *Food Chem.* 222, 1–5. doi: 10.1016/j.foodchem.2016.11.157

Dhakal, R., and Baek, K. H. (2014). Short period irradiation of single blue wavelength light extends the storage period of mature green tomatoes. *Postharvest Biol. Technol.* 90, 73–77. doi: 10.1016/j.postharvbio.2013.12.007

Dhindsa, R., Plumb-Dhindsa, P., and Thorpe, T. (1981). Leaf senescence: correlated with increased levels of membrane permeability and lipid peroxidation, and decreased levels of superoxide dismutase and catalase. *J. Exp. Bot.* 32, 93–101. doi: 10.1093/jxb/32.1.93

Elibox, W., and Umaharan, P. (2010). Cultivar differences in the deterioration of vase-life in cut-flowers of *Anthurium andraeanum* is determined by mechanisms that regulate water uptake. *Sci. Hortic.* 124, 102–108. doi: 10.1016/j.scienta.2009.12.005

Eskins, K., Jiang, C. Z., and Shibles, R. (1991). Light-quality and irradiance effects on pigments, light-harvesting proteins and Rubisco activity in a chlorophyll- and light- harvesting-deficient soybean mutant. *Physiol. Plant.* 83, 47–53. doi: 10.1111/j.1399-3054.1991.tb01280.x

Gangadhar, B. H., Mishra, R. K., Pandian, G., and Park, S. W. (2012). Comparative study of color, pungency, and biochemical composition in chili pepper (*Capsicum annuum*) under different light-emitting diode treatments. *HortScience* 47, 1729–1735. doi: 10.21273/hortsci.47.12.1729

Gong, D., Cao, S., Sheng, T., Shao, J., Song, C., Wo, F., et al. (2015). Effect of blue light on ethylene biosynthesis, signalling and fruit ripening in postharvest peaches. *Sci. Hortic.* 197, 657–664. doi: 10.1016/j.scienta.2015.10.034

Guo, Z., Ou, W., Lu, S., and Zhong, Q. (2006). Differential responses of antioxidative system to chilling and drought in four rice cultivars differing in sensitivity. *Plant Physiol. Biochem.* 44, 828–836. doi: 10.1016/j.plaphy.2006.10.024

Hajirezaei, M. R., Takahata, Y., Trethewey, R. N., Willmitzer, L., and Sonnewald, U. (2000). Impact of elevated cytosolic and apoplastic invertase activity on carbon metabolism during potato tuber development. *J. Exp. Bot.* 51, 439–445. doi: 10.1093/jexbot/51.suppl_1.439

Han, L. B., Song, G. L., and Zhang, X. (2008). Preliminary observation of physiological responses of three turfgrass species to traffic stress. *HortTechnology.* 18, 139–143. doi: 10.21273/horttech.18.1.139

Hasan, M., Bashir, T., Ghosh, R., Lee, S. K., and Bae, H. (2017). An overview of LEDs' effects on the production of bioactive compounds and crop quality. *Molecules.* 22:1420. doi: 10.3390/molecules22091420

Hasperué, J. H., Guardianelli, L., Rodoni, L. M., Chaves, A. R., and Martínez, G. A. (2016a). Continuous white–blue LED light exposition delays postharvest senescence of broccoli. *Food Sci. Technol.* 65, 495–502. doi: 10.1016/j.lwt.2015.08.041

Hasperué, J. H., Rodoni, L. M., Guardianelli, L. M., Chaves, A. R., and Martínez, G. A. (2016b). Use of LED light for Brussels sprouts postharvest conservation. *Sci. Hortic.* 213, 281–286. doi: 10.1016/j.scienta.2016.11.004

Heath, R. L., and Parker, L. (1968). Photoperoxidation in isolated chloroplasts kinetics and stoichiometry of fatty acid peroxidation. *Arch. Biophys.* 25, 189–198. doi: 10.1016/0003-9861(68)90654-1

Ho, L. C., and Nichols, R. (1975). The role of phloem transport in the translocation of sucrose along the stem of carnation cut flowers. *Ann. Bot.* 39, 439–446. doi: 10.1093/oxfordjournals.aob.a084958

Hogewoning, S. W., Trouwborst, G., Maljaars, H., Poorter, H., van Ieperen, W., and Harbinson, J. (2010). Blue light dose–responses of leaf photosynthesis, morphology, and chemical composition of *Cucumis sativus* grown under

different combinations of red and blue light. *J. Exp. Bot.* 61, 3107–3117. doi: 10.1093/jxb/erq132

Hotta, M., Hattori, H., Hirano, T., Kume, T., Okumura, Y., et al., (2016). Breeding and characteristics of spray-type carnation'Kaneainou 1 go'with a long vase life. *Res. Bull. Aichi Agric. Res. Ctr.* 48, 63–71.

Jerzy, M., Zakrzewski, P., and Schroeter-Zakrzewska, A. (2011). Effect of colour of light on the opening of inflorescence buds and post-harvest longevity of pot chrysanthemums (Chrysanthemum × grandiflorum (Ramat.) Kitam). *Acta Agrobot.* 64, 13–18. doi: 10.5586/aa.2011.025

Johkan, M., Shoji, K., Goto, F., Hashida, S., and Yoshihara, T. (2010). Blue light-emitting diode light irradiation of seedlings improves seedling quality and growth after transplanting in red leaf lettuce. *HortScience* 45, 1809–1814. doi: 10.21273/hortsci.45.12.1809

Kalhor, M., Aliniaeifard, S., Seif, M., Asayesh, E., Bernard, F., Hassani, B., et al., (2018). Enhanced salt tolerance and photosynthetic performance: implication of γ-amino butyric acid application in salt-exposed lettuce (*Lactuca sativa* L.) plants. *Plant Physiol. Biochem.* 130, 157–172. doi: 10.1016/j.plaphy.2018.07.003

Karami, O., Deljou, A., and Kordestani, G. K. (2008). Secondary somatic embryogenesis of carnation (*Dianthus caryophyllus* L.). *Plant Cell, Tissue Organ Cult.* 92, 273–280. doi: 10.1007/s11240-007-9332-2

Karimi, M., Asil, M. H., and Zakizadeh, H. (2012). Increasing plant longevity and associated metabolic events in potted carnation (*Dianthus caryophyllus* L. Clove Pink). *Braz. J. Plant Physiol.* 24, 247–252. doi: 10.1590/s1677-04202012000400003

Kim, K., Kook, H. S., Jang, Y. J., Lee, W. H., Kamala-Kannan, S., Chae, J. C., et al., (2013). The effect of blue-light-emitting diodes on antioxidant properties and resistance to *Botrytis cinerea* in tomato. *J. Plant Pathol. Microbiol.* 4:203.

Kopsell, D. A., and Sams, C. E. (2013). Increases in shoot tissue pigments, glucosinolates, and mineral elements in sprouting broccoli after exposure to short-duration blue light from light emitting diodes. *J. Amer. Soc. Hort. Sci.* 138, 31–37. doi: 10.21273/jashs.138.1.31

Krzymińska, A., and Karasiewicz, M. (2017). Postharvest longevity of cut hyacinths depending on light colour and types of lamps. *Nauka Przyr. Technol.* 11, 55–64.

Kumar, M., Singh, V. P., Arora, A., and Singh, N. (2014). The role of abscisic acid (ABA) in ethylene insensitive Gladiolus (*Gladiolus grandiflora* Hort.) flower senescence. *Acta Physiol. Plant.* 36, 151–159. doi: 10.1007/s11738-013-1395-6

Lee, M. K., Arasu, M. V., Park, S., Byeon, D. H., Chung, S. O., Park, S. U., et al., (2016). LED lights enhance metabolites and antioxidants in chinese cabbage and kale. *Braz. Arch. Biol. Technol.* 59:e16150546.

Lester, G. E., Makus, D. J., and Hodges, D. M. (2010). Relationship between fresh-packaged spinach leaves exposed to continuous light or dark and bioactive contents: effects of cultivar, leaf size, and storage duration. *J. Agric. Food Chem.* 58, 2980–2987. doi: 10.1021/jf903596v

Li, Q., and Kubota, C. (2009). Effects of supplemental light quality on growth and phytochemicals of baby leaf lettuce. *Environ. Expt. Bot.* 67, 59–64. doi: 10.1002/jsfa.6173

Liao, L. J., Lin, Y. H., Huang, K. L., Chen, W. S., and Cheng, Y. M. (2000). Postharvest life of cut rose flowers as affected by silver thiosulfate and sucrose. *Bot. Bull. Acad. Sin.* 41, 299–303.

Lichtenthaler, H. K., and Buschmann, C. (2001). Chlorophylls and carotenoids: measurement and characterization by UV-VIS spectroscopy. *Curr Protoc Food Anal Chem.* 1, 1–8.

Lu, P., Cao, J., He, S., Liu, J., Li, H., Cheng, G., et al., (2010). Nano-silver pulse treatments improve water relations of cut rose cv. Movie Star flowers. *Postharvest Biol. Technol.* 57, 196–202. doi: 10.1016/j.postharvbio.2010.04.003

Manivannan, A., Soundararajan, P., Halimah, N., Ko, C. H., and Jeong, B. R. (2015). Blue LED light enhances growth, phytochemical contents, and antioxidant enzyme activities of *Rehmannia glutinosa* cultured in vitro. *Hortic. Environ. Biotechnol.* 56, 105–113. doi: 10.1007/s13580-015-0114-1

Mastropasqua, L., Tanzarella, P., and Paciolla, C. (2016). Effects of postharvest light spectra on quality and health-related parameters in green *Asparagus officinalis* L. *Postharvest Biol. Technol.* 112, 143–151. doi: 10.1016/j.postharvbio.2015.10.010

Miao, Y., Chen, Q., Qu, M., Gao, L., and Hou, L. (2019). Blue light alleviates 'red light syndrome' by regulating chloroplast ultrastructure, photosynthetic traits and nutrient accumulation in cucumber plants. *Sci. Hortic.* 257:108680. doi: 10.1016/j.scienta.2019.108680

Mor, Y., Reid, M. S., and Kofranek, A. M. (1980). Role of the ovary in carnation senescence. *Sci. Hortic.* 13, 377–383. doi: 10.1016/0304-4238(80)90096-5

Muneer, S., Kim, E., Park, J., and Lee, J. (2014). Influence of green, red and blue light emitting diodes on multiprotein complex proteins and photosynthetic activity under different light intensities in lettuce leaves (*Lactuca sativa* L.). *Int. J. Mol. Sci.* 15, 4657–4670. doi: 10.3390/ijms15034657

Nascimento, L. B. S., Leal-Costa, M. V., Coutinho, M. A. S., Moreira, N.D. S., Lage, C. L. S., Barbi, N. D. S., et al., (2013). Increased antioxidant activity and changes in phenolic profile of *Kalanchoe pinnata* (Lamarck) persoon (crassulaceae) specimens grown under supplemental blue light. *Photochem. Photobiol.* 89, 391–399. doi: 10.1111/php.12006

Nichols, R., and Ho, L. C. (1975). Effects of ethylene and sucrose on translocation of dry matter and 14C-sucrose in the cut flower of the glasshouse carnation (*Dianthus caryophyllus*) during senescence. *Ann. Bot.* 39, 287–296. doi: 10.1093/oxfordjournals.aob.a084942

Noichinda, S., Bodhipadma, K., Mahamontri, C., Narongruk, T., and Ketsa, S. (2007). Light during storage prevents loss of ascorbic acid, and increases glucose and fructose levels in Chinese kale (*Brassica oleracea* var. alboglabra). *Postharvest Biol. Technol.* 44, 312–315. doi: 10.1016/j.postharvbio.2006.12.006

Ohashi-Kaneko, K., Takase, M., Kon, N., Fujiwara, K., and Kurata, K. (2007). Effect of light quality on growth and vegetable quality in leaf lettuce, spinach and komatsuna. *Environ. Control Biol.* 45, 189–198. doi: 10.2525/ecb.45.189

Oms-Oliu, G., Aguiló-Aguayo, I., Martín-Belloso, O., and Soliva-Fortuny, R. (2010). Effects of pulsed light treatments on quality and antioxidant properties of fresh mushrooms (*Agaricus bisporus*). *Postharvest Biol. Technol.* 56, 216–222. doi: 10.1016/j.postharvbio.2009.12.011

Paulin, A., Droillard, M. J., and Bureau, J. M. (1986). Effect of a free radical scavenger, 3,4,5- trichlorophenol, on ethylene production and on changes in lipids and membrane integrity during senescence of petals of cut carnations (*Dianthus caryophyllus*). *J. Plant Physiol.* 67, 465–471. doi: 10.1111/j.1399-3054.1986.tb05764.x

Perrin, P. W. (1982). Post storage effect of light, temperature and nutrient spray treatments on chlorophyll development in cabbage. *Can. J. Plant Sci.* 62, 1023–1026. doi: 10.4141/cjps82-151

Rodrigues, M. A., Bianchetti, R. E., and Freschi, L. (2014). Shedding light on ethylene metabolism in higher plants. *Front. Plant Sci.* 5:665. doi: 10.3389/fpls.2014.00665

Rogers, H. J. (2013). From models to ornamentals: how is flower senescence regulated? *Plant Mol. Biol.* 82, 563–574. doi: 10.1007/s11103-012-9968-0

Rubinstein, B. (2000). Regulation of cell death in flower petals. *Plant. Mol. Biol.* 44, 303–318.

Sairam, R. K., Deshmukh, P. S., and Shukla, D. S. (1997). Tolerance of drought and temperature stress in relation to increased antioxidant enzyme activity in wheat. *J Agron. Crop Sci.* 178, 171–177.

Satoh, S. (2011). Ethylene production and petal wilting during senescence of cut carnation (*Dianthus caryophyllus*) flowers and prolonging their vase life by genetic transformation. *J. Jpn. Soc. Hortic. Sci.* 80, 127–135. doi: 10.2503/jjshs1.80.127

Shibuya, K., and Ichimura, K. (2010). Depression of autocatalytic ethylene production by high-temperature treatment in carnation flowers. *J. Jpn. Soc. Hortic. Sci.* 79, 97–102. doi: 10.2503/jjshs1.79.97

Simlat, M., Lêzak, P., Mo's, M., Warcho, M., Skrzypek, E., and Ptak, A. (2016). The effect of light quality on seed germination, seedling growth and selected biochemical properties of *Stevia rebaudiana* Bertoni. *Sci. Hortic.* 211, 295–304. doi: 10.1016/j.scienta.2016.09.009

Singh, A., Kumar, J., and Kumar, P. (2008). Effects of plant growth regulators and sucrose on postharvest physiology, membrane stability and vase life of cut spikes of gladiolus. *Plant Growth Regul.* 55:221. doi: 10.1007/s10725-008-9278-3

Slootwet, G. (1995). Effect of water temperature on water uptake and vase life of different cut flowers. *Acta Hort.* 405, 67–74. doi: 10.17660/actahortic.1995.405.7

Solfanelli, C., Poggi, A., Loreti, E., Alpi, A., and Perata, P. (2006). Sucrose-specific induction of the anthocyanin biosynthetic pathway in *Arabidopsis*. *Plant Physiol.* 140, 637–646. doi: 10.1104/pp.105.072579

Strasser, R. J., Srivastava, A., and Tsimilli-Michael, M. G. (2000). The florescence transient as a tool to characterize and screen photosynthetic samples, in *Probing*

Photosynthesis: Mechanisms, Regulation and Adaptation, eds M. Yunus, U. Pathre, and P. Mohanty (Boca Raton, FL: CRC press), 445–483.

Strasser B. J., and Strasser, R. J. (1995). "Measuring fast florescence transients to address environmental questions: the JIP test," in *Photosynthesis: From Light to Biosphere*, Ed. P. Mathis (Amsterdam: Kluwer Academic Publishers).

Sugawara, H., Shibuya, K., Yoshioka, T., Hashiba, T., and Satoh, S. (2002). Is a cysteine proteinase inhibitor involved in the regulation of petal wilting in senescing carnation (*Dianthus caryophyllus* L.) flowers? *J. Exp. Bot.* 53, 407–413. doi: 10.1093/jexbot/53.368.407

Tanase, K., Onozaki, T., Satoh, S., Shibata, M., and Ichimura, K. (2008). Differential expression levels of ethylene biosynthetic pathway genes during senescence of long-lived carnation cultivars. *Postharvest Biol. Technol.* 47, 210–217. doi: 10.1016/j.postharvbio.2007.06.023

Tanase, K., Otsu, S., Satoh, S., and Onozaki, T. (2015). Expression levels of ethylene biosynthetic genes and senescence-related genes in carnation (*Dianthus caryophyllus* L.) with ultra-long-life flowers. *Sci. Hortic.* 183, 31–38. doi: 10.1016/j.scienta.2014.11.025

Trethewey, R. N., Geigenberger, P., Riedel, K., Hajirezaei, M. R., Sonnewald, U., Stitt, M., et al., (1998). Combined expression of glucokinase and invertase in potato tubers leads to a dramatic reduction in starch accumulation and a stimulation of glycolysis. *Plant J.* 15,109–118. doi: 10.1046/j.1365-313x.1998.00190.x

Van Doorn, W. G. (2011). Classes of programmed cell death in pants, compared to those in animals. *J. Exp. Bot.* 62, 4749–4761. doi: 10.1093/jxb/err196

Van Doorn, W. G., and Woltering, E. J. (2008). Physiology and molecular biology of petal senescence. *J. Exp. Bot.* 59, 453–480. doi: 10.1093/jxb/erm356

Van Geest, G., Choi, Y. H., Arens, P., Post, A., Liu, Y., and van Meeteren, U. (2016). Genotypic differences in metabolomic changes during storage induced-degreening of chrysanthemum disk florets. *Postharvest Biol. Technol.* 115, 48–59. doi: 10.1016/j.postharvbio.2015.12.008

Van Meeteren, U., and Aliniaeifard, S. (2016). "Stomata and postharvest physiology," in *Postharvest Ripening. Physiology of Crops*, Ed. S. Pareek (Boca Raton, FL: CRC Press), 157–216.

VBN (2005). *Evaluation Cards for Cut Flowers*. Leiden: VBN.

Wagstaff, C., Yang, T. J. W., Stead, A. D., Buchanan-Wollaston, V., and Roberts, J. A. (2009). A molecular and structural characterization of senescing petals and leaves. *Plant J.* 57, 690–705. doi: 10.1111/j.1365-313X.2008.03722.x

Woltering, E. J., and Seifu, Y. W. (2014). Low intensity monochromatic red, blue or green light increases the carbohydrate levels and substantially extends the shelf life of fresh-cut lettuce. *Acta Hortic.* 1079, 257–264. doi: 10.17660/actahortic.2015.1079.30

Xu, F., Shi, L., Chen, W., Cao, S., Su, X., and Yang, Z. (2014). Effect of blue light treatment on fruit quality, antioxidant enzymes and radical-scavenging activity in strawberry fruit. *Sci. Hortic.* 175, 181–186. doi: 10.1016/j.scienta.2014.06.012

Yagi, M., Kosugi, S., Hirakawa, H., Ohmiya, A., Tanase, K., Harada, T., et al., (2013). Sequence analysis of the genome of carnation (*Dianthus caryophyllus* L.). *DNA Res.* 21, 231–241.

Yamada, K., Ito, M., Oyama, T., Nakada, M., Maesaka, M., and Yamaki, S. (2007). Analysis of sucrose metabolism during petal growth of cut roses. *Postharvest. Biol. Technol.* 43, 174–177. doi: 10.1016/j.postharvbio.2006.08.009

Yamamoto, K., Saitoh, C., Yokoo, Y., Furukawa, T., and Oshima, K. (1992). Inhibition of wilting and autocatalytic ethylene production in cut carnation flowers by cispropenylphosphonic acid. *Plant Growth Regul.* 11, 405–409. doi: 10.1007/bf00130649

Ye, S., Shao, Q., Xu, M., Li, S., Wu, M., Tan, X., et al. (2017). Effects of light quality on morphology, enzyme activities, and bioactive compound contents in *Anoectochilus roxburghii*. *Front. Plant Sci.* 8:857. doi: 10.3389/fpls.2017.00857

Yu, W., Liu, Y., Song, L., Jacobs, D. F., Du, X., Ying, Y., et al., (2017). Effect of differential light quality on morphology, photosynthesis, and antioxidant enzyme activity in *Camptotheca acuminata* seedlings. *J. Plant Growth Regul.* 36, 148–160. doi: 10.1007/s00344-016-9625-y

Zeng, C. L., Liu, L., and Xu, G. Q. (2011). The physiological responses of carnation cut flowers to exogenous nitric oxide. *Sci. Hortic.* 127, 424–430. doi: 10.1016/j.scienta.2010.10.024

Zhan, L., Hu, J., Li, Y., and Panga, L. (2012). Combination of light exposure and low temperature in preserving quality and extending shelf-life offresh-cut broccoli (*Brassica oleracea* L.). *Postharvest Biol. Technol.* 72, 76–81. doi: 10.1016/j.postharvbio.2012.05.001

Zheng, L., and Van Labeke, M. C. (2017a). Chrysanthemum morphology, photosynthetic efficiency and antioxidant capacity are differentially modified by light quality. *J. Plant Physiol.* 213, 66–74. doi: 10.1016/j.jplph.2017.03.005

Zheng, L., and Van Labeke, M. C. (2017b). Long-term effects of red-and blue-light emitting diodes on leaf anatomy and photosynthetic efficiency of three ornamental pot plants. *Front. Plant Sci.* 8:917. doi: 10.3389/fpls.2017.00917

Conflict of Interest: The authors declare that the research was conducted in the absence of any commercial or financial relationships that could be construed as a potential conflict of interest.

frontiers in Plant Science

ORIGINAL RESEARCH
published: 12 June 2020
doi: 10.3389/fpls.2020.00846

Postharvest Spectral Light Composition Affects Chilling Injury in Anthurium Cut Flowers

Sasan Aliniaeifard[1*†], *Zahra Falahi*[1†], *Shirin Dianati Daylami*[1], *Tao Li*[2*] *and Ernst Woltering*[3,4]

[1] Photosynthesis Laboratory, Department of Horticulture, Aburaihan Campus, University of Tehran, Tehran, Iran, [2] Institute of Environment and Sustainable Development in Agriculture, Chinese Academy of Agricultural Sciences, Beijing, China, [3] Wageningen Food & Biobased Research, Wageningen, Netherlands, [4] Horticulture & Product Physiology Group, Department of Plant Sciences, Wageningen University, Wageningen, Netherlands

OPEN ACCESS

Edited by:
Margherita Irene Beruto, Istituto Regionale per la Floricoltura (IRF), Italy

Reviewed by:
Marcello Militello, Istituto Regionale per la Floricoltura (IRF), Italy
John Dole, North Carolina State University, United States

***Correspondence:**
Sasan Aliniaeifard
aliniaeifard@ut.ac.ir
Tao Li
litao06@caas.cn

[†]*These authors have contributed equally to this work*

Specialty section:
This article was submitted to Crop and Product Physiology, a section of the journal Frontiers in Plant Science

Received: *16 January 2020*
Accepted: *26 May 2020*
Published: *12 June 2020*

Citation:
Aliniaeifard S, Falahi Z, Dianati Daylami S, Li T and Woltering E (2020) Postharvest Spectral Light Composition Affects Chilling Injury in Anthurium Cut Flowers. Front. Plant Sci. 11:846. doi: 10.3389/fpls.2020.00846

The effect of the lighting environment during postharvest storage of ornamentals has largely been neglected in previous research. Anthurium is a cold-sensitive species originating from tropical climates and is widely cultivated all around the world for its colorful spathes. To investigate the effects of light spectrum on the performance of Anthurium cut flowers under cold storage, two cultivars [Calore (red spathe) and Angel (withe spathe)] were placed at low temperature (4°C), either in darkness (D) or under different light spectra [red (R), blue (B), 70:30% red:blue (RB), and white (W)] at an intensity of 125 μmol.m^{-2}.s^{-1}. In both cultivars, the longest and shortest vase lives were observed in spathes exposed to the R and B spectra, respectively. In both cultivars, electrolyte leakage (EL) of spathe was highest under the B and W spectra and lowest under the R spectrum. The highest rate of flower water loss from the spathes was observed under the B-containing light spectra, whereas the lowest rate of water loss was observed in D and under the R spectrum. Negative correlations were observed between EL and vase life and between anthocyanin concentration and EL for both Anthurium cultivars. A positive correlation was found between anthocyanin concentration and vase life. For both Anthurium cultivars, spectral light composition with higher percentage of B resulted in higher EL and as a result shorter vase life in cut flowers under cold storage condition. The negative effect of the B light spectrum on vase life of Anthurium can be explained through its effect on water loss and on oxidative stress and membrane integrity. The quality of Anthurium cut flowers should benefit from environments with restricted B light spectrum during postharvest handling.

Keywords: anthurium, water loss, transpiration rate, chilling stress, light spectrum

INTRODUCTION

Tropical flowers are produced worldwide because of their ornamental values. Postharvest handling of tropical flowers (*e.g.* Anthurium) is usually difficult due to their sensitivity to low temperatures. Anthurium (*Anthurium andraeanum*) is a tropical plant used in ornamental industry for its colorful spathes and green leaves. It is produced in wide ranges of climates; in locations far away from their

original habitats in greenhouses. Although cut Anthurium has a long vase life when compared to the vase life of many other cut flowers (Mujaffar and Sankat, 2003), postharvest exposure to low temperatures can reduce its vase life. Temperatures below 12°C induce symptoms of chilling injury such as brown spots on the Anthurium spathe (Promyou et al., 2012). In the winter time of temperate and cold climates, to prevent negative effects of cold temperatures on Anthurium cut flowers, the growers transfer the flowers to higher temperatures immediately after harvest. The importance of chilling stress for Anthurium flowers can be highlighted during their transport, storage, and distribution in the winter time. Anthurium flowers may be exposed to low temperatures as they are often part of mixed transport or storage with other flowers that need lower temperatures. This may cause a decrease in the quality of the spathe in customer locations. Browning and blueing of spathe and wilting of spadix are observed in Anthurium cut flowers when they face temperatures lower than 12°C (Promyou et al., 2012; Soleimani Aghdam et al., 2015).

Much effort has been made during the last decade to decrease the susceptibility of Anthurium cut flowers to low temperatures (Promyou et al., 2012; Soleimani Aghdam et al., 2015; Soleimani Aghdam et al., 2016b). These efforts were mainly focused on the application of chemical solutions to the stems of cut flowers. For instance, salicylic acid (Promyou et al., 2012) and γ-aminobutyric acid (GABA) (Soleimani Aghdam et al., 2015; Soleimani Aghdam et al., 2016b; Soleimani Aghdam et al., 2016c) have successfully decreased the negative effects of low temperatures on cut flower quality and vase life. Application of these chemicals caused approximately 10% reduction in occurrence of browning of Anthurium spathes. In the other cases no effect of chemical solutions was observed. For instance, using calcium in holding solution did not result in vase life improvement in cold-stored Anthurium cut flowers (Ketrodsakul et al., 2016). There is still a need for preventing the problems related to chilling injury beyond the use of chemicals.

In some cut flowers with long vase life such as Anthurium, long distance transport to customers is common. During the postharvest period the cut flowers are usually held in darkness and may be exposed to cold (<12°C). A positive role for the presence of light during postharvest storage has been proposed for keeping quality of flowers with photosynthetic leaves such as rose, chrysanthemum, and protea (Rajapakse and Kelly, 1994; Ranwala and Miller, 2000). To the best of our knowledge, no study has been done on the effect of light (spectra) on postharvest quality of cut flowers such as Anthurium.

Nowadays, light emitting diodes (LEDs) lighting technology is widely used in horticulture (Kozai et al., 2015). The LEDs have long lifetimes, small mass, low heat production, high radiant efficiency, physical robustness, and narrow spectrum (Tennessen et al., 1994; Kim et al., 2004; Breive et al., 2005; Morrow, 2008). By using LEDs it is possible to apply specific wavelengths to plant material to study particular plant responses. Red (R) and blue (B) wavelengths are the main light spectra influencing water relations and gas exchange features of the plants (Massa et al., 2008; Hogewoning et al., 2010; Ouzounis et al., 2014; Ouzounis et al., 2016). Research on the effect of spectral wavelengths on plant responses is still ongoing. After harvest, cut flowers still respond to environmental cues such as light spectra. Many plant processes are influenced by light spectrum in the range between 380 and 750 nm. For instance, B light induces water influx into the guard cells and thus, stomatal opening through activation of plasma membrane H^+-ATPases (Kinoshita and Hayashi, 2011). Red light increases phosphorylation levels of the H^+-ATPase in response to the B light and therefore has inductive effects on B light-dependent stomatal opening and water loss by the leaf (Olsen et al., 2002; Suetsugu et al., 2014).

The importance of spathe water loss during postharvest storage under different temperatures has been previously reported (Sankat and Mujaffar, 1994). It was shown that at temperatures above 13°C when transpiration is more than the water uptake; the product would not be marketable anymore. At 8°C both water uptake and transpiration will be hampered and chilling symptoms (*e.g.* blueing and browning of the spathes) will appear (Sankat and Mujaffar, 1994).

Spectrum is one of the light characteristics that considerably influence plant responses. Light quality not only influences photosynthesis but also cellular integrity, water relations, pigmentation, carbohydrate, and antioxidant status of the plants (Bayat et al., 2018; Hosseini et al., 2018; Hosseini et al., 2019). We hypothesized that different light spectra through their effects on cellular metabolism can influence the cold tolerance and quality of the spathe and hence the vase life of the Anthurium flower. The main aim of this study was to investigate the effects of different light spectra on postharvest performance of Anthurium cut flowers at a chilling temperature.

MATERIALS AND METHODS

Flowers and Lighting Treatments

Cut flowers of Anthurium (*Anthurium andraeanum*) cultivars with red ('Calore') and white ('Angel') spathes were obtained from a commercial Anthurium greenhouse in the morning. Both cultivars were said to have long vase life in temperatures over 13°C, but 'Angel' was considered more sensitive to cold than 'Calore' (personal communication with Anthurium growers).

Anthurium cut flowers were harvested at the commercial harvest stage when 40–50% of the spadix true flowers were fully opened (Promyou et al., 2012). In the greenhouse, flowers with no deformities, no bruises, and straight peduncles were cut and placed into 50 ml tubes containing water. They were immediately transported (within less than 1 h after harvest) at 21°C to the laboratory where the flower stems were recut to 30 cm length. Each flower was placed in flasks containing 500 ml tap water. Sixty flasks with cut flowers (30 cut flowers from each cultivar) were placed into the light treatment compartments (l × w × h = 0.8 m × 0.5m × 0.5m). Compartments were positioned in a climate room with relative humidity of 80–81% and fixed

temperature of 4°C provided by constant ventilation inside the cold rooms.

Twelve flasks (six per each cultivar) were placed in each of the aforementioned compartments in the dark (D) and under continuous light intensity of 125 ± 5 µmol m^{-2} s^{-1} photosynthetic photon flux density (PPFD) but with different light spectra including white (W), blue (B), red (R), and 70% R + 30% B (RB) provided by LED production modules (24W, Iran Grow Light Co, Iran). Light intensity and spectra were measured using a light meter (Sekonic C-7000, Japan) (**Figure 1**).

Visual Quality and Vase Life

Each flower was inspected daily, and its vase life was estimated based on the visual symptoms such as loss of spathe glossiness, desiccation of spadix, blackening and wilting of spathe (Paull and Goo, 1982) as well as browning and desiccation of spadix. Visual symptoms on the spathes were recorded using a scale from 1 to 5; 1 = no chilling injury; 2 = mild injury (1–20% of spathe affected); 3 = moderate injury (21–50% of spathe affected); 4 = severe injury (51–80% of spathe affected); 5 = very severe injury (81–100% of spathe affected).

Relative Water Loss Percentage

Every day during the experiment, fresh weight (FW) of individual Anthurium cut flower was measured. FW differences between two subsequent days were calculated (ΔFW). Accumulative water loss of the Anthurium cut flowers was expressed as percentage water loss relative to the initial weight.

Electrolyte Leakage

For measuring EL, 20 discs (8 mm) per spathe (three spathes) were floated in 10 ml deionized water in closed vials and incubated at 25°C on a rotary shaker for 24 h. Thereafter, electrical conductivity of the solution (C_1) was determined using a conductivity meter (Metrohm, Switzerland). Subsequently, samples were autoclaved at 120°C for 20 min, and the electrical conductivities of the solution (C_2) were again recorded after equilibration at 25°C. EL was calculated based on the following equation.

$$EL = \frac{C_1}{C_2} \times 100$$

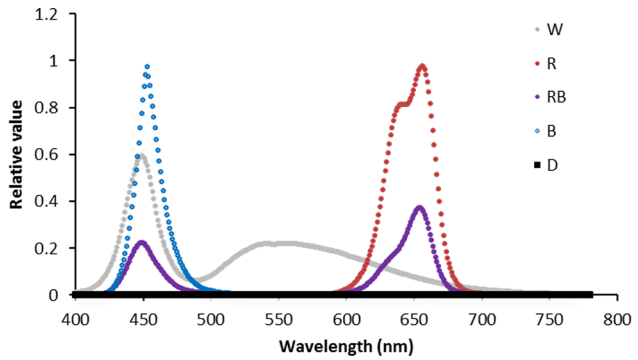

FIGURE 1 | Light spectra of white (W), red (R), red and blue (RB), blue (B), and dark (D) lighting environments measured at spathe level in the chambers at 4°C.

Osmotic Potential

Osmotic potential of the spathe was determined using the method described by Martìnez et al. (2004). The measurement was performed on three flowers per treatment. Spathes were cut into small segments; tissue pieces were placed in Eppendorf tubes perforated with four small holes and immediately frozen in liquid nitrogen. After being individually encased in a second intact Eppendorf tube, the samples were allowed to thaw for 30 min and centrifuged at 15,000 g for 15 min at 4°C. The extracted sap was collected and used for ψs determination. Osmolarity (c) was measured with a vapor pressure osmometer (Osmomat 030-gonatec) and converted from mOsmole kg^{-1} to MPa according to the Van't Hoff equation (Martìnez et al., 2004).

Proline Concentration

Free proline content was measured based on the method described by Bates et al. (1973). This measurement was performed on three spathes per treatment. Grounded spathe samples (0.5 g) were homogenized in 3% (w/v) sulphosalicylic acid and then filtered through filter papers. Following addition of acid-ninhydrin and glacial acetic acid, the mixture was heated at 100°C for 1 h in a water bath. Reaction was stopped using an ice bath. The mixture was extracted with toluene, and the absorbance of the fraction with toluene aspired from the liquid phase was read at 520 nm (Perkin Elmer Lambda 25 UV-VIS Spectrometer). Proline concentration was determined using a calibration curve and expressed as µmol proline g^{-1} FW (Bates et al., 1973).

Hydrogen Peroxide

Hydrogen peroxide (H_2O_2) content was spectrophotometrically (Perkin Elmer Lambda 25 UV-VIS Spectrometer) measured after reaction with potassium iodide (KI). Ground spathe samples (0.25 g) were homogenized in 0.1% trichloroacetic acid (TCA) and centrifuged at 5,000 g for 10 min. The reaction mixture contained 0.5 ml of 0.1% trichloroacetic acid (TCA), spathe extract supernatant, 0.5 ml of 100 mm K-phosphate buffer and 2 ml reagent (1 m KI w/v in fresh double-distilled H_2O). The blank contained 0.1% TCA in the absence of leaf extract. The reaction was developed for 1 h in darkness, and absorbance was measured at 390 nm. The amount of H_2O_2 was calculated using a standard curve prepared with known concentrations of H_2O_2 according to the method described by Patterson et al. (1984). This measurement was performed on three spathes per treatment.

Carbohydrate Contents

Ground spathe samples (300 mg FW) were mixed with 7 ml of 70% ethanol (w/v) for 5 min on ice and centrifuged at 6,700 *g* for 10 min at 4°C. After adding 200 ml of the supernatant to 1 ml of an anthrone solution (0.5 g anthrone, 250 ml 95% H_2SO_4, and 12.5 ml

distilled water), the absorbance was spectrophotometrically (Perkin Elmer Lambda 25 UV-VIS Spectrometer) recorded at 625 nm (van Doorn, 2012). This measurement was performed on three spathes per treatment.

Pigments

The Chl and carotenoid contents of the spathes were measured according to the method described by Arnon (1949). For measuring the anthocyanin content of the spathes, 1 g of ground spathe tissue was homogenized in 10 ml methanol, and the extract was incubated at 4°C in the dark overnight. The slurry was centrifuged (SIGMA-3K30) at 4,000 *g* for 10 min. The anthocyanin in the supernatant was spectrophotometrically (Perkin Elmer Lambda 25 UV-VIS Spectrometer) determined at 520 nm according to the method described by Wagner (1979). This measurement was performed on three spathes per treatment.

Statistical Analysis

Nondestructive measurements (water loss and vase life) were done on six spathes as six replicates. Destructive measurements were done on three spathes as three biological replicates. The experiment was repeated twice in precisely controlled cold room with fixed temperature of 4°C. Since the results of both experiments for the vase life were identical between the two experiments, part of the destructive measurements was performed in flowers from the first experiment and part of the measurements in flowers from the repeated experiment. In both experiments visual judgement of spathe quality and daily water loss were measured. Apart from these measurements, in the first experiment, EL, chlorophyll and carotenoids content, photosynthetic activity, and spathe characteristics were determined; in the second experiment osmotic potential, carbohydrates, anthocyanins, proline and hydrogen peroxide contents were determined after 14 days of treatment. Osmotic potential and EL were determined in fresh spathe samples; the other analyses were done in spathe samples ground in liquid nitrogen and kept in −80°C. In all the cases measurements were performed in three or more biological replications.

The data were subjected to two-way analysis of variance (ANOVA), and Tukey was used as a means separation test, and $P > 0.01$ was considered not significant. The percentage of spathe water loss data was fitted with linear regression, and F test was used for comparing the slopes of the curves. GraphPad Prism 7.01 for Windows (GraphPad software, Inc. San Diego, CA) was used for statistical analysis and comparisons among treatments.

TABLE 1 | Analysis of variance (*F* values) for assessed parameters for Anthurium cut flowers exposed to different light spectra under cold storage condition (4°C).

Dependent Variable	Independent variables		
	Light spectra	Cultivar	Interaction (Spectra × Cultivar)
Vase life	13.8**	18.2**	6.8**
EL	7.01***	57.6**	13.1**
Osmotic potential	4.5***	13.1***	1.4^{ns}
Proline	3.8*	71.1**	6.7**
Anthocyanin	17****	45****	4.7**
Carotenoids	0.55^{ns}	0.29^{ns}	0.54^{ns}
Soluble carbohydrates	2.9*	0.35^{ns}	13.8**
Hydrogen peroxide	16.01****	296****	17.39****

*ns, Nonsignificance. *Significance at 0.05 probability level. **Significance at 0.01 probability level. ***Significance at 0.001 probability level. ****Significance at 0.0001 probability level.*

RESULTS

Vase Life of Anthurium Depends on Postharvest Light Spectra and Cultivar

Vase life of Anthurium cut flowers at 4°C was significantly ($P \leq 0.01$, **Table 1**) influenced by the interaction between light spectra and cultivar (**Figures 2** and **3**). Among the light spectra, the longest vase life was observed in spathes exposed to R in both cultivars (**Figure 3**). In 'Angel', the shortest vase life was observed under W, B, and RB spectra (**Figures 2** and **3**). After 14 days exposure to B spectrum, the spathe and spadix of 'Angel' had become dark brown (**Figure 2**). In 'Calore', exposure to D, B, and RB spectra resulted in shorter vase life when compared to the vase life of flowers exposed to R and W spectra. These results indicate that R spectrum is able to prolong the vase life of Anthurium cut flowers in cold environments and that vase life under light was roughly dependent on the percentage of B

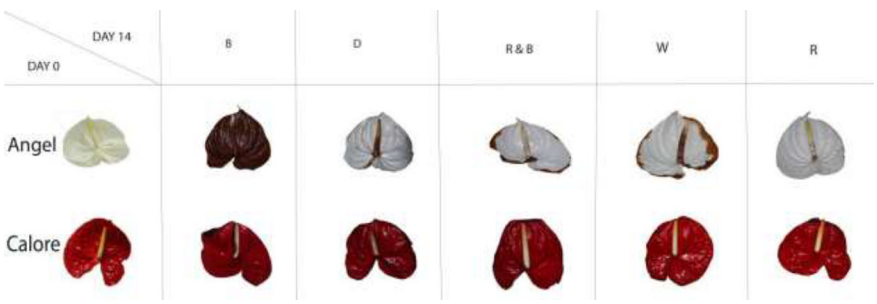

FIGURE 2 | Chilling injury symptoms in Anthurium cut flowers ('Angel' and 'Calore') held in the dark (D) or continuously exposed to 125 ± 5 μmol m^{-2} s^{-1} of different light spectra [white (W), red (R), red and blue (RB), blue (B)] after 14 days vase life at 4°C.

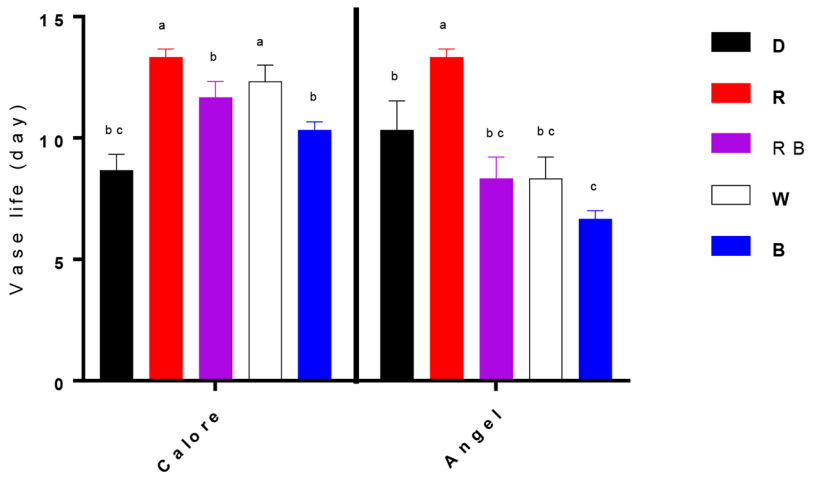

FIGURE 3 | Vase life of Anthurium cut flowers ('Angel' and 'Calore') held in the dark (D) or continuously exposed to 125 ± 5 µmol m^{-2} s^{-1} of different light spectra [white (W), red (R), red and blue (RB), blue (B)] at 4°C. End of vase life was determined by visual symptoms such as loss of spathe glossiness, desiccation of spadix, blackening and wilting of spathe as well as browning and desiccation of spadix. Vase life was terminated when flowers rated 3 for spathe browning or 4 for spadix necrosis. Values are the means of six biological replicates, and bars indicate means ± SEM. Bars with different letters are significantly different (ANOVA, $P < 0.01$).

wavelengths in the overall spectrum: the more B, the shorter the vase life.

Spathe Water Loss Is Controlled by Postharvest Light Spectra

Relative water loss percentage during 14 days of experiment was lowest under D and R spectrum in both cultivars (**Figure 4**). In 'Calore' (**Figure 4A**), the highest relative water loss percentage was observed under W; in 'Angel' under B spectrum (**Figure 4B**). The slope of the water loss curve under W light in 'Calore' and under B lights in 'Angel' was approximately doubled in comparison with the slope of the curves in D (**Table 2**). In both cultivars, no statistical differences for the slope of water loss were observed between D and R spectrum.

Cellular Integrity and Osmoregulation Is Influenced by Light Spectra and Cultivar

Electrolyte leakage (EL) after 14 days of treatment was considerably influenced by the interaction between the light spectra and cultivar ($P \leq 0.01$, **Table 1**). EL was generally higher in 'Angel' than in the 'Calore'. In 'Calore', EL was significantly lower under all light treatments compared to D. The lowest EL in 'Calore' was detected in spathes exposed to the R spectrum. In 'Angel' EL was highest in spathes exposed to W and B spectra and was lowest in spathes exposed to R spectrum (**Figure 5**).

Osmotic potential was influenced by the single effects of the light spectra ($P \leq 0.001$, **Table 1**) and cultivar ($P \leq 0.001$, **Table 1**). Osmotic potential of the spathe in 'Calore' after 14 days of treatment was 32% higher (more negative) than osmotic potential of spathe in 'Angel' (**Table 2**). Among the light spectra, osmotic potential of 'Calore' spathes under the B spectrum was the highest. Under the B spectrum, osmotic potential was 40% higher than the osmotic potential under the R spectrum. In 'Angel' osmotic potential was highest under the W and B spectra (**Table 2**).

Under all light spectra, proline concentration in the spathes of 'Calore' was higher than in 'Angel' (**Figure 6**). In the spathe of 'Calore' the highest proline concentration was detected under the R spectrum; in 'Angel' the lowest proline concentration was measured under R light. There was no clear trend in proline concentration with the proportion of B spectrum.

Concentration of soluble carbohydrates in the spathe was affected by the interaction between light spectra and cultivar ($P \leq 0.01$, **Table 1**). In 'Calore', the lowest concentration of soluble carbohydrates was detected under the R, B, and RB spectra; the highest concentration of carbohydrates was detected under the W spectrum and D. In 'Angel', the concentration of soluble carbohydrates in W was lower than in the other treatments (**Figure 7**). There was no clear trend in carbohydrate concentration with the proportion of B spectrum.

Hydrogen peroxide content of the spathe was influenced by the interaction between light spectra and cultivar ($P \leq 0.00001$, **Table 1**). Under all light spectra, higher hydrogen peroxide content was observed in 'Calore' in comparison with its content in 'Angel'. In 'Calore', the highest hydrogen peroxide content was detected under the W and RB spectra. The hydrogen peroxide content of 'Calore' spathes was respectively six and three times higher than its content in 'Angel' spathes under the W and RB spectra (**Figure 8**).

Spathe Anthocyanin Content Depends on Cultivar and Light Spectra

Chlorophyll was not detected in the two studied Anthurium cultivars. No significant difference in carotenoid content was detected between the two cultivars or among the light spectra

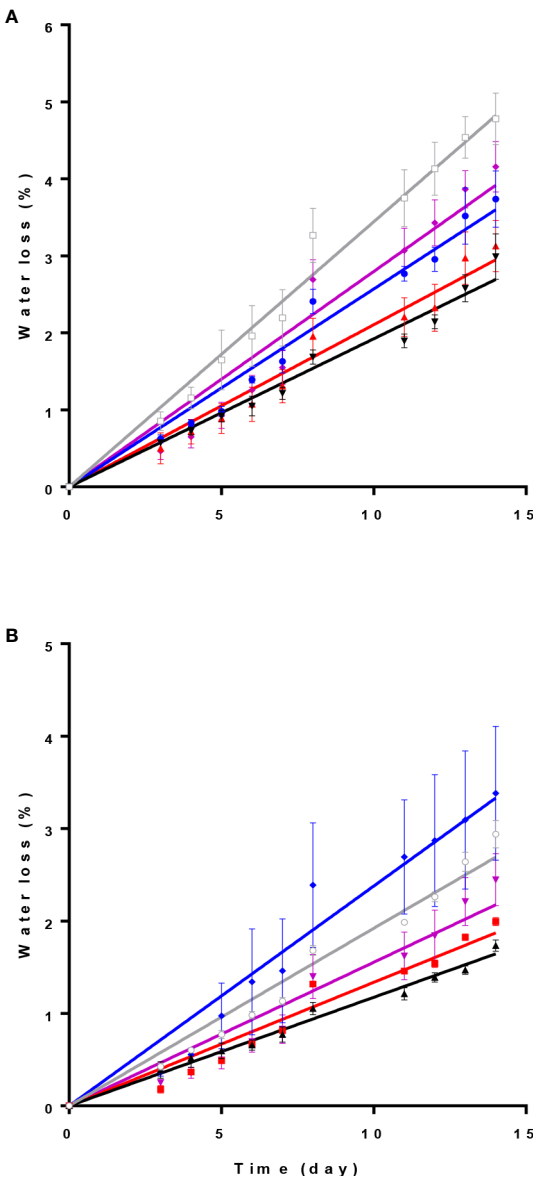

FIGURE 4 | Relative water loss percentage in Anthurium cut flowers ['Calore' **(A)** and 'Angel' **(B)**] held in the dark (D) or continuously exposed to 125 ± 5 µmol m^{-2} s^{-1} of different light spectra [white (W), red (R), red and blue (RB), blue (B)] during 14 days storage at 4°C. Values are the means of six biological replicates, and bars indicate means ± SEM. Data were fitted with linear regression, and the lines indicate the fitted line. Color of each line corresponds to the light spectrum of each treatment, gray stand for W spectrum.

and their interactions (**Table 1**). Anthocyanin content of the spathe was affected by the interaction between light spectra and cultivar ($P \leq 0.01$, **Table 1**). Under all light spectra, except B, higher anthocyanin concentration was detected in 'Calore' in comparison with 'Angel'. In 'Calore', the highest anthocyanin concentration was detected under R spectrum; the lowest concentration was found under W and B spectra. Similarly, in 'Angel', the lowest anthocyanin concentration was detected under W and B spectra (**Figure 9**).

TABLE 2 | Slope of the curve for accumulative percentage of water loss over time and spathe osmotic potential after 14 days of treatment in two Anthurium cut flowers ('Angel' and 'Calore') exposed to different light spectra [white (W), red (R), red and blue (RB), blue (B) and dark (D)] at 4°C.

Cultivar	Light spectrum	Slope	Osmotic potential (Mpa)
Calore	W	0.34 ± 0.007 ^{a}	−1.41 ± 0.32^{A,b}
	D	0.19 ± 0.005 ^{e}	−1.71 ± 0.27^{A,ab}
	R	0.21 ± 0.006 ^{de}	−1.13 ± 0.33^{A,b}
	B	0.26 ± 0.007 ^{bc}	−2.02 ± 0.12^{A,a}
	RB	0.28 ± 0.012 ^{b}	−1.03 ± 0.25^{A,b}
Angel	W	0.19 ± 0.006 ^{e}	−1.34 ± 0.02^{B,a}
	D	0.12 ± 0.002 ^{g}	−0.91 ± 0.05^{B,b}
	R	0.13 ± 0.005 ^{g}	−0.82 ± 0.13^{B,b}
	B	0.24 ± 0.005 ^{c}	−1.21 ± 0.08^{B,a}
	RB	0.15 ± 0.007 ^{f}	−0.71 ± 0.12^{B,b}

Values are the means of six biological replicates for the Slope and three biological replicates for the Osmotic potential, and bars indicate means ± SEM.
In the case of osmotic potential, different capital letters indicate the significant differences between cultivars and different small letters indicate significant difference among light spectra.

Vase Life of Anthurium Depended on Cellular Integrity and Anthocyanin Content

In 'Angel', after 14 days of light treatment, a positive relationship ($R^2 = 0.82$) was found between the light effects on the osmotic potential and the EL of the spathe (**Figure 10A**). The EL of the spathe tissue was positively correlated with the slope of the water loss curve ($R^2 = 0.87$) (**Figure 10B**). Both EL ($R^2 = 0.66$) and the slope of the water loss curve ($R^2 = 0.68$) were negatively correlated with the vase life (**Figures 10C, D**).

In contrast to 'Angel', in 'Calore', there were no clear relations between the above discussed parameters. Only a significant negative correlation was observed between the vase life and the EL ($R^2 = 0.89$) (**Figure 10C**).

In both cultivars, anthocyanin content of the spathe at day 14 was negatively correlated with EL ($R^2 = 0.55$ for the combined data); anthocyanin was positively correlated with the vase life ($R^2 = 0.65$ for the combined data) (**Figure 11**).

Blue Light Is a Determinate Factor for the Vase Life of Anthurium at Chilling Temperature

The relation between vase life and EL depended on the percentage of B (400–500 nm) in the light spectrum (**Figure 12**). A negative relationship was observed between the percentage of B in the light spectrum and the vase life in both Anthurium cultivars [$R^2 = 0.75$ for 'Angel' (**Figure 12A**) and $R^2 = 0.89$ for 'Calore' (**Figure 12B**)], and a positive relationship was found between the percentage of B in the light spectrum and EL [$R^2 = 0.69$ for 'Angel' (**Figure 12A**) and $R^2 = 0.72$ for 'Calore' (**Figure 12B**)].

DISCUSSION

Production of Anthurium cut flowers in cold seasons is challenged by the low temperatures during postharvest

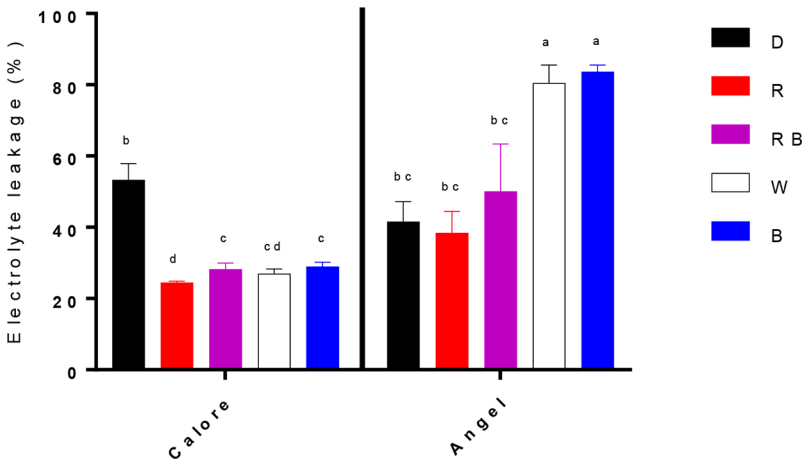

FIGURE 5 | Electrolyte leakage from two cultivars of Anthurium cut flowers ('Calore' and 'Angel') held in the dark (D) or continuously exposed to 125 ± 5 µmol m^{-2} s^{-1} of different light spectra [white (W), red (R), red and blue (RB), blue (B)] following 14 days storage at 4°C. Values are the means of three biological replicates, and bars indicate means ± SEM. Bars with different letters are significantly different (ANOVA, $P < 0.01$).

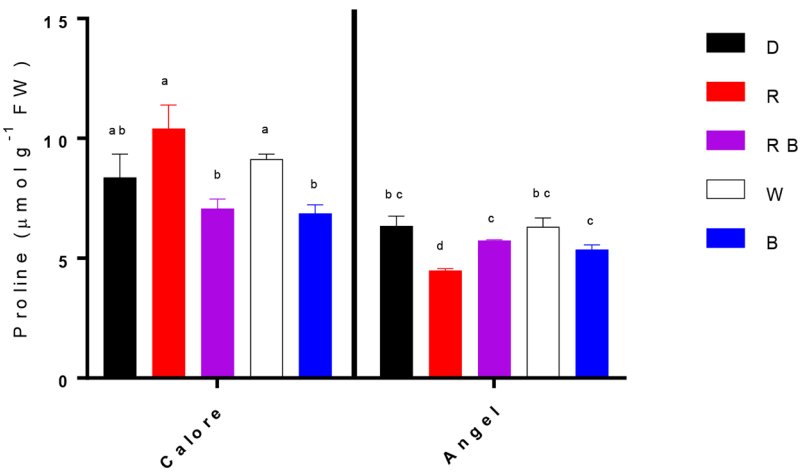

FIGURE 6 | Proline contents in the spathes of two cultivars of Anthurium cut flowers ('Calore' and 'Angel') held in the dark (D) or continuously exposed to 125 ± 5 µmol m^{-2} s^{-1} of different light spectra [white (W), red (R), red and blue (RB), blue (B)] following 14 days storage at 4°C. Values are the means of three biological replicates, and bars indicate means ± SEM. Bars with different letters are significantly different (ANOVA, $P < 0.01$).

(Kamemoto, 1962). Cold storage is usually used to regulate supply of cut flowers (Faragher et al., 1984). However, exposure to cold negatively affects quality of Anthurium (Promyou and Ketsa, 2014).

Results obtained from current experiment showed that postharvest lighting is an important aspect determining the quality of Anthurium cut flowers during exposure to cold. In most of the studies on postharvest quality, the different light treatments were applied before harvest (Gruda, 2005; Reid and Jiang, 2012; Darko et al., 2014). As far as we are aware there is no reported study on the effects of postharvest light spectra on quality of cut flowers especially under cold storage.

In the present study we have used two cultivars differing in spathe color; 'Calore' with red and 'Angel' with white spathe. Overall, the response to the postharvest light treatments was comparable in the two cultivars. More B in the spectrum correlated with a shorter vase life and higher EL (**Figure 12**). Lower anthocyanin content was correlated with higher EL and shorter vase life (**Figure 11**), and more water loss was correlated with the higher EL and shorter vase life (**Figure 10**). The latter aspect, however, was evident in 'Angel' but not in 'Calore'.

In the current study, postharvest exposure to B spectrum resulted in higher water loss from spathes of Anthurium especially when compared with R spectrum and D environment (**Figure 4**). Spathes of Anthurium contain

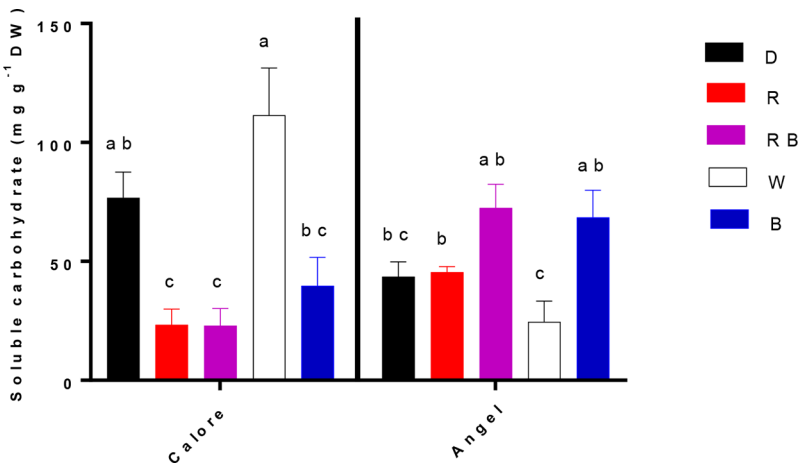

FIGURE 7 | Soluble carbohydrate concentrations in the spathes of two cultivars of Anthurium cut flowers ('Calore' and 'Angel') held in the dark (D) or continuously exposed to 125 ± 5 µmol m^{-2} s^{-1} of different light spectra [white (W), red (R), red and blue (RB), blue (B)] following 14 days vase life at 4°C. Values are the means of three biological replicates, and bars indicate means ± SEM. Bars with different letters are significantly different (ANOVA, $P < 0.01$).

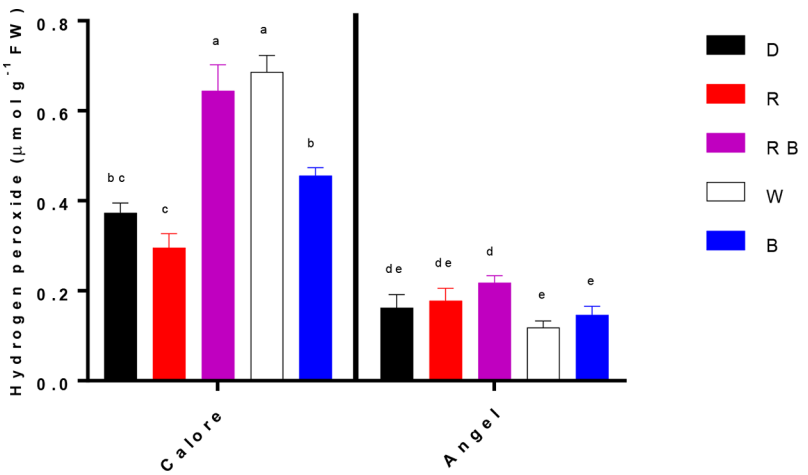

FIGURE 8 | Hydrogen peroxide content in the spathes of two cultivars of Anthurium cut flowers ('Calore' and 'Angel') held in the dark (D) or continuously exposed to 125 ± 5 µmol m^{-2} s^{v1} of different light spectra [white (W), red (R), red and blue (RB), blue (B)] following 14 days vase life at 4°C. Values are the means of three biological replicates, and bars indicate means ± SEM. Bars with different letters are significantly different (ANOVA, $P < 0.01$).

stomata (Elibox and Umaharan, 2008), and it has been shown that spathe water content depends on its stomatal conductance (Farrell et al., 2012). B spectrum can affect different processes in plants including stomatal opening and photosynthesis (Tibbitts et al., 1983; Mao et al., 2005; Whitelam and Halliday, 2008), and a wide range of publications supported the role of the B spectrum in stimulating stomatal opening (Kinoshita et al., 2001; Talbott et al., 2002; Hayashi et al., 2011). Although promotion of stomatal opening has been reported by both B and R spectra, the effect of R spectrum on stomatal opening is indirect. B spectrum can directly induce ion influx into the guard cells and as a result promotes stomatal opening (Kinoshita and Hayashi, 2011), whereas the promoting role of R spectrum on stomatal opening is *via* its effects on mesophyll photosynthesis and guard cell chloroplasts (Olsen et al., 2002; Suetsugu et al., 2014).

Although many studies reported the importance of light intensity during postharvest storage of horticultural crops, there are not many reports regarding the effects of light spectrum on quality of horticultural products (Kasim and Kasim, 2007; Noichinda et al., 2007; Martínez-Sánchez et al., 2011; Witkowska, 2013; van Meeteren and Aliniaeifard, 2016). Many of these studies related the effects of light on postharvest quality to its effects on photosynthesis process (Toledo et al.,

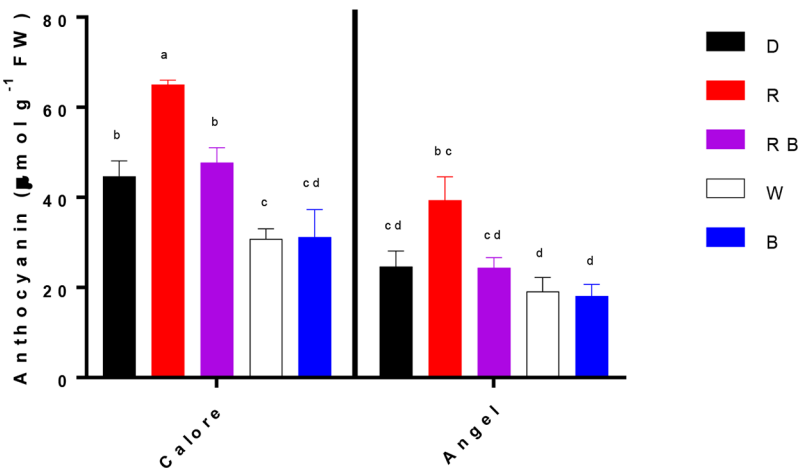

FIGURE 9 | Anthocyanin concentrations in the spathes of two cultivars of Anthurium cut flowers ('Calore' and 'Angel') held in the dark (D) or continuously exposed to 125 ± 5 μmol m^{-2} s^{-1} of different light spectra [white (W), red (R), red and blue (RB), blue (B)] following 14 days vase life at 4°C. Values are the means of three biological replicates, and bars indicate means ± SEM. Bars with different letters are significantly different (ANOVA, $P < 0.01$).

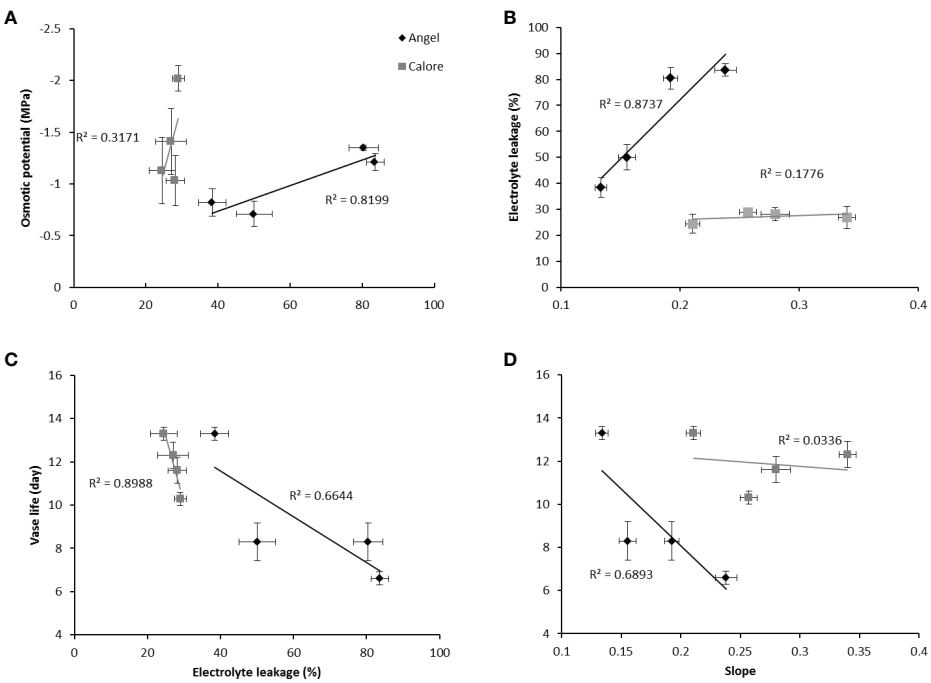

FIGURE 10 | Relationships between electrolyte leakage (EL) and osmotic potential **(A)**, EL and slope of the curve for accumulative percentage of water loss over time **(B)**, EL and vase life **(C)** and vase life and slope of the curve for percentage of water loss over time **(D)** for the spathes of two cultivars of Anthurium cut flowers ('Calore' and 'Angel') after 14 days of exposure to different light spectra at 4°C. Values are the means of six biological replicates for the vase life and slope and three biological replicates for electrolyte leakage and osmotic potential ± SEM.

2003; Noichinda et al., 2007; Martínez-Sánchez et al., 2011). In the current study we did not detect any photosynthetic activity in the spathe of Anthurium (data not shown), which is probably due to lack of chlorophyll pigments in the spathe of these two Anthurium cultivars. The observed effects of light therefore cannot be attributed to photosynthetic processes. As a consequence, the R spectrum cannot promote stomatal opening, which led to lower water loss from Anthurium spathes in comparison with B-containing spectral compositions (B, W, and RB) (**Figures 5** and **6**). In the present study,

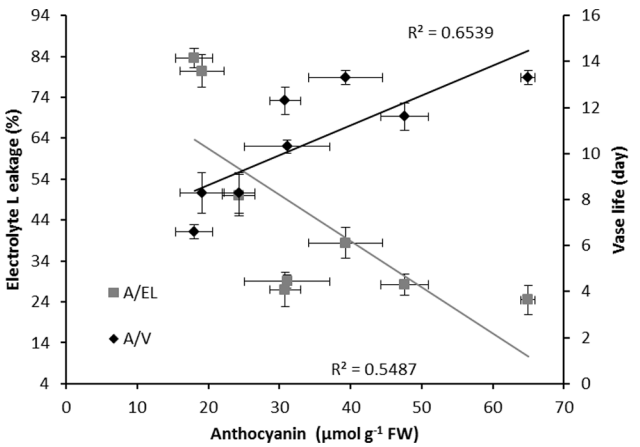

FIGURE 11 | Relationships between anthocyanin content (A), electrolyte leakage (EL) and vase life (V) of Anthurium cut flowers ('Calore' and 'Angel') after 14 days exposure to different light spectra at 4°C. Values are the means of six biological replicates for the vase life and three biological replicates for electrolyte leakage and anthocyanin ± SEM.

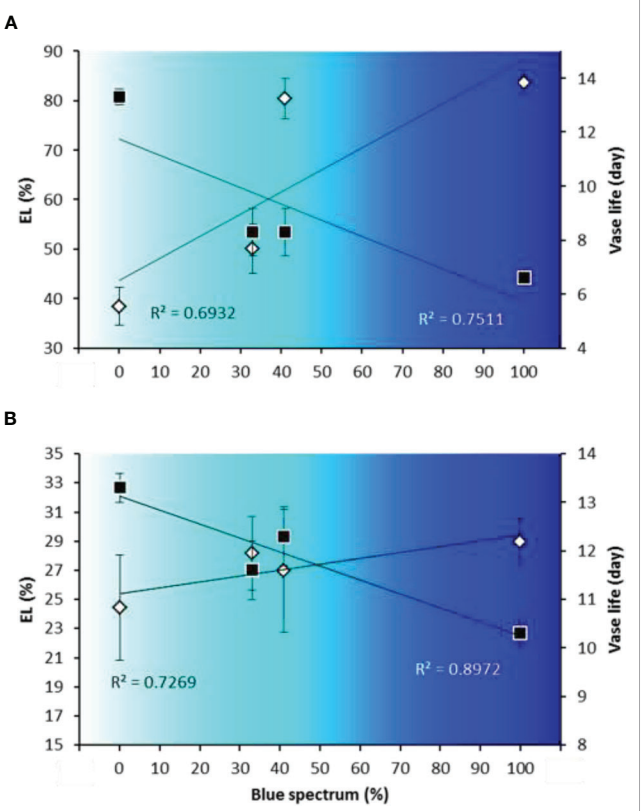

FIGURE 12 | Relationships between percentage of blue light (400–500 nm) in overall spectral light composition [B spectrum (%)] and electrolyte leakage (EL) at day 14 and vase life for spathes of Anthurium cut flowers ('Angel' [panel **(A)**] and 'Calore' [panel **(B)**]) at 4°C. Gray symbols stand for electrolyte leakage (EL), and black symbols stand for vase life. Values are the means of six biological replicates for the vase life and three biological replicates for EL ± SEM.

measuring stomatal conductance was not attainable due to low temperature. However, water loss is often closely related to stomatal conductance.

At first glance, it may be speculated that B spectrum triggers stomata opening and thus promotes water loss and EL, which is not favorable for the vase life. Although this idea holds true for 'Angel', it did not apply to 'Calore' where water loss was not correlated with the EL and vase life (**Figure 10**). Woltering and Paillart (2018) studied the relationships between stomatal functionality and vase life of two rose cultivars during low temperature storage. They found that depending on the cultivar, stomatal functionality (closing response following dehydration) is associated with water stress and vase life of the rose cultivars (Woltering and Paillart, 2018). Similar results were obtained for 'Angel'; however, no distinct correlation was found between water loss and vase life of 'Calore' (**Figure 10D**) indicating that other mechanisms are involved.

EL was correlated with osmotic potential (**Figure 10A**) and percentage of water loss (**Figure 10B**) in the spathe of Anthurium (especially for 'Angel'). Water loss induces alterations in cellular metabolism (Wang et al., 2014), resulting in accumulation of soluble carbohydrate and proline (Chaudhuri et al., 2017). In our experiment, no correlation was found between water loss percentage and proline or soluble carbohydrate concentrations among different light spectra. This partial contradiction in our findings compared to the previous reports can be due to the impact of low temperature on induction of osmotic solutes (Li, 2018). Accumulation of different osmotic substances results in a decline in osmotic potential (Chaudhuri et al., 2017) and as a result membrane deterioration (Shibairo et al., 2002). Loss of membrane integrity increases EL from the tissues. The relationship between the rate of water loss and changes in EL indicates that water loss in Anthurium spathes is associated with membrane injury and a decline in vase life (**Figure 10C**). However, the relationship between the rate of water loss with EL in 'Calore' was not the same as in 'Angel', and it seems the vase life is controlled by other mechanisms than those regulated with water loss. Farrell et al. (2012) showed that different mechanisms are involved in determining vase life of different cultivars of Anthurium cut flowers, and they concluded that compared to Anthurium cultivars with long vase life, cultivars with a short vase life have higher stomatal conductance and lower spathe RWC. Although, 'Angel' is considered as a long vase life Anthurium cultivar (more than 40 days), its vase life is dramatically decreased by exposure to low temperature during storage (3–20 days) (Promyou et al., 2012; Ketrodsakul et al., 2016). Therefore, it can be considered as a short vase life cultivar under cold storage conditions. Our results in the case of 'Angel' are in accordance with Farrell et al. (2012), who showed that spathes water holding capacity affects EL and as a result vase life of Anthurium spathes. In the current study, negative relationships (R^2 = 0.66 for 'Angel' and R^2 = 0.89 for 'Calore') were detected between EL and vase life for both Anthurium cultivars (**Figure 10C**). Similarly, increase in EL

due to low temperature exposure has been reported in spathes of different Anthurium cultivars (Farrell et al., 2012; Soleimani Aghdam et al., 2015; Soleimani Aghdam et al., 2016a).

ROS over-accumulation is one of the main reasons compromising cellular integrity (Mittler et al., 2004). However, no correlation was found between hydrogen peroxide levels and the vase life in Anthurium cultivars. 'Calore' with red spathe color had higher hydrogen peroxide content than 'Angel' under all studied light spectra (**Figure 8**), which further disapproves the involvement of hydrogen peroxide in determination of Anthurium vase life in cold storage.

Anthocyanins are plant pigments that usually accumulate in plant tissues in response to a wide range of stressors (Landi et al., 2015). These plant pigments can help plants to cope with light stress in two ways: by serving as a sun screen and through scavenging of free radicals (Landi et al., 2015). Apart from their sunscreen properties that restrict penetration of light into the plant tissues (Trojak and Skowron, 2017), anthocyanins through oxyradical scavenging activities can protect membranes and limit cell disruption (Takele, 2010; Zhang et al., 2012; Trojak and Skowron, 2017; Bayat et al., 2018). The ameliorative role of anthocyanins in different plant parts (*e.g.* leaf and fruit skin) in response to cold and light stresses has been reported (Sivankalyani et al., 2016; Bi et al., 2018). In Begonia leaves, elevation in transcript levels of the anthocyanin biosynthesis genes and as a consequence accumulation of anthocyanin was detected following six days of co-exposure to low temperature and light (300 µmol m^{-2} s^{-1}), while no increase in transcript levels of the anthocyanin biosynthesis genes and anthocyanin level was detected in plants exposed to the same condition and treated with 3-(3,4-dichlorophenyl)-1,1-dimethylurea (inhibitor of light mediated anthocyanin accumulation) or in plants exposed to 25/15°C (day/night) and 300 µmol m^{-2} s^{-1} light intensity (Bi et al., 2018). These findings are indicative of the production of anthocyanins possibly in response to light under low temperatures as protectants against excessive ROS production and subsequent chilling injury. In agreement with these findings, a negative relationship between anthocyanin concentration and EL of the spathe and a positive relationship between anthocyanin concentration and vase life were observed in the both studied Anthurium cultivars (**Figure 11**). The protective role of anthocyanins on cellular integrity has been previously reported in different plant species following exposure to different abiotic stresses (Takele, 2010; Trojak and Skowron, 2017; Bayat et al., 2018). Furthermore, the protective role of anthocyanins on membrane integrity during co-exposure of plant leaves to light and low temperature stresses has been reported (Krol et al., 1995; Hoch et al., 2001). However, in our research no significant relationship between anthocyanin concentration and H_2O_2 in the spathe was observed in both studied cultivars. It has been shown that anthocyanins mainly accumulate in the vacuole and not in the chloroplasts where ROS accumulation occurs (Wise, 1995). This suggests that antioxidant activity is not the main function of anthocyanins during cold–light stress (Hoch et al., 2001). In our study, the anthocyanins were mainly detected in the vacuole of the epidermal cells (**Supplemental Figure 1**). Confirming this result we did not detect any chlorophyll and as a result no photosystem II activity in both Anthurium cultivars. Therefore, due to the absence of chloroplast, we can conclude that anthocyanin mainly accumulated in the vacuole. It has been reported that anthocyanin accumulation is a response to high ROS level in the leaves (Xu and Rothstein, 2018). High original H_2O_2 content (**Supplemental Figure 2**) in the spathe of 'Calore' can be a reason for high anthocyanin content for this cultivar (**Supplemental Figure 3**).

Our result showed that a higher percentage of B in the spectral light composition during postharvest phase resulted in higher EL and as a result shorter vase life in Anthurium cut flowers under cold storage conditions (**Figure 4**). In accordance with our results, Yu et al. (2017) reported that in *Camptotheca acuminata* B spectrum can cause damage to the membrane and an increase in EL, while R spectrum can prevent ROS accumulation in the cells which prevents electrolyte leakage from the cells.

The different processes that are associated with the senescence in the two different cultivars in response to the percentage of B in the spectrum may be explained by assuming a dual role of B spectrum in cold stored Anthurium flowers (**Figure 13**). Original high ROS content causes accumulation of anthocyanins, as it is occurred for the Calore cultivar. Anthocyanin may be degraded by the B light but at the same time be used to neutralize the oxidative stress. B spectrum may induce oxidative stress, indirectly through its negative effects on anthocyanin content

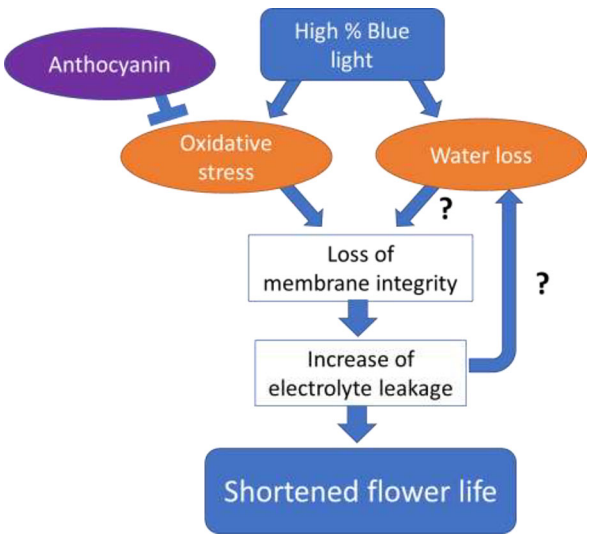

FIGURE 13 | Hypothetical model for the effect of Blue light spectrum on Anthuriun vase life under chilling conditions. Original high ROS content causes accumulation of anthocyanins, but cold-induced oxidative stress breaks down anthocyanins. Anthocyanin may be degraded by Blue light but at the same time be used to neutralize the oxidative stress. Blue spectrum may affect stomatal conductance leading to water loss, changes in osmotic potential, decreasing membrane integrity and finally spathe senescence. Blue spectrum may at the same time induce oxidative stress, leading to loss of membrane integrity, electrolyte leakage and spathe senescence. Both routes may interact with each other.

or directly leading to loss of membrane integrity, electrolyte leakage, and senescence. In both cultivars there were significant correlations between the vase life and ion leakage and anthocyanin. This indicates that this route is important in explaining the effect of B light. The magnitude of the effect of B light was less in 'Calore' than in 'Angel'; this may be related to the higher amount of anthocyanin naturally present in the spathe of 'Calore' (**Supplemental Figure 3**). On the other hand, the B spectrum may affect stomatal conductance leading to increased water loss, changes in osmotic potential and as a result loss of membrane integrity and senescence. Both routes may interact with each other.

In 'Angel', in addition to the oxidative stress route, there were also good correlations between the vase life and water loss, which was much less in the case of 'Calore'. This is caused by the relation between the percentage of the B light spectrum and the water loss. In 'Angel', water loss shows a linear relation with the percentage of the B light spectrum, indicating that stomatal conductance increases with increasing B spectrum; in 'Calore', however, maximum water loss occurs in 40% of B in the spectrum (**Figure 4**). The observations that in both cultivars there are good correlations between the vase life and the factors of the oxidative stress route indicate that the oxidative stress route is more important than the water loss route for the explanation of the effect of B light under these specific conditions (lighting in the cold condition).

This study is the first report showing the importance of light quality on determination of vase life of Anthurium under cold temperatures. However, further investigations regarding the effects of different temperatures, different intensities of light spectra and a wide range of Anthurium cultivars are needed to reach a practical solution for low temperature storage of cut Anthurium.

CONCLUSION

Anthurium is a tropical cold sensitive plant, which needs to be stored at 12.5–20°C. In the winter time and in cold environments, chilling injuries to Anthurium spathes decrease its marketability. Here, we showed that the spectral light composition during storage of Anthurium cut flowers is an important environmental factor determining postharvest flower performance. A high percentage of B in the light spectrum was associated with increased EL of the spathe and a shorter vase life. Therefore, postharvest handling of Anthurium cut flowers should preferably be performed in an environment with limited B spectrum when exposures to low temperatures are inevitable.

DATA AVAILABILITY STATEMENT

All datasets generated for this study are included in the article/ **Supplementary Material**.

AUTHOR CONTRIBUTIONS

SA made substantial contributions to conception and design, also performed statistical analysis, drafted the manuscript, and critically revised the final version. ZF carried out the experiments, collected and critically analyzed the scientific literature, and helped in the writing of the manuscript. SD took part in designing and planning the experiments, preparing of material for the experiment. TL helped in the preparation of material for the experiment and took part in designing and planning of the experiments and critical revision of the final manuscript. EW contributed to conception and design of the final manuscript, scientific discussion, and critical revision of the final manuscript.

ACKNOWLEDGMENTS

We thank Iran Grow light company for providing LEDs and projectors. We would also like to thank The National Natural Science Foundation of China (No.31872955), Iran National Science Foundation (INSF) (grant number 96006991), and University of Tehran for their support.

SUPPLEMENTARY MATERIAL

The Supplementary Material for this article can be found online at: https://www.frontiersin.org/articles/10.3389/fpls.2020.00846/full#supplementary-material

REFERENCES

Arnon, D. I. (1949). Copper enzymes in isolated chloroplasts. Polyphenoloxidase in *Beta vulgaris*. *Plant Physiol.* 24, 1–15. doi: 10.1104/pp.24.1.1

Bates, L., Waldren, R., and Teare, I. (1973). Rapid determination of free proline for water-stress studies. *Plant Soil.* 39, 205–207. doi: 10.1007/BF00018060

Bayat, L., Arab, M., Aliniaeifard, S., Seif, M., Lastochkina, O., and Li, T. (2018). Effects of growth under different light spectra on the subsequent high light tolerance in rose plants. *AoB Plants.* 10, ply052. doi: 10.1093/aobpla/ply052

Bi, H., Guo, M., Wang, J., Qu, Y., Du, W., and Zhang, K. (2018). Transcriptome analysis reveals anthocyanin acts as a protectant in *Begonia semperflorens* under low temperature. *Acta Physiol. Plant* 40, 10.

Breive, K., Tamulaitis, G., Duchovskis, P., Bliznikas, Z., Ulinskaite, R., Brazaityte, A., et al. (2005). High-power light-emitting diode based facility for plant cultivation. *J. Physics.* 38, 3182–3187. doi: 10.1088/0022-3727/38/17/S20

Chaudhuri, P., Rashid, N., and Thapliyal, C. (2017). "Osmolyte System and Its Biological Significance" in *Cellular Osmolytes*. Eds. L. Rajendrakumar Singh and T. Dar. (Singapore: Springer). doi: 10.1007/978-981-10-3707-8_1

Darko, E., Heydarizadeh, P., Schoefs, B., and Sabzalian, M. R. (2014). Photosynthesis under artificial light: the shift in primary and secondary metabolism. *Phil. Trans. R. Soc B.* 369, 20130243. doi: 10.1098/rstb.2013.0243

Elibox, W., and Umaharan, P. (2008). Morphophysiological characteristics associated with vase life of cut flowers of anthurium. *Hort. Sci.* 43, 825–831. doi: 10.21273/HORTSCI.43.3.825

Faragher, J. D., Mayak, S., Tirosh, T., and Halevy, A. H. (1984). Cold storage of rose flowers: Effects of cold storage and water loss on opening and vase life of 'Mercedes' roses. *Sci. Hortic.* 24, 369–378. doi: 10.1016/0304-4238(84)90122-5

Farrell, A. D., Evelyn, S., Lennon, A. M., and Umaharan, P. (2012). Genotypic variation in senescence and water relations in cut flowers of *Anthurium andraeanum* (Hort.). *Hort. Sci.* 47, 1333–1337. doi: 10.21273/HORTSCI.47.9.1333

Gruda, N. (2005). Impact of environmental factors on product quality of greenhouse vegetables for fresh consumption. *Crit. Rev. Plant Sci.* 24, 227–247. doi: 10.1080/07352680591008628

Hayashi, M., Inoue, S.-I., Takahashi, K., and Kinoshita, T. (2011). Immunohistochemical detection of blue light-induced phosphorylation of the plasma membrane H^+-ATPase in stomatal guard cells. *Plant Cell Physiol.* 52, 1238–1248. doi: 10.1093/pcp/pcr072

Hoch, W. A., Zeldin, E. L., and McCown, B. H. (2001). Physiological significance of anthocyanins during autumnal leaf senescence. *Tree Physiol.* 21, 1–8. doi: 10.1093/treephys/21.1.1

Hogewoning, S. W., Trouwborst, G., Maljaars, H., Poorter, H., van Ieperen, W., and Harbinson, J. (2010). Blue light dose–responses of leaf photosynthesis, morphology, and chemical composition of *Cucumis sativus* grown under different combinations of red and blue light. *J. Exp. Bot.* 61, 3107–3117. doi: 10.1093/jxb/erq132

Hosseini, A., Zare Mehrjerdi, M., and Aliniaeifard, S. (2018). Alteration of bioactive compounds in two varieties of Basil (*Ocimum basilicum*) grown under different light spectra. *J. Essent. Oil-Bear. Plants.* 21, 913–923. doi: 10.1080/0972060X.2018.1526126

Hosseini, A., Zare Mehrjerdi, M., Aliniaeifard, S., and Seif, M. (2019). Photosynthetic and growth responses of green and purple basil plants under different spectral compositions. *Physiol. Mol. Biol. Plants.* 25, 741–752. doi: 10.1007/s12298-019-00647-7

Kamemoto, H. (1962). Some factors affecting the keeping quality of anthurium flowers. *Hawaii Farm Sci.* 11, 204.

Kasim, R., and Kasim, M. U. (2007). Inhibition of yellowing in Brussels sprouts (*B. oleraceae* var. gemmifera) and broccoli (*B. oleraceae* var. italica) using light during storage. *J. Food Agric. Environ.* 5, 126.

Ketrodsakul, A., Choosung, P., Penchaiya, P., and Buanong, M. (2016). Effect of calcium on chilling injury of Anthurium'Angel'cut flower. *Acta Hortic.* 1131, 65–72. doi: 10.17660/ActaHortic.2016.1131.9

Kim, S. J., Hahn, E. J., Heo, J. W., and Paek, K. Y. (2004). Effects of LEDs on net photosynthetic rate, growth and leaf stomata of chrysanthemum plantlets *in vitro*. *Sci. Hortic.* 101, 143–151. doi: 10.1016/j.scienta.2003.10.003

Kinoshita, T., and Hayashi, Y. (2011). New insights into the regulation of stomatal opening by blue light and plasma membrane H^+-ATPase. *Int. Rev. Cell Mol. Biol.* 289, 89–115. doi: 10.1016/B978-0-12-386039-2.00003-1

Kinoshita, T., Doi, M., Suetsugu, N., Kagawa, T., Wada, M., and Shimazaki, K. I. (2001). Phot1 and phot2 mediate blue light regulation of stomatal opening. *Nature* 414, 656–660. doi: 10.1038/414656a

Kozai, T., Niu, G., and Takagaki, M. (2015). *Plant factory: an indoor vertical farming system for efficient quality food production* (Elsevier. Amesterdam: Academic Press).

Krol, M., Gray, G., Huner, N., Hurry, V., Öquist, G., and Malek, L. (1995). Low-temperature stress and photoperiod affect an increased tolerance to photoinhibition in *Pinus banksiana* seedlings. *Can. J. Bot.* 73, 1119–1127. doi: 10.1139/b95-122

Landi, M., Tattini, M., and Gould, K. S. (2015). Multiple functional roles of anthocyanins in plant-environment interactions. *Environ. Exp. Bot.* 119, 4–17. doi: 10.1016/j.envexpbot.2015.05.012

Li, P. H. (2018). *Low temperature stress physiology in crops* (New York: CRC press). doi: 10.1016/B978-0-124-60560-2.X5001-8

Mao, J., Zhang, Y.-C., Sang, Y., Li, Q.-H., and Yang, H.-Q. (2005). A role for Arabidopsis cryptochromes and *COP1* in the regulation of stomatal opening. *Proc. Natl. Acad. Sci. U. S. A.* 102, 12270–12275. doi: 10.1073/pnas.0501011102

Martínez-Sánchez, A., Tudela, J. A., Luna, C., Allende, A., and Gil, M. I. (2011). Low oxygen levels and light exposure affect quality of fresh-cut Romaine lettuce. *Postharvest Biol. Technol.* 59, 34–42. doi: 10.1016/j.postharvbio.2010.07.005

Martìnez, J.-P., Lutts, S., Schanck, A., Bajji, M., and Kinet, J.-M. (2004). Is osmotic adjustment required for water stress resistance in the Mediterranean shrub *Atriplex halimus* L? *J. Plant Physiol.* 161, 1041–1051. doi: 10.1016/j.jplph.2003.12.009

Massa, G. D., Kim, H.-H., Wheeler, R. M., and Mitchell, C. A. (2008). Plant productivity in response to LED lighting. *Hort. Sci.* 43, 1951–1956. doi: 10.21273/HORTSCI.43.7.1951

Mittler, R., Vanderauwera, S., Gollery, M., and Van Breusegem, F. (2004). Reactive oxygen gene network of plants. *Trends Plant Sci.* 9, 490–498. doi: 10.1016/j.tplants.2004.08.009

Morrow, R. C. (2008). LED lighting in horticulture. *Hort. Sci.* 43, 1947–1950. doi: 10.21273/HORTSCI.43.7.1947

Mujaffar, S., and Sankat, C. (2003). Effect of waxing on the water balance and keeping qualities of cut anthuriums. *Int. Agrophysics.* 17, 77–84.

Noichinda, S., Bodhipadma, K., Mahamontri, C., Narongruk, T., and Ketsa, S. (2007). Light during storage prevents loss of ascorbic acid, and increases glucose and fructose levels in Chinese kale (*Brassica oleracea* var. alboglabra). *Postharvest Biol. Technol.* 44, 312–315. doi: 10.1016/j.postharvbio.2006.12.006

Olsen, R. L., Pratt, R. B., Gump, P., Kemper, A., and Tallman, G. (2002). Red light activates a chloroplast-dependent ion uptake mechanism for stomatal opening under reduced CO_2 concentrations in *Vicia* spp. *New Phytol.* 153, 497–508. doi: 10.1046/j.0028-646X.2001.00337.x

Ouzounis, T., Fretté, X., Rosenqvist, E., and Ottosen, C.-O. (2014). Spectral effects of supplementary lighting on the secondary metabolites in roses, chrysanthemums, and campanulas. *J. Plant Physiol.* 171, 1491–1499. doi: 10.1016/j.jplph.2014.06.012

Ouzounis, T., Heuvelink, E., Ji, Y., Schouten, H., Visser, R., and Marcelis, L. (2016). Blue and red LED lighting effects on plant biomass, stomatal conductance, and metabolite content in nine tomato genotypes. *Acta Hortic.* 1134, 251–258. doi: 10.17660/ActaHortic.2016.1134.34

Patterson, B. D., MacRae, E. A., and Ferguson, I. B. (1984). Estimation of hydrogen peroxide in plant extracts using titanium (IV). *Anal. Biochem.* 139, 487–492. doi: 10.1016/0003-2697(84)90039-3

Paull, R., and Goo, T. (1982). Pulse treatment with silver nitrate extends vase life of anthuriums [flower handling, senescence]. *J. Am. Soci. Hortic. Sci.* 107, 842–44.

Promyou, S., and Ketsa, S. (2014). Cultivar difference in sensitivity to chilling injury of anthurium flowers (*Anthurium andraeanum*) during low temperature storage. *Acta Hortic.* 1025, 179–185. doi: 10.17660/ActaHortic.2014.1025.26

Promyou, S., Ketsa, S., and van Doorn, W. G. (2012). Salicylic acid alleviates chilling injury in anthurium (*Anthurium andraeanum* L.) flowers. *Postharvest Biol. Technol.* 64, 104–110. doi: 10.1016/j.postharvbio.2011.10.002

Rajapakse, N. C., and Kelly, J. W. (1994). Influence of spectral filters on growth and postharvest quality of potted miniature roses. *Sci. Hortic.* 56, 245–255. doi: 10.1016/0304-4238(94)90006-X

Ranwala, A. P., and Miller, W. B. (2000). Preventive mechanisms of gibberellin 4+7 and light on low-temperature-induced leaf senescence in *Lilium* cv. Stargazer. *Postharvest Biol. Technol.* 19, 85–92. doi: 10.1016/S0925-5214(00)00072-7

Reid, M. S., and Jiang, C. Z. (2012). Postharvest biology and technology of cut flowers and potted plants. *Hortic. Rev.* 40, 1–54. doi: 10.1002/9781118351871.ch1

Sankat, C. K., and Mujaffar, S. (1994). Water balance in cut anthurium flowers in storage and its effect on quality. *Acta Hortic.* 368, 723–732. doi: 10.17660/ActaHortic.1994.368.86

Shibairo, S. I., Upadhyaya, M. K., and Toivonen, P. M. A. (2002). Changes in water potential, osmotic potential, and tissue electrolyte leakage during mass loss in carrots stored under different conditions. *Sci. Hortic.* 95, 13–21. doi: 10.1016/S0304-4238(02)00034-1

Sivankalyani, V., Feygenberg, O., Diskin, S., Wright, B., and Alkan, N. (2016). Increased anthocyanin and flavonoids in mango fruit peel are associated with cold and pathogen resistance. *Postharvest Biol. Technol.* 111, 132–139. doi: 10.1016/j.postharvbio.2015.08.001

Soleimani Aghdam, M., Naderi, R., Sarcheshmeh, M. A. A., and Babalar, M. (2015). Amelioration of postharvest chilling injury in anthurium cut flowers by γ-aminobutyric acid (GABA) treatments. *Postharvest Biol. Technol.* 110, 70–76. doi: 10.1016/j.postharvbio.2015.06.020

Soleimani Aghdam, M., Jannatizadeh, A., Sheikh-Assadi, M., and Malekzadeh, P. (2016a). Alleviation of postharvest chilling injury in anthurium cut flowers by salicylic acid treatment. *Sci. Hortic.* 202, 70–76. doi: 10.1016/j.scienta.2016.02.025

Soleimani Aghdam, M., Naderi, R., Jannatizadeh, A., Sarcheshmeh, M. A. A., and Babalar, M. (2016b). Enhancement of postharvest chilling tolerance of anthurium cut flowers by γ-aminobutyric acid (GABA) treatments. *Sci. Hortic.* 198, 52–60. doi: 10.1016/j.scienta.2015.11.019

Soleimani Aghdam, M., Naderi, R., Malekzadeh, P., and Jannatizadeh, A. (2016c). Contribution of GABA shunt to chilling tolerance in anthurium cut flowers in response to postharvest salicylic acid treatment. *Sci. Hortic.* 205, 90–96. doi: 10.1016/j.scienta.2016.04.020

Suetsugu, N., Takami, T., Ebisu, Y., Watanabe, H., Iiboshi, C., Doi, M., et al. (2014). Guard cell chloroplasts are essential for blue light-dependent stomatal opening in Arabidopsis. *PloS One* 9, e108374. doi: 10.1371/journal.pone.0108374

Takele, A. (2010). Differential responses of electrolyte leakage and pigment compositions in maize and sorghum after exposure to and recovery from pre- and post-flowering dehydration. *Agr. Sci. China.* 9, 813–824. doi: 10.1016/S1671-2927(09)60159-0

Talbott, L. D., Nikolova, G., Ortiz, A., Shmayevich, I., and Zeiger, E. (2002). Green light reversal of blue-light-stimulated stomatal opening is found in a diversity of plant species. *Am. J. Bot.* 89, 366–368. doi: 10.3732/ajb.89.2.366

Tennessen, D. J., Singsaas, E. L., and Sharkey, T. D. (1994). Light-emitting diodes as a light source for photosynthesis research. *Photosynth. Res.* 39, 85–92. doi: 10.1007/BF00027146

Tibbitts, T., Morgan, D., and Warrington, I. (1983). Growth of lettuce, spinach, mustard, and wheat plants under four combinations of high-pressure sodium, metal halide, and tungsten halogen lamps at equal PPFD. *J. Amer. Soc Hortic. Sci.* 108, 622–630.

Toledo, M., Ueda, Y., Ayaki, M., Yamauchi, N., and Abe, K. (2003). Photosynthetic abilities of spinach (*Spinacia oleracea* L.) leaves during postharvest storage under light and dark conditions. *J. Hortic. Sci. Biotech.* 78, 375–380. doi: 10.1080/14620316.2003.11511634

Trojak, M., and Skowron, E. (2017). Role of anthocyanins in high-light stress response. *World Sci. News.* 81, 150–168.

van Doorn, W. G. (2012). Water relations of cut flowers: an update. *Hortic. Rev.* 40, 55–106. doi: 10.1002/9781118351871.ch2

van Meeteren, U., and Aliniaeifard, S. (2016). *Stomata and postharvest physiology. Postharvest ripening physiology of crops* (Boca Raton, FL, USA: CRC Press), 157–216.

Wagner, G. J. (1979). Content and vacuole/extravacuole distribution of neutral sugars, free amino acids, and anthocyanin in protoplasts. *Plant Physiol.* 64, 88–93. doi: 10.1104/pp.64.1.88

Wang, W.-H., Chen, J., Liu, T.-W., Han, A.-D., Simon, M., Dong, X.-J., et al. (2014). Regulation of the calcium-sensing receptor in both stomatal movement and photosynthetic electron transport is crucial for water use efficiency and drought tolerance in Arabidopsis. *J. Exp. Bot.* 65, 223–234. doi: 10.1093/jxb/ert362

Whitelam, G. C., and Halliday, K. J. (2008). *Annual plant reviews, light and plant development* (United Kingdom: John Wiley & Sons).

Wise, R. R. (1995). Chilling-enhanced photooxidation: the production, action and study of reactive oxygen species produced during chilling in the light. *Photosynth. Res.* 45, 79–97. doi: 10.1007/BF00032579

Witkowska, I. M. (2013). *Factors affecting the postharvest performance of fresh-cut lettuce. PhD thesis* (Netherlands: Wageningen University). ISBN 978-94-6173-574-4.

Woltering, E. J., and Paillart, M. J. M. (2018). Effect of cold storage on stomatal functionality, water relations and flower performance in cut roses. *Postharvest Biol. Technol.* 136, 66–73. doi: 10.1016/j.postharvbio.2017.10.009

Xu, Z., and Rothstein, S. J. (2018). ROS-induced anthocyanin production provides feedback protection by scavenging ROS and maintaining photosynthetic capacity in Arabidopsis. *Plant Signal. Behav.* 13, 1364–1377.

Yu, W., Liu, Y., Song, L., Jacobs, D. F., Du, X., Ying, Y., et al. (2017). Effect of differential light quality on morphology, photosynthesis, and antioxidant enzyme activity in *Camptotheca acuminata* seedlings. *J. Plant Growth Regul.* 36, 148–160. doi: 10.1007/s00344-016-9625-y

Zhang, Q., Su, L.-J., Chen, J.-W., Zeng, X.-Q., Sun, B.-Y., and Peng, C.-L. (2012). The antioxidative role of anthocyanins in Arabidopsis under high-irradiance. *Biol. Plant* 56, 97–104. doi: 10.1007/s10535-012-0022-5

Conflict of Interest: The authors declare that the research was conducted in the absence of any commercial or financial relationships that could be construed as a potential conflict of interest.

frontiers in Plant Science

ORIGINAL RESEARCH
published: 16 June 2020
doi: 10.3389/fpls.2020.00826

Isolation of Rhizosphere Bacteria That Improve Quality and Water Stress Tolerance in Greenhouse Ornamentals

*Nathan P. Nordstedt and Michelle L. Jones**

Department of Horticulture and Crop Science, Ohio Agricultural Research and Development Center, The Ohio State University, Wooster, OH, United States

Water deficit stress is a major contributor to the loss of ornamental crop value due to its negative effects on plant growth and flowering. In addition, post-production water stress can reduce the photosynthetic capacity of plants, negatively impacting crop quality at retail and in the consumer's home and garden. While the application of microbe-containing biostimulant products can increase stress tolerance and crop quality, the success of most commercially available biostimulants in greenhouse production systems is inconsistent. To identify beneficial bacteria with consistent biostimulant activity in greenhouse ornamentals, our study isolated bacteria from the rhizosphere of water stressed greenhouse ornamentals. Five species of popular ornamentals were obtained from 15 different commercial greenhouse facilities and then subjected to three cycles of water stress. Over 1,000 bacterial isolates were collected from the rhizosphere and screened *in vitro* for osmoadaptability and 1-aminocyclopropane-1-carboxylate (ACC) deaminase activity. Eighty selected isolates were evaluated in a high-throughput greenhouse trial for their ability to increase plant size and flower number of water-stressed *Petunia* × *hybrida*. Ten bacterial strains selected from the high-throughput trial were then evaluated in a greenhouse validation trial for their ability to increase plant growth and to mitigate the reduction in photosynthetic parameters of water stressed *P. hybrida* and *Pelargonium* × *hortorum*. Application of certain bacteria increased plant size in both species and flower number of *P. hybrida* after recovery from water stress when compared to untreated water stressed plants. In addition, bacteria application increased the chlorophyll fluorescence parameters including quantum yield and efficiency of photosystem II (PSII) and electron transport rate (ETR), while decreasing the extent of electrolyte leakage during water stress and recovery. Overall, this study identified bacterial strains that can increase tolerance to and recovery from water stress in two commercially important ornamental crop species.

Keywords: drought, floriculture, horticulture, photosynthesis, plant–microbe interaction, plant growth promoting rhizobacteria, post-production

OPEN ACCESS

Edited by:
Margherita Irene Beruto, Istituto Regionale per la Floricoltura (IRF), Italy

Reviewed by:
Renaud Canaguier, NIXE LABORATOIRE, France
Barbara De Lucia, University of Bari Aldo Moro, Italy

***Correspondence:**
Michelle L. Jones
jones.1968@osu.edu

Specialty section:
This article was submitted to Crop and Product Physiology, a section of the journal Frontiers in Plant Science

Received: *05 April 2020*
Accepted: *22 May 2020*
Published: *16 June 2020*

Citation:
Nordstedt NP and Jones ML (2020) Isolation of Rhizosphere Bacteria That Improve Quality and Water Stress Tolerance in Greenhouse Ornamentals. Front. Plant Sci. 11:826. doi: 10.3389/fpls.2020.00826

INTRODUCTION

Water stress during ornamental plant production impacts crop quality by reducing plant size and flower number, and increasing leaf yellowing and plant wilting (Sánchez-Blanco et al., 2009). These impacts are particularly detrimental to ornamental crops because their value is largely dependent on their appearance. In addition, water stress can have a long-term negative impact on photosynthetic parameters and plant health (Caser et al., 2017). Maintaining optimal photosynthetic efficiency, yield, and electron transport rate (ETR) are essential for protecting plants from photoinhibition during abiotic stress (Singh and Raja Reddy, 2011), and water deficits can lead to decreases in these parameters even before visible symptoms occur (Galmés et al., 2007; Naumann et al., 2007; Singh and Raja Reddy, 2011; Huang et al., 2013).

Plants unable to maintain health and quality under stressful conditions are likely to become unsalable at retail. It has been estimated that 20–30% of ornamental plants either become unmarketable or must be sold at a reduced price because of exposure to environmental extremes (i.e., abiotic stress) or poor post-production care and handling (Nelson and Carlson, 1987; Armitage, 1993; Healy, 2009). In addition to the more obvious impacts on visual qualities, abiotic stress can also permanently affect photosynthesis, such that plants are unable to fully recover and regain photosynthetic capacity equivalent to pre-stress levels (Armitage et al., 1983). Plants that have reduced photosynthetic efficiency may not grow as well in the consumer's home or garden, and their ability to survive under subsequent exposure to stresses will be reduced (Siddique et al., 2016). Therefore, growers need additional tools to make ornamental plants more tolerant of abiotic stresses and reduce crop losses.

A potential tool for growers to increase plant tolerance to abiotic stress is the application of plant growth promoting rhizobacteria (PGPR), a class of microorganisms that can colonize plant roots and produce enzymes and secondary metabolites that positively influence plant stress tolerance. Noteable PGPR include many genera such as *Acinetobacter*, *Agrobacterium*, *Arthobacter*, *Azospirillum*, *Bacillus*, *Bradyrhizobium*, *Burkholderia*, *Pseudomonas*, *Rhizobium*, and *Serratia* (Goswami et al., 2016). In particular, the application of PGPR in ornamental plant production can be used to enhance plant stress tolerance and increase plant health and quality under water deficient conditions. Recent studies have shown that the application of different PGPR can enhance plant quality by increasing plant size and flower number in greenhouse ornamental species when grown under normal conditions or subjected to abiotic stress (Göre and Altin, 2006; Flores et al., 2007; Hoda and Mona, 2014; Leoni et al., 2019; Nordstedt et al., 2020). However, to positively influence the quality of plants subjected to abiotic stress, the PGPR must first induce physiological changes that increase plant stress tolerance, allowing the plant to better overcome the stress during recovery (Yang et al., 2009).

Increased plant stress tolerance can be accomplished through a variety of mechanisms, many of which are likely interconnected. A key mechanism for PGPR to induce stress tolerance in plants is to modify hormone levels, resulting in enhanced growth. PGPR can reduce stress-induced ethylene in plants via the production of the enzyme 1-aminocyclopropane-1-carboxylate (ACC) deaminase, which acts by cleaving ACC, the direct precursor to ethylene (Klee et al., 1991). Through the activity of ACC deaminase, stress ethylene remains below inhibitory levels, allowing plants to maintain normal root growth and contributing to delayed senescence under water stress (Glick et al., 2007). The onset of water stress can also reduce the endogenous levels of auxin produced in plants (Nilsen and Orcutte, 1996), which can be partially mediated by bacterial auxin production (Ngumbi and Kloepper, 2016). Elevated levels of abscisic acid (ABA) modulate plant physiological processes during water stress such as stomatal closure and reduction in carboxylation, which temporarily saves resources by reducing energy production (Farooq et al., 2009). Application of PGPR can offset this energy loss by stimulating photosynthesis while also increasing ABA content and water use efficiency in water stressed arabidopsis (Bresson et al., 2013; Cohen et al., 2015).

In addition to regulating upstream processes such as phytohormone production, stomatal closure, and carboxylation levels, PGPR can also positively influence parameters such as membrane integrity and the quantum efficiency of photosystem II (PSII) in plants during water stress and recovery. PGPR reduce electrolyte leakage in water stressed plants by increasing membrane integrity, which leads to improved recovery after stress (Vardharajula et al., 2011; Jodeh et al., 2015; Tiwari et al., 2016). Measuring the quantum efficiency of PSII in plants under severe water stress can serve as an indicator of plant health during stress and recovery. Application of *Bacillus* spp. to potato and *Burkholderia phytofirmans* and *Enterobacter* sp. to maize significantly increased the quantum efficiency of PSII in these plants under severe water stress (Gururani et al., 2013; Naveed et al., 2014).

As resources like water become increasingly limited, all of agriculture, including the greenhouse industry, will need to adopt solutions that will allow them to continue producing high quality crops with fewer inputs. The application of PGPR in the form of commercial products (biostimulants) is a promising tool to produce more resilient crops with the ability to withstand severe water stress while maintaining health and quality during recovery. Unfortunately, most biostimulant research has focused on field crops, and the efficacy of these products in greenhouse production can be highly variable (Paulitz and Richard, 2001; Ngumbi and Kloepper, 2016). Noteable differences in greenhouse production compared to field production are the use of soilless media with less biodiversity, production in containerized systems, and increased frequency of fertilizer application (Montagne et al., 2017). Microbial inoculants have been isolated from a variety of natural environments, most of which are drastically different than controlled environment greenhouse production systems. The surrounding environment dramatically influences the root-associated bacterial communities, and results from other trials may not translate into practical applications if cultural inputs are not similar (Ngumbi and Kloepper, 2016).

Studies have shown that isolating bacteria from environments that are similar to ones they will be used in is an effective strategy

for identifying PGPR strains for a particular cropping system (Zahir et al., 2008; Ali et al., 2013). In particular, the isolation of bacteria directly from the rhizosphere of plants subjected to water deficit conditions can identify PGPR with the ability to confer water stress tolerance when applied to other plants (Liu et al., 2013; Wang et al., 2014; Huang et al., 2017; Yasmin et al., 2017; Raheem et al., 2018). Therefore, the aim of this study was to establish a novel collection of bacteria for the purpose of identifying strains that improve ornamental plant tolerance to water stress. The bacteria were isolated from the rhizosphere of plants grown in controlled environment greenhouse systems and subjected to severe water deficit. The isolated bacteria were screened using a previously established pipeline (Nordstedt et al., 2020) and then evaluated for their ability to improve the growth, quality, and overall health of two economically important ornamental plant species.

MATERIALS AND METHODS

Isolation of Rhizospheric Bacteria From Greenhouse-Grown Ornamental Plants

Solenostemon scutellarioides (coleus), *Petunia* × *hybrida* (petunia), *Pelargonium* × *hortorum* (geranium), *Catharanthus roseus* (vinca), and *Zinnia elegans* (zinnia) plants at the mature flowering stage, which had been grown alongside other plants throughout their production cycle, were collected from 15 greenhouse ornamental production facilities in Ohio and West Virginia. These greenhouse facilities were selected for their diversity in environmental and cultural practices (i.e., water source, substrate composition, and chemical inputs). Irrigation water sources between greenhouse facilities varied between municipal/city, well, and recirculated pond water. Fertilizer rates and timing varied between greenhouses; however, each facility fertilized with at least 100 mg L^{-1} N at each fertilization. The soilless growing media components were vastly different between growers and consisted of a variety of formulations using peat, perlite, rice hulls, pine bark, and wood fiber. Plants were brought to the Ohio Agricultural Research and Development Center (Wooster, OH, United States) research greenhouses and subjected to water stress by removing all irrigation until plants were visibly wilted, and then rewatering so that plants regained turgidity. This cycle of wilting and recovery was repeated three times. The stress was repeated to induce plant stress signaling responses and changes to the rhizospheric environment. These changes can alter the microbial population in the rhizosphere, providing a higher likelihood of selecting strains with the ability to withstand water stress (Naylor and Coleman-Derr, 2018).

Following the third water stress cycle, excess potting media was removed from the root system and a 5-g root sample was collected. Samples were vortexed for 1 min in 25 mL sterile H_2O and then sonicated at 117 V for 1 min (Branson 2200 Ultrasonic Cleaner, Shelton, CT, United States). A 1-mL aliquot of this sample was serial diluted in sterile H_2O and 100 μL of 10^{-2}, 10^{-3}, and 10^{-4} diluted solutions were plated onto 1X King's Media B (KMB) agar plates supplemented with 100 μg/mL cycloheximide to prevent fungal growth. In addition, a 1-mL aliquot of each sample was added to 4 mL 0.1X Tryptic Soy Broth (TSB) and incubated at 65°C for 30 min to select for spore-forming bacteria, while preventing growth of film-producing bacteria such as *Pseudomonas* sp. (Fall et al., 2004; Gutierrez, 2004). The heat-treated samples were serial diluted in sterile H_2O and 100 μL of 10^{-2}, 10^{-3}, and 10^{-4} diluted solutions were plated onto 0.1X TSB agar plates supplemented with 100 μg/mL cycloheximide. Agar plates were incubated at 28°C for 48 h followed by 48 h at 4°C to allow for any color development between different isolates. Following incubation, bacterial isolates of unique morphology were struck into single cultures and then stored in 25% glycerol stocks at −80°C. This collection is referred to as the greenhouse rhizosphere collection.

In vitro Selection of Osmoadaptive Bacteria

An *in vitro* osmoadaptability bioassay was conducted according to Nordstedt et al. (2020) for the selection of the most osmotic stress tolerant bacteria within the greenhouse rhizosphere collection. Briefly, a sterile 96-well microplate replicator (Boekel Scientific, Feasterville, PA, United States, Model 140500) was used to transfer glycerol freezer stocks of each isolate into separate wells of a 96-well microtiter plate pre-filled with 200 μL Luria-Bertani (LB) media for inoculation. Bacteria were incubated at 28°C with shaking at 120 r/min for 18 h. The optical density at 595 nm (OD_{595}) was measured using a spectrophotometer (DTX880, Beckman Coulter, Brea, CA, United States) and adjusted to OD_{595} of 0.8 with LB. Ten microliters of the bacteria cultures were transferred to a microtiter plate prefilled with yeast extract mannitol (YEM) broth amended with 30% PEG_{8000} (w/v). Each bacterial isolate was assayed on three separate microtiter plates (n = 3). Strains *Pseudomonas poae* 29G9 and *Pseudomonas fluorescens* 90F12-2 were used for comparison, because they were previously reported to withstand osmotic stress and increase plant tolerance to abiotic stress (Nordstedt et al., 2020). Plates were incubated at 28°C with shaking at 120 r/min. After 96 h, the OD_{595} was measured to quantify the growth of the bacteria under osmotic stress.

Selection of ACC Deaminase-Producing Bacteria

To identify ACC deaminase-producing bacteria, bacteria were first grown in media containing ACC as the sole nitrogen source. A sterile 96-well microplate replicator was used to transfer freezer glycerol stocks of each isolate to individual wells in a 96-well microtiter plate containing 200 μL of amended Dworkin and Foster (DF) minimal media (Dworkin and Foster, 1958). For a liter of DF minimal media, the following was added to water: 4.0 g of KH_2PO_4, 6.0 g of Na_2HPO_4, 0.2 g of $MgSO_4.7H_20$, 2.0 g of glucose, 2.0 g of gluconic acid, 2.0 g of citric acid, 1.0 mg of $FeSO_4.7H_20$, 10 μg of H_3BO_3, 10 μg of $MnSO_4$, 70 μg of $ZnSO_4$, 50 μg of $CuSO_4$, and 10 μg of MoO_3; supplemented with 3 mM ACC as the sole source of nitrogen. Bacterial isolates were incubated at 28°C for 48 h shaking at 120 r/min. The OD_{595} was measured using a spectrophotometer (DTX880, Beckman Coulter) to select bacteria able to grow in the DF-ACC media.

ACC deaminase activity was then quantified for each bacterial isolate able to grow in the media.

ACC deaminase activity from the selected isolates was quantified using a colorimetric enzyme activity assay adapted from Penrose and Glick (2003) and optimized for the high-throughput evaluation in a 96-well plate format. *Pseudomonas putida* UW4^{+} was used as the positive bacteria control because it has been well studied as an ACC deaminase producer with beneficial effects on plant stress tolerance (Hontzeas et al., 2004). Bacteria were cultured in 12 mL TSB divided between four culture tubes and incubated at 28°C for 48 h shaking at 200 r/min. Cultures were combined into two tubes and bacteria were harvested by centrifugation at 4,000 *g* for 10 min at 4°C. The cells were washed with 5 mL DF media and the centrifugation was repeated. Cells were resuspended in 3 mL DF media supplemented with ACC at a final concentration of 3 mM and incubated at 28°C for 24 h shaking at 200 r/min. The cultures were then combined into a single tube and harvested by centrifugation at 4,000 *g* for 10 min at 4°C. The supernatant was decanted, and the cells were washed three times in 6 mL of 0.1 M Tris-HCl (pH 7.6) and resuspended in 1.8 mL of 0.1 M Tris-HCl (pH 8.5). Toluene (90 μL) was added to each tube and samples were vortexed three times for 1 min and then stored on ice. A 190 μL aliquot of the toluenized cells was added to each of three wells (n = 3) in a 96-well 2 mL plate containing 19 μL of 0.5 M ACC. Two wells in each plate contained 19 μL distilled H_2O to serve as the negative control. Samples were incubated in a 30°C water bath for 15 min. Following the addition of 950 μL 0.56 M HCl to each well, 800 μL of each sample was transferred to a 1.7 mL centrifuge tube, and samples were centrifuged at 13,000 *g* for 5 min. Three-hundred microliters of the supernatant was mixed with 240 μL of 0.56 HCl and 90 μL of 2,4-dinitrophenylhydrazine reagent (0.2% 2,4-dinitrophenylhydrazine in 2 M HCl), and samples were incubated in a 30°C water bath for 30 min. Following incubation, 600 μL of 2 M NaOH was added to each sample and the absorbance of the mixture was measured at 540 nm (A_{540}) using a spectrophotometer (DTX880, Beckman Coulter). An increase in absorbance served as an indicator of α-ketobutyrate production, and confirmation of the cleavage of ACC by ACC deaminase.

High-Throughput Greenhouse Evaluation of *in vitro*-Selected Bacterial Isolates

A high-throughput greenhouse trial pipeline developed by Nordstedt et al. (2020) was used for the *in planta* evaluation of the *in vitro*-selected osmoadaptive and ACC deaminase-producing bacteria. The bacteria were evaluated for their ability to stimulate growth of *Petunia* × *hybrida* 'Picobella Blue' under water stress conditions. Seeds were sown in Pro-Mix PGX media (Premier Tech Horticulture, Quakertown, PA, United States) and fertilized at each irrigation with 50 mg L^{-1} N from 15N–2.2P–12.5K–2.9Ca–1.2Mg water soluble fertilizer (JR Peters Inc., Allentown, PA, United States). Seedlings were transplanted 3 weeks after sowing to 6.4 cm pots containing Pro-Mix PGX media. Plants were arranged in a randomized complete block design (RCBD) with six blocks, and two replicates per block (n = 12). Due to the large number of bacterial isolates to be tested, three independent greenhouse trials were conducted, and results were analyzed separately. The greenhouse was equipped with supplementary lighting powered by high-pressure sodium and metal halide lamps (GLX/GLS e-systems GROW lights, PARSource, Petaluma, CA, United States) for a 16-h photoperiod. During the light period, the supplementary lighting system was turned on when the PAR flux was below 250 μmol m^{-2} s^{-1} at bench level and turned off when the PAR flux reached 350 μmol m^{-2} s^{-1}. Air temperature at canopy height was maintained at 25/19 [standard deviation (SD) ± 3]°C day/night.

Bacterial inoculum was prepared by inoculating LB media with individual bacteria cultures (selected from the *in vitro* osmoadaptability and ACC deaminase activity assays) and incubating at 28°C for 16 h with shaking at 250 r/min. Cultures were then adjusted to an OD_{595} = 0.8 with LB. Inoculum for treating plants was prepared by diluting each culture 1:100 in reverse osmosis (RO) water. Uninoculated LB diluted 1:100 with RO water was used as the negative control. Plants were treated weekly with a media drench of 40 mL bacterial inoculum.

Water stress was induced 3 weeks post-transplant by discontinuing irrigation and bacteria treatments until all plants in the experiment showed a visible loss of turgidity across the plant. Plants were then rewatered and bacteria treatments were resumed. Plant performance of previously water stressed plants was evaluated 6 weeks post-transplant. Flower numbers (open flowers and buds showing color) and shoot (stems and leaves) biomass were used as indicators of plant performance. Shoot tissue was dried at 49°C for at least 96 h and then weighed to measure dry biomass.

Sequencing and Taxonomic Classification of Selected Bacteria

Genomic DNA was extracted from bacteria selected in the high-throughput greenhouse trial using the Quick-DNA Bacterial Miniprep kit (Zymo Research, Irvine, CA, United States) and samples were submitted to CoreBiome (St. Paul, MN, United States) for whole-genome sequencing. Samples were quantified with Qiant-iT Picogreen dsDNA Assay (Invitrogen, Carlsbad, CA, United States). Libraries were prepared with a procedure adapted from the Nextera Library Prep kit (Illumina, San Diego, CA, United States). Libraries were sequenced on an Illumina NovaSeq using singled-end 1 × 100 reads with a NovaSeq SP flowcell. DNA sequences were filtered for low quality (Q-Score < 20) and length (<50), and adapter sequences were trimmed using cutadapt (v.1.15). The sequences for each sample were assembled into contigs using SPAdes (v3.11.0). Contigs greater than 1,000 bases in length were used in a QUAST (QUAST v4.5) analysis. Prokka (v 1.12) was used to annotate genes for each strain using the contigs > 1,000 bases as described above. Sequence files were uploaded to the Microbial Genome Atlas (MiGA) for taxonomic classification. MiGA allows for the computing of average nucleotide identity (ANI) between the query sequence and the NCBI prokaryotic genome database (Rodriguez-R et al., 2018). Query sequences sharing greater than 94% ANI with a species in the database were considered the

same species. Bacteria that did not share at least 94% ANI with another sequence were considered to not have a species-level match in the database and were given the "species" designation (i.e., *Pseudomonas* sp.) (Konstantinidis and Tiedje, 2005).

Data Deposition

The whole-genome sequence data were deposited in the NCBI database under the BioProject no PRJNA631210.

Evaluation of Quality and Stress Tolerance of Water Stressed Ornamental Plants Treated With Bacteria

Greenhouse Validation Trial

A greenhouse validation trial was used to evaluate the effect of applying individual bacteria selected from the high throughput trial (**Table 1**) on the quality and water stress tolerance of *P. hybrida* (petunia) and *Pelargonium* × *hortorum* (geranium) plants. *P. putida* UW4^{+} was included because it is well-documented to increase quality and stress tolerance of plants subjected to abiotic stress (Hontzeas et al., 2004). The negative control plants were treated with uninoculated LB and subjected to water stress. The positive control plants were also treated with uninoculated LB but were continually irrigated and not subjected to water stress. *P. hybrida* 'Picobella Blue' and *P. hortorum* 'Maverick Red' seeds were sown and cultivated as described for the high-throughput trial, with the exception that seedlings were transplanted to 11.4 cm pots to simulate common production practices. Greenhouse conditions were maintained similar to the high-throughput trial. Plants grown for the evaluation of quality were arranged in a RCBD with 16 blocks and one replicate per block (n = 16). Additional plants were grown in a RCBD to evaluate plant stress tolerance with six blocks and one replicate per block (n = 6).

Bacterial inoculum was prepared similar to the high-throughput trial, and the plants were treated weekly with 120 mL diluted inoculum to account for the larger pot size and media volume. Water stress began 5 weeks after transplant by discontinuing all irrigation and bacteria treatments. Water stress was induced for 7 and 10 days for petunia and geranium, respectively, to the point of loss of turgidity across the plant. Plants were rewatered and weekly bacteria treatments were resumed for 3 weeks, at which point all plants were at the final marketable stage (i.e., flowering).

Plant Growth and Quality

Flower number and plant biomass were measured as indicators of plant growth and quality (n = 16). When plants reached the final marketable stage, flower number (open flowers and buds showing color) was recorded, and flowers and shoots (stems and leaves) were individually harvested, dried at 49°C for at least 96 h, and weighed to measure dry biomass.

Plant Stress Tolerance

Electron transport rate, quantum yield, and quantum efficiency of PSII were measured to evaluate differences in photosynthetic health involved in plant stress tolerance (n = 6). ETR, quantum yield, and quantum efficiency of PSII were measured using an open gas-exchange system (Li-6400 XT; Li-Cor Inc., NE, USA, United States) with an integrated fluorescence chamber head (Li-6400-40 leaf chamber fluorometer; Li-Cor Inc., Lincoln, NE, United States). A lower, fully expanded leaf was used, and all measurements were taken the day prior to water stress (T_1), at severe water stress (T_2), and 3 days after rewatering to assess recovery from water stress (T_3). To identify bacterial strains that improved the photosynthetic health of plants during recovery, the mean of each treatment was ranked for each measurement, and the individual ranking values were summed together to provide an overall ranking (**Table 2**). Electrolyte leakage was measured from plants at T_1 and T_3 by collecting three 6-mm leaf punches from the same leaf used for photosynthetic measurements.

Electron Transport Rate, Quantum Yield, and Efficiency of Photosystem II

Chlorophyll fluorescence measurements were taken between 10:00 and 12:00. The instrument conditions were set as follows: 25°C cuvette temperature, 150 μmol photon m^{-2} s^{-1} to ensure light saturation, CO_2 concentration of 400 μmol CO_2 mol^{-1}, air and leaf vapor pressure deficit between 2 and 2.5 kPa. After inducing photosynthesis under the above conditions and once steady state was reached, the following parameters were measured of light-adapted leaves: ETR, PSII efficiency (Fv'/Fm'), and quantum yield of PSII (φ PSII).

Electron transport rate was calculated by assuming a leaf absorption of 0.85 and a PSII:PSI ratio of 1:1 (ETR = PPFD × φPSII × 0.85 × 0.5). The efficiency of PSII was calculated as: Fv'/Fm' = (Fm' – Fo')/Fm', where Fo' is the minimal fluorescence in the light-adapted state and Fm' is the maximal value. Relative quantum yield of PSII (φPSII) was calculated as: φ_{PSII} = (Fm' - Fs)/Fm', where Fs is the steady state parameter (Huang et al., 2013).

Electrolyte Leakage

Leaf tissue was stored in a 15 mL plastic tube on ice during collection. Tissue was triple rinsed with 1 mL nanopure H_2O and then stored in 4 mL nanopure H_2O. Tubes were gently agitated with shaking at 120 r/min for 2 h and electrolyte content (EL_1) was measured using the Accumet AB30 Conductivity Meter (Fisher Scientific, Oslo, Norway). Tissue was then autoclaved for 20 min and final electrolyte content (EL_2) was measured. Total electrolyte leakage percentage was defined as: $(EL\%) = (EL_1/EL_2) \times 100$.

Statistical Analysis

Results from each of the three high-throughput greenhouse trials were analyzed independently. Data for each phenotype (flower number and shoot dry weight) were analyzed using a linear mixed effect model with lme4 (Bates et al., 2015), and fixed effect estimates (FEE) for treatment effect were used to rank each treatment best to worst compared to the negative control using the highest to lowest FEE, respectively. Rankings of both phenotypes (flower number and shoot biomass) were summed and these values were again ranked best to worst. Treatments

TABLE 1 | The 10 bacterial strains selected from the high-throughput greenhouse trial for their ability to increase flower number or plant biomass of water stressed *Petunia* × *hybrida* 'Picobella Blue.'

			In vitro selection		
Strain	**Host plant isolated from**	**Heat- treated isolation**	**YEM + PEG**	**ACC deaminase activity**	**Taxonomic classification**
C9C5	Coleus	X	X		*Arthrobacter* sp.
C4D7	Geranium	X	X		*Pseudarthrobacter* sp.
C5G2	Coleus		X		*Leifsonia* sp.
C2B4	Zinnia			X	*Pseudomonas* sp.
C6C2	Coleus			X	*Herbaspirillum robiniae*
C2F7	Petunia			X	*Pseudomonas brassicacearum*
C7D2	Zinnia			X	*Pseudomonas corrugata*
C9C3	Coleus			X	*Herbaspirillum* sp.
C1C7	Geranium			X	*Pseudomonas* sp.
C8A5	Coleus			X	*Pseudomonas corrugata*

These bacteria were isolated from the rhizosphere of greenhouse ornamental plants and previously selected for their ability to grow under PEG-mediated osmotic stress (YEM + PEG) or activity of ACC deaminase in vitro.

TABLE 2 | Influence of bacterial application on the photosynthetic health of *Petunia* × *hybrida* 'Picobella Blue' plants under severe water stress (T_2) and following recovery (T_3).

Severe water stress (T_2)					**Recovery (T_3)**				
Strain	**ETR**	**Fv'/Fm'**	**ΦPSII**	**Rank**	**Strain**	**ETR**	**Fv'/Fm'**	**ΦPSII**	**Rank**
C7D2	44.07	0.75	0.67	1	C7D2	43.23	0.751	0.659	1
C1C7	43.44	0.738	0.66	2	C9C3	42.93	0.743	0.653	2
C2B4	43.25	0.737	0.656	3	C2B4	42.92	0.742	0.653	3
C2F7	41.21	0.706	0.625	4	C9C5	42.86	0.744	0.653	4
C8A5	40.64	0.699	0.617	5	C1C7	42.91	0.741	0.653	5
C4D7	40.37	0.694	0.614	6	C6C2	42.62	0.747	0.649	6
C5G2	39.48	0.684	0.599	7	C5G2	42.4	0.741	0.646	7
UW4 +	38.53	0.671	0.585	8	C4D7	42.15	0.729	0.642	8
C9C3	38.14	0.664	0.58	9	UW4 +	42.1	0.735	0.641	9
(−) Control	38.15	0.626	0.579	10	C8A5	41.79	0.728	0.636	10
C9C5	35.6	0.628	0.54	11	C2F7	40.97	0.721	0.623	11
C6C2	33.18	0.609	0.504	12	(−) Control	40.79	0.694	0.621	12
Mean	39.67	0.684	0.602		Mean	42.31	0.735	0.644	
SD	3.23	0.046	0.049		SD	0.79	0.016	0.012	

Electron transport rate (ETR), efficiency of photosystem II (Fv'/Fm'), and quantum yield of photosystem II (ΦPSII) were measured on a single leaf of each plant per treatment (n = 6) and the mean value for each is shown. Plants treated with strains from the greenhouse rhizosphere collection were compared to the bacterial treatment control strain UW4$^+$ and the uninoculated negative control. Measurements were taken 7 days after withholding water for water stress (T_2) and 3 days after rewatering for recovery (T_3), respectively. Means are organized based on if they are more than one standard deviation (SD) greater than the overall mean (light gray), greater than the mean but less than one SD (gray), lower than the mean but not by more than one SD (dark gray), and more than one SD lower than the mean (black). The mean values for each photosynthetic measurement were ranked from highest to lowest value, and the individual ranks were summed together to get the overall rank. Treatments with the lowest ranking sum were given the best overall rank.

ranking in the top 10% for each individual greenhouse trial were selected for further evaluation.

For the greenhouse validation trial, statistical analyses were conducted in R Studio version 3.5.2 using an analysis of variance (ANOVA) with the model: $Y = \mu + \text{treatment} + \text{block}$. Factors that had a significant p-value ($p < 0.05$) were analyzed using Dunnett's test with the negative control used for comparison.

RESULTS

Isolation of the Greenhouse Rhizosphere Collection

A total of 1,056 bacterial isolates were collected from the rhizosphere of greenhouse-produced coleus, petunia, geranium, vinca, and zinnia plants. Of the total isolates,

609 were selected on KMB and 447 were selected on TSB following heat treatment.

In vitro Selection of Osmoadaptive and ACC Deaminase Producing Bacteria

From the greenhouse rhizosphere collection, a total of 80 isolates were selected from the *in vitro* bioassays. Of these isolates, 21 had an OD_{595} greater than 0.2 and were identified as the most osmoadaptive, although the growth of each isolate was less than the comparison strains 29G9 and 90F12-2 (**Figure 1**). The greenhouse rhizosphere collection was also tested for ACC deaminase activity, and 59 isolates tested positive for enzyme activity (**Figure 2**). There were no isolates that were selected by both assays (osmoadaptability and ACC deaminase activity).

High-Throughput Greenhouse Evaluation of *in vitro*-Selected Bacteria

The 80 bacterial isolates selected from the *in vitro* bioassays were evaluated in three independent greenhouse trials for their ability to increase plant size and/or flower number of water-stressed petunia plants when compared to the negative control. Treatments ranking in the top 10% for each individual greenhouse trial were selected for further evaluation (**Supplementary Table S1**).

From the high-throughput greenhouse trials, 10 isolates were selected for increasing plant size and/or flower number when compared to the negative control: C4D7, C7D2, C1C7, C5G2, C6C2 C8A5, C9C3, C9C5, C2B4, and C2F7. Following taxonomic identification (see below), these strains were evaluated in a validation greenhouse trial under water stress (**Table 1**).

Taxonomic Classification

The 10 bacterial isolates selected from the high-throughput greenhouse trial were sequenced and taxonomic classification was assigned (**Table 1**). These bacteria are from five different genera, with five of them belonging to the genus *Pseudomonas*.

Shoot Biomass and Flower Number of Water Stressed Plants When Treated With Beneficial Bacteria

The 10 bacterial strains selected from the high-throughput trial were evaluated for their ability to increase water stress tolerance in petunia and geranium plants. Application of bacteria had broad beneficial effects on the shoot biomass of petunia plants recovering from water stress. Each bacterial application significantly increased shoot biomass compared to the negative control, an average increase of 21% (**Figure 3A**). In addition to shoot biomass, seven of the greenhouse rhizosphere strains (C8A5, C4D7, C7D2, C1C7, C6C2, C9C5, C2F7) and $UW4^+$ significantly increased flower number, with an average increase of five flowers per plant compared to the negative control (**Figure 3B**). Treatment with strain C9C5 had the greatest effect on plant quality, increasing shoot biomass by 36% and increasing flower number by at least eight flowers per plant when compared to the negative control. Plants treated with C6C2 and C9C5 had greater shoot biomass than plants treated with $UW4^+$ and the positive control that did not undergo water stress. In addition, plants treated with C9C5 also had greater flower number than $UW4^+$ and the positive control (**Figures 3A,B**).

Bacteria application also had a beneficial effect on the quality of water stressed geranium. Application of eight of the greenhouse rhizosphere strains (C8A5, C4D7, C1C7, C9C3, C5G2, C6C2, C9C5, C2F7) and $UW4^+$ significantly increased shoot biomass when compared to the negative control (**Figure 4**). The increase in shoot biomass was not as great as the positive control; however, application of the eight strains still ameliorated the negative effects of water stress on plant size when compared to the negative control. There was not an increase in geranium flower number or biomass, likely due to their habit of producing very few but large inflorescences (data not shown).

Chlorophyll Fluorescence Parameters and Electrolyte Leakage of Bacteria Treated Plants Subjected to Water Stress

Electron Transport Rate, Quantum Yield, and Quantum Efficiency of PSII in Petunia

Out of the 11 bacterial strains tested (including $UW4^+$), C7D2 was identified as the best strain for increasing overall photosynthetic health of petunia plants. C7D2 increased the ETR, ΦPSII, and Fv'/Fm' more than one SD greater than the treatment means in petunia throughout severe water stress (T_2) and recovery (T_3) (**Table 2**). Strain C2B4 also showed consistent results in both severe water stress (T_2) and recovery (T_3), being ranked in the top three strains under both conditions. Strain C1C7 also increased the photosynthetic health of petunia plants under severe stress (T_2); however, the effects were not as evident in plants recovering from water stress (T_3). Plants treated with the control strain $UW4^+$ did not have increased photosynthetic health compared to plants treated with most other bacterial strains; however, petunia plants treated with bacteria from the greenhouse rhizosphere collection did tend to rank higher in photosynthetic health than the untreated negative control in terms of ETR, Fv'/Fm', and ΦPSII (**Table 2**). Overall, petunia plants treated with bacteria from the collection also recovered from water stress better than the negative control in terms of electrolyte leakage, ETR, Fv'Fm, and ΦPSII. Treated plants had lower percent differences when comparing recovery measurements (T_3) to measurements prior to water stress (T_1) (**Table 3**).

Electron Transport Rate, Quantum Yield, and Quantum Efficiency of PSII in Geranium

Unlike the observed results in petunia, the effect of bacteria application on the photosynthetic health (ETR, Fv'/Fm', and ΦPSII) of geranium was not as consistent throughout water stress and recovery. The strain C6C2 was ranked in the top three strains under severe water stress (T_2) and recovery (T_3), being the most consistent treatment to increase the ETR, Fv'/Fm', and ΦPSII of geranium under both conditions. The control treatment $UW4^+$ was the best at increasing overall photosynthetic health of geranium plants under severe water stress (T_2), as plants treated with $UW4^+$ had an increase in

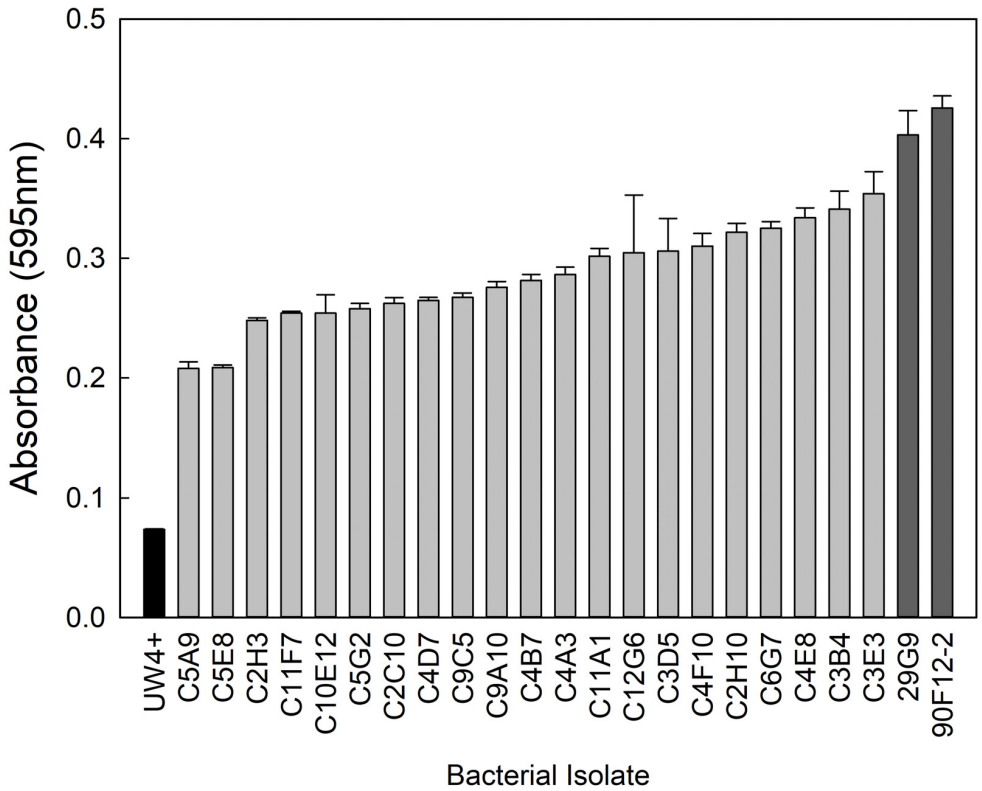

FIGURE 1 | Growth of bacterial isolates in YEM media containing 30% polyethylene glycol to induce osmotic stress. Bars represent the mean (±SE) optical density (OD_{595}) of the isolates after 96 h incubation at 28°C (n = 3). Isolates with an absorbance greater than 0.2 (light gray) were selected for further evaluation. Strains 29G9 and 90F12-2 (dark gray) were used for comparison because they were previously reported to increase plant tolerance to abiotic stress.

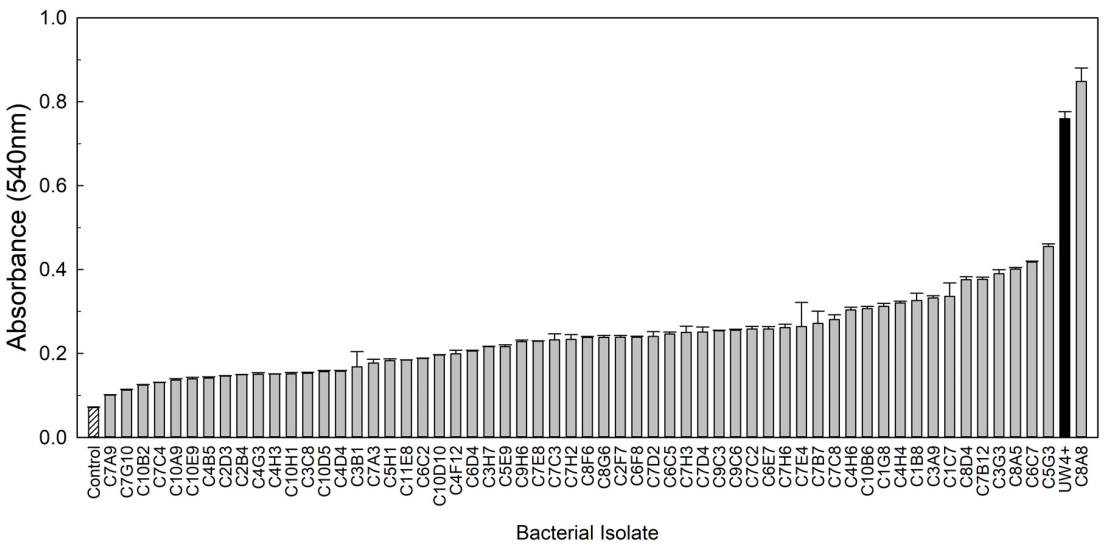

FIGURE 2 | ACC deaminase activity of bacterial isolates measured by a 2,4-dinitrophenylhydrazine assay after induction in a Dworkin and Foster (DF) media containing ACC as the sole nitrogen source. Bars represent the mean (±SE) absorbance (A_{540}) of the ACC byproduct, α-ketobutyrate, following the enzymatic reaction (n = 3). Bacterial cultures (light gray) were compared to the uninoculated control (white with lines) and the positive bacteria control *Pseudomonas putida* $UW4^+$ (black).

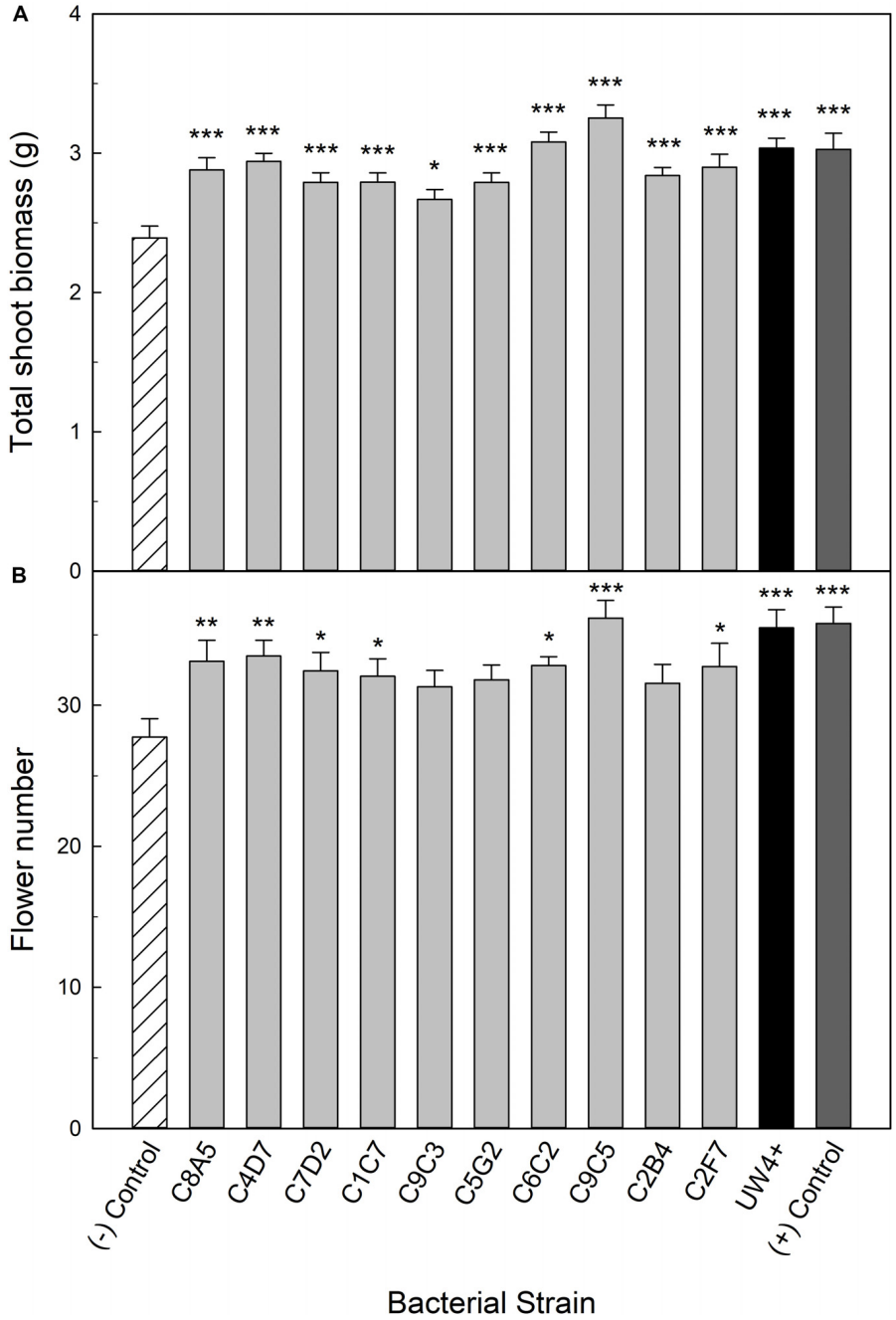

FIGURE 3 | Plant growth performance parameters for *Petunia* × *hybrida* 'Picobella Blue,' plants subjected to water stress 5 weeks after transplant (n = 16). Plants were treated with bacterial inoculum weekly starting at transplant. Plants treated with strains from the greenhouse rhizosphere collection (light gray), were compared to the bacterial treatment control strain UW4^{+} (black), the uninoculated negative control (white with lines), and the uninoculated positive control (dark gray). The negative control plants were subjected to water stress similar to the inoculated plants, whereas the positive control plants were irrigated regularly throughout the experiment. Total shoot biomass (dry weight) **(A)** and number of flowers **(B)** was measured 3 weeks after rewatering following severe water stress. Bars represent mean (±SE). The asterisks indicate significance between the treatments compared to the uninoculated negative control using the Dunnett's test; *, **, *** significant at $P \leq 0.05$, 0.01, or 0.001, respectively.

ETR, ΦPSII, and Fv'/Fm' more than one SD greater than the treatment means. Strains C2F7 and C4D7 had the greatest effect on increasing overall photosynthetic health of geranium after recovering from water stress (T_3). Treatment with each of the strains increased plant ETR, ΦPSII, and Fv'/Fm' measurements more than one SD greater than their respective means (**Table 4**). Similar to petunia plants, geranium plants treated with bacteria from the greenhouse rhizosphere collection recovered from

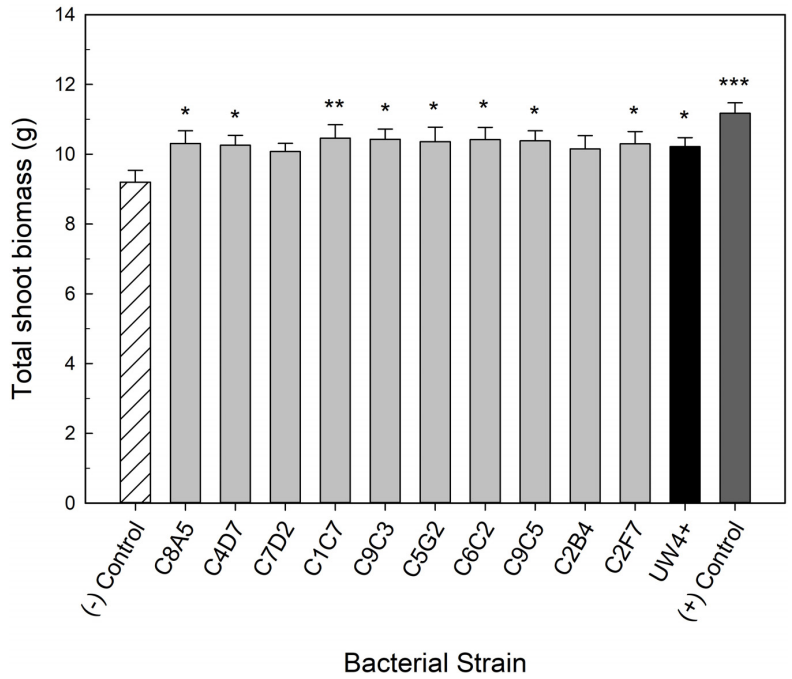

FIGURE 4 | Plant growth performance parameters for *Pelargonium* × *hortorum* 'Maverick Red,' plants subjected to water stress 5 weeks after transplant (n = 16). Plants were treated with bacterial inoculum weekly starting at transplant. Plants treated with strains from the greenhouse rhizosphere collection (light gray) were compared to the bacterial treatment control strain UW4$^+$ (black), the uninoculated negative control (white with lines), and the uninoculated positive control (dark gray). The negative control plants were subjected to water stress similar to the inoculated plants, whereas the positive control plants were irrigated regularly throughout the experiment. Total shoot biomass (dry weight) was measured 3 weeks after rewatering following water stress. Bars represent mean (±SE). The asterisks indicate significance between the treatments compared to the uninoculated negative control using the Dunnett's test; *, **, *** significant at $P \leq 0.05$, 0.01, or 0.001, respectively.

water stress better than the negative control when comparing recovery measurements (T_3) to measurements prior to water stress (T_1) (**Table 5**).

TABLE 3 | Percent change in physiological measurements of *Petunia* × *hybrida* 'Picobella Blue' after 3 days of recovery (T_3) from being subjected to 7 days of water stress, when compared to measurements prior to water stress (T_1).

Strain	Electrolyte leakage	ETR	Fv'/Fm'	ΦPSII
(–) Control	54.5	−10.2	−9.5	−9.8
C8A5	7.8	−8.3	−5.0	−8.3
C4D7	10.9	−7.2	−4.7	−6.6
C7D2	10.5	−4.9	−1.4	−3.9
C1C7	16.5	−5.8	−3.1	−5.1
C9C3	17.0	−4.5	−3.5	−4.6
C5G2	13.0	−6.4	−2.9	−5.9
C6C2	−4.9	−6.3	−2.4	−5.8
C9C5	14.1	−5.2	−2.8	−4.7
C2B4	9.3	−6.3	−3.1	−5.4
C2F7	13.5	−9.8	−5.6	−9.5
UW4+	8.8	−7.5	−3.8	−6.6

Plants treated with strains from the greenhouse rhizosphere collection were compared to the bacterial treatment control strain UW4$^+$ and the uninoculated negative control.

Electrolyte Leakage in Petunia and Geranium

Application of five bacterial strains significantly decreased the percentage of electrolyte leakage in both petunia and geranium after recovery from water stress (T_3). These included the greenhouse rhizosphere strains C8A5, C4D7, C9C3, C9C5, and the treatment control strain UW4$^+$ (**Figures 5A,B**). Application of beneficial bacteria ameliorated the negative effects of water stress on the electrolyte leakage of petunia and geranium plants after recovering from stress (T_3). The electrolyte leakage of negative control petunia plants increased by 54% when compared to plants before water stress, whereas plants treated with bacteria from the greenhouse rhizosphere collection and UW4$^+$ had an average increase of only 11% (**Table 3**). The negative control geranium plants had an electrolyte leakage increase of 87% after recovery, whereas plants treated with bacteria from the greenhouse rhizosphere collection and UW4$^+$ had an average increase of only 36% (**Table 5**) when compared to measurements pre-stress (T_1).

DISCUSSION

Greenhouse ornamentals can be subjected to water deficit throughout different stages of production, shipping, and retail. There is a need to find solutions that increase plant tolerance to stress, allowing production of horticulture crops that

TABLE 4 | Influence of bacterial application on the photosynthetic health of *Pelargonium* × *hortorum* 'Maverick Red' plants under severe water stress (T_2) and following recovery (T_3).

Severe water stress (T_2)					Recovery (T_3)				
Strain	**ETR**	**Fv'/Fm'**	**ΦPSII**	**Rank**	**Strain**	**ETR**	**Fv'/Fm'**	**ΦPSII**	**Rank**
UW4 +	20.44	0.516	0.313	1	C2F7	41.63	0.745	0.636	1
C9C5	19.39	0.541	0.297	2	C4D7	41.47	0.742	0.633	2
C6C2	18.25	0.495	0.279	3	C6C2	41.45	0.739	0.633	3
C8A5	18.27	0.468	0.278	4	C9C5	40.77	0.732	0.622	4
C2F7	17.59	0.496	0.269	5	C5G2	39.61	0.725	0.604	5
C7D2	17.84	0.462	0.273	6	UW4 +	38.83	0.724	0.592	6
C5G2	17.43	0.477	0.266	7	C9C3	38.64	0.726	0.59	7
C9C3	17.06	0.487	0.261	8	C2B4	38.21	0.72	0.584	8
C1C7	17.37	0.446	0.265	9	C1C7	36.74	0.705	0.561	9
C4D7	16.85	0.465	0.258	10	C7D2	36.41	0.694	0.557	10
C2B4	16.09	0.448	0.246	11	(–) Control	35.93	0.678	0.547	11
(–) Control	12.03	0.369	0.183	12	C8A5	35.69	0.701	0.545	12
Mean	17.38	0.472	0.266		Mean	38.78	0.719	0.592	
SD	2.04	0.043	0.031		SD	2.24	0.021	0.034	

Electron transport rate (ETR), efficiency of photosystem II (Fv'/Fm'), and quantum yield of photosystem II (ΦPSII) were measured on a single leaf of each plant per treatment (n = 6) and the mean value for each is shown. Plants treated with strains from the greenhouse rhizosphere collection were compared to the bacterial treatment control strain UW4$^+$ and the uninoculated negative control. Measurements were taken 7 days after withholding water for water stress (T_2) and 3 days after rewatering for recovery (T_3). Means are organized based on if they are more than one standard deviation (SD) greater than the overall mean (light gray), greater than the mean but less than one SD (gray), lower than the mean but not by more than one SD (dark gray), and more than one SD lower than the mean (black). The mean values for each photosynthetic measurement were ranked from highest to lowest value, and the individual ranks were summed together to get the overall rank. Treatments with the lowest ranking sum were given the best overall rank.

satisfy quality demands under limited resource availability. In this study, we have established a novel collection of bacteria from the rhizosphere of greenhouse ornamentals. We then used *in vitro* and *in planta* selection methods to screen the entire greenhouse rhizosphere collection and identify strains with the ability to increase water stress tolerance in petunia and geranium. We selected petunia and geranium for this study because they are two of the most popular ornamental greenhouse crops with a combined annual wholesale value in the United States greater than $190 million (National Agricultural Statistics, 2019).

TABLE 5 | Percent change in physiological measurements of *Pelargonium* × *hortorum* 'Maverick Red' after 3 days of recovery (T_3) from being subjected to 10 days of water stress, when compared to measurements prior to water stress (T_1).

Strain	Electrolyte leakage	ETR	Fv'/Fm'	ΦPSII
(–) Control	87.5	−18.6	−8.8	−19.0
C8A5	39.1	−18.8	−6.3	−18.9
C4D7	16.5	−4.3	−0.6	−4.2
C7D2	43.0	−14.1	−6.0	−13.8
C1C7	41.6	−11.3	−4.0	−11.0
C9C3	37.1	−10.7	−2.6	−10.5
C5G2	26.9	−7.7	−1.8	−7.6
C6C2	29.8	−2.8	0.1	−2.7
C9C5	35.5	−8.7	−2.5	−8.6
C2B4	47.2	−13.1	−3.3	−12.9
C2F7	33.7	−3.5	0.5	−3.4
UW4+	43.4	−11.7	−3.1	−11.9

Plants treated with strains from the greenhouse rhizosphere collection were compared to the bacterial treatment control strain UW4$^+$ and the uninoculated negative control.

Water stress directly impacts the soil microbiome by selecting for stress-tolerant taxa. In addition, plants influence their rhizosphere microbiome during stress by altering their root exudate profile (Naylor and Coleman-Derr, 2018). We took advantage of this principle by imitating the environment that plants would go through during post-harvest water stress and selecting culturable bacteria from these plants. We isolated the general culturable bacteria from the rhizosphere as well as those able to form spores through heat treatment and selection. Sporulation allows bacteria to enter dormancy under periods of water stress, serving as an advantage over other bacteria that are less likely to persist in these environments (Hayden et al., 2012).

The application of PGPR to greenhouse ornamental crops is a useful tool to increase plant stress tolerance. The onset of water stress in greenhouse crops is rapid and can occur throughout production, making it difficult for plants to adapt to the stress and maintain superior quality. Therefore, the ability for PGPR to colonize plant roots and then stimulate plant stress responses is an attractive solution to prime ornamental crops before the onset of stress. Using

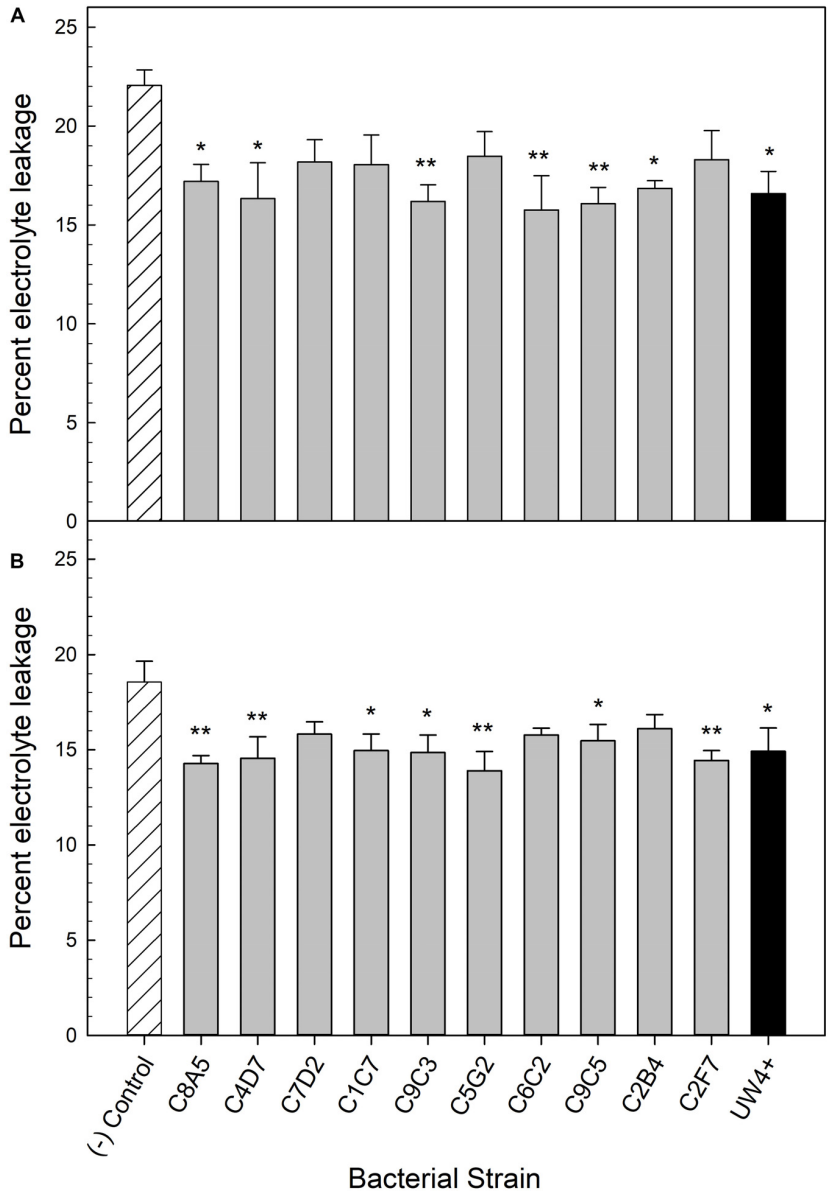

FIGURE 5 | Percent electrolyte leakage of *Petunia* × *hybrida* 'Picobella Blue' **(A)** and *Pelargonium* × *hortorum* 'Maverick Red' **(B)** after 3 days of recovery from water stress ($n = 6$). Plants were treated with bacterial inoculum weekly starting at transplant and were subjected to severe water stress 5 weeks after transplant. Plants treated with strains from the greenhouse rhizosphere collection (light gray) were compared to the bacterial treatment control strain UW4^{+} (black), and the uninoculated negative control (white with lines). Bars represent mean (±SE). The asterisks indicate significance between the treatments compared to the uninoculated negative control using the Dunnett's test; *, ** significant at $P \leq 0.05$, and 0.01, respectively.

previously established methods, we utilized high-throughput bioassays to identify bacteria within our collection that were able to withstand osmotic stress in PEG or produce the enzyme ACC deaminase. The use of PEG to select osmotic stress tolerant bacteria, and the ability of these bacteria to then confer water stress tolerance to plants has been well established (Forchetti et al., 2007; Vardharajula et al., 2011; Hussain et al., 2014; Asghar et al., 2015). In addition, the treatment of tomato and pepper plants with ACC-deaminase producing *Achromobacter piechaudii* stimulates plant growth during water stress, contributing to larger plant size (Mayak et al., 2004).

Many PGPR studies are conducted in greenhouses; however, these results can be difficult to relate to horticulture crop production due to the use of agronomic crop species and soil-based growing media. A previously established high-throughput greenhouse trial (Nordstedt et al., 2020) was an effective method to screen the *in vitro* selected bacteria in our collection and identify those that increased plant size or flower number of water stressed petunia plants in a greenhouse production system. In this

study, the high-throughput trial was used to evaluate 80 isolates and select 10 for the validation trial with petunia and geranium.

Inhibition of shoot growth is a common plant response to water stress because it limits the leaf area available for evaporative loss. However, this decrease in plant size can lower ornamental crop quality and profitability. Application of bacteria can stimulate plant growth under severe water deficit, ameliorating the negative effects of water stress. PGPR application had the most consistent effect on water stressed petunias. Application of all ten bacterial strains significantly increased plant size. In the case of *Arthrobacter* sp. C9C5, plant size was comparable to our positive control that did not undergo any water stress (**Figure 3A**). These results are similar to other studies that have shown *Arthrobacter* sp. to increase the size of arabidopsis, tomato, and wheat plants grown under high saline conditions (Barriuso et al., 2008; Upadhyay and Singh, 2015; Fan et al., 2016). In addition, eight strains significantly increased plant size of water-stressed geranium (**Figure 4**). These eight strains consist of five different genera, including *Arthrobacter*, *Pseudarthrobacter*, *Leifsonia*, *Pseudomonas*, and *Herbaspirillum*. There is currently little evidence for *Pseudarthrobacter* spp. as a plant growth promoter other than phytoremediation (Ghasemi et al., 2018) and *in vitro* plant growth promoting properties (Mesa-Marín et al., 2019). To our knowledge, our study is the first to document a *Pseudarthrobacter* strain as a plant growth promoting bacteria under water stressed conditions. *Leifsonia* has also not been extensively studied as a PGPR, although the strain *Leifsonia xyli* SE134 has been shown to increase plant growth of cucumber, tomato, and radish under non-stressed conditions (Kang et al., 2014). *Herbaspirillum* spp. are well-documented as biological N_2-fixer (Hayat et al., 2012). Although *Herbaspirillum seropedicae* has been shown to increase the plant size of maize under water stress (Cura et al., 2017), to our knowledge, we are the first to document *Herbaspirillum robiniae* as a PGPR under water stressed conditions. This work provides evidence of multiple bacterial species that have not been previously characterized as PGPR, adding to the diversity of PGPR that can be studied to stimulate plant growth under water stress.

Plant growth promoting rhizobacteria that can increase flower number even under water stressed conditions are of interest to the horticulture industry, and seven strains significantly increased flower number in water stressed petunia (**Figure 3B**). These results are similar to our previous work that identified two *Pseudomonas* spp. that increase the flower number of water-stressed petunia (Nordstedt et al., 2020). Half of the PGPR strains identified in the current study also belong to the genus *Pseudomonas* (**Table 1**). Many species within *Pseudomonas* have been extensively studied under a variety of conditions as plant growth promoters (Goswami et al., 2016), and our results add to the current literature by showing the species *Pseudomonas brassicacearum* and *Pseudomonas corrugata* can increase the quality of water stressed greenhouse ornamentals. Overall, this work shows that improvements in water stress tolerance allow for visual quality to be maintained longer, which can reduce plant mortality following wholesale production (Eakes et al., 1991).

Different *Pseudomonas* spp. have been shown to increase water stress tolerance in maize by reducing electrolyte leakage (Sandhya et al., 2010). This increase in membrane stability allows plants to recover more efficiently from stress, often increasing plant size (Sandhya et al., 2010; Vardharajula et al., 2011). The present study identified nine strains that decreased the electrolyte leakage in plants recovering from water stress (**Figures 5A,B**). Plants tended to have greater plant biomass when their electrolyte leakage was decreased after recovering from water stress (**Figures 3A**, **4**). PSII efficiency is inversely proportional to damage in the open PSII reaction centers (Farquhar et al., 1989). Therefore, an increase in photosynthetic health via application of PGPR can delay mortality of plants. *P. brassicacearum* that delayed the decline in photosynthetic health of water stressed arabidopsis also increased the probability of plant survival (Bresson et al., 2014). In our study, we measured three different parameters of photosynthetic health: PSII efficiency (Fv'/Fm'), quantum yield of PSII (ΦPSII), and ETR. Utilizing a ranking system, we were able to select the strains with the best effect on overall photosynthetic health in our two plant species during severe water stress and recovery. The best strains were more consistent between severe water stress and recovery in petunia (**Table 2**). Strains C7D2, C2B4, and C1C7 were the best treatments for increasing overall photosynthetic health in petunia, while also improving plant quality of water-stressed petunias (**Figures 3A,B**). Noteably, these strains were originally isolated from zinnia (C7D2 and C2B4) and geranium (C1C7) rhizosphere samples. The best strains for geranium photosynthetic health were different depending on if the plants were under severe water stress or recovering from stress (**Table 4**). These results are consistent with Arzanesh et al. (2011) that showed different strains of *Azospirillum* had a positive influence on wheat plants that was dependent on the severity of the water stress. Strain C6C2 was identified as the best strain for increasing the overall photosynthetic health of water stressed geranium plants and also significantly increased the biomass of geranium plants after recovery from water stress. However, this strain was originally isolated from a coleus rhizosphere sample. These results, in combination with the origin of strains that increased the health of petunia, show that bacteria isolated from one plant species can have a beneficial effect on other plant species. This provides evidence of the generalist nature of these PGPR to stimulate plant growth of multiple plant species in one system, a common occurance in ornamental plant production. It is likely that environmental conditions (i.e., growing media composition, fertilizer rates, and temperature fluctuations) play a more important role than plant host in beneficial plant–microbe interactions.

We utilized *P. putida* $UW4^+$ as a positive treatment control for comparison because it has been documented as an ACC deaminase producer that stimulates plant growth under abiotic stress (Grichko and Glick, 2001; Cheng et al., 2007; Farwell et al., 2007; Jodeh et al., 2015). $UW4^+$ had the highest ACC deaminase activity compared to the other ten strains evaluated in the greenhouse validation trial (**Figure 2**). $UW4^+$ also increased the quality of water stressed petunia and geranium plants when

compared to the negative control, yet many of our strains performed as well or better than UW4$^+$ (**Figures 3AB**, **4**). In regard to overall photosynthetic parameters, petunia treated with UW4$^+$ ranked higher than the negative control but ranked below most of our strains during water stress and recovery (**Table 2**). UW4$^+$ had the best influence on geranium photosynthetic health during water stress and was ranked in the middle of all treatments for plants during recovery (**Table 4**).

Our study contributes to the current literature by establishing a large collection of diverse bacterial isolates originating from the rhizosphere of water stressed greenhouse ornamental species. In addition, we evaluated the effect of bacterial application on two economically important ornamental species, grown in a soilless peat-based media, and subjected to severe water stress. This water deficit is similar to what plants may be subjected to after production, when market-ready plants are shipped or sold at retail garden centers. Utilizing cultural inputs and inducing water stress similar to what would be experienced in greenhouse production further validates the potential for these bacteria to be used by the industry as a tool to increase plant stress tolerance and overall quality.

The commercialization of biostimulant products from isolation to formulation is timely and resource intensive (Backer et al., 2018). In addition to contributing to the scientific community, the work outlined in this study contributes significantly to the biostimulant commercialization pipeline. The methods used for isolation, screening, and validation of the PGPR strains can be used by other groups to identify beneficial strains specific to their system of interest. In conclusion, *in vitro* bioassays are effective at selecting candidate PGPR with the ability to withstand osmotic stress or produce beneficial enzymes; however, their ability to stimulate plant growth must also be validated *in planta*. PGPR can positively influence plant health and quality differently across plant species. Therefore, future research should focus on developing consortia of PGPR that can be formulated into products with broad effects across different ornamental plant species.

DATA AVAILABILITY STATEMENT

The whole-genome sequence data were deposited in the NCBI database under the BioProject no. PRJNA631210.

AUTHOR CONTRIBUTIONS

NN and MJ conceived the experimental design. NN collected the data, performed all analyses, and led the writing of the manuscript. MJ edited the manuscript.

FUNDING

Salaries and research support were provided in part by State and Federal funds appropriated to the OARDC, The Ohio State University. Journal Article Number HCS 20-03. This work was financially supported by the American Floral Endowment and the OSU D.C. Kiplinger Floriculture Endowment. Support was also provided by The Ohio State University Distinguished Fellowship and the OARDC Director's Graduate Associateship.

ACKNOWLEDGMENTS

We thank Laura Chapin for help with the greenhouse experiments and Dr. David Francis for his help with statistical analysis. We also thank Ball Horticultural Company (West Chicago, IL, United States) and Syngenta Flowers (Gilroy, CA, United States) for providing seeds.

SUPPLEMENTARY MATERIAL

The Supplementary Material for this article can be found online at: https://www.frontiersin.org/articles/10.3389/fpls.2020.00826/full#supplementary-material

REFERENCES

Ali, S. Z., Sandhya, V., and Rao, L. V. (2013). Isolation and characterization of drought-tolerant ACC deaminase and exopolysaccharide-producing fluorescent *Pseudomonas* sp. *Ann. Microbiol.* 64, 493–502. doi: 10.1007/s13213-013-0680-683

Armitage, A. M. (1993). *Bedding Plants: Prolonging Shelf Performance: Postproduction Care & Handling*. Batavia, IL: Ball Publishing.

Armitage, A. M., Vines, H. M., Tu, Z.-P., and Black, C. C. (1983). Water relations and net photosynthesis in hybrid geranium. *J. Am. Soc. Hortic. Sci.* 108, 310–314.

Arzanesh, M. H., Alikhani, H. A., Khavazi, K., Rahimian, H. A., and Miransari, M. (2011). Wheat (*Triticum aestivum* L.) growth enhancement by *Azospirillum* sp. under drought stress. *World J. Microbiol. Biotechnol.* 27, 197–205. doi: 10.1007/s11274-010-0444-441

Asghar, H. N., Zahir, Z. A., Akram, M. A., Ahmad, H. T., and Hussain, M. B. (2015). Isolation and screening of beneficial bacteria to ameliorate drought stress in wheat. *Soil Environ.* 34, 100–110.

Backer, R., Rokem, J. S., Ilangumaran, G., Lamont, J., Praslickova, D., Ricci, E., et al. (2018). Plant growth-promoting rhizobacteria: context, mechanisms of action, and roadmap to commercialization of biostimulants for sustainable agriculture. *Front. Plant Sci.* 871:1473. doi: 10.3389/fpls.2018.01473

Barriuso, J., Ramos Solano, B., and Gutiérrez Mañero, F. J. (2008). Protection against pathogen and salt stress by four plant growth-promoting rhizobacteria isolated from *Pinus* sp. on *Arabidopsis thaliana*. *Phytopathology* 98, 666–672. doi: 10.1094/PHYTO-98-6-0666

Bates, D., Mächler, M., Bolker, B. M., and Walker, S. C. (2015). Fitting linear mixed-effects models using lme4. *J. Stat. Softw.* 67:jssv067. doi: 10.18637/jss.v067.i01

Bresson, J., Varoquaux, F., Bontpart, T., Touraine, B., and Vile, D. (2013). The PGPR strain *Phyllobacterium brassicacearum* STM196 induces a reproductive delay and physiological changes that result in improved drought tolerance in *Arabidopsis*. *New Phytol.* 200, 558–569. doi: 10.1111/nph.12383

Bresson, J., Vasseur, F., Dauzat, M., Labadie, M., Varoquaux, F., Touraine, B., et al. (2014). Interact to survive: *Phyllobacterium brassicacearum* improves *Arabidopsis* tolerance to severe water deficit and growth recovery. *PLoS One* 9:e0107607. doi: 10.1371/journal.pone.0107607

Caser, M., Lovisolo, C., and Scariot, V. (2017). The influence of water stress on growth, ecophysiology and ornamental quality of potted *Primula vulgaris*

'Heidy' plants. New insights to increase water use efficiency in plant production. *Plant Growth Regul.* 83, 361–373. doi: 10.1007/s10725-017-0301-304

Cheng, Z., Park, E., and Glick, B. R. (2007). 1-aminocyclopropane-1-carboxylate deaminase from *Pseudomonas putida* UW4 facilitates the growth of canola in the presence of salt. *Can. J. Microbiol.* 918, 912–918. doi: 10.1139/W07-050

Cohen, A. C., Bottini, R., Pontin, M., Berli, F. J., Moreno, D., Boccanlandro, H., et al. (2015). *Azospirillum brasilense* ameliorates the response of *Arabidopsis thaliana* to drought mainly via enhancement of ABA levels. *Physiol. Plant.* 153, 79–90. doi: 10.1111/ppl.12221

Cura, J. A., Franz, D. R., Filosofia, J. E., Balestrasse, K. B., and Burgueno, L. E. (2017). Inoculation with *Azospirillum* sp. and *Herbaspirillum* sp. bacteria increases the tolerance of maize to drought stress. *Microorganisms* 5:41. doi: 10.3390/microorganisms5030041

Dworkin, M., and Foster, J. W. (1958). Experiments with some microorganisms which utilize ethane and hydrogen. *J. Bacteriol.* 75, 592–603. doi: 10.1016/j.sbspro.2010.03.167

Eakes, D. J., Wright, R. D., and Seiler, J. R. (1991). Moisture stress conditioning effects on Salvia splendens 'Bonfire'. *J. Am. Soc. Hortic. Sci.* 116, 716–719. doi: 10.21273/jashs.116.4.716

Fall, R., Kinsinger, R. F., and Wheeler, K. A. (2004). A simple method to isolate biofilm-forming *Bacillus subtilis* and related species from plant roots. *Syst. Appl. Microbiol.* 27, 372–379. doi: 10.1078/0723-2020-2267

Fan, P., Chen, D., He, Y., Zhou, Q., Tian, Y., and Gao, L. (2016). Alleviating salt stress in tomato seedlings using *Arthrobacter* and *Bacillus megaterium* isolated from the rhizosphere of wild plants grown on saline-alkaline lands. *Int. J. Phytoremed.* 18, 1113–1121. doi: 10.1080/15226514.2016.1183583

Farooq, M., Wahid, A., Kobayashi, N., Fujita, D., and Basra, S. M. A. (2009). Plant drought stress: effects, mechanisms and management. *Agron. Sustain. Dev.* 29, 185–212. doi: 10.1051/agro:2008021

Farquhar, G. D., Ehleringer, J. R., and Hubick, K. T. (1989). Carbon isotope discrimination and photosynthesis. *Annu. Rev. Plant Physiol. Plant Mol. Biol.* 40, 503–537. doi: 10.1146/annurev.pp.40.060189.002443

Farwell, A. J., Vesely, S., Nero, V., Rodriguez, H., Mccormack, K., Shah, S., et al. (2007). Tolerance of transgenic canola plants (*Brassica napus*) amended with plant growth-promoting bacteria to flooding stress at a metal-contaminated field site. *Environ. Pollut.* 147, 540–545. doi: 10.1016/j.envpol.2006.10.014

Flores, A. C., Luna, A. A. E., and Portugal, V. O. (2007). Yield and quality enhancement of marigold flowers by inoculation with *Bacillus subtilis* and *Glomus fasciculatum*. *J. Sustain. Agric.* 31, 21–31. doi: 10.1300/J064v31n01

Forchetti, G., Masciarelli, O., Alemano, S., Alvarez, D., and Abdala, G. (2007). Endophytic bacteria in sunflower (*Helianthus annuus* L.): isolation, characterization, and production of jasmonates and abscisic acid in culture medium. *Appl. Microbiol. Biotechnol.* 76, 1145–1152. doi: 10.1007/s00253-007-1077-1077

Galmés, J., Medrano, H., and Flexas, J. (2007). Photosynthesis and photoinhibition in response to drought in a pubescent (var. *minor*) and a glabrous (var. palaui) variety of Digitalis minor. *Environ. Exp. Bot.* 60, 105–111. doi: 10.1016/j.envexpbot.2006.08.001

Ghasemi, Z., Ghaderian, S. M., Rodríguez-Garrido, B., Prieto-Fernández, A., and Kidd, P. S. (2018). Plant species-specificity and effects of bioinoculants and fertilization on plant performance for nickel phytomining. *Plant Soil* 425, 265–285. doi: 10.1007/s11104-017-3553-x

Glick, B. R., Cheng, Z., Czarny, J., and Duan, J. (2007). Promotion of plant growth by ACC deaminase-producing soil bacteria. *Eur. J. Plant Pathol.* 119, 329–339. doi: 10.1007/978-1-4020-6776-1_8

Göre, M. E., and Altin, N. (2006). Growth promoting of some ornamental plants by root treatment with specific fluorescent pseudomonads. *J. Biol. Sci.* 6, 610–615. doi: 10.3923/jbs.2006.610.615

Goswami, D., Thakker, J. N., and Dhandhukia, P. C. (2016). Portraying mechanics of plant growth promoting rhizobacteria (PGPR): a review. *Cogent Food Agric.* 2, 1–19. doi: 10.1080/23311932.2015.1127500

Grichko, V. P., and Glick, B. R. (2001). Amelioration of flooding stress by ACC deaminase-containing plant growth-promoting bacteria. *Plant Physiol. Biochem.* 39, 11–17. doi: 10.1016/s0981-9428(00)01212-2

Gururani, M. A., Upadhyaya, C. P., Baskar, V., Venkatesh, J., Nookaraju, A., and Park, S. W. (2013). Plant growth-promoting rhizobacteria enhance abiotic stress tolerance in Solanum tuberosum through inducing changes in the expression of ROS-scavenging enzymes and improved photosynthetic performance. *J. Plant Growth Regul.* 32, 245–258. doi: 10.1007/s00344-012-9292-9296

Gutierrez, L. J. (2004). *Fungicide Sensitivity and Biological Control Potential of Tomato Fruit rot Pathogens in Ohio.* Master's thesis. Wooster, OH: The Ohio State University.

Hayat, R., Ahmed, I., and Sheirdil, R. A. (2012). "An overview of plant growth promoting rhizobacteria (PGPR) for sustainable agriculture," in *Crop Production for Agricultural Improvement*, ed. M. Ashraf, (Dordrecht: Springer), 557–578. doi: 10.1007/978-94-007-4116-4_22

Hayden, H. L., Mele, P. M., Bougoure, D. S., Allan, C. Y., Norng, S., Piceno, Y. M., et al. (2012). Changes in the microbial community structure of bacteria, archaea and fungi in response to elevated CO2 and warming in an Australian native grassland soil. *Environ. Microbiol.* 14, 3081–3096. doi: 10.1111/j.1462-2920.2012.02855.x

Healy, W. (2009). *Piles of Money*. West Chicago, IL: Growertalks.

Hoda, E. E.-M., and Mona, S. (2014). Effect of bio and chemical fertilizers on growth and flowering of *Petunia hybrida* plants. *Am. J. Plant Physiol.* 9, 68–77. doi: 10.3923/ajpp.2014.68.77

Hontzeas, N., Zoidakis, J., Glick, B. R., and Abu-Omar, M. M. (2004). Expression and characterization of 1-aminocyclopropane-1-carboxylate deaminase from the rhizobacterium *Pseudomonas putida* UW4: a key enzyme in bacterial plant growth promotion. *Biochim. Biophys. Acta Proteins Proteom.* 1703, 11–19. doi: 10.1016/j.bbapap.2004.09.015

Huang, C., Zhao, S., Wang, L., Anjum, S. A., Chen, M., Zhou, H., et al. (2013). Alteration in chlorophyll fluorescence, lipid peroxidation and antioxidant enzymes activities in hybrid ramie (*Boehmeria nivea* L.) under drought stress. *Aust. J. Crop Sci.* 7, 594–599.

Huang, X. F., Zhou, D., Lapsansky, E. R., Reardon, K. F., Guo, J., Andales, M. J., et al. (2017). *Mitsuaria* sp. and *Burkholderia* sp. from *Arabidopsis rhizosphere* enhance drought tolerance in *Arabidopsis thaliana* and maize (*Zea mays* L.). *Plant Soil* 419, 523–539. doi: 10.1007/s11104-017-3360-3364

Hussain, M. B., Zahir, Z. A., Asghar, H. N., and Asgher, M. (2014). Can catalase and exopolysaccharides producing rhizobia ameliorate drought stress in wheat? *Int. J. Agric. Biol.* 16, 3–13.

Jodeh, S., Alkowni, R., Hamed, R., and Samhan, S. (2015). The study of electrolyte leakage from barley (*Hordeum vulgare* L) and pearlmillet using plant growth promotion (PGPR) and reverse osmosis. *J. Food Nutr. Res.* 3, 422–429. doi: 10.12691/jfnr-3-7-3

Kang, S. M., Khan, A. L., You, Y. H., Kim, J. G., Kamran, M., and Lee, I. J. (2014). Gibberellin production by newly isolated strain leifsonia soli SE134 and its potential to promote plant growth. *J. Microbiol. Biotechnol.* 24, 106–112. doi: 10.4014/jmb.1304.04015

Klee, H. J., Hayford, M. B., Kretzmer, K. A., Barry, G. F., and Kishore, G. M. (1991). Control of ethylene synthesis by expression of a bacterial enzyme in transgenic tomato plants. *Plant Cell* 3, 1187–1193. doi: 10.2307/3869226

Konstantinidis, K. T., and Tiedje, J. M. (2005). Genomic insights that advance the species definition for prokaryotes. *Proc. Natl. Acad. Sci. U.S.A.* 102, 2567–2572. doi: 10.1073/pnas.0409727102

Leoni, B., Loconsole, D., Cristiano, G., and Lucia, B. (2019). Comparison between chemical fertilization and integrated nutrient management: yield, quality, N, and P contents in *Dendranthema grandiflorum* (Ramat.) Kitam. cultivars. *Agronomy* 9, 1–16. doi: 10.3390/agronomy9040202

Liu, F., Xing, S., Ma, H., Du, Z., and Ma, B. (2013). Cytokinin-producing, plant growth-promoting rhizobacteria that confer resistance to drought stress in *Platycladus orientalis* container seedlings. *Appl. Microbiol. Biotechnol.* 97, 9155–9164. doi: 10.1007/s00253-013-5193-5192

Mayak, S., Tirosh, T., and Glick, B. R. (2004). Plant growth-promoting bacteria that confer resistance to water stress in tomatoes and peppers. *Plant Sci.* 166, 525–530. doi: 10.1016/j.plantsci.2003.10.025

Mesa-Marín, J., Pérez-Romero, J. A., Mateos-Naranjo, E., Bernabeu-Meana, M., Pajuelo, E., Rodríguez-Llorente, I. D., et al. (2019). Effect of plant growth-promoting rhizobacteria on *Salicornia ramosissima* seed germination under salinity, CO_2 and temperature stress. *Agronomy* 9, 1–14. doi: 10.3390/agronomy9100655

Montagne, V., Capiaux, H., Barret, M., Cannavo, P., Charpentier, S., Grosbellet, C., et al. (2017). Bacterial and fungal communities vary with the type of organic substrate: implications for biocontrol of soilless

crops. *Environ. Chem. Lett.* 15, 537–545. doi: 10.1007/s10311-017-0628-620

National Agricultural Statistics, (2019). *Floriculture Crops 2018 Summary*. Washington, D.C: United States Department of Agriculture.

Naumann, J. C., Young, D. R., and Anderson, J. E. (2007). Linking leaf chlorophyll fluorescence properties to physiological responses for detection of salt and drought stress in coastal plant species. *Physiol. Plant.* 131, 422–433. doi: 10.1111/j.1399-3054.2007.00973.x

Naveed, M., Mitter, B., Reichenauer, T. G., Wieczorek, K., and Sessitsch, A. (2014). Increased drought stress resilience of maize through endophytic colonization by *Burkholderia phytofirmans* PsJN and *Enterobacter* sp. FD17. *Environ. Exp. Bot.* 97, 30–39. doi: 10.1016/j.envexpbot.2013.09.014

Naylor, D., and Coleman-Derr, D. (2018). Drought stress and root-associated bacterial communities. *Front. Plant Sci.* 8:2223. doi: 10.3389/fpls.2017.02223

Nelson, L., and Carlson, W. (1987). *Improve the Marketability Of Bedding Plants*. Calverton, NY: Green Grow Farms.

Ngumbi, E., and Kloepper, J. (2016). Bacterial-mediated drought tolerance: current and future prospects. *Appl. Soil Ecol.* 105, 109–125. doi: 10.1016/j.apsoil.2016.04.009

Nilsen, E. T., and Orcutte, D. M. (1996). "Phytohormones and plant responses to stress," in *Physiology Of Plants Under Stress: Abiotic Factors*, ed. G. K. Pandey, (New York, NY: John Wiley and Sons), 183–198.

Nordstedt, N. P., Chapin, L. J., Taylor, C. G., and Jones, M. L. (2020). Identification of *Pseudomonas* Spp. that increase ornamental crop quality during abiotic stress. *Front. Plant Sci.* 10:1754. doi: 10.3389/fpls.2019.01754

Paulitz, T. C., and Richard, R. B. (2001). Biological control in greenhouse systems. *Annu. Rev. Phytopathol.* 39, 103–133.

Penrose, D. M., and Glick, B. R. (2003). Methods for isolating and characterizing ACC deaminase-containing plant growth-promoting rhizobacteria. *Physiol. Plant.* 118, 10–15. doi: 10.1034/j.1399-3054.2003.00086.x

Raheem, A., Shaposhnikov, A., Belimov, A. A., Dodd, I. C., and Ali, B. (2018). Auxin production by rhizobacteria was associated with improved yield of wheat (*Triticum aestivum* L.) under drought stress. *Arch. Agron. Soil Sci.* 64, 574–587. doi: 10.1080/03650340.2017.1362105

Rodriguez-R, L. M., Gunturu, S., Harvey, W. T., Rosselló-Mora, R., Tiedje, J. M., Cole, J. R., et al. (2018). The microbial genomes atlas (MiGA) webserver: taxonomic and gene diversity analysis of archaea and bacteria at the whole genome level. *Nucleic Acids Res.* 46:gky467. doi: 10.1093/nar/gky467

Sánchez-Blanco, M. J., Álvarez, S., Navarro, A., and Bañón, S. (2009). Changes in leaf water relations, gas exchange, growth and flowering quality in potted geranium plants irrigated with different water regimes. *J. Plant Physiol.* 166, 467–476. doi: 10.1016/j.jplph.2008.06.015

Sandhya, V., Ali, S. Z., Grover, M., Reddy, G., and Venkateswarlu, B. (2010). Effect of plant growth promoting *Pseudomonas* spp. on compatible solutes, antioxidant status and plant growth of maize under drought stress. *Plant Growth Regul.* 62, 21–30. doi: 10.1007/s10725-010-9479-9474

Siddique, Z., Jan, S., Imadi, S. R., Gul, A., and Ahmad, P. (2016). *Water Stress And Crop Plants: A Sustainable Approach*. West Sussex: Wiley.

Singh, S. K., and Raja Reddy, K. (2011). Regulation of photosynthesis, fluorescence, stomatal conductance and water-use efficiency of cowpea (*Vigna unguiculata* L. Walp.) under drought. *J. Photochem. Photobiol. B Biol.* 105, 40–50. doi: 10.1016/j.jphotobiol.2011.07.001

Tiwari, S., Lata, C., Chauhan, P. S., and Nautiyal, C. S. (2016). *Pseudomonas putida* attunes morphophysiological, biochemical and molecular responses in *Cicer arietinum* L. during drought stress and recovery. *Plant Physiol. Biochem.* 99, 108–117. doi: 10.1016/j.plaphy.2015.11.001

Upadhyay, S. K., and Singh, D. P. (2015). Effect of salt-tolerant plant growth-promoting rhizobacteria on wheat plants and soil health in a saline environment. *Plant Biol.* 17, 288–293. doi: 10.1111/plb.12173

Vardharajula, S., Ali, S. Z., Grover, M., Reddy, G., and Bandi, V. (2011). Drought-tolerant plant growth promoting *Bacillus* spp.: effect on growth, osmolytes, and antioxidant status of maize under drought stress. *J. Plant Interact.* 6, 1–14. doi: 10.1080/17429145.2010.535178

Wang, S., Ouyang, L., Ju, X., Zhang, L., Zhang, Q., and Li, Y. (2014). Survey of plant drought-resistance promoting bacteria from *Populus euphratica* tree living in arid area. *Indian J. Microbiol.* 54, 419–426. doi: 10.1007/s12088-014-0479-473

Yang, J., Kloepper, J. W., and Ryu, C. M. (2009). Rhizosphere bacteria help plants tolerate abiotic stress. *Trends Plant Sci.* 14, 1–4. doi: 10.1016/j.tplants.2008.10.004

Yasmin, H., Nosheen, A., Naz, R., Bano, A., and Keyani, R. (2017). L-tryptophan-assisted pgpr-mediated induction of drought tolerance in maize (*Zea mays* L.). *J. Plant Interact.* 12, 567–578. doi: 10.1080/17429145.2017.1402212

Zahir, Z. A., Munir, A., Asghar, H. N., Shaharoona, B., and Arshad, M. (2008). Effectiveness of rhizobacteria containing ACC deaminase for growth promotion of peas (*Pisum sativum*) under drought conditions. *J. Microbiol. Biotechnol.* 18, 958–963.

Conflict of Interest: The authors declare that the research was conducted in the absence of any commercial or financial relationships that could be construed as a potential conflict of interest.

frontiers in Plant Science

ORIGINAL RESEARCH
published: 24 June 2020
doi: 10.3389/fpls.2020.00825

Raising the pH of the Pulsing Solution Improved the Acropetal Transport of NAA and 2,4-D and Their Efficacy in Reducing Floret Bud Abscission of Red Cestrum Cut Flowers

Bekele Abebie[1,2], Sonia Philosoph-Hadas[1], Joseph Riov[2], Moshe Huberman[2], Raphael Goren[2] and Shimon Meir[1]*

[1] Department of Postharvest Science, Agricultural Research Organization, The Volcani Center, Rishon LeZion, Israel, [2] The Robert H. Smith Institute of Plant Sciences and Genetics in Agriculture, The Robert H. Smith Faculty of Agriculture, Food and Environment, The Hebrew University of Jerusalem, Rehovot, Israel

OPEN ACCESS

Edited by:
Antonio Ferrante, University of Milan, Italy

Reviewed by:
Barbara De Lucia, University of Bari Aldo Moro, Italy
Yunus Effendi, Leibniz University Hannover, Germany

***Correspondence:**
Sonia Philosoph-Hadas
vtsoniap@volcani.agri.gov.il

Specialty section:
This article was submitted to Crop and Product Physiology, a section of the journal Frontiers in Plant Science

Received: *06 March 2020*
Accepted: *22 May 2020*
Published: *24 June 2020*

Citation:
Abebie B, Philosoph-Hadas S, Riov J, Huberman M, Goren R and Meir S (2020) Raising the pH of the Pulsing Solution Improved the Acropetal Transport of NAA and 2,4-D and Their Efficacy in Reducing Floret Bud Abscission of Red Cestrum Cut Flowers. Front. Plant Sci. 11:825. doi: 10.3389/fpls.2020.00825

The use of auxins to improve the vase life of cut flowers is very limited. Previous studies demonstrated that a pulse treatment of Red Cestrum (*Cestrum elegans* Schlecht.) cut flowers with 2,4-dichlorophenoxyacetic acid (2,4-D) significantly reduced floret bud abscission, whereas 1-naphthaleneacetic acid (NAA) was ineffective. This difference resulted, at least in part, from the higher acropetal transport capability of 2,4-D compared to that of NAA. The present research focused on examining the factors affecting the acropetal transport, and hence the efficacy of the two auxins in reducing floret bud abscission of Red Cestrum cut flowers. We assumed that the differential acropetal transport capability of the two auxins results from the difference in their dissociation constants (pKa), with values of 2.75 and 4.23 for 2,4-D and NAA, respectively, which affects their pH-dependent physicochemical properties. Thus, increasing the pH of the pulsing solution above the pKa of both auxins might improve their acropetal movement. Indeed, the results of the present research show that raising the pH of the pulsing solution to pH 7.0 and above improved the efficacy of the two auxins in reducing floret bud abscission, with a higher effect on 2,4-D than that on NAA. Raising the pH of the pulsing solution decreased the adsorption and/or uptake of the two auxins by the cells adjacent to the xylem vessels, leading to an increase in their acropetal transport. The high pH of the pulsing solution increased the dissociation and hence decreased the lipophilicity of the auxin molecules, leading to improved acropetal movement. This effect was corroborated by the significant reduction in their 1-octanol/water partition coefficient (K_{OW}) values with the increase in the pH. A significant increase in the *CelAA1* transcript level was obtained in response to 2,4-D pulsing at pH

7.0 and 8.25 and to NAA pulsing at pH 8.25, indicating that the acropetally transported auxins were taken up by the cells under these conditions. Our data suggest that raising the pH of the pulsing solution would significantly contribute to the increased efficacy of auxins in improving the vase life of cut flowers.

Keywords: acropetal auxin transport, *Cestrum elegans*, *CelAA1* transcript level, cut flowers, floret bud abscission, NAA, 2,4-D, pH

INTRODUCTION

The vase life of cut flowers is limited by the acceleration of several processes, such as senescence and abscission or wilting of their various organs after harvest (Reid and Jiang, 2012). Application of growth regulators is one of the various technologies developed to improve the vase life of cut flowers. Treatments with cytokinins and gibberellins were reported to have a positive effect on the vase life of a wide range of cut flowers, by retarding leaf senescence and/or flower senescence or abscission, and by improving flower opening (Ascough et al., 2005; Reid and Jiang, 2012). Although auxins play a major role in the control of the abscission process by rendering the abscission zone (AZ) insensitive to ethylene (Meir et al., 2015), and they were also reported to retard petal senescence (Wojciechowska et al., 2018), they are seldom being used to improve the vase life of cut flowers. There are only a very few reports on the improvement of the vase life of cut flowers by auxins, applied either by pulsing or a quick dip of the whole flowers in the treatment solution. These reports include treatments with 2,4-dichlorophenoxyacetic acid (2,4-D) in carnations (Sacalis and Nichols, 1980) and 1-naphthaleneacetic acid (NAA) in Alstroemeria (Bagheri et al., 2012). Other reports demonstrated that auxin alone was ineffective, but when applied together with cytokinins or ethylene inhibitors, the combined treatment improved the vase life of cut flowers. These reports include a combined treatment of 2,4-D and benzyladenine in daffodils (*Narcissus pseudonarcissus*) (Ballantyne, 1965), 2,4-D and silver thiosulfate (STS) in Red Cestrum (Meir et al., 1999), and NAA and aminoethoxyvinylglycine (AVG) in lisianthus (*Eustoma grandiflorum*) (Shimizu-Yumoto and Ichimura, 2010a). Based on the results of the latter report, the above authors stated that auxin treatment might have a potential to improve the vase life of cut flowers (Shimizu-Yumoto and Ichimura, 2010b).

Application of chemicals to cut flowers is usually performed by pulsing, which is the common method used by growers. However, application of auxins by this method might be ineffective, since their acropetal transport might be limited. There are two main pathways of auxin transport in plants (Petrášek and Friml, 2009). The first is carrier-regulated cell-to-cell polar transport, and the second is non-directional transport in the phloem, which is commonly related to the transport of indole-3-acetic acid (IAA) from source organs. However, the above-mentioned reports demonstrating improved vase life of cut flowers by various auxins applied by pulsing, indicate that auxins are also transported acropetally, presumably in the xylem. Acropetal transport of auxins was also demonstrated in other systems by using radiolabeled auxins, including transport of IAA and indole-3-butyric acid (IBA) in shoot sections of *Arabidopsis thaliana* (Ludwig-Müller et al., 1995), NAA in loblolly pine (*Pinus taeda* L.) cuttings (Diaz-Sala et al., 1996), and IAA and IBA in mung bean cuttings (Weisman et al., 1988). Our research group demonstrated a significant fast acropetal transport of 2,4-D in cut Red Cestrum shoot sections, whereas NAA moved mostly polarly in this system (Abebie et al., 2005, 2006).

There are acceptable insights about the factors affecting the acropetal transport of weak acids in the xylem, which are relevant to most common auxins (Trapp, 2004; Kramer, 2006). Indolic auxins and NAA have a dissociation constant (pKa) between 4 and 5. In the weak acidic xylem sap, part of the molecules of these auxins will be protonated, and hence membrane permeable. Upon entering the cells adjacent to the xylem vessels, these molecules will be dissociated in the almost neutral cytoplasm, and accumulate within the cells. This mechanism, known as ion trapping (Sterling, 1994), limits the acropetal movement of auxins in the xylem, particularly if trans-membrane efflux carriers are not present. The pKa also affects the adsorption rate of various molecules onto plant cell wall components, namely lignin (Barak et al., 1983; Trapp et al., 2001), a process that might also reduce the acropetal movement of auxins. The pKa of 2,4-D (2.75) is significantly lower than that of indolic auxins and NAA, and hence 2,4-D is expected to have a relatively higher capability of acropetal transport when applied by pulsing by the commercial acidic preservative solutions, as indeed demonstrated in our previous studies (Abebie et al., 2005, 2006). The acropetal transport of auxins in the xylem is a passive process, so that the involvement of auxin transporters in this process is indirect, and could be carried out by an effect on the ion trapping mechanism. It is a common view that the accumulation of weakly acidic auxins in cells is mainly regulated by the activity of influx and efflux carriers (Grones and Friml, 2015). However, there are indications that there is a tendency of weak acids present in the extracellular space to be trapped by adjacent cells due to dissociation in the almost neutral cellular pH (Kramer, 2006).

The transport of a molecule in the plant vascular systems is often related to the relationship between its pKa and its lipophilicity (Grimm et al., 1986; Rigitano et al., 1987). Lipophilicity of a compound is commonly expressed by its *n*-octanol/water partition coefficient (K_{OW}), whose value is mostly determined by its pKa (Briggs et al., 1987; Chamberlain et al., 1996). The K_{OW} value determines the lipophilic-hydrophilic balance, which in turn determines the ease of movement across plant membranes. The importance of K_{OW} as an indicator of lipophilicity in biological studies has been well established (Leo et al., 1971; Leo, 2000). Organic compounds can be classified as lipophilic when the log $K_{OW} > 0$, and

as hydrophilic when the log $K_{OW} < 0$ (Popp et al., 2005). According to Bertosa et al. (2003), the lipophilicity positively correlates with membrane permeability and receptor binding of auxin molecules. Although the K_{OW} is a good indicator for measuring lipophilicity and adsorption of a xenobiotic, there are some anomalies when it comes to hydrophilic compounds. For example, the adsorption of the hydrophilic compounds onto cuticular membranes is significantly higher than expected from their K_{OW} values (Kerler and Schönherr, 1988).

We previously observed that 2,4-D exhibited a high efficacy in improving the vase life of Red Cestrum cut flowers by inhibiting their floret bud abscission, whereas NAA had almost no effect (Abebie et al., 2005, 2006, 2007). Similarly, a combined treatment of STS and 2,4-D inhibited floret bud abscission in Red Cestrum cut flowers, whereas a combination of STS and NAA was ineffective (Meir et al., 1999). Based on the above mentioned observations regarding the higher acropetal transport capability of 2,4-D in Red Cestrum compared to that of NAA (Abebie et al., 2005, 2006), we assumed that the difference in the response to the above treatments resulted from the differential acropetal transport capability of the two auxins. The difference in the acropetal transport capability is undoubtedly related to different physicochemical characteristics of the two auxins, namely the significantly higher pKa of NAA (4.23) than that of 2,4-D (2.75), which affect their membrane permeability and adsorption onto plant cell wall components, and possibly also apoplastic proteins. Hence, increasing the pH of the pulsing solution well above the pKa might decrease the efficacy of the ion trapping mechanism of the applied auxins and their adsorption onto plant cell wall components, resulting in their increased acropetal transport.

The aims of the present study were: (a) to examine the effect of the pH of the pulsing solutions of NAA and 2,4-D on their differential acropetal transport in relation to their efficacy in reducing floret bud abscission in Red Cestrum cut flowers; (b) to study the effect of pH on the physicochemical properties of these auxins in relation to their differential acropetal transport capability. The data of the present study indeed confirmed our assumption. Raising the pH of the pulsing solution of the two auxins well above their pKa, with the required raise in the pH being higher for NAA than that for 2,4-D, significantly increased their acropetal transport in Red Cestrum cut flowers, resulting in reduced bud abscission. Therefore, adjusting the pH of the pulsing solution of auxins might significantly increase their efficacy in improving the vase life of cut flowers, and therefore might enable the use of mild and hence less phytotoxic auxins, such as NAA, for treating cut flowers.

MATERIALS AND METHODS

Plant Material

Red Cestrum (*Cestrum elegans* Schlecht cv. "Red Flame") cut flowers were obtained from plants grown in a local commercial plantation. A typical cestrum cut flower shoots has an inflorescence composed of alternate racemes bearing a cluster of florets at different stages of development (**Figure 1A**). The florets in the upper shoot apex and the raceme apexes are chronologically older and open first, while those in the lower positions are chronologically younger and open last. Each individual inflorescence head contains also florets at different stages of development (**Figures 1B,C**). Generally, the experiments were performed with commercial size cut flowers bearing a few open florets, except for one experiment in which shoot segments were used.

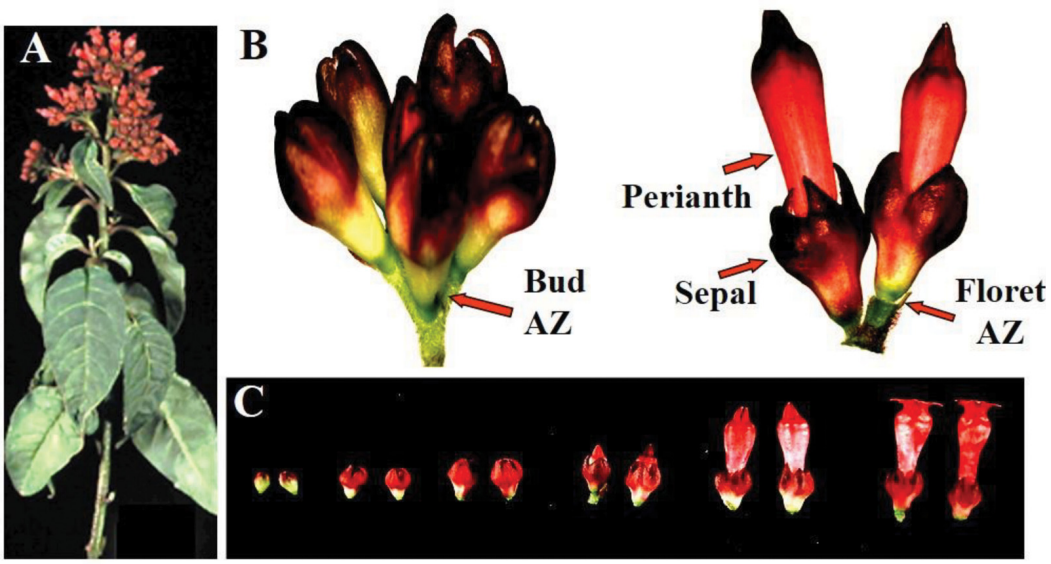

FIGURE 1 | Morphology of floret developmental stages in Red Cestrum cut flowers. A typical cut flowering shoot **(A)**; definition of floral parts in an individual cluster of florets from an inflorescence head composed of florets at two developmental stages **(B)**; and classification of floret buds developmental stages **(C)**.

Radiochemicals

[1-^{14}C]NAA (specific activity 344 MBq mmol^{-1}) and [1-^{14}C]2,4-D (specific activity 592 MBq mmol^{-1}) were obtained from Sigma, United States. The purity of the radiochemicals was checked periodically by thin-layer chromatography, using silica gel GF_{254} plates developed with chloroform-ethyl acetate-formic acid (5:4:1, v/v).

Pulsing Treatments

Cut flowers were incubated at room temperature for about 2 h until they lost 3–5% of their fresh weight (FW), in order to increase the uptake of the applied auxins. For the experiments, 30-cm-long cut flowers were used. The leaves were removed up to 12 cm from the base of the shoots, and each shoot was placed in a 50-mL Falcon tube containing 7 mL of the pulsing solution composed of 0.2 M buffer for obtaining the desired pH, and 0.2 mM of NAA or 2,4-D with or without the corresponding radiolabeled auxins as tracers. The buffers used were Na_2HPO_4-citrate buffer for obtaining pH levels up to 7.0, and Tris–HCl buffer for obtaining pH levels above 7.0. The cut flowers were pulsed for 24 h in an observation room maintained at 20°C, 60–70% relative humidity, and 12-h photoperiod at a light intensity of 14 μmol m^{-2} s^{-1}. In one experiment, the pulsing treatment was performed for 4 h at 20°C followed by additional 20 h at 4°C. After pulsing, the lower 2-cm section of each shoot was trimmed off, and the pulsing solution was replaced with 20 mL of a disinfectant aqueous solution containing 50 μL L^{-1} sodium dichloroisocyanurate, pH 6.0 (TOG-6®, Gadot-Agro Ltd., Israel). The shoots were incubated in the observation room under the conditions specified above for vase life evaluation. Additional TOG-6 solution was added during vase life when necessary to replace the amount lost by transpiration.

Monitoring Floret Bud Abscission

For monitoring floret bud abscission during vase life, individual inflorescence heads were removed from the cut flowers at different time points, placed in polyethylene bags, tapped gently, and the abscised floret buds were collected and counted. At the end of the experiment, the floret buds that did not abscise were counted, and their number was summed up to the number of abscised ones to determine the percentage of accumulated floret bud abscission during vase life.

Autoradiography of the Acropetal Transport of NAA and 2,4-D in Cut Flowers

For determining the acropetal transport of NAA or 2,4-D by autoradiography, cut flowers were pulsed for 24 h with the standard auxin pulsing solutions containing 16.0 KBq of either [1-^{14}C]NAA or [1-^{14}C]2,4-D as tracers. At the end of a 24-h pulsing treatment (0 h), the lower part of each cut flower shoot was thoroughly washed with distilled water, and the cut flowers were dried off by pressing them for 1 week between 20 × 40-cm blotting papers at room temperature. The dried samples were exposed to Fujifilm Imaging Plates for 48 h, the images were then analyzed by a Fujifilm Fla-5000 phospho-imager, and processed with Photoshop version 7.0.

Measuring the Adsorption and/or Uptake of NAA and 2,4-D by Xylem Shoot Cells

Adsorption and/or uptake of radiolabeled NAA or 2,4-D by shoot xylem sections were measured as previously described by Huberman et al. (2005) with some modifications. Samples of 200 mg of 2-3-mm-long sections of xylem tissue were pre-incubated for 5 min in 25-mL Erlenmeyer flasks containing 5 mL of 20 mM Na_2HPO_4-citrate buffer (for pH 3.0, 5.0, and 7.0), or 20 mM Tris–HCl buffer (for pH 9.0) to equilibrate the extracellular pH to the desired values. The above pre-incubation procedure was repeated three times. The pre-incubation buffers were removed by suction, and 2 mL of the corresponding incubation buffers containing 0.2 mM of NAA or 2,4-D and 3.6 KBq of [1-^{14}C]NAA or 3.8 KBq of [1-^{14}C]2,4-D as tracers were added. The sections were then incubated for 1 h at 25°C in a shaking water bath. At the end of the incubation, the incubation buffers were removed by suction, and the samples were extensively washed three times with 5 mL of the same buffer for 5 min to remove the label from the apoplast. After the final wash, the samples were blotted onto a paper towel, and then the radioactivity was extracted with 10 mL of Opti-Fluor® high performance flash-point liquid scintillation cocktail for aqueous samples (Packard BioScience, United States) by shaking overnight in darkness. The extracted radioactivity was then monitored by a Liquid Scintillation Analyzer (Packard Tri-Carb 1600 TR, United States). The calculated auxin adsorption and/or uptake is expressed as nmol g^{-1} FW.

Determination of *CeIAA1* RNA Transcript Level

Total RNA was extracted from the floret AZ following the cetyltrimethylammonium bromide (CTAB) extraction procedure, as described by Liao et al. (2004) with some modifications, following the LiCl overnight precipitation and centrifugation (20,000 × *g* for 20 min at 4°C). After a subsequent centrifugation (20,000 × *g* for 40 min at 4°C), the pellet was resuspended in 0.5 mL of sterile water and transferred to sterile Eppendorf tubes. Then, 1.8 volume of absolute ethanol and 0.1 volume of 3.0 M sodium acetate (pH 5.5) were added, and the RNA was precipitated by an overnight incubation at −20°C, pelleted by centrifugation (20,000 × *g* for 20 min at 4°C), washed twice with 75% ethanol, and resuspended in an appropriate amount of sterile water. The RNA was quantified by NanoDrop® ND-1000 spectrophotometer (NanoDrop Technologies, Inc., Rockland, DE, United States), and stored at −80°C for further use. Equal amounts of total RNA (20 μg) were run on a formaldehyde agarose gel and blotted onto Hybond N$^+$ membranes (Amersham Pharmacia Biotech, United States) by the standard capillary transfer methods (Ausubel et al., 1995). Membranes were hybridized with ^{32}P-labeled *CeIAA1* (Gene bank accession no. DQ900819) gene specific probe amplified

from the 3′UTR of the clone. The transcript level of this gene was compared by quantitative real time PCR (qRT-PCR) analysis performed as described by Abebie et al. (2007). The sequences of the forward and reverse primers used for the qRT-PCR analysis were 5′-CACCAACATATGAAGACAAGG-3′, and 5′-GCTTCAGAACCCTTCATG-3′, respectively. Two separate experiments were performed with similar results, in which the qRT-PCR reactions were performed in duplicates, thus representing overall four biological replicates.

Determination of Physicochemical Properties of NAA and 2,4-D

The partition coefficient (K_{OW}) values of NAA and 2,4-D were determined using the shake-flask method, as described by the Organization for Economic Cooperation and Development (OECD, 1987) guidelines for testing of chemicals. *n*-Octanol saturated with 20 mM Na_2HPO_4-citrate buffer (pH 3.0, 5.0, and 7.0), or 20 mM Tris–HCl buffer (pH 9.0) were used as the organic phase, and the above buffers saturated with *n*-octanol were used as the aqueous phase. The ratio of the organic phase to the aqueous phase was 1:1 (v/v), and the final concentration of NAA or 2,4-D dissolved in the aqueous phase was 2 mM. Each treatment was performed in four repetitions. Blanks were prepared in an identical manner, except that no auxin was added. The organic and the aqueous phases were allowed to reach equilibrium on a horizontal shaker for 24 h at 20°C. After equilibrium was achieved, the mixed solutions were centrifuged at 1,500 rpm for 15 min. The aqueous phase was carefully removed with a pasture pipette, and the absorbance of NAA or 2,4-D in the two phases was determined at 280 nm with a UV 2201 UV-VIS spectrophotometer against the above blanks. When required, the samples were diluted before measuring the absorbance. K_{OW} values were calculated from the equilibrium ratio of the auxin concentrations in the *n*-octanol and the aqueous phases, as extrapolated from standard curves.

Percent ionization was calculated by rearranging the Henderson–Hasselbalch equation at a known pH and pKa of a xenobiotic,[1] as follows:

$$\% \text{ ionization} = \frac{10^{\text{pH}-\text{pKa}}}{1 + 10^{\text{pH}-\text{pKa}}} \times 100$$

Statistical Analysis

The statistical analysis was performed using JMP 5.0 software (SAS Institute). The data were analyzed using one-way ANOVA. Significant differences between treatment means were determined by Tukey's HSD test ($P \leq 0.01$). Experiments were repeated at least twice, and the data from one representing experiment are presented. The number of replicates in each experiment is specified in the legends of the table and figures.

[1]https://basicmedicalkey.com/physical-and-chemical-properties-of-drug-molecules/

RESULTS

Effect of the pH of the Pulsing Solution on the Efficacy of NAA and 2,4-D in Inhibiting Floret Bud Abscission

The effect of the pH of the pulsing solution on the inhibitory effect of NAA and 2,4-D on floret bud abscission was determined at different time points after a 24-h pulsing treatment. When the pH of the NAA pulsing solution was equal to its pKa (4.23), about 60% of the floret buds already abscised at 2 days after pulsing, and the abscission rate reached 100% after 4 days (**Figure 2A**). Pulsing with 2,4-D at pH equal to its pKa (2.75) resulted in a similar abscission pattern to that obtained with NAA. Raising the pH of the NAA pulsing solution to 7.0 slightly reduced the abscission rate compared to that obtained at the pH equal to its pKa, particularly during the initial 3 days after pulsing (**Figure 2B**). In contrast, at pH 7.0, 2-4-D significantly reduced the abscission rate compared to that obtained at the pH equal to its pKa, and the inhibitory effect was significantly higher than that observed with NAA at all the time points. Only pulsing with NAA at pH 8.25 significantly increased its inhibitory effect on floret bud abscission at all the time points compared to that obtained at pH 7.0, but the inhibitory effect of 2,4-D at this pH was again higher than that obtained with NAA (**Figure 2C**). It is noteworthy, that neither of the buffers used to obtain the various pH levels had any effect on floret bud abscission (data not shown).

Autoradiography of the Acropetal Transport of NAA and 2,4-D

The effect of the pH of the pulsing solution on the acropetal transport of NAA and 2,4-D to the various organs of the cut flowers was evaluated by autoradiography conducted at the end of a 24-h pulsing. At the pH equal to the pKa, a strong label of NAA was observed in the lower shoot section, and only a trace of labeled NAA was detected in the upper shoot section and the lower leaves (**Figure 3A**). At pH 7.0, more NAA moved to the upper shoot section, and some label was also detected in the lateral shoots and particularly in the midribs of the lower leaves (**Figure 3B**). A much stronger label of NAA was observed in the above organs at pH 8.25, and a weak label was also detected at this pH in the rachises and the florets (**Figure 3C**). 2,4-D exhibited a different distribution pattern at the various pH levels than that obtained with NAA. Thus, some label of 2,4-D was already observed in the upper shoot section, lateral shoots, and midribs of the lower leaves at the pH equal to the pKa (**Figure 3D**). At pH 7.0 (**Figure 3E**) and particularly at pH 8.25 (**Figure 3F**), a strong label was detected in all organs of the cut flowers, including the sepals and florets of the open flowers.

Effect of the pH on the Adsorption and/or Uptake of NAA and 2,4-D by Xylem Shoot Cells

The effect of the pH on the adsorption of NAA and 2,4-D onto the cell wall of the xylem shoot cells and/or on their uptake by these cells was determined immediately after a 1-h incubation at

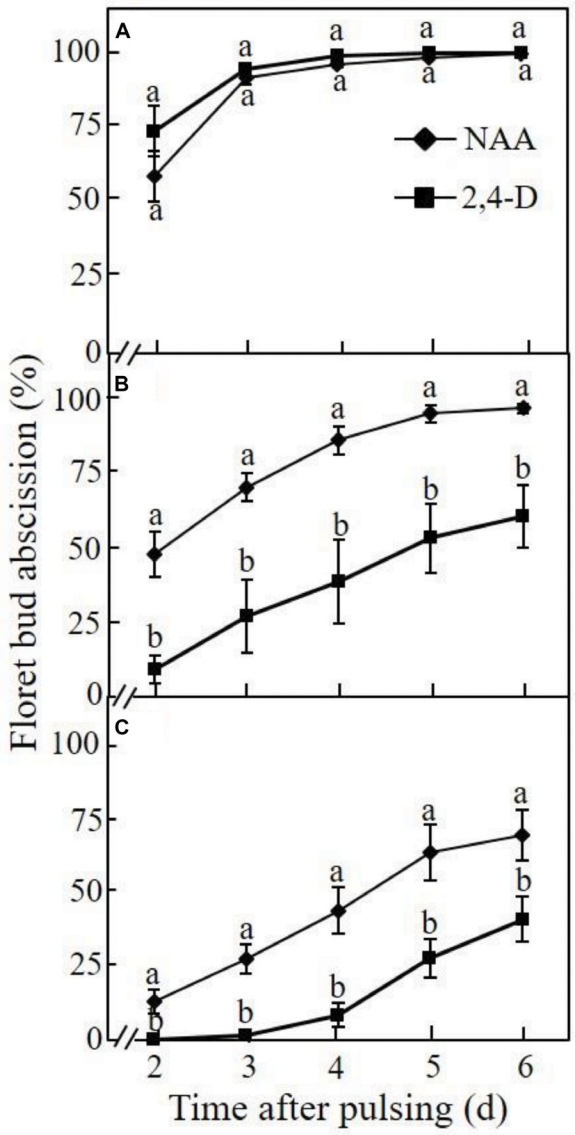

FIGURE 2 | Effect of the pH of the auxin pulsing solution on the efficacy of NAA and 2,4-D to retard floret bud abscission in Red Cestrum cut flowers during vase life. The cut flowers were pulsed for 24 h at 20°C with either 0.2 mM NAA or 2,4-D at pH = pKa **(A)**, pH = 7.0 **(B)**, or pH = 8.25 **(C)** and then placed in TOG-6 solution under vase life conditions for monitoring bud abscission. The percentage of abscised floret buds was determined relative to the total number of floret buds (abscised and intact) per inflorescence. Each value represents means of five replicates ± SE. Different letters indicate significant differences between treatments at each pH separately, at $P \leq 0.01$ according to the Tukey–Kramer HSD test using one-way ANOVA. The pKa values of NAA and 2,4-D are 4.23 and 2.75, respectively.

various pH levels. A gradual decrease in the adsorption and/or uptake of both auxins by the xylem shoot cells occurred with the increase in the pH of the pulsing solution from pH 3.0 to pH 9.0 (**Figure 4**). It should be noted that at all the pH levels, the amount of 2,4-D adsorbed and/or taken up by the xylem shoot cells was significantly lower than that of NAA.

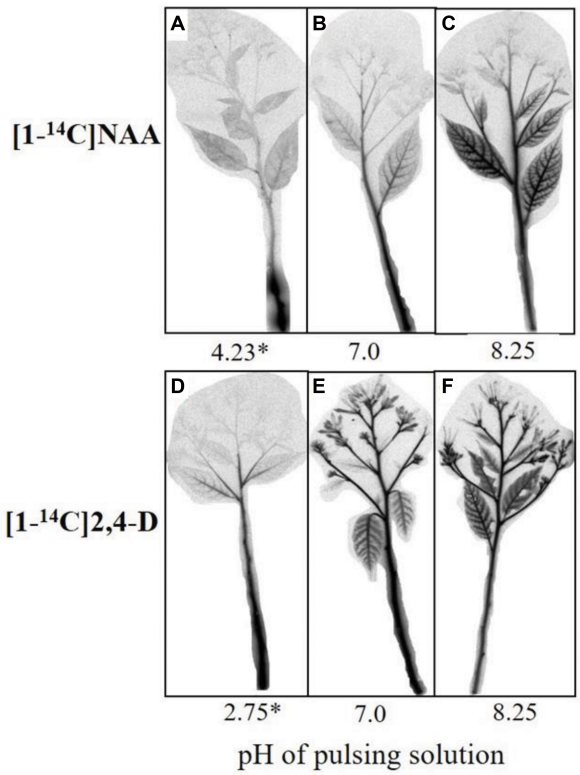

FIGURE 3 | Autoradiography images of the acropetal transport of labeled NAA **(A–C)** or 2,4-D **(D–F)** in Red Cestrum cut flowers after pulsing at different pH levels. The cut flowers were pulsed for 24 h at 20°C with either 0.2 mM NAA or 2,4-D containing radiolabeled standards, at the indicated pH values. After pulsing the shoots were dried and exposed to a Fujifilm Imaging Plate for 48 h. Asterisk, the pH = pKa values of each auxin.

Expression of *CeIAA1* in the Floret AZ Following Pulsing With NAA and 2,4-D at Different pH Levels

In order to examine the uptake of NAA and 2,4-D by the floret bud AZ cells following pulsing of cut flowers with either one of these auxins at different pH levels, we evaluated the expression of *CeIAA1* at various time points after pulsing. This gene was one of the six *Aux/IAA* homologous genes cloned in the floret bud AZ of Red Cestrum cut flowers following auxin application, as reported in our previous study (Abebie et al., 2007). It was selected for the present study since it exhibited the highest increase in expression in response to applied NAA or 2,4-D, and it peaked 2 days after the initiation of the auxin treatments. The results demonstrate that at the pH equal to the pKa, the expression of *CeIAA1* in the floret bud AZ cells of the NAA-treated cut flowers remained low during the entire experimental period (**Figure 5**). The expression of *CeIAA1* in the floret bud AZ cells of the 2,4-D-treated cut flowers pulsed at pH equal to the pKa exhibited a different pattern. *CeIAA1* expression increased 2 days after pulsing, remained high on the third day, and decreased later on to the basal level. Raising the pH of the NAA pulsing solution from 4.23 (its pKa) to 8.25

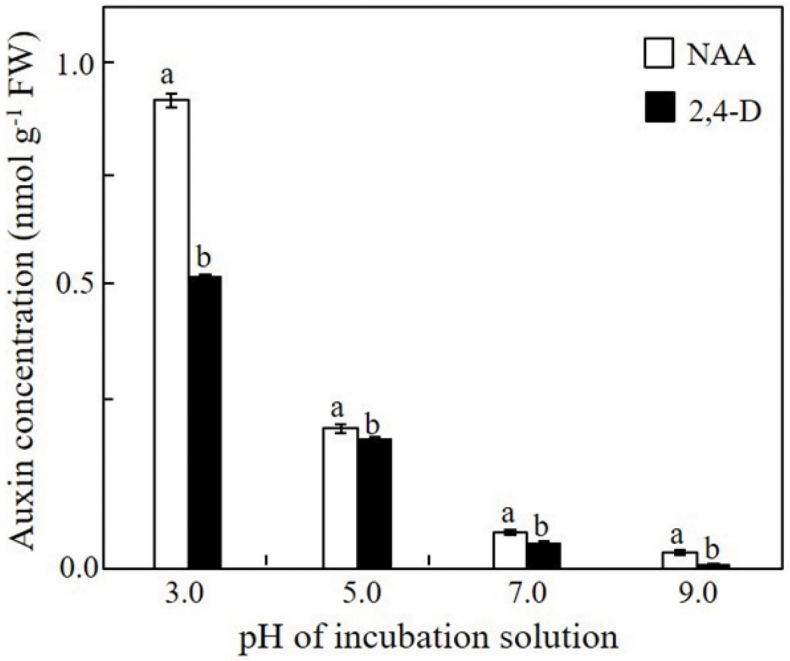

FIGURE 4 | Effect of the pH of the incubation solution on the uptake/adsorption of NAA or 2,4-D by the xylem shoot sections excised from Red Cestrum cut flowers. Samples of 2- to 3-mm-long sections of xylem tissue were incubated for 1 h in 0.2 mM NAA or 2,4-D containing radiolabeled standards at the indicated pH. The extracted radiolabeled auxins served for determination of the auxin concentration in the treated xylem sections. Each value represents means of three replicates ± SE. Different letters indicate significant differences between treatments at each pH separately, at $P \leq 0.01$ according to the Tukey–Kramer HSD test using one-way ANOVA.

increased by fourfold the expression of *CeIAA1* in the floret bud AZ cells one day after pulsing, and it gradually decreased later on to the basal level. Similar to NAA, *CeIAA1* expression increased considerably in the floret bud AZ cells of cut flowers pulsed with 2,4-D at pH 8.25, as compared to its pulsing at pH 2.75 (its pKa), reaching a peak of a fourfold increase 1 day after pulsing. However, unlike in NAA-treated flowers, *CeIAA1* expression in the 2,4-D-treated flowers at pH 8.25 decreased to a constant level, which remained about twofold higher than the basal level up to the end of the experiment. It should be noted that in our previous report we demonstrated that the expression of *CeIAA1* remained almost unchanged in the AZ of floret buds during vase life of the untreated cut flowers (Abebie et al., 2007).

Effect of the pH on Physicochemical Properties of NAA and 2,4-D

The effect of the pH on the ionization rates and K_{OW} values of NAA and 2,4-D was studied in order to elucidate the effect of the pH on their adsorption onto cell wall components of xylem shoot cells and/or uptake by these cells. The data presented in **Table 1** demonstrate that increasing the pH from 3.0 to 7.0 caused almost a complete ionization of the two auxins, with a significant concomitant decrease in their K_{OW} values. However, at the two lower pH levels, the ionization rates of 2,4-D were significantly higher than those of NAA, and its K_{OW} values were significantly lower.

DISCUSSION

Previous studies of our group demonstrated that 2,4-D applied by the standard pulsing method (pH 3.4) had a higher acropetal transport capability, and hence a higher efficacy in inhibiting abscission of floret buds and florets in Red Cestrum cut flowers during vase life, than those of NAA (Abebie et al., 2005, 2006, 2007). Based on the common view on the factors which affect the acropetal transport capacity of week acids (Trapp, 2004; Kramer, 2006), it seemed quite reasonable that the differential acropetal transport capacity of the two auxins resulted from the difference in their pKa values. We hypothesized that because of this difference, raising the pH of the pulsing solution of Red Cestrum cut flowers would differentially affect the physicochemical properties of the two auxins. This could in turn affect their lipophilicity, which determines the rate of adsorption onto plant cell wall components and/or uptake by cells, and hence their acropetal transport capability. The data of the present research demonstrated that raising the pH of the pulsing solution of NAA and 2,4-D increased their transport capacity (**Figure 3**), resulting in a higher efficacy in inhibiting floret bud abscission (**Figure 2**). But as expected, the increase in 2,4-D transport capacity was significantly higher than that of NAA. Similarly, the pKa was reported to be an important factor in determining the phloem transport capability of acidic herbicides (Bromilow et al., 1990). The difference in the pKa of the two auxins was also demonstrated in their differential

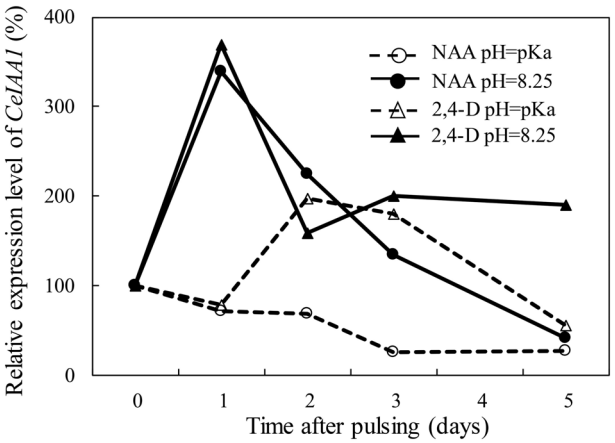

FIGURE 5 | Effect of the pH of the pulsing solution on the influence of NAA and 2,4-D on the transcript level of *CelAA1* gene in the floret AZ of Red Cestrum cut flowers during vase life. The cut flowers were pulsed for 4 h at 20°C and for additional 20 h at 4°C with 0.2 mM NAA or 2,4-D at pH = pKa or at pH = 8.25, and then placed in TOG-6 solution for further incubation under vase life conditions at 20°C. The qRT-PCR analysis was performed with RNA extracted from 2- to 3-mm-long floret AZ sections, excised at the indicated time points after pulsing during vase life. The expression level of *CelAA1* was calculated relative to its basal level at the end of pulsing (0 time). The pKa values of NAA and 2,4-D are 4.23 and 2.75, respectively. The results represent average values of four biological replicates (two replicates of qRT-PCR reactions in each one of the two separate experiments performed).

adsorption and/or uptake by xylem cells (**Figure 4**), which have a significant impact on the acropetal transport capability. It is noteworthy, that besides increasing the dissociation of the auxin molecules, which decreases their membrane permeability and adsorption onto cell wall components, the high pH can also inhibit the activity of 2,4-D influx carriers (see below), thus decreasing its ion trapping in cells adjacent to the vascular system.

Studying the effect of the pH on the physicochemical properties of NAA and 2,4-D indicates that a high pulsing solution pH led to a significant reduction in the log K_{OW}, i.e., in the lipophilicity of both auxins (**Table 1**), so that the dissociated hydrophilic molecules failed to adsorb onto cell wall components and/or taken up by the cells. This leads in turn to their increased accumulation in the xylem, and hence to increased acropetal transport. A significant decline in the lipophilicity of weak acids with increasing pH was previously reported (Coupland, 1989). These data are in accordance with the observations showing the importance of the hydrophilic-lipophilic balance of xenobiotics for their transport capability in the vascular systems, for example in the phloem (Bromilow et al., 1990). Although both auxins exhibited a decrease in lipophilicity in response to the increase in the pH, the decrease in the lipophilicity of 2,4-D along the pH range studied was more significant than that of NAA, leading to a higher transport capability (**Figure 3**). It is noteworthy, that while the log K_{OW} of NAA at pH 3.0 (2.12) is comparable to the value reported in the literature (2.20), that of 2,4-D (1.30) was significantly lower than the reported value (2.90) (Jafvert et al., 1990). This could result from the fact that we determined the log K_{OW} of 2,4-D at a pH range higher than its pKa (2.75), in which more than 60% of its molecules are presumed to be dissociated (**Table 1**).

The relatively high lipophilicity of NAA led to its higher adsorption and/or uptake by the xylem cells compared to 2,4-D, particularly at the low pH level (**Figure 4**), indicating that lipophilicity of NAA is one of the major factors which hindered its acropetal movement compared to 2,4-D under the standard pulsing conditions (pH 3.4). Adsorption of lipophilic compounds onto plant material limits their movement (Barak et al., 1983; Trapp et al., 2001). For example, the more lipophilic herbicide trifluralin failed to move freely in the phloem because of its strong adsorption onto plant cells (Bromilow et al., 1990).

The data obtained in the present paper raise two questions. The first is related to the transport capability of NAA with the increase in the pH of the pulsing solution. The observations that the transport capability of NAA at pH 7.0, at which it was completely ionized (**Table 1**), was still limited (**Figure 3**), suggest that additional factors might affect its transport capability. One possible factor is the binding of NAA to apoplastic proteins, which reduces its level in the xylem. An example for these proteins is the Auxin Binding Protein 1 (ABP1). Although ABP1 is mostly localized in the endoplasmic reticulum (ER), there is evidence that a small fraction of it is localized in the apoplast, i.e., in the extracellular space between the plasma membrane and the cell wall (Feng and Kim, 2015; Grones and Friml,

TABLE 1 | Effect of the pH on physicochemical properties of NAA and 2,4-D.

Auxin $_{(pKa)}$	Parameter	pH			
		3.0	**5.0**	**7.0**	**9.0**
$NAA_{(4.23)}$	Percent ionization	5.60	86.00	99.80	99.99
	K_{OW}	130.88 ± 5.09	6.93 ± 0.15	0.92 ± 0.01	0.07 ± 0.01
	log K_{OW}	2.12	0.84	−0.03	−1.16
$2,4\text{-}D_{(2.75)}$	Percent ionization	64.00	99.00	99.80	99.99
	K_{OW}	20.04 ± 1.80	2.04 ± 0.04	0.69 ± 0.02	0.25 ± 0.01
	log K_{OW}	1.30	0.31	−0.16	−0.60

Percent ionization was determined by using the Henderson–Hasselbalch equation. K_{OW} values were calculated from the equilibrium ratio of the auxin concentrations in the n-octanol and the aqueous phases. The results of K_{OW} represent means of four replicates ± SE.

2015). In Arabidopsis for example, Xu et al. (2014) reported that about 22% of ABP1 was secreted from the ER to the apoplast. There are reports showing that the apoplast pH (5.5) is more favorable for auxin binding to ABP1 than the ER pH (7.5) (Grones and Friml, 2015). Nevertheless, NAA is expected to bind to some extend to ABP1 also at pH 7.0. In addition, it was reported that ABP1 has a much higher affinity for NAA binding than for 2,4-D binding (Badescu and Napier, 2006). Various other auxin binding proteins might also differentially interfere with the acropetal transport of the two auxins. Riederer (2004) claimed that lipophilic substances, which are present along the transport pathway, might be an additional barrier to transport. If a molecule is not sufficiently hydrophilic, it could be partitioned into the lipophilic substances, thereby being trapped by them. Our data show that, based on the physicochemical characteristics of the two auxins, NAA is less hydrophilic than 2,4-D at pH 7.0 (**Table 1**), so that this process might interfere with its acropetal transport more than with 2,4-D transport.

The second question is related to the uptake of auxins at high pH levels. Theoretically, a high pH in the xylem is expected to inhibit the uptake of auxins by the target cells, which in the present study were the floret bud AZ cells. This however was not the case in this system, since the inhibitory effect of NAA and 2,4-D on floret bud abscission (**Figure 2**) and their induction of *CeIAA1* expression in the AZ cells (**Figure 5**) were considerably higher at pH 8.25 than those obtained at lower pH levels. In our previous study performed with Red Cestrum cut flowers, we cloned six *Aux/IAA* homologous genes, designated as *CeIAA1* to *CeIAA6,* in the floret bud AZ (Abebie et al., 2007). The *CeIAA1* gene was characterized as a late auxin-responsive gene, as its mRNA peaked in the floret bud AZ 2 days after the initiation of the NAA or 2,4-D pulsing treatments. These results suggest that this gene may also have a regulatory role in the abscission process of floret buds. Therefore, the highly expressed *CeIAA1* gene in the floret bud AZ in response to auxin treatments can serve as a marker of auxin activity in this system. It should be noted that increased expression of the *Aux/IAA* homologous genes in our previous study occurred only in response to NAA or 2,4-D treatments, and was positively correlated with the efficacy of these treatments to inhibit floret bud abscission.

Auxin uptake at the high pH used for pulsing might be explained by re-attainment of the normal pH (pH homeostasis) in the xylem following the termination of the pulsing treatment, as described in various plant systems (Savchenko and Heber, 2000; Geilfus, 2017). For example, Peters and Felle (1991) demonstrated that the apoplast pH of corn coleoptile segments changed quickly during incubation, reaching a constant level irrespective of the initial incubation medium pH. Another common example of the apoplastic pH regulation is related to auxin-induced growth (Hager, 2003). Auxin induces the activation of the plasma membrane-localized H^+-ATPase, which leads to acidification of the apoplast, resulting in increased activity of cell wall-loosening enzymes, followed by cellular expansion by the turgor pressure. It is possible that the post pulsing TOG-6 disinfectant incubation solution (about pH 6.0) also contributed to the reduction of the xylem pH following pulsing at high pH levels, due to its relatively low pH. It is noteworthy that plant hormones, including auxins, can also move across cell membranes by means of transporters (Grones and Friml, 2015; Park et al., 2017). Delbarre et al. (1996) demonstrated that in suspension-cultured tobacco cells, uptake of NAA occurred mostly by diffusion, whereas that of 2,4-D occurred mostly by influx carriers. Similar to the penetration of auxins into cells by diffusion, the uptake of auxins by influx carriers is also dependent on the apoplast pH. Rubery (1978) reported that the pH optima of the carrier-mediated uptake of IAA and 2,4-D by suspension-cultured crown gall cells were pH 5.0 and 4.0, respectively. A later study approved the above data related to IAA uptake, by demonstrating that IAA binding to the Arabidopsis influx transporter AUX1 occurred in a pH-dependent manner, with maximum binding taking place between pH 5.0 and 6.0, and below and above this pH range the binding ability was very low (Carrier et al., 2008). The fact that none of the two auxin uptake processes, i.e., diffusion and influx carrier-mediated uptake, could operate at a high pH, supports our assumption that the xylem pH is adjusted to the normal one after pulsing, enabling the uptake of both auxins by the target cells.

The data of the present research indicate that the relatively high acropetal transport capability of 2,4-D is an important factor in determining its higher efficacy in inhibiting floret bud abscission compared to that of NAA. However, additional factors, namely a high auxin activity and a slow rate of metabolism in the plant tissues might contribute to the relatively high activity of 2,4-D (Enders and Strader, 2015; Peterson et al., 2016). 2,4-D was also demonstrated to be metabolized at a much slower rate than that of NAA in Red Cestrum cut flowers and leaf tissues (Abebie et al., 2005). However, the relatively high activity of 2,4-D might limit its use in various species due to phytotoxic effects. For example, pulsing of Red Cestrum cut flowers with 0.15 mM 2,4-D, which inhibited floret bud abscission, caused leaf yellowing (Meir et al., 1999). This was related to the increased ethylene production induced by 2,4-D, as the leaf yellowing was inhibited by STS, the ethylene action inhibitor. Similarly, Sacalis and Nichols (1980) reported that 2,4-D retarded petal senescence in carnation cut flowers, but caused damage to the vegetative tissues.

CONCLUSION

From our data it can be concluded that the higher acropetal transport capability of 2,4-D compared to that of NAA results from its lower pKa value. Since the pKa affects the pH-dependent physicochemical properties of these two auxins, raising the pH of the pulsing solution improved significantly their acropetal transport, and contributed to their increased efficacy in reducing floret bud abscission of Red Cestrum cut flowers. Based on these results, increasing the pH can be practically used for pulsing application of weakly acidic compounds for agricultural purposes, such as improving the vase life of cut flowers. Considering the possible phytotoxic effects of 2,4-D, raising the pH of the auxin pulsing solution might be mainly important for increasing the efficacy of mild auxins such as NAA.

DATA AVAILABILITY STATEMENT

All datasets generated for this study are included in the article.

AUTHOR CONTRIBUTIONS

BA, SM, SP-H, JR, and RG were responsible for the conception, design of the experiments, and interpretation of the data. BA performed the laboratory experiments and the analyses of the data. MH assisted in the performance of the experiments. BA, JR, SM, and SP-H were involved in drafting the work, responsible for the writing, editing, and final approval of the version to be published. All authors revised and approved the final version.

FUNDING

The research was supported by the Chief Scientist Fund of the Israeli Ministry of Agriculture (Project No. 409-0056-00 to SM, SP-H, and JR).

REFERENCES

Abebie, B., Goren, R., Huberman, M., Meir, S., Philosoph-Hadas, S., and Riov, J. (2005). Prevention of bud and floret abscission in *Cestrum* cut flowers is related to the mode of transport and metabolism of synthetic auxins. *Acta Hort.* 682, 789–794. doi: 10.17660/actahortic.2005.682.102

Abebie, B., Lers, A., Philosoph-Hadas, S., Goren, R., Riov, J., and Meir, S. (2007). Differential effects of NAA and 2,4-D in reducing floret abscission in *Cestrum* (*Cestrum elegans*) cut flowers are associated with their differential activation of *Aux/IAA* homologous genes. *Ann. Bot.* 101, 249–259. doi: 10.1093/aob/mcm115

Abebie, B., Philosoph-Hadas, S., Lers, A., Goren, R., Huberman, M., Riov, J., et al. (2006). "The differential effectiveness of two synthetic auxins in delaying floret abscission in Red *Cestrum* cut flowers depends on their transport and metabolism," in *Proceedings of the 33rd PGRSA Annual Meeting*, Sarasota, FL, 75–80.

Ascough, G. D., Nogemane, N., Mtshall, N. P., and van Staden, J. (2005). Flower abscission: environmental control, internal regulation and physiological responses of plants. *South Afr. J. Bot.* 71, 287–301. doi: 10.1016/s0254-6299(15)30101-0

Ausubel, F. M., Brent, R., Kingston, R. F., Moore, D. D., Seidman, J. G., Smith, J. A., et al. (1995). *Short Protocols in Molecular Biology*, 3rd Edn, New York, NY: John Wiley & Sons, Inc.

Badescu, G. O., and Napier, R. M. (2006). Receptors for auxin: will it end in TIRs. *Trends Plant Sci.* 11, 217–223.

Bagheri, H., Hashemabadi, D., and Sedaghahhoor, S. (2012). Improvement of vase life and postharvest quality of Alstroemeria hybrida flowers via naphthalene acetic acid (NAA). *Eur. J. Exp. Biol.* 2, 2481–2484.

Ballantyne, D. J. (1965). Senescence of daffodil (*Narcissus pseudonarcissus*) cut flowers treated with benzyladenine and auxin. *Nature* 205:819. doi: 10.1038/205819a0

Barak, E., Dinoor, A., and Jacoby, B. (1983). Adsorption of systemic fungicides and a herbicide by some components of plant tissues, in relation to some physicochemical properties of the pesticides. *Pestic. Sci.* 14, 213–219. doi: 10.1002/ps.2780140302

Bertosa, B., Kojic-Prodic, B., Wade, R. C., Ramek, M., Piperaki, S., Tsantili-Kakoulidou, A., et al. (2003). A new approach to predict the biological activity of molecules based on similarity of their interaction fields and the log P and log D values: application to auxins. *J. Chem. Info. Comp. Sci.* 43, 1532–1541. doi: 10.1021/ci034063n

Briggs, G. G., Rigitano, R. L. O., and Bromilow, R. H. (1987). Physicochemical factors affecting uptake by roots and translocation to shoots of weak acids in barley. *Pestic. Sci.* 19, 101–112. doi: 10.1002/ps.2780190203

Bromilow, R. H., Chamberlain, K., and Evans, A. A. (1990). Physicochemical aspects of phloem translocation of herbicides. *Weed Sci.* 38, 305–314. doi: 10.1017/s0043174500056575

Carrier, D. J., Abu Baker, N. T., Swarup, R., Callaghan, R., Napier, R. M., Bennett, M. J., et al. (2008). The binding of auxin to the *Arabidopsis influx* transporter AUX1. *Plant Physiol.* 148, 529–535. doi: 10.1104/pp.108.122044

Chamberlain, K., Evans, A. A., and Bromilow, R. H. (1996). 1-Octanol/water partition coefficient (KOW) and pKa for ionisable pesticides measured by a pH-metric method. *Pestic. Sci.* 47, 265–271. doi: 10.1002/(sici)1096-9063(199607)47:3<265::aid-ps416>3.0.co;2-f

Coupland, D. (1989). "Factors affecting the phloem translocation of foliage-applied herbicides," in *Mechanism and Regulation of Transport Processes*, eds R. K. Atkin, and D. R. Clifford, (Berlin: Springer), 85–112.

Delbarre, A., Muller, P., Imhoff, V., and Guern, J. (1996). Comparison of mechanisms controlling uptake and accumulation of 2,4-dichlorophenoxy acetic acid, naphthalene-1-acetic acid, and indole-3-acetic acid in suspension-cultured tobacco cells. *Planta* 198, 532–541. doi: 10.1007/bf00262639

Diaz-Sala, C., Hutchison, K. W., Goldfarb, B., and Greenwood, M. S. (1996). Maturation-related loss in rooting competence by loblolly pine stem cuttings: the role of auxin transport, metabolism and tissue sensitivity. *Physiol. Plant.* 97, 481–490. doi: 10.1034/j.1399-3054.1996.970310.x

Enders, T. A., and Strader, L. C. (2015). Auxin activity: past, present, and future. *Am. J. Bot.* 102, 180–196. doi: 10.3732/ajb.1400285

Feng, M., and Kim, J.-Y. (2015). Revisiting apoplastic auxin signaling mediated by AUXIN BINDING PROTEIN 1. *Mol. Cells* 38, 829–835. doi: 10.14348/molcells.2015.0205

Geilfus, C.-M. (2017). The pH of the apoplast: dyanamic factor with functional impact under stress. *Mol. Plant* 10, 1371–1386. doi: 10.1016/j.molp.2017.09.018

Grimm, E., Neumann, S., and Jacob, F. (1986). Transport of xenobiotics in higher plants. III. Absorption of 2,4-D and 2,4-dichloroanisole by isolated conducting tissue of Cyclamen. *Biochem. Physiol. Pflanzen.* 181, 69–82.

Grones, P., and Friml, J. (2015). Auxin transporters and binding proteins at a glance. *J. Cell Sci.* 128, 1–7. doi: 10.1242/jcs.159418

Hager, A. (2003). Role of plasma membrane H+-ATPase in auxin-induced elongation of growth: Historical and new aspects. *J. Plant Res.* 116, 483–505. doi: 10.1007/s10265-003-0110-x

Huberman, M., Zehavi, U., Stein, W. D., Etxeberria, E., and Goren, R. (2005). In vitro sugar uptake by grapefruit (*Citrus paradisi*) juice-sac cells. *Func. Plant Biol.* 32, 357–366.

Jafvert, C. T., Westall, J. C., Grieder, E., and Schwarzenbach, R. P. (1990). Distribution of hydrophobic ionogenic organic compounds between octanol and water: organic acids. *Environ. Sci. Technol.* 24, 1795–1803. doi: 10.1021/es00082a002

Kerler, F., and Schönherr, J. (1988). Accumulation of lipophilic chemicals in plant cuticles: prediction from octanol/water partition coefficients. *Arch. Environ. Contam. Toxicol.* 17, 1–6. doi: 10.1007/bf01055146

Kramer, E. M. (2006). How far can a molecule of weak acid travel in the apoplast or the xylem? *Plant Physiol.* 141, 1233–1236. doi: 10.1104/pp.106.083790

Leo, A. (2000). "Octanol/water partition coefficients," in *Handbook of Property Estimation Methods for Chemicals*, eds R. S. Boethling, and D. Mackay, (Boca Raton, FL: Lewis Publishers), 89–114.

Leo, A., Hansch, C., and Elkins, D. (1971). Partition coefficients and their uses. *Chem. Rev.* 71, 525–616. doi: 10.1021/cr60274a001

Liao, Z. H., Chen, M., Guo, L., Gong, Y. F., Tang, F., Sun, X. F., et al. (2004). Rapid isolation of high quality total RNA from taxus and ginkgo. *Prep. Biochem. Biotech.* 34, 209–214. doi: 10.1081/pb-200026790

Ludwig-Müller, J., Raisig, A., and Hilgenberg, W. (1995). Uptake and transport of indole-3-butyric acid in *Arabidopsis thaliana*: comparison with other natural and synthetic auxin. *J. Plant Physiol.* 147, 351–354. doi: 10.1016/s0176-1617(11)82166-8

Meir, S., Philosoph-Hadas, S., Salim, S., Davidson, H., Tamari, Y., and Gutman, S. (1999). Prevention of floret abscission in Cestrum cut flowers by pulsing

treatments with synthetic chlorophenoxy auxins and STS. *Bulletin of Israeli Flower Growers* 4, 83–89. In Hebrew.

Meir, S., Sundaresan, S., Riov, J., Agarwal, I., and Philosoph-Hadas, S. (2015). Role of auxin depletion in abscission control. *Stewart Postharvest. Rev.* 11, 1–15. doi: 10.2212/spr.2015.2.2

OECD (1987). *OECD Guidelines for the Testing of Chemicals, Section 4*. Paris: OECD Publishing.

Park, J., Lee, Y., Martinoia, E., and Geisler, M. (2017). Plant hormone transporters: What we know and what we would like to know? *BMC Biol.* 15:93. doi: 10.1186/s12915-017-0443-x

Peters, W. S., and Felle, H. (1991). Control of apoplast pH in corn coleoptile segments. I: the endogenous regulation of cell wall pH. *J. Plant Physiol.* 137, 655–661. doi: 10.1016/s0176-1617(11)81217-4

Peterson, M. A., McMaster, S. A., Riechers, D. E., Skelton, J., and Stahlman, P. W. (2016). 2,4-D: past, present, and future: a review. *Weed Technol.* 30, 303–345.

Petrášek, J., and Friml, J. (2009). Auxin transport routes in plant development. *Development* 136, 2675–2688. doi: 10.1242/dev.030353

Popp, C., Burghardt, M., Friedmann, A., and Riederer, M. (2005). Characterization of hydrophilic and lipophilic pathways of *Hedera helix* L. cuticular membranes: permeation of water and uncharged organic compounds. *J. Exp. Bot.* 56, 2797–2806. doi: 10.1093/jxb/eri272

Reid, M. S., and Jiang, C.-Z. (2012). Postharvest biology and technology of cut flowers and potted plants. *Hort. Rev.* 40, 1–54. doi: 10.1002/9781118351871.ch1

Riederer, M. (2004). "Uptake and Transport of *Xenobiotics*," in *Plant Toxicology*, 4th Edn, eds B. Hook, and E. F. Elstner, (Boca Raton: CRC Press), 131–150. doi: 10.1201/9780203023884

Rigitano, R. L. O., Bromillow, R. H., Briggs, G. G., and Chamberlain, K. (1987). Phloem translocation of weak acids in *Ricinus communis*. *Pestic. Sci.* 19, 113–133.

Rubery, P. H. (1978). Hydrogen ion dependence of carrier-mediated auxin uptake by suspension-cultured crown gall cells. *Planta* 142, 203–206. doi: 10.1007/bf00388213

Sacalis, J. N., and Nichols, R. (1980). Effect of 2,4-D uptake on petal senescence in cut carnation flowers. *Hortscience* 15, 499–500.

Savchenko, G., and Heber, V. (2000). pH regulation in apoplastic and cytoplastic cell compartments of leaves. *Planta* 211, 246–255. doi: 10.1007/s004250000280

Shimizu-Yumoto, H., and Ichimura, K. (2010a). Combination pulse treatment of 1-naphthaleneacetic acid and aminoehoxyvinyl glycine greatly improves postharvest life in cut Eustoma flowers. *Postharvest. Biol. Technol.* 56, 104–107. doi: 10.1016/j.postharvbio.2009.10.001

Shimizu-Yumoto, H., and Ichimura, K. (2010b). Postharvest physiology and technology of cut Eustoma flowers. *J. Jpn. Soc. Hort. Sci.* 79, 227–238. doi: 10.2503/jjshs1.79.227

Sterling, T. M. (1994). Mechanisms of herbicide absorption across plant membranes and accumulation in plant cells. *Weed Sci.* 42, 263–276. doi: 10.1017/s0043174500080383

Trapp, S. (2004). Plant uptake and transport models for neutral and ionic chemicals. *Environ. Sci. Pollut. Res.* 11, 33–39. doi: 10.1065/espr2003.08.169

Trapp, S., Miglioranza, K. S. B., and Mosbaek, H. (2001). Sorption of lipophilic organic compounds to wood and implications for their environmental fate. *Environ. Sci. Technol.* 35, 1561–1566. doi: 10.1021/es000204f

Weisman, Z., Riov, J., and Epstein, E. (1988). Comparison of movement and metabolism of indole-3-acetic acid and indole-3-butyric acid in mung bean cuttings. *Physiol. Plant.* 74, 556–560. doi: 10.1111/j.1399-3054.1988.tb02018.x

Wojciechowska, N., Sobieszczuk-Nowicka, E., and Bagniewska-Zadworna, A. (2018). Plant organ senescence – regulation by manifold pathways. *Plant Biol.* 20, 167–181. doi: 10.1111/plb.12672

Xu, T., Dai, N., Chen, J., Nagawa, S., Cao, M., and Li, H. (2014). Cell surface ABP1-TMK auxin-sensing complex activates ROP GTPase signaling. *Science* 343, 1025–1028. doi: 10.1126/science.1245125

Conflict of Interest: The authors declare that the research was conducted in the absence of any commercial or financial relationships that could be construed as a potential conflict of interest.

frontiers in Plant Science

PERSPECTIVE
published: 30 June 2020
doi: 10.3389/fpls.2020.00907

Overcoming Physiological Bottlenecks of Leaf Vitality and Root Development in Cuttings: A Systemic Perspective

*Uwe Druege**

Erfurt Research Centre for Horticultural Crops (FGK), University of Applied Sciences Erfurt, Erfurt, Germany

Each year, billions of ornamental young plants are produced worldwide from cuttings that are harvested from stock plants and planted to form adventitious roots. Depending on the plant genotype, the maturation of the cutting, and the particular environment, which is complex and often involves intermediate storage of cuttings under dark conditions and shipping between different climate regions, induced senescence or abscission of leaves and insufficient root development can impair the success of propagation and the quality of generated young plants. Recent findings on the molecular and physiological control of leaf vitality and adventitious root formation are integrated into a systemic perspective on improved physiologically-based control of cutting propagation. The homeostasis and signal transduction of the wound responsive plant hormones ethylene and jasmonic acid, of auxin, cytokinins and strigolactones, and the carbon-nitrogen source-sink balance in cuttings are considered as important processes that are both, highly responsive to environmental inputs and decisive for the development of cuttings. Important modules and bottlenecks of cutting function are identified. Critical environmental inputs at stock plant and cutting level are highlighted and physiological outputs that can be used as quality attributes to monitor the functional capacity of cuttings and as response parameters to optimize the cutting environment are discussed. Facing the great genetic diversity of ornamental crops, a physiologically targeted approach is proposed to define bottleneck-specific plant groups. Components from the field of machine learning may help to mathematically describe the complex environmental response of specific plant species.

Keywords: internal quality, senescence, adventitious rooting, plant development, phytohormones, primary metabolism, environment, modeling

OPEN ACCESS

Edited by:
Margherita Irene Beruto, Istituto Regionale per la Floricoltura (IRF), Italy

Reviewed by:
Francisco Perez-Alfocea, Spanish National Research Council, Spain
Carmen Diaz-Sala, University of Alcalá, Spain

***Correspondence:**
Uwe Druege
uwe.druege@fh-erfurt.de

Specialty section:
This article was submitted to Crop and Product Physiology, a section of the journal Frontiers in Plant Science

Received: *24 April 2020*
Accepted: *03 June 2020*
Published: *30 June 2020*

Citation:
Druege U (2020) Overcoming Physiological Bottlenecks of Leaf Vitality and Root Development in Cuttings: A Systemic Perspective. Front. Plant Sci. 11:907. doi: 10.3389/fpls.2020.00907

INTRODUCTION

Plant propagation is the initial process of producing ornamental crops that already sets the first benchmark for the whole cultivation process by determining the quality of the young plant. Many ornamental plant species are propagated vegetatively by rooting of shoot tip cuttings. Depending on the plant genotype, the developmental stage of the cutting, and specific constellation of environmental factors, impaired vitality of cuttings or insufficient adventitious root (AR) formation in the stem base can cause leaf losses and dying of cuttings or failures in rooting

and delayed or uneven root formation among individuals that impairs synchronous subsequent growth. Furthermore, the increasing demand on sustainability of young plant production requires improved propagation protocols that should provide maximum utilization of the genetically determined endogenous potential of the crop.

Propagation of ornamental plants by cuttings can be characterized as follows:

(1) It involves control of plant development in highly equipped ecosystems, that are mainly determined by technically controlled environmental inputs, for example in greenhouses, growth and storage rooms etc. I propose the term "technoecosystems" for such systems.
(2) Environmental inputs are highly dynamic, because propagation involves a complex chain of subsequent processes that occur in different environments. Stock plant cultivation and harvest of cuttings occurs in diverse climatic regions far remote from the market of young plants and is followed by packaging, storage, transport, sticking and cultivation of cuttings close to the market.
(3) The chain is continuously changing, because new priorities in the society and developing technologies provide new demands and options. Examples are the increasing demand for saving energy and reducing pollution, the changing lighting technology and the up-coming rooting systems that are compatible with transport logistics and sticking robots.
(4) There is a great genetic diversity of plants that are propagated by cuttings. This results from the high number of species used in floriculture and also from the high breeding activities bringing more than thousand new cultivars to the European market year by year. For example, in 2018, 140 applications for protection of *Chrysanthemum* varieties were submitted to the Community Plant Variety Office (Anonymus, 2019).

Considering this complex and highly dynamic situation, there is the need for a general concept, which helps to understand the limitation of and how to optimize cutting propagation in a specific system of interest, as characterized by the particular plant genotype and the environmental inputs that can be technically controlled during the specific chain. In this context, endogenous quality attributes of a cutting should reflect its current capacity to develop into a young plant. Recently, comprehensive review articles have provided detailed views on the molecular, hormonal and metabolic control of AR formation (Steffens and Rasmussen, 2016; Druege et al., 2019; Lakehal and Bellini, 2019). In this perspective article, the essential knowledge concerning this process is brought into context with the problem of leaf senescence and abscission, and further integrated into a systemic approach that faces the demands and the complex environment of ornamental horticulture. A physiologically based model of crucial processes determining the success in cutting propagation, their linkages to critical environmental inputs as well as those physiological outputs that can be used to monitor cutting function are introduced.

SYSTEMIC MODEL OF PROPAGATION BY CUTTINGS

The Cutting Function

The cutting is considered as functional unit in the center of the propagation system (**Figure 1**). Leaf retention and greenness and AR formation are the two targets of cutting function that determine the final quality of the young plant. Depending on the initial status of the AR source cells [cells, in which adventitious rooting starts (Druege et al., 2019)], their dedifferentiation may be involved first to gain competence for AR induction. Induction of AR competent cells leads to cell specification toward subsequent initiation (ending with the formation of primordia) and final expression of ARs from the stem base (SB). There, homeostasis of wound-responsive ethylene (ET) and jasmonic acid (JA), of the auxin indole-3-acetic acid (IAA), cytokinins (CK) and strigolactones (SL), and hormone signaling and function are core processes regulating AR formation, which is further dependent on sink establishment and C and N utilization. Fully developed leaves (FL) constitute important source tissues for N and C re-mobilization, while the developing leaves (DL) and shoot apex (SA) compete with the stem base (SB) for these resources. IAA accumulation in the SB is dependent on auxin re-mobilization from the upper shoot with polar auxin transport (PAT) as main driving process. The changed hormone homeostasis of the cutting may affect leaf senescence and abscission. Further explanation is given in **Box 1**.

The Bottlenecks

Depending on the plant genotype and configuration of environmental inputs at stock plant and cutting level, different processes may constitute the bottleneck (B) of cutting function (**Figure 1**).

B1: General Auxin Responsiveness in the Stem Base

If auxin signaling is generally low in the candidate AR source cells and not stimulated by the changed hormone homeostasis after cutting (see B2), no or few ARs will be formed. Cuttings, particularly of woody ornamentals such as *Rosa* or *Hydrangea macrophylla*, can exhibit low rooting capacity in dependence on the specific genotype (Dubois and Vries, 1991) or when they have been collected from mature parts of the stock plant (Galopin et al., 1996). The underlying principles are only fragmentary understood. A recent genome-wide association study of 95 rose genotypes indicated functions of the auxin and ET signal transduction (see also B2) in the diversity of AR formation, pointing to one auxin response factor (ARF), to cell fate regulating transcription factors (CTF), e.g., of the WOX- and GRAS-families that act down-stream of auxin, and to one positive regulator of the ET response pathway (Nguyen et al., 2020). In some forest tree species, the maturation-related decline in rooting capacity was related to divergences in expression of specific ARFs or CTF of the GRAS-family (Diaz-Sala, 2014, 2019). In *Eucalyptus grandis,* the maturation-induced decline in auxin-induced rooting was related to disturbed microtubule remodeling, which functional relevance was proven by chemical

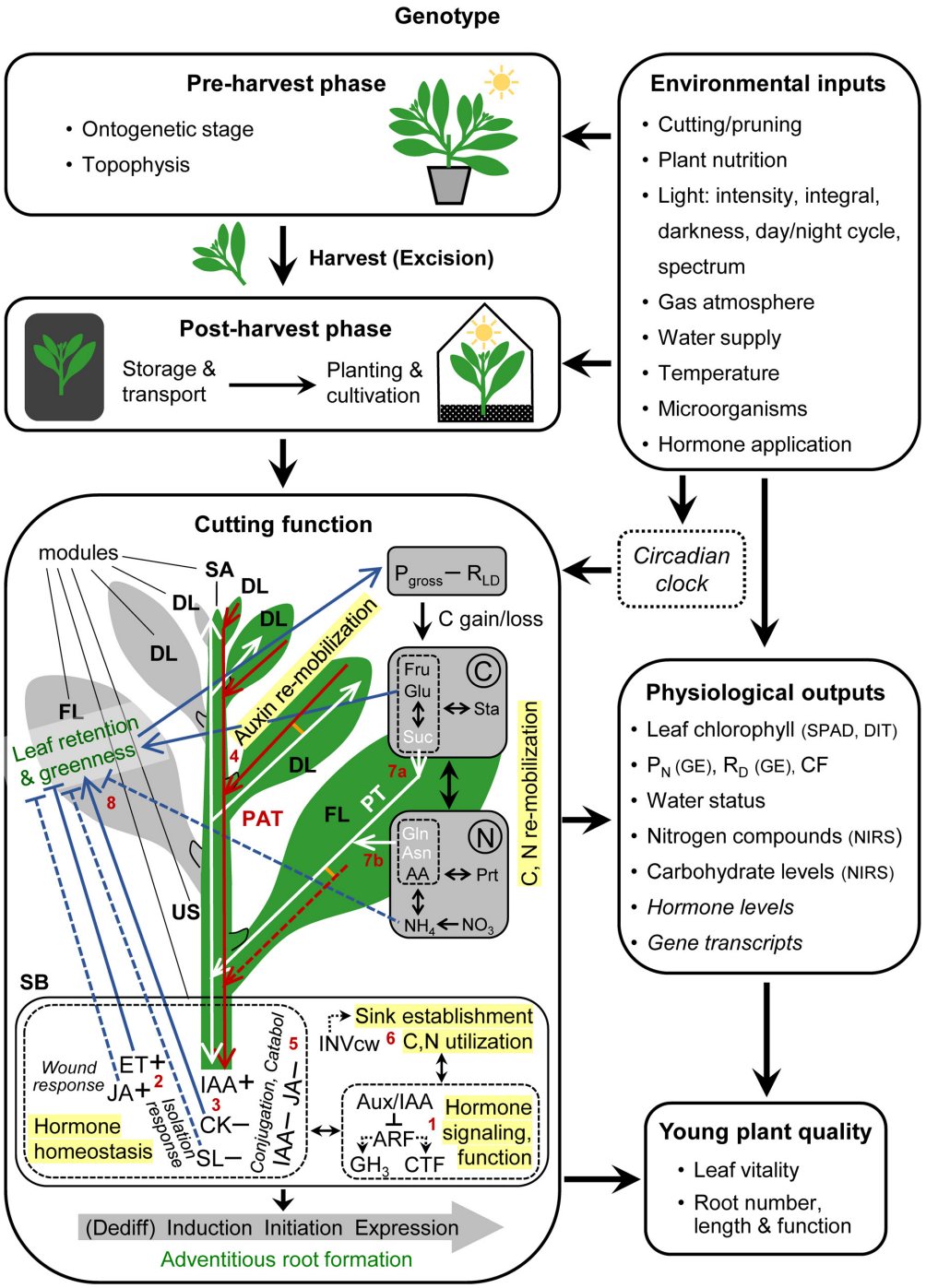

FIGURE 1 | Systemic, process-based model of clonal propagation by utilization of adventitious root formation in cuttings. Red and white lines and arrow heads indicate the pathways and directions of polar auxin transport (PAT) and phloem transport (PT), respectively. Lines in orange indicate PAT-PT connections. Blue lines ending with arrow heads or crossbars indicate positive or negative effects of increasing concentrations and of leaf retention and greenness, respectively. Plus versus minus signs indicate increased versus decrease of hormone concentrations, respectively, in response to excision. Red numbers indicate the bottlenecks explained in the text. *Italic letters* mark those physiological outputs, which are currently not accessible to routine analysis under practical conditions. Abbreviations between brackets indicate currently available measuring principles. AA, amino acids; ARF, auxin responsive factors; Aux/IAA, auxin/indole-3-acetic acid repressors; Asn, asparagine; CTF, cell fate regulating transcription factors; Catabol, catabolism; CK, cytokinins; Dediff, dedifferentiation; CF, chlorophyll fluorescence; DIT, digital image technology; DL, developing leaf; ET, ethylene; FL, fully developed leaf; GE, gas exchange analysis; GH3, Gretchen Hagen 3; Gln, glutamine; Glu, glucose; IAA, indole-3-acetic acid; INWcw, cell wall invertase; JA, jasmonic acid; NIRS, near infrared reflectance spectroscopy; P_N, net photosynthesis; P_{gross}, gross photosynthesis; Prt, proteins; R_D, dark respiration; R_{LD}, light and dark respiration; SA, shoot apex; SB, stem base; SL, strigolactones; SPAD, Soil Plant Analysis Development-chlorophyll meter; Sta, starch; suc, sucrose. Further explanations see **Box 1** and the text.

BOX 1 | Targets, modules and processes of cutting function.
Leaf retention and greenness and **adventitious root formation** in the stem base are the **two targets** of cutting function that determine the final **quality of the young plant**, while **physiological outputs** can be used to monitor the cutting performance.
Plant genotype and environmental inputs, which act pre-harvest during the stock plant phase and after the harvest of cuttings, control the function of cuttings. This may also involve the circadian clock. The function of the cutting is further subject to the **ontogenetic stage** of the stock plant and to the cutting position within the stock plant (**topophysis**), which determines the specific developmental stage as well as the source-sink and hormonal status of the cutting tissues at time of harvest.
Important functional modules are the **stem base (SB)** as zone of root regeneration and of C and N utilization, the **upper stem (US)** as transport unit for all compounds and as intermediate storage unit of C and N, the **fully developed leaves (FL)** as source organs for providing C, N and possibly auxin, and the **developing leaves (DL)** and **shoot apex (SA)** as competitive utilization sinks for C and N and as potential source (DL) or sink (SA) of auxin.
In the SB, **hormone homeostasis**, **signaling and function** control the **dedifferentiation (Dediff)**, **induction**, **initiation** and **expression** of adventitious roots, with Aux/IAA proteins, auxin responsive factor (ARF) transcription factors, GH3 proteins, and cell fate regulating transcription factors (CTF) such as GRAS, AP2/ERF and WOX as important components. **Sink establishment and C and N utilization** provide building blocks, energy and metabolic signals. Wound-induced accumulation of ethylene (ET) and jasmonic acid (JA), a decrease in levels of root-sourced cytokinins (CK) and strigolactones (SL) due to isolation from the stock plant, and accumulation of IAA contribute to dedifferentiation and induction of ARs. IAA accumulation in the stem base is dependent on **auxin re-mobilization** from the upper shoot, with DL and FL as potential auxin sources and **polar auxin transport (PAT)** as important process of translocation.
Depending on the sensitivity of the leaves, systemic effects of the changed plant hormone homeostasis may control **leaf retention and greenness** by affecting **leaf senescence** and **abscission**, with ethylene (ET) and cytokinins (CK) as classical trigger and inhibitors of leaf senescence or abscission, respectively. Whether the principally known agonistic effects of jasmonic acid (JA) and strigolactones (SL) on leaf senescence have relevance to cuttings, requires further investigation. High sugar levels, particularly of glucose can counteract leaf senescence/abscission, possibly via depressed ET signalling.
The earliness of **establishment and the strength of the new utilization sink in the stem base** as compared to the competing sink in the upper shoot limits the influx of C and N resources into the stem base. Activity of cell wall invertase (INVcw) as crucial driver of initial sink activity may be under positive control by IAA and JA.
C and N re-mobilization from the upper shoot, particularly from fully developed leaves is an important process for the delivery of sugars and amino acids (AA) to the utilization sink in the stem base, with sucrose (Suc), asparagine (Asn) and glutamine (Gin) as important components of **phloem transport (PT)**.
The balance **of gross photosynthesis (P_{gross})** and **respiration** in the light and in the dark (R_{LD}) determines the **carbon gain or loss** of the leaf and thus its **carbohydrate pool**, with starch (Sta) and Suc as intermediate storage and main export fraction, respectively, while glucose (Glu) and Fructose (Fru) are locally utilized.
Light-dependent **assimilation of nitrate and ammonium**, that have been initially delivered from the root system of the stock plant, determines one influx of N into the **AA and protein (Prt) pools**, while competing with the sugar pool for C skeletons. Under prolonged dark conditions of whole cuttings that deplete the carbohydrate pool of leaves, leaf metabolism is readjusted towards a survival strategy, resulting in **accumulation of AA**, while proteolysis contributes to this process. If the released AAs are further catabolized to free **ammonium**, this may trigger leaf senescence.

manipulation (Abu-Abied et al., 2014). However, whether these relationships are based on bottleneck functions of the auxin signal transduction *per se* or rather reflect upstream limitations of cellular plasticity that is under further control of microRNAs and epigenetic factors (Poethig, 2013; Diaz-Sala, 2014; Druege et al., 2019) requires further investigation (see also B2).

B2: Initial ET-JA-CK Interaction in the Stem Base

If AR source cells require dedifferentiation before AR induction, early wound induced accumulation of ET and JA, together with CKs may contribute to this process by enhancing auxin responsiveness (Druege et al., 2019) (see B1).

B3: Early Rise of Auxin/CK-SL Ratio in the Stem Base

If AR source cells are root competent (see also B2), AR induction is dependent on local accumulation of IAA and further supported by a decrease in levels of the antagonistic CKs and SLs. Cutting off from (a) the root-ward auxin-drain and (b) the root-sourced delivery of CKs and SLs initiates these changes which may be supported by local IAA biosynthesis or release from auxin conjugates (Druege et al., 2019).

B4: Auxin Re-mobilization From the Upper Shoot

In intact plants, IAA is synthesized in young expanding leaves and is in the stem either transported root-ward by polar auxin transport (PAT) in xylem parenchyma and cambium cells or co-transported in the phloem associated with assimilate transport (AT) (Kramer and Bennett, 2006; Petrasek and Friml, 2009; Leyser, 2011; van Rongen et al., 2019), while in leaves both pathways can be interconnected (Cambridge and Morris, 1996; **Figure 1**). These auxin routes are supplemented with a low conductance and less polar "connective auxin transport," linking the PAT route to the surrounding tissues (Bennett et al., 2016; van Rongen et al., 2019). In shoot tip cuttings, PAT has important functions in auxin translocation toward the SB and, depending on the plant genotype and environmental condition, cutting leaves of different age may constitute important auxin sources (Guerrero et al., 1999; Garrido et al., 2002; Ahkami et al., 2013; Yang et al., 2019; **Figure 1**). Wounding and isolation of cuttings may trigger specific auxin biosynthetic pathways in addition to the pathways of the intact plant (Chen et al., 2016), possible via action of JA (Zhang et al., 2019).

B5: Late Decrease in Auxin and JA Levels in the Stem Base

Initiation and expression of ARs requires a decrease of IAA and probably also of the physiologically active conjugate of JA after the induction phase. Obviously, upregulation of specific GH3 proteins that function as acyl acid amido synthetases conjugating IAA or JA to specific AAs has an important role for this dynamic (Druege et al., 2019; Lakehal and Bellini, 2019). IAA level can be reduced also by catabolism, with oxidation as important route that can be triggered by JA (Lakehal et al., 2019; **Figure 1**).

B6: Sink Establishment and C and N Utilization in the Stem Base

Temporal courses of carbohydrates and amino acids (AA) in the stem base of cuttings during rooting (Ahkami et al., 2009) and the

positive response of AR formation to applications of sugars and AA reveal that AR formation utilizes both resources (Orlikowska, 1992; Takahashi et al., 2003; Correa et al., 2005; Schwambach et al., 2005; Yasodha et al., 2008). After excision of cuttings, the transport route of these resources has to be directed toward the developing ARs, while the DLs and SA constitute competitive sink organs. Provided C or N sources are not the limiting factors (see B7), the strength of the new utilization sink in the SB limits the influx of C and N into the SB (**Figure 1** and **Box 1**). This is determined by the activities of invertases, in particular cell wall invertase which can be up-regulated by IAA and JA (Roitsch and Gonzalez, 2004; Ahkami et al., 2009, 2013; Albacete et al., 2011; Agulló-Antón et al., 2014).

B7: Surplus of C and N in Source Leaves

If the sink in the SB is sufficiently high to attract resources (B6), their influx can be limited by the source capacity of the upper shoot, with the fully developed leaves (FL) as main source organs (**Figure 1**). Depending on the plant genotype and the particular environmental conditions during the chain, the magnitudes of either the C (*B7a*) or N source (*B7b*) may limit rooting (Druege et al., 2000, 2004; Zerche et al., 2016). The available surplus of carbohydrates in cutting leaves depends on the initial carbohydrate level at time of planting and the current C gain during cutting cultivation (Rapaka et al., 2005), while current photosynthesis and C gain of cuttings is obviously dependent on plant species (Druege and Kadner, 2008; Klopotek et al., 2012). The level in leaves of total sugars, particularly of sucrose, during the rooting period reflects the carbohydrate source limitation of rooting in cuttings (Rapaka et al., 2005; Druege and Kadner, 2008; Klopotek et al., 2010).

B8: Hormone Sensitivity of Leaves

Senescence or abscission of leaves can impair the visual quality and vitality of cuttings and may finally cause decay and loss of whole cuttings. Changed concentrations in cuttings particularly of ET, JA, and CK in response to their excision have consequences for leaf senescence and/or abscission when the changed hormone homeostasis meets the respective responsiveness of the leaf (**Figure 1** and **Box 1**). Both, the change in hormone levels and the leaf response are dependent on the plant genotype. Stimulation of ET biosynthesis by wounding or other stresses may promote leaf senescence in cuttings of sensitive plant species, particularly when packaging and storage of cuttings entraps the ET in the surrounding air (Müller et al., 1998; Rapaka et al., 2007a,b; Leatherwood et al., 2016). Depletion of CK in cuttings in response to the cut off from the root system can contribute to post-harvest leaf senescence, since CK application rescued leaf greenness antagonizing ET effects (Mutui et al., 2005). Observed agonistic effects of JA and SL on leaf senescence in intact plants (Ueda and Kusaba, 2015; Zhuo et al., 2020) may also be relevant to cuttings. Free ammonium can promote leaf senescence (Britto and Kronzucker, 2002), whereas high sugar levels obviously protect cutting leaves from senescence or abscission, while agonistic and antagonistic effects on ET signaling may be involved, respectively (Yanagisawa et al., 2003; Druege et al., 2004; Rapaka et al., 2007a,b; Druege and Kadner, 2008; Li et al., 2019).

Critical Environmental Inputs

Diverse environmental factors at stock plant and cutting level modify the function of cuttings and thereby control the quality of the young plant as final output of the system (**Figure 1**). Mechanisms of plant nutritional factors and effects of controlled atmosphere storage are largely unexplored. In addition to the effects of light intensity and integral and of CO_2 on the C gain of cuttings, distinct effects of light spectrum may involve changes of auxin homeostasis and signaling (Ruedell et al., 2015; Christiaens et al., 2019). Dark-induced carbohydrate depletion in cuttings can impair AR formation via reduced C source. However, if high photosynthetic activity of cuttings after the dark period allows fast recovery of the C source, dark storage can promote AR formation (Klopotek et al., 2010). In addition to the enhancement of AA levels in cuttings following carbohydrate depletion (**Box 1**), dark storage of cuttings may promote sink establishment in the stem base via up-regulation of invertases (Klopotek et al., 2016) and stimulate auxin signaling by enhanced auxin mobilization from the upper shoot (Yang et al., 2019). There is indication from growth analyses of petunia plants, that also the circadian clock, which coordinates plant metabolism with the environment, has important functions in carbon allocation toward roots (Feller et al., 2015). The mechanisms underlying the recently observed stimulation of AR formation by targeting of water to the rooting zone (sub-misting) when compared to overhead misting are not understood. There is indication that beneficial effects of inoculations of specific root endophytes, such as arbuscular mycorrhizal fungi or *Serendipita indica* (former *Piriformospora indica*) at stock plant or cutting level on leaf vitality and AR formation may involve changed C source and hormone signaling in cuttings. However, effects of such inoculations are highly variable and even include negative effects on AR formation, when comparing different environmental conditions, modes of inoculation and plant genotype (Druege et al., 2006, 2007; Justice et al., 2018). This highlights the need for future research on the underlying mechanisms and key factors in the plant-microorganism-abiotic environment continuum. More details about the modes of action of the distinct environmental inputs (**Figure 1**) on cutting function consider also findings and concepts of Kadner and Druege (2004), Husen and Pal (2007), Rapaka et al. (2008), Bredmose and Nielsen (2009), Agulló-Antón et al. (2011), Osterc and Stampar (2011), Franken (2012), da Costa et al. (2013), Bauerfeind et al. (2015), Rasmussen et al. (2015), Otiende et al. (2017), Zhang et al. (2017), Ferrari et al. (2018), Peterson et al. (2018), Taylor and Hoover (2018), Cho et al. (2019), Heide (2019), Sanchez et al. (2020) and are summarized in **Supplementary Table S1**.

Physiological Outputs

Distinct physiological parameters of cuttings can be used to monitor their function, which means to determine the efficiency of the processes contributing to leaf vitality and AR formation in the stem base (**Figure 1**). These parameters may be used to define the functional capacity of the cuttings as important internal

quality attribute of cuttings or to adjust the environmental factors toward optimum cutting performance.

Even though the distinct effects of different levels and locations of water supply (top vs. bottom) on rooting of cuttings are unclear (**Supplementary Table S1**), monitoring the water status of cuttings can help to avoid water deficit induced limitation of leaf function (e.g., the reduction of carbon gain by stomatal closure) and AR formation at early rooting stages and to acclimate cuttings to moderate stress conditions at later rooting stages when ARs have already been formed. Water status of cuttings can be assessed by measuring transpiration *viz*. the water loss through the leaves, stomatal conductance representing the guard cell vapor conductivity, and the relative water content or water potential both reflecting the dehydration state of leaves or whole cuttings (Aminah et al., 1997; LeBude et al., 2005; Wilkerson et al., 2005). In addition to direct measurements of such parameters e.g., by use of gas exchange cuvettes, porometers etc., indirect methods and tools for real-time sensing of plant water status are increasingly available. These use for example stem thickness, leaf compressibility and thermal or spectral signatures of leaves (Millan-Almaraz et al., 2010; Steppe, 2015; Gerhards et al., 2019; Gautam and Pagay, 2020). However, the use of thermal signatures, which utilizes the dependency of leaf temperature on transpiration is complex in top-misting systems, where leaf temperature is decreased with each mist application.

Leaf chlorophyll content of leaves can be used to monitor leaf senescence and may also limit the C gain of cuttings by restriction of P_{gross}. One of the most frequently used non-invasive tools for chlorophyll analysis in plant leaves is the Soil Plant Analysis Development (SPAD) (**Figure 1**) chlorophyll meter (SPAD-502, Konica Minolta, Osaka, Japan), that measures leaf transmittance in the red (650 nm; the measuring wavelength) and infrared (940 nm; a reference wavelength), while the output gives a relative value that is proportional to the chlorophyll content of the leaf (Ling et al., 2011). This tool has also been used in studies on ornamental crops, where nitrogen content as building block of chlorophyll was mostly the target (Bracke et al., 2019 and references therein) and also in some descriptive studies on cuttings (Rufai et al., 2016; Chater et al., 2017). Very high correlations can be found between chemically analyzed chlorophyll concentrations and SPAD values within a certain plant species as shown for Arabidopsis (Ling et al., 2011). However, the plant matrix obviously can affect these relationships as reflected by lower correlations, when ten different species of leafy vegetables were compared (Limantara et al., 2015). Digital image technology (DIT, **Figure 1**) is one alternative to analyze leaf color and also selectively chlorophyll contents, for example by use of the Red Green Blue color model. Such technologies may even provide a better estimation of chlorophyll than SPAD (Riccardi et al., 2014) and are further compatible to smartphones (Rigon et al., 2016).

Infrared gas analyzers can be used to determine the current carbon gain of cuttings or cutting leaves under the condition of measurement, which may, however, differ from the real conditions of rooting depending on the used measuring system (Druege and Kadner, 2008; Klopotek et al., 2012; Currey and Lopez, 2015; Tombesi et al., 2015). Use of chlorophyll fluorescence technology may provide information about the functional integrity of the photosynthetic apparatus. Quantum yield of PSII or quenching parameters in cutting leaves have already been used to determine their photosynthetic function as dependent on light acclimation (Rapaka et al., 2005), plant genotype (Druege and Kadner, 2008) and duration and temperature of dark storage (Faust and Enfield, 2010). Considering their relevance to the carbon gain and their stress response, online measurements of both leaf gas exchange and photosystem operating efficiency may be combined to optimize dynamic greenhouse control regimes during rooting of cuttings.

Considering that sugars and of AA in source tissues of cuttings reveal important fractions for the crucial C and N re-mobilization, analysis of their levels provides important information about the C and N source limitation of rooting (Druege et al., 2004; Rapaka et al., 2005; Zerche and Druege, 2009; Tombesi et al., 2015; Zerche et al., 2016). The N source availability in cuttings as affected by nitrogen fertilization of stock plants and by dark incubation is reflected not only by the levels of AA but also by the soluble organic nitrogen fraction (sum of amide- and amino-N) (Zerche et al., 2019). Lohr et al. (2016, 2017) have recently established protocols for non-invasive quantification of (a) soluble nitrogen fractions and total nitrogen in cuttings and (b) total non-structural carbohydrates, starch and total sugars (sum of glucose+fructose+sucrose) in cutting leaves by use of near infrared reflectance spectroscopy (NIRS). These methods provide a new basis for the control of cutting quality as affected by their C and N source availability during the propagation chain. Considering the progress in NIRS measuring systems during recent years (Ishikawa et al., 2014) and the potential of hyperspectral imaging for detection of individual metabolites in plant tissues (Vergara-Diaz et al., 2020), more selective non-invasive monitoring of the cutting metabolome should become possible in future.

Since hormone levels in the cutting tissues have decisive functions in leaf senescence and AR formation, their analysis can discover important bottlenecks of cutting function. Whereas commercial systems are available to measure ET emission by plants in closed environments such as storage packages or boxes (Caprioli and Quercia, 2014; Tolentino et al., 2018), analysis of plant hormones in plant tissues requires cutting edge laboratory equipment (Novak et al., 2017) and highly skilled analysts. Polymerase chain reaction (PCR) is standard in detection of plant pathogens (Lau and Botella, 2017) and Reverse Transcriptase (RT) PCR is a frequently used tool in human medicine to detect the expression of critical genes, e.g., in cancer diagnosis (Sager et al., 2015). To my knowledge, up to date no RNA-based tools are available for routine determination of internal quality of plant products such as cuttings. Nevertheless, considering that environmentally and genetically mediated AR formation in cuttings can depend on plant hormones, especially of IAA or the transcript levels of signaling components such as *ARF* and *GH3* genes (Ruedell et al., 2015; Yang et al., 2019), RNA-based quantitative diagnostic tools seem to have a high potential for next-generation functional diagnostics in cutting propagation. Considering the great diversity of ornamental plant species, such an approach must either be species-specific or focus on conserved

DNA, respective RNA sequences that have same functions in several plant species.

OUTLOOK

The high complexity of highly dynamic environmental inputs in young plant production by cuttings and responding metabolic and hormonal pathways (**Figure 1**) is a challenge for the development of general rules or even mechanistic models to support a process-based management of cutting propagation. However, in a targeted approach the relevance of each potential bottleneck can be analyzed for selected plant species or cultivars and those can be grouped according to their identified bottlenecks. Further, the recently discussed concept of "plant perceptron" that implements components from the field of machine learning (Scheres and van der Putten, 2017) may help to mathematically describe these processes for model plant species. In such an approach, the early responding plant hormones JA, ET or IAA and the Aux/IAA-ARF modules (**Figure 1**) would constitute important environment-responsive factors of the so-called "top-hidden" and "bottom-hidden" layers of the information-processing system, respectively, that are weighted and integrated in the "output layer," where the transcription of genes that control cell division, expansion and fate is regulated (Scheres and van der Putten, 2017). Because the cutting function provides the core of the conception (**Figure 1**), the presented model is open for and may stimulate the use of new environmental inputs to control propagation by cuttings. Some of the discussed physiological outputs are currently utilizable only for researchers and experimental conditions, because their monitoring requires high technical input and very specific skills. However, we can expect that the continuous technological progress, e.g., in the application of molecular tools will open more possibilities in future for the propagation industry to utilize physiological and molecular outputs of cuttings for optimizing the young plant production chain. Nevertheless, there will be the challenge to compromise between the specificity of targets, which increases with zooming from the crop to individual cuttings to individual organs such as FL or SB, and the relevance to the whole crop.

DATA AVAILABILITY STATEMENT

All datasets generated for this study are included in the article/**Supplementary Material**, further inquiries can be directed to the corresponding author.

AUTHOR CONTRIBUTIONS

UD wrote the article.

FUNDING

This work was funded by the German Federal Ministry of Food and Agriculture (BMEL) based on a decision of the Parliament of the Federal Republic of Germany, granted by the Federal Office for Agriculture and Food (BLE; grant no. 2818HSE02).

SUPPLEMENTARY MATERIAL

The Supplementary Material for this article can be found online at: https://www.frontiersin.org/articles/10.3389/fpls.2020.00907/full#supplementary-material

TABLE S1 | Modes of action of environmental inputs on cutting function.

REFERENCES

Abu-Abied, M., Szwerdszarf, D., Mordehaev, I., Yaniv, Y., Levinkron, S., Rubinstein, M., et al. (2014). Gene expression profiling in juvenile and mature cuttings of *Eucalyptus grandis* reveals the importance of microtubule remodeling during adventitious root formation. *BMC Genomics* 15:826. doi: 10.1186/1471-2164-15-826

Agulló-Antón, M. A., Ferrandez-Ayela, A., Fernandez-Garcia, N., Nicolas, C., Albacete, A., Perez-Alfocea, F., et al. (2014). Early steps of adventitious rooting: morphology, hormonal profiling and carbohydrate turnover in carnation stem cuttings. *Physiol. Plant* 150, 446–462. doi: 10.1111/ppl.12114

Agulló-Antón, M. A., Sanchez-Bravo, J., Acosta, M., and Druege, U. (2011). Auxins or sugars: what makes the difference in the adventitious rooting of stored carnation cuttings? *J. Plant Growth Regul.* 30, 100–113. doi: 10.1007/s00344-010-9174-8

Ahkami, A. H., Lischewski, S., Haensch, K.-T., Porfirova, S., Hofmann, J., Rolletschek, H., et al. (2009). Molecular physiology of adventitious root formation in *Petunia hybrida* cuttings: involvement of wound response and primary metabolism. *New Phytol.* 181, 613–625. doi: 10.1111/j.1469-8137.2008.02704.x

Ahkami, A. H., Melzer, M., Ghaffari, M. R., Pollmann, S., Javid, M. G., Shahinnia, F., et al. (2013). Distribution of indole-3-acetic acid in *Petunia hybrida* shoot tip cuttings and relationship between auxin transport, carbohydrate metabolism and adventitious root formation. *Planta* 238, 499–517. doi: 10.1007/s00425-013-1907-z

Albacete, A., Grosskinsky, D. K., and Roitsch, T. (2011). Trick and treat: a review on the function and regulation of plant invertases in the abiotic stress response. *Phyton* 50, 181–204.

Aminah, H., Dick, J. M., and Grace, J. (1997). Influence of irradiance on water relations and carbon flux during rooting of *Shorea leprosula* leafy stem cuttings. *Tree Physiol.* 17, 445–452. doi: 10.1093/treephys/17.7.445

Anonymus (2019). *CPVO Annual Report 2018*. Luxembourg: Publications Office of the European Union.

Bauerfeind, M. A., Winkelmann, T., Franken, P., and Druege, U. (2015). Transcriptome, carbohydrate, and phytohormone analysis of *Petunia hybrida* reveals a complex disturbance of plant functional integrity under mild chilling stress. *Front. Plant Sci.* 6:583. doi: 10.3389/fpls.2015.00583

Bennett, T., Hines, G., van Rongen, M., Waldie, T., Sawchuk, M. G., Scarpella, E., et al. (2016). Connective auxin transport in the shoot facilitates communication between shoot apices. *PLoS Biol.* 14:e1002446. doi: 10.1371/journal.pbio.1002446

Bracke, J., Eisen, A., Adriaenssens, S., Vandendriessche, H., and van Labeke, M. C. (2019). Utility of proximal plant sensors to support nitrogen fertilization in *Chrysanthemum*. *Sci. Hortic.* 256:108544. doi: 10.1016/j.scienta.2019.108544

Bredmose, N. B., and Nielsen, K. L. (2009). Controlled atmosphere storage at high CO_2 and low O_2 levels affects stomatal conductance and influence root

formation in kalanchoe cuttings. *Sci. Hortic.* 122, 91–95. doi: 10.1016/j.scienta.2009.03.017

Britto, D. T., and Kronzucker, H. J. (2002). NH4+ toxicity in higher plants: a critical review. *J. Plant Physiol.* 159, 567–584. doi: 10.1078/0176-1617-0774

Cambridge, A. P., and Morris, D. A. (1996). Transfer of exogenous auxin from the phloem to the polar auxin transport pathway in pea (*Pisum sativum* L). *Planta* 199, 583–588.

Caprioli, F., and Quercia, L. (2014). Ethylene detection methods in post-harvest technology: a review. *Sensor Actuat. B Chem.* 203, 187–196. doi: 10.1016/j.snb.2014.06.109

Chater, J. M., Merhaut, D. J., Preece, J. E., and Blythe, E. K. (2017). Rooting and vegetative growth of hardwood cuttings of 12 pomegranate (*Punica granatum* L) cultivars. *Sci. Hortic.* 221, 68–72. doi: 10.1016/j.scienta.2017.04.025

Chen, L. Q., Tong, J. H., Xiao, L. T., Ruan, Y., Liu, J. C., Zeng, M. H., et al. (2016). YUCCA-mediated auxin biogenesis is required for cell fate transition occurring during de novo root organogenesis in *Arabidopsis*. *J. Exp. Bot.* 67, 4273–4284. doi: 10.1093/jxb/erw213

Cho, K. H., Laux, V. Y., Wallace-Springer, N., Clark, D. G., Folta, K. M., and Colquhoun, T. A. (2019). Effects of light quality on vegetative cutting and *in vitro* propagation of Coleus (*Plectranthus scutellarioides*). *Hortscience* 54, 926–935. doi: 10.21273/Hortsci13903-19

Christiaens, A., Gobin, B., van Huylenbroeck, J., and van Labeke, M. C. (2019). Adventitious rooting of *Chrysanthemum* is stimulated by a low red: far-red ratio. *J. Plant Physiol.* 236, 117–123. doi: 10.1016/j.jplph.2019.03.008

Correa, L. D., Paim, D. C., Schwambach, J., and Fett-Neto, A. (2005). Carbohydrates as regulatory factors on the rooting of *Eucalyptus saligna* Smith and *Eucalyptus globulus* labill. *Plant Growth Regul.* 45, 63–73. doi: 10.1007/s10725-004-6125-z

Currey, C. J., and Lopez, R. G. (2015). Biomass accumulation and allocation, photosynthesis, and carbohydrate status of New Guinea impatiens, geranium, and petunia cuttings are affected by photosynthetic daily light integral during root development. *J. Am. Soc. Hortic. Sci.* 140, 542–549. doi: 10.21273/jashs.140.6.542

da Costa, C. T., Almeida, M. R., de Ruedell, C. M., Schwambach, J., Maraschin, F. S., and Fett-Neto, A. G. (2013). When stress and development go hand in hand. *Front. Plant Sci.* 4:133. doi: 10.3389/fpls.2013.00133

Diaz-Sala, C. (2014). Direct reprogramming of adult somatic cells toward adventitious root formation in forest tree species. *Front. Plant Sci.* 5:310. doi: 10.3389/fpls.2014.00310

Diaz-Sala, C. (2019). Molecular dissection of the regenerative capacity of forest tree species: special focus on conifers. *Front. Plant Sci.* 9:1943. doi: 10.3389/fpls.2018.01943

Druege, U., Baltruschat, H., and Franken, P. (2007). *Piriformospora indica* promotes adventitious root formation in cuttings. *Sci. Hortic.* 112, 422–426. doi: 10.1016/j.scienta.2007.01.018

Druege, U., Hilo, A., Perez-Perez, J. M., Klopotek, Y., Acosta, M., Shahinnia, F., et al. (2019). Molecular and physiological control of adventitious rooting in cuttings: phytohormone action meets resource allocation. *Ann. Bot.* 123, 929–949. doi: 10.1093/aob/mcy234

Druege, U., and Kadner, R. (2008). Response of post-storage carbohydrate levels in pelargonium cuttings to reduced air temperature during rooting and the relationship with leaf senescence and adventitious root formation. *Postharv. Biol. Technol.* 47, 126–135. doi: 10.1016/j.postharvbio.2007.06.008

Druege, U., Xylaender, M., Zerche, S., and Alten, H. (2006). Rooting and vitality of poinsettia cuttings was increased by *Arbuscular mycorrhiza* in the donor plants. *Mycorrhiza* 17, 67–72. doi: 10.1007/s00572-006-0074-5

Druege, U., Zerche, S., and Kadner, R. (2004). Nitrogen- and storage-affected carbohydrate partitioning in high-light-adapted *Pelargonium* cuttings in relation to survival and adventitious root formation under low light. *Ann. Bot.* 94, 831–842. doi: 10.1093/aob/mch210

Druege, U., Zerche, S., Kadner, R., and Ernst, M. (2000). Relation between nitrogen status, carbohydrate distribution and subsequent rooting of chrysanthemum cuttings as affected by pre-harvest nitrogen supply and cold-storage. *Ann. Bot.* 85, 687–701. doi: 10.1006/anbo.2000.1132

Dubois, L. A. M., and Vries, D. P. (1991). Variation in adventitious root formation of softwood cuttings of *Rosa chinensis minima* (Sims) Voss cultivars. *Sci. Hortic.* 47, 345–349. doi: 10.1016/0304-4238(91)90018-t

Faust, J. E., and Enfield, A. L. (2010). Effect of temperature and storage duration on quality and rooting performance of poinsettia (*Euphorbia pulcherrima* 'Prestige Red') cuttings. *Acta Hortic.* 877, 1799–1807. doi: 10.17660/actahortic.2010.877.247

Feller, C., Favre, P., Janka, A., Zeeman, S. C., Gabriel, J. P., and Reinhardt, D. (2015). Mathematical modeling of the dynamics of shoot-root interactions and resource partitioning in plant growth. *PLoS One* 10:e0127905. doi: 10.1371/journal.pone.0127905

Ferrari, A., Hagedorn, F., and Niklaus, P. A. (2018). Disentangling effects of air and soil temperature on C allocation in cold environments: a C-14 pulse-labelling study with two plant species. *Ecol. Evol.* 8, 7778–7789. doi: 10.1002/ece3.4215

Franken, P. (2012). The plant strengthening root endophyte *Piriformospora indica*: potential application and the biology behind. *Appl. Microbiol. Biotech.* 96, 1455–1464. doi: 10.1007/s00253-012-4506-1

Galopin, G., Beaujard, F., and Gendraud, M. (1996). Intensive production of juvenile cuttings by mother microplant culture in *Hydrangea macrophylla* "Leuchtfeuer". *Can. J. Bot.* 74, 561–567. doi: 10.1139/b96-071

Garrido, G., Guerrero, J. R., Cano, E. A., Acosta, M., and Sanchez-Bravo, J. (2002). Origin and basipetal transport of the IAA responsible for rooting of carnation cuttings. *Physiol. Plant* 114, 303–312. doi: 10.1034/j.1399-3054.2002.1140217.x

Gautam, D., and Pagay, V. (2020). A review of current and potential applications of remote sensing to study the water status of horticultural crops. *Agronomy* 10:140. doi: 10.3390/agronomy10010140

Gerhards, M., Schlerf, M., Mallick, K., and Udelhoven, T. (2019). Challenges and future perspectives of multi-/hyperspectral thermal infrared remote sensing for crop water-stress detection. *Remote Sens.* 11:1240. doi: 10.3390/rs11101240

Guerrero, J. R., Garrido, G., Acosta, M., and Sanchez-Bravo, J. (1999). Influence of 2,3,5-triiodobenzoic acid and 1-N-naphthylphthalamic acid on indoleacetic acid transport in carnation cuttings: relationship with rooting. *J. Plant Growth Regul.* 18, 183–190. doi: 10.1007/Pl00007068

Heide, O. M. (2019). Juvenility, maturation and rejuvenation in plants: adventitious bud formation as a novel rejuvenation process. *J. Hortic. Sci. Biotech.* 94, 2–11. doi: 10.1080/14620316.2018.1482795

Husen, A., and Pal, M. (2007). Effect of branch position and auxin treatment on clonal propagation of *Tectona grandis Linn. f. New Forest* 34, 223–233. doi: 10.1007/s11056-007-9050-y

Ishikawa, D., Shinzawa, H., Genkawa, T., Kazarian, S. G., and Ozaki, Y. (2014). Recent progress of near-infrared (NIR) imaging -development of novel instruments and their applicability for practical situations. *Anal. Sci.* 30, 143–150. doi: 10.2116/analsci.30.143

Justice, A. H., Faust, J. E., and Kerrigan, J. L. (2018). Evaluating a novel method to introduce a mycorrhizal-like fungus, *Piriformospora indica*, via an inoculated rooting substrate to improve adventitious root formation. *Horttechnology* 28, 149–153. doi: 10.21273/Horttech03914-17

Kadner, R., and Druege, U. (2004). Role of ethylene action in ethylene production and poststorage leaf senescence and survival of pelargonium cuttings. *Plant Growth Regul.* 43, 187–196. doi: 10.1023/b:grow.0000045999.61765.7e

Klopotek, Y., Franken, P., Klaering, H. P., Fischer, K., Hause, B., Hajirezaei, M. R., et al. (2016). A higher sink competitiveness of the rooting zone and invertases are involved in dark stimulation of adventitious root formation in *Petunia hybrida* cuttings. *Plant Sci.* 243, 10–22. doi: 10.1016/j.plantsci.2015.11.001

Klopotek, Y., George, E., Druege, U., and Klaering, H.-P. (2012). Carbon assimilation of petunia cuttings in a non-disturbed rooting environment: response to environmental key factors and adventitious root formation. *Sci. Hortic.* 145, 118–126. doi: 10.1016/j.scienta.2012.08.004

Klopotek, Y., Haensch, K.-T., Hause, B., Hajirezaei, M.-R., and Druege, U. (2010). Dark exposure of petunia cuttings strongly improves adventitious root formation and enhances carbohydrate availability during rooting in the light. *J. Plant Physiol.* 167, 547–554. doi: 10.1016/j.jplph.2009.11.008

Kramer, E. M., and Bennett, M. J. (2006). Auxin transport: a field in flux. *Trends Plant Sci.* 11, 382–386. doi: 10.1016/j.tplants.2006.06.002

Lakehal, A., and Bellini, C. (2019). Control of adventitious root formation: insights into synergistic and antagonistic hormonal interactions. *Physiol. Plant* 165, 90–100. doi: 10.1111/ppl.12823

Lakehal, A., Dob, A., Novák, O., and Bellini, C. (2019). DAO1-mediated circuit controls auxin and jasmonate crosstalk robustness during adventitious root

initiation in *Arabidopsis*. *Int. J. Mol. Sci.* 20:4428. doi: 10.3390/ijms20184428

Lau, H. Y., and Botella, J. R. (2017). Advanced DNA-based point-of-care diagnostic methods for plant diseases detection. *Front. Plant Sci.* 8, 2016. doi: 10.3389/fpls.2017.02016

Leatherwood, W. R., Dole, J. M., Bergmann, B. A., and Faust, J. E. (2016). 1-methylcyclopropene improves ethylene tolerance of unrooted herbaceous cuttings but delays adventitious root development in *Angelonia*, *Calibrachoa*, *Impatiens*, *Portulaca*, *Sutera*, and *Verbena* cultivars. *Hortscience* 51, 164–170. doi: 10.21273/hortsci.51.2.164

LeBude, A. V., Goldfarb, B., Blazich, F. A., Frampton, J., and Wise, F. C. (2005). Mist level influences vapor pressure deficit and gas exchange during rooting of juvenile stem cuttings of loblolly pine. *Hortscience* 40, 1448–1456. doi: 10.21273/Hortsci.40.5.1448

Leyser, O. (2011). Auxin, self-organisation, and the colonial nature of plants. *Curr. Biol.* 21, R331–R337. doi: 10.1016/j.cub.2011.02.031

Li, G. J., Zhang, L., Wang, M., Di, D. W., Kronzucker, H. J., and Shi, W. M. (2019). The *Arabidopsis* AMOT1/EIN3 gene plays an important role in the amelioration of ammonium toxicity. *J. Exp. Bot.* 70, 1375–1388. doi: 10.1093/jxb/ery457

Limantara, L., Dettling, M., Indrawati, R., Hardo, T., and Brotosudarmo, T. H. P. (2015). Analysis on the chlorophyll content of commercial green leafy vegetables. *Proc. Chem.* 14, 225–231. doi: 10.1016/j.proche.2015.03.032

Ling, Q. H., Huang, W. H., and Jarvis, P. (2011). Use of a SPAD-502 meter to measure leaf chlorophyll concentration in *Arabidopsis thaliana*. *Photosynth. Res.* 107, 209–214. doi: 10.1007/s11120-010-9606-0

Lohr, D., Tillmann, P., Druege, U., Zerche, S., Rath, T., and Meinken, E. (2017). Non-destructive determination of carbohydrate reserves in leaves of ornamental cuttings by near-infrared spectroscopy (NIRS) as a key indicator for quality assessments. *Biosyst. Engin.* 158, 51–63. doi: 10.1016/j.biosystemseng.2017.03.005

Lohr, D., Tillmann, P., Zerche, S., Druege, U., Rath, T., and Meinken, E. (2016). Non-destructive measurement of nitrogen status of leafy ornamental cuttings by near infrared reflectance spectroscopy (NIRS) for assessment of rooting capacity. *Biosyst. Engin.* 147, 157–167. doi: 10.1016/j.biosystemseng.2016.06.003

Millan-Almaraz, J. R., Romero-Troncoso, R. D., Guevara-Gonzalez, R. G., Contreras-Medina, L. M., Carrillo-Serrano, R. V., Osornio-Rios, R. A., et al. (2010). FPGA-based fused smart sensor for real-time plant-transpiration dynamic estimation. *Sensors* 10, 8316–8331. doi: 10.3390/s100908316

Müller, R., Serek, M., Sisler, E. C., and Andersen, A. S. (1998). Ethylene involvement in leaf abscission, chlorosis, and rooting of *Codiaeum variegatum* var. pictum (Lodd) Muell '*Aucubaefolia*'. *Gartenbauwiss* 63, 66–71.

Mutui, T. M., Mibus, H., and Serek, M. (2005). Effects of thidiazuron, ethylene, abscisic acid and dark storage on leaf yellowing and rooting of *Pelargonium* cuttings. *J. Hortic. Sci. Biotech.* 80, 543–550. doi: 10.1080/14620316.2005.11511975

Nguyen, T. H. N., Tänzer, S., Rudeck, J., Winkelmann, T., and Debener, T. (2020). Genetic analysis of adventitious root formation in vivo and in vitro in a diversity panel of roses. *Sci. Hortic.* 266:109277. doi: 10.1016/j.scienta.2020.109277

Novak, O., Napier, R., and Ljung, K. (2017). Zooming in on plant hormone analysis: tissue- and cell-specific approaches. *Ann. Rev. Plant Biol.* 68, 323–348. doi: 10.1146/annurev-arplant-042916-040812

Orlikowska, T. (1992). Effect of amino acids on rooting of apple dwarf rootstocks in vitro. *Biol. Plant* 34, 39–44. doi: 10.1007/bf02925788

Osterc, G., and Stampar, F. (2011). Differences in endo/exogenous auxin profile in cuttings of different physiological ages. *J. Plant. Physiol.* 168, 2088–2092. doi: 10.1016/j.jplph.2011.06.016

Otiende, M. A., Nyabundi, J. O., Ngamau, K., and Opala, P. (2017). Effects of cutting position of rose rootstock cultivars on rooting and its relationship with mineral nutrient content and endogenous carbohydrates. *Sci. Hortic.* 225, 204–212. doi: 10.1016/j.scienta.2017.07.009

Peterson, B. J., Sanchez, O., Burnett, S. E., and Hayes, D. J. (2018). Comparison of four systems for propagation of *Coleus* by stem cuttings. *Horttechnology* 28, 143–148. doi: 10.21273/Horttech03926-17

Petrasek, J., and Friml, J. (2009). Auxin transport routes in plant development. *Development* 136, 2675–2688. doi: 10.1242/dev.030353

Poethig, R. S. (2013). Vegetative phase change and shoot maturation in plants. *Curr. Top. Dev. Biol.* 105, 125–152. doi: 10.1016/B978-0-12-396968-2.00005-1

Rapaka, V. K., Bessler, B., Schreiner, M., and Druege, U. (2005). Interplay between initial carbohydrate availability, current photosynthesis and adventitious root formation in *Pelargonium* cuttings. *Plant Sci.* 168, 1547–1560. doi: 10.1016/j.plantsci.2005.02.006

Rapaka, V. K., Faust, J. E., Dole, J. M., and Runkle, E. S. (2007a). Diurnal carbohydrate dynamics affect postharvest ethylene responsiveness in portulaca (*Portulaca grandiflora* 'Yubi Deep Rose') unrooted cuttings. *Postharv. Biol. Technol.* 44, 293–299. doi: 10.1016/j.postharvbio.2006.12.004

Rapaka, V. K., Faust, J. E., Dole, J. M., and Runkle, E. S. (2007b). Effect of time of harvest on postharvest leaf abscission in lantana (*Lantana camara* L. 'Dallas Red') unrooted cuttings. *Hortscience* 42, 304–308. doi: 10.21273/hortsci.42.2.304

Rapaka, V. K., Faust, J. E., Dole, J. M., and Runkle, E. S. (2008). Endogenous carbohydrate status affects postharvest ethylene sensitivity in relation to leaf senescence and adventitious root formation in *Pelargonium c* uttings. *Postharv. Biol. Technol.* 48, 272–282. doi: 10.1016/j.postharvbio.2007.10.001

Rasmussen, A., Hosseini, S. A., Hajirezaei, M. R., Druege, U., and Geelen, D. (2015). Adventitious rooting declines with the vegetative to reproductive switch and involves a changed auxin homeostasis. *J. Exp. Bot.* 66, 1437–1452. doi: 10.1093/jxb/eru499

Riccardi, M., Mele, G., Pulvento, C., Lavini, A., d'Andria, R., and Jacobsen, S. E. (2014). Non-destructive evaluation of chlorophyll content in quinoa and amaranth leaves by simple and multiple regression analysis of RGB image components. *Photosynth. Res.* 120, 263–272. doi: 10.1007/s11120-014-9970-2

Rigon, J. P. G., Capuani, S., Fernandes, D. M., and Guimaraes, T. M. (2016). A novel method for the estimation of soybean chlorophyll content using a smartphone and image analysis. *Photosynthetica* 54, 559–566. doi: 10.1007/s11099-016-0214-x

Roitsch, T., and Gonzalez, M. C. (2004). Function and regulation of plant invertases: sweet sensations. *Trends Plant Sci.* 9, 606–613. doi: 10.1016/j.tplants.2004.10.009

Ruedell, C. M., de Almeida, M. R., and Fett-Neto, A. G. (2015). Concerted transcription of auxin and carbohydrate homeostasis-related genes underlies improved adventitious rooting of microcuttings derived from far-red treated *Eucalyptus globulus* Labill mother plants. *Plant Physiol. Biochem.* 97, 11–19. doi: 10.1016/j.plaphy.2015.09.005

Rufai, S., Hanafi, M. M., Rafii, M. Y., Mohidin, H., and Omar, S. R. S. (2016). Growth and development of moringa (*Moringa oleifera* L) stem cuttings as affected by diameter magnitude, growth media, and indole-3-butyric acid. *Ann. For. Res.* 59, 209–218. doi: 10.15287/afr.2016.686

Sager, M., Yeat, N. C., Pajaro-Van der Stadt, S., Lin, C., Ren, Q. Y., and Lin, J. (2015). Transcriptomics in cancer diagnostics: developments in technology, clinical research and commercialization. *Expert Rev. Mol. Diagn.* 15, 1589–1603. doi: 10.1586/14737159.2015.1105133

Sanchez, O., Burnett, S. E., and Peterson, B. J. (2020). Environment, photosynthesis, and adventitious rooting of manchurian lilac cuttings propagated in overhead mist, submist, and combination systems. *Hortscience* 55, 78–82. doi: 10.21273/Hortsci14473-19

Scheres, B., and van der Putten, W. H. (2017). The plant perceptron connects environment to development. *Nature* 543, 337–345. doi: 10.1038/nature22010

Schwambach, J., Fadanelli, C., and Fett-Neto, A. G. (2005). Mineral nutrition and adventitious rooting in microcuttings of *Eucalyptus globulus*. *Tree Physiol.* 25, 487–494. doi: 10.1093/treephys/25.4.487

Steffens, B., and Rasmussen, A. (2016). The physiology of adventitious roots. *Plant Physiol. Biochem.* 170, 603–617. doi: 10.1104/pp.15.01360

Steppe, K. (2015). Contribution of plant sensors to new developments in horticulture. *Acta Hortic.* 1099, 55–61. doi: 10.17660/actahortic.2015.1099.2

Takahashi, F., Sato-Nara, K., Kobayashi, K., Suzuki, M., and Suzuki, H. (2003). Sugar-induced adventitious roots in *Arabidopsis* seedlings. *J. Plant Res.* 116, 83–91. doi: 10.1007/s10265-002-0074-2

Taylor, B. D., and Hoover, B. K. (2018). Foliar auxin application improves adventitious rooting of wall germander cuttings. *Horttechnology* 28, 17–21. doi: 10.21273/Horttech03891-17

Tolentino, M. A. K. P., Albano, D. R. B., and Sevilla, F. B. (2018). Piezoelectric sensor for ethylene based on silver(I)/polymer composite. *Sensor Actuat. B Chem.* 254, 299–306. doi: 10.1016/j.snb.2017.07.015

Tombesi, S., Palliotti, A., Poni, S., and Farinelli, D. (2015). Influence of light and shoot development stage on leaf photosynthesis and carbohydrate status during the adventitious root formation in cuttings of *Corylus avellana* L. *Front. Plant Sci.* 6:973. doi: 10.3389/fpls.2015.00973

Ueda, H., and Kusaba, M. (2015). Strigolactone regulates leaf senescence in concert with ethylene in *Arabidopsis*. *Plant Physiol.* 169, 138–147. doi: 10.1104/pp.15.00325

van Rongen, M., Bennett, T., Ticchiarelli, F., and Leyser, O. (2019). Connective auxin transport contributes to strigolactone-mediated shoot branching control independent of the transcription factor BRC1. *PLoS Genet.* 15:e1008023. doi: 10.1371/journal.pgen.1008023

Vergara-Diaz, O., Vatter, T., Kefauver, S. C., Obata, T., Fernie, A. R., and Araus, J. L. (2020). Assessing durum wheat ear and leaf metabolomes in the field through hyperspectral data. *Plant J.* 102:14636. doi: 10.1111/tpj.14636

Wilkerson, E. G., Gates, R. S., Zolnier, S., Kester, S. T., and Geneve, R. L. (2005). Predicting rooting stages in poinsettia cuttings using root zone temperature-based models. *J Am. Soc. Hortic. Sci.* 130, 302–307. doi: 10.21273/Jashs.130.3.302

Yanagisawa, S., Yoo, S. D., and Sheen, J. (2003). Differential regulation of EIN3 stability by glucose and ethylene signalling in plants. *Nature* 425, 521–525. doi: 10.1038/nature01984

Yang, H. Y., Klopotek, Y., Hajirezaei, M. R., Zerche, S., Franken, P., and Druege, U. (2019). Role of auxin homeostasis and response in nitrogen limitation and dark stimulation of adventitious root formation in petunia cuttings. *Ann. Bot.* 124, 1053–1066. doi: 10.1093/aob/mcz095

Yasodha, R., Kamala, S., Kumar, S. R. A., Kumar, R. D., and Kalaiarasi, K. (2008). Effect of glucose on in vitro rooting of mature plants of *Bambusa nutans*. *Sci. Hortic.* 116, 113–116. doi: 10.1016/j.scienta.2007.10.025

Zerche, S., and Druege, U. (2009). Nitrogen content determines adventitious rooting in *Euphorbia pulcherrima* under adequate light independently of pre-rooting carbohydrate depletion of cuttings. *Sci. Hortic.* 121, 340–347. doi: 10.1016/j.scienta.2009.02.012

Zerche, S., Haensch, K. T., Druege, U., and Hajirezaei, M. R. (2016). Nitrogen remobilisation facilitates adventitious root formation on reversible dark-induced carbohydrate depletion in *Petunia hybrida*. *BMC Plant Biol.* 16:219. doi: 10.1186/s12870-016-0901-6

Zerche, S., Lohr, D., Meinken, E., and Druege, U. (2019). Metabolic nitrogen and carbohydrate pools as potential quality indicators of supply chains for ornamental young plants. *Sci. Hortic.* 247, 449–462. doi: 10.1016/j.scienta.2018.12.029

Zhang, G. F., Zhao, F., Chen, Y. Q., Pan, Y., Sun, L. J., Bao, N., et al. (2019). Jasmonate-mediated wound signalling promotes plant regeneration. *Nat. Plants* 5, 491–497. doi: 10.1038/s41477-019-0408-x

Zhang, W. X., Fan, J. J., Tan, Q. Q., Zhao, M. M., and Cao, F. L. (2017). Mechanisms underlying the regulation of root formation in *Malus hupehensis* stem cuttings by using exogenous hormones. *J. Plant Growth Regul.* 36, 174–185. doi: 10.1007/s00344-016-9628-8

Zhuo, M. N., Sakuraba, Y., and Yanagisawa, S. (2020). A jasmonate-activated MYC2-Dof2.1-*MYC2* transcriptional loop promotes leaf senescence in *Arabidopsis*. *Plant Cell* 32, 242–262. doi: 10.1105/tpc.19.00297

Conflict of Interest: The author declares that the research was conducted in the absence of any commercial or financial relationships that could be construed as a potential conflict of interest.

frontiers in Plant Science

ORIGINAL RESEARCH
published: 17 July 2020
doi: 10.3389/fpls.2020.01093

A Genomewide Scan for Genetic Structure and Demographic History of Two Closely Related Species, *Rhododendron dauricum* and *R. mucronulatum* (*Rhododendron*, Ericaceae)

Baiming Yang[1,2], *Guoli Zhang*[1], *Fengping Guo*[3], *Manqi Wang*[1], *Huaying Wang*[1] *and Hongxing Xiao*[1*]

[1] Key Laboratory of Molecular Epigenetics of Ministry of Education, Northeast Normal University, Changchun, China, [2] Changchun Guoxin Modern Agricultural Technology Development Co., Ltd., Changchun, China, [3] Biology Group, No. 30 Middle School of Shenyang, Shenyang, China

OPEN ACCESS

Edited by:
Renato Paiva,
Universidade Federal de Lavras, Brazil

Reviewed by:
Yoshiko Shimono,
Kyoto University, Japan
Robin Van Velzen,
Wageningen University and Research, Netherlands

***Correspondence:**
Hongxing Xiao
xiaohx771@nenu.edu.cn

Specialty section:
This article was submitted to Crop and Product Physiology, a section of the journal Frontiers in Plant Science

Received: 13 December 2019
Accepted: 02 July 2020
Published: 17 July 2020

Citation:
Yang B, Zhang G, Guo F, Wang M, Wang H and Xiao H (2020) A Genomewide Scan for Genetic Structure and Demographic History of Two Closely Related Species, Rhododendron dauricum and R. mucronulatum (Rhododendron, Ericaceae). Front. Plant Sci. 11:1093. doi: 10.3389/fpls.2020.01093

Understanding the processes of divergence and speciation is an important task for evolutionary research, and climate oscillations play a pivotal role. We estimated the genetic structure and demographic history of two closely related species of *Rhododendron*, *R. dauricum*, and *R. mucronulatum*, distributed in northeastern China using 664,406 single nucleotide polymorphic loci of specific-locus amplified fragment sequencing (SLAF-seq) and 4 chloroplast DNA (cpDNA) fragments, sampling 376 individuals from 39 populations of these two species across their geographic distributions. The geographical distribution of cpDNA haplotypes revealed that *R. dauricum* and *R. mucronulatum* have different spatial genetic structures and haplotype diversity. Analysis of molecular variance (AMOVA) results showed that these two species have significant genetic differentiation and that the phylogeny demonstrates that these two species clustered a monophyletic group based on SLAF data, respectively, but not in cpDNA data. The evidence of significant gene flow was also detected from *R. mucronulatum* to *R. dauricum*. A deep divergence between the two species was observed and occurred during the early Oligocene. The niche models showed that the two species have different demographic histories. Thus, our results imply that geography and climate changes played important roles in the evolutionary process of *R. dauricum* and *R. mucronulatum*, and although there was an interspecific gene flow, the divergence was maintained by natural selection.

Keywords: specific-locus amplified fragment, nucleotide differentiation, gene flow, niche simulation, climate changes

INTRODUCTION

Past climate oscillations and historical tectonism had a huge impact on the genetic structure and demographic histories of many species, even triggering divergence and speciation (Milne, 2006). Understanding the factors that promote species divergence is of major interest in ecological and evolutionary research (Papadopulos et al., 2011; Butlin et al., 2012). Species divergences are frequently driven by geographic isolation, environmental heterogeneity (ecological speciation) or a combination of both (Orr and Smith, 1998; Schluter, 2001; Nosil, 2012). Geographic isolation is generally considered an allopatric speciation, where gene flow among splitting populations is disrupted by physical barriers, and genetic divergence occurs between taxa by local adaptation, mutation, and genetic drift (Coyne and Orr, 2004). In contrast, under ecological speciation, divergence is driven by divergent natural selection between environments, giving rise to reproductive isolation between subsets of a single population by adaptation to different environments or ecological niches. (Schluter, 2000; Schluter, 2001; Rundle and Nosil, 2005).

Gene flow played an important role in the evolution of species, having both positive and negative effects on adaptation (Palme et al., 2004). Itis expected due to secondary contact when physical barriers disappear (under allopatric speciation) or range expansions and contractions in response to climatic fluctuation, which is generally regarded as a force counteracting population divergence (Runemark et al., 2012). When the rate of gene flow between species exceeds that among populations within the species, hybridization might occur. These phenomena have been demonstrated not only in animals (Taylor et al., 2005; Seehausen, 2006; Webb et al., 2011), but also in plants (Marczewski et al., 2015; Ma et al., 2016). Interspecies gene flow after speciation can reduce genetic differentiation among species and even achieve homogenization (Vonlanthen et al., 2012; Bhat et al., 2014). However, when the homogenization of interspecific gene flow is weaker than the disproportionation of natural selection, species genetic differentiation may still be maintained (Rundell and Prince, 2009; Ribera et al., 2011).

Rhododendron (Ericaceae L.) is a taxonomically complex genus with approximately 1,000 species (Chamberlain et al., 1996) distributed in Himalayan flora. It is one of the major genera of China and includes approximately 571 species, of which 402 species are endemic to China (Wu et al., 2003; Fang et al., 2005). Northeast Asia is an area with complex topographic and climatic gradients (Lopez-Pujol et al., 2011), and recent research supports a northeastern Asian origin of *Rhododendron* (Shrestha et al., 2018). Among *Rhododendron* species, *Rhododendron* subgen. *Rhodorastrum*, including four taxa, *R. ledebourii*, *R. dauricum*, *R. mucronulatum*, and *R. sichotense*, are distributed in this area. The four species exhibit similar phenotypic characteristics, such as leaf, petiole and flower shapes, thus making taxonomy difficult. *R. ledebourii*, *R. mucronulatum*, and *R. sichotense* were regarded as populations, varieties or subspecies of *R. dauricum* in previous studies (Voroshilov, 1982; Mazurenko and Hohryakov, 1991; Koropachinskii and Vstovskaya, 2002). In contrast, phylogenetic analysis supports the species status of these four species-based cpDNA regions (Tikhonova et al., 2012; Polezhaeva et al., 2018). Additionally, two well-distinguished groups were determined for these four species, including *R. ledebourii* and *R. dauricum* as the Siberian group and *R. sichotense* and *R. mucronulatum* as the Far Eastern group (Polezhaeva et al., 2018), demonstrating good agreement with the geographical positions of the species collected. However, a main haplotype of *R. mucronulatum* was clustered with the haplotypes of *R. sichotense*, and the two species were joined together based on SAMOVA, Furthermore, samples were only from Russia and located in Northeast China (NEC) were lacking. In addition, phylogenetic reconstruction of the genus *Rhododendron* based on the ITS region showed that *R. dauricum* and *R. mucronulatum* were sister species (Kutsev and Karakulov, 2010; Baranova et al., 2014).

These four species have different geographical distribution, covering Mongolia, Northeast China, Japan, Korean Peninsula, and Russian (including the southern part of western Siberia, eastern Siberia, and the Russian Far East), and Northeast China (NEC) is in the center of these areas (**Figure 1C**), among which *R. dauricum* is widely distributed. *R. dauricum* and *R. mucronulatum* have different geographical distribution in NEC, although they both occur along mountain slopes. *R. dauricum* is distributed along the Great Khingan Mountains (GKM), Lesser Khingan Mountains (LKM) and Changbai Mountain (CBM), while *R. mucronulatum* is found in the south of the Changbai Mountain and other locations in North China.

Therefore, in this study, to test the genetic divergence and demographic history of *R. dauricum* and *R. mucronulatum* driven by possible roles of geological or climate events, we first combined specific-locus amplified fragment sequencing (SLAF-seq) and cpDNA markers. We assessed the genetic diversity, phylogeny, and genetic structures of the two species. The divergence time and ecological niche modeling were also tested to infer the possible population demographic history in light of past climate changes. In addition, gene flow between the species was also detected to further elucidate the role of either climate oscillations or geological processes in shaping nucleotide variation and triggering divergence. Together, these analyses not only provide insights into the evolutionary history of two closely related species but also contribute to understanding biodiversity in northern and northeastern China.

MATERIALS AND METHODS

Plant Materials and Sequencing

On the basis of 23 populations in Jiang et al. (2016), we have newly collected some populations and individuals of *R. dauricum*. After removing and merging some populations that were close to each other or for which the haplotypes were completely consistent, we newly added 127 *R. dauricum* individuals in this study. Of these, 88 individuals were from newly added 9 populations and 39 were extensions to the existing populations. Finally, there were a total of 247 *R. dauricum*

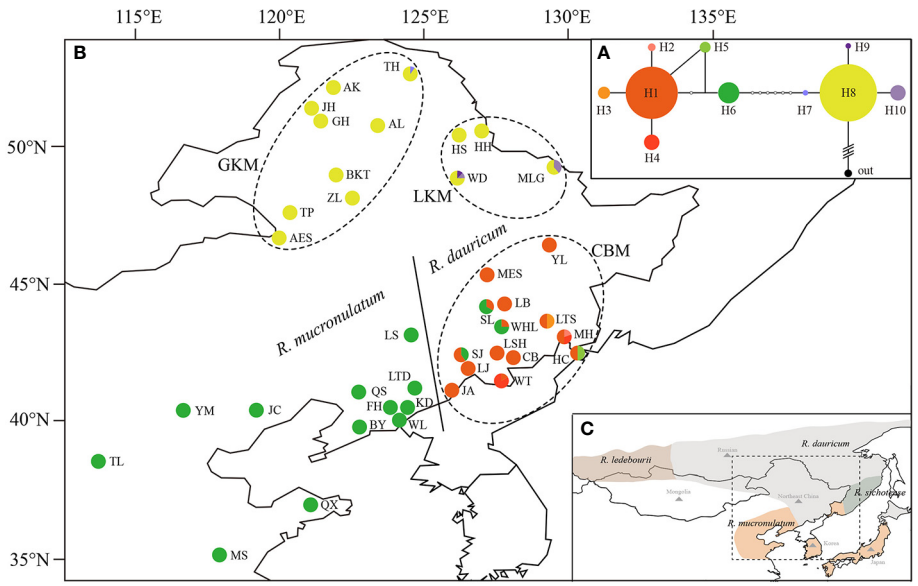

FIGURE 1 | (A) The Network of haplotypes in *R. dauricum*. The size of haplotype circle represents relative frequency. **(B)** Geographical distribution of haplotypes within *R. dauricum* and *R. mucronulatum*. The regions of GKM, LKM, and CBM were indicated by dotted ellipses. The populations of *R. dauricum* and *R. mucronulatum* were distinguished by solid line. **(C)** The distribution of four species in subgen. *Rhodorastrum*. It was drawn based on Polezhaeva (2018) and the sites information collected in ecological niche model simulation. Each color represents a species.

individuals in 27 populations (**Table 1**). Moreover, we newly collected 12 populations of 129 individuals with *R. mucronulatum* across all the current relevant regions in China. 5 to 23 individuals for each population, only one individual for LB. We distinguished these two species mainly based on geographical distribution and morphological characteristics. Firstly, *R. dauricum* is mainly distributed in Inner Mongolia, Heilongjiang and Jilin Provinces of China, and *R. mucronulatum* is mainly distributed in Liaoning Province, Hebei Province, Beijing, Shandong Province, and northern Jiangsu Province. Secondly, the main differences in morphology between the two are the characteristic of scales on the leaves abaxial surface and whether there are hairs on the branchlets. The leaves abaxial surface of *R. dauricum* densely covered with scales, imbricate or adjacent to each other, spacing 1/2 or 1.5 times their diameter, and branchlets pilose; the spacing of the scales in *R. mucronulatum* was two to four times its diameter and branchlets glabrous. Sampled individuals were located at least 50 m apart. Additionally, samples of *R. micranthum* and *R. schlippenbachii* were also collected to serve as outgroups for cpDNA phylogenetic analyses. All fresh leaf materials were desiccated in silica gel, and voucher specimens were stored in the Northeast Normal University Herbarium (NENU).

Total genomic DNA was extracted using a modified 4 × CTAB procedure (Doyle and Doyle, 1987). The concentration and quality of genomic DNA were tested by agarose gel electrophoresis (1%) and an ND-1000 spectrophotometer (Thermo Fisher Scientific, USA). Qualified DNA samples were stored at −20°C for polymerase chain reaction (PCR) amplification and high-throughput sequencing.

To obtain the orthologous regions of *R. dauricum* individuals from *R. mucronulatum* samples, we selected four pairs of primers (*trnS-trnG*, *trnS-trnfM*, *TabE-ndhJ*, *trnK-matK*) used in a previous study (Jiang et al., 2016), which were most informative for *R. dauricum* populations. The reagent concentrations, polymerase chain reaction (PCR) process, and sequencing followed Jiang et al. (2016).

Analyses of cpDNA Sequences

DNA sequence alignment was performed using ClustalX 2.0 (Larkin et al., 2007), and alignments were edited manually in BioEdit 7.0.1 (Hall, 1999) before being concatenated. The number of polymorphic sites (S), nucleotide diversity (π), number of haplotypes (h), and haplotype diversity (Hd) were calculated by DnaSP v5 (Librado and Rozas, 2009). We also calculated Tajimas' D (Tajima, 1989), Fu and Li' s D and F (Fu and Li, 1993) separately for the two species using this software to test how well the data conformed to the neutral model of evolution. The population differentiation statistic (F_{ST}) (Wright, 1984) was calculated by AMOVA in ARLEQUIN 3.5 (Excoffier et al., 2005). Furthermore, the cpDNA haplotype, representing unique DNA sequences or alleles separated by mutational steps, was constructed by TCS v1.2.1 (Clement et al., 2000) with genetic distance and statistical parsimony methods. We chose 'Gaps = missing' and set the Fix Connection Limit to 50 steps to ensure that all haplotypes were connected to each other. In order to compare with the phylogenetic tree constructed by SLAF data, we chose the same individuals as SLAF to construct the phylogenetic tree based on cpDNA. A maximum likelihood (ML) tree was constructed in RAxML 8.2.9 software (Stamatakis et al., 2008) under GTRGAMMA selected by

TABLE 1 | Sampling information and genetic diversity for SLAF data and cpDNA of *R. dauricum* and *R. mucronulatum*.

pop	Location	Long (°E)	Lat (°N)	size	S	h	Hd	$\pi \times 10^{-3}$	voucher
R. dauricum				247 (40)	15	10	0.6610	1.8000 (0.2450)	
GKM									
AES^{+}	Aersha, IM	120.562	47.410	20 (2)	0	1	0.0000	0.0000	NENU00042001
TP	Taipingling, IM	120.491	47.488	10 (1)	0	1	0.0000	0.0000	NENU00042002
ZL	Zhalant, IM	122.700	48.083	10	0	1	0.0000	0.0000	NENU00042003
BKT*	Boktu, IM	122.105	48.832	10 (3)	0	1	0.0000	0.0000	NENU00042004
GH	Genhe City, IM	121.492	50.775	5 (1)	0	1	0.0000	0.0000	NENU00042005
JH	Jinhe Town, IM	121.294	51.041	5 (1)	0	1	0.0000	0.0000	NENU00042006
AK	Oakley Hill, IM	122.037	51.838	10 (1)	0	1	0.0000	0.0000	NENU00042007
AL	Ali River, IM	123.533	50.550	5	0	1	0.0000	0.0000	NENU00042008
TH*	Tahe County, HLJ	124.710	52.334	10 (3)	1	2	0.2000	0.0001	NENU00042009
LKM									
HS	Big black mountain, HLJ	126.448	50.241	5 (3)	0	1	0.0000	0.0000	NENU00042010
HH	Heihe, HLJ	127.516	50.233	5	0	1	0.0000	0.0000	NENU00042011
MLG^{+}	Maolangou, HLJ	129.771	49.098	18 (3)	1	2	0.5033	0.0002	NENU00042012
WD*	Longmen Shizhai, HLJ	126.335	48.695	8 (3)	2	3	0.4643	0.0002	NENU00042013
CBM									
YL	Yilan County, HLJ	129.568	46.325	9 (3)	0	1	0.0000	0.0000	NENU00042014
MES	Maoer Mountain, HLJ	127.449	45.259	5 (1)	0	1	0.0000	0.0000	NENU00042015
SL*	Shulan City, JL	127.452	44.247	12 (3)	2	2	0.4850	0.0004	NENU00042016
LB	Old white mountain, JL	127.919	44.242	1	–	–	–	–	NENU00042017
WHL*	Weihuling, JL	127.866	43.483	10	2	2	0.3560	0.0003	NENU00042018
LTS*	Camel Mountain, JL	129.540	43.645	10 (2)	1	2	0.5560	0.0002	NENU00042019
MH*	Manhe Village, JL	130.055	43.189	10 (2)	2	3	0.6890	0.0003	NENU00042020
HC*	Jiushaping, JL	130.633	42.417	8 (1)	1	2	0.5710	0.0002	NENU00042021
CB^{+}	Changbai Mountain, JL	127.787	42.052	11 (3)	0	1	0.0000	0.0000	NENU00042022
LSH	Lushihe, JL	127.883	42.533	6	0	1	0.0000	0.0000	NENU00042023
WT	Wangtian'e Scenic Area, JL	127.943	41.547	6 (1)	1	2	0.3330	0.0001	NENU00042024
SJ	Triangular Bay, JL	126.433	42.350	5	2	2	0.6000	0.0004	NENU00042025
LJ^{+}	Pearl Gate Village, JL	126.156	42.278	23 (3)	0	1	0.0000	0.0000	NENU00042026
JA*	Ji'an, JL	126.283	41.250	10	0	1	0.0000	0.0000	NENU00042027
R. mucronulatum				129 (25)	0	1	0.0000	0.0000 (0.1850)	
LTD*	Lao Baldingzi, LN	124.908	41.298	21 (2)	0	1	0.0000	0.0000	NENU00042028
LS*	Sitaizi Forest Farm, JL	124.702	43.189	10 (3)	0	1	0.0000	0.0000	NENU00042029
QS*	Qianshan, LN	123.091	41.589	9	0	1	0.0000	0.0000	NENU00042030
FH*	Phoenix Mountain, LN	124.078	40.413	21 (3)	0	1	0.0000	0.0000	NENU00042031
WL*	Wulong Mountain, LN	124.336	40.255	10 (3)	0	1	0.0000	0.0000	NENU00042032
KD*	Kuandian, JL	124.483	40.500	10	0	1	0.0000	0.0000	NENU00042033
BY*	Bingyugou, LN	122.950	39.983	8	0	1	0.0000	0.0000	NENU00042034
JC*	Sandaogou, LN	119.345	40.583	15 (3)	0	1	0.0000	0.0000	NENU00042035
YM*	Yunmeng Mountain, BJ	116.686	40.555	10 (3)	0	1	0.0000	0.0000	NENU00042036
TL*	Tuoliang Scenic Spot,HB	113.812	38.740	5 (3)	0	1	0.0000	0.0000	NENU00042037
QX*	Leshan Park, SD	121.066	37.226	8 (3)	0	1	0.0000	0.0000	NENU00042038
MS*	Mengshan Forest Park, SD	117.969	35.557	2 (2)	0	1	0.0000	0.0000	NENU00042039
Total				376 (65)	16	10	0.5198	0.0014	

*S, number of polymorphic sites (SNPs); h, number of haplotypes; Hd, haplotype diversity; π, nucleotide diversity. *represents the newly added populations of R. dauricum and R. mucronulatum in this study, $^{+}$represents the populations of individual expansion based on previous studies (the number of newly added: AES, 10; MLG, 8; CB, 9; LJ, 12). The size in brackets represents the individuals used for SLAF; the π in brackets represents the nucleotide diversity based on SLAF. GKM, Great Khingan Mountains; LKM, Lesser Khingan Mountains; CBM, Changbai Mountain; IM, Inner Mongolia; HLJ, Heilongjiang Province; JL, Jilin Province; LN, Liaoning Province; BJ, Beijing; HB, Hebei Province; SD, Shandong Province.*

jModeltest 2.0 (Darriba et al., 2012) based on Akaike information criterion (AIC) values and bootstrap supports for clades calculated using 1000 bootstrap replicates.

SLAF Sequencing, Read Alignment and SNP Calling

To obtain all haplotypes of cpDNA and represent the distribution of the two species as evenly as possible, we selected 65 individuals (including 40 *R. dauricum* samples and 25 *R. mucronulatum* samples) for subsequent SLAF sequencing (**Table 1**). Samples of *R. redowskianum* and *R. delavayi* were used as outgroup. The genome of *R. delavayi* (ftp://parrot.genomics.cn/gigadb/pub/10.5524/100001_101000/100331/) was selected as the reference genome for enzyme cutting site prediction. After strict filtering, *Hae*III and *Hpy*166II restriction enzymes were finally used to digest the qualified DNA of the sampled individuals according to the results of prerestriction enzyme digestion. To evaluate the accuracy of the enzyme digestion experiment, *Oryza sativa* subsp. *indica* was

used as a control to ensure the effectiveness of the enzyme-cutting scheme. The obtained SLAF tags with an A-tail added to the 3′ ends were ligated with Dual-index sequencing adaptors, amplified by PCR, screened, and then used to construct the SLAF library (for detailed processes of the SLAF library construction, refer to the methods of Sun et al. (2016). The selected tags were then subjected to pair-end sequencing using an Illumina Hiseq™ 2500 at Biomarker Technologies Corporation in Beijing. Sequencing insert size was 314 to 414 bp and paired-end reads were 126 bp in length.

Clear reads were aligned against the reference genome using Burrows-Wheeler Aligner (BWA) (Li and Durbin, 2009) with parameters defined as missed match = 3; opening gap = 11 and gap extension = 4. False alignment was always detected near Indels; therefore, local alignment was performed. The Genome Analysis Toolkit (GATK) (DePristo et al., 2011) and Sequence Alignment/Map tools (SAMtools) (Li et al., 2009) were used for variant calling under the default setting. Raw SNPs were filtered with a minimum depth (DP) of 3 and minimum mapping quality (MQ) of 30 by our custom Perl scripts, and then PLINK 2 (Purcell et al., 2007) was used to further filter with the minor allele frequency (MAF) of 0.04 and maximum missing rate of 0.5, and SNPs that were out of Hardy-Weinberg equilibrium (HWE) were removed with a p-value threshold < 0.01. Later, considering the linkage disequilibrium (LD) between SNPs, we used the -r2 function in PLINK to quantify pairwise LD between all pairs of SNPs located within 1000 kb of each other, and the results showed that the LD of both species decayed rapidly (**Supplementary Figure S1**). Thus, we did not further filter SNPs according to LD. All non-biallelic SNPs, which may be caused by sequencing, were filtered using our custom Perl scripts. The final screened SNPs were subjected to subsequent data analyses.

Genetic Diversity, Phylogeny, and Population Structure Analyses

The genetic diversity parameter π and the neutral test of Tajima's D, Fu and Li' s D and F values were calculated by PopGenome in R (Bastian et al., 2014) based on SNPs. F_{ST} was also calculated by AMOVA in ARLEQUIN 3.5. The ML tree was constructed in the same way as above. The population structure analyses were performed using ADMIXTURE software (Alexander et al., 2009). The number of subgroups (K value) was set as 1 to 10 in advance for clustering, and the clustering results were cross-verified to determine the optimal number of subgroups according to the valley value of the cross-validation error rate. We further performed principal component analysis (PCA) to determine the clustering status of samples using EIGENSOFT (Price et al., 2006).

Divergence Time and Gene Flow

A Bayesian relaxed molecular clock approach was used to estimate species divergence time by MCMCTREE in PAML (Yang, 2007). When using previously published calibration times, the split of *Oryza sativa* (https://phytozome.jgi.doe.gov/pz//portal.html#!info?alias=Org_Osativa) and *Arabidopsis thaliana* (https://phytozome.jgi.doe.gov/pz/portal.html#!info?alias=Org_Athaliana_er) was fixed as 130~200 Mya, and the split of *R. delavayi* and *Actinidia chinensis* (http://bioinfo.bti.cornell.edu/cgi-bin/kiwi/download.cgi) was estimated to be in the range of 56.1~120.8 Mya (Zhang et al., 2017). The 150 bp sequences before and after the SNPs were used for BLASTN (Altschul et al., 1990) against the reference genomes with an E-value threshold of 1e-3, and then obtained the sequence with a total length of 12,936,348 bp as an input file. *R. dauricum* and *R. mucronulatum* individuals were selected from populations TP and MS, respectively, based on the cpDNA haplotype. The data set was modeled under a correlated rates clock, and the HKY85 nucleotide substitution model was determined by ModelFinder (Kalyaanamoorthy et al., 2017). The first 2000 iterations were discarded as burn-in, and every 10 iterations were sampled until 20000 samples were obtained. Furthermore, to account for gene flow among the groups, we used TREEMIX 1.12 (Pickrell and Pritchard, 2012), which infers patterns of population splitting and mixing accessing the covariance structure of allele frequencies between populations and performing a Gaussian approximation for genetic drift.

Ecological Niche Modeling

MaxEnt software (Phillips et al., 2006) was used to predict the distribution models for *R. dauricum* and *R. mucronulatum* in the last interglacial (LIG) (0.14–0.12 Mya), the last maximum glacial (LGM) (0.02–0.018 Mya) and current time based on modern distribution records and bioclimatic variables. The occurrence data of species were mainly collected from the following three sources: Chinese Virtual Herbarium (CVH) (http://www.cvh.ac.cn/) and relevant literature; Global Biodiversity Information Facility (GBIF) (http://www.gbif.org); and sampling point information obtained from our field survey. 316 sites of *R. dauricum* and 214 sites of *R. mucronulatum* worldwide were obtained. Then, the distribution data obtained in these three ways were manually checked and proofread, and duplicate records within each 2.5-arc-minute cell and artificially planted species distribution points were removed. Finally, 238sites of *R. dauricum* and 214 sites of *R. mucronulatum* worldwide were obtained.

The 19 bioclimatic environmental variables were downloaded from the world climate data website (http://www.worldclim.org) with a 30 arc-second resolution for the present and LIG and 2.5 arc-minute for LGM. Then, ArcGIS software (Johnston et al., 2001) was used to perform pairwise correlations among the 19 variables. If r > 0.8, only one of the variables was selected based on the relative contribution to the model to minimize biased fitting of niche models. Accordingly, seven environmental variables were used to simulate species distribution areas for *R. dauricum* and *R. mucronulatum*. Model evaluation statistics were produced from 15 replicate runs with 60% of the data used for training and 40% for model testing. Finally, the accuracy of the predicted distribution results was tested by the ROC curve analysis method, and the AUC value (the area under the ROC curve) was obtained. The closer the AUC value is to 1, the farther it is from a random distribution, the greater the correlation

between environmental variables and the predicted geographical distribution of species, and the more accurate the model prediction results will be.

RESULTS

Genetic Diversity and Neutrality Test

The concatenated cpDNA sequences (including indels) had an aligned length of 2,711 bp, in which 15 SNPs and 10 haplotypes were identified (**Table 1**). Excluding the 5 haplotypes published by Jiang et al. (2016), the new 5 haplotypes sequences were deposited in the GenBank database (MT603719–MT603738). In 376 individuals from 39 populations, the haplotype diversity (Hd) and nucleotide diversity (π) ranged from 0 to 0.5198 and from 0 to 0.0014, respectively. Independently, 15 SNPs and 10 haplotypes were identified in *R. dauricum* populations, and the Hd was 0.6610 and π was 0.0018. The results of the neutrality test showed no significant positive or negative value (Tajima's D = 1.3348, Fu and Li's D = −0.1766, Fu and Li's F = 0.3798; P > 0.1). In contrast, only one haplotype (H6) was detected in *R. mucronulatum* populations and shared with *R. dauricum*; that is, there was no variation. The pairwise F_{ST} values (0.3541) showed significant genetic differentiation between *R. dauricum* and *R. mucronulatum*.

After SLAF library construction and high-throughput sequencing, a total of 735,337 SLAF tags was developed, and the average depth was 16.33x, which generated 328.74 Mb reads, with a mean Q30 of 92.02% and a GC content of approximately 41.53%. The numbers of SLAF markers in each individual ranged from 95,609 to 282,183. Among the SLAFs that were detected in total, 79,696 SLAFs were mapped to the *R. delavayi* genome and were distributed equally on each chromosome (**Supplementary Figure S2A**). Then, a total of 6,514,510 SNPs across the 65 accessions were identified by both GATK and SAMtools, which were considered to be reliable and equally well spread across all chromosomes (**Supplementary Figure S2B**). After various filtering, 664,406 SNPs were finally selected for downstream analyses. The SLAF data have been submitted to the Sequence Read Archive (SRA) database in the NCBI and the accession number was PRJNA589346. The average nucleotide diversity of *R. dauricum* was 0.2450×10^{-3}, which was lower than that of the cpDNA (**Table 2**). In contrast, the average nucleotide diversity of *R. mucronulatum* (0.1850×10^{-3}) was higher than that of cpDNA. The results of the neutrality test showed a significant positive value (Tajima's D = 0.8196, Fu and Li' s D = 1.5824, Fu and Li' s F = 1.5494 in *R. dauricum*; Tajima's D = 0.6661, Fu and Li' s D = 0.9743, Fu and Li' s F = 0.9989 in *R. mucronulatum*; P < 0.1), which might indicate that these species experienced a bottleneck in their evolutionary history or balancing selection of these loci.

TABLE 2 | Summary results of AMOVA and F_{ST}.

Locus	cpDNA		SLAF	
	% of variation	P	% of variation	P
Among species	28.57	<0.01	57.98	<0.01
Among populations within species	68.06	<0.01	18.59	<0.01
Within populations	3.37	<0.01	23.43	<0.01
F_{ST} Among species	0.3541		0.2886	

Population Structure

The topology obtained from TCS based on cpDNA was used to infer relationships among the 10 cpDNA haplotypes (**Figure 1A**), of which H1, H6, H8 were the most frequent haplotypes and were located in the center of the haplotype network. However, these three major haplotypes are geographically segregated: H1 from the Changbai Mountains populations of *R. dauricum*, H6 from *R. mucronulatum* populations and H8 exclusive to the Great/Lesser Khingan Mountains populations of *R. dauricum*. Eight mutational steps differentiate H6 from H8, while only two steps separate haplotype H1 from H6 (**Figure 1A**). In addition, some low-frequency haplotypes were found in a few populations of *R. dauricum*.

To further understand the evolutionary history of the two species, we used a Bayesian clustering algorithm to estimate the population genetic structure. The results of ADMIXTURE showed that K=2 was the optimal value when the cross-validation (CV) errors were applied(**Supplementary Figure S3**). When K=2, *R. dauricum* and *R. mucronulatum* clustered into distinct groups and showed majority populations collected from the Changbai Mountains (MES, SL, LTS, MH, HC, LJ, CB, WT) of *R. dauricum* with some admixture from *R. mucronulatum* (**Figure 2A**). When K=3, the admixture *R. dauricum* samples were separate. PCA results also showed that samples from *R. dauricum* and *R. mucronulatum* clustered into different groups by PC1, while the samples of *R. dauricum* from Great/Lesser Khingan Mountains and Changbai Mountains were clustered into distinct groups by PC2 (**Figure 2B**), consistent with the result of the ADMIXTURE analysis.

Phylogeny and Divergence Time

The maximum-likelihood (ML) phylogenetic tree of all samples based on the 664,406 SNPs showed that *R. dauricum* and *R. mucronulatum* formed a well-supported clade, respectively. (**Figure 3A**). In the *R. dauricum* clade, the individuals from Changbai Mountain formed a subclade, and others formed another clade, with a high support value (bootstrap values > 90%). However, the ML tree based on cpDNA (**Figure 3B**, note that it represents a bootstrap consensus tree and therefore does not show all individual cpDNA haplotypes) presented multiple incongruences with the phylogenetic tree based on SLAF data. The cpDNA phylogeny identified three main lineages: *R. mucronulatum*, *R. dauricum* from Changbai Mountain and *R. dauricum* from elsewhere. *R. dauricum* did not constitute a monophyletic group.

Based on the two previously published calibration time points, the divergence time was calculated based on the maximum-likelihood (ML) tree using MCMCTREE (**Figure 4**), which pointed toward the divergence time of outgroup *R. redowskianum* from the most recent common ancestor of *R. dauricum*, and *R. mucronulatum* was dated to have occurred

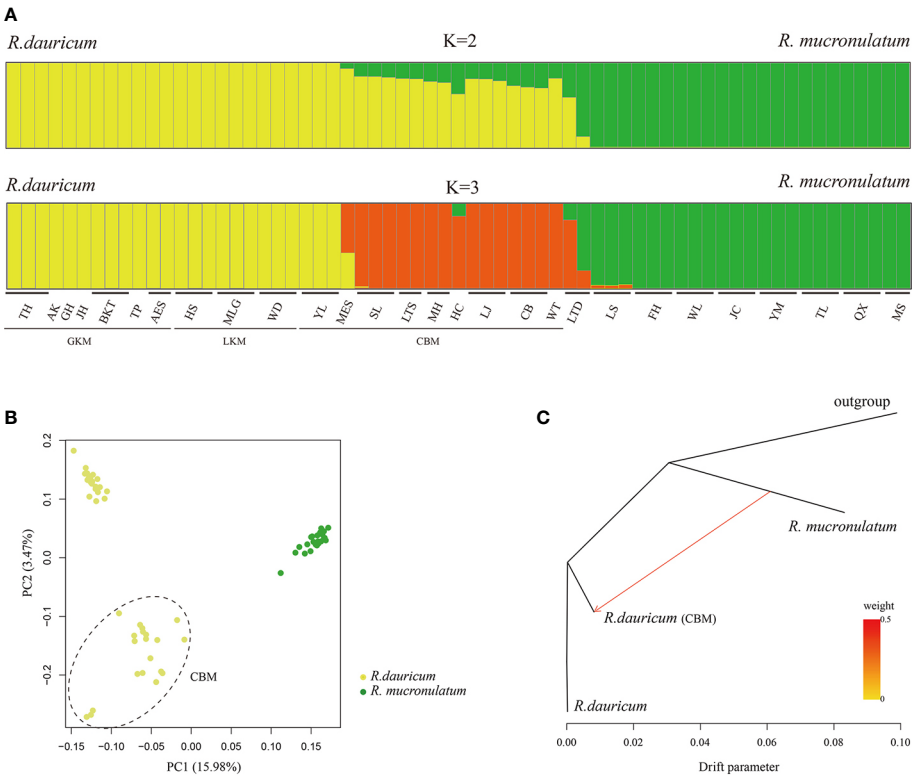

FIGURE 2 | (A) Bayesian clustering of all *R. dauricum* and *R. mucronulatum* individuals. Each rectangle represents an individual. The population and region codes were placed at the bottom. **(B)** Plot of principle component analysis (PCA). The dotted ellipse represents the individuals of *R. dauricum* from the Changbai Mountains. **(C)** TREEMIX analysis of population splitting and migration events. Colored arrows represent migration events from *R. mucronulatum* to *R. dauricum* (CBM) with color ramp indicating the magnitude of gene flow.

68.65 Mya (95% HPD interval: 71.42–120.48 Mya), while the divergence time of *R. dauricum* and *R. mucronulatum* was estimated at 32.41 Mya (95% HPD interval: 17.54–53.11 Mya) during the early Oligocene. This was in effect also the divergence time between the Siberian and the Far Eastern clades of subgen. *Rhodorastrum*.

Genetic Differentiation and Gene Flow

Our hierarchical AMOVA showed that the percentage of variation among species was 28.57% and was significant in terms of cpDNA ($P < 0.01$) (**Table 2**). In general, the variations among species in SLAF were 57.98% higher than cpDNA and were the main source of variation, while the main source of variation in cpDNA was found among populations within species (68.06%). The pairwise F_{ST} values between *R. dauricum* and *R. mucronulatum* showed significant genetic differentiation among species (F_{ST} = 0.3541 in cpDNA; F_{ST} = 0.2886 in SLAF). The results of TREEMIX suggested a higher proportion of gene flow in populations of *R. dauricum* and *R. mucronulatum* from Changbai Mountain (**Figure 2C**), which may be a major reason for the lack of complete species divergence and the shared haplotype (H6) between *R. dauricum* (SJ, SL, and WHL) and *R. mucronulatum* (**Figure 1B**).

Distribution Model Analysis

Based on the model fitting of the *R. mucronulatum* and *R. dauricum* distribution areas by MaxEnt software, the high ROC values (*R. dauricum*: 0.896, 0.881, 0.881, 0.909; *R. mucronulatum*: 0.910, 0.945, 0.959, 0.948) indicate the good accuracy of our model predictions. *R. mucronulatum* in China is mainly distributed in Liaoning, Beijing, Hebei, and Shandong, and the simulated result of the current potential distribution areas is basically consistent with the current distribution areas (**Figure 5H**), although some areas of southern China were also predicted to be suitable. Based on the paleoclimate information simulation, this species had a relatively large distribution range in the LIG period (**Figure 5E**), while in the subsequent LGM period (**Figures 5F, G**), both the CCSM and MIROC models showed that the distribution areas shrank and migrated to the southeast. From LGM until now (**Figures 5F–H**), the distribution range had neither obvious shrinkage or expansion. In contrast, *R. dauricum* populations showed the opposite trend, with a relatively small distribution range in the LIG (**Figure 5A**) and expansion during the LGM (**Figures 5B, C**), with subsequent shrinkage when the climate was warm (**Figure 5D**). This is probably related to the fact that *R. dauricum* is a cold-tolerant plant.

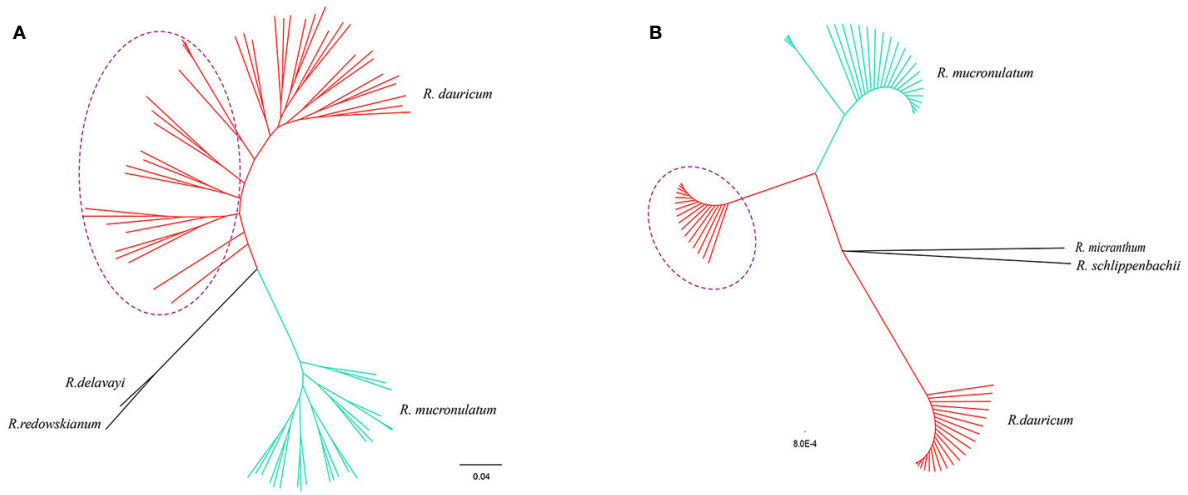

FIGURE 3 | (A) Phylogenetic trees using the maximum-likelihood (ML) method on the basis of 664,406 SNPs. **(B)** The maximum-likelihood (ML) tree based on 4 cpDNA (the same individuals as SLAF). Bootstrap support values all >90%. The red represents the individuals of *R. dauricum*; the green represents the individuals of *R. mucronulatum*. The purple dotted ellipse represents the individuals from the Changbai Mountains.

DISCUSSION

Differences in Genetic Diversity Between *R. dauricum* and *R. mucronulatum*

Based on the genetic diversity values obtained in the present study, the total nucleotide diversity (π = 0.0014, **Table 1**) is relatively high at the subgen. *Rhodorastrum* level, and the haplotype diversity (Hd = 0.5198) is at a medium level. These two species showed different levels of nucleotide diversity based on SLAF and cpDNA data. The analysis results of SLAF data showed that *R. dauricum* and *R. mucronulatum* have similar nucleotide diversity, but a higher level of species-wide nucleotide diversity was found in *R. dauricum*, consistent with a previous report (Jiang et al., 2016) and that of *R. mucronulatum* was zero in cpDNA. The nucleotide diversity of *R. dauricum* was higher than that of other species of *Rhododendron*, such as *R. simsii* (π = 1.06×10^{-3}) (Li et al., 2012). In addition, *R. dauricum* contained all 10 haplotypes, while *R. mucronulatum* had only one haplotype (H6) and shared it with *R. dauricum*. Compared to other temperate species, such as *R. delavayi* (Hd = 0.5570) (Sharma et al., 2014), *R. simsii* (Hd = 0.749) (Li et al., 2012), and *Platycrater arguta* (Hd = 0.8820) (Qiu et al., 2009), *R. dauricum* was in the middle (Hd = 0.6610), but fewer than 170 angiosperms indicate cpDNA haplotype diversity (Hd = 0.6700) (Petit et al., 2005).

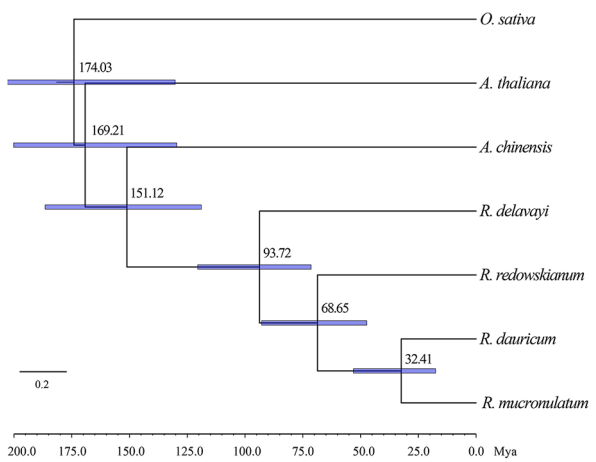

FIGURE 4 | Phylogenetic tree showing result from divergence time analysis using MCMCTREE. Numbers at nodes are divergence age, timescale is in million years ago (Mya). A geological time scale is shown below the tree. Node bars indicate the intervals of 95% HPD.

As noted by Wright and Gaut (2005), a series of factors may contribute to genetic diversity in plant species. The niche simulation analysis showed that *R. dauricum* and *R. mucronulatum* occupy different niches (**Figures 5D, H**), so climate may be an important driver that causes genetic diversity between the two species (Wang et al., 2015). For the extreme situation where *R. mucronulatum* has only one cpDNA haplotype, similarly low cpDNA diversity has been found in *Acer mono* (Guo et al., 2014) and *Juglans mandshurica* (Bai et al., 2016) distributed in NEC. These provide evidence that many of these northern populations may have experienced a bottleneck during LGM. Also, the limitation of marker sampling cannot be excluded. Furthermore, due to the ornamental value of this species, the influence of human factors on diversity cannot be ignored.

Oligocene Divergent Event and Demographic Histories of Two Species

Climate changes and tectonic events have had a profound influence on the evolution of different lineages and have often been associated

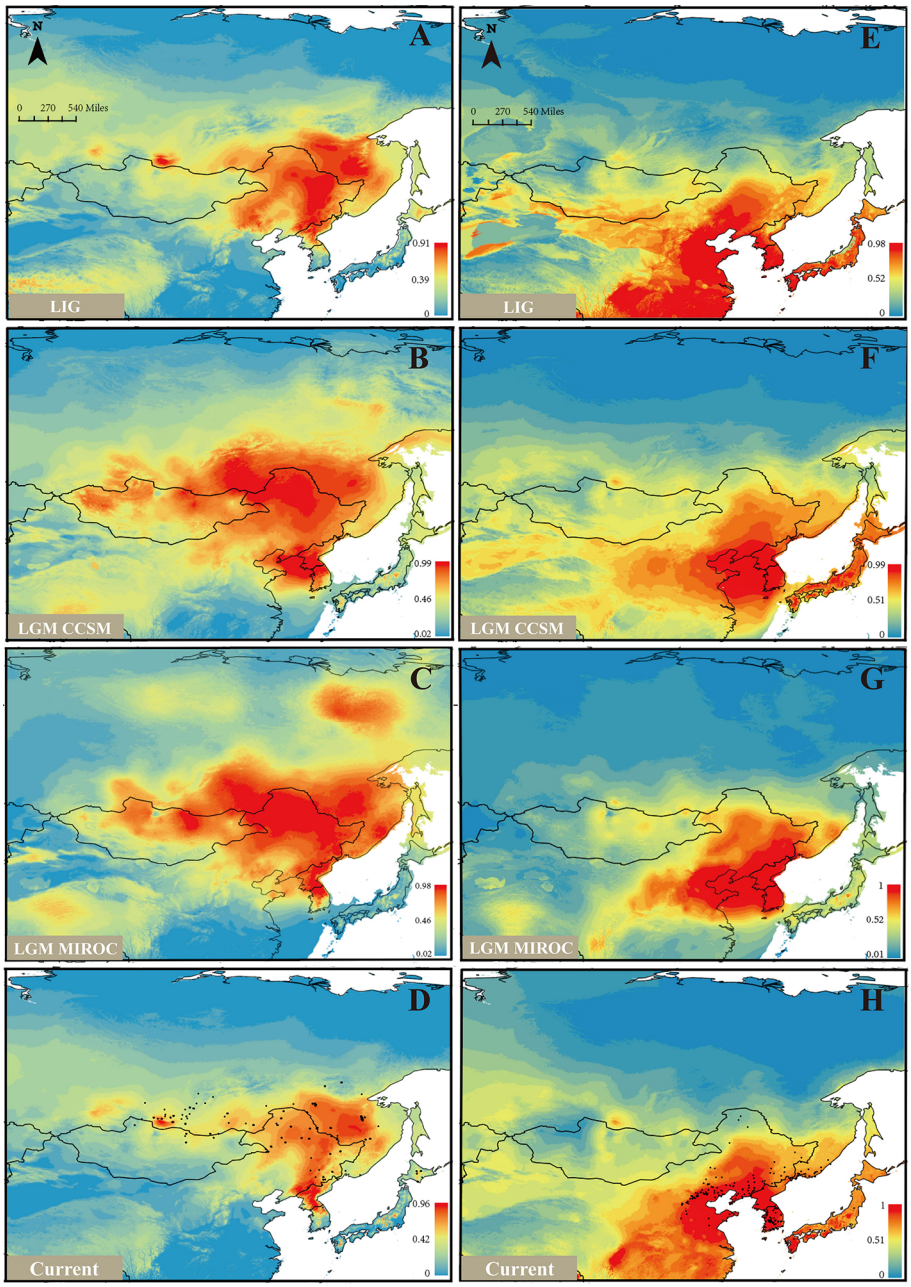

FIGURE 5 | Ecological niche models (ENMs) for *R. dauricum* and *R. mucronulatum*. **(A–D)** represents the distribution of *R. dauricum*; **(E–H)** represents the distribution of *R. mucronulatum*. The black dots in D and H represent the sites of *R. dauricum* and *R. mucronulatum* used for simulation.

with rapid divergence or speciation (Milne and Abbott, 2002; Milne, 2006; Mao et al., 2012; Zou et al., 2013). Previous studies showed drastic global cooling after the early Eocene Climatic Optimum (EECO; 52–50 Ma) (Zachos et al., 2001). Our study inferred that the divergence of *R. dauricum* and *R. mucronulatum* occurred at 32.41 Mya (i.e., the divergence between the Siberian and the Far Eastern clades, **Figure 4**). This may be driven by the global dramatic climate cooling and reduced sea level (Ivany et al., 2000; Katz et al., 2008; Liu et al., 2009; Buerki et al., 2013) during the late Eocene to the early Oligocene (40–30 Mya). In addition, the separation of most continents and the collision between the plates have a direct or indirect impact on speciation (Hall, 2009). During the North China tectonic period of the Middle Eocene-Oligocene (52–23.3 Mya), the Pacific plate displaced in the NWW (West-Northwest) direction. At approximately 34 Mya, the direction of motion suddenly changed from NNW (West-Northwest) to NWW, causing severe deformation

in the eastern part of the Eurasian plate, and mainland China was squeezed in an east-west direction, simultaneously resulting in a series of near-south-north folds (Wan and Cao, 1992). Thus, the divergence between Siberian and the Far Eastern clades was likely to be directly impacted by geomorphological changes.

Based on the cpDNA haplotype geographical distribution (**Figure 1**), we found that the two populations of MLG and WD of *R. dauricum* located in LKM have the ancient haplotype H8, special haplotypes H9, H10, and a higher haplotype diversity. The populations of *R. dauricum* in CBM also have special haplotypes and higher haplotype diversity. In addition, the results of the niche model showed that the populations of *R. dauricum* clustered to the LKM and CBM in the LIG, with subsequent local expansion during the LGM. Therefore, it is speculated that multiple refugias were maintained in *R. dauricum*. Li et al. (2012) and Bao et al. (2015) also found similar situations for *R. simsii* and *Pinus koraiensis*. In contrast, *R. mucronulatum* is currently mainly distributed in North China. The niche model showed that its distribution shrank back to the Korean Peninsula during the LGM; thus, the Korean Peninsula may be a glacial refugia for *R. mucronulatum* (Watanabe et al., 2016).

The Relative Effectiveness of Natural Selection and Gene Flow in the Evolution of the Two Species

Natural selection and gene flow are two important influential factors in the evolution of species. Gene flow generally occurs within a species, but there are numerous examples of interspecific gene flow. Gene flow can achieve homogenizing effects between gene pools (Coyne and Orr, 2004), while natural selection can weaken this effect. When natural selection overcomes the homogenizing effects of gene flow, populations or species are able to evolve separately. Our results of the species tree estimated by TREEMIX suggested a higher proportion of gene flow in populations of *R. dauricum* from *R. mucronulatum* (**Figure 2C**), and the main hybrid zone was observed in the CBM region. Higher levels of migration were suggested from populations of *R. mucronulatum* to populations of *R. dauricum* located in the CBM. The divergence time analysis shows a pre-LGM divergence of the two species (**Figure 4**), and ecological niche modeling revealed the distribution from LGM to now of the two species overlapped in the CBM region (**Figure 5**). Therefore, gene flow may occur due to the overlap of regions (Li et al., 2010; Abbott et al., 2013; Sun et al., 2016).

In the haplotype geographical distribution, the range-edge populations (SJ, SL, and WHL) of *R. dauricum* contained the haplotype (H6) from *R. mucronulatum* (**Figure 1B**). Consistent with this, the phylogeny tree based on cpDNA showed that the *R. dauricum* individuals from CBM did not cluster with others that was assigned to the *R. mucronulatum* clade (**Figure 3B**). This suggests that there may be seed-mediated unidirectional gene flow from *R. mucronulatum* to the populations of *R. dauricum* in the CBM. However, the phylogeny tree based on markers sampled across the SLAF data present the correct topology that *R. dauricum* and *R. mucronulatum* form a monophyly, respectively. In addition, the results of clustering analysis based on the SLAF data (K=2) showed that individuals from the CBM experienced introgression from *R. mucronulatum*, and that group was separate when K=3 (**Figure 2**), but the optimal K value was 2. The AMOVA results showed that the main source of variation occurred among species in the SLAF data. In general, the main source of variation in cpDNA was among populations within species (**Table 2**), which may be due to the gene flow from *R. mucronulatum* increasing genetic differences between populations of *R. dauricum*. Furthermore, the F_{ST} value showed that the genetic differentiation between *R. dauricum* and *R. mucronulatum* was generally significant (**Table 2**). Therefore, all our results suggest that interspecies gene flow exists, but the role of gene flow is not sufficient to offset the disproportionation of natural selection, and the status of the two species has been maintained (Sun et al., 2016). Therefore, we support Tikhonova's point mentioned above regarding the relationship between the two species that acted as two independent species.

On the other hand, the inconsistency between SLAF and cpDNA also indirectly illustrates the limitations of cpDNA for studying the genetic differentiation and speciation of closely related species, especially the presence of gene flow. Previous research has also demonstrated low species discrimination (24%) for *Rhododendron* based on cpDNA for both coding and noncoding gene regions when used singly or in combination (Li et al., 2011).

CONCLUSION

Numerous studies have shown that speciation and diversification cannot be adequately explained only by geographic isolation. Factors such as local selection and gene flow may likely and prevalently influence the divergence and diversification of closely related species. Our study investigated the genetic structure and demographic history of two closely related species distributed in northeastern China and revealed that divergence was strongly influenced by early the Oligocene climatic shift. Despite the deep differentiation of the two species, gene flow was not completely interrupted. The significantly different biogeographic structures indicated that the two species experienced divergent selection since their differentiation and overcame the homogenizing effect of gene flow. Our study provides an additional case of the evolutionary history of two closely related species and contributes to understanding the factors affecting this process.

DATA AVAILABILITY STATEMENT

The original contributions presented in the study are publicly available. The SLAF data can be found in NCBI : [PRJNA589346], the cpDNA data can be found here: [MT603719-MT603738]. Publicly available datasets were analyzed in this study. This data can be found here: [https://www.ncbi.nlm.nih.gov/genbank/ KT696944-KT697615].

AUTHOR CONTRIBUTIONS

BY and HX designed the research and wrote the manuscript. GZ conducted data analysis and figures made. FG performed the experiments. GZ, FG, MW, and HW collected experimental samples.

FUNDING

This work was supported by the Natural Science Foundation of the Science and Technology Department of Jilin Province (Subject layout project: 20190201184JC).

ACKNOWLEDGMENTS

The authors wish to thank Mingzhou Sun for his assistance with field sampling.

SUPPLEMENTARY MATERIAL

The Supplementary Material for this article can be found online at: https://www.frontiersin.org/articles/10.3389/fpls.2020.01093/full#supplementary-material

REFERENCES

Abbott, R., Albach, D., Ansell, S., Arntzen, J. W., Baird, S. J. E., Bierne, N., et al. (2013). Hybridization and speciation. *J. Evol. Biol.* 26, 229–246. doi: 10.1111/j.1420-9101.2012.02599.x

Alexander, D. H., Novembre, J., and Lange, K. (2009). Fast model-based estimation of ancestry in unrelated individuals. *Genome Res.* 19, 1655–1664. doi: 10.1101/gr.094052.109

Altschul, S. F., Gish, W., Miller, W., Myers, E. W., and Lipman, D. J. (1990). Basic local alignment search tool. *J. Mol. Biol.* 215, 403–410. doi: 10.1016/S0022-2836(05)80360-2

Bai, W. N., Wang, W. T., and Zhang, D. Y. (2016). Phylogeographic breaks within Asian butternuts indicate the existence of a phytogeographic divide in East Asia. *New Phytol.* 209, 1757–1772. doi: 10.1111/nph.13711

Bao, L., Ayijiamali, K., Bai, W. N., Chen, R. Z., Wang, T. M., Wang, H. F., et al. (2015). Contributions of multiple refugia during the last glacial period to current mainland populations of Korean pine (*Pinus koraiensis*). *Sci. Rep.* 5:18608. doi: 10.1038/srep18608

Baranova, T. V., Kalendar, R. N., and Kalaev, V. N. (2014). K voprosu flogenii roda *Rhododendron* L. na osnove posledovatelnosti speisera ITS1-ITS2. *Sibirsk Lesn. Zhur.* 6, 29–45.

Bastian, P. R., Ulrich, W., Sebastian, E. R.-O., and Martin, J. (2014). PopGenome: An Efficient Swiss Army Knife for Population Genomic Analyses in *R. Mol. Biol. Evol.* 31, 1929–1936. doi: 10.1093/molbev/msu136

Bhat, S., Amundsen, P. A., Knudsen, R., Gjelland, K. Ø., Fevolden, S. E., Bernatchez, L., et al. (2014). Speciation reversal in European whitefish (*Coregonus lavaretus* (L.)) caused by competitor invasion. *PLoS One* 9, e91208. doi: 10.1371/journal.pone.0091208

Buerki, S., Forest, F., Stadler, T., and Alvarez, N. (2013). The abrupt climate change at the Eocene-Oligocene boundary and the emergence of South-East Asia triggered the spread of sapindaceous lineages. *Ann. Bot.* 112, 151–160. doi: 10.1093/aob/mct106

Butlin, R., Debelle, A., Kerth, C., Snook, R. R., Beukeboom, L. W., Cajas, R. F. C., et al. (2012). What do we need to know about speciation? *Trends Ecol. Evol.* 27, 27–39. doi: 10.1016/j.tree.2011.09.002

Chamberlain, D. F., Hyam, R., Argent, G., Fairweather, G., and Walter, K. S. (1996). *The genus Rhododendron—its classification and synonymy* (Edinburgh: Royal Botanical Garden of Edinburgh Press).

Clement, M., Posada, D., and Crandall, K. A. (2000). TCS: a computer program to estimate gene genealogies. *Mol. Ecol.* 9, 1657–1659. doi: 10.1046/j.1365-294x.2000.01020.x

Coyne, J. A., and Orr, H. A. (2004). *Speciation* (Sunderland, MA: Sinauer Associates).

Darriba, D., Taboada, G. L., Doallo, R., and Posada, D. (2012). jModelTest 2: more models, new heuristics and parallel computing. *Nat. Methods* 9, 772. doi: 10.1038/nmeth.2109

DePristo, M. A., Banks, E., Poplin, R., Garimella, K. V., Maguire, J. R., Hartl, C., et al. (2011). A framework for variation discovery and genotyping using next-generation DNA sequencing data. *Nat. Genet.* 43, 491–498. doi: 10.1038/ng.806

Doyle, J., and Doyle, J. L. (1987). Genomic plant DNA preparation from fresh tissue-CTAB method. *Phytochem. Bull.* 19, 11–15.

Excoffier, L., Laval, G., and Schneider, S. (2005). Arlequin (version 3.0): an integrated software package for population genetics data analysis. *Evol. Bioinform.* 1, 47–50. doi: 10.1177/117693430500100003

Fang, M. Y., Fang, R. C., He, M. Y., Hu, L. Z., Yang, H. B., and Chamberlain, D. (2005). *Rhododendron* (Beijing & St. Louis: Science Press & Missouri Botanical Garden Press).

Fu, Y. X., and Li, W. H. (1993). Statistical tests of neutrality of mutations. *Genetics* 133, 693–709. doi: 10.0000/PMID8454210

Guo, X. D., Wang, H. F., Bao, L., Wang, T. M., Bai, W. N., Ye, J. W., et al. (2014). Evolutionary history of a widespread tree species *Acer mono* in East Asia. *Ecol. Evol.* 4, 4332–4345. doi: 10.1002/ece3.1278

Hall, T. A. (1999). BioEdit: a user-friendly biological sequence alignment editor and analysis program for Windows 95/98/NT. *Nucleic Acids Symp Ser.* 41, 95–98. doi: 10.1021/bk-1999-0734.ch008

Hall, R. (2009). Southeast Asia's changing palaeogeography. *Blumea* 54, 148–161. doi: 10.3767/000651909X475941

Ivany, L. C., Patterson, W. P., and Lohmann, K. C. (2000). Cooler winters as a possible cause of mass extinctions at the Eocene/Oligocene boundary. *Nature* 407, 887–890. doi: 10.1038/35038044

Jiang, N., Man, L., Zhang, W., Dong, H. X., Wang, H. Y., Li, M. R., et al. (2016). Chloroplast View of the Population Genetics and Phylogeography of a Widely Distributed Shrub Species, *Rhododendron dauricum* (Ericaceae). *Syst. Bot.* 41, 626–633. doi: 10.1600/036364416X692343

Johnston, K., Ver, H. J. M., Krivoruchko, K., and Lucas, N. (2001). Using ArcGIS geostatistical analyst. *Redlands: Esri.* 300.

Kalyaanamoorthy, S. M., Wong, B. Q., Thomas, K. F., Haeseler, A. V., and Jermiin, L. S. (2017). modelfinder: fast model selection for accurate phylogenetic estimates. *Nat. Methods*. 14, 587–589. doi: 10.1038/nmeth.4285

Katz, M. E., Miller, K. G., Wright, J. D., Wade, B. S., Browning, J. V., Cramer, B. S., et al. (2008). Stepwise transition from the Eocene greenhouse to the Oligocene icehouse. *Nat. Geosci.* 1, 329–334. doi: 10.1038/ngeo179

Koropachinskii, I. Y., and Vstovskaya, T. N. (2002). *Drevesnye rasteniya aziatskoi Rossii* (Novosibirsk: Publisher House of SB RAS).

Kutsev, M. G., and Karakulov, A. V. (2010). Rekonstruktsiya flogenii roda *Rhododendron* L. (Ericaceae) fory Rossii na osnove posledovatelnostei speiserov ITS1-ITS2. *Turczaninowia* 13, 59–62.

Larkin, M. A., Blackshields, G. N., Brown, P., Chenna, R., McGettigan, P. A., McWilliam, H., et al. (2007). Clustal W and clustal X version 2.0. *Bioinformatics* 23, 2947–2948. doi: 10.1093/bioinformatics/btm404

Li, H., and Durbin, R. (2009). Fast and accurate short read alignment with Burrows-Wheeler transform. *Bioinformatics* 25, 1754–1760. doi: 10.1093/bioinformatics/btp324

Li, H., Handsaker, B., Wysoker, A., Fennell, T., and Ruan, J. (2009). The sequence alignment/map format and SAMtools. *Bioinformatics* 25, 2078–2079. doi: 10.1093/bioinformatics/btp352

Li, J. W., Yeung, C. K. L., Tsai, P. W., Lin, R. C., Yeh, C. F., Yao, C. T., et al. (2010). Rejecting strictly allopatric speciation on a continental island: prolonged postdivergence gene flow between Taiwan (*Leucodioptron taewanus*, Passeriformes Timaliidae) and Chinese (*L. canorum canorum*) hwameis. *Mol. Ecol.* 19, 494–507. doi: 10.1111/j.1365-294X.2009.04494.x

Li, D. Z., Gao, L. M., Li, H. T., Wang, H., Ge, S. J., Liu, J. Q., et al. (2011). Comparative analysis of a large dataset indicates that internal transcribed

spacer (ITS) should be incorporated into the core barcode for seed plants. *Proc. Nat. Acad. Sci. U. S. A.* 108, 19641–19646. doi: 10.1073/pnas.1104551108

Li, Y., Yan, H. F., and Ge, X. J. (2012). Phylogeographic analysis and environmental niche modeling of widespread shrub *Rhododendron simsii* in China reveals multiple glacial refugia during the last glacial maximum. *J. Sys. Evol.* 50, 362–373. doi: 10.1111/j.1759-6831.2012.00209.x

Librado, P., and Rozas, J. (2009). DnaSP v5: a software for comprehensive analysis of DNA polymorphism data. *Bioinformatics* 25, 1451–1452. doi: 10.1093/bioinformatics/btp187

Liu, Z. H., Pagani, M., Zinniker, D., DeConto, R., Huber, M., Brinkhuis, H., et al. (2009). Global cooling during the Eocene-Oligocene climate transition. *Science* 323, 1187–1190. doi: 10.1126/science.1166368

Lopez-Pujol, J., Zhang, F. M., Sun, H. Q., Ying, T. S., and Ge, S. (2011). Centres of plant endemism in China: places for survival or for speciation? *J. Biogeogr.* 38, 1267–1280. doi: 10.1111/j.1365-2699.2011.02504.x

Ma, Y. P., Xie, W. J., Sun, W. B., and Marczewski, T. (2016). Strong reproductive isolation despite occasional hybridization between a widely distributed and a narrow endemic *Rhododendron* species. *Sci. Rep.* 6, 19146. 10. doi: 10.1038/srep19146

Mao, K., Milne, R.II, Zhang, L., Peng, Y. L., Liu, J. Q., Philip, T., et al. (2012). Distribution of living Cupressaceae reflects the breakup of Pangea. *Proc. Nat. Acad. Sci. U. S. A.* 109, 7793–7798. doi: 10.1073/pnas.1114319109

Marczewski, T., Chamberlain, D. F., and Milne, R.II (2015). Hybridization in closely related *Rhododendron* species: half of all species-differentiating markers experience serious transmission ratio distortion. *Ecol. Evol.* 5, 3003–3022. doi: 10.1002/ece3.1570

Mazurenko, M. T., and Hohryakov, A. P. (1991). *Ericaceae Juss* (St. Petersburg: Sosudistye rasteniya sovetskogo Dalnego Vostoka. Nauka Press).

Milne, R.II, and Abbott, R. J. (2002). The origin and evolution of Tertiary relict floras. *Adv. Bot. Res.* 38, 281–314. doi: 10.1016/S0065-2296(02)38033-9

Milne, R.II (2006). Northern Hemisphere plant disjunctions: a window on tertiary land bridges and climate change? *Ann. Bot.* 98, 465–472. doi: 10.1093/aob/mcl148

Nosil, P. (2012). *Ecological Speciation* (New York: Oxford University Press).

Orr, M. R., and Smith, T. B. (1998). Ecology and speciation. *Trends Ecol. Evol.* 13, 502–506. doi: 10.1016/S0169-5347(98)01511-0

Palme, A. E., Su, Q., Palsson, S., and Lascoux, M. (2004). Extensive sharing of chloroplast haplotypes among European birches indicates hybridization among *Betula pendula*, *B. pubescens* and *B. nana*. *Mol. Ecol.* 13, 167–178. doi: 10.1046/j.1365-294X.2003.02034.x

Papadopulos, A. S. T., Baker, W. J., Crayn, D., Butlin, R. K., Kynast, R. G., Hutton, I., et al. (2011). Speciation with gene flow on Lord Howe Island. *Proc. Nat. Acad. Sci. U. S. A.* 108, 13188–13193. doi: 10.1073/pnas.1106085108

Petit, R. J., Duminil, J., Fineschi, S., Hampe, A., Salvini, D., and Vendramin, G. G. (2005). Invited review: comparative organization of chloroplast, mitochondrial and nuclear diversity in plant populations. *Mol. Ecol.* 14, 689–701. doi: 10.1111/j.1365-294X.2004.02410.x

Phillips, S. J., Anderson, R. P., and Schapire, R. E. (2006). Maximum entropy modeling of species geographic distributions. *Ecol. Model.* 190, 231–259. doi: 10.1016/j.ecolmodel

Pickrell, J. K., and Pritchard, J. K. (2012). Inference of population splits and mixtures from genome-wide allele frequency data. *PLoS Genet.* 8, e1002967. doi: 10.1371/journal.pgen.1002967

Polezhaeva, M. A., Pimenova, E. A., Tikhonova, N. A., and Korchagina, O. S. (2018). Plastid DNA diversity and genetic divergence within *Rhododendron dauricum* s.l. (*R. dauricum* s.s., *R. ledebourii*, *R. sichotense* and *R. mucronulatum*; Ericaceae). *Plant Sys. Evol.* 304, 763–774. doi: 10.1007/s00606-018-1508-1

Price, A. L., Patterson, N. J., Plenge, R. M., Weinblatt, M. E., Shadick, N. A., and Reich, D. (2006). Principal components analysis corrects for stratification in genome-wide association studies. *Nat. Genet.* 38, 904–909. doi: 10.1038/ng1847

Purcell, S., Neale, B., Todd-Brown, K., Thomas, L., Ferreira, M. A. R., and Bender, D. (2007). PLINK: a tool set for whole-genome association and population-based linkage analyses. *Am. J. Hum. Genet.* 81, 559–575. doi: 10.1086/519795

Qiu, Y. X., Qi, X. S., Tao, X. Y., Fu, C. X., Naiki, A., and Comes, H. P. (2009). Population genetic structure, phylogeography, and demographic history of *Platycrater argute* (Hydrangeaceae) endemic to East China and South Japan, inferred from chloroplast DNA sequence variation. *Taxon* 58, 1226–1241. doi: 10.1016/j.jallcom.2006.08.275

Ribera, I., Castro, A., Diaz, J. A., Garrido, J., Izquierdo, A., Jaech, M. A., et al. (2011). The geography of speciation in narrow-range endemics of the 'Haenydra' lineage (Coleoptera, Hydraenidae, Hydraena). *J. Biogeogr.* 38, 502–516. doi: 10.1111/j.1365-2699.2010.02417.x

Rundell, R. J., and Price, T. D. (2009). Adaptive radiation, nonadaptive radiation, ecological speciation and nonecological speciation. *Trends Ecol. Evol.* 24, 394–399. doi: 10.1016/j.tree.2009.02.007

Rundle, H. D., and Nosil, P. (2005). Ecological speciation. *Ecol. Lett.* 8, 336–352. doi: 10.1111/j.1461-0248.2004.00715.x

Runemark, A., Hey, J., Hansson, B., and Svensson, E.II (2012). Vicariance divergence and gene flow among islet populations of an endemic lizard. *Mol. Ecol.* 21, 117–129. doi: 10.1111/j.1365-294X.2011.05377.x

Schluter, D. (2000). *The Ecology of Adaptive Radiation* (Oxford: Oxford University Press).

Schluter, D. (2001). Ecology and the origin of species. *Trends Ecol. Evol.* 16, 372–380. doi: 10.1016/S0169-5347(01)02198-X

Seehausen, O. (2006). Sympatric speciation: Why the controversy? *Curr. Biol.* 16, R333–R334. doi: 10.1016/j.cub.2006.03.077

Sharma, A., Poudel, R. C., Li, A., Xu, J. C., and Guan, K. Y. (2014). Genetic diversity of *Rhododendron delavayi* var. *delavayi* (C. B. Clarke) Ridley inferred from nuclear and chloroplast DNA: implications for the conservation of fragmented populations. *Plant Syst. Evol.* 300, 1853–1866. doi: 10.1007/s00606-014-1012-1

Shrestha, N., Wang, Z. H., Su, X. Y., Xu, X. T., Lyu, L., Liu, Y. P., et al. (2018). Global patterns of *Rhododendron* diversity: The role of evolutionary time and diversification rates. *Global Ecol. Biogeogr.* 27, 913–924. doi: 10.1111/geb.12750

Stamatakis, A., Hoover, P., and Rougemont, J. (2008). A rapid bootstrap algorithm for the RAxML web servers. *Syst. Biol.* 57, 758–771. doi: 10.1080/10635150802429642

Sun, Y., Surget-Groba, Y., and Gao, S. X. (2016). Divergence maintained by climatic selection despite recurrent gene flow: a case study of *Castanopsis carlesii* (Fagaceae). *Mol. Ecol.* 25, 4580–4592. doi: 10.1111/mec.13764

Tajima, F. (1989). Statistical method for testing the neutral mutation hypothesis by DNA polymorphism. *Genetics* 123, 585–595.

Taylor, E. B., Boughman, J. W., Groenenboom, M., Sniatynski, M., Schluter, D., and Gow, J. L. (2005). Speciation in reverse: Morphological and genetic evidence of the collapse of a three-spined stickleback (*Gasterosteus aculeatus*) species pair. *Mol. Ecol.* 15, 343–355. doi: 10.1111/j.1365-294X.2005.02794.x

Tikhonova, N. A., Polezhaeva, M. A., and Pimenova, E. A. (2012). AFLP analysis of the genetic diversity of closely related *Rhododendron* species of the section *Rhodorastra* (Ericaceae) from Siberia and the Far East of Russia. *Russ J. Genet.* 48, 1153–1161. doi: 10.1134/S1022795412100110

Vonlanthen, P., Bittner, D., Hudson, A. G., Young, K. A., M€uller, , R., Lundsgaard-Hansen, B., et al. (2012). Eutrophication causes speciation reversal in whitefish adaptive radiations. *Nature* 482, 357–362. doi: 10.1038/nature10824

Voroshilov, V. N. (1982). *Opredelitel rastenii sovetskogo DalhegoVostoka* (Moscow: Nauka Press).

Wan, T. F., and Cao, R. P. (1992). Middle Eocene-Early Pleistocene tectonic events and stress fields in China. *GEOCIECE* 6, 3.

Wang, X., Li, Y., Liang, Q., Zhang, L., Wang, Q., Hu, H., et al. (2015). Contrasting responses to Pleistocene climate changes: a case study of two sister species *Allium cyathophorum* and *A. spicata* (Amaryllidaceae) distributed in the eastern and western Qinghai-Tibet Plateau. *Ecol. Evol.* 5, 1513–1524. doi: 10.1002/ece3.1449

Watanabe, Y., Ichiro, T., Shota, S., Song, J. S., Yamamoto, S., and Tomaru, N. (2016). Population demographic history of a temperate shrub, *Rhododendron weyrichii* (Ericaceae), on continental islands of Japan and South Korea. *Ecol. Evol.* 6, 8800–8810. doi: 10.1002/ece3.2576

Webb, W. C., Marzluff, J. M., and Omland, K. E. (2011). Random interbreeding between cryptic lineages of the Common Raven: Evidence for speciation in reverse. *Mol. Ecol.* 20, 2390–2402. doi: 10.1111/j.1365-294X.2011.05095.x

Wright, S.II, and Gaut, B. S. (2005). Molecular population genetics and the search for adaptive evolution in plants. *Mol. Biol. Evol.* 22, 506–519. doi: 10.1093/molbev/msi035

Wright, S. (1984). *Evolution and the genetics of populations* (Chicago: University of Chicago press).

Wu, C. Y., Lu, A. M., Tang, Y. C., and Li, D. Z. (2003). *The Families and Genera of Angiosperms in China (A Comprehensive Analysis)* (Beijing: Science Press).

Yang, Z. (2007). PAML 4: phylogenetic analysis by maximum likelihood. *Mol. Biol. Evol.* 24, 1586–1591. doi: 10.1093/molbev/msm088

Zachos, J., Pagani, M., Sloan, L., Thomas, E., and Billups, K. (2001). Trends, rhythms, and aberrations in global climate 65 Ma to present. *Science* 292, 686–693. doi: 10.1126/science.1059412

Zhang, L., Xu, P., Cai, Y., Ma, L., Zhang, C., Gao, Q., et al. (2017). The draft genome assembly of *Rhododendron delavayi* Franch. var. *delavayi*. *Gigascience* 6, 1–11. doi: 10.1093/gigascience/gix076

Zou, X. H., Yang, Z., Doyle, J. J., and Ge, S. (2013). Multilocus estimation of divergence times and ancestral effective population sizes of *Oryza* species and implications for the rapid diversification of the genus. *New Phytol.* 198, 1155–1164. doi: 10.1111/nph.12230

Conflict of Interest: Author Baiming Yang was employed by company Changchun Guoxin Modern Agricultural Technology Development Co., Ltd.,.

The remaining authors declare that the research was conducted in the absence of any commercial or financial relationships that could be construed as a potential conflict of interest.

frontiers in Plant Science

ORIGINAL RESEARCH
published: 28 July 2020
doi: 10.3389/fpls.2020.01036

Blue Light Improves Stomatal Function and Dark-Induced Closure of Rose Leaves (*Rosa* x *hybrida*) Developed at High Air Humidity

Meseret Tesema Terfa[1,2], *Jorunn Elisabeth Olsen*[1] *and Sissel Torre*[1]*

[1] Department of Plant Sciences (IPV), Faculty of Biosciences, Norwegian University of Life Sciences, Aas, Norway, [2] School of Plant and Horticulture Science, College of Agriculture, Hawassa University, Hawassa, Ethiopia

Plants developed under constant high (>85%) relative air humidity (RH) have larger stomata that are unable to close completely in response to closing stimuli. Roses (*Rosa* x *hybrida*) developed in high RH have previously been shown to have high water loss during leaf dehydration and reduced dark-induced closure resulting in a shorter postharvest life. In this study, the effect of B-light on stomatal function under high RH conditions was investigated. The ability of rose leaves developed under continuous high (90%) or moderate (60%) RH to close their stomata in response to darkness and leaf dehydration assay was studied. Moreover, the level and regulation of ABA in light and darkness in relation to B-light was measured. Our results show that increased B-light proportion improved stomatal function and dark-induced stomatal closure under high RH conditions and that was associated with increased [ABA] in general and a dynamic ABA peak during darkness. Furthermore, increased B-light during the day was associated with the presence of high β-glucosidase activity during night. This indicates that B-light is important as a signal to activate the β-glucosidase enzyme and release ABA during night. Altogether, the improved stomatal function and reduced transpiration in combination with increased [ABA] indicate that preharvest B-light plays an important role in governing stomatal functionality and ABA homeostasis under high RH and can be a useful method to improve postharvest water balance of roses.

Keywords: abscisic acid, blue light, darkness, relative air humidity (RH), stomata, postharvest

OPEN ACCESS

Edited by:
Julian C. Verdonk, Wageningen University and Research, Netherlands

Reviewed by:
Caspar Christian Cedric Chater, University of Sheffield, United Kingdom
Hanna Hõrak, University of Tartu, Estonia

***Correspondence:**
Sissel Torre
sissel.torre@nmbu.no

Specialty section:
This article was submitted to Crop and Product Physiology, a section of the journal Frontiers in Plant Science

Received: *05 March 2020*
Accepted: *24 June 2020*
Published: *28 July 2020*

Citation:
Terfa MT, Olsen JE and Torre S (2020) Blue Light Improves Stomatal Function and Dark-Induced Closure of Rose Leaves (Rosa x hybrida) Developed at High Air Humidity. Front. Plant Sci. 11:1036. doi: 10.3389/fpls.2020.01036

INTRODUCTION

In greenhouse production systems, the relative air humidity (RH) can exceed 85% in certain periods of the year (e.g. during winter) when heating costs are high and ventilation of humid air is avoided to save energy. High RH, or low aerial vapor pressure deficit (VPD), decreases the evaporative demand and transpiration rates of plants. Leaf anatomy, stomatal morphology, density, and function are reported to be modified in response to elevated RH (Torre et al., 2003; Arve et al., 2013). Plants develop larger stomata, sometimes more stomata (higher density/frequency) that are less responsive to environmental closing signals. Typically, stomata developed in high RH respond

slower and do not close fully in response to darkness and/or drought resulting in plants with reduced dehydration tolerance and higher nocturnal transpiration (Torre and Fjeld, 2001; Arve, 2013; Fanourakis et al., 2013a). Excessive water loss postharvest, reduces the postharvest life and overall quality of pot roses and cut roses (Fanourakis et al., 2012; Fanourakis et al., 2013b; Carvalho et al., 2015a; Carvalho et al., 2015b). Furthermore, poor stomata control leads to early wilting during shipping and retailing and reduces marketability of ornamentals (Waterland et al., 2010a; Waterland et al., 2010b). Insight into the influence of preharvest greenhouse environment on stomatal functionality is important for enabling growth of robust, drought tolerant plants of high quality.

Different strategies to counteract the negative effects of high RH on stomatal function are reported. Some of the strategies involve technical greenhouse installations like dehumidification systems (Lim et al., 2017), selecting tolerant cultivars (Giday et al., 2013a), or modifying cultivation techniques (Fjeld et al., 1994; Fanourakis et al., 2011; Terfa et al., 2013; Giday et al., 2014; Arve et al., 2015b; Carvalho et al., 2015a; Fanourakis et al., 2016; Arve et al., 2017). Numerous studies have shown that different cultivation strategies can alleviate the negative consequences of high RH (reviewed by Fanourakis et al. (2016), such as foliar applications of the plant hormone abscisic acid (ABA) during growth (Fanourakis et al., 2011; Kim and van Iersel, 2011) and grafting on a rootstock with natural high ABA content (Giday et al., 2013a). Furthermore, modifying aerial environment such as: simultaneous changes in RH and temperature to manipulate VPD (Pettersen et al., 2007), daily changes in VPD (Arve et al., 2017); high air speed (Carvalho et al., 2015a), and changes in light quality (Terfa et al., 2012; Ahmadi et al., 2019) and irradiance (Fanourakis et al., 2019). This stimulation of stomatal functioning has been discussed to be linked to increased leaf [ABA] or changed ABA sensitivity (Aliniaeifard and van Meeteren, 2013), however it has been less pursued so far to come up with conclusive results.

The plant hormone ABA is generally known as a stress hormone, is involved in abiotic and biotic stress responses and plays an important role in the control of stomatal movement and transpiration (Wilkinson and Davies, 2002). However, ABA is also synthesized under well-watered conditions, and low concentrations of ABA affects plant metabolism and growth also under non-stressed conditions (Li et al., 2019; Yoshida et al., 2019). The endogenous level of ABA in plant tissues is dynamically regulated by the balance between its biosynthesis and inactivation (Zeevaart, 1980; Cutler and Krochko, 1999). The inactivation of free ABA involves either hydroxylation of ABA to the ABA catabolites phaseic acid (PA) and dihydrophaseic acid (DPA) or conjugation of ABA with glucose, creating ABA-glucose ester (ABA-GE) (Lim et al., 2005; Priest et al., 2006). ABA-GE is believed to be a storage form of ABA, and can be stored in the vacuoles and hydrolyzed to free ABA when required (Dietz et al., 2000; Arve, 2013). In many plant species it has been shown that ABA-GE is hydrolyzed in response to water stress, RH and darkness by β-glucosidase, leading to an increase in the pool of active ABA (Dietz et al., 2000; Sauter et al., 2002; Lee et al., 2006; Arve, 2013; Allen et al., 2019). In roses, conjugation of ABA with glucose, creating ABA-GE seems to be a more important inactivation pathway than hydroxylation of ABA to PA (Arve et al., 2013).

Numerous reports show that light regulates ABA biosynthesis and degradation directly or indirectly (Xiong and Zhu, 2002; Tallman, 2004; Novakova et al., 2005). Specific light qualities like B-light are also reported to regulate endogenous ABA levels during different plant developmental processes (Fellner and Sawhney, 2002; Ahmadi et al., 2019). Furthermore, the diurnal pattern of stomatal movements is affected by the diurnal alterations in metabolism of endogenous ABA, which is partly associated with the effect of light on ABA precursors such as violaxanthin (Tallman, 2004). During the day the ABA biosynthesis in guard cells is restricted by the removal of the ABA precursor, violaxanthin, through light-driven xanthophyll cycling (e.g. B light), which converts violaxanthin to zeaxanthin (Eskling et al., 1997). In light driven stomatal movements the blue (B)/Ultraviolet A (UVA) light-absorbing cryptochromes, zeaxanthin, and phototropins are the suggested receptors for B-light specific stomatal responses (Frechilla et al., 1999; Kinoshita et al., 2003; Kinoshita and Hayashi, 2011). Zeaxanthin is proposed to be a B-light-specific photoreceptor of guard cells (Talbott et al., 2003). These interconversion between xanthophyll cycles (violaxanthin and zeaxanthin) for B-light and ABA, as discussed above, shows the common denominator between the two processes. That is, both actions (B-light perception and ABA biosynthesis) could affect each other and in turn regulate stomatal movements. Hence, to understand the interactions between ABA and B-light is highly important to elucidate their implications.

In Northern greenhouse production, supplementary light is common when the natural solar radiation is low. The light is mainly supplied by gas-discharge lamp-types like high pressure sodium (HPS) lamps containing only 5% B-light in comparison to the natural solar radiation which has 15–18% B-light. It constituents of the light wavelength within the range of 565 to 700 nm, primarily yellow (565 to 590 nm) and orange (590 to 625 nm), with a peak at 589 nm (Currey and Lopez, 2013). However, during the last decade the progress in solid-state lighting, based on light-emitting diodes (LEDs) has facilitated the research on light quality responses of plants in general, and attracted much interest as a light source for assimilation lighting in greenhouses and plant factories. An important aspect of the commercial application of LEDs as supplementary lighting is how plant production can be optimized. However, attention has also been placed on other important processes like content of phytochemicals, water use efficiency (WUE), field performance and postharvest behavior (Arve et al., 2015b; Riikonen, 2016; Lanoue et al., 2017; Ahmadi et al., 2019; Leonardos et al., 2019). In spite of the progress in research on light regulation of stomatal movement, there is a lack of information on the interaction between light quality and other environmental factors. RH is economically the most difficult climate factor to control in closed

production systems and the most important climate factor in determining postharvest water loss (Fanourakis et al., 2013b; Fanourakis et al., 2016). Hence, the aim of this study was to investigate the role of B-light during production in improving postharvest transpiration of roses grown under higher RH. Further, since ABA is believed to be an important signal in stress responses and stomatal movement of roses, its content and regulation in light and darkness in relation to B-light was studied.

MATERIAL AND METHODS

Plant Materials and Growing Conditions

Rosa x hybrida, cv. Toril plants were grown from a single node stem segment with one mature leaf as is commercially practiced. The cuttings were taken from the middle and lower position of fully developed stems with open flowers. After 2–3 weeks, the cuttings were rooted and transferred to 12 cm pots containing a standard fertilized *Sphagnum* peat media (Floralux, Nittedal, Norway). The pH and electrical conductivity (EC) level were 5.7 and 1.75, respectively, in all experiments (Superba: NPK 9-5-25+Mg+S+Mikro and calcinit, Yara, Oslo, Norway). During pre-cultivation, the plants were kept in a greenhouse compartment (glass roof and polycarbonate walls) at a temperature of 21°C, and average daily relative air humidity (RH) of 70% [corresponding to a water vapour deficit (vpd) of 0.74 KPa], at the Center for plant research in controlled climate at the Norwegian University of Life Sciences, Ås, Norway (N 59° 40.120', E 10° 46.232'). Supplementary light by high pressure sodium lamps (HPS, Osram NAVT- 400W, Munich, Germany) was given 20 h every day at a photon flux density of 100 (± 10) µmol m^{-2} s^{-1} at 400–700 nm (measured with a Li-Cor, Model L1-185, quantum sensor, Li-Cor Inc., Lincoln, NE, USA). The pre-cultivation ended when the plants had 1–1.5 cm long shoots. Thereafter, the plants were transferred to different air humidity treatments in growth chambers.

Two different experiments were carried out in controlled growth chambers and both experiments were repeated twice. The temperature set point was 20 ± 0.5°C, for all experiments during the experimental period. The RH in the growth chambers was either 60 ± 3% (moderate RH, vpd: 0.7 KPa) or 90 ± 2% (high RH, vpd: 0.23 KPa) and the CO_2 was 400 ppm in all experiments. In *experiment I* plants were exposed to 100 µmol m^{-2} s^{-1} irradiance in a 20 h photoperiod provided either by LED lamps (round LED-light with 3 chains, Sola-co, Guangdong, China) containing 80% red (R; peak wavelength at 630 nm) and 20% blue (B) light (peak wavelength at 465 nm) or HPS lamps containing 5% B-light (HPS, Osram NAVT- 400W) in high (90%) and moderate (60%) RH (**Figure 1**). In *experiment II*, the plants were grown at high RH (90%) and subjected to 100 µmol m^{-2} s^{-1} irradiance in a 20 h photoperiod provided by a mixture of B and R LEDs with different proportions of B and R with dominant wavelength peaks at 465 and 630 nm, respectively

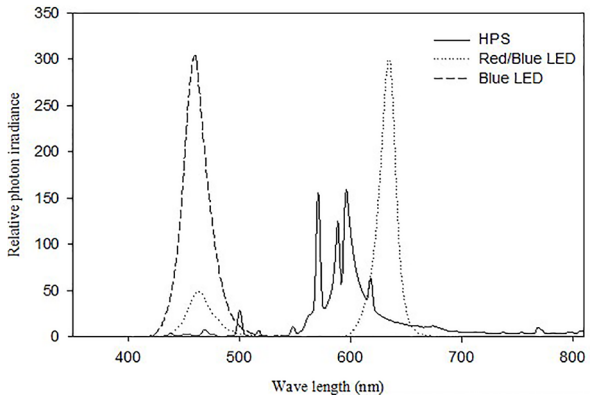

FIGURE 1 | Relative spectra of the lamps used in the experiments: High pressure sodium (HPS) lamps Osram NAV T-400W (Solid lines), Light emitting diode (LED) lamps (Round LED-light 92W with 3 chains, SoLa-Co) (Dotted lines) and pure blue LED (Round LED-light 92W with three chains, SoLa-Co) (Dashed lines).

(round LED-light with 3 chains, Sola-co, Guangdong, China). Three different spectral treatments expressed as the B-light percentage 5% B, 20% B, and 100% B were given while the remaining percentage was R. The spectra of the lamps were measured with an OceanOptics SD2000 spectrometer (**Figure 1**) (model SD2000, OceanOptics, Eerbeek, The Netherlands). The spectrometer was calibrated against a NIST-traceable calibration lamp (model LS-1-CAL, OceanOptics). Leaf temperature during growth was measured by a thermocouple thermometer (model HD 9016; Delta OHM SRL, Caselle Di Selvazzano, Italy) and was measured to be in average 1.5 °C higher under HPS compared to LED.

Stomata Morphology Analysis

To study stomata morphology, impressions of the epidermal layer were made of fresh intact upper leaves in the middle of the day and middle of the night by Suzuki's Universal Micro-Printing (SUMP) method using SUMP liquid and SUMP plate B (SUMP Laboratory, Tokyo, Japan) as described previously (Tanaka et al., 2005). Samples were taken interveinally close to the mid-rib on the abaxial side of the leaf from the first fully developed leaves of each plant from each air humidity and light quality treatment during both light and darkness. The SUMP imprints were observed under a light microscope (Leitz, Labolux K, Type 0.2, Wetzlar, Germany) and stomata images were obtained with a Leica camera (Leica DC200, Heerbrugg, Switzerland). Stomata morphology (length, width and area) and density were analyzed with the use of UTHSCSA ImageTool for windows version 3.00 (The University of Texas Health Science center, San Antonio, Texas, USA). The experiment was repeated twice, and twelve imprints were made from each experiment and three images were taken from each imprint for image analysis.

Measurement of Stomata Conductance, Water Usage, and Dehydration Assay

To study the diurnal pattern of stomata conductance, measurements were done on intact fully expanded leaves for 24 h in experiment I using a CIRAS-2 Portable Photosynthesis System with PLC6 (U) Automatic Universal Leaf Cuvette (PP Systems, 2001, Amesbury, MA, USA). During all measurements, the RH and light in the leaf cuvette were the same as in the growth chamber, the CO_2 was 400 mmol mol^{-1}, the airflow 250 mmol s^{-1}, and the temperature 22°C. Measurements were taken every 15 min for 24 h. The experiment was repeated twice and the measurement was taken from three plants in each repeat.

To analyze the water usage capacity, plants with intact roots were transferred from the different treatments to a test chamber with 40–50% RH, 100 µmol m^{-2} s^{-1} irradiance for 20 h photoperiod provided by Mercury lamps (Osram NAV T-400W, Munich, Germany), and a temperature of 20 ± 0.5°C. The pots were covered with plastic bags to prevent water loss through evaporation from the soil. The pots were then weighed right before dark and right after the dark period for three consecutive days. After the measurements the leaf area was determined with a leaf area meter (LI-COR, LI-3100). Leaf stomata conductance of these plants was also measured on intact fully expanded leaves using an AP4 leaf porometer (Delta-T devices LTD, Cambridge, UK). The rate of water loss (transpiration rate) per leaf area per hour was calculated as per the following equation:

$$water\ usage = \frac{Change\ in\ plant\ weight\ before\ and\ after\ dark\ period}{leafarea * \text{hour}}$$

Leaf dehydration assay were also done to study the stomatal response to dehydration. Detached upper leaves from eight plants grown under different RH and light quality treatments were tested in a test room with 50% RH, an irradiance of 15 µmol m^{-2} s^{-1} and 22°C. The leaves were weighed after 0, 5, 10, 15, 20, 25, 30, 40, 50, 60, 90, 120, and 180 min after detachment and their relative weight after the leaf dehydration assay were determined.

ABA and β-Glucosidase Quantification

For analysis of ABA, β-glucosidase activity, fully developed leaves were sampled in the middle of the light and dark period for all treatments after 6 weeks of treatment when the plants had 1–3 open flowers. The leaf samples were immediately frozen in liquid nitrogen and stored at -80°C prior to extraction for ABA and β-glucosidase quantification.

Frozen leaf tissue was freeze-dried and finely ground and extracted in distilled deionized water with an extraction ratio of 1:70 (g dry weight: ml water) overnight at 5°C. [ABA] of the extract was determined using a radioimmunoassay technique as previously described (Quarrie et al., 1988).

β-glucosidase analysis was done based on the procedure described by Arve et al. (2013). The leaf samples were taken from the freezer (-80°C) and immediately homogenized in liquid nitrogen using a mortar and pestle. 700 mg samples were extracted for 1.5 h at 4°C in 10 ml 100 mm citrate buffer, containing 5% (w/v) PVPP, 1 mm EDTA, 14 mm mercaptoethanol, and 10% (w/v) glycerol. Samples were then centrifuged at 1,000 rpm for 4 min (Eppendorf 5810 centrifuge, Hamburg, Germany). One hundred µl of the supernatant was mixed with 1 ml 100 mm citrate buffer containing 4 mM p-nitrophenol-β-D-glucopyranoside (pNPG) and incubated at 37°C for 60 min (Termaks B 8054 Incubator, Bergen, Norway). The reaction was then terminated with 2 ml 1M Na_2CO_3 and the amount of liberated p-nitrophenol was measured spectrophotometrically at 405 nm (Helios Alpha Spectrophotometer, Thermo Scientific, Surrey, UK). The concentration was calculated using the Beer-Lambert law, Absorbance=ϵ*length*concentration, and the molar extinction coefficient for p-nitrophenol ϵ=18,300 (Dietz et al., 2000). One unit of enzyme is then defined as the amount of enzyme needed to yield 1 nmol of p-nitrophenol per hour at 37°C. The samples were collected from five plants at the middle of the light and dark periods. Each sample consisted of 5–6 young and mature leaves from a single plant.

Statistical Analyses

Both experiments (*Experiment I and II)* were repeated twice and since the trends of the results in the experiments were similar the data are presented as combined experimental repeats unless otherwise are stated. Significant differences between means were tested for normally distributed general linear models (GLM) and Tukey's test. Differences with $p < 0.05$ were considered significantly different. All statistical tests were performed in Minitab 16.1.1 (Minitab 16.1.1, windows version, State College, PA, USA).

RESULTS

Effect of Light Source: LED (20% B and 80% R) Reduces the Transpiration Rate and Improves Stomatal Closure in Plants Grown Under High RH Compared to HPS

RH and light quality (LED; 20% B and HPS; 5% B) during growth significantly affected the diurnal stomata conductance (*gs*) of

TABLE 1 | Average stomatal conductance (mmol m^{-2} s^{-1}) measured by CIRAS-2 during darkness and light periods for rose leaves grown under different relative air humidity (RH) regimes (moderate RH, 60% and high RH, 90%) and light qualities provided by light emitting diodes (LED; 20% B) or high pressure sodium (HPS; 5%B) lamps.

	Moderate RH (60%)		High RH (90%)	
	LED	HPS	LED	HPS
Light	21.9^{d} ± 0.4	26.5^{d} ± 0.4	50.5^{b} ± 1.0	60.5^{a} ± 0.9
Dark	12.0^{e} ± 1.5	15.4^{de} ± 1.7	30.1^{c} ± 1.5	48.6^{b} ± 1.5
Light/Dark ratio	1.8^{a} ± 0.8	1.7^{a} ± 0.9	1.7^{a} ± 0.7	1.2^{b} ± 0.7

Data are the mean values ± SE of measurements from two experimental repeats with three replications in each and three sampling points per hour as a technical repeat (n=6). Different superscript letters indicate significant differences (P<0.05).

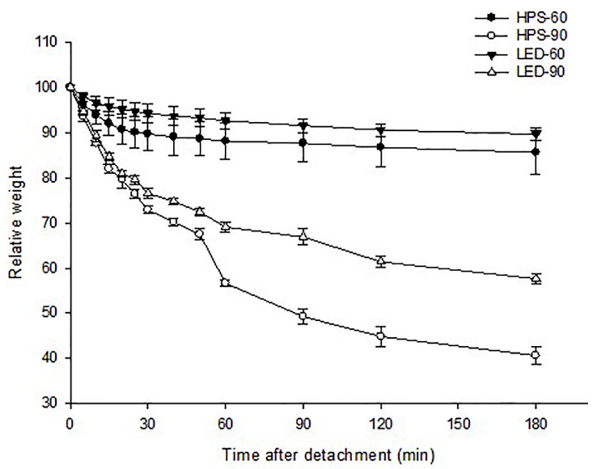

FIGURE 2 | Change in relative weight (%) of detached rose leaves grown under different relative air humidity (RH) (moderate RH; 60% and high RH; 90%) and blue light proportions provided by light emitting diodes (LED; 20% B) and high pressure sodium (HPS; 5% B) lamps during 3 h of leaf dehydration assay. Data points and error bars indicate: B: leaf dehydration assay: mean ± SE from two experimental repeats with eight replications from each repeat (n=16).

rose leaves (**Table 1**; $P < 0.01$). The *gs* throughout day and night was higher for leaves of rose plants under high RH-grown as compared to moderate RH (**Table 1**). However, also light source had an effect. If plants were grown under LED with a high B-light proportion (20% B) at high RH, they had 10% lower *gs* throughout the day and reached their average lowest *gs* (30 $mmol^{-2}$ s^{-1}) during the darkness as compared to plants grown under HPS with a lower B proportion (5% B), which still had higher average *gs* (48 mol^{-2} s^{-1}) during dark (**Table 1**). In moderate RH however, the difference in *gs* between plants grown under LED and HPS was statistically insignificant, but still slightly lower *gs* was measured throughout the day in plants grown under LED (**Table 1**). The percent reduction in *gs* between light and darkness for LED-grown plants at high RH was higher (20%) as compared to HPS-grown plants, which was 9.6% only (**Table 1**). In addition, the calculated day: night ratio of *gs* was higher (1.7) for LED-grown plants than HPS (1.2). To understand if the change in *gs* was due to the change in stomata aperture, we analyzed the ratio of stomata size between light and darkness. In high RH the change in aperture was much higher (37.6%) in LED-grown plants than HPS where there was no significant difference (**Figure 3**). The reduced aperture in darkness in LED-plants partly explains the decrease in transpiration during darkness, entailing an improvement in stomatal function due to the prevailing environmental condition during the day.

Stomatal response to dehydration was tested to further analyze the degree to which the detached leaves close their stomata and retain water during a 3 h water loss test. The test showed that plants grown at moderate RH closed their stomata during the first 30 min and lost only 10% of their weight irrespective of the light quality (**Figure 2**). However, high RH-grown plants at both light qualities had lost much of their weight (40–57%), and showed a continuous transpiration throughout the testing hours as compared to moderate RH. Nevertheless, a better stomatal closure and water retaining ability was observed for the plants grown under LED. They showed about 20% less weight loss as compared to HPS-grown plants (**Figure 2**).

Stomata imprints of rose leaves made during the light and dark periods showed that the stomata pore length and aperture were significantly larger at high RH than moderate RH, regardless of the light source (**Figure 3** and **Table 2**; $P<0.05$). The stomata pore length and aperture of high RH-grown plants was on average 1.8 and 1.7 times higher than in moderate RH and this affected the stomata area (**Figure 3** and **Table 2**). However, for the high RH-grown plants these stomatal characteristics were much smaller for LED-grown plants than

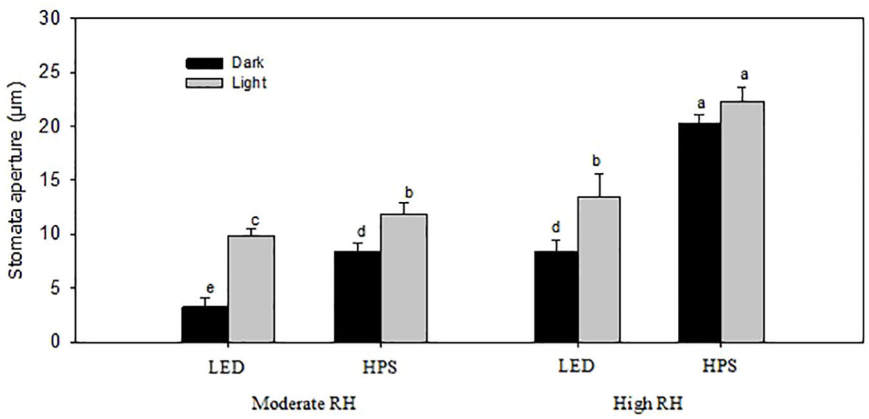

FIGURE 3 | Stomatal aperture of rose leaves grown under different relative air humidity (RH) regimes (moderate RH, 60% and high RH, 90%) and light qualities provided by light emitting diodes (LED; 20% Blue) and high pressure sodium (HPS; 5% Blue) lamps. Data are the mean values ± SE from two experimental repeats with five imprint samples from each repeat and three images from each sample as technical repeat (n=1). Different letters indicate significant differences ($p<0.05$).

TABLE 2 | Stomatal characteristics of rose leaves grown under different relative humidity regimes (RH) (moderate RH; 60% and High RH; 90%) and blue (B) light proportions provided by light emitting diodes LED (20% B) and high pressure sodium HPS (5% B) lamps.

		Moderate RH (60%)		High RH (90%)	
		LED	HPS	LED	HPS
Pore length (μm)	Light	26.2 ± 1.0^{d}	32.8 ± 1.6^{c}	40.1 ± 0.4^{b}	48.2 ± 0.7^{a}
	Dark	21.5 ± 0.3^{e}	24.4 ± 0.3^{d}	34.2 ± 0.9^{c}	42.9 ± 1.3^{b}
Pore area (μm^{2})	Light	176.7 ± 9.2^{d}	267.3 ± 8.4^{c}	325.0 ± 12.7^{b}	373.1 ± 18^{a}
	Dark	111.3 ± 3.5^{e}	166.7 ± 11.8^{d}	234.5 ± 5.6^{c}	370.7 ± 10.9^{a}
Stomata number (μm^{-2})		75 ± 2.5 ^{b}	60 ± 3.4 ^{c}	85 ± 5.2 ^{a}	70 ± 3.1 ^{b}

Data are the mean values ± SE from two experimental repeats with five imprint samples from each repeat and three images from each sample as a technical repeat (n=10). Different letters indicate significant differences (P<0.05).

HPS (**Figure 3** and **Table 2**). The pores length and aperture were even smaller during darkness for LED-grown plants compared to HPS. The stomata pore length of high RH and HPS-grown plants was 1.2 and 1.6 times larger during light and darkness, respectively, compared to those of LED-grown plants (**Table 2**). Correspondingly, the stomata aperture of HPS-grown plants was 2.4 and 1.7 times larger than LED-grown plants during light and darkness, respectively (**Figure 3**). Consequently, this led to a larger pore area for plants grown at high RH under HPS light than LED-grown plants (**Table 2**). However, plants grown under LED had a higher number of stomata per area as compared to HPS-grown plants (**Table 2**). This indicates that, in spite of the higher number of stomata in a high B-light proportion, the stomata have a better capability to close in response to darkness.

The [ABA] and β-Glucosidase Activity Is Highly Affected by RH and Light Quality

In HPS-grown plants the [ABA] was significantly higher in plants from moderate RH compared to high RH (**Figure 4A**; P= 0.011). In moderate RH the highest [ABA] was measured during darkness in both HPS and LED grown plants (**Figure 4A**). However, in high RH the highest [ABA] was measured in LED-grown plants, which had 40% higher total ABA level as compared to HPS-grown plants (**Figure 4A**; P= 0.001). The [ABA] for LED-grown plants from high RH was very much comparable to the amount of ABA measured in moderate RH (**Figure 4A**). Nevertheless, there was no significant change in ABA level between light and darkness in high RH for any of the light treatments, except a slight trend of higher ABA level during the night under LED. Hence, for plants grown under high RH and LED this slight change in ABA during light and darkness might be an important signal to induce closure in the darkness.

To further study if the increase in ABA level during darkness was related to ABA conjugation, we quantified the β-glucosidase activity during darkness. In our recent work with roses grown under moderate and high RH it was shown that ABA-GE, which is degraded by β-glucosidase, is the main catabolite playing a major role in affecting the diurnal ABA pool turnover (Arve et al., 2013). The level of β-glucosidase activity was significantly higher in moderate RH compared to high RH-grown plants irrespective of the light quality difference (**Figure 4B**; P<0.05). Furthermore, at high RH the activity of this enzyme was significantly higher under LED compared to HPS (**Figure 4B**). This could partly explain the slight trend of an increase in [ABA] in the darkness under LED.

Effects of B-Light: Transpiration Rate, Water Usage, and Stomatal Function Is Improved as B-Light Proportion is Increased

Since HPS contains other wave lengths like yellow and orange in addition to R and B, and increases leaf temperature compared to LED (Nelson and Bugbee, 2015), another experiment

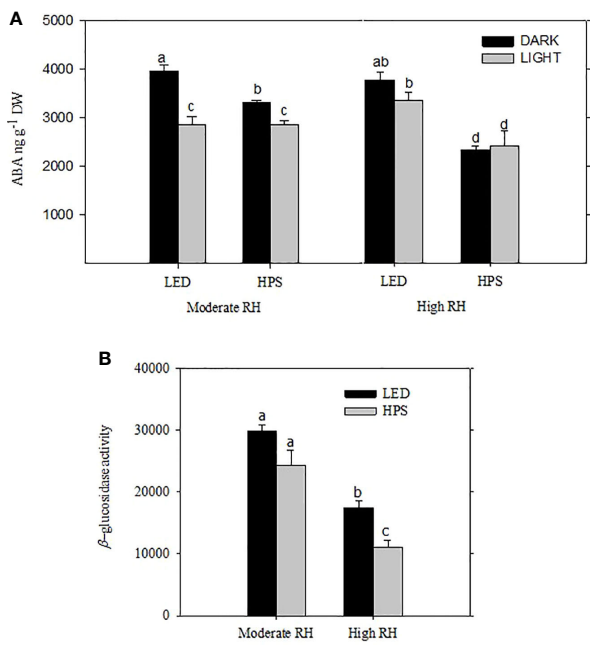

FIGURE 4 | The effect of different relative air humidity (RH; Moderate RH, 60% and High RH; 90%) and blue **(B)** light proportions provided by light emitting diodes (LED; 20% B) and high pressure sodium (HPS; 5% B) lamps on the abscisic acid (ABA) content **(A)** and β-glucosidase activity **(B)** of freeze-dried rose leaves. For ABA quantification the samples were collected and measurements were done in the middle of the light and dark period. For β-glucosidase quantification, only samples from dark period were used. For both ABA and β-glucosidase analysis data are the mean values ± SE of 5 samples, each consisting of 5–6 leaves from each of five plants. Different letters within each figure indicate significantly different values (P < 0.05).

(experiment II) was carried out to elucidate the sole effect of B-light on stomatal function under high RH. Plants grown under high RH were then exposed to pure B or different B-light proportions using LED lamps with distinct wavelengths of B and R-light only (**Figure 1**).

Stomatal morphology and water relations of rose leaves grown at high RH were notably affected by different B-light proportions (**Figures 5** and **6**; **Table 3**, $P<0.01$). The transpiration during the light period did not differ significantly between the different B-light proportions, only a slightly higher transpiration in the highest B proportion was observed. However, during the dark period the transpiration decreased significantly with lower *gs* (165 mmol on average) at 20% B and 100% B compared to 5% B (**Figure 5A**; $P<0.05$). The transpiration ratio between day and night under 20% B or 100% B were 2.0 and 2.2 respectively, and this was higher than for plants grown under 5% B, which was only 1.2. This indicates a reduction in transpiration during night due to improved stomatal dark closure ability in the two highest B-light proportions.

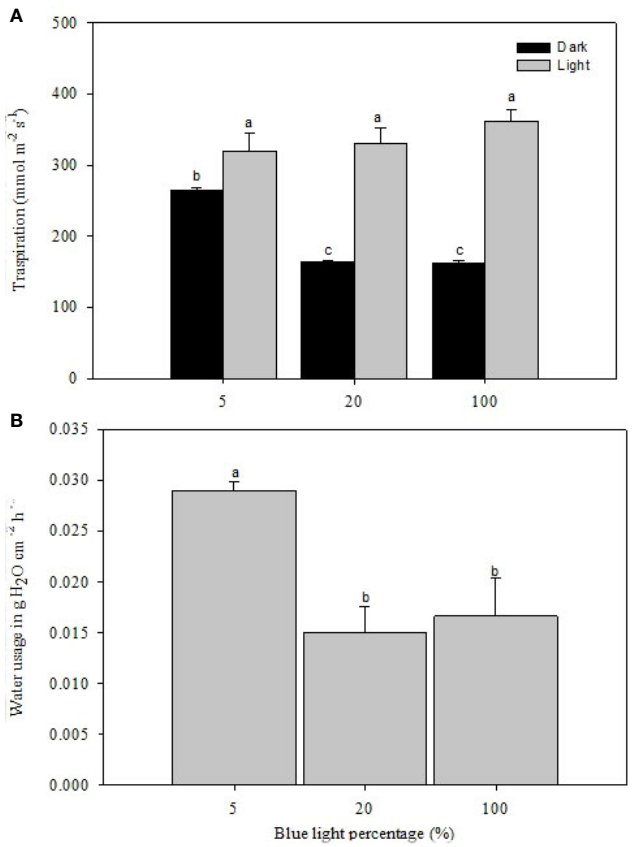

FIGURE 5 | Transpiration rate during the light and dark cycle (**A**; measured by porometer) and water usage (**B**; measured gravimetrically right before and after the dark period, and data are put as a reduction in weight) of rose plants grown under high relative air humidity (RH; 90%) with different blue **(B)** light proportions provided by light emitting diodes (LED). The transpiration rate and water usage were measured for three consecutive days after plants were moved from their respective chambers to a common environment with a temperature of 20°C RH of 40% and 100 µmol m^{-2} s^{-1} irradiance for 20 h photoperiod provided by mercury lamps. The data are mean ± SE of measurements on the first fully developed leaf from ten plants. Different letters within each subfigure indicate significant differences ($P < 0.05$).

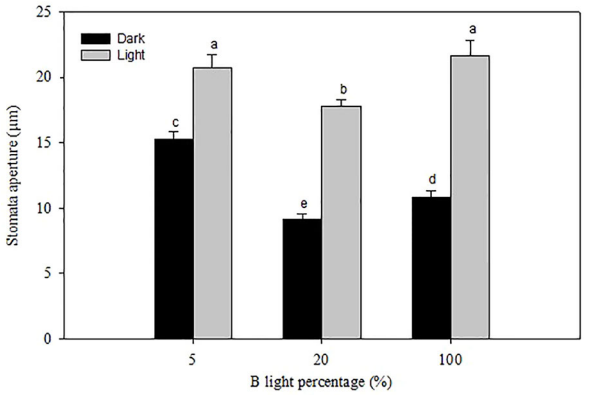

FIGURE 6 | Stomatal pore aperture of rose leaves grown under and high relative air humidity (RH) with different blue **(B)** light proportions. Data are the mean values ± SE from two experimental repeats with five imprint samples from each repeat and three images from each sample as a technical repeats (n=1). Different letters indicate significant differences ($P<0.05$).

TABLE 3 | Stomatal pore characteristics of rose leaves grown under high relative air humidity (RH; 90%) and different B-light proportions.

Stomatal characteristics		B-light proportion (%)		
		5	20	100
Pore Length (µm)	ight	42.9 ± 1.4^{a}	35.9 ± 1.5^{c}	43.6 ± 0.6^{a}
	Dark	40.7 ± 1.6^{ab}	30.1 ± 0.7^{d}	35.1 ± 1.1^{c}
Pore Area (µm^2)	Light	378.6 ± 21.5^{a}	287.1 ± 9.4^{c}	332.8 ± 12.2^{b}
	Dark	265.0 ± 4.8c^{d}	196.6 ± 7.2^{e}	195.4 ± 8.2^{e}
Stomata Number (µm^{-2})		70 ± 7.1 ^{c}	85 ± 5.1^{b}	113 ± 9.2^{a}

Data are the mean values ± SE from two experimental repeats with five imprint samples from each repeat and three images from each sample as a technical repeat (n=1). Different letters indicate significant differences (P<0.05).

[ABA] During Darkness Is Increased as B-Light Proportion Increases for Plants Grown Under High RH

A significant difference was observed in the [ABA] in rose leaves grown at high RH under the different B-light proportions (**Figure 7**; $P<0.05$). The highest level of ABA was recorded during the dark period when plants had grown at 20 and 100% B, which was 1.2 times higher than 5% B grown plants. Whilst the lowest level was recorded during the light period for plants grown at 100% B, there was no significant difference in the amount of ABA between 5 and 20% B ($P<0.05$) during light period (**Figure 7A**). However, similar to plants grown under HPS (experiment 1, **Figure 4**), there was no significant change in the level of ABA between light and darkness for plants grown at 5% B (**Figure 7A**). The change in diurnal ABA level between light and darkness for 20 and 100% B-grown plants suggests the change in the ABA pool either by altered biosynthesis or release

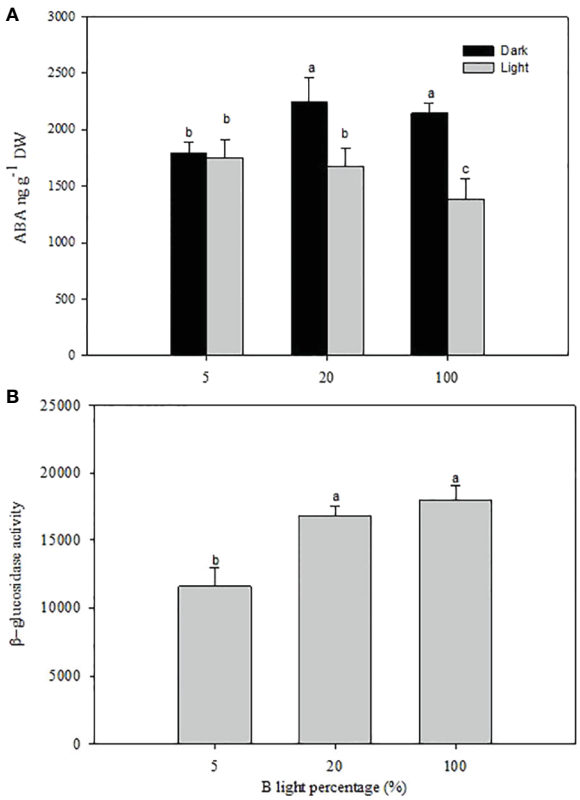

FIGURE 7 | The effect of different blue **(B)** light proportions supplemented by light emitting diodes (LED) on the abscisic acid (ABA) content **(A)** and *β*-glucosidase (B) activity of freeze-dried rose leaves grown under high relative air humidity (RH; 90%). For ABA quantification the samples were collected in the middle of the light and dark period. For *β*-glucosidase quantification, only samples from dark period were used. Data are the mean values ± SE of 5 samples each consisting of 5–6 leaves from each of plants. Different letters within each figure indicate significantly different values ($P < 0.05$).

from conjugated ABA. To verify this, we quantified the *β*-glucosidase activity during darkness (**Figure 7B**). Hence, the quantified level of *β*-glucosidase activity was significantly higher in plants grown under 20% B or more (**Figure 7B**). *β*-glucosidase activity in 20 and 100% B plants was 1.5 and 1.6 fold higher than that of 5 % B-grown plants, respectively. This correlates with the increase in the [ABA] during darkness in plants grown under 20 and 100% B.

Postharvest Transpiration and Responsiveness to Dry Air and Darkness as Signals for Stomatal Closure

At marketing stage (flowering), plants from the different B-light treatments were moved to a common environment with dry air (40% RH), and 100 μmol m^{-2} s^{-1} for 20 h (provided by Mercury lamps and 20 ± 0.5°C) to test the effect on preharvest light conditions on stomatal functionality and water usage. The porometer data (transpiration rate) was correlated with water usage measured gravimetrically right before and after the dark period (**Figure 5B**). Plants grown under 5% B showed 49 and 45% higher weight loss during the dark period as compared to 20 and 100% B, respectively, indicating higher transpiration rate under 5% B even during the darkness (**Figure 5B**). Thus, the data on water usage as well as transpiration suggested improvement in stomatal sensitivity during darkness in response to increased B proportions during light. To further verify this, we analyzed the stomata imprints of rose plants grown at high RH with different B proportions (**Figure 6** and **Table 3**). In all treatments the plants had open stomata during the light period and closed their stomata during darkness. During the light the stomata aperture and length were larger for plants grown under 5% B than 20% B (**Figure 6** and **Table 3**). However, no significant difference in stomata aperture or pore length during light in 100% B compared to 5% B was observed. During the night the smallest stomata aperture and length were recorded for plants grown under 20% B and 100% B (**Figure 6** and **Table 3**). The maximum percent reduction in the stomata size was recorded for plants grown under 100% B (50.1%), followed by 20% B (46.8%) and the smallest reduction was observed under 5% B (25%). This lead to smaller stomata pore area for leaves grown under 20 and 100% B as compared to leaves of 5% B-grown plants. However, the highest number of stomata per area was counted when plants were grown under more B-light (**Table 3**). Plants grown under 100% B had 1.6 and 1.3 time higher number of stomata per area than 5% B and 20% B, respectively. This might explain the slight trend of higher transpiration during day. However, the interesting point is the ability of these stomata to close during darkness so that the transpiration was reduced by more than 50% in plants grown under 20% B or more.

DISCUSSION

Uncontrolled water loss from plants grown at high RH leading to early wilting of leaves and flowers postharvest is common in ornamentals like cut flowers and pot plants produced in greenhouses (Mortensen, 2000; Torre and Fjeld, 2001; Fanourakis, 2011). This scenario has been suggested to have association with ABA and the diurnal pattern of stomatal response (Fanourakis, 2011; Aliniaeifard and van Meeteren, 2013; Arve, 2013; Giday et al., 2013a; Giday et al., 2014; Fanourakis et al., 2016). Preharvest factors like RH and light quality can affect the speed and degree to which stomata close or/and open after harvest. In this study we showed that a high portion of B-light (≥20%) can improve the stomatal function, a better dark-induced stomatal closure of roses grown under high RH conditions, and in turn improve postharvest water relations and product longevity.

Blue Light Reduces the Transpiration and Improves the Stomatal Function of Roses Grown Under High RH

In the present study, the rose plants which were grown under constant high RH during leaf development clearly showed a poor stomatal closure in response to darkness and dehydration similar

to what was found previously (Fanourakis et al., 2011). Nevertheless, we found that the stomatal characteristics and transpiration rates were significantly different in high RH plants exposed to LED with 20% B and 80% R as compared to under HPS (5% B) (**Figures 2** and **3**; **Tables 1** and **2**; $P<0.05$). Continuous measurements of stomata conductance during day and night and a leaf dehydration assay further confirmed that roses grown under high RH under LED had lower transpiration rate and improved dehydration tolerance (**Figure 2**; **Table 1**) as compared to plants grown with HPS lamps. Plants grown at moderate RH did not show big differences in transpiration rate and/or dehydration tolerance in response to light sources (**Figure 2**). In conclusion, the transpiration rate and the stomatal function of plants developed under high RH seems to be more dependent on the light quality than plants grown under moderate RH.

As a response to stomata-closing stimuli, the stomata of rose plants grown at high RH and 20% B and 80% R responded strongly to darkness by closing and eventually reducing transpiration compared to HPS as a light source. To further verify the role of B-light and to separate the effects of leaf temperature (Nelson and Bugbee, 2015) and the other wave lengths provided by HPS lamps, an experiment was carried out with distinct wavelengths of only B or R-light. This showed similar B-light-induced improvement in stomatal function and reduced water usage and transpiration during darkness as the light source experiment (**Figure 5**). The transpiration rate was the highest during the light period for all the treatments, but the rate was decreased during darkness by 50 and 55%, respectively, for the plants grown under 20 and 100% B as compared to those grown under 5% B (**Figure 4A**). Accordingly, the water usage recorded during the darkness, when stomata are expected to close, was lower for plants grown under 20 and 100% B (**Figure 5B**). The higher transpiration rate during the day for all treatments and a significant reduction in transpiration rate during the darkness for plants grown under a higher B-light proportion indicates B-light-induced improvement in dark closure of stomata. This suggests that stomata of plants grown under a higher B proportion have a better control of water loss when subjected to stimuli that normally induces stomatal closure. This is similar to (Blom-Zandstra et al., 1995), showing a significant reduction in water usage and *gs* during darkness for rose plants grown at 70% RH and monochromatic supplementary B-light than those grown under orange light.

In general, rose plants grown under high RH had larger stomata length and aperture, which in turn resulted in a larger stomata area as compared to moderate RH (**Figure 3**, **Table 2**). This is similar to previous studies in a number of species (Fordham et al., 2001; Torre et al., 2003; Karbulkova et al., 2008; Arve et al., 2013). Nevertheless, plants developed at high RH and higher B proportion had smaller stomata aperture and length, which in turn resulted in smaller stomata area as compared to those developed under HPS (**Figures 3** and **5**, **Tables 2** and **3**). The decreased stomata area and aperture in plants grown under 20 and 100% B partly explains the reduced transpiration rate and better water usage (Giday et al., 2013b). Furthermore, the stomata of plants developed under high RH and 20 and 100% B closed their stomata better when subjected to darkness or dehydration as compared to those grown under 5% B. However, plants grown at higher B-light proportion (20 and 100% B) had higher number of stomata as compared to 5% B (**Tables 2** and **3**). This is in agreement with the literature, including our previous work with roses (Terfa et al., 2013) where a higher B-light proportion increased the number of stomata per area as compared to HPS. Interestingly, although plants grown under higher B-light proportion had higher number of stomata which correlated with higher day time transpiration; they were able to close their stomata better during the dark period, avoiding night-time water loss (**Table 1**; **Figures 1** and **5**). The ability of the leaves of plants grown under 20% B and more to close their stomata when subjected to darkness or leaf dehydration tests shows the improved stomata ability to quickly adapt and respond to the prevailing environmental stimuli.

Blue Light increases the Activity of β-glucosidase under High RH Conditions and affects the Diurnal [ABA]

The lack of stomatal response in plants developed under high RH is discussed to be partly due to low leaf [ABA] and/or ABA insensitivity of the leaves (Aliniaeifard and van Meeteren, 2013). In another study, we showed that roses growing under high RH regulate their ABA differently during day and night than plants grown at moderate RH (Arve et al., 2013). A higher [ABA] during night was found in rose leaves exposed to moderate RH, but not in rose leaves from high RH (Arve et al., 2013).

In the present study, we quantified higher total [ABA] in plants grown under a higher B-light proportion (20% B and more) regardless of the RH regime. However, the highest [ABA] was measured for the samples collected during the dark period. Previously, it was suggested that the increased [ABA] during darkness for plants grown under moderate RH act as a signal for stomatal closure during darkness (Tallman, 2004; Novakova et al., 2005; Arve et al., 2013). A study on the diurnal variation of ABA in *Nicotiana tabaccum* showed an increase in [ABA] after 3 h of exposure to darkness (Novakova et al., 2005). Similarly, our previous study on *Rosa x hybrida* also demonstrated an increase in [ABA] during the darkness as compared to light period in moderate RH-grown plants, but there was no change in the [ABA] for high RH-grown plants (Arve et al., 2013). In this experiment, however, we observed a significant increase in [ABA] during darkness for plants grown under high RH and higher B-light proportion (20% B and more). This showed that the light quality is influencing the diurnal ABA levels (**Figures 4** and **7**). The increase in ABA during darkness might arise either from increased ABA biosynthesis or release from ABA-conjugate. This ABA might also have been transported from the root as a long distance chemical signal (Wilkinson and Davies, 2002) or from leaf cells (as short distance signal) (Cutler and Krochko, 1999).

The diurnal pattern of stomatal movements are suggested to be affected by the altering endogenous ABA metabolism during

the day (Tallman, 2004). The author also discussed that light is one of the factors affecting sources of ABA during the day. The observed lower [ABA] during light and a sharp increase during darkness in the leaves of rose plants grown under 20% B or more in this study also indicate a dynamic change of the ABA pool either by degradation, biosynthesis, or conjugation. A possible explanation could be as Tallman (2004) indicated, guard cell ABA biosynthesis restricted by the removal of the ABA precursor, violaxanthin through light-driven xanthophyll cycling which converts violaxanthin to zeaxanthin in B-light perception during the light period; since Zeaxanthin is proposed to be a B-light-specific photoreceptor of guard cells (Frechilla et al., 2002; Talbott et al., 2003). This partly explains the lower [ABA] during light in plants grown under higher proportions of B-light (20% B or more). Plausibly, during the dark period, conditions favoring endogenous guard cell ABA biosynthesis would prevail once again to maintain stomata in closed position, hence the accumulated zeaxanthin during day as a result of B-light photoreception might start to convert to violaxanthin, which would favor endogenous ABA biosynthesis by guard cells (Tallman, 2004). However, the direct relationship between B-light and ABA biosynthesis needs further studies.

In the case of high RH, it has been shown that it is mainly the inactivation of ABA which is affected rather than the biosynthesis (Okamoto et al., 2011; Arve et al., 2015a). Our previous result showed that the ABA metabolite ABA-GE is the predominant factor in changing the ABA pool during light and darkness in different RH regimes (Arve, 2013). Based on this knowledge, we assayed the β-glucosidase-activity to get insight if there is any inter-conversion between ABA and ABA-GE under the different light qualities. Clearly, the β-glucosidase assay showed a high activity of the enzyme in moderate RH compared to high RH, similarly to what was found in Arve et al. (2013). Interestingly, although plants grown at high RH generally had lower β-glucosidase activity, those grown under 20% B and more had a higher activity of this enzyme as compared to those grown at lower B-light proportion. The result was consistent in both experiments (exp 1and 2). This was associated with increased ABA during darkness pointing out that the increase in [ABA] during darkness might arise from ABA-GE conversion. The decreasing trend in transpiration and stomata size during darkness for plants grown under high RH and 20% B- was also linked with increased [ABA], which improved stomatal closure during darkness. Some of this increase in ABA might be root-derived ABA. However, it is also logical to assume that the stored ABA (in the form of ABA-GE) is a rapid and easy way to regulate available ABA in guard cells to quickly induce stomatal closure in response to external stimuli, whereas the bulk of transported ABA from the root might help to inhibit stomatal opening throughout the dark period/until stomata receives an over-riding signal inducing opening. This indicated an involvement of Blight in β-glucosidase activity which was also observed in other processes, such as phototropic responses of *Zea mays* coleoptiles (Jabeen et al., 2006).

Blue Light Improves Dark-Induced Stomatal Closure

Night time transpiration is potentially an important factor affecting whole-plant water balance and water use efficiency (Caird et al., 2007). Attention has been given to energy consumption in greenhouses because the lack of dark-induced stomatal closure may lead to evaporative heat loss at night. Besides, when the product continues to transpire during dark storage, this may lead to aggravated water loss and a shorter postharvest life. However, from different studies it is obvious that the magnitude of water loss occurring during the night depends on the daytime growth conditions such as RH, photoperiod, light quality, and irradiance (Blom-Zandstra et al., 1995; Caird et al., 2007; Fanourakis et al., 2012; Arve et al., 2017). In the present study, we found that high RH-grown plants had higher night time transpiration compared to moderate RH plants regardless of the light quality. Nonetheless, for high RH-grown plants, dark transpiration and water usage was reduced by 50% if the plants were grown under 20% B or more (**Table 1** and **Figure 5**). This significant reduction in transpiration and water usage correlates with decreases in stomata aperture and area during darkness (**Figures 3** and **6**; **Tables 2** and **3**). Blom-Zandstra et al. (1995) also showed that higher daytime irradiance resulted in faster stomatal closure upon transition to darkness in roses, although closure was still incomplete. The spectrum of the low intensity supplementary light (25 μmol m^{-2} s^{-1}) also affected gs at night, with orange supplementary light resulted in 100 and 50% higher gs as compared to control and B-light, respectively (Blom-Zandstra et al., 1995).

The increased level of [ABA] during darkness in higher B proportion might be important in the development of functional stomata. It has been shown that, the variation in the diurnal ABA is important to develop functional stomata, similar to a daily spray with ABA (Fanourakis, 2011). In our previous (Arve et al., 2013) and present studies it has been shown that the absence of a significant change in [ABA] between light and dark period in high RH-grown plants correlated with absence of stomatal closure. Hence, this absence of a dynamic ABA peak at the beginning of the dark period in high RH-grown plants might be an important closing stimulus, and vice versa for moderate RH-grown plants. In another study, we observed that detached full developed leaves produced under high RH from roses ('Toril'), the same cultivar as used in the present study, did not respond to exogenous ABA treatment (100 μm) while the moderate RH leaves responded and closed their stomata (Carvalho et al., 2015a). This shows that the sensitivity to ABA is reduced when leaves are developed under high RH. In the study of (Giday et al., 2013a) it was found that a rose cultivar tolerant to high RH closed its stomata better during darkness than a rose cultivar less tolerant to high RH. Hence, roses grown under high RH and a higher B-light fraction behave similar as a high RH tolerant cultivar. Furthermore, the fact that B-light itself (in addition to its effect on ABA) plays a major role as a signal in stomatal movements, it can directly affect the stomatal functionality. That is, the stomata that are adapted to regular

opening and closing during development under B-light would be able to close better when they are subjected to signals important for stomatal closure such as darkness, drought or ABA. Thereby, it can be suggested that both increased level of ABA and B-light in combination or individually would contribute to the improved stomatal functionality directly or indirectly.

CONCLUSION

The present study shows that B-light improves the stomatal function under high RH conditions. The ABA content was higher in darkness under a light source with a high B-light proportion and this correlates with the presence of high β-glucosidase activity. Taken together, the improved stomatal function in combination with increased ABA level, indicate that B-light plays an important role in governing stomatal functionality and ABA homeostasis under high RH. This result has both practical and experimental implication in such a way that, lighting sources in production systems can be improved by adding extra B to reduce the water usage during growth and to minimize postharvest losses due to an improved water balance.

DATA AVAILABILITY STATEMENT

The datasets generated for this study are available on request to the corresponding author.

AUTHOR CONTRIBUTIONS

Conceptualization, methodology, investigation, formal analysis, and interpretation (MT, ST, JO). Validation (ST, JO). Original draft preparation (MT, ST). Review and editing (MT, ST, JO). Supervision (ST, JO). Funding acquisition and resource administration (ST).

ACKNOWLEDGMENTS

We would like to thank Lancaster University and Xiaoqing Li for technical help in ABA analysis. Thanks also to Ida Hagen at Norwegian University of Life Sciences for the technical assistance. This research was supported by Norwegian Research Council and Norwegian Growers Association "VEKSTHUS" project number 190395. The Norwegian State Educational Loan Fund is also acknowledged for financial support.

SUPPLEMENTARY MATERIAL

The Supplementary Material for this article can be found online at: https://www.frontiersin.org/articles/10.3389/fpls.2020.01036/full#supplementary-material

SUPPLEMENTARY FIGURE 1 | Relative spectra of Mercury Lamps (Hg lamps, Osram NAV T-400W, Munich, Germany) used in the test rooms to measure post harvest water usage and analyze dark responses of Rose plants.

REFERENCES

Ahmadi, T., Shabani, L., and Sabzalian, M. R. (2019). Improvement in drought tolerance of lemon balm, Melissa officinalis L. under the pre-treatment of LED lighting. *Plant Physiol. Biochem.* 139, 548–557. doi: 10.1016/j.plaphy.2019.04.021

Aliniaeifard, S., and van Meeteren, U. (2013). Can prolonged exposure to low VPD disturb the ABA signalling in stomatal guard cells? *J. Exp. Bot.* 64, 3551–3566. doi: 10.1093/jxb/ert192

Allen, J., Guo, K., Zhang, D. X., Ince, M., and Jammes, F. (2019). ABA-glucose ester hydrolyzing enzyme ATBG1 and PHYB antagonistically regulate stomatal development. *PloS One* 14, 19. doi: 10.1371/journal.pone.0218605

Arve, L. E., Terfa, M. T., Gislerød, H. R., Olsen, J. E., and Torre, S. (2013). High relative air humidity and continuous light reduce stomata functionality by affecting the ABA regulation in rose leaves. *Plant Cell Environ.* 36, 382–392. doi: 10.1111/j.1365-3040.2012.02580.x

Arve, L. E., Kruse, O. M. O., Tanino, K. K., Olsen, J. E., Futsæther, C., and Torre, S. (2015a). ABA regulation and stomatal malfunctioning in *Arabidopsis thaliana* developed in continuous high air humidity. *Environ. Exp. Bot.* 115, 11–19. doi: 10.1016/j.envexpbot.2015.02.004

Arve, L. E., Terfa, M. T., Suthaparan, A., Poudel, M. S., Gislerod, H. R., Torre, S., et al. (2015b). Aerial environment and light quality during production affect postharvest transpiration of ornamentals. *Acta Hortic.* 1104, 197–203.

Arve, L. E., Kruse, O. M. O., Tanino, K. K., Olsen, J. E., Futsaether, C., and Torre, S. (2017). Daily changes in VPD during leaf development in high air humidity increase the stomatal responsiveness to darkness and dry air. *J. Plant Physiol.* 211, 63–69. doi: 10.1016/j.jplph.2016.12.011

Arve, L. E. (2013). Stomatal functioning and abscisic acid (ABA) regulation in plants developed in different air humidity regimes. PhD thesis 2013:29. (Ås: Norwegian University of Life Sciences). pp. 142.

Blom-Zandstra, M., Pot, C. S., Maas, F. M., and Schapendonk, H. C. M. (1995). Effects of different light treatments on the nocturnal transpiration and dynamics of stomatal closure of two rose cultivars. *Sci. Hortic.* 61, 251–262. doi: 10.1016/0304-4238(94)00751-Z

Caird, M. A., Richards, J. H., and Donovan, L. A. (2007). Nighttime stomatal conductance and transpiration in C-3 and C-4 plants. *Plant Physiol.* 143, 4–10. doi: 10.1104/pp.106.092940

Carvalho, D. R. A., Torre, S., Kraniotis, D., Almeida, D. P. F., Heuvelink, E., and Carvalho, S. M. P. (2015a). Elevated air movement enhances stomatal sensitivity to abscisic acid in leaves developed at high relative air humidity. *Front. Plant Sci.* 6, 11. doi: 10.3389/fpls.2015.00383

Carvalho, D. R. A., Torre, S., Vasconcelos, M. W., Almeida, D. P. F., Heuvelink, E., and Carvalho, S. M. P. (2015b). "Effects of Air Humidity and Air Movement on Growth, Visual Quality and Post-Production Stress Tolerance of Pot Rose 'Toril'," in *Vi International Symposium on Rose Research and Cultivation*. Eds. T. Debener and M. Linde, 273–278.

Currey, C. J., and Lopez, R. G. (2013). Cuttings of Impatiens, Pelargonium, and Petunia Propagated under Light-emitting Diodes and High-pressure Sodium Lamps Have Comparable Growth, Morphology, Gas Exchange, and Post-transplant Performance. *Hortscience* 48, 428–434. doi: 10.21273/HORTSCI.48.4.428

Cutler, A. J., and Krochko, J. E. (1999). Formation and breakdown of ABA. *Trends Plant Sci.* 4, 472–478. doi: 10.1016/S1360-1385(99)01497-1

Dietz, K. J., Sauter, A., Wichert, K., Messdaghi, D., and Hartung, W. (2000). Extracellular beta-glucosidase activity in barley involved in the hydrolysis of ABA glucose conjugate in leaves. *J. Exp. Bot.* 51, 937–944. doi: 10.1093/jexbot/51.346.937

Eskling, M., Arvidsson, P. O., and Akerlund, H. E. (1997). The xanthophyll cycle, its regulation and components. *Physiol. Plant* 100, 806–816. doi: 10.1111/j.1399-3054.1997.tb00007.x

Fanourakis, D., Carvalho, S. M. P., Almeida, D. P. F., and Heuvelink, E. (2011). Avoiding high relative air humidity during critical stages of leaf ontogeny is decisive for stomatal functioning. *Physiol. Plant* 142, 274–286. doi: 10.1111/j.1399-3054.2011.01475.x

Fanourakis, D., Carvalho, S. M. P., Almeida, D. P. F., van Kooten, O., van Doorn, W. G., and Heuvelink, E. (2012). Postharvest water relations in cut rose cultivars with contrasting sensitivity to high relative air humidity during growth. *Postharvest Biol. Technol.* 64, 64–73. doi: 10.1016/j.postharvbio.2011.09.016

Fanourakis, D., Heuvelink, E., and Carvalho, S. M. P. (2013a). A comprehensive analysis of the physiological and anatomical components involved in higher water loss rates after leaf development at high humidity. *J. Plant Physiol.* 170, 890–898. doi: 10.1016/j.jplph.2013.01.013

Fanourakis, D., Pieruschka, R., Savvides, A., Macnish, A. J., Sarlikioti, V., and Woltering, E. J. (2013b). Sources of vase life variation in cut roses: A review. *Postharvest Biol. Technol.* 78, 1–15. doi: 10.1016/j.postharvbio.2012.12.001

Fanourakis, D., Bouranis, D., Giday, H., Carvalho, D. R. A., Rezaei Nejad, A., and Ottosen, C.-O. (2016). Improving stomatal functioning at elevated growth air humidity: A review. *J. Plant Physiol.* 207, 51–60. doi: 10.1016/j.jplph.2016.10.003

Fanourakis, D., Hyldgaard, B., Giday, H., Alilik, I., Bouranis, D., Korner, O., et al. (2019). Stomatal anatomy and closing ability is affected by supplementary light intensity in rose (Rosa hybrida L.). *Hortic. Sci.* 46, 81–89. doi: 10.17221/144/2017-HORTSCI

Fanourakis, D. (2011). Stomatal Response Characteristics as Affected by Long-term Elevated Humidity Levels. PhD thesis. Wageningen, the Netherlands: Wageningen University. pp. 169.

Fellner, M., and Sawhney, V. K. (2002). The 7B-1 mutant in tomato shows blue-light-specific resistance to osmotic stress and abscisic acid. *Planta* 214, 675–682. doi: 10.1007/s004250100671

Fjeld, T., Gislerød, H. R., Revhaug, V., and Mortensen, L. M. (1994). Keeping quality of cut roses as affected by high supplementary irradiation. *Sci. Hortic.* 57, 157–164. doi: 10.1016/0304-4238(94)90043-4

Fordham, M. C., Harrison-Murray, R. S., Knight, L., and Evered, C. E. (2001). Effects of leaf wetting and high humidity on stomatal function in leafy cuttings and intact plants of Corylus maxima. *Physiol. Plant* 113, 233–240. doi: 10.1034/j.1399-3054.2001.1130211.x

Frechilla, S., Zhu, J. X., Talbott, L. D., and Zeiger, E. (1999). Stomata from npq1, a zeaxanthin-less arabidopsis mutant, lack a specific response to blue light. *Plant Cell Physiol.* 40, 949–954. doi: 10.1093/oxfordjournals.pcp.a029627

Frechilla, S., Talbott, L. D., and Zeiger, E. (2002). The CO2 response of Vicia guard cells acclimates to growth environment. *J. Exp. Bot.* 53, 545–550. doi: 10.1093/jexbot/53.368.545

Giday, H., Fanourakis, D., Kjaer, K. H., Fomsgaard, I. S., and Ottosen, C. O. (2013a). Foliar abscisic acid content underlies genotypic variation in stomatal responsiveness after growth at high relative air humidity. *Ann. Bot.* 112, 1857–1867. doi: 10.1093/aob/mct220

Giday, H., Kjaer, K. H., Fanourakis, D., and Ottosen, C. O. (2013b). Smaller stomata require less severe leaf drying to close: A case study in Rosa hydrida. *J. Plant Physiol.* 170, 1309–1316. doi: 10.1016/j.jplph.2013.04.007

Giday, H., Fanourakis, D., Kjaer, K. H., Fomsgaard, I. S., and Ottosen, C.-O. (2014). Threshold response of stomatal closing ability to leaf abscisic acid concentration during growth. *J. Exp. Bot.* 65 (15), 4361–4370. doi: 10.1093/jxb/eru216

Jabeen, R., Yamada, K., Shigemori, H., Hasegawa, T., Hara, M., Kuboi, T., et al. (2006). Induction of beta-glucosidase activity in maize coleoptiles by blue light illumination. *J. Plant Physiol.* 163, 538–545. doi: 10.1016/j.jplph.2005.05.004

Karbulkova, J., Schreiber, L., Macek, P., and Santrucek, J. (2008). Differences between water permeability of astomatous and stomatous cuticular membranes: effects of air humidity in two species of contrasting drought-resistance strategy. *J. Exp. Bot.* 59, 3987–3995. doi: 10.1093/jxb/ern238

Kim, J., and van Iersel, M. W. (2011). Abscisic acid drenches can reduce water use and extend shelf life of Salvia splendens. *Sci. Hortic.* 127, 420–423. doi: 10.1016/j.scienta.2010.10.020

Kinoshita, T., and Hayashi, Y. (2011). "New Insights Into The Regulation Of Stomatal Opening By Blue Light And Plasma Membrane H+-Atpase," in *International Review of Cell and Molecular Biology*, vol. 289 . Ed. K. W. Jeon (San Diego: Elsevier Academic Press Inc), 89–115.

Kinoshita, T., Emi, T., Tominaga, M., Sakamoto, K., Shigenaga, A., Doi, M., et al. (2003). Blue-light- and phosphorylation-dependent binding of a 14-3-3 protein to phototropins in stomatal guard cells of broad bean. *Plant Physiol.* 133, 1453–1463. doi: 10.1104/pp.103.029629

Lanoue, J., Leonardos, E. D., Ma, X., and Grodzinski, B. (2017). The Effect of Spectral Quality on Daily Patterns of Gas Exchange, Biomass Gain, and Water-Use-Efficiency in Tomatoes and Lisianthus: An Assessment of Whole Plant Measurements. *Front. Plant Sci.* 8, 1076. doi: 10.3389/fpls.2017.01076

Lee, K. H., Piao, H. L., Kim, H. Y., Choi, S. M., Jiang, F., Hartung, W., et al. (2006). Activation of glucosidase via stress-induced polymerization rapidly increases active pools of abscisic acid. *Cell* 126, 1109–1120. doi: 10.1016/j.cell.2006.07.034

Leonardos, E. D., Ma, X., Lanoue, J., and Grodzinski, B. (2019). Leaf and whole-plant gas exchange and water-use efficiency of chrysanthemums under HPS and LEDs during the vegetative and flower-induction stages. *Can. J. Plant Sci.* 99, 639–653. doi: 10.1139/cjps-2018-0245

Li, X. Y., Wu, L. T., Qiu, Y., Wang, T., Zhou, Q., Zhang, Q., et al. (2019). Abscisic Acid Receptors Modulate Metabolite Levels and Phenotype in Arabidopsis Under Normal Growing Conditions. *Metabolites* 9, 9. doi: 10.3390/metabo9110249

Lim, E. K., Doucet, C. J., Hou, B., Jackson, R. G., Abrams, S. R., and Bowles, D. J. (2005). Resolution of (+)-abscisic acid using an Arabidopsis glycosyltransferase. *Tetrahedron-Asymmetry* 16, 143–147. doi: 10.1016/j.tetasy.2004.11.062

Lim, J. H., Choi, H. W., Ha, S. T. T., and In, B. C. (2017). Greenhouse Dehumidification Extends Postharvest Longevity of Cut Roses in Winter Season. *Hortic. Sci. Technol.* 35, 737–746. doi: 10.12972/kjhst.20170078

Mortensen, L. M. (2000). Effects of air humidity on growth, flowering, keeping quality and water relations of four short-day greenhouse species. *Sci. Hortic.* 86, 299–310. doi: 10.1016/S0304-4238(00)00155-2

Nelson, J. A., and Bugbee, B. (2015). Analysis of Environmental Effects on Leaf Temperature under Sunlight, High Pressure Sodium and Light Emitting Diodes. *PloS One* 10 (10), e0138930. doi: 10.1371/journal.pone.0138930

Novakova, M., Motyka, V., Dobrev, P. I., Malbeck, J., Gaudinova, A., and Vankova, R. (2005). Diurnal variation of cytokinin, auxin and abscisic acid levels in tobacco leaves. *J. Exp. Bot.* 56, 2877–2883. doi: 10.1093/jxb/eri282

Okamoto, M., Kushiro, T., Jikumaru, Y., Abrams, S. R., Kamiya, Y., Seki, M., et al. (2011). ABA 9 '-hydroxylation is catalyzed by CYP707A in Arabidopsis. *Phytochemistry* 72, 717–722. doi: 10.1016/j.phytochem.2011.02.004

Pettersen, R. I., Moe, R., and Gislerød, H. R. (2007). Growth of pot roses and post-harvest rate of water loss as affected by air humidity and temperature variations during growth under continuous light. *Sci. Hortic.* 114, 207–213. doi: 10.1016/j.scienta.2007.06.009

Priest, D. M., Ambrose, S. J., Vaistij, F. E., Elias, L., Higgins, G. S., Ross, A. R. S., et al. (2006). Use of the glucosyltransferase UGT71B6 to disturb abscisic acid homeostasis in Arabidopsis thaliana. *Plant J.* 46, 492–502. doi: 10.1111/j.1365-313X.2006.02701.x

Quarrie, S. A., Whitford, P. N., Appleford, N. E. J., Wang, T. L., Cook, S. K., Henson, I. E., et al. (1988). A monoclonal antibody to (S)-abscisic acid: its characterisation and use in a radioimmunoassay for measuring abscisic acid in crude extracts of cereal and lupin leaves. *Planta* 173, 330–339. doi: 10.1007/BF00401020

Riikonen, J. (2016). Pre-cultivation of Scots pine and Norway spruce transplant seedlings under four different light spectra did not affect their field performance. *New For* 47, 607–619. doi: 10.1007/s11056-016-9533-9

Sauter, A., Dietz, K. J., and Hartung, W. (2002). A possible stress physiological role of abscisic acid conjugates in root-to-shoot signalling. *Plant Cell Environ.* 25, 223–228. doi: 10.1046/j.1365-3040.2002.00747.x

Talbott, L. D., Rahveh, E., and Zeiger, E. (2003). Relative humidity is a key factor in the acclimation of the stomatal response to CO2. *J. Exp. Bot.* 54, 2141–2147. doi: 10.1093/jxb/erg215

Tallman, G. (2004). Are diurnal patterns of stomatal movement the result of alternating metabolism of endogenous guard cell ABA and accumulation of ABA delivered to the apoplast around guard cells by transpiration? *J. Exp. Bot.* 55, 1963–1976. doi: 10.1093/jxb/erh212

Tanaka, Y., Sano, T., Tamaoki, M., Nakajima, N., Kondo, N., and Hasezawa, S. (2005). Ethylene inhibits abscisic acid-induced stomatal closure in Arabidopsis. *Plant Physiol.* 138, 2337–2343. doi: 10.1104/pp.105.063503

Terfa, M. T., Poudel, M. S., Roro, A. G., Gislerod, H. R., Olsen, J. E., and Torre, S. (2012). "Light Emitting Diodes with a High Proportion of Blue Light Affects External and Internal Quality Parameters of Pot Roses Differently than the Traditional High Pressure Sodium Lamp," in *Vii International Symposium on Light in Horticultural Systems*. Eds. S. Hemming and E. Heuvelink (Leuven 1: Int Soc Horticultural Science), 635–641.

Terfa, M. T., Solhaug, K. A., Gislerod, H. R., Olsen, J. E., and Torre, S. (2013). A high proportion of blue light increases the photosynthesis capacity and leaf formation rate of Rosa x hybrida but does not affect time to flower opening. *Physiol. Plant* 148, 146–159. doi: 10.1111/j.1399-3054.2012.01698.x

Torre, S., and Fjeld, T. (2001). Water loss and postharvest characteristics of cut roses grown at high or moderate relative air humidity. *Sci. Hortic.* 89, 217–226. doi: 10.1016/S0304-4238(00)00229-6

Torre, S., Fjeld, T., Gislerød, H. R., and Moe, R. (2003). Leaf anatomy and stomatal morphology of greenhouse roses grown at moderate or high air humidity. *J. Am. Soc. Hortic. Sci.* 128, 598–602. doi: 10.21273/JASHS.128.4.0598

Waterland, N. L., Campbell, C. A., Finer, J. J., and Jones, M. L. (2010a). Abscisic Acid Application Enhances Drought Stress Tolerance in Bedding Plants. *Hortscience* 45, 409–413. doi: 10.21273/HORTSCI.45.3.409

Waterland, N. L., Finer, J. J., and Jones, M. L. (2010b). Abscisic Acid Applications Decrease Stomatal Conductance and Delay Wilting in Drought-stressed Chrysanthemums. *Horttechnology* 20, 896–901. doi: 10.21273/HORTTECH.20.5.896

Wilkinson, S., and Davies, W. J. (2002). ABA-based chemical signalling: the co-ordination of responses to stress in plants. *Plant Cell Environ.* 25, 195–210. doi: 10.1046/j.0016-8025.2001.00824.x

Xiong, L., and Zhu, J. K. (2002). Molecular and genetic aspects of plant responses to osmotic stress. *Plant Cell Environ.* 25, 131–139. doi: 10.1046/j.1365-3040.2002.00782.x

Yoshida, T., Christmann, A., Yamaguchi-Shinozaki, K., Grill, E., and Fernie, A. R. (2019). Revisiting the Basal Role of ABA - Roles Outside of Stress. *Trends Plant Sci.* 24, 625–635. doi: 10.1016/j.tplants.2019.04.008

Zeevaart, J. A. D. (1980). Changes in the levels of abscisic-acid and its metabolites in excised leaf blades of Xanthium-strumarium during and after water-stress. *Plant Physiol* 66, 672–678. doi: 10.1104/pp.66.4.672

Conflict of Interest: The authors declare that the research was conducted in the absence of any commercial or financial relationships that could be construed as a potential conflict of interest.

frontiers in Plant Science

ORIGINAL RESEARCH
published: 10 September 2020
doi: 10.3389/fpls.2020.566824

Effects of Exogenous Putrescine on Delaying Senescence of Cut Foliage of *Nephrolepis cordifolia*

Ying Qu[1], *Lu Jiang*[1], *Tana Wuyun*[2*], *Shouyuan Mu*[1], *Fuchun Xie*[1], *Yajun Chen*[1] *and Lu Zhang*[1*]

[1] College of Horticulture and Landscape Architecture, Northeast Agricultural University, Harbin, China, [2] Chair of Crop Science and Plant Biology, Estonian University of Life Sciences, Tartu, Estonia

OPEN ACCESS

Edited by:
Antonio Ferrante, University of Milan, Italy

Reviewed by:
Giuseppina P. P. Lima, São Paulo State University, Brazil
Weibiao Liao, Gansu Agricultural University, China
Gustavo A. Martinez, Consejo Nacional de Investigaciones Científicas y Técnicas (CONICET), Argentina

***Correspondence:**
Lu Zhang
caszhanglu@hotmail.com
Tana Wuyun
wuyuntana@emu.ee

Specialty section:
This article was submitted to Crop and Product Physiology, a section of the journal Frontiers in Plant Science

Received: *01 June 2020*
Accepted: *24 August 2020*
Published: *10 September 2020*

Citation:
Qu Y, Jiang L, Wuyun T, Mu S, Xie F, Chen Y and Zhang L (2020) Effects of Exogenous Putrescine on Delaying Senescence of Cut Foliage of Nephrolepis cordifolia. Front. Plant Sci. 11:566824. doi: 10.3389/fpls.2020.566824

Senescence is the main limitation for cut foliage display in vase. Naturally occurring polyamines such as putrescine (Put) have been considered effective anti-senescence agents. However, effect of Put on cut foliage in vase in a realistic indoor environment has not yet been revealed. In the present study, effects of Put spraying on the postharvest performance of cut foliage of *Nephrolepis cordifolia* L. were investigated. Cut fronds sprayed with deionized water (Put0) showed visible injuries after 10 days in vase. Meanwhile, chlorophyll (Chl), soluble protein (Sp), and proline (Pro) content were decreased by 60.15, 57.93, and 73.09% respectively, photochemical activity reflected by Chl fluorescence parameters was inhibited, whereas electrolyte leakage (EL), contents of soluble sugar (Ss), malondialdehyde (MDA), and hydrogen peroxide (H_2O_2) were increased (+194.29, +44.83, +34.06, and +178.01%, respectively). Put spraying extended the vase life of the cut foliage and the 2.0 mM Put had a longer vase life (21 days) than 0.2 mM (15 days). Leaf spraying of 2.0 mM Put for 10 days significantly ameliorated the losses of Chl, Sp, and Pro content (–10.72, –26.29, and –42.64%, respectively), followed by 0.2 mM Put (–27.36, –36.24, and –60.55%, respectively). Put spraying also improved photochemical capability and prevented membrane impairment as well as visible injury in comparison with Put0. In addition, 2.0 mM Put had a better mitigating ability than that of 0.2 mM. Leaf spraying of 2.0 mM Put greatly reduced the decline of the effective quantum yield of photochemical energy conversion in PSII (ΦPSII), the maximal quantum yield of PSII photochemistry measured in the dark-adapted state (Fv/Fm) and electron transport rate (ETR) (–7.89, –12.91, and –10.06%, respectively), and also inhibited the increases of EL, MDA, Ss, and H_2O_2 (+31.87, +6.43, +16.22, and +49.40%, respectively). Overall, Put played important roles in deterring the degradation of Chl, Ss, and Pro, detoxifying the H_2O_2, weakening the sugar signaling, mitigating the decline of photochemical activity, and eventually postponing the leaf senescence. The present study gives new insights into effects of Put on leaf senescence and provides a strategy for preserving post-harvest cut foliage.

Keywords: antioxidant enzyme, biochemical, chlorophyll fluorescence imaging, polyamines, sword fern

INTRODUCTION

In recent decades, with continuous improvement of standard of living and increasing desire for a better indoor environment, indoor greening and decoration has emerged, with a strong demand for cut flowers and foliage. The short vase life and the low ability to cope with unsuitable environment during floral arrangement and display are the most important constraints for the commercialization of cut flowers and foliage (Zamani et al., 2011; Zhao et al., 2017).

For cut flowers and foliage, senescence is the main reason for short vase life (Shabanian et al., 2018). Although cut foliage plays important roles in floriculture industry, studies on its postharvest senescence are very limited compared with cut flowers (Malakar et al., 2017; Che-Husin et al., 2018; Lin et al., 2019). Senescence caused by the detachment of leaves from plants is associated with various biochemical and physiological changes. Leaf yellowing is often the first visible symptom of senescence, mainly due to the loss of chlorophyll (Chl) (Skutnik et al., 2004). It has been reported that after leaves were detached from rabbit's foot fern (*Phlebodium aureum*), Chl *a* and Chl *b* contents decreased (Teerarak and Laosinwattana, 2019). Chl breakdown often occurs due to the remobilization of nitrogen from Chl-binding proteins to other processes during leaf senescence (Hörtensteiner, 2006). Besides Chl, protein is also considered as a marker of senescence since it degrades during leaf senescence (Breeze et al., 2011). Furthermore, many studies have found that reactive oxygen species (ROS) level increases during leaf senescence (Merzlyak and Hendry, 1994; Breusegem and Dat, 2006). Plants orchestrate a myriad of antioxidants such as ascorbic acid (AsA) as a strategy to cope with the detrimental ROS. For instance, it has been observed that increases in peroxidase (POD) and superoxide dismutase (SOD) activity occur in senescing leaves (Kim et al., 2004). Moreover, senescence induces an increase in the content of polyamines such as putrescine (Put), spermidine (Spd), and spermine (Spm) (Serrano et al., 2001; Sobieszczuk-Nowicka et al., 2016). Study on the maximum quantum yield of photosystem II (PSII) photochemistry measured in the dark-adapted state (Fv/Fm) shows that it decreases in *Sorghum bicolor* during leaf senescence (Chen et al., 2015).

Polyamines (PAs) are biodegradable organic compounds and have no adverse environmental effects (Sharma et al., 2017). Naturally occurring PAs such as Put have been reported as effective anti-senescence agents and lower Put content was found in aged cell (Paschalidis and Roubelakis-Angelakis, 2005; Kusano et al., 2008). The addition of PAs (Put, Spd, and Spm) increases the longevity of isolated flowers of *Nicotiana plumbaginifolia* (Nisar et al., 2015). Conditioning of cut stems of rose in Put solution results in a higher Chl *a* and Chl *b* content (Rubinowska et al., 2012). Exogenously supplied Put reduces hydrogen peroxide (H_2O_2) accumulation, electrolyte leakage (EL) and malondialdehyde (MDA) content, while increasing the activities of catalase (CAT) and ascorbate peroxidase (APX), thereby prolonging the vase life of cut lisianthus flowers (Ataii et al., 2015). Leaf senescence is different from petal senescence. For example, cut foliage can still sustain photosynthesis and do not need energy to maintain its survival at the late stage of senescence process (Zhang and Becker, 2015). However, information about the effects of PAs on cut foliage is very limited. In the limited studies, scientists focused on the roles of PAs in Chl and protein loss and antioxidant system with or without light (Altman, 1982; Cho and Hong, 1988). Generally, these studies have uncoupled the dark and light responses to investigate the senescence mechanisms. However, to reveal how Put affects postharvest quality of cut foliage, the holistic effects on leaf senescence should be considered in a realistic light-dark cycle. To our best knowledge, relevant reports are very few (Sood and Nagar, 2003). Furthermore, the state of art technology supplies novel insights to reveal the mechanism of leaf senescence. For example, Chl fluorescence imaging provides a non-destructive method to detect the photochemical damage in a whole leaf scale and very suitable for studying the anti-aging effect of Put. However, this method has not yet been applied in this field.

Sword fern (*N. cordifolia* L.) is commonly used in the garden and its cut green foliage has a high decorative value in floral arrangements due to it providing a vertical accent to floral designs (Safeena et al., 2019). In addition, it is available throughout the year. Therefore, in the present study, we selected sword fern as plant material and aimed to investigate the potential mitigating effects of Put on the senescence of cut foliage under realistic indoor environment and to reveal the underlying physiological and biochemical mechanisms. These results could provide a theoretical basis for prolonging the vase life of cut foliage using exogenous Put.

MATERIALS AND METHODS

Plant Material

Sword fern (*N. cordifolia* L.) was selected as plant material. A total of 50 pots of plants were bought from Harbin Flower Market, CN. The diameter of the pots was 16 cm and the average height of the plants was ca. 30 cm. Before treatments, the plants were adapted for one week in a greenhouse where the average temperature was ca. 25 °C and relative humidity ca. 65%. During this period, the light period was 16/8 h (day/night), and the average light intensity was ca. 800 μmol (photon) m^{-2} s^{-1}. The plants were irrigated to the soil water capacity every day.

Treatment and Vase Life Observation

A total of 72 healthy fronds with similar size (ca. 20 cm long, in which both the lamina and the stipe were 10 cm) were cut from the plants using a sharp knife, then each frond was immediately placed upright into one individual conical flask containing 100 ml of deionized water. The conical flasks were covered with transparent plastic films to decrease water evaporation and placed on a table in the laboratory. Fronds together with conical flasks were randomly and equally divided into four groups (18 cut fronds for each group). For the control group,

the cut fronds were observed and sampled immediately, then the samples were stored in -80 °C for the following measurements. The other three groups were sprayed with 0.2 mM Put (Put0.2), 2.0 mM Put (Put2.0), or deionized water (Put0), respectively. The Put concentrations were selected based on references (Yiu et al., 2009; Rubinowska et al., 2012) and a preliminary assay. During the preliminary assay, we used 0.2, 2.0, 4.0 mM Put to test whether they can extend the vase life of cut fronds and found that the frond sprayed with 4.0 mM Put had a shorter vase life than that with Put0 (data not shown). Spraying treatments (2 ml for each frond) were conducted every day in the morning (09:00 am) for consecutive 10 days till 50% of the fronds in Put0 group showed leaflet drop. Then 12 cut fronds of each group were observed and sampled immediately. The samples were also stored in -80 °C for the following measurements. The remaining six cut fronds in each group continue to be sprayed as before to observe the vase life. When 50% of the fronds in each group showed leaflet drop, the vase life was recorded. During the treatment period, the range of relative humidity was ca. 40–55%, the temperature ca. 28/24 °C (day/night), the light period 16/8 h (day/night), and the average light intensity ca. 100 μmol (photon) m^{-2} s^{-1}.

Leaf Appearance

The cut foliage was photographed before and after 10 days of treatment in different groups. Six intact fronds in each treatment group were selected. The percentage of injured area on each cut frond was observed and recorded by three surveyors using a 5 and 1% step scale independently (Paoletti et al., 2009).

Chl Content

Fresh leaflet (0.3 g, n = 6) was sampled and ground with quartz sand and ethanol (95%, v/v), then the extract was filtered into a 25 ml brown volumetric flask, in which the volume was kept at 25 ml using ethanol (95%, v/v). Absorbance of the extracting solution was measured at 470, 649, 665 nm using an Ultraviolet-Visible spectrophotometer (*T6 New Century*, CN). Contents of Chl *a*, Chl *b*, and total Chl, were calculated according to Scrob et al. (2019).

Membrane Integrity

EL was determined according to the method of Lutts et al. (1996). Fresh leaf sample (0.1 g, n = 6) was put into test tubes containing 10 ml of deionized water at 25 °C. After 24 h, EL was determined using a conductivity meter as EL_1. Then samples were maintained in boiling water bath (100 °C) for 20 min. After cooling to 25 °C, a last EL reading (EL_2) was obtained. The EL was defined as: $EL_1/EL_2 \times 100\%$.

Fresh leaflet sample (0.15 g, n = 6) was ground with trichloroacetic acid (10%). Then the homogenate was centrifuged at 4,000×g for 10 min. The supernatant (1 ml) was mixed with 1 ml of thiobarbituric acid (0.6%) and then maintained in boiling water bath for 15 min. After cooling, the mixture was centrifuged at 4,000×g for 10 min. The absorbance of supernatant was detected at 450, 532, 600 nm using an Ultraviolet-Visible spectrophotometer (*T6 New Century*, CN). The MDA content was calculated according to Li et al. (2018).

Reactive Oxygen Species (ROS)

Fresh leaflet sample (0.5 g, n = 6) was put in an ice-cold mortar and ground with 50 mM phosphate extraction buffer (PBS, 3 ml, pH 7.8). Thereafter the homogenate was centrifuged at 12,000×g for 15 min at 4 °C and the supernatant was used to measure the content of superoxide anion ($O_2^{\bullet -}$). The content of $O_2^{\bullet -}$ was determined according to the method of Tian et al. (2003). The concentration of H_2O_2 was determined by the method of Patterson et al. (1984). To determine the H_2O_2 content, the leaflet sample (1.0 g, n = 6) was put in a mortar and ground in cold acetone (5 ml). The homogenate was centrifuged at 5,000×g for 5 min at 4 °C and the supernatant was used to determine the content of H_2O_2.

Antioxidant System

Preparation of SOD and CAT sample solution is the same as $O_2^{\bullet -}$. SOD activity (U g^{-1} fresh weight, FW) was quantified according to the method of Syeed et al. (2011). One unit of SOD activity (U) was defined as the amount of enzyme that inhibited the photoreduction of 50% nitro blue tetrazolium (NBT). Activity of CAT was quantified based on the method described by Díaz-Vivancos et al. (2008). One unit of CAT activity represented the amount of enzyme catalyzing the decomposition of 1 μmol (H_2O_2) min^{-1} g^{-1} FW. Ascorbic acid (AsA) content was measured according to Law et al. (1983). The method is based on the reduction of Fe^{3+} to Fe^{2+} by AsA in acidic solution. Then Fe^{2+} forms complexes with bipyridyl, which appears pink at an absorption of 525 nm.

Cellular Macromolecules

Soluble sugar (Ss), soluble protein (Sp), and proline (Pro) levels were estimated. Anthrone-sulfuric acid method (Leng et al., 2016) was employed to measure Ss. Finally, the absorbance of solution was detected at 620 nm. The Sp content was measured based on the binding of Coomassie Brilliant Blue G-250 to protein according to the Bradford method (Bradford, 1976). Fresh leaf (0.5 g, n = 6) was homogenized using 3% sulfosalicylic acid solution (5 ml) and then maintained in boiling water bath (100 °C) for 10 min (stirred often). After cooling, Pro extract was obtained by filtering the mixture. According to the method (Teklić et al., 2010), the supernatant was used to determine the Pro content.

Chl a Fluorescence

In the early morning of sampling date, Chl *a* fluorescence of cut frond was measured using an IMAGING-PAM Chlorophyll Fluorometer (*Heinz Walz*, Effeltrich, Germany). Six intact fronds per treatment were used. The selected cut fronds were adapted in the dark for 20 min. Thereafter fluorescence induction curves were automatically recorded using the slow kinetic program in the saturation pulse analysis mode. The values of the minimal fluorescence yield in the dark-adapted state (Fo) and the maximal fluorescence yield of the dark-

adapted state (Fm) were obtained with a modulated light [650 nm, 0.5 μmol (photon) m^{-2} s^{-1}] and a 0.8 s saturating pulse [650 nm, 3,700 μmol (photon) m^{-2} s^{-1}], respectively. After 40s, an actinic light irradiation [650 nm, 196 μmol (photon) m^{-2} s^{-1}] was turned on. Then, a saturating pulse was imposed every 20 s until 5 min to determine the maximal fluorescence in the irradiation-adapted state (Fm'). Fv/Fm was calculated as: Fv/Fm=(Fm−Fo)/Fm (Kitajima and Butler, 1975). Stern-Volmer non-photochemical quenching coefficient (NPQ), coefficient of photochemical quenching of variable fluorescence based on the puddle model of PSII (qP), effective quantum yield of photochemical energy conversion in PSII (ΦPSII), quantum yield of regulated energy dissipation in PSII (ΦNPQ), quantum yield of non-regulated energy dissipation in PSII (ΦNO), and electron transport rate (ETR) were calculated by the ImagingPamGigE software (*Heinz Walz*, Effeltrich, Germany). Values of four circular areas (from the top to the bottom positions) on each cut frond were recorded, then averaged as a replicate for statistical analysis.

Images of the fluorescence parameters were stored in the ImagingPamGigE software and displayed by means of a false color code ranging from black (0.0) to purple (ending at 1.0) *via* red, yellow, green, and blue.

Statistical Analysis

All data were analyzed using SPSS (v.12, SPSS, Chicago, IL, USA). One-way analysis of variance (ANOVA) was used to identify the effect of Put solution. Post-hoc Duncan's test was used to compare means of each parameter among different treatments. The relative effect of Put spraying on each parameter was calculated as $[(Value_{treatment}-Value_{control})/Value_{control}]$.

RESULTS

Vase Life of Cut Foliage

According to the experimental observation, when sprayed with deionized water for 10 days, 50% of the cut fronds in the deionized water group showed leaflet drop, whereas the vase life was extended by 5 days in Put0.2 group and by 11 days in Put2.0 group.

Leaf Appearance and Visible Symptoms

The foliage before treatment (Control) exhibited no visible injury (**Figure 1**). After 10 days of treatment, six cut fronds were starting to shed the leaflets and the other six had chlorotic blades under Put0 (15.92% of the total fronds area). Compared with Put0 treatment, the average percentages of visible yellowing area over the leaf surface under Put0.2 and Put2.0 were significantly lower, 2.40 and 1.18%, respectively (**Table 1**).

Chl Content

After 10 days of treatment, Chl *a* (−50.98%), Chl *b* (−72.69%), and total Chl (−60.15%) content of cut leaves under Put0 decreased significantly compared with control (**Figure 2**). Put2.0 spraying greatly alleviated the losses of Chl *a* (−7.68%), Chl *b* (−14.86%), and total Chl (−10.72%). Cut fronds sprayed with Put0.2 also had higher Chl *a* (−15.89%), Chl *b* (−43.05%), and total Chl content (−27.36%) than those sprayed with deionized water (Put0), further supporting its anti-senescence effect.

Membrane Integrity

Compared to control, fronds sprayed with deionized water had significantly higher EL (+194.29%, **Figure 3A**). The relative increase of EL in leaves sprayed with Put0.2 and Put2.0 were lower (+69.90 and +31.87%, respectively), showing a better membrane integrity. Fronds sprayed with deionized water had a higher MDA (+34.06%) in comparison to control (**Figure 3B**), whereas in the leaves sprayed with Put (Put0.2 and Put2.0),

TABLE 1 | Visible injury on the cut foliage of *Nephrolepis cordifolia* before (Control) and after 10 days spraying with deionized water (Put0), 0.2 mM Put (Put0.2), and 2.0 mM Put (Put2.0).

Treatment	Visible injury (%)
Control	0
Put0	15.92 ± 0.61[a]
Put0.2	2.40 ± 0.22[b]
Put2.0	1.18 ± 0.14[c]

Data were shown as means ± S.E. (n = 6). Values with different letters indicate significant differences between treatments (Duncan's test, $p \leq 0.05$).

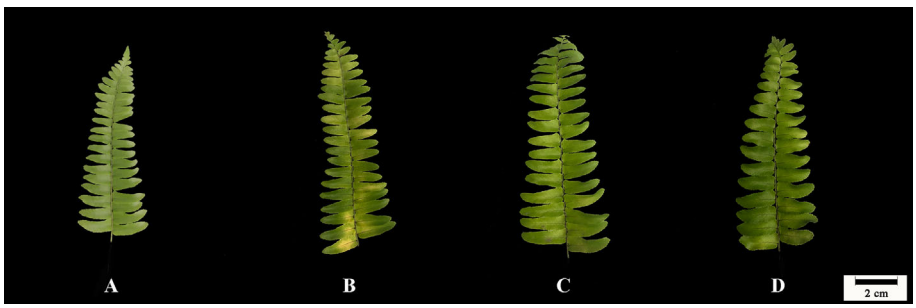

FIGURE 1 | Leaf appearance of cut foliage of *N. cordifolia* before (Control, **A**) and after 10 days spraying with deionized water (Put0, **B**), 0.2 mM Put (Put0.2, **C**), and 2.0 mM Put (Put2.0, **D**).

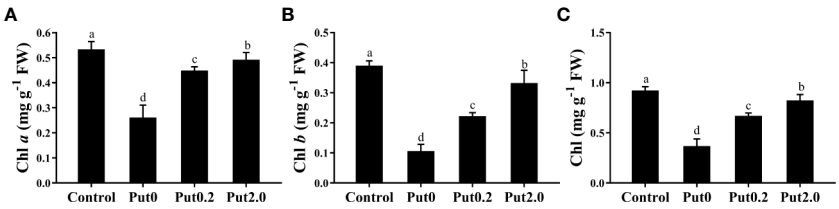

FIGURE 2 | Mean (+ S.E., n = 6) contents of chlorophyll (Chl) *a* **(A)**, Chl *b* **(B)**, and total Chl **(C)**, of cut foliage of *N. cordifolia* before (Control) and after 10 days spraying with deionized water (Put0), 0.2 mM Put (Put0.2), and 2.0 mM Put (Put2.0). FW is the fresh weight of the sample. Different letters show significant differences among bars (Duncan's test, $p \leq 0.05$).

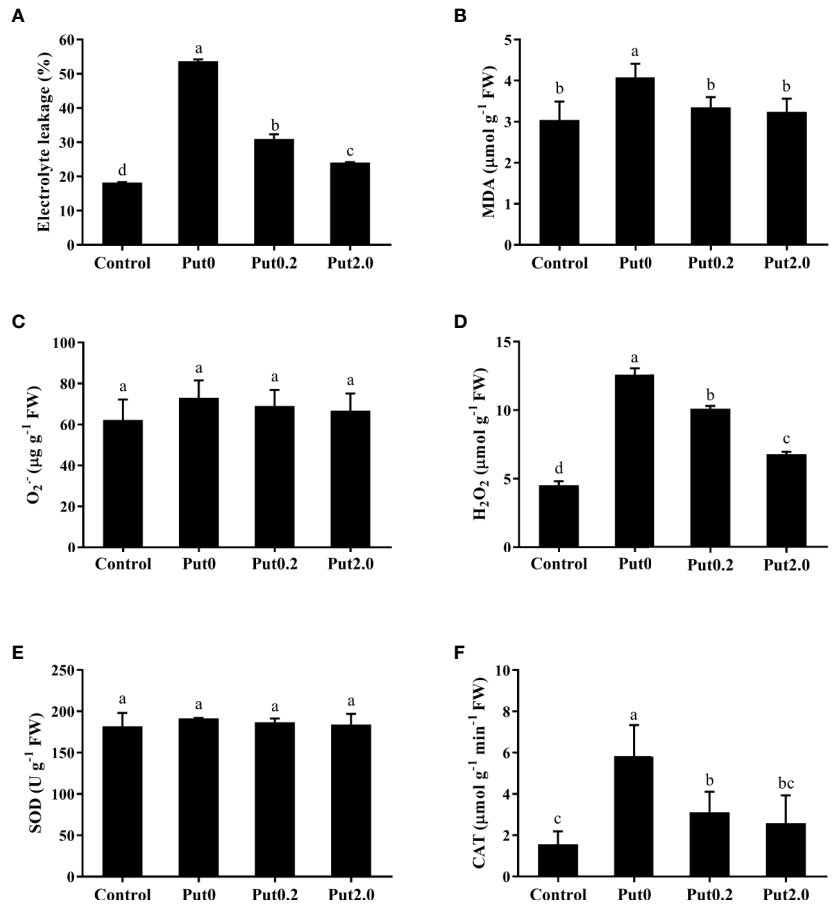

FIGURE 3 | Electrolyte leakage **(A)**, malondialdehyde content (MDA, **B**), superoxide anion content ($O_2^{\bullet -}$, **C**), hydrogen peroxide content (H_2O_2, **D**), and activities of superoxide dismutase (SOD, **E**) and catalase (CAT, **F**) of cut foliage of *N. cordifolia* before (Control) and after 10 days spraying with deionized water (Put0), 0.2 mM Put (Put0.2), and 2.0 mM Put (Put2.0). FW is the fresh weight of the sample. Data were shown as means + S.E. (n = 6). Different letters show significant differences among bars (Duncan's test, $p \leq 0.05$).

MDA levels were not significantly different from control, indicating that Put could protect the plasma membrane from the ROS attack.

Reactive Oxygen Species (ROS)

There was no significant difference of $O_2^{\bullet -}$ content between treatments (**Figure 3C**). H_2O_2 content significantly increased in the fronds treated with deionized water (+178.01%) compared to control. Put0.2 and Put2.0 inhibited the increase of H_2O_2 (+122.89 and +49.40%, respectively) (**Figure 3D**).

Antioxidant System

There was no significant change in SOD activity between treatments (**Figure 3E**). Compared to control, fronds sprayed

with deionized water had significantly higher CAT activity (+273.33%, **Figure 3F**) and Put spraying inhibited the increase. The relative increase of CAT activity in the Put2.0-sprayed (+66.67%) fronds were the lowest, followed by the Put0.2-sprayed fronds (+100%). After 10 days of treatment, AsA contents of cut fronds under Put0, Put0.2, and Put2.0 decreased significantly compared with control (−54.71, −76.24, and −72.87%, respectively) (**Figure 4D**). However, the AsA content was not significantly different between Put0.2 and Put2.0.

Cellular Macromolecules

After 10 days of treatment, Sp (−57.93%) and Pro (−73.09%) content of cut fronds under Put0 decreased significantly compared with control (**Figure 4**). Put2.0 spraying greatly alleviated the losses of Sp (−26.29%) and Pro (−42.64%). Cut fronds sprayed with Put0.2 also had lower losses of Sp (−36.24%) and Pro content (−60.55%). Cut fronds sprayed with deionized water had higher Ss content (+44.83%, **Figure 4B**) than control and Put spraying inhibited the increase. The relative increase of Ss content in the Put2.0-sprayed fronds was the lowest (+16.22%), followed by the Put0.2 (+26.92%).

Chl a Fluorescence

Both Fm (−50.02%) and variable fluorescence (Fv, −59.12%) decreased in the fronds under Put0 after 10 days of spraying with deionized water in comparison to control, whereas these values were higher in the fronds sprayed with Put0.2 (−46.05 and −53.34%, respectively) and Put2.0 (−35.19 and −43.55%, respectively) relative to Put0 (**Figure 5**). Fv/Fm (−18.80%), ΦPSII (−31.21%), ΦNPQ (−12.98%), NPQ (−47.88%), qP (−31.09%), and ETR (−30.28%) of the cut fronds sprayed with deionized water decreased relative to control, while ΦNO increased (+54.84%) (**Figure 6**). The relative losses of Fv/Fm

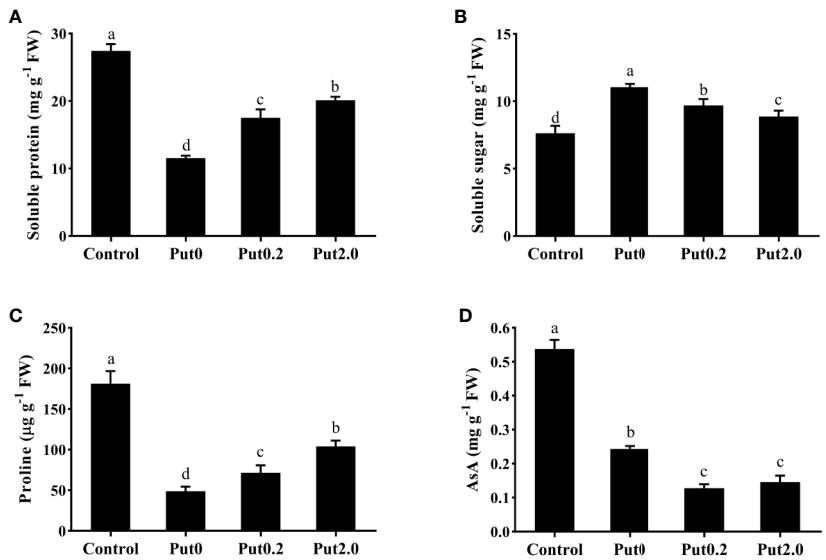

FIGURE 4 | Soluble protein **(A)**, soluble sugar **(B)**, proline **(C)**, and ascorbic acid (AsA, **D**) contents of cut foliage of *N. cordifolia* before (Control) and after 10 days spraying with deionized water (Put0), 0.2 mM Put (Put0.2), and 2.0 mM Put (Put2.0). FW is the fresh weight of the sample. Data were shown as means + S.E. (n = 6). Different letters show significant differences among bars (Duncan's test, $p \leq 0.05$).

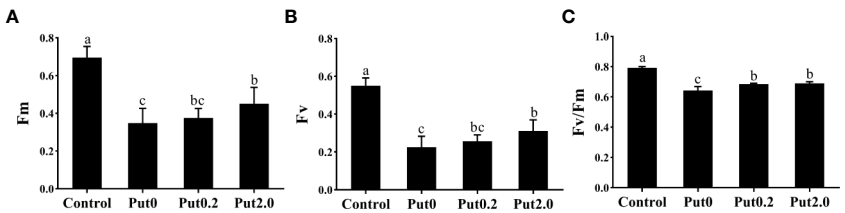

FIGURE 5 | The maximal fluorescence yield of the dark-adapted state (Fm, **A**), variable fluorescence (Fv, **B**), the maximal quantum yield of PSII photochemistry measured in the dark-adapted state (Fv/Fm, **C**) of cut foliage of *N. cordifolia* before (Control) and after 10 days spraying with deionized water (Put0), 0.2 mM Put (Put0.2), and 2.0 mM Put (Put2.0). Data were shown as means + S.E. (n = 6). Different letters show significant differences between bars (Duncan's test, $P \leq 0.05$).

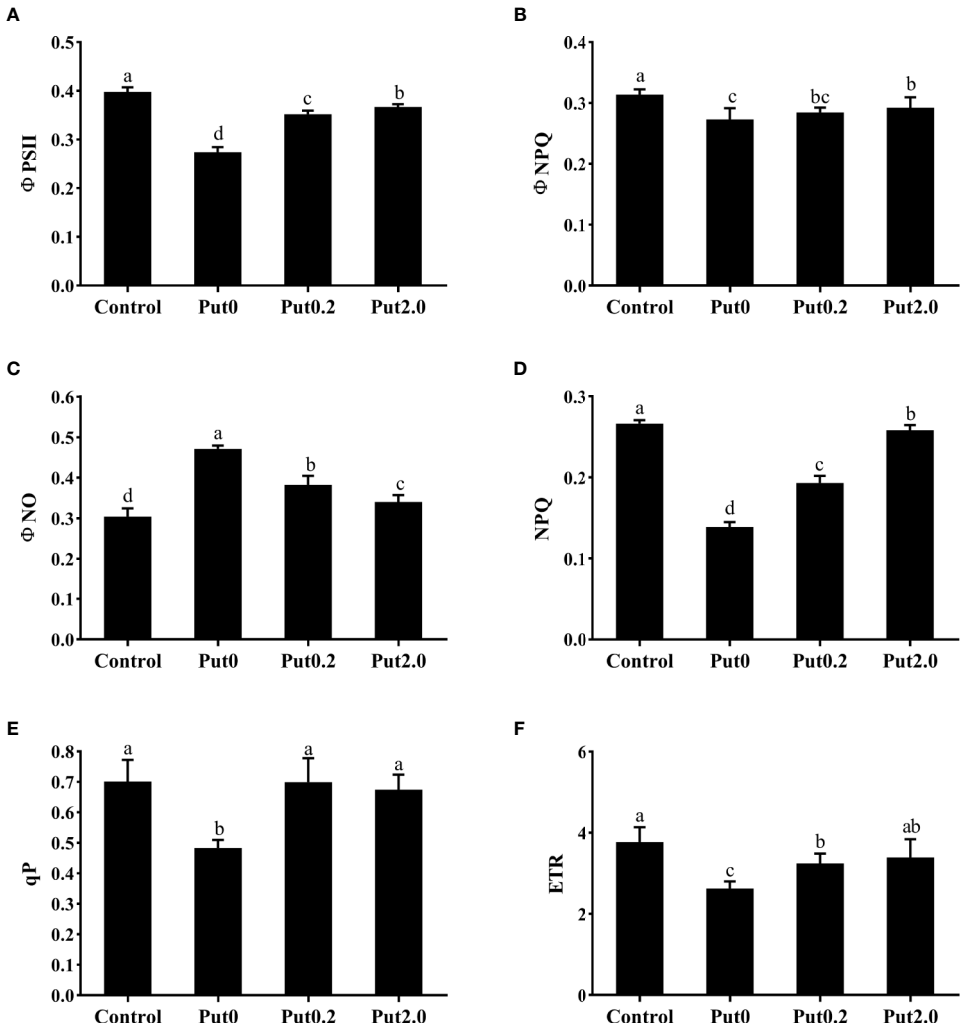

FIGURE 6 | The effective quantum yield of photochemical energy conversion in PSII (ΦPSII, **A**), quantum yield of regulated energy dissipation in PSII (ΦNPQ, **B**), quantum yield of non-regulated energy dissipation in PSII (ΦNO, **C**), non-photochemical quenching coefficient (NPQ, **D**), coefficient of photochemical quenching of variable fluorescence based on the puddle model of PSII (qP, **E**), and electron transport rate (ETR, **F**) of cut foliage of *N. cordifolia* before (Control) and after 10 days spraying with deionized water (Put0), 0.2 mM Put (Put0.2), and 2.0 mM Put (Put2.0). Data were shown as means + S.E. (n = 6). Different letters show significant differences between bars (Duncan's test, $P \leq 0.05$).

(−12.91%), NPQ (−3.13%), and ETR (−10.06%) in the fronds treated with Put2.0 were lower than those with other treatments. The relative increases of ΦNO (+11.76%) in fronds treated with Put2.0 were lower than those upon other treatments.

Chl fluorescence imaging presents an instantaneous overview of the fluorescence emission pattern of the whole leaf surface (Gorbe and Calatayud, 2012). The images of Fv/Fm, ΦPSII, ΦNO, and ΦNPQ showed that the fronds were stressed under Put0 after 10 days of deionized water spraying (**Figure 7**). Compared with Put0 treatment, foliar application of Put exerted significant mitigating effect. Distinct effects of Put0.2 and Put2.0 spraying on Fv/Fm, ΦNO, and ΦNPQ were found. Put2.0 seems to be more efficient in mitigating the negative effects of photoinhibition or photodamage than Put0.2. In the present study, heterogeneous distributions of these four parameters over the screened leaf area were observed especially in leaves sprayed with deionized water and Put0.2.

DISCUSSION

Half of the replicates in the cut foliage of sword fern treated with deionized water were beginning to shed pinnae after 10 days of treatment. Meanwhile leaf yellowing appeared, which is a normal symptom of leaf senescence. It has been reported that abscission of the leaflets of sword fern started from the fourth days in vase (Banthoengsuk et al., 2011). The discrepancy between this previous study and our result is probably due to the different ways for treatment. Spraying deionized water every day could postpone the water deficit and the following pinnae abscission

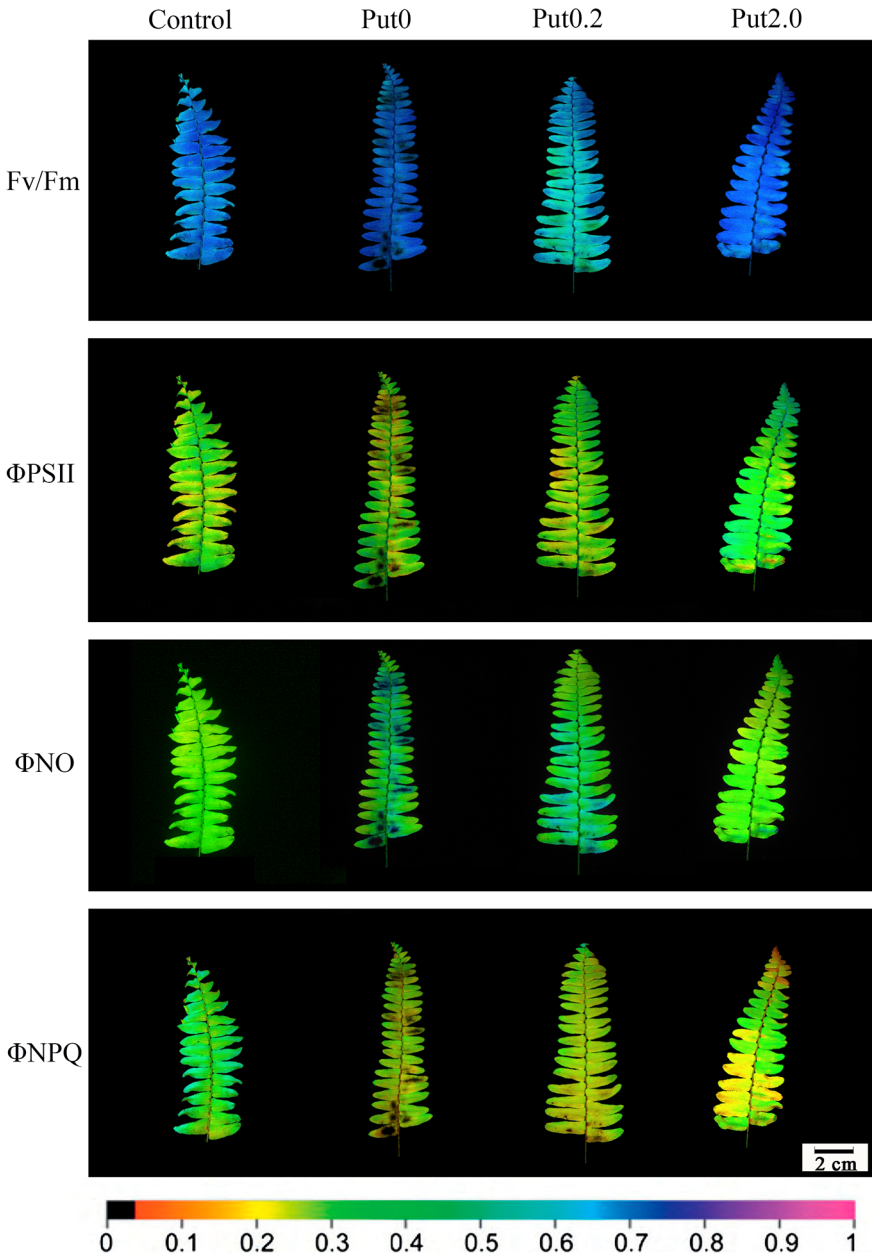

FIGURE 7 | Detection of the effects of exogenous putrescine (Put) on cut foliage of *N. cordifolia* using a chlorophyll fluorescence imaging technique. Images of Fv/Fm, ΦPSII, ΦNO, and ΦNPQ, with actinic illumination of 196 μmol m^{-2} s^{-1} are shown. Each image in the same column represents the same frond. From left to right: Control, Put0, Put0.2, and Put2.0. The color scale at the bottom indicates values from 0 (black) to 1 (pink).

and Chl degradation. In our experiment, Put (0.2 and 2.0 mM) alleviated Chl (Chl *a*, Chl *b*, and total Chl) loss significantly and higher concentration had a stronger effect (**Figure 2**). Our results are in agreement with some previous studies, in which application of Put on leaves of *Thymus vulgaris* (Mohammadi et al., 2018) and flower head of broccoli (Zheng et al., 2019) increased Chl *a*, Chl *b*, and total Chl content compared to those under natural senescence. It might be due to PAs could alleviate the loss of Chl in thylakoid membranes by stabilizing photosystem complexes during storage (Beigbeder et al., 1995).

During leaf senescence ROS level increases (Breusegem and Dat, 2006). In the present study, the $O_2^{\bullet -}$ contents were similar between treatments, but the H_2O_2 was much higher under Put0 in comparison to control. Fronds sprayed with Put had lower increase of H_2O_2, suggesting it could play direct or indirect roles in scavenging H_2O_2. Both SOD and CAT are key antioxidant

enzymes that have high ability of scavenging ROS under stress (Pan et al., 2006). SOD could convert $O_2^{\bullet -}$ into H_2O_2 in cells and CAT converts H_2O_2 into H_2O and O_2 (Hossain et al., 2006; Liu et al., 2015). In the current study, SOD activities of the cut foliage under spraying treatments were not significantly different in comparison to control, probably due to the similar $O_2^{\bullet -}$ contents between treatments. The activity of CAT was significantly elevated after 10 days in foliage sprayed with deionized water (Put0), suggesting the increase in CAT activity may be used to remove H_2O_2. It has been reported that an increase in PA content up-regulated the expression of genes encoding antioxidant enzymes and enhanced the activities of SOD, APX, and CAT under stress (Nayyar and Chander, 2004; Tang and Newton, 2005; Wi et al., 2006; Kuznetsov and Shevyakova, 2010). However, our results show that the SOD and CAT activities in Put-sprayed foliage were not significantly higher, even lower than those in Put0-sprayed foliage. Furthermore, the AsA content decreased with the leaf senescence, even lower in Put-sprayed foliage than that in Put0 treatment. These results indicate that Put detoxified the H_2O_2 directly or indirectly by triggering other pathways such as the γ-aminobutyric acid (GABA) shunt pathway (Groppa and Benavides, 2008; Palma et al., 2015; Palma et al., 2019).

Cellular membrane is very important for maintaining the osmotic balance of cells. ROS can attack the membrane and disrupt its integrity (Lim et al., 2007; Mohammadi et al., 2018). EL and MDA content are indicators of plasma membrane permeability and stability (Liu et al., 2015; Palma et al., 2016; Torabian et al., 2018). In the present study, foliage sprayed with deionized water had higher EL and MDA content while foliage sprayed with Put had slightly higher values or no significant difference compared to control, suggesting lower lipid peroxidation and higher membrane stability in Put-treated leaves (Wilhelmová et al., 2006). This result could be partly explained by the change of H_2O_2. In addition, this result could also be due to Put's polycationic nature and it can directly bind to phospholipids to stabilize the membrane (Tiburcio et al., 1994; Bouchereau et al., 1999). During leaf senescence, the degradation of macromolecules and disassembly of cellular contents are often observed. In this study, Sp and Pro contents were decreased whereas Ss content was increased. This result indicates that protein degradation and Pro catabolism occurred after 10 days in vase (Zhang and Becker, 2015). However, Put spraying deterred this process. It is probably because Put is polycationic and could bind and stabilize these macromolecules (Tassoni et al., 1996). Another reason might be due to Put could enter the cell nuclear and produce thermospermine, then upregulate the prosurvival genes and activate ribosomal protein, finally produce more protein (Breeze et al., 2011; Moschou and Roubelakis-Angelakis, 2014). It has been proposed that the high level of Ss is the cause of senescence because of its repression of photosynthesis (van Doorn, 2008). Put spraying alleviated the increase of Ss content, suggesting that it could weaken the sugar signaling for anti-aging which is similar to the role of melatonin (Wang et al., 2013).

Generally, Fv/Fm, ΦPSII, and qP decrease under stresses and regulated-energy dissipation indicated by NPQ and ΦNPQ increase at first but decrease when the stress is more severe, while ΦNO increases (Gorbe and Calatayud, 2012). The decreased value of Fv/Fm often indicates photoinhibition (Thwe et al., 2014). In the present study, the fronds sprayed with deionized water (Put0) had a lower Fv/Fm compared with control, indicating the emergence of photoinhibition. The increase of ΦNO further confirmed that photodamage had occurred (Zhang et al., 2018). We found that the changes of Fv/Fm and ΦNO, indicators of photoinhibition and photodamage, respectively, were mitigated by the Put spraying. The values of ΦPSII, qP, and ETR were significantly reduced in fronds sprayed with deionized water (Put0) compared with control. The malfunction of the electron transport chain probably further induced the generation of H_2O_2 (Gupta et al., 2016). However, qP of the fronds sprayed with Put was not significantly different from qP in control. This result is in accord with a previous study showing that both ΦPSII and qP of cucumber plants under NaCl stress were reduced, while the reductions were alleviated to the control level by treatment with Put (Zhang et al., 2009). The mitigating effect of Put could be due to its polycationic nature, which induces the electrostatic screening, causes the stacking of thylakoid membrane and increases a spatial segregation of PSII and PSI (Barber, 1982; Ioannidis et al., 2006). In addition, Put can act as a permeant buffer to stimulate the synthesis of ATP, which can be used for PSII recovery after stress (Ioannidis et al., 2006; Ioannidis and Kotzabasis, 2007; Wu et al., 2019). The high value of NPQ indicates that plant has a high photo-protective ability and can protect itself from the damage *via* dissipation of excessive energy (Shu et al., 2013). In our study, we observed that NPQ in Put0 was significantly lower than that in control, suggesting the foliage was aging very serious after 10 days of treatment. Exogenous Put spraying significantly increased NPQ in the fronds compared with Put0. These results indicate that Put protects PSII against over-excitation by regulating heat dissipation probably through the aggregation of light harvest complex II (LHCII) (Pascal et al., 2005).

Chl fluorescence imaging is a non-destructive and easy operating technique that can rapidly detect spatial heterogeneities in fluorescence emission pattern and photosynthetic capacity across the leaf surface, even before visual injury appears (Omasa and Takayama, 2003; Calatayud et al., 2006; Gorbe and Calatayud, 2012). This technique is very useful for identifying early stress-induced damage. In the present study, the visible injury on frond surface was not severe and could not be detected easily by naked eye, except for fronds treated with Put0 (**Figure 1**), but the images of chlorophyll fluorescence parameters showed that the photochemical activity had already been inhibited and photodamage had occurred under both Put0 and Put0.2 treatments (**Figure 7**). In addition, there was obvious spatial heterogeneity in the fluorescence emission patterns over the frond surface under these two treatments. Mesophyll cells near the midrib in some leaflets under Put0 and Put0.2 treatments had lower Fv/Fm, ΦPSII, and ΦNPQ, but had higher ΦNO than mesophyll cells in other parts of the leaf. There is a report suggesting that leaf section next to the midrib has a more severe change of chlorophyll fluorescence parameters

(Gorbe, 2009). They also find that the capacity of photoprotection of PSII, indicated by the ratio ΦNPQ/ΦNO decreases progressively as flower shoots wilt and vase life ends in cut rose flowers (Gorbe, 2009). Our results showed that the leaflets under Put0 and Put0.2 treatments lost the photoprotection ability due to the decreased ΦNPQ and increased ΦNO, while those sprayed with 2.0 mM Put still had this capability of dissipating excess energy. From the image of ΦNPQ, a significant difference among treatments was observed while the average values of this parameter among treatments were not different significantly. This result suggests that it is better to combine the qualitative and quantitative chlorophyll fluorescence analysis together to describe leaf senescence.

In conclusion, we investigated the effects of Put on senescence of cut foliage in sword fern. After fronds were detached from the plants, the Chl, Sp, and Pro contents were decreased, EL, MDA, and H_2O_2 contents were increased, plasma membrane was impaired, photochemical activity was inhibited, and photoinhibition and photodamage happened. Both 0.2 and 2.0 mM Put spraying extended the vase life of the cut foliage and alleviated the changes of parameters caused by senescence. In addition, 2.0 mM Put had a better mitigating ability than that of 0.2 mM. Leaf spraying of 2.0 mM Put for 10 days significantly ameliorated the losses of Chl, Sp, and Pro content (−10.72, −26.29, and −42.64%, respectively), followed by 0.2 mM Put (−27.36, −36.24, and −60.55%, respectively). Put spraying also improved photochemical capability and prevented membrane impairment as well as visible injury in comparison with cut fronds sprayed with deionized water. Leaf spraying of 2.0 mM Put greatly reduced the decline of the effective quantum yield of photochemical energy conversion in PSII (ΦPSII), the maximal quantum yield of PSII photochemistry measured in the dark-adapted state (Fv/Fm) and electron transport rate (ETR) (−7.89, −12.91, and −10.06%, respectively), and also inhibited the increases of EL, MDA, Ss, and H_2O_2 (+31.87, +6.43, +16.22, and +49.40%, respectively). Overall, Put played important roles in deterring the degradation of Chl, Ss, and Pro, detoxifying the H_2O_2, weakening the sugar signaling, mitigating the decline of photochemical activity, and postponing the leaf senescence. The present study gives new insights into effects of Put on leaf senescence and provides a strategy for preserving post-harvest cut foliage.

DATA AVAILABILITY STATEMENT

All datasets presented in this study are included in the article.

AUTHOR CONTRIBUTIONS

LZ and TW designed research. YQ, LJ, and SM conducted experiments. YQ, FX, and YC analyzed data. LZ, YQ, and TW wrote the manuscript. All authors contributed to the article and approved the submitted version.

FUNDING

This research was supported financially by National Natural Science Foundation of China (No. 31711530648), the open funding of State Key Laboratory of Tree Genetics and Breeding (TGB2019004), Northeast Agricultural University of China (Academic backbone Project, No.18XG07), and Achimedes Foundation of Estonia.

ACKNOWLEDGMENTS

The authors thank Dr. Hanna Hõrak for her kind editing of this manuscript.

REFERENCES

Altman, A. (1982). Retardation of radish leaf senescence by polyamines. *Physiol. Plant.* 54 (2), 189–193. doi: 10.1111/j.1399-3054.1982.tb06324.x

Ataii, D., Naderi, R., and Khandan-Mirkohi, A. (2015). Exogenous putrescine delays senescence of Lisianthus cut flowers. *J. Ornam. Plants* 5 (3), 167–174.

Banthoengsuk, S., Ketsa, S., and van Doorn, W. G. (2011). 1-MCP partially alleviates dehydration-induced abscission in cut leaves of the fern *Nephrolepis cordifolia*. Postharvest Biol. *Technolology* 59 (3), 253–257. doi: 10.1016/j.postharvbio.2010.10.001

Barber, J. (1982). Influence of surface charges on thylakoid structure and function. *Annu. Rev. Plant Physiol.* 33, 261–295. doi: 10.1146/annurev.pp.33.060182.001401

Beigbeder, A., Vavadakis, M., Navakoudis, E., and Kotzabasis, K. (1995). Influence of polyamine inhibitors on light-independent and light-dependent chlorophyll biosynthesis and on the photosynthetic rate. *J. Photochem. Photobiol.* 28 (3), 235–242. doi: 10.1016/1011-1344(95)07113-G

Bouchereau, A., Aziz, A., Larher, F., and Martin-Tanguy, J. (1999). Polyamines and environmental challenges: recent development. *Plant Sci.* 140 (2), 103–125. doi: 10.1016/S0168-9452(98)00218-0

Bradford, M. M. (1976). A rapid and sensitive method for the quantitation of microgram quantities of protein utilizing the principle of protein-dye binding. *Anal. Biochem.* 72, 248–254. doi: 10.1016/0003-2697(76)90527-3

Breeze, E., Harrison, E., McHattie, S., Hughes, L., Hickman, R., Hill, C., et al. (2011). High-resolution temporal profiling of transcripts during Arabidopsis leaf senescence reveals a distinct chronology of processes and regulation. *Plant Cell* 23 (3), 873–894. doi: 10.1105/tpc.111.083345

Breusegem, F. V., and Dat, J. F. (2006). Reactive oxygen species in plant cell death. *Plant Physiol.* 141 (2), 384–390. doi: 10.1104/pp.106.078295

Calatayud, A., Roca, D., and Martínez, P. F. (2006). Spatial-temporal variations in rose leaves under water stress conditions studied by chlorophyll fluorescence imaging. *Plant Physiol. Biochem.* 44 (10), 564–573. doi: 10.1016/j.plaphy.2006.09.015

Che-Husin, N. M., Joyce, D. C., and Irving, D. E. (2018). Gel xylem occlusions decrease hydraulic conductance of cut *Acacia holosericea* foliage stems. *Postharvest Biol. Technol.* 135, 27–37. doi: 10.1016/j.postharvbio.2017.08.015

Chen, D. Q., Wang, S. W., Xiong, B. L., Cao, B. B., and Deng, X. P. (2015). Carbon/nitrogen imbalance associated with drought-induced leaf senescence in *Sorghum bicolor*. *PloS One* 10 (8), e0137026. doi: 10.1371/journal.pone.0137026

Cho, H. T., and Hong, Y. N. (1988). Effects of putrescine on senescence in detached leaves of Chinese cabbage in the light. *Korean J. Bot.* 31 (3), 227–237.

Díaz-Vivancos, P., Clemente-Moreno, M. J., Rubio, M., Olmos, E., García, J. A., Martínez-Gómez, P., et al. (2008). Alteration in the chloroplastic metabolism leads to ROS accumulation in pea plants in response to plum pox virus. *J. Exp. Bot.* 59, 2147–2160. doi: 10.1093/jxb/ern082

Gorbe, E., and Calatayud, A. (2012). Applications of chlorophyll fluorescence imaging technique in horticultural reaearch: a review. *Sci. Hortic.* 138, 24–35. doi: 10.1016/j.scienta.2012.02.002

Gorbe, E. (2009). *Study of nutrient solution management in soilless rose cultivation through the analysis of physiological parameters and nutrient absorption. PhD thesis* (Polytechnical University of Valencia). doi: 10.4995/Thesis/10251/6921

Groppa, M. D., and Benavides, M. P. (2008). Polyamines and abiotic stress: recent advances. *Amino Acids* 34 (1), 35–45. doi: 10.1007/s00726-007-0501-8

Gupta, K., Sengupta, A., Chakraborty, M., and Gupta, B. (2016). Hydrogen peroxide and polyamines act as double edged swords in plant abiotic stress responses. *Front. Plant Sci.* 7, 1343. doi: 10.3389/fpls.2016.01343

Hörtensteiner, S. (2006). Chlorophyll degradation during senescence. *Annu. Rev. Plant Biol.* 57, 55–77. doi: 10.1146/annurev.arplant.57.032905.105212

Hossain, Z., Mandal, A. K. A., Datta, S. K., and Biswas, A. K. (2006). Decline in ascorbate peroxidase activity–A prerequisite factor for tepal senescence in gladiolus. *J. Plant Physiol.* 163 (2), 186–194. doi: 10.1016/j.jplph.2005.03.004

Ioannidis, N. E., and Kotzabasis, K. (2007). Effects of polyamines on the functionality of photosynthetic membrane in vivo and in vitro. *BBA* 1767, 1372–1382. doi: 10.1016/j.bbabio.2007.10.002

Ioannidis, N. E., Sfichi, L., and Kotzabasis, K. (2006). Putrescine stimulates chemiosmotic ATP synthesis. *BBA-Bioenergetics* 1757 (7), 821–828. doi: 10.1016/j.bbabio.2006.05.034

Kim, J. S., Yun, B. W., Choi, J. S., Kim, T. J., Kwak, S. S., and Cho, K. Y. (2004). Death mechanisms caused by carotenoid biosynthesis inhibitors in green and in undeveloped plant tissues. *Pestic. Biochem. Physiol.* 78 (3), 127–139. doi: 10.1016/j.pestbp.2003.12.001

Kitajima, M., and Butler, W. L. (1975). Quenching of chlorophyll fluorescence and primary photochemistry in chloroplasts by dibromothymoquinone. *BBA-Bioenergetics* 376 (1), 105–115. doi: 10.1016/0005-2728(75)90209-1

Kusano, T., Berberich, T., Tateda, C., and Takahashi, Y. (2008). Polyamines: essential factors for growth and survival. *Planta* 228 (3), 367–381. doi: 10.1007/s00425-008-0772-7

Kuznetsov, V. V., and Shevyakova, N. I. (2010). "Polyamines and plant adaptation to saline environments," in *Desert plants* (Berlin, Heidelberg: Springer), 261–298. doi: 10.1007/978-3-642-02550-1_13

Law, M. Y., Charles, S. A., and Halliwell, B. (1983). Glutathione and ascorbic acid in spinach (*Spinacia oleracea*) chloroplasts. The effect of hydrogen peroxide and of Paraquat. *Biochem. J.* 210, 899–903. doi: 10.1042/bj2100899

Leng, F., Sun, S., Jing, Y., Wang, F., Wei, Q., Wang, X., et al. (2016). A rapid and sensitive method for determination of trace amounts of glucose by anthrone-sulfuric acid method. *Bulg. Chem. Commun.* 48 (1), 109–113.

Li, X., Zhang, X. M., Wu, Y. S., Li, B. Q., and Yang, Y. P. (2018). Physiological and biochemical analysis of mechanisms underlying cadmium tolerance and accumulation in turnip. *Plant Divers.* 40 (1), 19–27. doi: 10.1016/j.pld.2017.12.005

Lim, P. O., Kim, H. J., and Gil Nam, H. (2007). Leaf senescence. *Annu. Rev. Plant Biol.* 58 (1), 115–136. doi: 10.1146/annurev.arplant.57.032905.105316

Lin, S., Li, H., Xian, X., Lin, X., Pang, Z., Liu, J., et al. (2019). Nano-silver pretreatment delays wilting of cut gardenia foliage by inhibiting bacterial xylem blockage. *Sci. Hortic.* 246, 791–796. doi: 10.1016/j.scienta.2018.11.050

Liu, X., Sui, L. H., Huang, Y. Z., Geng, C. M., and Yin, B. H. (2015). Physiological and visible injury responses in different growth stages of winter wheat to ozone stress and the protection of spermidine. *Atmos. Pollut. Res.* 6 (4), 596–604. doi: 10.5094/APR.2015.067

Lutts, S., Kinet, J. M., and Bouharmont, J. (1996). NaCl-induced senescence in leaves of rice (*Oryza sativa* L.) cultivars differing in salinity resistance. *Ann. Bot.* 78 (3), 389–398. doi: 10.1006/anbo.1996.0134

Malakar, M., Acharyya, P., and Biswas, S. (2017). Effect of certain chemicals on post harvest life of some cut foliages. *Int. J. Agric. Environ. Biotechnol.* 10 (2), 199–207. doi: 10.5958/2230-732X.2017.00023.7

Merzlyak, M. N., and Hendry, G. A. F. (1994). Free radical metabolism, pigment degradation and lipid peroxidation in leaves during senescence. *P. R. Soc B.-Biol. Sci.* 102, 459–471. doi: 10.1017/S0269727000014482

Mohammadi, H., Ghorbanpour, M., and Brestic, M. (2018). Exogenous putrescine changes redox regulations and essential oil constituents in field-grown *Thymus vulgaris* L. under well-watered and drought stress conditions. *Ind. Crop Prod.* 122, 119–132. doi: 10.1016/j.indcrop.2018.05.064

Moschou, P. N., and Roubelakis-Angelakis, K. A. (2014). Polyamines and programmed cell death. *J. Exp. Bot.* 65 (5), 1285–1296. doi: 10.1093/jxb/ert373

Nayyar, H., and Chander, S. (2004). Protective effects of polyamines against oxidative stress induced by water and cold stress in chickpea. *J. Agron. Crop Sci.* 190, 355–365. doi: 10.1111/j.1439-037X.2004.00106.x

Nisar, S., Tahir, I., and Ahmad, S. S. (2015). Modulation of flower senescence in *Nicotiana plumbaginifolia* L. by polyamines. *Indian J. Plant Physiol.* 20 (2), 186–190. doi: 10.1007/s40502-015-0154-7

Omasa, K., and Takayama, K. (2003). Simultaneous measurement of stomatal conductance, non-photochemical quenching, and photochemical yield of photosystem II in intact leaves by thermal and chlorophyll fluorescence imaging. *Plant Cell Physiol.* 44 (12), 1290–1300. doi: 10.1093/pcp/pcg165

Palma, F., Carvajal, F., Ramos, J. M., Jamilena, M., and Garrido, D. (2015). Effect of putrescine application on maintenance of zucchini fruit quality during cold storage: contribution of GABA shunt and other related nitrogen metabolites. *Postharvest Biol. Technol.* 99, 131–140. doi: 10.1016/j.postharvbio.2014.08.010

Palma, F., Carvajal, F., Jamilena, M., and Garrido, D. (2016). Putrescine treatment increases the antioxidant response and carbohydrate content in zucchini fruit stored at low temperture. *Postharvest Biol. Technol.* 118, 68–70. doi: 10.1016/j.postharvbio.2016.03.009

Palma, F., Carvajal, F., Jiménez-Muñoz, R., Pulido, A., Jamilena, M., and Garrido, D. (2019). Exogenous γ-aminobutyric acid treatment improves the cold tolerance of zucchini fruit during postharvest storage. *Plant Physiol. Biochem.* 136, 188–195. doi: 10.1016/j.plaphy.2019.01.023

Pan, Y., Wu, L. J., and Yu, Z. L. (2006). Effect of salt and drought stress on antioxidant enzymes activities and SOD isoenzymes of liquorice (*Glycyrrhiza uralensis Fisch*). *Plant Growth Regul.* 49, 157–165. doi: 10.1007/s10725-006-9101-y

Paoletti, E., Ferrara, A. M., Calatayud, V., Cerveró, J., Giannetti, F., Sanz-Sanchez, M. J., et al. (2009). Deciduous shrubs for ozone bioindication *Hibiscus syriacus* as an example. *Environ. Pollut.* 157 (3), 865–870. doi: 10.1016/j.envpol.2008.11.009

Pascal, A. A., Liu, Z., Broess, K., van Oort, B., van Amerongen, H., Wang, C., et al. (2005). Molecular basis of photoprotection and control of photosynthetic light-harvesting. *Nature* 436, 134–137. doi: 10.1038/nature03795

Paschalidis, K. A., and Roubelakis-Angelakis, K. A. (2005). Spatial and temporal distribution of polyamine levels and polyamine anabolism in different organs/tissues of the tobacco plant. Correlations with age, cell division/expansion, and differentiation. *Plant Physiol.* 138 (1), 142–152. doi: 10.1104/pp.104.055483

Patterson, B. D., Macrae, E. A., and Ferguson, I. B. (1984). Estimation of hydrogen peroxide in plant extracts using titanium (IV). *Anal. Biochem.* 139 (2), 487–492. doi: 10.1016/0003-2697(84)90039-3

Rubinowska, K., Pogroszewska, E., and Michalek, W. (2012). The effect of polyamines on physiological parameters of post-harvest quality of cut stems of *Rosa* 'Red Berlin'. *Acta Sci. Pol. Hortorum Cultus* 11 (6), 81–93.

Safeena, S. A., Thangam, M., and Singh, N. P. (2019). Conservation and evaluation of different cut foliage species comprising pteridophytes (ferns and fern allies) of west coast regions of India. *J. Indian Soc Coastal Agric. Res.* 37 (1), 7–13.

Scrob, T., Hosu, A., and Cimpoiu, C. (2019). The Influence of in Vitro Gastrointestinal Digestion of *Brassica oleracea* Florets on the Antioxidant Activity and Chlorophyll, Carotenoid and Phenolic Content. *Antioxidants* 8 (7), 212. doi: 10.3390/antiox8070212

Serrano, M., Amorós, A., Pretel, M. T., Martínez-Madrid, M. C., and Romojaro, F. (2001). Preservative solutions containing boric acid delay senescence of carnation flowers. *Postharvest Biol. Technol.* 23 (2), 133–142. doi: 10.1016/S0925-5214(01)00108-9

Shabanian, S., Esfahani, M. N., Karamian, R., and Tran, L. S. P. (2018). Physiological and biochemical modifications by postharvest treatment with sodium nitroprusside extend vase life of cut flowers of two gerbera cultivars. *Postharvest Biol. Technol.* 137, 1–8. doi: 10.1016/j.postharvbio.2017.11.009

Sharma, S., Pareek, S., Sagar, N. A., Valero, D., and Serrano, M. (2017). Modulatory effects of exogenously applied polyamines on postharvest physiology, antioxidant system and shelf life of fruits: a review. *Int. J. Mol. Sci.* 18 (8), 1789. doi: 10.3390/ijms18081789

Shu, S., Yuan, L. Y., Guo, S. R., Sun, J., and Yuan, Y. H. (2013). Effects of exogenous spermine on chlorophyll fluorescence, antioxidant system and ultrastructure of chloroplasts in *Cucumis sativus* L. under salt stress. *Plant Physiol. Biochem.* 63, 209–216. doi: 10.1016/j.plaphy.2012.11.028

Skutnik, E., Rabiza-Świder, J., Wachowicz, M., and Łukaszewska, A. J. (2004). Senescence of cut leaves of *Zantedeschia aethiopica* and *Z. elliottiana.* part I. chlorophyll degradation. *Acta Sci. Pol. Hortorum Cultus* 3 (2), 57–65.

Sobieszczuk-Nowicka, E., Kubala, S., Zmienko, A., Małecka, A., and Legocka, J. (2016). From accumulation to degradation: reprogramming polyamine metabolism facilitates dark-induced senescence in barley leaf cells. *Front. Plant Sci.* 6, 1198. doi: 10.3389/fpls.2015.01198

Sood, S., and Nagar, P. K. (2003). The effect of polyamines on leaf senescence in two diverse rose species. *Plant Growth Regul.* 39 (2), 155–160. doi: 10.1023/A:1022514712295

Syeed, S., Anjum, N. A., Nazar, R., Iqbal, N., Masood, A., and Khan, N. A. (2011). Salicylic acid-mediated changes in photosynthesis, nutrients content and antioxidant metabolism in two mustard (*Brassica juncea* L.) cultivars differing in salt tolerance. *Acta Physiol. Plant* 33 (3), 877–886. doi: 10.1007/s11738-010-0614-7

Tang, W., and Newton, R. J. (2005). Polyamines reduce salt-induced oxidative damage by increasing the activities of antioxidant enzymes and decreasing lipid peroxidation in Virginia pine. *Plant Growth Regul.* 46, 31–43. doi: 10.1007/s10725-005-6395-0

Tassoni, A., Antognoni, F., and Bagni, N. (1996). Polyamine binding to plasma membrane vesicles isolated from zucchini hypocotyls. *Plant Physiol.* 110 (3), 817–824. doi: 10.1104/pp.110.3.817

Teerarak, M., and Laosinwattana, C. (2019). Essential oil from ginger as a novel agent in delaying senescence of cut fronds of the fern (*Davallia solida* (G. Forst.) Sw.). *Postharvest Biol. Technol.* 156, 110927. doi: 10.1016/j.postharvbio.2019.06.001

Teklić, T., Špoljarević, M., Stanisavljević, A., Lisjak, M., Vinković, T., Paradiković, N., et al. (2010). Assessment of the influence of different sample processing and cold storage duration on plant free proline content analyses. *Phytochem. Anal.* 21, 561–565. doi: 10.1002/pca.1233

Thwe, A. A., Vercambre, G., Gautier, H., Gay, F., Phattaralerphong, J., and Kasemsap, P. (2014). Response of photosynthesis and chlorophyll fluorescence to acute ozone stress in tomato (*Solanum lycopersicum* Mill.). *Photosynthetica* 52 (1), 105–116. doi: 10.1007/s11099-014-0012-2

Tian, M., Gu, Q., and Zhu, M. Y. (2003). The involvement of hydrogen peroxide and antioxidant enzymes in the process of shoot organogenesis of strawberry callus. *Plant Sci.* 165, 701–707. doi: 10.1016/S0168-9452(03)00224-3

Tiburcio, A. F., Besford, R. T., Capell, T., Borrell, A., Testillano, P. S., and Risueno, M. C. (1994). Mechanisms of polyamine action during senescence responses induced by osmotic stress. *J. Exp. Bot.* 45 (12), 1789–1800. doi: 10.1093/jxb/45.12.1789

Torabian, S., Shakiba, M. R., Dabbagh, M. N. A., and Toorchi, M. (2018). Leaf gas exchange and grain yield of common bean exposed to spermidine under water stress. *Photosynthetica* 56, 1387–1397. doi: 10.1007/s11099-018-0834-4

van Doorn, W. G. (2008). Is the onset of senescence in leaf cells of intact plants due to low or high sugar levels? *J. Exp. Bot.* 59 (8), 1963–1972. doi: 10.1093/jxb/ern076

Wang, P., Sun, X., Chang, C., Feng, F., Liang, D., Cheng, L., et al. (2013). Delay in leaf senescence of *Malus hupehensis* by long-term melatonin application is associated with its regulation of metabolic status and protein degradation. *J. Pineal Res.* 55 (4), 424–434. doi: 10.1111/jpi.12091

Wi, S. J., Kim, W. T., and Park, K. Y. (2006). Overexpression of carnation S-adenosylmethionine decarboxylase gene generates a broad-spectrum tolerance to abiotic stresses in transgenic tobacco plants. *Plant Cell Rep.* 25, 1111–1121. doi: 10.1007/s00299-006-0160-3

Wilhelmová, N., Domingues, P. M. D. N., Srbová, M., Fuksová, H., and Wilhelm, J. (2006). Changes in non-polar aldehydes in bean cotyledons during aging. *Biol. Plantarum* 50 (4), 559–564. doi: 10.1007/s10535-006-0088-z

Wu, X., Shu, S., Wang, Y., Yuan, R., and Guo, S. (2019). Exogenous putrescine alleviates photoinhibition caused by salt stress through cooperation with cyclic electron flow in cucumber. *Photosynth. Res.* 141 (3), 303–314. doi: 10.1007/s11120-019-00631-y

Yiu, J. C., Juang, L. D., Fang, D. Y. T., Liu, C. W., and Wu, S. J. (2009). Exogenous putrescine reduces flooding-induced oxidative damage by increasing the antioxidant properties of Welsh onion. *Sci. Horti.* 120 (3), 306–314. doi: 10.1016/j.scienta.2008.11.020

Zamani, S., Kazemi, M., and Aran, M. (2011). Postharvest life of cut rose flowers as affected by salicylic acid and glutamine. *World Appl. Sci. J.* 12, 1621–1624.

Zhang, L., and Becker, D. (2015). Connecting proline metabolism and signaling pathways in plant senescence. *Front. Plant Sci.* 6, 552. doi: 10.3389/fpls.2015.00552

Zhang, R. H., Li, J., Guo, S. R., and Tezuka, T. (2009). Effects of exogenous putrescine on gas-exchange characteristics and chlorophyll fluorescence of NaCl-stressed cucumber seedlings. *Photosynth. Res.* 100 (3), 155–162. doi: 10.1007/s11120-009-9441-30

Zhang, L., Jia, L. L., Sui, J. X., Wen, M. X., and Chen, Y. J. (2018). Ameliorating effects of three kinds of antioxidants to ozone- polluted painted nettle (*Coleus blumei* Benth.). *Photosynthetica* 56 (2), 623–632. doi: 10.1007/s11099-017-0693-4

Zhao, D. Q., Wang, R., Meng, J. S., Li, Z. Y., Wu, Y. Q., and Tao, J. (2017). Ameliorative effects of melatonin on dark-induced leaf senescence in gardenia (*Gardenia jasminoides* Ellis): leaf morphology, anatomy, physiology and transcriptome. *Sci. Rep.* 7, 10423. doi: 10.1038/s41598-017-10799-9

Zheng, Q. L., Zuo, J. H., Gu, S. T., Gao, L. P., Hu, W. Z., Wang, Q., et al. (2019). Putrescine treatment reduces yellowing during senescence of broccoli (*Brassica oleracea* L. var. *italica*). *Postharvest Biol. Technol.* 152, 29–35. doi: 10.1016/j.postharvbio.2019.02.014

Conflict of Interest: The authors declare that the research was conducted in the absence of any commercial or financial relationships that could be construed as a potential conflict of interest.

frontiers in Plant Science

ORIGINAL RESEARCH
published: 09 November 2020
doi: 10.3389/fpls.2020.584822

Digital Image Analysis Using *FloCIA* Software for Ornamental Sunflower Ray Floret Color Evaluation

Martina Zorić[1], Sandra Cvejić[2], Emina Mladenović[3], Siniša Jocić[2], Zdenka Babić[4], Ana Marjanović Jeromela[2] and Dragana Miladinović[2]*

[1] Institute of Lowland Forestry and Environment, University of Novi Sad, Novi Sad, Serbia, [2] Sunflower Department, Institute of Field and Vegetable Crops, Novi Sad, Serbia, [3] Faculty of Agriculture, University of Novi Sad, Novi Sad, Serbia, [4] Faculty of Electrical Engineering, University of Banja Luka, Banja Luka, Bosnia and Herzegovina

As an esthetic trait, ray floret color has a high importance in the development of new sunflower genotypes and their market value. Standard methodology for the evaluation of sunflower ray florets is based on International Union for the Protection of New Varieties of Plants (UPOV) guidelines for sunflower. The major deficiency of this methodology is the necessity of high expertise from evaluators and its high subjectivity. To test the hypothesis that humans cannot distinguish colors equally, six commercial sunflower genotypes were evaluated by 100 agriculture experts, using UPOV guidelines. Moreover, the paper proposes a new methodology for sunflower ray floret color classification – digital UPOV (dUPOV), that relies on software image analysis but still leaves the final decision to the evaluator. For this purpose, we created a new *Flower Color Image Analysis* (*FloCIA*) software for sunflower ray floret digital image segmentation and automatic classification into one of the categories given by the UPOV guidelines. To assess the benefits and relevance of this method, accuracy of the newly developed software was studied by comparing 153 digital photographs of F_2 genotypes with expert evaluator answers which were used as the ground truth. The *FloCIA* enabled visualizations of segmentation of ray floret images of sunflower genotypes used in the study, as well as two dominant color clusters, percentages of pixels belonging to each UPOV color category with graphical representation in the CIE (International Commission on Illumination) L*a*b* (or simply Lab) color space in relation to the mean vectors of the UPOV category. Precision (repeatability) of ray flower color determination was greater between dUPOV based expert color evaluation and software evaluation than between two UPOV based evaluations performed by the same expert. The accuracy of *FloCIA* software used for unsupervised (automatic) classification was 91.50% on the image dataset containing 153 photographs of F_2 genotypes. In this case, the software and the experts had classified 140 out of 153 of images in the same color categories. This visual presentation can serve as a guideline for evaluators to determine the dominant color and to conclude if more than one significant color exists in the examined genotype.

Keywords: sunflower, breeding, ornamental value, digital UPOV, software, classification

OPEN ACCESS

Edited by:
Patrícia Duarte De Oliveira Paiva, Federal University of Lavras, Brazil

Reviewed by:
Bruno Trevenzoli Favero, University of Copenhagen, Denmark
Diogo Pedrosa Correa Silva, Universidade Federal de Lavras, Brazil

****Correspondence:***
Sandra Cvejić
sandra.cvejic@ifvcns.ns.ac.rs

Specialty section:
This article was submitted to Crop and Product Physiology, a section of the journal Frontiers in Plant Science

Received: *18 July 2020*
Accepted: *20 October 2020*
Published: *09 November 2020*

Citation:
Zorić M, Cvejić S, Mladenović E, Jocić S, Babić Z, Marjanović Jeromela A and Miladinović D (2020) Digital Image Analysis Using FloCIA Software for Ornamental Sunflower Ray Floret Color Evaluation. Front. Plant Sci. 11:584822. doi: 10.3389/fpls.2020.584822

INTRODUCTION

Sunflower (*Helianthus annuus* L.), is a common plant species that is grown for different purposes. Following its introduction into Europe by Spanish sailors, the 'flower of the sun' or 'the New World flower,' as it was called at the time, quickly gained popularity as an ornamental plant (Kaya et al., 2012). For almost 200 years, sunflowers were grown in Europe exclusively as ornamental plants (Cvejić et al., 2016). Today, most of the cultivated sunflower plants are used for oil production, as confectionery sunflowers, or as bird feed. In recent years, sunflower has been "rediscovered" as an interesting ornamental plant due to its beauty and possibility to be used both as an ornamental cut flower and as potted plant (Mladenović et al., 2016). Since sunflower has moderate drought tolerance and can be grown in different agroecological conditions (Miladinović et al., 2019), its utilization, as ornamental plant, that is based upon floral and vegetative characteristics rather than seed production, permits its cultivation under even wider spectrum of agroecological conditions (Vuppalapti, 2005).

The main esthetic quality of ornamental sunflower is high variation in shape and texture, as well in the color of the flower. Sunflower inflorescence consists of fertile disk florets, located in the internal part of the flower head and circular arranged sterile ray florets around them. The color of sunflower disk florets can vary from dark red to completely white. Ray florets are mostly yellow, but may also appear in different shades of red, orange, lemon-yellow, white, or combination of these colors (Cvejić et al., 2016). New types of floricultural crops are in demand at the market and among consumers eager for new varieties with ornamental value, such as flowers with new shapes and colors (Shibata, 2008). According to Jocić et al. (2015), ornamental sunflower producers are, considering market requirements, mostly interested in the variation of flower color, and the structure of ray florets. As in most of the cultivated plants, the market also defines the breeding objectives in ornamental sunflower, where the focus is on desirable plant architecture, colors of ray and disk florets, and a prolonged duration of flowering (Cvejić and Jocić, 2010).

The quality of new plant genotypes can be evaluated using numerous criteria, but for ornamental plants, the most important criterion is flower color, hence extensive selection and breeding is done to develop new phenotypes (Bohorquez-Restrepo, 2015). The same stands for ornamental sunflower breeding, where the most important feature in terms of ornamental value is the color of ray florets (Divita et al., 2012). Phenotyping during creation of new genotypes is done using UPOV descriptor for sunflower (UPOV, 2000), and the complete process of phenotypic traits evaluation, including ray floret color determination, is done subjectively. Considering the fact that people see colors differently, the subjective approach to the description of crucial ornamental sunflower traits, such as ray floret color, could lead to inconsistency between how ray floret color is observed by breeders as opposed to catalog description of a commercial variety. This discrepancy could potentially have a negative influence on further research of new genotypes, ornamental sunflower market, and customer preferences, as well as protection of breeders' rights.

In this paper, we have described a new methodology for ornamental sunflower ray floret color classification, based on in-house developed *Flower Color Image Analysis* (*FloCIA*) software performed in Lab color space. Based on the UPOV descriptor for sunflower, we have developed a new, digital UPOV for sunflower ray floret color classification (dUPOV), that relies on software image analysis but still leaves to evaluator the possibility of making the final decision.

MATERIALS AND METHODS

Plant Material

Images of six proprietary ornamental sunflower genotypes were used for the evaluation of the ray floret colors, as well as segmentation of UPOV categories (**Table 1**), while images of 153 F_2 genotypes were used for testing of *FloCIA* software accuracy[1].

Experimental Trial

The material was collected during the 2017 and 2018 growing seasons, in Serbia (45.26°N, 19.83°E). Observations of ray floret color were carried out in the flowering phase F 3.2 as recommended by the UPOV guidelines for sunflower (UPOV, 2000). Visual assessment based on the UPOV guidelines was performed in the field. All examined genotypes were photographed using Nikon 3300 camera, with 6000 × 4000 resolution, in.png format. The photographs of each sunflower flower were taken without flash, during early morning with the sun facing the flowers to ensure environmental conditions as uniform as possible for each photograph taken. The white background (cloth) was placed behind each flower in order to facilitate background subtraction and ray floret segmentation. Ray floret color evaluation was performed using the data collected and analyzed from two separate studies; assessments based on the UPOV descriptor for sunflower (UPOV, 2000) and the proposed methodology based on in-house designed software for digital image processing for image segmentation, petals' pixels classification into UPOV color groups and statistical analysis.

Methodology Based on UPOV Guidelines

The UPOV descriptor for sunflower provides guidelines for the assessment of 11 characteristics related to ray and disk sunflower florets. Descriptor is supported by the *Description of Components and Varieties of Sunflower*, created by GEVES, the French Variety and Seed Study and Control Group in 2000, which provides a set of pictures to facilitate the calibration of scale notation for each characteristic. In the descriptor, color of ray florets has been defined as *yellowish white, light yellow, medium yellow, orange yellow, orange, purple, reddish brown,* and *multicolored*, and the set of photographs was provided (**Table 2**).

Evaluation of the ray floret colors of the examined ornamental sunflower genotypes was done by 100 people with the use of

[1]https://zenodo.org/record/4068475#.X31utGgza71

TABLE 1 | Ray floret color evaluation of studied ornamental sunflower genotypes.

Genotypes	Main characteristics	Ray floret color		
		Subjective	Catalog	Image analysis
'Ring of Fire' 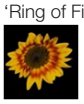	Commercial, branched, suitable as cut flower	Multicolored (98%)	Unique bicolor flower Yellow/Orange	Orange (29.64%) Medium yellow (21.97%) Reddish brown (21.42 %)
'CMS1 30' 	Standard oil type line, unbranched	Medium yellow (86%)	Yellow	Medium yellow (38.09%) Orange yellow (20.81%)
'Heliopa' 	Commercial, branched, suitable for gardens and as cut flower	Orange Yellow (79%)	Yellow	Medium yellow (40.60 %) Orange (28.44%) Orange yellow (24.84%)
'Dwarf' 	Commercial, very short, branched	Orange Yellow (50%) Medium yellow (28%)	Yellow	Orange yellow (39.40%) Medium yellow (34.01%)
'Neoplanta' 	Commercial, branched, suitable for gardens and as cut flower	Reddish Brown (88%),	Bordeaux	Reddish brown (67.04%) Purple (30.18%)
'Pacino Gold' 	Commercial, very short, branched, suitable for pots	Medium Yellow (59%),	Bright yellow	Medium yellow (58.12%) Orange yellow (28.63%)

Subjective – evaluation done by 100 evaluators. Data presented in the percentages for values over 20%. Catalog – color description in commercial catalog. Image analysis – Color evaluation with the use of FloCIA software. Data presented in the percentages for values over 20%.

the UPOV guidelines. The evaluators were mainly employees in the Institute of Field and Vegetable Crops or professors and students at different levels of horticulture studies at the Faculty of Agriculture, University of Novi Sad. During 2018, the evaluators were given a questionnaire containing photographs from UPOV descriptor for each ray floret color category and photographs of examined sunflower genotypes (**Table 1**, column Genotypes, rows A–F). Before the assessment, the evaluation process has been thoroughly explained to each evaluator. The evaluators were asked to define one or more colors present in ray florets of examined sunflower genotypes, based on the provided UPOV guidelines.

Methodology Based on FloCIA Software

Flower Color Image Analysis (*FloCIA*) software was used for segmentation of the UPOV categories. Segmentation included separation of flowers from the background and removing disk florets to get only ray florets. After the segmentation, color clouds in HSV (H-hue, S-saturation and V-value of light intensity) and Lab color space were analyzed (**Table 2**). In HSV color model V component was omitted (2D presentation) for better visualization of colors., and all the pixels with hue outside the range of 17.99-66.95 (yellow and red color area) and with saturation lower than 12.5% of the maximum saturation were removed.

For the purpose of classification into one of seven UPOV classes (UPOV 1 - UPOV 7) in Lab color space, mean vectors of UPOV categories of sunflower ray florets have been calculated. Lab color space is used when is necessary to determine color differences, and where each pixel of the image is written with three values: L*, a*, b*. Pixels are linked to the UPOV category by the nearest neighbor method (Altman, 1992), where Euclidean distance was calculated for each pixel from all seven mean vectors, and the pixels were classified into the category for which the distance is the shortest. Value of each category was calculated by counting the pixels from the same category of the test sunflower and dividing them by the total number of pixels of the segmented test sunflower ray florets. The mean vector numerical values are given in the **Table 2**. The centers of the cluster (middle vectors) of the UPOV category (seven larger dots) were visually presented in 3D representation (**Figure 1A**), and in 2D color distribution (**Figure 1B**).

Finally, software *FloCIA* was used for segmentation and classification of the six examined genotypes. The basic techniques used for this purpose were smoothing and standard deviation filtering and color and texture segmentation. Clustering of ray florets included their grouping into three clusters by using the k-means algorithm. Visually, images of two dominant clusters (dominant colors) were shown in the form of images of sunflowers, with separate colors. Additionally, the pixel layout was displayed in the Lab color space (blue dot in the 3D image Lab color space). The closest UPOV category to blue dot shows dominant color of the examined sunflower.

TABLE 2 | Segmentation of the International Union for the Protection of New Varieties of Plants (UPOV) color categories with *Flower Color Image Analysis* (*FloCIA*) and color clouds obtained by analysis with HSV (H-hue, S-saturation and V-value of light intensity) and Lab color space.

UPOV images	UPOV images segmented	HSV color space, HS components	Lab color space, ab components	Mean vectors		
				L	a	b
				207.959	128.5699	180.9511
				220.7627	119.1718	196.9132
				194.3196	131.934	195.4371
				187.9894	147.3313	195.7025
			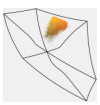	187.4147	151.3149	196.4400
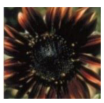				32.28135	133.7543	131.8849
		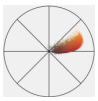		86.7722	163.5352	155.0404

UPOV images – Color groups based on UPOV descriptor for sunflower. From top to the bottom of the column: yellowish white, light yellow, medium yellow, orange yellow, orange, purple, reddish brown.

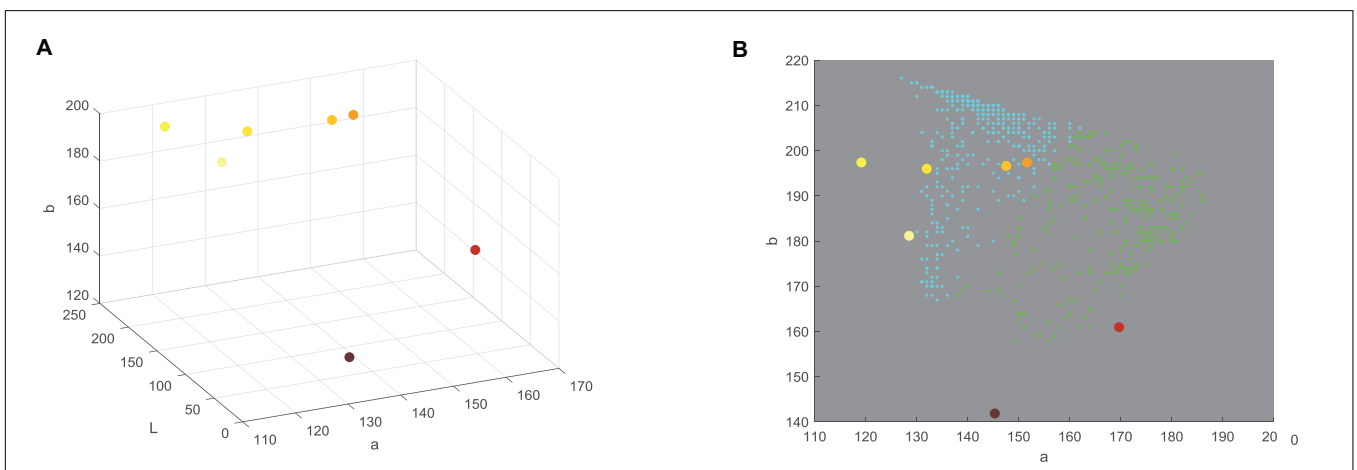

FIGURE 1 | Determined mean vectors for International Union for the Protection of New Varieties of Plants (UPOV) color categories in **(A)** 3D Lab color space and **(B)** 2D ab color space.

The accuracy of the software was tested based on the results of segmentation and colors classification of 153 images of F_2 ornamental sunflower genotypes and compared with the answers of an expert in two replications. The first replication was on a day of evaluation and the second one after 7 days.

The data and code that support the findings of this study are publicly available on https://zenodo.org/record/4068475#.X31utGgza71.

Data Analysis

Reliability coefficients were calculated in order to assess the reliability of UPOV methodology for sunflower ray floret color evaluation. Result of all evaluators' answers were processed and analyzed statistically in the R environment (R Development Core Team, 2011), with the use of Fleiss Kappa statistical model (Fleiss, 1971). This model is commonly used to evaluate the validity of multiple raters which are classifying a subject in multiple categories based on kappa (k) value. Considering that possible values of kappa are in range from −1 to 1, basic opinion is that if value of kappa is closer to 1, the agreement among raters is stronger, the validity of results is higher, and vice-versa, if the value of k is closer to −1, the agreement among raters is weaker and the validity of the obtained results is lower. According to Xie et al. (2017), Kappa values in ranges of (0–0.2), (0.2–0.4), (0.4–0.6), (0.6–0.8), (0.8–1) are an indication of slight, fair, moderate, substantial and almost perfect consistency, respectively.

Based on 100 evaluator scores of ray floret color of six tested sunflower genotypes, the percentages of evaluators who associated ray floret color to any of the UPOV color categories was correlated with the percentages of pixels in the corresponding UPOV color categories for all genotypes.

Objectivity of the *FloCIA* software, as well as its accuracy and precision (repeatability) were estimated using matching and confusion matrix (Visa et al., 2011). Expert annotations were used as the ground truth (evaluator's scores). They were made after the evaluator was presented with original sunflower images followed by images of two clusters of dominant colors, percentages of pixels belonging to individual UPOV categories and pixel distribution in the ab plane of the Lab color space, and the positions of the mean vectors of examined sunflowers in Lab color space in relation to the mean vectors of the UPOV categories. Two scenarios were examined. In the first one (matching matrix), the *FloCIA* was used as a tool in assisted decision-making methodology, to show subjectivity of evaluator due to a high number of photos and the time distance. In this scenario, the algorithm was applied to match the results of the same evaluator on 153 photographs of F_2 sunflower genotypes using traditional UPOV method for sunflower ray floret color classification in two replications. The first replication was marked as UPOV_EP1 and the second one, comprising classifications of the same evaluators after 7 days, as UPOV_EP2. The second scenario (confusion matrix) was created to visualize matching of an expert evaluator result using the *FloCIA* software assistance as a ground truth, and automatic sunflower color classification. Data in the *FloCIA assisted* rows were presented as real (*actual*) color categories in which the analyzed genotypes were classified (ground truth), and the data belonging to the *Automatic classification* were determined by an algorithm (*predicted*). The data gave information on how many sunflower genotypes were classified in an appropriate color category that match ground truth data, and how many were mistakenly automatically classified in another color category by an algorithm. From this confusion matrix, the accuracy of the automatic classification and precision (repeatability) for each UPOV category was calculated. Accuracy was calculated as the ratio of the number of correct classifications (sum of all diagonal values) to the total number of classifications. Precision was calculated in the same way that was used for the matching matrix.

RESULTS

Color Evaluation by UPOV Guideline

Based on the evaluators' answers by UPOV guidelines, genotypes 'CMS1 30' and 'Neoplanta' had a high percentage of the same answers (more than 80%) (**Table 1**). 'Neoplanta' was classified as *reddish brown* (88% respondents), although some of the answers suggest more than one color (11%), while 'CMS1 30' was classified as *medium yellow* (86%). Based on the highest answer percentage, both 'Heliopa' and 'Dwarf' were classified as *orange yellow* with 79% and 50% of answers, respectively. With the highest percentage of 59%, 'Pacino Gold' was classified as *medium yellow*. Sunflower genotype 'Ring of Fire' was classified as *multicolored*, with 98% of evaluators matched it with this category. Considering that the *multicolored* color category in UPOV guidelines was not clearly defined, evaluators were asked during the assessment if they can determine two or more colors of this genotype based on UPOV color guidelines. Out of 100 evaluators, 77% reported that they were able to determine two or more colors, but only 3.96% of them observed three or more colors. Most of the evaluators reported that this multicolored sunflower variety could be described by two dominant color categories: *medium yellow* and *reddish brown*. In order to examine the validity of the test, the agreement among evaluators has been calculated, as k-value. Based on this value and strength of agreement, the obtained results can be described as moderate agreement (k = 0.542).

Digital Image Analysis (dUPOV) Using FloCIA Software

In the process of color segmentation, ray and disk florets were extracted from the background. Disk florets of investigated sunflower genotypes were mostly characterized by different shades of similar colors as their ray florets, but the texture was different. The difference among textures of ray and disk florets allowed design of software for image segmentation and removal of sunflower disk florets in test images. Image segmentation was conducted by designing a texture segmentation algorithm based on histogram equalization, standard deviation filtering, and morphology operation. Step by step segmentation of parental line sunflower's images were shown in **Figures 2B,C**. A white cloth was used behind sunflowers during image recording and no manual correction was used (**Figure 2A**). After segmentation, k-Means clustering in Lab color space was used to determine the dominant ray floret color clusters. Lab color space was perceptually uniform to the human color vision, meaning that the same amount of numerical change in these values corresponds to about the same amount of the visually perceived change. Luminance component (L) was neglected so as to avoid unfavorable ambient illumination conditions. The results are given in **Figures 2D,E**.

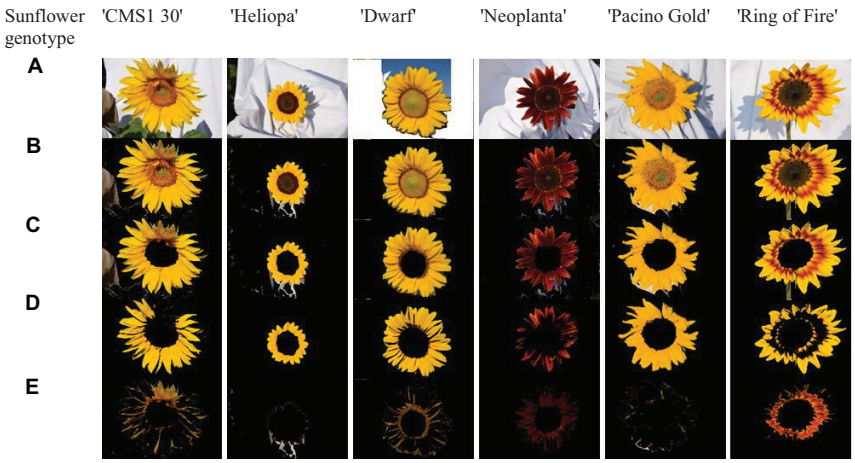

FIGURE 2 | The images of six examined sunflower (H. annus) genotypes ('CMS1 30,' 'Heliopa,' 'Dwarf,' 'Neoplanta,' 'Pacino Gold,' and 'Ring of Fire') were segmented (excluded background and disk florets) and clustered using the k-means algorithm: **(A)** original images, **(B)** color segmentation, **(C)** texture segmentation, **(D,E)** two dominant clusters.

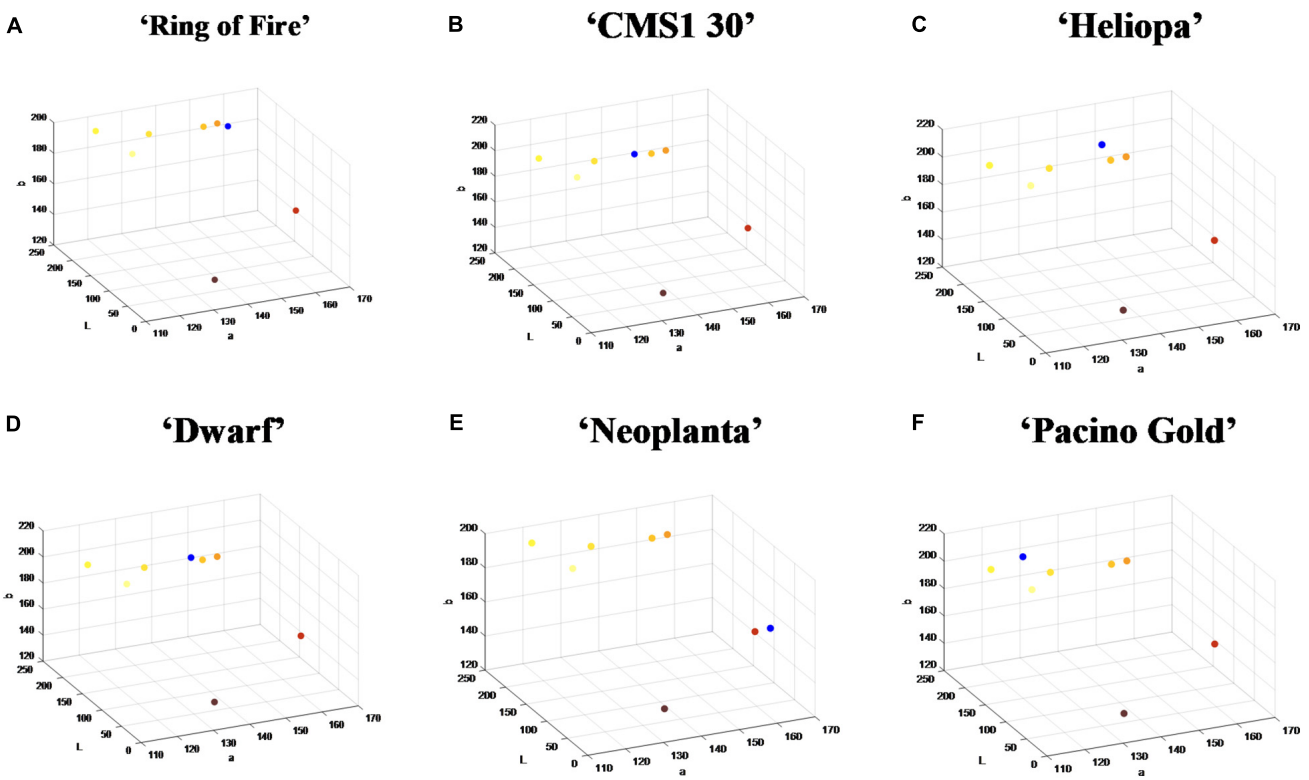

FIGURE 3 | The position of dominant color clusters for each examined genotype. Dots in yellowish white, light yellow, medium yellow, orange yellow, orange, purple, and reddish brown represent one of the seven International Union for the Protection of New Varieties of Plants (UPOV) color categories. The dominant color in tested genotypes is marked with blue dot. **(A–F)** Represent each tested sunflower genotype.

Finally, ray florets of six tested genotypes were segmented, and pixels of ray florets of each genotype were clustered into two dominant colors. Visualization of this process was presented in **Figures 2C–E**. The columns from left to right show segmented ray florets, pixels belonging to the first dominant color cluster, and pixels belonging to the second dominant color cluster.

The nearest neighborhood methodology of classification was used thereafter, so that Euclidean distances from the mean vectors of UPOV color categories were calculated for each pixel from

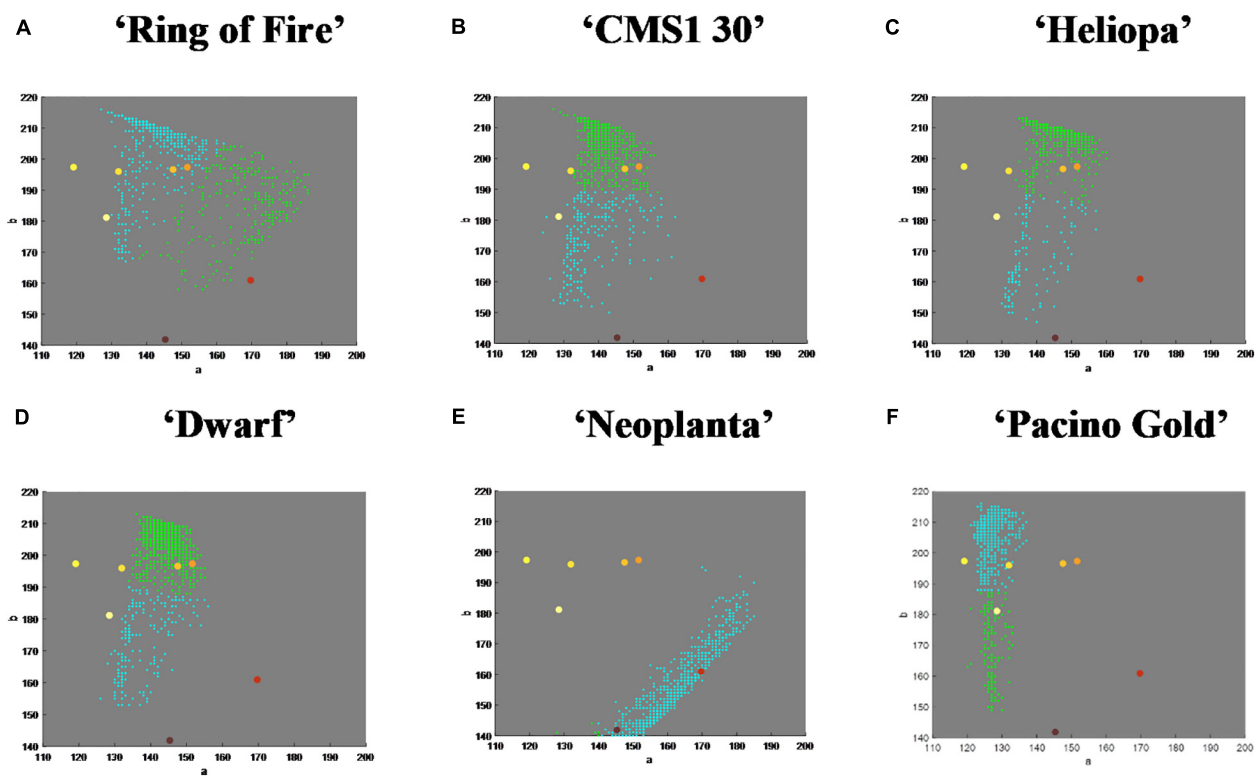

FIGURE 4 | The amount and distribution of pixels of each International Union for the Protection of New Varieties of Plants (UPOV) color category in Lab color space. Dots in yellowish white, light yellow, medium yellow, orange yellow, orange, purple, and reddish brown represent one of the seven UPOV color categories. The dominant color in tested genotypes is marked with blue dots. Pixels belonging to two dominant color clusters in tested genotypes in ab color space are roughly represented with blue and green dots. **(A–F)** Represent each tested sunflower genotype.

the two dominant clusters, and pixels were classified using the smallest Euclidean distance. Visualization of this process for six commercial sunflower genotypes was presented in **Figures 3A–F**. Along with visual representation of mean vectors of the seven UPOV color categories (dots in *yellowish white*, *light yellow*, *medium yellow*, *orange yellow*, *orange*, *purple,* and *reddish brown*), that were obtained by processing the original UPOV images, a dominant color in tested genotypes was marked with blue dots. This process guides the visual determination of sunflower ray florets color category: by comparing the distances of blue dot from the dots of UPOV colors in the Lab color space, it becomes clearer which of the seven UPOV colors were dominant in a tested genotype (**Figures 3A–F**).

Additional visualization of mean vectors of clusters showed distribution and number of pixels in chrominance "ab" plane of Lab color space (**Figures 4A–F**). For example, genotype 'Ring of Fire' presented disperse pixel layout, showing presents of all UPOV color categories, while 'Neoplanta' presented narrow distribution of pixels focused around *purple* and *reddish brown* UPOV color categories.

Quantification of the main color of ray florets of the six examined sunflower genotypes was performed using Lab color space. The mean vectors of sunflower ray florets have been calculated (**Table 3**). The final results of image analysis were presented in the percentage of pixels per each UPOV color category (**Table 1**). Finally, the percentage of pixels per UPOV category and visual representation of two dominant colors and their mean vectors are used by humans in the decision-making process.

TABLE 3 | Quantification of the main color of ray florets of the six examined sunflower genotypes with mean vectors obtained with Lab color space.

Genotype	L	a	b
'Ring of Fire'	169.0986	152.4655	197.8293
'CMS1 30'	179.3181	141.6079	200.0990
'Heliopa'	195.4105	145.8504	205.7754
'Dwarf'	181.1503	143.4153	200.9932
'Neoplanta'	68.3184	165.5987	159.9250
'Pacino Gold'	184.7126	139.0641	201.5160

L – lightness; a – component which varies from green to red; b – component which varies from blue to yellow.

Correlation Between UPOV and dUPOV Values

The correlation between evaluator scores and number of pixels follows the trend line (**Figure 5**) for only three color categories (*medium yellow*, *orange yellow* and *reddish brown*). Other colors

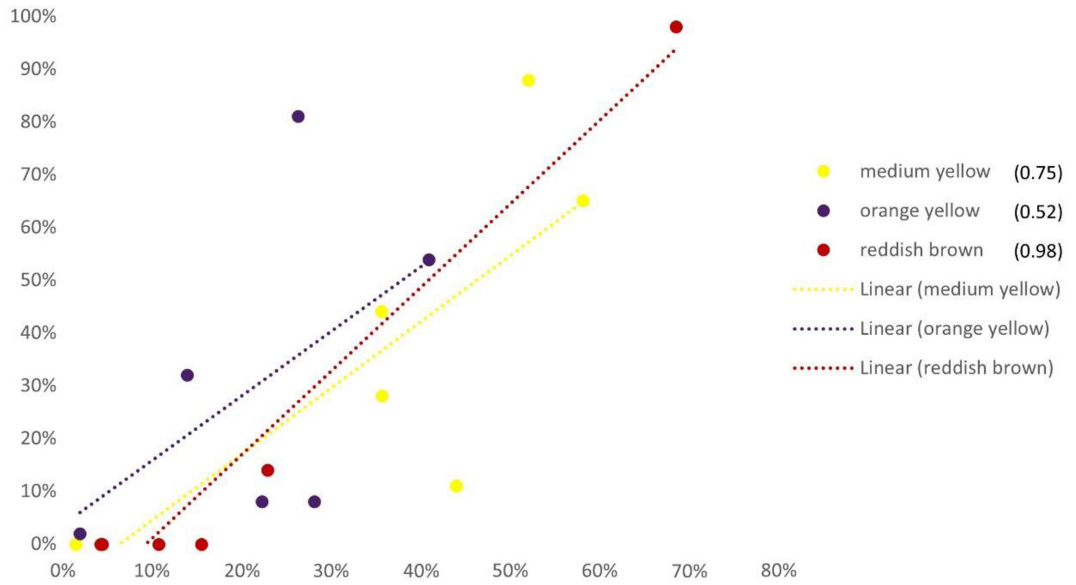

FIGURE 5 | Correlation among evaluators' score and number of pixels of each International Union for the Protection of New Varieties of Plants (UPOV) color category of six examined sunflower genotypes ('Neoplanta,' 'Heliopa,' 'CMS1 30,' 'Ring of Fire,' 'Pacino Gold,' and 'Dwarf'). X-axis represents the percentage of pixels for all genotypes; y-axis represents the percentage of evaluators scores of all genotypes.

did not have a sufficient number of pixels and therefore were not recognized by evaluators.

FloCIA Software Accuracy Testing

FloCIA software's accuracy and repeatability has been tested on the image set containing 153 photographs of F_2 ornamental sunflower genotypes.

In order to examine the objectivity of the software, its accuracy and precision (repeatability) were calculated using the confusion matrix. To assess if the software is more accurate and precise than the human evaluation, the same parameters were calculated using the matching matrix on expert color evaluation based on the traditional UPOV guidelines. The results of the matching matrix (**Table 4**) and confusion matrix (**Table 5**) presented a visualization of accuracy and precision (repeatability) of these two processes of sunflower color evaluation.

The matching matrix was used to visualize the matching of the results of two replications: the first UPOV_EP1 and the second after 7 days UPOV_EP2 (**Table 4**). The values on the diagonal of the matching matrix indicate the number of the same evaluations (0,1,30,18,13,2), while the values outside the diagonal indicate the number of evaluations that differ in two replications, carried out by the same expert evaluator using the traditional UPOV color evaluation method. The matching matrix visualization mostly showed scattered answers given by the experts, whereas the highest number of replications was characteristic of the *medium yellow* (MY) color group (30) and *orange yellow* (OY) color group (18), as confirmed by the calculated values of precision 57.69%, 51.43%, respectively (**Table 6**). The calculated accuracy of single expert evaluator using the traditional UPOV method in two replications seven days apart was 41.83%.

TABLE 4 | Matching matrix of expert answers on the dominant color classification by the International Union for the Protection of New Varieties of Plants (UPOV) guidelines in two replications (UPOV_EP1 and UPOV_EP2), 7 days apart.

		UPOV_EP2					
		YW	***LY***	***MY***	***OY***	***O***	***RB***
UPOV_EP1	***YW***	0	0	3	0	2	0
	LY	1	1	2	4	5	1
	MY	0	1	30	8	7	1
	OY	2	2	10	18	13	0
	O	0	3	4	2	13	0
	RB	3	5	3	3	4	2

The values on the diagonal of the matching matrix indicate the number of the same evaluations, while the values outside the diagonal indicate the number of evaluations that differ in two replications. Color categories from UPOV guidelines: YW – yellowish white, LY – light yellow, MY – medium yellow, OY – orange yellow, O – orange, RB – reddish brown.

The confusion matrix (**Table 5**) was created to visualize the matching of the data in *FloCIA assisted* methodology. The rows present real (*actual*) color categories that analyzed genotypes were classified in (ground truth), and the data belonging to the *Automatic classification* were determined by an algorithm (*predicted*). The values on the diagonal of the confusion matrix indicate the number of evaluations that were the same for *FloCIA* assisted color evaluation (ground truth) and automatic evaluation (7,7,49,41,17,19), and the values outside the diagonal indicate the number of evaluations that differ. The calculated accuracy of automatic sunflower color classification was 91.50%, which was supported by the high precision of matching color categories above 60% (**Table 6**).

TABLE 5 | Confusion matrix of evaluator answers obtained with the assistance of *FloCIA* software and automatic sunflower color category classification.

		Automatic classification					
		YW	***LY***	***MY***	***OY***	***O***	***RB***
FloCIA assisted	***YW***	7	2	1	0	0	0
	LY	0	7	0	0	0	0
	MY	0	2	49	5	0	0
	OY	0	0	1	41	1	0
	O	0	0	0	1	17	0
	RB	0	0	0	0	1	19

The data in FloCIA assisted rows present real (actual) color categories that analyzed genotypes were classified in (ground truth), and the data belonging to the Automatic classification were determined by an algorithm (predicted). The values on the diagonal of the confusion matrix indicate the number of evaluations that were the same for FloCIA assisted color evaluation (ground truth) and automatic evaluation, and the values outside the diagonal indicate the number of evaluations that differ. Color categories from the International Union for the Protection of New Varieties of Plants (UPOV) guidelines: YW – yellowish white, LY – light yellow, MY – medium yellow, OY – orange yellow, O – orange, RB – reddish brown.

DISCUSSION

Accurate phenotype classification is one of the requirements of the ornamental plant market, which is becoming increasingly more sophisticated and demanding (Guerra Mattos et al., 2020). The same stands for ornamental sunflower breeding and marketing which is expected to adopt automatic classification, in order to improve breeding efficiency and quality of products offered to consumers (Lino et al., 2011). Color determination is highly subjective, and can possibly even lead to misunderstandings, wrong genotype descriptions and unsatisfied producers. Digital imaging in combination with efficient analytic software could be a powerful tool efficient and accurate transformation of qualitative measurements of phenotypic traits like color and shape into quantitative data (Bohorquez-Restrepo, 2015).

In this paper we describe the first attempt to use digital image analysis for ray floret color evaluation in ornamental sunflower. Based on image analysis algorithms, in-house created software, *FloCIA* automatically detected dominant colors of ray florets in six ornamental sunflower genotypes, thus offering novel methodology for objective and more precise ornamental sunflower phenotyping. In ornamental plants, digital image technology has been used for gerbera flower classification (Lino et al., 2011), rose shape analysis (Miao et al., 2006), bedding plant species quality assessment (Parsons et al., 2009), flower color pattern determination in *Primula sieboldii* E. Morren (Yoshioka et al., 2004), as well as evaluation of *Anthurium* 'Tropical' postharvest quality (Guerra Mattos et al., 2020). In sunflower, image analysis so far has been used for early detection of broomrape infection (Cochavi et al., 2017; Ortiz-Bustos et al., 2017; Lati et al., 2019), weed mapping (López-Granados et al., 2016), architecture-based organ segmentation (Gélard et al., 2016) and floral dimension determination (Sunoj et al., 2018). Common for all image analysis studies is that they can either replace the currently used parameters or provide additional characteristics with good discriminating power, determined in an objective and standardized way (Lootens et al., 2013).

Our study proposes using dUPOV to eliminate shortcomings of the UPOV-based methodology, such as subjectivity and inability of evaluators to differentiate colors, as well as the quality of photographs in the UPOV guidelines. For example, evaluators could not say with the certainty if some genotypes, such as 'Neoplanta,' should be described as single colored or multi-colored, while being certain that 'Ring of Fire' could be described as multicolored. Although digital image results also showed this color as the dominant, the *FloCIA* software recognized the presence of *purple* in this genotype which covers 30.18% of its color (**Table 1**). Results for the other tested genotypes, such are 'CMS1 30' and 'Heliopa,' showed the dominance of one color - for 'CMS1 30' *medium yellow* with 86%, and for 'Heliopa' *orange yellow* with 79%. In both cases only 6% of the evaluators observed the presence of the second dominant color which, according to the results of the *FloCIA* software, was *orange yellow* (20.81%) for 'CMS1 30' and *orange* (28.44%) for 'Heliopa.' Genotype 'Pacino Gold' seemed to be easy for color evaluation. However, the presence of different shades of yellow and orange misguided the evaluators, but its color was clearly identified by the *FloCIA* software. Results of image analysis of this genotype showed the dominance of *medium yellow* (58.12%), but also the presence of *orange yellow* (28.63%) which evaluators failed to observe. Most of the evaluators defined 'Ring of Fire' as a *multicolored*, with *reddish brown* and *medium yellow* as two dominant colors. Based on the results of image analysis using *FloCIA* software, this genotype was characterized with three colors: *orange*, *medium yellow, and reddish brown*, with percentages of 29.64, 21.97, and 21.42, respectively. Statistical analysis confirmed the uncertainty of evaluators with moderate value of kappa for the agreement among evaluators. Similar to the results of our study, Kendal et al. (2013) found that analysis of digital images of plants of eleven grassland species taken with digital cameras was

TABLE 6 | Calculated precision for each International Union for the Protection of New Varieties of Plants (UPOV) color category found as a dominant color of tested sunflower genotypes.

Precision of matching color categories	**YW *yellowish white***	**LY *light yellow***	**MY *medium yellow***	**OY *orange yellow***	**O *orange***	**RB *reddish brown***
Expert evaluator in two replications by UPOV guidelines	0.00%	8.33%	57.69%	51.43%	29.55%	50.00%
Expert evaluator supported by *FloCIA* software and automatic classification	100.00%	63.64%	96.08%	89.13%	89.47%	100.00%

a practicable method for quantifying color and estimating color difference between flowers both in the field and in the laboratory. The same stands for Garcia et al. (2014), who used digital imaging to map flower colors and concluded that this method presents a significant new opportunity to reliably map flower colors.

A quantitative and objective measure of plant color has the potential to improve plant management through improved estimation of plant dynamics and improved modeling of human-plant interactions (Kendal et al., 2013). Digital images can provide information on the color patterns of objects; this information is composed of pixels, their locations and color depths (Yoshioka et al., 2004). Based on image analysis algorithms, we have created the *FloCIA* software that automatically classifies image pixels and gives guidelines to a person who makes the final conclusion. Using *FloCIA*, none of the tested genotypes can be described as single colored, while visual estimation placed all six tested genotypes into one dominant color. Although the base color of ray florets was visually scored, the *FloCIA* enabled the detection of different shades of the same color. In the case of sunflower, using digital image, we could distinguish hues of yellow, orange and red color. For example, genotype 'CMS1 30' had predominant *medium yellow* (38.09%) but all other colors from the UPOV guideline we were also detected by *FloCIA* software. We have also tested the accuracy of the *FloCIA* software trough matching and confusion matrixes. The results showed that there is scattering of the data obtained by evaluations based on UPOV guidelines, compared to *FloCIA* software automatic color classification. Both calculated parameters, accuracy and precision (repeatability) of matching of each color category, were unequivocally higher with the use of *FloCIA* software. Singh et al. (2011) also pointed out the advantages of the use of image analysis in the flower color study, as it enables increased precision in estimation of variation by differentiating color groups into sub-groups, which in turn allowed for determination of variations within the sub-groups in a reliable manner. This fine color determination opens up new possibilities in ornamental sunflower breeding, production, marketing and trade, since Behe et al. (1999) in their study of consumer preferences revealed that flower color, followed by leaf variation, and the price, was the most important factor affecting consumer's decision to buy certain ornamental variety and has direct influence on its commercial value. Hence developing precise flower color phenotyping methods for color analysis is essential for providing accurate, quantitative information useful both in breeding and variety marketing and commercialization.

CONCLUSION

The main advantages of digital image analysis methods are their accuracy as well as clear and concise information for color evaluation in a breeding process. The proposed digital image (dUPOV) methodology using *FloCIA* software for sunflower ray floret color evaluation offers objective information supported with quantitative data regarding the dominant color category of ray florets, making the final evaluations made either by breeders or traders more accurate and carried out with more confidence. dUPOV groups the pixels of segmented ray florets into two dominant clusters and graphically presents the position of their mean vectors in Lab color space, thus providing the breeders with objective information on ray floret color of the newly created varieties. Since color patterning contributes to important plant traits that influence ecological interactions, ornamental plants breeding, and agricultural performance, the proposed dUPOV image analysis methodology could be adapted and applied for similar tasks in different fields of horticulture, agriculture and plant research.

DATA AVAILABILITY STATEMENT

The raw data supporting the conclusions of this article will be made available by the authors, without undue reservation.

ETHICS STATEMENT

The requirement for ethics approval for this study was waived by Ethics Committee Board of the Faculty of Agriculture, University of Novi Sad. All participants provided their written informed consent.

AUTHOR CONTRIBUTIONS

MZ, SC, and EM performed conceptualization. MZ and ZB performed methodology. MZ, SC, EM, and ZB performed formal analysis and investigation. MZ prepared original draft. SC, EM, and DM wrote, reviewed, and edited the manuscript. AM and DM acquired funding. SC and SJ performed resources. EM and SC performed supervision. All authors contributed to the article and approved the submitted version.

FUNDING

This study was supported by Ministry of Education, Science and Technological Development of Republic of Serbia, project TR31025, Provincial Secretariat for Higher Education and Science of Vojvodina, project 114-451-2126/2016-03, and project number 19/6-020/961-143/18, supported by the Ministry of Scientific-Technological Development, Higher Education and Information Society, Republic of Srpska, Bosnia and Herzegovina.

ACKNOWLEDGMENTS

The authors would like to thank the technicians of the Institute for Field and Vegetable Crops who took great care of the sunflowers and all evaluators who assessed the sunflower ray florets color.

REFERENCES

Altman, N. S. (1992). An introduction to kernel and nearest-neighbor nonparametric regression. *Am. Static.* 46, 175–185. doi: 10.1080/00031305.1992.10475879

Behe, B., Nelson, R., Barton, S., Hall, C., Safley, C. D., and Turner, S. (1999). Consumer preferences for geranium flower color, leaf variegation, and price. *Hort. Sci.* 34, 740–742. doi: 10.21273/hortsci.34.4.740

Bohorquez-Restrepo, A. (2015). *Biochemical and Colorimetric Study of Flower Color in Phlox Species*. master's thesis, The Ohio State University, Columbus, OH.

Cochavi, A., Rapaport, T., Gendler, T., Karnieli, A., Eizenberg, H., Rachmilevitch, S., et al. (2017). Recognition of *Orobanche cumana* below-ground parasitism through physiological and hyper spectral measurements in sunflower (*Helianthus annuus* L.). *Front. Plant Sci.* 8:909. doi: 10.3389/fpls.2017.00909

Cvejić, S., and Jocić, S. (2010). Development of ornamental sunflower hybrids. *Ratar. Povrtar.* 47, 147–152.

Cvejić, S., Jocić, S., and Mladenović, E. (2016). Inheritance of floral colour and type in four new inbred lines of ornamental sunflower (*Helianthus annuus* L.). *J. Hortic. Sci. Biotech.* 91, 30–35. doi: 10.1080/14620316.2015.1110989

Divita, M. E., Salaberry, M. T., Echeverría, M. M., and Rodríguez, R. H. (2012). "Genetic and environmental effects of some traits of ornamental value in sunflower (*Helianthus annuus* L.)," in *Proceedings of the 18th International Sunflower Conference*, Mar del Plata, 159.

Fleiss, J. L. (1971). Measuring nominal scale agreement among many raters. *Psychologic. Bull.* 76, 378–382. doi: 10.1037/h0031619

Garcia, J. E., Greentree, A. D., Shrestha, M., Dorin, A., and Dyer, A. G. (2014). Flower colours through the lens: quantitative measurement with visible and ultraviolet digital photography. *PLoS One* 9:e96646. doi: 10.1371/journal.pone.0096646

Gélard, W., Burger, P., Casadebaig, P., Langlade, N., Debaeke, P., Devy, M., et al. (2016). "3D plant phenotyping in sunflower using architecture-based organ segmentation from 3D point clouds," in *Proceedings of the International Workshop on Image Analysis Methods for the Plant Sciences (IAMPS)*, Angers.

Guerra Mattos, D., Duarte de Oliveira Paiva, P., Silva Mundim, A., Valquíria, dos Reis, M., Mateus Nery, E., et al. (2020). Digital images and *in-person* evaluation of *Anthurium* 'Tropical' postharvest quality. *Ornam. Hortic.* 26, 166–176. doi: 10.1590/2447-536x.v26i2.2123

Jocić, S., Miladinović, D., and Kaya, Y. (2015). "Breeding and genetics of sunflower," in *Sunflower: Chemistry, Production, Processing, and Utilization*, Vol. 7, eds E. Martínez-Force, N. T. Dunford, and J. J. Salas (Urbana, IL: AOCS Press), 547–558.

Kaya, Y., Jocić, S., and Miladinović, D. (2012). "Sunflower," in *Technological Innovations in Major Oil Crops*, ed. S. K. Gupta (New York, NY: Springer), 85–129.

Kendal, D., Hauser, C. E., Garrard, G. E., Jellinek, S., Giljohann, K. M., and Moore, J. L. (2013). Quantifying plant colour and colour difference as perceived by humans using digital images. *PLoS One* 8:e72296. doi: 10.1371/journal.pone.0072296

Lati, R. N., Filin, S., Elnashef, B., and Eizenberg, H. (2019). 3-D image-driven morphological crop analysis: a novel method for detection of sunflower broomrape initial subsoil parasitism. *Sensors* 19:1569. doi: 10.3390/s19071569

Lino, A. C. L., Sanches, J., Moraes, G., Dias-Tagliacozzo, I. M. D., Augusto, F., Lima, B., et al. (2011). Flower classification supported by digital imaging techniques. *J. Inform. Technol. Agric.* 4, 1–6.

Lootens, P., Chaves, B., Baert, J., Pannecoucque, J., Van Waes, J., and Roldan-Ruiz, I. (2013). Comparison of image analysis and direct measurement of UPOV taxonomic characteristics for variety discrimination as determined over five growing seasons, using industrial chicory as a model crop. *Euphytica* 189, 329–341. doi: 10.1007/s10681-012-0750-9

López-Granados, F., Torres-Sánchez, J., Serrano-Pérez, A., de Castro, A. I., Mesas-Carrascosa, F. J., and Pena, J. M. (2016). Early season weed mapping in sunflower using UAV technology: variability of herbicide treatment maps against weed thresholds. *Prec. Agric.* 17, 183–199. doi: 10.1007/s11119-015-9415-8

Miao, Z., Gandelin, M. H., and Yuan, B. (2006). A new image shape analysis approach and its application to flower shape analysis. *Image Vis. Comput.* 24, 1115–1122. doi: 10.1016/j.imavis.2006.04.004

Miladinović, D., Hladni, N., Radanović, A., Jocić, S., and Cvejić, S. (2019). "Sunflower and climate change: possibilities of adaptation through breeding and genomic selection," in *Genomic Designing of Climate-Smart Oilseed Crops*, ed. S. K. Gupta (New York, NY: Springer), 173–238. doi: 10.1007/978-3-319-93536-2_4

Mladenović, E., Cvejić, S., Čukanović, J., Žeravica, G., and Jocić, S. (2016). Evaluation of sunflower genotypes for ornamental use. *Contemp. Agric.* 65, 39–43. doi: 10.1515/contagri-2016-0007

Ortiz-Bustos, C. M., Pérez-Bueno, M. L., Barón, M., and Molinero-Ruiz, L. (2017). Use of blue-green fluorescence and thermal imaging in the early detection of sunflower infection by the root parasitic weed *Orobanche cumana* Wallr. *Front. Plant Sci.* 8:833. doi: 10.3389/fpls.2017.00833

Parsons, N. R., Edmondson, R. N., and Song, Y. (2009). Image analysis and statistical modelling for measurement and quality assessment of ornamental horticulture crops in glasshouses. *Biosys. Engineer.* 104, 161–168. doi: 10.1016/j.biosystemseng.2009.06.015

R Development Core Team (2011). *R: A Language and Environment for Statistical Computing*. Vienna: R Foundation for Statistical Computing.

Shibata, M. (2008). Importance of genetic transformation in ornamental plant breeding. *Plant Biotechnol.* 25, 3–8. doi: 10.5511/plantbiotechnology.25.3

Singh, S., Dhyani, D., Ashok, K. Y., and Rajkumar, S. (2011). Flower colour variations in gerbera (*Gerbera jamesonii*) population using image analysis. *Indian J. Agric. Sci.* 81, 1130–1136.

Sunoj, S., Subhashree, S. N., Dharani, S., Igathinathane, C., Franco, J. G., Mallinger, R. E., et al. (2018). Sunflower floral dimension measurements using digital image processing. *Comp. Electron. Agric.* 151, 403–415. doi: 10.1016/j.compag.2018.06.026

UPOV (2000). *Guidelines for the Conduct of Tests for Distinctness, Uniformity and Stability: Sunflower (Helianthus annuus* L.). TG/81/6. Geneva: International Union for the Protection of New Varieties of Plants.

Visa, S., Ramsay, B., Ralescu, A. L., and Van Der Knaap, E. (2011). Confusion matrix-based feature selection. *MAICS* 710, 120–127.

Vuppalapti, P. (2005). *Sunflower, Helianthus annuus L., cut flower variety trial*. master's thesis, Western Kentucky University, Bowling Green, KY.

Xie, Z., Gadepalli, C., and Cheetham, B. M. (2017). Reformulation and generalization of the Cohen and Fleiss kappas. *LIFE Int. J. Health Life Sci.* 3, 1–15. doi: 10.20319/lijhls.2017.32.115

Yoshioka, Y., Iwata, H., Ohsawa, R., and Ninomiya, S. (2004). Quantitative evaluation of flower colour pattern by image analysis and principal component analysis of *Primula sieboldii* E. *Morren. Euphytica* 139, 179–186. doi: 10.1007/s10681-004-3031-4

Conflict of Interest: The authors declare that the research was conducted in the absence of any commercial or financial relationships that could be construed as a potential conflict of interest.

frontiers in Plant Science

ORIGINAL RESEARCH
published: 09 December 2020
doi: 10.3389/fpls.2020.595376

Magnesium Hydride-Mediated Sustainable Hydrogen Supply Prolongs the Vase Life of Cut Carnation Flowers via Hydrogen Sulfide

Longna Li[1†], Yuhao Liu[1†], Shu Wang[1†], Jianxin Zou[2†], Wenjiang Ding[2†] and Wenbiao Shen[1,2†]*

[1] Laboratory Center of Life Sciences, College of Life Sciences, Nanjing Agricultural University, Nanjing, China, [2] Center of Hydrogen Science, Shanghai Jiao Tong University, Shanghai, China

OPEN ACCESS

Edited by:
Antonio Ferrante,
University of Milan, Italy

Reviewed by:
Hua Zhang,
Hefei University of Technology, China
Chao Ma,
China Agricultural University, China

***Correspondence:**
Wenbiao Shen
wbshenh@njau.edu.cn

†ORCID:
Longna Li
orcid.org/0000-0003-0007-3165
Yuhao Liu
orcid.org/0000-0002-1666-208X
Shu Wang
orcid.org/0000-0002-4417-9386
Jianxin Zou
orcid.org/0000-0003-1041-121X
Wenjiang Ding
orcid.org/0000-0003-0948-8025
Wenbiao Shen
orcid.org/0000-0003-1525-9472

Specialty section:
This article was submitted to Crop and Product Physiology, a section of the journal Frontiers in Plant Science

Received: 17 August 2020
Accepted: 13 October 2020
Published: 09 December 2020

Citation:
Li L, Liu Y, Wang S, Zou J, Ding W and Shen W (2020) Magnesium Hydride-Mediated Sustainable Hydrogen Supply Prolongs the Vase Life of Cut Carnation Flowers via Hydrogen Sulfide. Front. Plant Sci. 11:595376. doi: 10.3389/fpls.2020.595376

Magnesium hydride (MgH_2) is a promising solid-state hydrogen source with high storage capacity (7.6 wt%). Although it is recently established that MgH_2 has potential applications in medicine because it sustainably supplies hydrogen gas (H_2), the biological functions of MgH_2 in plants have not been observed yet. Also, the slow reaction kinetics restricts its practical applications. In this report, MgH_2 (98% purity; 0.5–25 μm size) was firstly used as a hydrogen generation source for postharvest preservation of flowers. Compared with the direct hydrolysis of MgH_2 in water, the efficiency of hydrogen production from MgH_2 hydrolysis could be greatly improved when the citrate buffer solution is introduced. These results were further confirmed in the flower vase experiment by showing higher efficiency in increasing the production and the residence time of H_2 in solution, compared with hydrogen-rich water. Mimicking the response of hydrogen-rich water and sodium hydrosulfide (a hydrogen sulfide donor), subsequent experiments discovered that MgH_2-citrate buffer solution not only stimulated hydrogen sulfide (H_2S) synthesis but also significantly prolonged the vase life of cut carnation flowers. Meanwhile, redox homeostasis was reestablished, and the increased transcripts of representative senescence-associated genes, including *DcbGal* and *DcGST1*, were partly abolished. By contrast, the discussed responses were obviously blocked by the inhibition of endogenous H_2S with hypotaurine, an H_2S scavenger. These results clearly revealed that MgH_2-supplying H_2 could prolong the vase life of cut carnation flowers via H_2S signaling, and our results, therefore, open a new window for the possible application of hydrogen-releasing materials in agriculture.

Keywords: magnesium hydride, hydrogen gas, hydrogen sulfide, vase life, cut carnation flowers

INTRODUCTION

Hydrogen is an ideal energy carrier that is being increasingly used in both power generation applications and transportation. Besides, hydrogen gas (H_2) has been documented having a range of biological effects and gradually utilized in medicine and agriculture (Ohsawa et al., 2007; Xie et al., 2012; Zeng et al., 2013; Wu et al., 2019). Clearly, the storage of hydrogen is one of the key challenges in developing a hydrogen economy. The storage methods include pressurized gas, a cryogenic

liquid, and solid fuel as chemically or physically combination with materials, such as metal hydrides (Sakintuna et al., 2007). At present, the supplementation of H_2 for biological research includes a gas cylinder and water electrolysis, and H_2 is normally dissolved in water and saline (Ohta, 2011; Xie et al., 2014; Li et al., 2018; Su et al., 2018). However, the extensive application of the hydrogen-rich liquid solution is limited due to the low solubility and short residence time of H_2 in water. Fortunately, the growing development of solid hydrogen-storage materials may provide ways to improve the issues about production and storage of H_2, considering portable, safety, large hydrogen contents, and sustainable hydrogen supply of solid-state storage (Hirscher et al., 2020).

Magnesium hydride (MgH_2) stands as a promising hydrogen source because of its high hydrogen-storage capacity (7.6 wt%), abundant resources, and low cost (Grochala and Edwards, 2004). The research on applications of MgH_2 and its related compounds has focused on thermal storage for solar power stations and hydrogen supply for vehicles (Bogdanović et al., 1995; Schlapbach and Zuttel, 2001; Baricco et al., 2017; Lototskyy et al., 2018; Hirscher et al., 2020). It is well documented that MgH_2 can produce a desired quantity of H_2 by the following hydrolysis reaction at room temperature: $MgH_2 + 2H_2O \rightarrow Mg(OH)_2 + 2H_2$, the by-product of which is environmentally friendly. This property of MgH_2 makes a possible for biological application. Amazingly, Kamimura et al. (2016) discovered that orally given MgH_2 could increase the content of blood H_2 and decrease the level of plasma triglyceride in rats, thus extending their average lifespan. These results indicated that MgH_2 with biosafety might also have potential roles in medical applications.

In fact, there are two disadvantages of MgH_2 restricting its further practical application: (1) the reaction kinetics of MgH_2 hydrolysis is extremely slow in pure water; (2) the insoluble layer of magnesium hydroxide [$Mg(OH)_2$] rapidly coated on the outer surface of the unreacted MgH_2 to further hide reaction as the pH increases (Hiraki et al., 2012). Subsequently, some organic acids (including citric acid, ethylenediamine-tetraacetic acid, and tartaric acid) were found as good buffer agents to effectively accelerate the reaction, finally improving H_2 generation by decreasing the pH and suppressing $Mg(OH)_2$ formation (Hiraki et al., 2012; Chao, 2018). On the other hand, it is well-known that organic acid-induced decrease in pH of vase solutions inhibits bacterial growth and increases the water conduction in the xylem of cut flowers, thus prolonging the vase life (van Doorn, 2010).

The postharvest senescence of cut flowers results in significant commercial losses, which is closely associated with a series of signaling molecules, including ethylene (Kumar et al., 2008), reactive oxygen species (ROS; van Doorn and Woltering, 2008), nitric oxide (NO; Naing et al., 2017), and hydrogen sulfide (H_2S; Zhang et al., 2011). Highly coordinated changes in gene expression are also involved (Shahri and Tahir, 2011). Many senescence-associated genes (*SAGs*) have been cloned from carnation petals, and their expression patterns were examined as well. For example, transcripts of representative genes encoding β-galactosidase (*DcbGal*) and glutathione-*S*-transferase (*DcGST1*), previously described as *SR12* and *SR8*, are increased during flower senescence (Lawton et al., 1989; Meyer et al., 1991).

Recently, the usage of H_2 in the form of hydrogen-rich water (HRW) was observed to delay postharvest senescence and improve the quality of cut flowers (Ren et al., 2017; Su et al., 2019; Wang et al., 2020). Subsequent biochemical analysis showed that H_2 prolonged the vase life of cut rose and lily was mediated by maintaining water balance, increasing antioxidant defense, and prolonging cell membranes stability (Ren et al., 2017). Meanwhile, H_2 can inhibit ethylene synthesis and corresponding signal transduction via regulating the expressions of related genes (such as ethylene synthesis genes *Rh-ACS3* and *Rh-ACO1* and ethylene receptor genes *Rh-ETR1*), thus delaying rose senescence during the vase period (Wang et al., 2020). In addition, H_2-stimulated NO, another gaseous molecule, can act as a downstream signal molecule involving keeping postharvest freshness in cut lily (Huo et al., 2018). However, the effects of sustained hydrogen supply on prolonging the vase life of cut flowers and related mechanisms are still elusive.

In this study, we firstly aim to find an optimized condition for using MgH_2 in the flower vase experiment. It was confirmed that the application of citrate buffer solution (CBS) could greatly accelerate the reaction rate of MgH_2 hydrolysis, confirmed by the rapid and sustainable increased H_2 generation, thus showing more efficiency in the residence time of H_2 in solution, compared with HRW. By using pharmacological and molecular approaches, we discovered that the combined treatment of MgH_2 and CBS could remarkably prolong the vase life of a cut carnation flower, compared with either treatment with MgH_2 or HRW, or CBS alone. It is a new finding. Further results suggested that the discussed MgH_2-CBS response is mediated by influencing H_2S signaling. Together, this work will not only extend the application of MgH_2 to agricultural practices but also provide a new idea for the development of new plant growth regulators.

MATERIALS AND METHODS

Chemicals

All chemicals used in our experiments were purchased from Sigma-Aldrich (St. Louis, MO, United States) unless stated otherwise. MgH_2 was obtained from the Center of Hydrogen Science, Shanghai Jiao Tong University (Ma et al., 2019). MgH_2 was further characterized by using scanning electron microscopy (SU-8010, Hitachi, Tokyo, Japan), X-ray diffraction (D/MAX-Ultima III, Rigaku, Tokyo, Japan) with Cu K radiation source, differential scanning calorimetry (STA449F3, Netzsch, Selb, Germany), and thermogravimetry (TG209F3, Netzsch, Selb, Germany). In addition, sodium hydrosulfide (NaHS) and hypotaurine (HT) were used as an H_2S releasing compound and a specific H_2S-scavenger, respectively (Ortega et al., 2008). H_2S fluorescent probe 3-oxo-3H-spiro[isobenzofuran-1,9'-xanthene]-3',6'-diyl bis(2-(pyridin-2-yldisulfanyl)benzoate) (WSP-5; MKBio, Shanghai, China) was used to monitored endogenous H_2S in cut flowers (Peng et al., 2014). The

concentrations of these chemicals were selected based on the results of pilot experiments.

Plant Material and Treatments

Cut carnation "Pink Diamond" flowers at the typical commercial stage (the petals form a right angle with the stem axis) were purchased from a flower market in Nanjing City, Jiangsu Province, China, from July to September of 2019. They were transported within 1 h to the laboratory. Subsequently, the cut flower stems were placed in distilled water and re-cut underwater to a length of 25 cm. The top two leaves were kept as well.

The cut flower stems were incubated in glass bottles with 150-ml distilled water (control) and 0.1-M CBS (pH 3.4) containing 0.01, 0.1, and 1 g L^{-1} MgH_2. Because the treatment with 0.1-M CBS (pH 3.4) plus 0.1 g L^{-1} MgH_2 showed the most obvious effects on prolonging the vase life of a cut flower in a pilot experiment (**Supplementary Figures 1A–C**), this combined treatment was applied subsequently. Meanwhile, 0.1 g L^{-1} MgH_2, 0.1 M CBS (pH 3.4), or 10% HRW (obtained by water electrolysis) alone was, respectively, regarded as controls, and HRW was prepared according to the previous method (Su et al., 2019).

To confirm the possibility that the effect of MgH_2 was only due to molecular hydrogen and not associated with magnesium ion, MgH_2-CBS solution was boiled for three times, 5 min each to remove the generated H_2, followed by keeping under the normal temperature condition for 1 day until no H_2 was detected.

Because 600-μM NaHS and 10-mM HT showed the obviously promoting and repressing effects on prolonging the vase life of a cut flower in pilot experiments, respectively (**Supplementary Figures 1D,E**), these treatments were also chosen. For further tests, the cut flower stems were incubated in treatment solutions (150 ml) containing distilled water (control), 0.1 g L^{-1} MgH_2-CBS, 600-μM NaHS, or 10-mM HT, alone and in combination. For the entire tests, all stems were continuously kept in the treatment solutions throughout the vase period at 25 ± 2°C, 60–70% relative humidity, and 12 h per day of light (20 μmol m^{-2} s^{-1}). All treatment solutions were renewed daily as well.

Determination of Hydrogen Gas Concentration

The concentration of H_2 in solutions was measured by a portable dissolved hydrogen meter (ENH-1000, TRUSTLEX, Osaka, Japan) that was calibrated by gas chromatography (Su et al., 2019).

Vase Life, Relative Fresh Weight, and Flower Diameter

The vase life of each flower was calculated as the number of days from the day that the stems were placed in the vase solutions (recorded as day 0) until the day that 50% of petals had wilted or the stems had bent (bent-neck angle greater than 45°). During the vase period, the fresh weight of each sample was measured daily using an analytical balance. The relative fresh weight (RFW) was calculated as following: $RFW\% = (FW_t/Fw_0) \times 100$, where W_t is the fresh weight of the sample (g) at day t (t = 0, 1, 2, 3, etc.), and W_0 is the fresh weight of the same sample (g) at day 0. Additionally, flower diameter was defined as the maximum width of each flower and measured daily using a digital caliper. In each experiment, 10 flowers were placed per treatment with three replications, and the means of the vase life, RFW, and flower diameter were determined.

Measurement of Endogenous Hydrogen Sulfide

With the aid of laser scanning confocal microscopy, H_2S level *in vivo* was determined as described previously with minor modification (Kou et al., 2018). The petals were incubated with 20-μM WSP5 (an H_2S fluorescent probe) in 20-mM 4-(2-hydroxyethyl)-1-piperazineethanesulfonic acid–sodium hydroxide buffer (pH 7.5) for 30 min in the dark (25°C). After three washes (10 min per time) with fresh 4-(2-hydroxyethyl)-1-piperazineethanesulfonic acid–sodium hydroxide buffer, the samples were observed using an LSM 710 microscope (Carl Zeiss, Oberkochen, Germany) with excitation at 495 nm and emission at 525 nm. The bright-field images were shown at the lower right corners of their corresponding fluorescent images. The relative fluorescence was presented as relative units of pixel intensities calculated by the ZEN software to the control samples. At least five sections per sample were determined, and three samples in each treatment were used.

Histochemical Staining and Corresponding Measurement of Hydrogen Peroxide Content

The hydrogen peroxide (H_2O_2) in petal was visually detected according to the method of Thordal-Christensen et al. (1997). The petals were stained with 0.1% 3,3-diaminobenzidine for 12 h at room temperature in the dark. Afterward, the petals were detected under a light microscope (Stemi 2000-C; Carl Zeiss, Germany).

The H_2O_2 content was measured by the spectrophotography (Mei et al., 2017). The samples were incubated with assay reagent (containing 50-mM H_2SO_4, 200-μM xylenol orange, and 200-mM sorbitol) for 45 min in the dark at 25°C. Then, the absorbance values were determined at 560 nm. A standard curve was obtained by adding a variable amount of H_2O_2.

Analysis of Senescence-Associated Genes Transcription

Quantitative real-time RT-PCR (qPCR) was used to analyze the expression of *SAGs*. Total RNA was extracted from petals using the SparkZol Reagent (SparkJade, Shandong, China). The concentration and quality of RNA were determined using a NanoDrop 2000 (Thermo Fisher Scientific, Wilmington, DE, United States), and RNA was treated with RNase-free DNase (TaKaRa Bio Inc., Dalian, China) to eliminate traces of DNA. Afterward, complementary DNAs were synthesized using HiScript III RT SuperMix (Vazyme, Nanjing, China). By using specific primers (**Supplementary Table 1**), qPCR was performed using a Mastercycler ep® *realplex* real-time PCR system (Eppendorf, Hamburg, Germany) with

2 × SYBR Green qPCR Mix (SparkJade, Shandong, China). Relative expression levels were calculated using the $2^{-\Delta\Delta CT}$ method (Livak and Schmittgen, 2001) and presented as values relative to the control samples (0 days) after the normalization with the transcript levels of an internal control gene *DcActin*.

Statistical Analysis

All values are means ± standard error (SE) of three independent experiments with three biological replicates for each. Data were analyzed by SPSS 22.0 software (IBM Corporation, Armonk, NY, United States). Differences among treatments were analyzed by one-way analysis of variance (ANOVA) followed by Duncan's multiple range test or *t*-test, and $P < 0.05$ or 0.01 were considered as statistically significant.

RESULTS

Characterization of Magnesium Hydride

As shown in the scanning electron microscopy images (**Figure 1A**), the as-received MgH_2 particles are spherical with a diameter of 0.5–25 μm (mean diameter = 15 μm; Ma et al., 2019). The X-ray diffraction patterns (**Figure 1B**) confirmed that MgH_2 is the majority phase with a small amount of unhydrided magnesium. The dehydriding properties of MgH_2 were investigated by using differential scanning calorimetry and thermogravimetry. It was observed that the peak temperature of decomposition is 405°C at a heating rate of 10°C min^{-1} with a mass loss of about 7.2 wt% (**Figure 1C**).

The amount of H_2 generated from complete hydrolysis of MgH_2 was about 1,800 ml g^{-1} (**Figure 1D**); namely, the concentration of H_2 in unit volume (1 m^3) was 0.18% (v v^{-1}). It is not flammable and explosive when the H_2 concentration is less than 4% by volume (lower flammability limit of H_2). Thus, it is generally safe by using MgH_2 as a vase regent.

Magnesium Hydride–Citrate Buffer Solution Prolongs the Vase Life of Cut Carnation Flowers

In our experimental conditions, when 0.1 g L^{-1} MgH_2 was dissolved in 0.1-M CBS (pH 3.4), this combined treatment (also abbreviated as MgH_2-CBS in the following experiments) was observed as the most obvious effect on prolonging the vase life of carnation cut flowers, compared with different doses of MgH_2, various CBS, or 10% HRW alone (**Supplementary Figures 1A–C** and **Figures 2A,B**). In the presence of 0.1 g L^{-1} MgH_2-CBS (0.1 M, pH 3.4), for example, the vase life of the fresh cut flowers was the longest among all the treatment and was 11.4 days, which prolonged 3.9 days compared with the control, which was also significantly different from the treatments of 0.1 g L^{-1} MgH_2 (prolonged about 2.0 days), 0.1-M CBS (pH 3.4; about 1.6 days), or 10% HRW (about 1.5 days) alone. This conclusion correlates with the data from other phenotypic parameters, including RFW and flower diameter in carnation (**Figures 2C,D**). By contrast, the removal of H_2 by heating solution impaired the positive effects of MgH_2-CBS. It was also confirmed that the boiling used in our experiment was sufficient to remove H_2 from solutions (**Figure 2E**), thus suggesting the function of MgH_2-CBS is H_2-dependent.

Consistently, the contents of dissolved H_2 in MgH_2-CBS and 0.1 g L^{-1} MgH_2 solutions ranked the first and second (rapidly peaking at 0.80 and 0.48 ppm) and remained in higher levels until 6 and 12 h, respectively. Meanwhile, H_2 existing in 10% HRW progressively decreased, just from an initial 0.16 ppm to the basal level after 6 h (**Figure 2E**).

Hydrogen Sulfide Is Involved in Magnesium Hydride–Citrate Buffer Solution-Prolonged Vase Life of Cut Carnation Flowers

To investigate whether H_2S is involved in MgH_2-CBS-prolonged vase life of carnation cut flowers, both MgH_2-CBS and HT (a specific H_2S scavenger; Ortega et al., 2008) were applied alone and in combination. Meanwhile, NaHS (an H_2S releasing compound) was used as a positive control. The response of the endogenous H_2S level in the petal was monitored by labeling H_2S using an H_2S-specific fluorescent probe (WSP-5; Peng et al., 2014) and imaging by laser scanning confocal microscopy (Kou et al., 2018). As shown in **Figure 3**, the WSP-5-dependent fluorescent intensity was increased by NaHS but was greatly impaired by HT. In addition, HT alone decreased fluorescent intensity in comparison with the chemical-free control. It was confirmed that some, if not most, of the WSP-5-related fluorescence is caused by H_2S. Further results demonstrated that MgH_2-CBS significantly increased endogenous H_2S production. Consistently, the inducing effect achieved by MgH_2-CBS could be prevented by HT. Moreover, there was no additive response in fluorescence when MgH_2-CBS was added together with NaHS.

The subsequent experiment was to assess the contribution of H_2S in prolonging carnation vase-life achieved by MgH_2-CBS. Consistently, three parameters, in terms of vase life, RFW, and flower diameter, were used. As expected, compared with the responses of NaHS, the prolonged vase life of cut carnation flowers was intensified in the presence of MgH_2-CBS, which was abolished when HT was added (**Figure 4**). In contrast, compared with control, HT alone shortened the vase life. However, MgH_2-CBS co-treated with NaHS cannot result in an additive extension of carnation vase-life. Correlating with the changes in endogenous H_2S production (**Figure 3**), the results indicated that endogenous H_2S might participate in MgH_2-CBS-prolonged the vase life of cut carnation flowers.

Magnesium Hydride–Citrate Buffer Solution Maintains Redox Homeostasis via Hydrogen Sulfide

Histochemical staining of ROS (H_2O_2) accumulation was then adopted to reveal the detailed mechanism underlying MgH_2-CBS-prolonged carnation vase-life. As expected, it was observed that a gradual increase of 3,3-diaminobenzidine-dependent staining in the control during the vase period (**Figure 5A**). The change of endogenous H_2O_2 level determined

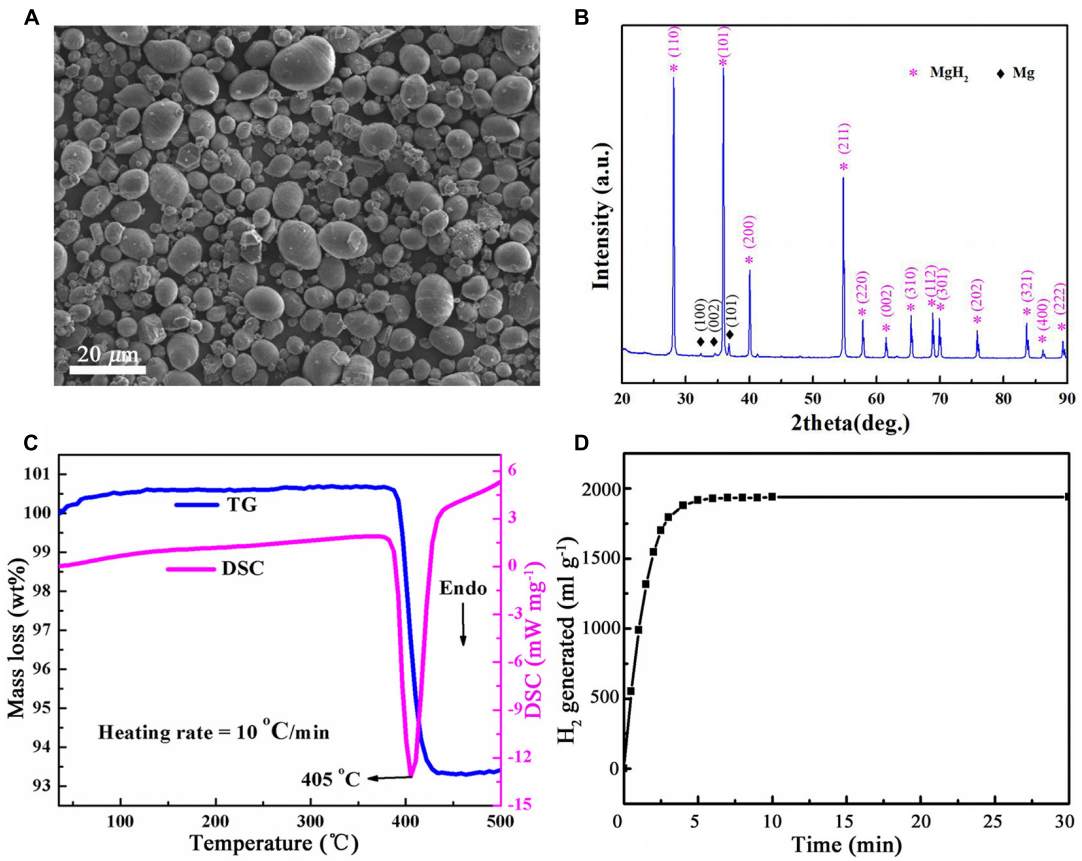

FIGURE 1 | Characterization of MgH_2 used in this work. **(A)** Scanning electron microscopy (SEM) micrographs of MgH_2 (Scale bar = 20 μm). **(B)** X-ray diffraction (XRD) pattern of MgH_2 powers. **(C)** Thermogravimetric (TG) and differential scanning calorimetry (DSC) curves of MgH_2. **(D)** H_2 generated from hydrolysis of MgH_2.

with spectrophotography displayed a similar tendency (**Figure 5B**), indicating that redox homeostasis was disrupted during senescence.

Compared with the control, the treatments with MgH_2-CBS and NaHS individually resulted in slight staining patterns (**Figure 5A**). By contrast, the mentioned responses elicited by MgH_2-CBS, and NaHS was reversed by the removal of endogenous H_2S when HT was applied. Alone, HT brought out extensive straining compared with the control (5 days). No additive responses were observed in MgH_2-CBS plus NaHS. Meanwhile, changes in endogenous H_2O_2 contents showed similar patterns (**Figure 5B**). These results suggested that MgH_2-CBS could reestablish redox homeostasis in carnation flowers, which might be mediated by H_2S.

Role of Hydrogen Sulfide in Magnesium Hydride–Citrate Buffer Solution-Modulated Senescence-Associated Genes During Postharvest Senescence

To further elucidate the molecular mechanism of how H_2S is involved in MgH_2-CBS-prolonged carnation vase-life, several molecular probes responsible for senescence, including *DcbGal* and *DcGST1*, were analyzed by qPCR. The time-course experiment showed that the expression levels of *DcbGal* and *DcGST1* were increased during postharvest senescence, and those in petals of control were much higher than those in the presence of MgH_2-CBS (**Figures 6A,B**). Similar to the responses of H_2S, MgH_2-CBS could also downregulate the transcripts of *DcbGal* and *DcGST1* (5 days; **Figures 6C,D**). In contrast, the inhibition mentioned earlier was attenuated by the depletion of H_2S with HT. Additionally, HT alone could greatly increase the expression levels of these two genes. No additive inhibition responses occurred in co-treatment of MgH_2-CBS and H_2S as well. Therefore, H_2S was involved in MgH_2-CBS-induced reduction of *DcbGal* and *DcGST1* expression in carnation during the vase period.

DISCUSSION

At present, HRW is a major route of H_2 administration (Shen and Sun, 2019). Ample evidence showed that HRW has positive effects on postharvest physiology. For example, HRW can prolong the shelf life (Hu et al., 2014) and decrease nitrite accumulation of fruits during storage (Zhang et al., 2019), as

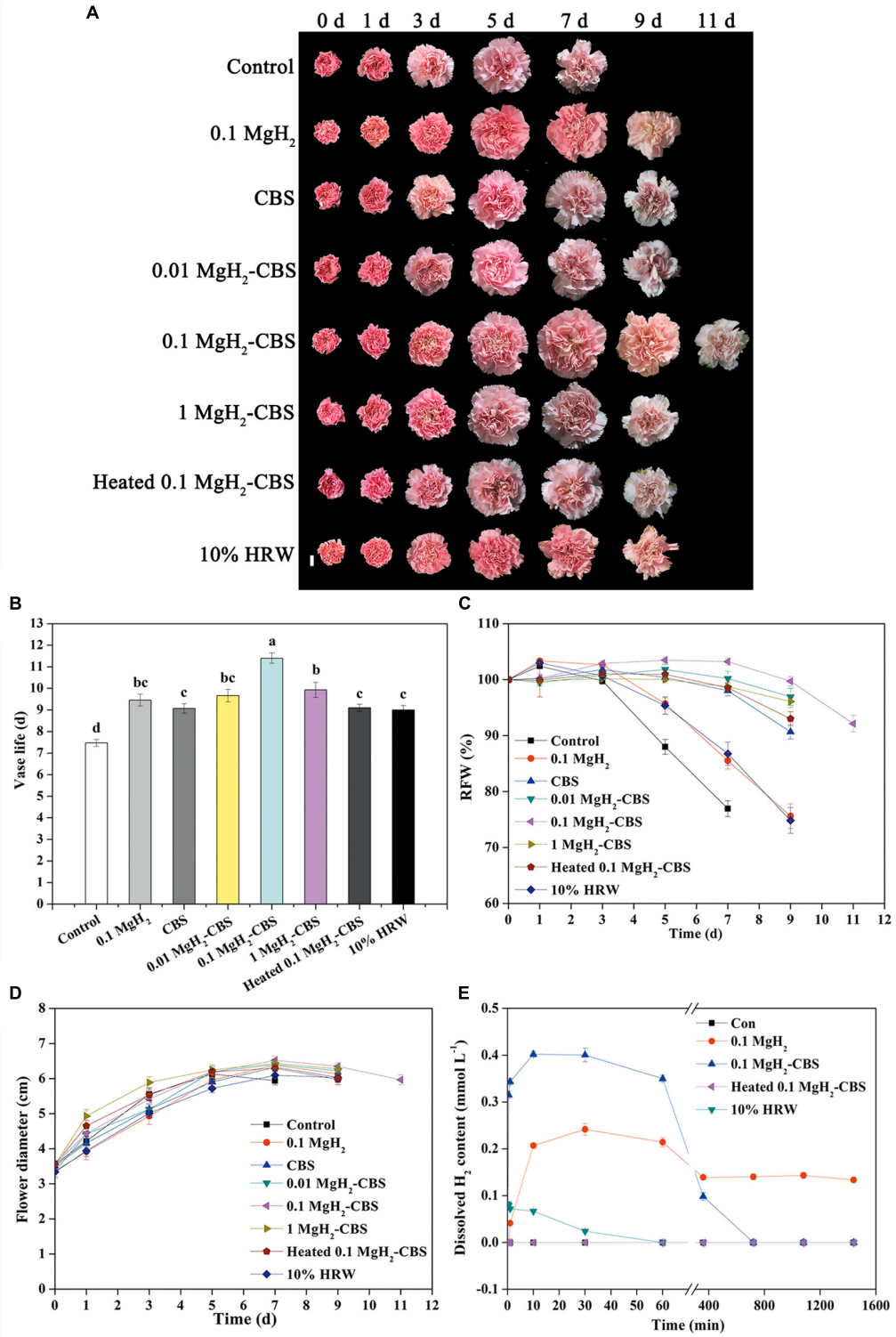

FIGURE 2 | Changes in vase life, relative fresh weight (RFW), and flower diameter of cut carnations and dissolved H_2 in solution subjected to MgH_2, citrate buffer solution (CBS), MgH_2-CBS, heated MgH_2-CBS, and hydrogen-rich water (HRW). **(A)** Representative photographs of cut flowers (scale bar = 2 cm). Cut flower stems were incubated in untreated (control) and treatment solutions containing 0.1 g L^{-1} MgH_2, 0.1-M CBS (pH 3.4) with or without 0.01, 0.1, and 1 g L^{-1} MgH_2, 10% electrolytic HRW during vase period. Afterward, vase life **(B)**, RFW **(C)**, maximum flower diameter **(D)**, and H_2 content in solutions **(E)** were expressed as mean ± standard error (SE). There were three replicates and 10 flowers per each for **(A–D)**, and three replicates per each for **(E)**. Experiments were conducted for three times. Bars with different letters are significantly different ($P < 0.05$), as determined by Duncan's multiple range test.

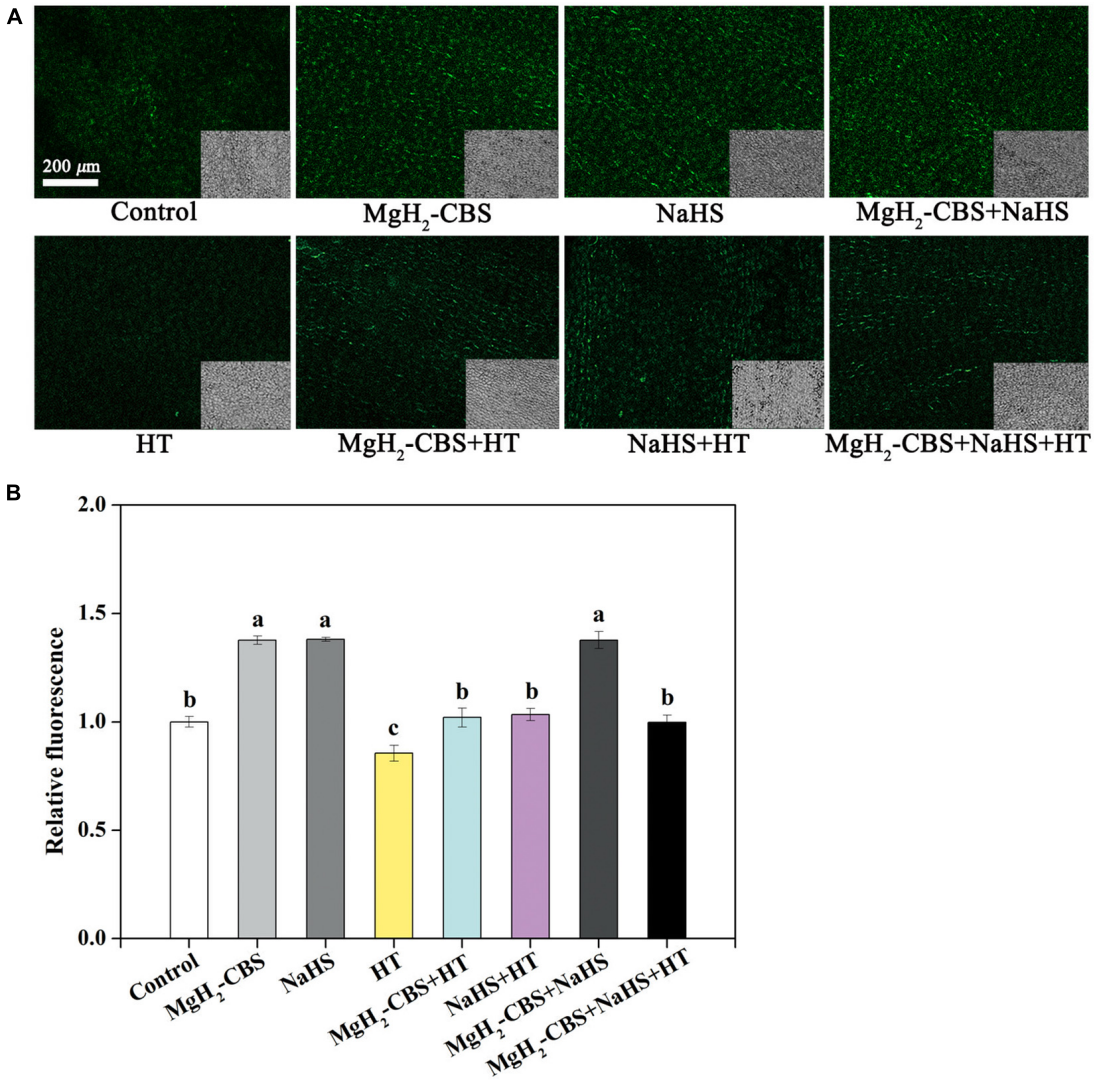

FIGURE 3 | MgH_2-CBS triggers H_2S accumulation. **(A)** Cut flower stems were incubated in untreated (control) and treatment solutions containing 0.1 g L^{-1} MgH_2-CBS, 600-μM NaHS, 10-mM HT (a scavenger of H_2S), alone or their combinations for 3 days. Afterward, epidermis of petals was loaded with 20-μM WSP5 (an H_2S fluorescent probe) and detected by laser scanning confocal microscopy (scale bar = 200 μm). Bright-field images corresponding to the fluorescent images were at the bottom right corner. **(B)** Relative fluorescence was also presented as values relative to control. Mean and SE values were calculated. At least five sections per sample were determined, and three samples in each treatment were used. Bars with different letters denoted significant differences in comparison with control at $P < 0.05$, according to Duncan's multiple range test.

well as prolong the vase life of cut flowers (Ren et al., 2017; Su et al., 2019; Wang et al., 2020). Importantly, the HRW is presently mainly obtained by water electrolysis, which requires a hydrogen gas generator. Moreover, the solubility of H_2 in water is very low (approximately 1.84 ml in 100-g H_2O at 20°C, 1 atm; Safonov and Khitrin, 2013), and especially, the residence time of H_2 in HRW is shorter, as the half-time of dissolved H_2 in HRW is less than 1 h (**Figure 2E**), at least under our experimental conditions. The discussed disadvantages may restrict the practical applications of the electrolytic produced HRW.

In this study, H_2 was generated by MgH_2 hydrolysis, which was intensified when dissolved in CBS. Additionally, it can remain in higher amounts of dissolved H_2 over a relatively longer period than the electrolytic HRW (**Figure 2E**). It has been reported that hydrolysis of magnesium particles can produce hydrogen nanobubbles that can exist in the water solution of a dietary supplement for a sufficiently long time (Bunkin et al., 2009; Safonov and Khitrin, 2013). A balance between surface tension and repulsive forces between surface electric charges is responsible for the stabilization of nanobubbles (Bunkin et al., 2009). We also found that the dissolution of MgH_2 in water and CBS (in particular) was accompanied by a large number of small bubbles in the first 1–2 min. Thus, MgH_2 may also produce hydrogen nanobubbles that increase the solubility and the residence time of H_2. However, the dissolution of MgH_2 in water led to a strongly

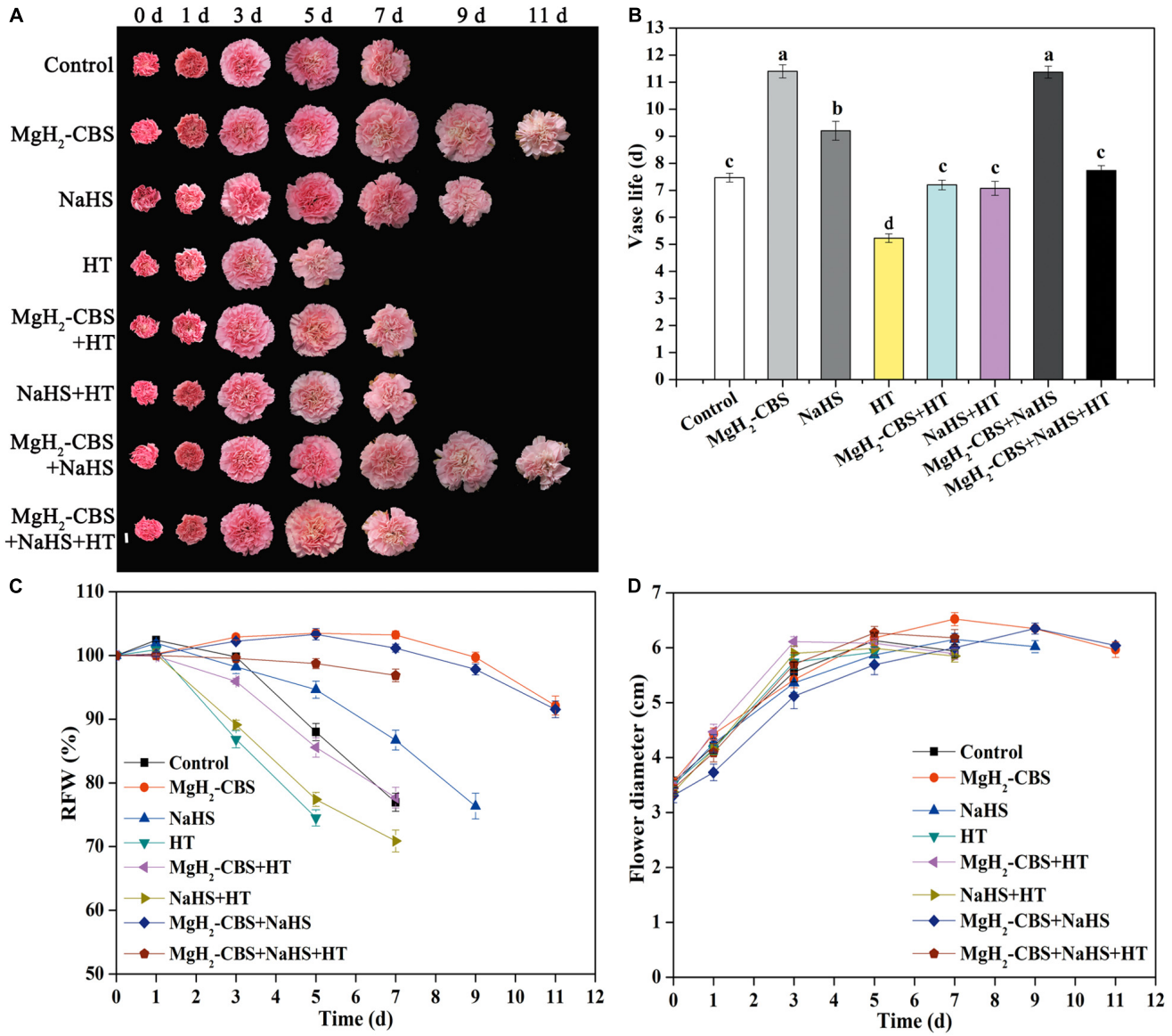

FIGURE 4 | MgH_2-CBS-prolonged vase life of cut carnation flowers is sensitive to the scavenger of H_2S. **(A)** Cut flower stems were incubated in untreated (control) and treatment solutions containing 0.1 g L^{-1} MgH_2-CBS, 600-μM NaHS, 10-mM HT (a scavenger of H_2S), alone or their combinations throughout the vase period. Representative photographs of cut flowers were taken (scale bar = 2 cm). Vase life **(B)**, relative fresh weight (RFW; **C**), and maximum flower diameter **(D)** were expressed as mean and SE values. There were three replicates and 10 flowers per each. Experiments were conducted for three times. Bars with different letters are significantly different ($P < 0.05$), as determined by Duncan's multiple range test.

alkaline environment (approximately pH 10; **Supplementary Figure 1F**). By contrast, the administration with CBS significantly accelerated the reaction of MgH_2 hydrolysis and increased H_2 generation (**Figure 2E**) by decreasing the pH, which is consistent with the previous studies (Hiraki et al., 2012; Chao, 2018).

It is worth noting the safety of MgH_2 use. In fact, the concentration of H_2 generated from MgH_2 hydrolysis is far less than the lower flammability limit of H_2 (4% in air). Therefore, it is safe by using MgH_2 as a vase regent. It has been reported that the citric acid buffered around pH 3 can effectively prolong the vase life of cut flowers by reducing bacterial growth and maintaining the water balance (van Doorn, 2010). A similar result was observed in this study (**Supplementary Figures 1B,C** and **Figures 2A,B**). Although the combination of MgH_2 and acid solutions is impractical for industry application because it causes equipment corrosion, it precisely favors postharvest preservation. We also observed that combining MgH_2 with CBS may produce additive or synergistic effects in prolonging the vase life of cut carnation flowers. Together, MgH_2 might be used as a promising chemical for producing a hydrogen-rich solution in horticulture.

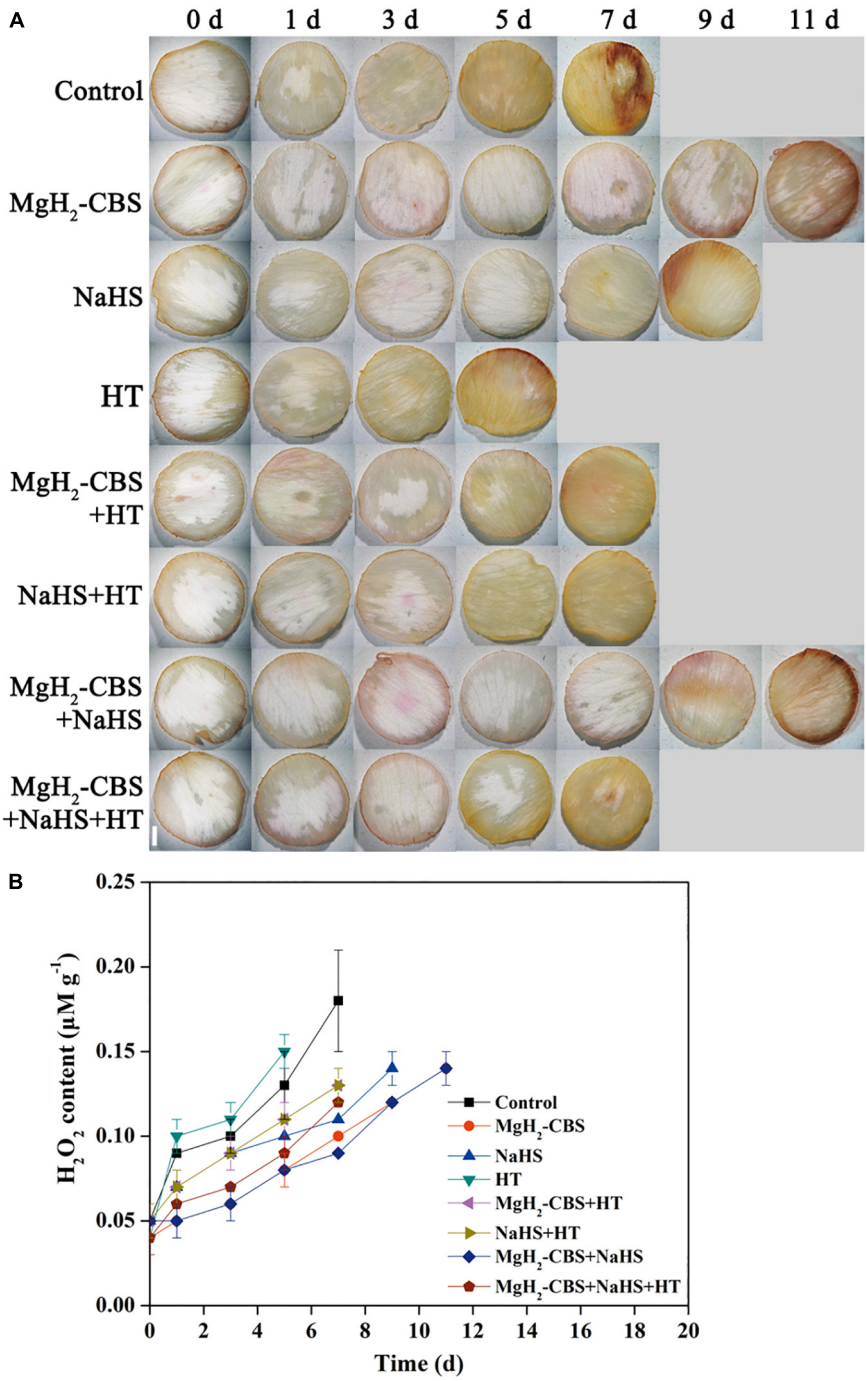

FIGURE 5 | MgH_2-CBS maintains redox homeostasis via H_2S. **(A)** Cut flower stems were incubated in solutions containing 0.1 g L^{-1} MgH_2-CBS, 600-μM NaHS, 10-mM HT, alone or their combinations throughout the vase period. The petals were stained with 3,3-diaminobenzidine (DAB), then photographed under a light microscope (scale bar = 1 mm). **(B)** Spectrophotography also determined H_2O_2 contents. Values are mean ± SE of three independent experiments with three replicated for each.

H_2S is a well-known important gaseous signaling molecule involved in plant developmental and environmental responses, such as root organogenesis, response to abiotic stresses, and delayed senescence of vegetables, fruits, and flowers (Zhang et al., 2011; Li et al., 2012, 2013; Wang et al., 2012; Ali et al., 2019; Corpas, 2019; Mei et al., 2019). It has been confirmed that L-cysteine desulfhydrase-dependent H_2S acts as the downstream signal molecule involved in NO-induced heat tolerance of maize seedlings (Li et al., 2013) and methane-induced tomato and *Arabidopsis* lateral root formation (Mei et al., 2019). Interestingly,

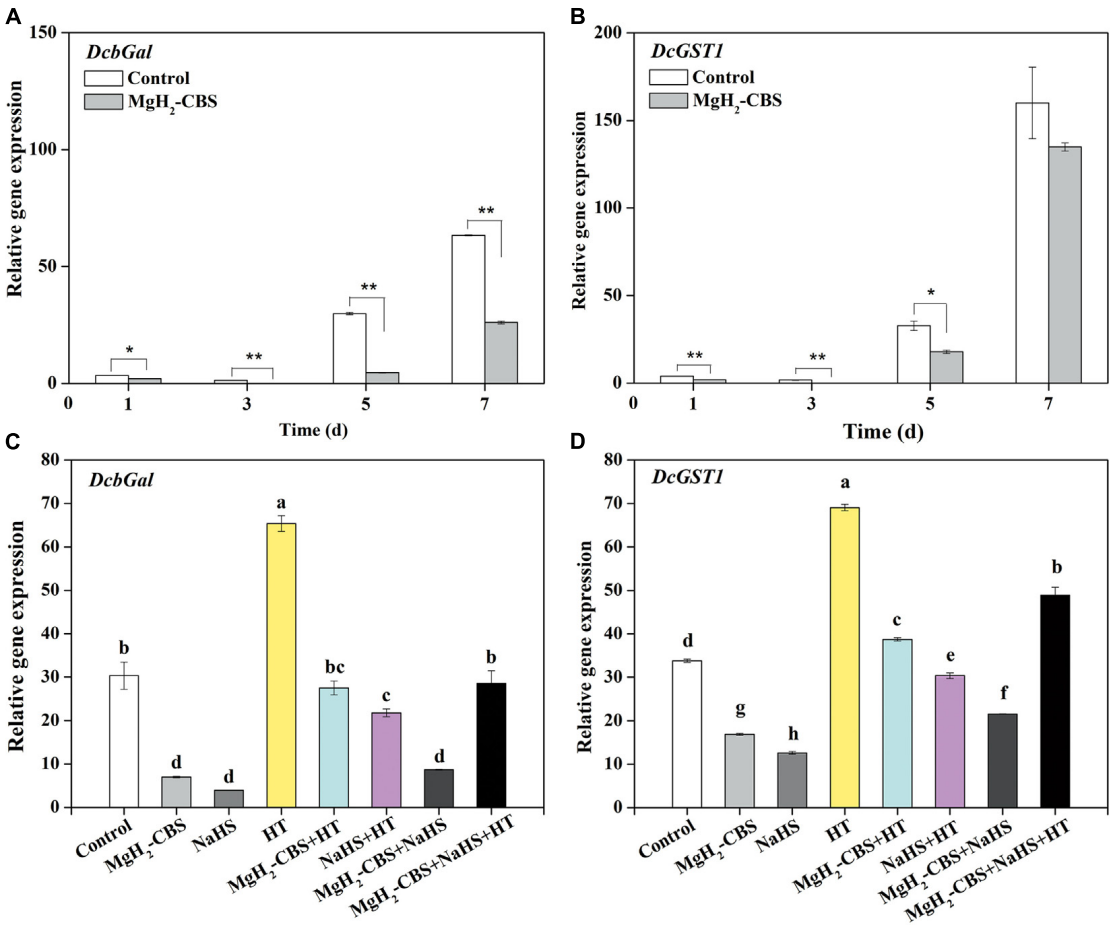

FIGURE 6 | Changes in the transcripts of senescence-associated genes. Cut flower stems were incubated in solutions containing 0.1 g L^{-1} MgH_2-CBS, 600-μM NaHS, 10-mM HT, alone or their combinations throughout the vase period. After treatments for the indicated time points or 5 days, the transcript levels of *DcbGal* **(A,C)** and *DcGST1* **(B,D)** in petals were analyzed by qPCR and presented as values relative to the control samples (0 days) after the normalization with the transcript levels of an internal control gene *DcActin*. Values are mean ± SE of three independent experiments with three replicated for each. Bars with asterisks were significantly different in comparison with control at $^*P < 0.05$ and $^{**}P < 0.01$ according to *t*-test. Bars with different letters are significantly different ($P < 0.05$), as determined by Duncan's multiple range test.

a similar requirement of H_2S for MgH_2-prolonged vase life of cut carnation flowers was discovered in this work. The conclusion is supported by the following pharmacologic and molecular evidence.

HT, a scavenger of H_2S (Ortega et al., 2008; Fang et al., 2014; Mei et al., 2019), was used in our experiments, and its inhibitory role was confirmed. The increase in endogenous H_2S accumulation triggered by MgH_2-CBS was observed to be sensitive by HT (**Figure 3**). Correlating with the changes in the phenotypes of vase life, relative fresh weight, and flower diameter (**Figure 4**), the results presented here further revealed a requirement for endogenous H_2S in MgH_2-CBS-prolonged carnation vase-life.

Furthermore, ROS (especially H_2O_2) has been observed to increasingly produce during the senescence process in cut flower (Hossain et al., 2006; Kumar et al., 2007; Su et al., 2019). It has been demonstrated that H_2S could inhibit ROS overproduction by increasing activities of antioxidant enzymes (Zhang et al., 2011; Hu et al., 2012, 2015). In this study, the contents of H_2O_2 gradually increased during the normal senescence of cut carnation flowers, which indicated the disruption of redox homeostasis (**Figure 5B**). The lower H_2O_2 levels maintained by MgH_2-CBS might be, at least partially, responsible for delaying senescence. By contrast, the discussed responses of MgH_2-CBS were reversed by the removal of endogenous H_2S with HT (**Figure 5B**). Changes in histochemical staining showed a similar pattern (**Figure 5A**). The discussed results, therefore, confirmed that MgH_2-CBS-reestablished redox homeostasis was closely associated with the alteration in endogenous H_2S.

Recent evidence proved that H_2S decreased the expression levels of *SAGs*, resulting in delaying the postharvest senescence of broccoli (Li et al., 2014). Furthermore, sucrose and silver thiosulphate (an inhibitor of ethylene receptor) could repress the upregulation of *SAGs* (including *DcbGal* and *DcGST*) in petals of carnation (Hoeberichts et al., 2007). Similarly, our further

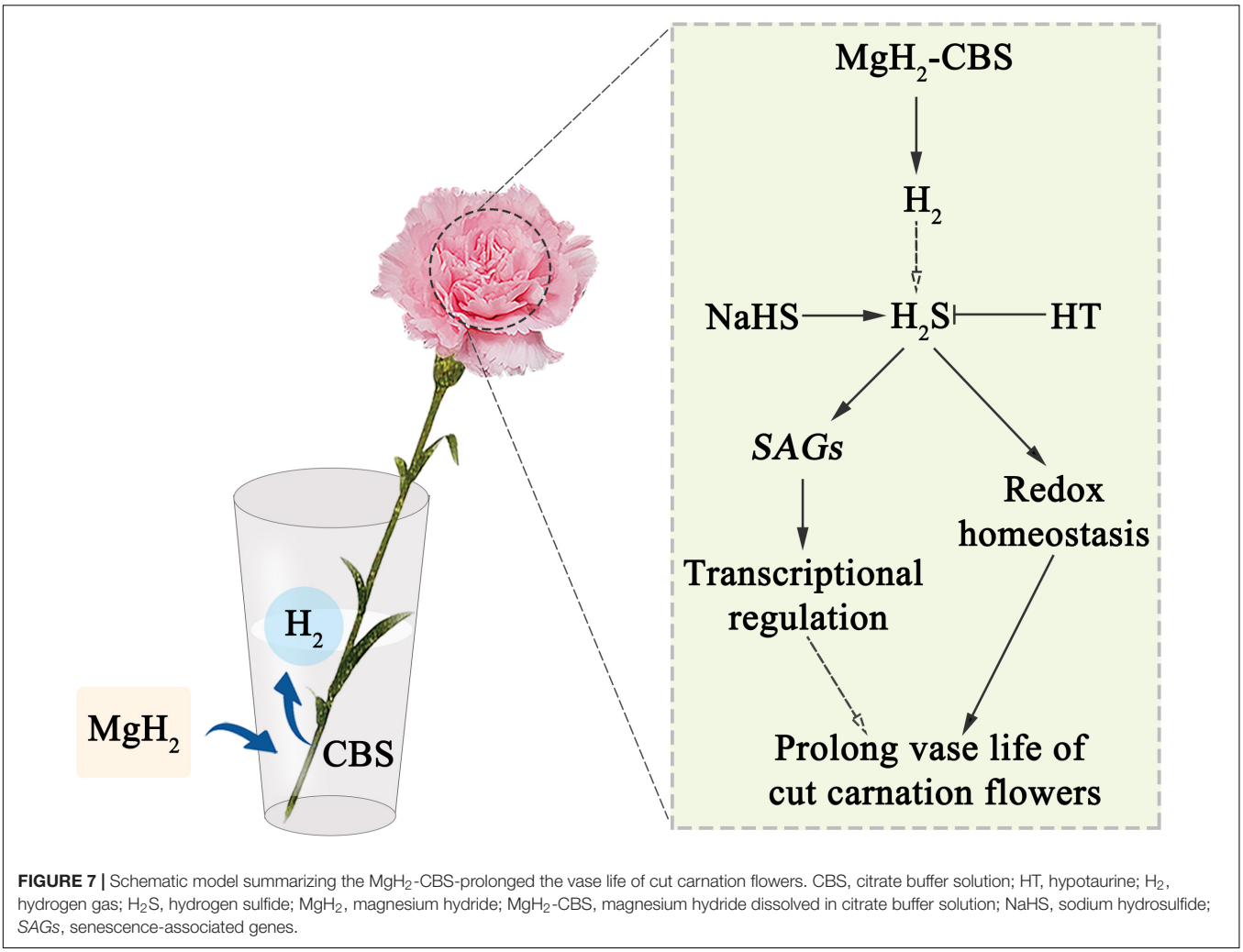

FIGURE 7 | Schematic model summarizing the MgH_2-CBS-prolonged the vase life of cut carnation flowers. CBS, citrate buffer solution; HT, hypotaurine; H_2, hydrogen gas; H_2S, hydrogen sulfide; MgH_2, magnesium hydride; MgH_2-CBS, magnesium hydride dissolved in citrate buffer solution; NaHS, sodium hydrosulfide; *SAGs*, senescence-associated genes.

molecular data revealed that MgH_2-CBS could downregulate the expression of *DcbGal* and *DcGST* (**Figure 6**). By contrast, such inhibition effects of MgH_2-CBS were alleviated by HT. Combined with the changes in phenotypes and endogenous H_2S level (**Figures 3**, **4**), we also speculated that *SAGs* might be the target genes responsible for MgH_2-CBS-triggered H_2S-prolonged vase life of cut flowers.

Accordingly, a schematic model shown in **Figure 7** summarizes the role of H_2S in the MgH_2-CBS-prolonged the vase life of cut carnation flowers.

CONCLUSION

This study revealed the effectiveness of MgH_2-mediated H_2 sustainable supply in postharvest preservation of cut flowers. Compared with hydrogen-rich water, the utilization efficiency of MgH_2 was improved by buffering with CBS. Thus, MgH_2 may have great potential for application in horticulture. In addition, it also demonstrated a vital role of H_2S in MgH_2-CBS-prolonged the vase life of cut flowers by modulating the expression of *SAGs*.

DATA AVAILABILITY STATEMENT

All datasets generated for this study are included in the article/**Supplementary Material**, further inquiries can be directed to the corresponding author.

AUTHOR CONTRIBUTIONS

WS and LL conceived and designed the research. LL, YL, and SW performed the experiments and analyzed the data. JZ and WD provided advice and materials for these experiments. LL, YL, SW, and WS wrote and revised the manuscript. All authors contributed to the article and approved the submitted version.

FUNDING

The work was financially supported by the funding from the Center of Hydrogen Science, Shanghai Jiao Tong University, China, and the Foshan Agriculture Science and Technology Project (Foshan City budget no. 140, 2019).

ACKNOWLEDGMENTS

We would like to thank Evan Evans (University of Tasmania; tassiebeerdr@gmail.com) for the English editing of this manuscript.

SUPPLEMENTARY MATERIAL

The Supplementary Material for this article can be found online at: https://www.frontiersin.org/articles/10.3389/fpls.2020.595376/full#supplementary-material

REFERENCES

Ali, S., Nawaz, A., Ejaz, S., Haider, S. T., Alam, M. W., and Javed, H. U. (2019). Effects of hydrogen sulfide on postharvest physiology of fruits and vegetables: an overview. *Sci. Hortic.* 243, 290–299. doi: 10.1016/j.scienta.2018.08.037

Baricco, M., Bang, M., Fichtner, M., Hauback, B., Linder, M., Luetto, C., et al. (2017). SSH2S: hydrogen storage in complex hydrides for an auxiliary power unit based on high temperature proton exchange membrane fuel cells. *J. Power Sourc.* 342, 853–860. doi: 10.1016/j.jpowsour.2016.12.107

Bogdanović, B., Ritter, A., Spliethoff, B., and Straβburger, K. (1995). A process steam generator based on the high temperature magnesium hydride/magnesium heat storage system. *Int. J. Hydrogen Energ.* 20, 811–822. doi: 10.1016/0360-3199(95)00012-3

Bunkin, N. F., Suyazov, N. V., Shkirin, A. V., Ignatiev, P. S., and Indukaev, K. V. (2009). Nanoscale structure of dissolved air bubbles in water as studied by measuring the elements of the scattering matrix. *J. Chem. Phys.* 130:476. doi: 10.1063/1.3095476

Chao, C. (2018). "Clinical applications of magnesium hydride," in *Magnesium Alloys - Selected Issue*, eds T. Tański, W. Borek, and M. Król (London: IntechOpen), 115–128. doi: 10.5772/intechopen.79507

Corpas, F. J. (2019). Hydrogen sulfide: a new warrior against abiotic stress. *Trends Plant Sci.* 24, 983–988. doi: 10.1016/j.tplants.2019.08.003

Fang, T., Cao, Z., Li, J., Shen, W., and Huang, L. (2014). Auxin-induced hydrogen sulfide generation is involved in lateral root formation in tomato. *Plant Physiol. Biochem.* 76, 44–51. doi: 10.1016/j.plaphy.2013.12.024

Grochala, W., and Edwards, P. P. (2004). Thermal decomposition of the non-interstitial hydrides for the storage and production of hydrogen. *Chem. Rev.* 104, 1283–1315. doi: 10.1021/cr030691s

Hiraki, T., Hiroi, S., Akashi, T., Okinaka, N., and Akiyama, T. (2012). Chemical equilibrium analysis for hydrolysis of magnesium hydride to generate hydrogen. *Int. J. Hydrogen Energ.* 37, 12114–12119. doi: 10.1016/j.ijhydene.2012.06.012

Hirscher, M., Yartys, V. A., Baricco, M., Bellosta Von Colbe, J., Blanchard, D., Bowman, R. C., et al. (2020). Materials for hydrogen-based energy storage-past, recent progress and future outlook. *J. Alloy Compd.* 827:153548. doi: 10.1016/j.jallcom.2019.153548

Hoeberichts, F. A., van Doorn, W. G., Vorst, O., Hall, R. D., and van Wordragen, M. F. (2007). Sucrose prevents up-regulation of senescence-associated genes in carnation petals. *J. Exp. Bot.* 58, 2873–2885. doi: 10.1093/jxb/erm076

Hossain, Z., Mandal, A., Datta, S. K., and Biswas, A. K. (2006). Decline in ascorbate peroxidase activity-a prerequisite factor for tepal senescence in gladiolus. *J. Plant Physiol.* 163, 186–194. doi: 10.1016/j.jplph.2005.03.004

Hu, H., Li, P., Wang, Y., and Gu, R. (2014). Hydrogen-rich water delays postharvest ripening and senescence of kiwifruit. *Food Chem.* 156, 100–109. doi: 10.1016/j.foodchem.2014.01.067

Hu, H., Liu, D., Li, P., and Shen, W. (2015). Hydrogen sulfide delays leaf yellowing of stored water spinach (*Ipomoea aquatica*) during dark-induced senescence by delaying chlorophyll breakdown, maintaining energy status and increasing antioxidative capacity. *Postharvest Biol. Technol.* 108, 8–20. doi: 10.1016/j.postharvbio.2015.05.003

Hu, L., Hu, S., Wu, J., Li, Y., Zheng, J., Wei, Z., et al. (2012). Hydrogen sulfide prolongs postharvest shelf life of strawberry and plays an antioxidative role in fruits. *J. Agric. Food Chem.* 60, 8684–8693. doi: 10.1021/jf300728h

Huo, J., Huang, D., Zhang, J., Fang, H., Wang, B., Wang, C., et al. (2018). Comparative proteomic analysis during the involvement of nitric oxide in hydrogen gas-improved postharvest freshness in cut lilies. *Int. J. Mol. Sci.* 19:3955. doi: 10.3390/ijms19123955

Kamimura, N., Ichimiya, H., Iuchi, K., and Ohta, S. (2016). Molecular hydrogen stimulates the gene expression of transcriptional coactivator PGC-1α to enhance fatty acid metabolism. *NPJ Aging Mech. Dis.* 2:16008. doi: 10.1038/npjamd.2016.8

Kou, N., Xiang, Z., Cui, W., Li, L., and Shen, W. (2018). Hydrogen sulfide acts downstream of methane to induce cucumber adventitious root development. *J. Plant Physiol.* 228, 113–120. doi: 10.1016/j.jplph.2018.05.010

Kumar, N., Srivastava, G. C., and Dixit, K. (2007). Role of superoxide dismutases during petal senescence in rose (*Rosa hybrida* L.). *J. Hortic. Sci. Biotechnol.* 82, 673–678. doi: 10.1080/14620316.2007.11512290

Kumar, N., Srivastava, G. C., and Dixit, K. (2008). Hormonal regulation of flower senescence in roses (*Rosa hybrida* L.). *Plant Growth Regul.* 55, 65–71. doi: 10.1007/s10725-008-9259-6

Lawton, K. A., Huang, B., Goldsbrough, P. B., and Woodson, W. R. (1989). Molecular cloning and characterization of senescence-related genes from carnation flower petals. *Plant Physiol.* 90, 690–696. doi: 10.1104/pp.90.2.690

Li, H., Bai, G., Ge, Y., Zhang, Q., Kong, X., Meng, W., et al. (2018). Hydrogen-rich saline protects against small-scale liver ischemia-reperfusion injury by inhibiting endoplasmic reticulum stress. *Life Sci.* 194, 7–14. doi: 10.1016/j.lfs.2017.12.022

Li, L., Wang, Y., and Shen, W. (2012). Roles of hydrogen sulfide and nitric oxide in the alleviation of cadmium-induced oxidative damage in alfalfa seedling roots. *Biometals* 25, 617–631. doi: 10.1007/s10534-012-9551-9

Li, S., Hu, K., Hu, L., Li, Y., Jiang, A., Xiao, F., et al. (2014). Hydrogen sulfide alleviates postharvest senescence of broccoli by modulating antioxidant defense and senescence-related gene expression. *J. Agric. Food Chem.* 62, 1119–1129. doi: 10.1021/jf4047122

Li, Z., Yang, S., Long, W., Yang, G., and Shen, Z. (2013). Hydrogen sulphide may be a novel downstream signal molecule in nitric oxide-induced heat tolerance of maize (*Zea mays* L.) seedlings. *Plant Cell Environ.* 36, 1564–1572. doi: 10.1111/pce.12092

Livak, K. J., and Schmittgen, T. D. (2001). Analysis of relative gene expression data using real-time quantitative PCR and the $2-\Delta\Delta CT$ method. *Methods* 25, 402–408. doi: 10.1006/meth.2001.1262

Lototskyy, M., Nyallang, N. S., Pasupathi, S., Wærnhus, I., Vik, A., Ilea, C., et al. (2018). A concept of combined cooling, heating and power system utilising solar power and based on reversible solid oxide fuel cell and metal hydrides. *Int. J. Hydrogen Energ.* 43, 1865–1866. doi: 10.1016/j.ijhydene.2018.05.075

Ma, Z., Zou, J., Hu, C., Zhu, W., Khan, D., Zeng, X., et al. (2019). Effects of trimesic acid-Ni based metal organic framework on the hydrogen sorption performances of MgH2. *Int. J. Hydrogen Energ.* 44, 29235–29248. doi: 10.1016/j.ijhydene.2019.01.288

Mei, Y., Chen, H., Shen, W., Shen, W., and Huang, L. (2017). Hydrogen peroxide is involved in hydrogen sulfide-induced lateral root formation in tomato seedlings. *BMC Plant Biol.* 17:162. doi: 10.1186/s12870-017-1110-7

Mei, Y., Zhao, Y., Jin, X., Wang, R., Xu, N., Hu, J., et al. (2019). L-Cysteine desulfhydrase-dependent hydrogen sulfide is required for methane-induced lateral root formation. *Plant Mol. Biol.* 99, 283–298. doi: 10.1007/s11103-018-00817-3

Meyer, J. R. C., Goldsbrough, P. B., and Woodson, W. R. (1991). An ethylene-responsive flower senescence-related gene from carnation encodes a protein homologous to glutathione S-transferases. *Plant Mol. Biol.* 17, 277–281. doi: 10.1007/BF00039505

Naing, A. H., Lee, K., Arun, M., Lim, K. B., and Kim, C. K. (2017). Characterization of the role of sodium nitroprusside (SNP) involved in long vase life of different carnation cultivars. *BMC Plant Biol.* 17:149. doi: 10.1186/s12870-017-1097-0

Ohsawa, I., Ishikawa, M., Takahashi, K., Watanabe, M., Nishimaki, K., Yamagata, K., et al. (2007). Hydrogen acts as a therapeutic antioxidant by selectively reducing cytotoxic oxygen radicals. *Nat. Med.* 13, 688–694. doi: 10.1038/nm1577

Ohta, S. (2011). Recent progress toward hydrogen medicine: potential of molecular hydrogen for preventive and therapeutic applications. *Curr. Pharm. Design* 17:2241. doi: 10.2174/138161211797052664

Ortega, J. A., Ortega, J. M., and Julian, D. (2008). Hypotaurine and sulfhydryl-containing antioxidants reduce H2S toxicity in erythrocytes from a marine invertebrate. *J. Exp. Biol.* 211, 3816–3825. doi: 10.1242/jeb.021303

Peng, B., Chen, W., Liu, C., Rosser, E. W., Pacheco, A., Zhao, Y., et al. (2014). Fluorescent probes based on nucleophilic substitution-cyclization for hydrogen sulfide detection and bioimaging. *Chem. Eur.* 20, 1010–1016. doi: 10.1002/chem.201303757

Ren, P., Jin, X., Liao, W., Wang, M., Niu, L., Li, X., et al. (2017). Effect of hydrogen-rich water on vase life and quality in cut lily and rose flowers. *Hortic. Environ. Biotechnol.* 58, 576–584. doi: 10.1007/s13580-017-0043-2

Safonov, V. L., and Khitrin, A. K. (2013). Hydrogen nanobubbles in a water solution of dietary supplement. *Colloid Surf. A* 436, 333–336. doi: 10.1016/j.colsurfa.2013.06.043

Sakintuna, B., Lamaridarkrim, F., and Hirscher, M. (2007). Metal hydride materials for solid hydrogen storage: a review. *Int. J. Hydrogen Energ.* 32, 1121–1140. doi: 10.1016/j.ijhydene.2006.11.022

Schlapbach, L., and Zuttel, A. (2001). Hydrogen-storage materials for mobile applications. *Nature* 414, 353–358. doi: 10.1038/35104634

Shahri, W., and Tahir, I. (2011). Flower senescence-strategies and some associated events. *Bot. Rev.* 77, 152–184. doi: 10.1007/s12229-011-9063-2

Shen, W., and Sun, X. (2019). Hydrogen biology: it is just beginning. *Chin. J. Biochem. Mol. Biol.* 35, 1037–1050. doi: 10.13865/j.cnki.cjbmb.2019.10.01

Su, J., Nie, Y., Zhao, G., Cheng, D., Wang, R., Chen, J., et al. (2019). Endogenous hydrogen gas delays petal senescence and extends the vase life of lisianthus cut flowers. *Postharvest Biol. Technol.* 147, 148–155. doi: 10.1016/j.postharvbio.2018.09.018

Su, J., Zhang, Y., Nie, Y., Cheng, D., Wang, R., Hu, H., et al. (2018). Hydrogen-induced osmotic tolerance is associated with nitric oxide-mediated proline accumulation and reestablishment of redox balance in alfalfa seedlings. *Environ. Exp. Bot.* 147, 249–260. doi: 10.1016/j.envexpbot.2017.12.022

Thordal-Christensen, H., Zhang, Z., Wei, Y., and Collinge, D. B. (1997). Subcellular localization of H_2O_2 in plants. H_2O_2 accumulation in papillae and hypersensitive response during the barley—powdery mildew interaction. *Plant J.* 11, 1187–1194. doi: 10.1046/j.1365-313X.1997.11061187.x

van Doorn, W. G. (2010). "Water relations of cut flowers," in *Horticultural Reviews*, ed. J. J. Janick (New York, NY: John Wiley & Sons), 1–85. doi: 10.1002/9780470650608.ch1

van Doorn, W. G., and Woltering, E. J. (2008). Physiology and molecular biology of petal senescence. *J. Exp. Bot.* 59, 453–480. doi: 10.1093/jxb/erm356

Wang, C., Fang, H., Gong, T., Zhang, J., Niu, L., Huang, D., et al. (2020). Hydrogen gas alleviates postharvest senescence of cut rose 'Movie star' by antagonizing ethylene. *Plant Mol. Biol.* 102, 271–285. doi: 10.1007/s11103-019-00946-3

Wang, Y., Li, L., Cui, W., Xu, S., Shen, W., and Wang, R. (2012). Hydrogen sulfide enhances alfalfa (*Medicago sativa*) tolerance against salinity during seed germination by nitric oxide pathway. *Plant Soil* 351, 107–119. doi: 10.1007/s11104-011-0936-2

Wu, Y., Yuan, M., Song, J., Chen, X., and Yang, H. (2019). Hydrogen gas from inflammation treatment to cancer therapy. *ACS Nano* 13, 8505–8511. doi: 10.1021/acsnano.9b05124

Xie, Y., Mao, Y., Lai, D., Zhang, W., and Shen, W. (2012). H2 enhances *Arabidopsis* salt tolerance by manipulating ZAT10/12-mediated antioxidant defence and controlling sodium exclusion. *PLoS One* 7:e49800. doi: 10.1371/journal.pone.0049800

Xie, Y., Mao, Y., Zhang, W., Lai, D., Wang, Q., and Shen, W. (2014). Reactive oxygen species-dependent nitric oxide production contributes to hydrogen-promoted stomatal closure in *Arabidopsis*. *Plant Physiol.* 165, 759–773. doi: 10.1104/pp.114.237925

Zeng, J., Zhang, M., and Sun, X. (2013). Molecular hydrogen is involved in phytohormone signaling and stress responses in plants. *PLoS One* 8:e71038. doi: 10.1371/journal.pone.0071038

Zhang, H., Hu, S., Zhang, Z., Hu, L., Jiang, C., Wei, Z., et al. (2011). Hydrogen sulfide acts as a regulator of flower senescence in plants. *Postharvest Biol. Technol.* 60, 251–257. doi: 10.1016/j.postharvbio.2011.01.006

Zhang, Y., Zhao, G., Cheng, P., Yan, X., Li, Y., Cheng, D., et al. (2019). Nitrite accumulation during storage of tomato fruit as prevented by hydrogen gas. *Int. J. Food Prop.* 22, 1425–1438. doi: 10.1080/10942912.2019.1651737

Conflict of Interest: The authors declare that the research was conducted in the absence of any commercial or financial relationships that could be construed as a potential conflict of interest.

frontiers in Plant Science

MINI REVIEW
published: 17 December 2020
doi: 10.3389/fpls.2020.584698

Selenium-Ethylene Interplay in Postharvest Life of Cut Flowers

Lucas C. Costa[1], Luana M. Luz[2], Vitor L. Nascimento[3], Fernanda F. Araujo[1], Mirelle N. S. Santos[1], Christiane de F. M. França[4], Tania P. Silva[5], Karen K. Fugate[6] and Fernando L. Finger[1]*

[1] Departamento de Fitotecnia, Universidade Federal de Viçosa, Viçosa, Brazil, [2] Laboratório de Genética e Biotecnologia – Campus Capanema, Universidade Federal Rural da Amazônia, Capanema, Brazil, [3] Setor de Fisiologia Vegetal – Departamento de Biologia, Universidade Federal de Lavras, Lavras, Brazil, [4] Departamento de Tecnologia Agroindustrial e Socioeconomia Rural, Universidade Federal de São Carlos, Araras, Brazil, [5] Instituto de Ciências Agrárias, Universidade Federal dos Vales do Jequitinhonha e Mucuri, Unaí, Brazil, [6] USDA-ARS, Edward T. Schafer Agricultural Research Center, Fargo, ND, United States

Selenium (Se) is considered a beneficial element in higher plants when provided at low concentrations. Recently, studies have unveiled the interactions between Se and ethylene metabolism throughout plant growth and development. However, despite the evidence that Se may provide longer shelf life in ethylene-sensitive flowers, its primary action on ethylene biosynthesis and cause-effect responses are still understated. In the present review, we discuss the likely action of Se on ethylene biosynthesis and its consequence on postharvest physiology of cut flowers. By combining Se chemical properties with a dissection of ethylene metabolism, we further highlighted both the potential use of Se solutions and their downstream responses. We believe that this report will provide the foundation for the hypothesis that Se plays a key role in the postharvest longevity of ethylene-sensitive flowers.

Keywords: ethylene inhibitors, vase life, flower quality, preservative solutions, Se metabolism

OPEN ACCESS

Edited by:
Margherita Irene Beruto, Istituto Regionale per la Floricoltura (IRF), Italy

Reviewed by:
Izabela Michalak, Wrocław University of Science and Technology, Poland
John Dole, North Carolina State University, United States

****Correspondence:***
Lucas C. Costa
costalc@ymail.com

Specialty section:
This article was submitted to Crop and Product Physiology, a section of the journal Frontiers in Plant Science

Received: *17 July 2020*
Accepted: *26 November 2020*
Published: *17 December 2020*

Citation:
Costa LC, Luz LM, Nascimento VL, Araujo FF, Santos MNS, França CFM, Silva TP, Fugate KK and Finger FL (2020) Selenium-Ethylene Interplay in Postharvest Life of Cut Flowers. Front. Plant Sci. 11:584698. doi: 10.3389/fpls.2020.584698

INTRODUCTION

Selenium (Se) is an essential nutrient for humans, bacteria, and most of the chlorophyte species (Lobanov et al., 2009; Nancharaiah and Lens, 2015). In higher plants, the beneficial effect of Se occurs in a concentration-dependent manner (Hawrylak-Nowak et al., 2014; Saidi et al., 2014; Boldrin et al., 2016; Sattar et al., 2019). At low concentrations, ranging from 0.1 to 1.0 mg L^{-1}, Se stimulates plant growth and activates components of the reactive oxygen species (ROS) scavenge system, thereby protecting against multiple abiotic and biotic stresses (Feng et al., 2013; Ahmad et al., 2016; Lapaz et al., 2019). On the other hand, Se can be also toxic at concentrations ranging from 1 to 5 mg L^{-1}, but the degree of tolerance varies among species (Freeman et al., 2010; Feng et al., 2013). Biological functions of Se occur primarily through selenoproteins which contain this element as part of the amino acids, selenocysteine (SeCys) and selenomethionine (SeMet) (Daniels, 1996), but also as a component of antioxidants, co-enzymes, specialized metabolites, and lipids (Khan M.I.R. et al., 2014; Khan N.A. et al., 2014). Therefore, the multiple presence of Se in plant metabolites evidences the unlimited possibilities of its action on plant metabolism, which has not been entirely explored.

Ethylene is a plant hormone mainly known for its role in affecting leaf and flower senescence, and fruit ripening. However, this simple gaseous molecule is also involved with other elemental processes throughout the plant's life cycle, including seed germination (Corbineau et al., 2014;

Miransari and Smith, 2014; Wilson et al., 2014), root initiation and development (Ivanchenko et al., 2008; Lima et al., 2009; Huang et al., 2013), floral development (O'Neill, 1997; Wuriyanghan et al., 2009), sexual determination (Iwahori et al., 1970; Yamasaki et al., 2001; Salman-Minkov et al., 2008), fruit ripening (Giovannoni, 2001; Barry and Giovannoni, 2007; Lim et al., 2007; De Martinis et al., 2015), plant senescence (Kim et al., 2014; De Martinis et al., 2015; Ueda and Kusaba, 2015), and response to biotic and abiotic stresses (Morgan and Drew, 1997; Wang et al., 2007; Lin et al., 2013; Steffens, 2014). Recently, several studies have uncovered evidence of a relationship between Se and ethylene metabolism in plants (Malorgio et al., 2009; Iqbal et al., 2015; Zhu et al., 2017; Hajiboland et al., 2019; Malheiros et al., 2019). In this vein, Malheiros et al. (2019) demonstrated that Se partially inhibits ethylene biosynthesis in roots of rice seedlings. Likewise, Iqbal et al. (2015) evidenced that Se inhibits 1-aminocyclopropane-1-carboxylate synthase (ACS) activity in wheat, the main limiting step of ethylene production in higher plants.

The production of flowers is one of the most important segments of horticulture in the field of agroindustry in many countries. The increased demand for high-quality products, however, requires postharvest technologies to improve floral vase life longevity. In recent years, the biological importance of ethylene on ornamental plant production and development of methods to alleviate its deleterious consequences in the overall ornamental value have been well explored. Nevertheless, many chemicals currently used to lessen ethylene responses present raised environmental and public health concerns. Thus, the development of methods that are environmentally friendly has become crucial (Scariot et al., 2014). Selenium presents suitable proprieties to be an eco-friendly (Cochran et al., 2018) and inexpensive (Haug et al., 2008) alternative to composing ethylene-sensitive flower preservative solutions. Recently, it was demonstrated that Se (6 mg L^{-1}) increases the vase life of Easter Lily (*Lilium longiflorum*) by alleviating cell damage via the ROS scavenging system and osmotic adjustment (Lu et al., 2020). However, it seems that Se may have additional functions affecting the postharvest life of cut flowers that have yet to be investigated. Based on the current literature, herein we propose a novel model of interaction between Se metabolism and ethylene biosynthesis, which likely underlies positive consequences on postharvest life of cut flowers.

AN OVERVIEW OF Se CHEMICAL CHARACTERISTICS AND METABOLISM

As part of the chalcogen group of chemical elements, Se is normally found in soils at concentrations from 0.01 to 2.0 mg kg^{-1} (Fordyce, 2005). This element exists in different oxidative states in soil conditions, such as elemental selenium (Se^0), selenide (Se^{2-}), thioselenate ($Se_2O_3^{2-}$), selenite (SeO_3^{2-}), and selenate (SeO_4^{2}) (Neal et al., 1987; White et al., 2004). Among the different forms of Se, selenate is the most soluble and bioavailable for plants; additionally, it is the most predominant form of transport through the xylem, as compared to selenite (Asher et al., 1977; Gupta and Gupta, 2017). The essentiality of Se in plants has not been proven, but it seems to affect several aspects of plant metabolism. Discovered in 1817, this trace element is actively absorbed by root cells through the sulfur (S) transporters SULTR1;2 and SULTR1; however SULTR1;2 seems to be the preferential transporter for the uptake of Se (Gupta and Gupta, 2017). Once absorbed, all synthesized organoselenium compounds are derived from pathways associated with S metabolism (Terry et al., 2000) and accumulate in roots (Galeas et al., 2007), leaves, stems (Liang et al., 2019), flowers (Quinn et al., 2011), and seeds (Liang et al., 2019).

The metabolism of Se is partially dependent on chloroplast metabolic machinery, where the reduction of selenate to selenite occurs under the sequential action of two enzymes that incorporate Se into amino acids (Terry et al., 2000). The accumulation of selenoamino acids allows non-specific incorporation of SeCys or SeMet in plant proteins since SeCys insertion machinery has allegedly been lost through evolution (Lobanov et al., 2009; Pilon-Smits and Quinn, 2010). Moreover, selenoamino acids can be converted to volatile compounds or Se^0 from the action of enzymes, such as methionine *S*-methyltransferase (Tagmount et al., 2002; Gupta and Gupta, 2017), SeCys methyltransferase (SMT) (Neuhierl and Boeck, 1996; Brummell et al., 2011; Chen et al., 2019) and SeCys lyase (SCL) (Pilon-Smits and Quinn, 2010). Because of this, most plants prevent excessive selenoamino acid accumulation to avoid metabolic impairments, especially those that may affect structural integrity and protein functions (Burnell, 1981; Brown and Shrift, 1982). The presence of Se in excess causes serious disruption at the metabolic level, including major changes in energy metabolism and ATP production, starch mobilization, and cell wall extension, which explains how Se causes a plant growth reduction (Ribeiro et al., 2016).

Selenoamino acids appear to be beneficial to growth in some conditions with an underlying influence on the oxidative protection networks in plants (Pilon-Smits and Quinn, 2010; Feng et al., 2013; Ahmad et al., 2016). Different strategies have been adopted to evaluate the role of Se in response to stress, including the application of Se as a seed priming treatment (Hasanuzzaman and Fujita, 2011; Nawaz et al., 2013; Hussain et al., 2016), soil fertilizer (Kumar et al., 2014; Khan et al., 2015; Atarodi et al., 2018), and foliar drench (Iqbal et al., 2015; Shahverdi et al., 2020). Treatment with Se at low concentrations is known to alleviate several stresses in plants, including those ones caused by drought (Hasanuzzaman and Fujita, 2011; Nawaz et al., 2013), heat (Iqbal et al., 2015), arsenic (Kumar et al., 2014), cadmium (Khan et al., 2015), low phosphorus (Jia et al., 2018), salinity (Shahverdi et al., 2020), as well as lead and aluminum (Feng et al., 2013). In addition to positive results in responding to several stresses, low concentrations of Se can also induce plant growth (Lehotai et al., 2012; Boldrin et al., 2016), via an effect on mitochondrial metabolism (Dimkovikj and Van Hoewyk, 2014) and molecular switches (Lehotai et al., 2012; Khan et al., 2015; Jia et al., 2018).

Concerning specific organs, several studies have demonstrated that this element delays fruit ripening (Zhu et al., 2017; Choudhary and Jain, 2018) and senescence

(Pezzarossa et al., 2012, 2014), leading to reductions in postharvest losses. Its ability to alter these processes is related to increased glutathione peroxidase (GSH-Px) activity (Rayman, 2002; Hasanuzzaman et al., 2010; Feng et al., 2013), neutralization of oxidative stress through the inhibition of lipid peroxidation (Cartes et al., 2005), and ethylene biosynthesis downregulation (Pezzarossa et al., 2014). However, despite some studies had examined the effect of Se on postharvest vase life in cut flowers (Tognon et al., 2016; Lu et al., 2020), none of them investigated yet the relationship between Se and ethylene biosynthesis directly.

ETHYLENE METABOLISM AND ITS INHIBITORS

As a simple gaseous hormone, ethylene acts in many fundamental processes in the plant's life cycle, including regulation of leaf and root development, senescence, fruit ripening, and germination. Ethylene also acts in response to several abiotic stresses such as heat (Savada et al., 2017), heavy metals damage (Thao et al., 2015), salinity (Zhang et al., 2016; Silva et al., 2018), low soil pH (Brito et al., 2018; Ribeiro et al., 2018), and water deficiency (Dubois et al., 2017), triggering adaptive responses (Wang et al., 2002).

The complete elucidation of the ethylene biosynthetic pathway by Yang and Hoffman (1984) was a notable episode for the progress of studies of this hormone in higher plants. Ethylene is synthesized from carbons C3 and C4 of methionine (Met) through three key enzymatic reactions: (i) conversion of Met into *S*-adenosyl-L-methionine (SAM) by the enzyme SAM synthetase (SAMS); (ii) conversion of SAM to 1-aminocyclopropane-1-carboxylic acid (ACC) by the enzyme ACC synthase (ACS); and (iii) conversion of ACC to ethylene by the enzyme ACC oxidase (ACO). The 2nd step in this process, i.e., the formation of ACC from SAM is considered the rate-limiting step, since the formation of ethylene is strongly controlled by the ACS enzyme (Yang and Hoffman, 1984; Alonso and Ecker, 2001; Pattyn et al., 2020). The final conversion of ACC to ethylene is oxygen-dependent (Kende, 1993) and yields CO_2 and cyanide as by-products. Once it is synthesized and perceived, the ethylene signaling pathway involves both positive and negative regulators, with the initial steps of signal transduction occurring at the endoplasmic reticulum membrane. The signal transduction involves ethylene receptors and transcription factors, with negative regulators inhibiting downstream responses via protein phosphorylation under the absence of ethylene (Azhar et al., 2019; Binder, 2020).

Ethylene biosynthesis/action inhibitors and ethylene removal technologies can mitigate premature senescence and abscission caused by exposure to exogenous or endogenous ethylene (Martínez-Romero et al., 2007). Interference in ethylene biosynthesis in ornamental plants can be achieved by blocking components of the ethylene synthesis pathway. Inhibition of the conversion of SAM to ACC by the compounds 1-aminoethoxyvinylglicine (AVG) and aminooxy acetic acid (AOA) effectively blocks the increase in ethylene production that accompanies senescence in a variety of ethylene sensitive flowers (Broun and Mayak, 1981; Serek and Andersen, 1993).

The inhibition of ethylene action is achieved by the use of antagonist molecules that bind to ethylene receptors, thus preventing downstream signaling. Among them, 2,5-norbornadiene (2,5-NBD) (Wang and Woodson, 1989), diazocyclopentadiene (DACP) (Blankenship and Sisler, 1993; Sisler et al., 1993; Serek et al., 1994), silver thiosulphate (Veen, 1979; Celikel and Reid, 2002), and 1-methyl cyclopropane (1-MCP) (Serek et al., 1995, 2006a; Sisler et al., 1999) are the most commonly studied and exploited. 1-MCP is the most commonly-used compound to control ethylene action during postharvest handling of fruits, flowers and vegetables commercially (Sisler and Serek, 1997). Its inhibitory mechanism is a result of competitive interaction with the ethylene receptors, since the ligand-binding site affinity is higher for 1-MCP than that of the gaseous hormone itself (Blankenship and Dole, 2006; Serek et al., 2006a). Nevertheless, it is thought that the development of new receptors recovers tissue sensitivity to ethylene in some plant materials, which can be treated with multiple applications of 1-MCP (Feng et al., 2004; Blankenship and Dole, 2006; In et al., 2013). On the other hand, 2,5-NBD also competes with ethylene for binding to ethylene receptors; however, high concentrations of ethylene can overcome the inhibitory effect of 2,5-NBD (Sisler and Yang, 1984). Moreover, 2,5-NBD is limitedly useful commercially as an ethylene inhibitor since it requires continuous exposure to be effective, and presents a strong and disagreeable odor (Sisler et al., 1990). Similarly, DACP is unlikely to be used commercially due to its instability and hazardous characteristics (Serek et al., 2006b). Finally, silver ions (Ag^+) may also block ethylene action, perhaps by replacing the metal component in the receptor. However, commercial use of silver is limited due to its heavy metal toxicity (Atta-Aly et al., 1987). Furthermore, the use of solutions containing silver íon by florists has raised environmental concerns, mostly regarding disposal issues (Sisler and Serek, 1997).

MODEL FOR Se-INDUCED DOWNREGULATION OF ETHYLENE BIOSYNTHESIS IN CUT FLOWER

Recently, a direct interaction between Se and ethylene was elegantly demonstrated in experiments involving cadmium stress alleviation in wheat (Iqbal et al., 2015), tomato fruit ripening (Zhu et al., 2017), and control of primary root growth in the rice system (Malheiros et al., 2019). These independent but complementary studies generated shreds of evidence that such responses were a consequence of an ethylene biosynthesis downregulation induced by Se. In close agreement with this, Se was also reported to improve minimally processed vegetable life span through ethylene depletion (Malorgio et al., 2009).

In this review, we propose the action of Se on ethylene biosynthesis in a cut flower model system through selenate (**Figure 1**) – the main form of Se to be transported in the xylem (Asher et al., 1977; Terry et al., 2000). The first

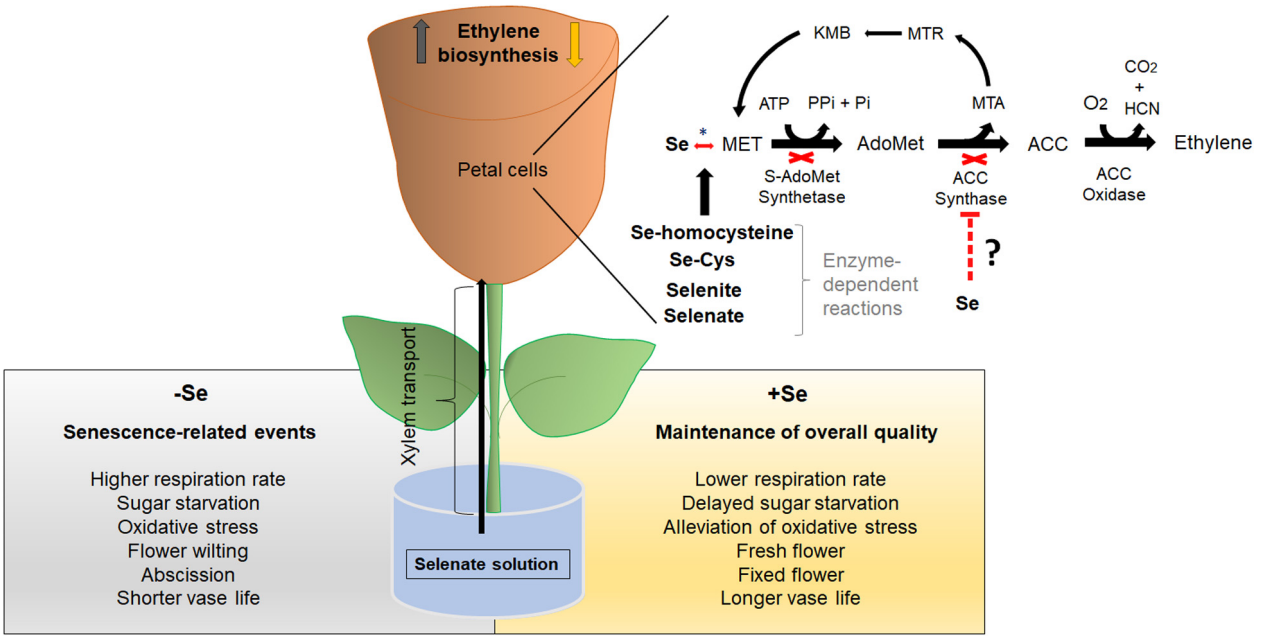

FIGURE 1 | Model for Se-induced ethylene biosynthesis downregulation in a cut flower system. Firstly, Se is provided as selenate – the main transported form in the xylem. In petal cells, selenate is converted to selenite and subsequently to Se-homocysteine by a series of enzymatic reactions. In a third stage, Se-homocysteine forms SeMet, reducing free Met levels toward to biosynthesis ethylene pathway. This event affects subsequently SAMS and ACS activities by reducing substrate (Met) availability to sustain ethylene biosynthesis pathway. Finally, the decreased ethylene biosynthesis may lead to the maintenance of overall quality on the postharvest life of cut flowers. Ethylene biosynthesis pathway: ACC, 1-aminocyclopropane-1-carboxylate; ACS, ACC synthase; MTR, *S*-methyl-5-thio-D-ribose; MTA, *S*-methyl-5′-this adenosine; KMB, 2-keto-4-methylthiobutyrate; Se, Selenium; SAM, *S*-adenosylmethionine; SAM synthetase, SAMS; HCN, Hydrogen cyanide; CO_2, Carbon dioxide; O_2, Oxygen; Met, Methionine; Pi, inorganic phosphate; and PPi, inorganic pyrophosphate. Se metabolism: Se, Selenium; SeCys, selenocysteine; SeMet, selenomethionine. *Enzymatic reaction.

step of Se metabolism in the cells involves the reduction of selenate to selenite under the sequential action of two enzymes, ATP sulfurylase (ATPS) and APS reductase (APR) (Shaw and Anderson, 1972; Sors et al., 2005; Pilon-Smits and Quinn, 2010; Quinn et al., 2011; Gupta and Gupta, 2017). ATPS catalyzes the hydrolysis of ATP, coupling ATP to selenate to form adenosine phosphoselenate (APSe), being subsequently reduced to selenite by APR (Sors et al., 2005; Pilon-Smits and Quinn, 2010). Both enzymes are present in the cytosol and plastids, but this process occurs primarily in the plastids, as observed in S metabolism (Kolosova et al., 2001). The reduction from selenite to selenide is also carried out in an enzyme-independent way by reduced glutathione (GSH) (Terry et al., 2000; Wallenberg et al., 2010). In the presence of the cysteine synthase (CS) enzyme, selenide can be converted into SeCys by coupling with *O*-acetylserine (OAS) (Ng and Anderson, 1978).

Selenocysteine may be incorporated into proteins, thereby impairing their activities (Burnell, 1981; Brown and Shrift, 1982; Terry et al., 2000). On the other hand, SeCys can be also transferred to Met, forming MeSeCys by selenocysteine methyltransferase (SMT) (Sors et al., 2005; Gupta and Gupta, 2017). In this case, a critical point arises since Met is shared with the ethylene biosynthesis pathway (**Figure 1**). For such convergences, it has been suggested that SeMet reduces free Met, which in turn diminishes internal ethylene levels by limiting the substrate for SAMS and ACS activities (Konze and Kende, 1979; Malorgio et al., 2009; Iqbal et al., 2013, 2015). The improvement of cut flowers vase life by manipulating ethylene biosynthesis has been addressed in several previous studies (Baker et al., 1977; Wang et al., 1977; Reid and Wu, 1992; Zeng et al., 2012). Kosugi et al. (2002), for instance, demonstrated that the suppression of ethylene biosynthesis in the *ACO* antisense line prolonged the vase life of carnation by 1.6-fold, as compared to its counterpart. In our proposed model (**Figure 1**), we hypothesize that Se diminishes ethylene levels in cut flowers by reducing the presence of free precursor Met to sustain ethylene biosynthesis, leading to extended postharvest life in ethylene-sensitive species.

DOWNSTREAM RESPONSES ASSOCIATED WITH Se USE IN VASE SOLUTION

Senescence is a complex, critical, and coordinated event that determines the longevity of cut flowers (Wu et al., 2017; Aalifar et al., 2020). The final phase of flower vase life, for instance, is characterized by time-dependent petal wilting, flower withering (Su et al., 2019), and flower or petal abscission (Van Doorn, 2001). Some flowers usually show symptoms of color change and desiccation of petals before abscission (Ma et al., 2005; Shibuya et al., 2016).

Ethylene is one of the most important hormones involved in the regulation of flower senescence (Ma et al., 2018; Wang et al., 2020) and elicits responses at concentrations as low as 0.1 $\mu L\ L^{-1}$ in highly sensitive flowers (Macnish et al., 2011). Sensitivity to ethylene differs between species and cultivars (Macnish et al., 2010; Costa and Finger, 2016; Wu et al., 2017). In ethylene-sensitive species, ethylene induces endogenous and autocatalytic ethylene biosynthesis that triggers petal and flower senescence. Ethylene causes petal and flower wilting during senescence by inhibiting cell expansion through the regulation of aquaporins (Ma et al., 2008), proteins that promote water transport through biological membranes (Xue et al., 2020). This causes subsequently a negative water balance, a key limiting event in the vase life of cut flowers (Van Meeteren and Aliniaeifard, 2016).

High rates of respiration are also one of the main causes of short vase life in cut flowers (Jones et al., 2009). Ethylene is known to induce respiratory activity, thereby depleting carbohydrates levels (Gonzalez-Candelas et al., 2010; John-Karuppiah and Burns, 2010). On the other hand, ethylene is also involved with flower abscission by triggering abscission zone formation (Van Doorn, 2002) and by oxidative stress promoted by ROS, including the overproduction of superoxide anion (O_2^-) and hydrogen peroxide (H_2O_2) (Rogers and Munné-Bosch, 2016; Ren et al., 2017; Jędrzejuk et al., 2018; Bayanati et al., 2019).

Therefore, we suggest that Se increases vase life directly by downregulating ethylene synthesis and indirectly by reducing flower senescence-related events, such as respiration rate, sugar starvation, petal and flower wilting and abscission, and oxidative stress (**Figure 1**).

CONCLUSION AND BROADER PERSPECTIVES

Herein, we have proposed a new model of interaction between Se metabolism and ethylene biosynthesis, and pointed out the positive effects of this event on the postharvest life of cut flowers. We believe the use of Se can provide a commercially viable and environmentally friendly alternative to current methods applied to ethylene-sensitive cut flowers. Practical aspects such as doses and standard use methods should be further investigated for each species under study.

AUTHOR CONTRIBUTIONS

LC, LL, and VN conceptualized and organized all this manuscript. LC, LL, VN, and MS contributed in survey and writing for selenium metabolism. VN, FA, CF, and TS performed a survey and writing for ethylene metabolism and postharvest quality of flowers. KF and FF supervised all the surveys and writing. All authors equally contributed to the development of the article's theoretical framework and approved the submitted version.

ACKNOWLEDGMENTS

The authors are grateful to Coordenação de Aperfeiçoamento de Pessoal de Nível Superior (CAPES) and Fundação de Amparo à Pesquisa do Estado de Minas Gerais (FAPEMIG) for financial support.

REFERENCES

Aalifar, M., Aliniaeifard, S., Arab, M., Mehrjerdi, M., and Serek, M. (2020). Blue light postpones senescence of carnation flowers through regulation of ethylene and abscisic acid pathway-related genes. *Plant Physiol. Biochem.* 151, 103–112. doi: 10.1016/j.plaphy.2020.03.018

Ahmad, R., Waraich, E. A., Nawaz, F., Ashraf, M. Y., and Khalid, M. (2016). Selenium (Se) improves drought tolerance in crop plants- a myth or fact? *J. Sci. Food Agric.* 96, 372–380. doi: 10.1002/jsfa.7231

Alonso, J. M., and Ecker, J. R. (2001). The ethylene pathway: a paradigm for plant hormone signalling and interaction. *Sci. Signal.* 70:re1. doi: 10.1126/stke.2001.70.re1

Asher, C. J., Butler, G. W., and Peterson, P. J. (1977). Selenium transport in root systems of tomato. *J. Exp. Bot.* 28, 279–291. doi: 10.1093/jxb/28.2.279

Atarodi, B., Fotovat, A., Khorassani, R., Keshavarz, P., and Hammami, H. (2018). Interaction of selenium and cadmium in wheat at different salinities. *Toxicol. Environ. Chem.* 100, 348–360. doi: 10.1080/02772248.2018.1524472

Atta-Aly, M. A., Saltveit, M. E., and Hobson, G. E. (1987). Effect of silver ions on ethylene biosynthesis by tomato fruit tissue. *Plant Physiol.* 83, 44–48. doi: 10.1104/pp.83.1.44

Azhar, B. J., Zulfiqar, A., Shakeel, S. N., and Schaller, G. E. (2019). Amplification and adaptation in the ethylene signaling pathway. *Small Methods* 4:1900452. doi: 10.1002/smtd.201900452

Baker, J. E., Wang, C. Y., Lieberman, M., and Hardenburg, R. (1977). Delay of senescence in carnations by rhizobitoxine analog and sodium benzoate. *HortScience* 12, 38–39.

Barry, C. S., and Giovannoni, J. J. (2007). Ethylene and fruit ripening. *J. Plant Growth Regul.* 26, 143–159. doi: 10.1007/s00344-007-9002-y

Bayanati, M., Tehranifar, A., Razavi, K., Nemati, S. H., Lohrasebi, T., and Ahmadi, N. (2019). Expression patterns analysis of SOD genes in responses to ethylene-induced oxidative stress in rose (Rosa hybrida) during flower development. *S. Afr. J. Bot.* 127, 265–270. doi: 10.1016/j.sajb.2019.09.009

Binder, B. M. (2020). Ethylene signaling in plants. *J. Biol. Chem.* 295, 7710–7725. doi: 10.1074/jbc.REV120.010854

Blankenship, S. M., and Dole, J. M. (2006). 1-Methylcyclopropene: a review. *Postharvest Biol. Technol.* 28, 1–25. doi: 10.1016/S0925-5214(02)00246-6

Blankenship, S. M., and Sisler, E. C. (1993). Response of apples to diazocyclopentadiene inhibition of ethylene binding. *Postharvest Biol. Technol.* 3, 95–101. doi: 10.1016/0925-5214(93)90001-J

Boldrin, P. F., de Figueiredo, M. A., Yang, Y., Luo, H., Giri, S., Hart, J. J., et al. (2016). Selenium promotes sulfur accumulation and plant growth in wheat (*Triticum aestivum*). *Physiol. Plant.* 158, 80–91. doi: 10.1111/ppl.12465

Brito, F. A. L., Costa, L. C., Gasparini, K., Pimenta, T. M., Araujo, W. L., Zsögön, A., et al. (2018). Low soil pH modulates ethylene biosynthesis and germination response of Stylosanthes humilis seeds. *Plant Signal Behav.* 13:e1460186. doi: 10.1080/15592324.2018.1460186

Broun, R., and Mayak, S. (1981). Aminooxyacetic acid as an inhibitor of ethylene synthesis and senescence in carnation flowers. *Sci. Hortic.* 15, 277–282. doi: 10.1016/0304-4238(81)90038-8

Brown, T. A., and Shrift, A. (1982). Selenium: toxicity and tolerance in higher plants. *Biol. Rev.* 57, 59–84. doi: 10.1111/j.1469-185X.1982.tb00364.x

Brummell, D. A., Watson, L. M., Pathirana, R., Joyce, N. I., West, P. J., Hunter, D. A., et al. (2011). Biofortification of tomato (*Solanum lycopersicum*) fruit with the anticancer compound methylselenocysteine using a selenocysteine

methyltransferase from a selenium hyperaccumulator. *J. Agric. Food Chem.* 59, 10987–10994. doi: 10.1021/jf202583f

Burnell, J. N. (1981). Selenium metabolism in *Neptunia amplexicaulis*. *Plant Physiol.* 67, 316–324. doi: 10.1104/pp.67.2.316

Cartes, P., Gianfreda, L., and Mora, M. L. (2005). Uptake of selenium and its antioxidant activity in ryegrass when applied as selenate and selenite forms. *Plant Soil* 276, 359–367. doi: 10.1007/s11104-005-5691-9

Celikel, F. G., and Reid, M. S. (2002). Postharvest handling of stock (*Matthiola incana*). *HortScience* 37, 144–147. doi: 10.21273/HORTSCI.37.1.144

Chen, M., Zeng, L., Luo, X., Mehboob, M. Z., Tegenbaiyin, A. O., and Lang, M. (2019). Identification and functional characterization of a novel selenocysteine methyltransferase from *Brassica juncea* L. *J. Exp. Bot.* 70, 6401–6416. doi: 10.1093/jxb/erz390

Choudhary, P., and Jain, V. (2018). Effect of post-harvest treatments of selenium on physico-chemical quality in guava (*Psidium guajava* L.) fruit. *Hortic. Int. J.* 2, 41–44. doi: 10.15406/hij.2018.02.00024

Cochran, A. T., Bauer, J., Metcalf, J. L., Lovecka, P., Sura-de Jong, M., Warris, S., et al. (2018). Plant selenium hyperaccumulation affects rhizosphere: enhanced species richness and altered species composition. *Phytobiomes J.* 2, 82–91. doi: 10.1094/pbiomes-12-17-0051-R

Corbineau, F., Xia, Q., Bailly, C., and El-Maarouf-Bouteau, H. (2014). Ethylene, a key factor in the regulation of seed dormancy. *Front. Plant Sci.* 10:539. doi: 10.3389/fpls.2014.00539

Costa, L. C., and Finger, F. L. (2016). Flower opening and vase life of gladiolus cultivars: the sensitivity to ethylene and the carbohydrate content. *Ornam. Hortic.* 22, 147–153. doi: 10.14295/oh.v22i2.901

Daniels, L. A. (1996). Selenium metabolism and bioavailability. *Biol. Trace Elem. Res.* 54, 185–199. doi: 10.1007/BF02784430

De Martinis, D., Koyama, T., and Chang, C. (2015). Ethylene is all around. *Front. Plant Sci.* 6:76. doi: 10.3389/fpls.2015.00076

Dimkovikj, A., and Van Hoewyk, D. (2014). Selenite activates the alternative oxidase pathway and alters primary metabolism in *Brassica napus* roots: evidence of a mitochondrial stress response. *BMC Plant Biol.* 14:259. doi: 10.1186/s12870-014-0259-6

Dubois, M., Claeys, H., Van den Broeck, L., and Inzé, D. (2017). Time of day determines *Arabidopsis transcriptome* and growth dynamics under mild drought. *Plant Cell Environ.* 40, 180–189. doi: 10.1111/pce.12809

Feng, R. W., Wei, C. Y., and Tu, S. X. (2013). The roles of selenium in protecting plants against abiotic stresses. *Environ. Exp. Bot.* 87, 58–68. doi: 10.1016/j.envexpbot.2012.09.002

Feng, X. Q., Apelbaum, A., Sisler, E. C., and Goren, R. (2004). Control of ethylene activity in various plant systems by structural analogues of 1-methylcyclopropene. *Plant Growth Regul.* 42, 29–38.

Fordyce, F. M. (2005). "Selenium deficiency and toxicity in the environment," in *Essentials of Medical Geology*, ed. O. Selinus (Dordrecht: Springer), 373–415.

Freeman, J. L., Tamaoki, M., and Stushnoff, C. (2010). Molecular mechanisms of selenium tolerance and hyperaccumulation in *Stanleya pinnata*. *Plant Physiol.* 153, 1630–1652. doi: 10.1104/pp.110.156570

Galeas, M. L., Zhang, L. H., Freeman, J. L., Wegner, M., and Pilon-Smits, E. A. H. (2007). Seasonal fluctuations of selenium and sulfur accumulation in selenium hyperaccumulators and related non-accumulators. *New Phytol.* 173, 517–525. doi: 10.1111/j.1469-8137.2006.01943.x

Giovannoni, J. J. (2001). Molecular biology of fruit maturation and ripening. *Annu. Rev. Plant Physiol. Plant Mol. Biol.* 52, 725–749. doi: 10.1146/annurev.arplant.52.1.725

Gonzalez-Candelas, L., Alamar, S., Sanchez-Torres, P., Zacarias, L., and Marcos, J. F. (2010). A transcriptomic approach highlights induction of secondary metabolism in citrus fruit in response to Penicillium digitatum infection. *BMC Plant Biol.* 10:194. doi: 10.1186/1471-2229-10-194

Gupta, M., and Gupta, S. (2017). An overview of selenium uptake, metabolism, and toxicity in plants. *Front. Plant Sci.* 7:2074. doi: 10.3389/fpls.2016.02074

Hajiboland, R., Rahmat, S., Zeinalzadeh, N., Farsad-Akhtar, N., and Hosseinpour-Feizi, M.-A. (2019). Senescence is delayed by selenium in oilseed rape plants. *J. Trace Elem. Med. Biol.* 55, 96–106.

Hasanuzzaman, M., and Fujita, M. (2011). Selenium pretreatment upregulates the antioxidant defense and methylglyoxal detoxification system and confers enhanced tolerance to drought stress in rapeseed seedlings. *Biol. Trace Elem. Res.* 143, 1758–1776. doi: 10.1007/s12011-011-8998-9

Hasanuzzaman, M., Hossain, M. A., and Fujita, M. (2010). Selenium in higher plants: physiological role, antioxidant metabolism and abiotic stress tolerance. *J. Plant Sci.* 4, 354–375. doi: 10.3923/jps.2010.354.375

Haug, A., Graham, R. D., Christopherson, O. A., and Lyons, G. H. (2008). How to use the world's scarce selenium resources efficiently to increase the selenium concentration in food. *Microb. Ecol. Health Dis.* 19, 209–228. doi: 10.1080/08910600701698986

Hawrylak-Nowak, B., Dreslerb, S., and Wójcik, M. (2014). Selenium affects physiological parameters and phytochelatins accumulation in cucumber (*Cucumis sativus* L.) plants grown under cadmium exposure. *Sci. Hort.* 172, 10–18. doi: 10.1016/j.scienta.2014.03.040

Huang, W. N., Liu, H. K., Zhang, H. H., Chen, Z., Guo, Y. D., and Kang, Y. F. (2013). Ethylene-induced changes in lignification and cell wall-degrading enzymes in the roots of mungbean (*Vigna radiata*) sprouts. *Plant Physiol. Biochem.* 73, 412–419. doi: 10.1016/j.plaphy.2013.10.020

Hussain, S., Khan, F., Cao, W., Wu, L., and Geng, M. (2016). Seed priming alters the production and detoxification of reactive oxygen intermediates in rice seedlings grown under sub-optimal temperature and nutrient supply. *Front. Plant Sci.* 7:439. doi: 10.3389/fpls.2016.00439

In, B. C., Strable, J., Binder, B. M., Falbel, T. G., and Patterson, S. E. (2013). Morphological and molecular characterization of ethylene binding incarnations. *Post. Harvest Biol. Technol.* 86, 272–279. doi: 10.1016/j.postharvbio.2013.07.007

Iqbal, M., Hussain, I., Liaqat, H., Arslan Ashraf, M., Rasheed, R., and Ur Rehman, A. (2015). Exogenously applied selenium reduces oxidative stress and induces heat tolerance in spring wheat. *Plant Physiol. Biochem.* 94, 95–103. doi: 10.1016/j.plaphy.2015.05.012

Iqbal, N., Trivellini, A., Masood, A., Ferrante, A., and Khan, N. A. (2013). Current understanding on ethylene signaling in plants: the influence of nutrient availability. *Plant Physiol. Biochem.* 73, 128–138. doi: 10.1016/j.plaphy.2013.09.011

Ivanchenko, M. G., Muday, G. K., and Dubrovsky, J. G. (2008). Ethylene-auxin interactions regulate lateral root initiation and emergence in *Arabidopsis thaliana*. *Plant J.* 55, 335–347. doi: 10.1111/j.1365-313X.2008.03528.x

Iwahori, S., Lyons, J. M., and Smith, O. E. (1970). Sex expression in cucumber plants as affected by 2-chloroethylphosphonic acid, ethylene, and growth regulators. *Plant Physiol.* 46, 412–415. doi: 10.1104/pp.46.3.412

Jędrzejuk, A., Rabiza-Świder, J., Skutnik, E., and Łukaszewska, A. (2018). Growing conditions and preservatives affect longevity, soluble protein, H2O2 and MDA contents, activity of antioxidant enzymes and DNA degradation in cut lilacs. *Sci. Hortic.* 228, 122–131. doi: 10.1016/j.scienta.2017.10.026

Jia, H., Song, Z., Wu, F., Ma, M., Li, Y., Han, D., et al. (2018). Low selenium increases the auxin concentration and enhances tolerance to low phosphorous stress in tobacco. *Environ. Exp. Bot.* 153, 127–134. doi: 10.1016/j.envexpbot.2018.05.017

John-Karuppiah, K., and Burns, J. K. (2010). Degreening behavior in 'Fallglo' and 'Lee×Orlando' is correlated with differential expression of ethylene signaling and biosynthesis genes. *Postharvest Biol. Technol.* 58, 185–193. doi: 10.1016/j.postharvbio.2010.07.013

Jones, M. L., Stead, A. D., and Clark, D. G. (2009). "Petunia flower senescence," in *Petunia*, eds T. Gerats and J. Strommer (New York, NY: Springer), 301–324.

Kende, H. (1993). Ethylene biosynthesis. *Annu. Rev. Plant Physiol. Plant Mol. Biol.* 44, 283–307. doi: 10.1146/annurev.pp.44.060193.001435

Khan, M. I. R., Asgher, M., and Khan, N. A. (2014). Alleviation of salt-induced photosynthesis and growth inhibition by salicylic acid involves glycinebetaine and ethylene in mung bean (*Vigna radiata* L.). *Plant Physiol. Biochem.* 80, 67–74. doi: 10.1016/j.plaphy.2014.03.026

Khan, M. I. R., Nazir, F., Asgher, M., Per, T. S., and Khan, N. A. (2015). Selenium and sulfur influence ethylene formation and alleviate cadmium-induced oxidative stress by improving proline and glutathione production in wheat. *J. Plant Physiol.* 173, 9–18. doi: 10.1016/j.jplph.2014.09.011

Khan, N. A., Khan, M. I. R., Asgher, M., Fatma, M., Masood, A., and Syeed, S. (2014). Salinity tolerance in plants: revisiting the role of sulfur metabolites. *J. Plant Biochem. Physiol.* 2:120. doi: 10.4172/2329-9029.1000120

Kim, H. J., Hong, S. H., Kim, Y. W., Lee, I. H., Jun, J. H., Phee, B. K., et al. (2014). Gene regulatory cascade of senescence-associated NAC transcription factors

activated by ETHYLENE-INSENSITIVE2-mediated leaf senescence signalling in *Arabidopsis*. *J. Exp. Bot.* 65, 4023–4036. doi: 10.1093/jxb/eru112

Kolosova, N., Sherman, D., Karlson, D., and Dudareva, N. (2001). Cellular and subcellular localization of S-adenosyl-L-methionine:benzoic acid carboxyl methyltransferase, the enzyme responsible for biosynthesis of the volatile ester methylbenzoate in snapdragon flowers. *Plant Physiol.* 126, 956–964. doi: 10.1104/pp.126.3.956

Konze, J. R., and Kende, H. (1979). Interactions of methionine and selenomethionine with methionine adenosyltransferase and ethylene-generating systems. *Plant Physiol.* 63, 507–510. doi: 10.1104/pp.63.3.507

Kosugi, Y., Waki, K., Iwazaki, Y., Tsuruno, N., Mochizuki, A., Yoshioka, T., et al. (2002). Senescence and gene expression of transgenic non-ethylene-producing carnation flowers. *J. Jpn. Soc. Hortic. Sci.* 71, 638–642.

Kumar, A., Singh, R. P., Singh, P. K., Awasthi, S., Chakrabarty, D., Trivedi, P. K., et al. (2014). Selenium ameliorates arsenic induced oxidative stress through modulation of antioxidant enzymes and thiols in rice (*Oryza sativa* L.). *Ecotoxicology* 23, 1153–1163. doi: 10.1007/s10646-014-1257-z

Lapaz, A. M., Santos, L. F. M., Yoshida, C. H. P., Heinrichs, R., Campos, M., and Reis, A. R. (2019). Physiological and toxic effects of selenium on seed germination of cowpea seedlings. *Bragantia.* 4, 1–11. doi: 10.1590/1678-4499.20190114

Lehotai, N., Kolbert, Z., Peto, A., Feigl, G., Ordog, A., Kumar, D., et al. (2012). Selenite-induced hormonal and signalling mechanisms during root growth of *Arabidopsis thaliana* L. *J. Exp. Bot.* 63, 5677–5687. doi: 10.1093/jxb/err313

Liang, Y., Yang, S. U., Ling, L. I., Xin, H., Panhwar, F., Zheng, T., et al. (2019). Quick selenium accumulation in the selenium-rich rice and its physiological responses in changing selenium environments. *BMC Plant Biol.* 19:559. doi: 10.1186/s12870-019-2163-6

Lim, P. O., Kim, H. J., and Nam, H. G. (2007). Leaf senescence. *Annu. Rev. Plant Biol.* 58, 115–136. doi: 10.1146/annurev.arplant.57.032905.105316

Lima, J. E., Benedito, V. A., Figueira, A., and Peres, L. E. P. (2009). Callus, shoot and hairy root formation in vitro as affected by the sensitivity to auxin and ethylene in tomato mutants. *Plant Cell Rep.* 28, 1169–1177. doi: 10.1007/s00299-009-0718-y

Lin, Y., Yang, L., Paul, M., Zu, Y., and Tang, Z. (2013). Ethylene promotes germination of Arabidopsis seed under salinity by decreasing reactive oxygen species: Evidence for the involvement of nitric oxide simulated by sodium nitroprusside. *Plant Physiol. Biochem.* 73, 211–218. doi: 10.1016/j.plaphy.2013.10.003

Lobanov, A. V., Hatfield, D. L., and Gladyshev, V. N. (2009). Eukaryotic selenoproteins and selenoproteomes. *BBA Gen. Subjects* 1790, 1424–1428. doi: 10.1016/j.bbagen.2009.05.014

Lu, N., Wu, L., and Shi, M. (2020). Selenium enhances the vase life of Lilium longiflorum cut flower by regulating postharvest physiological characteristics. *Sci. Hortic.* 264:109172. doi: 10.1016/j.scienta.2019.109172

Ma, N., Cai, L., Wangjin, L., Tan, H., and Gao, J. (2005). Exogenous Ethylene influences flower opening of cut roses (Rosa hybrida) by regulating the genes encoding ethylene biosynthesis enzymes. *Sci. Shina Ser. B* 48:434. doi: 10.1360/062004-37

Ma, N., Ma, C., Liu, Y., Shahid, M., Wang, C., and Gao, J. (2018). Petal senescence: a hormone view. *J. Exp. Bot.* 69, 719–732. doi: 10.1093/jxb/ery009

Ma, N., Xue, J., Li, Y., Liu, X., Dai, F., Jia, et al. (2008). Rh-PIP2;1, a rose aquaporin gene, is involved in ethylene-regulated petal expansion. *Plant Physiol.* 148, 894–907. doi: 10.1104/pp.108.120154

Macnish, A. J., Leonard, R. T., Borda, A. M., and Nell, T. A. (2010). Genotypic variation in the postharvest performance and ethylene sensitivity of cut rose flowers. *Hortscience.* 45, 790–796. doi: 10.21273/hortsci.45.5.790

Macnish, A. J., Leonard, R. T., and Nell, T. A. (2011). Sensitivity of potted foliage plant genotypes to ethylene and 1-methylcyclopropene. *Hortscience* 46, 1127–1131. doi: 10.21273/hortsci.46.8.1127

Malheiros, R. S. P., Costa, L. C., Ávila, R. T., Pimenta, T. M., Teixeira, L. S., Brito, F. A. L., et al. (2019). Selenium downregulates auxin and ethylene biosynthesis in rice seedlings to modify primary metabolism and root architecture. *Planta* 250, 333–345. doi: 10.1007/s00425-019-03175-6

Malorgio, F., Diaz, K. E., Ferrante, A., Mensuali-Sodi, A., and Pezzarossa, B. (2009). Effects of selenium addition on minimally processed leafy vegetables grown in a floating system. *J. Sci. Food Agric.* 89, 2243–2251. doi: 10.1002/jsfa.3714

Martínez-Romero, D., Bailén, G., Serrano, M., Guillén, F., Valverde, J. M., Zapata, P., et al. (2007). Tools to maintain postharvest fruit and vegetable quality through the inhibition of ethylene action: a review. *Crit. Rev. Food Sci. Nutr.* 47, 543–560. doi: 10.1080/10408390600846390

Miransari, M., and Smith, D. L. (2014). Plant hormones and seed germination. *Environ. Exp. Bot.* 99, 110–121. doi: 10.1016/j.envexpbot.2013.11.005

Morgan, P. W., and Drew, M. C. (1997). Ethylene and plant responses to stress. *Physiol. Plant* 100, 620–630. doi: 10.1034/j.1399-3054.1997.1000325.x

Nancharaiah, Y. V., and Lens, P. N. (2015). Ecology and biotechnology of selenium-respiring bacteria. *Microbiol. Mol. Biol. R.* 79, 61–80. doi: 10.1128/MMBR.00037-14

Nawaz, F., Ashraf, M. Y., Ahmad, R., and Waraich, E. A. (2013). Selenium (Se) seed priming induced growth and biochemical changes in wheat under water deficit conditions. *Biol. Trace Elem. Res.* 151, 284–293. doi: 10.1007/s12011-012-9556-9

Neal, R. H., Sposito, G., Holtzclaw, K. M., and Traina, S.l (1987). Selenite adsorption on alluvial soils. I. Soil composition and pH effects. *Soil Sci. Soc. Am. J.* 51, 1161–1165. doi: 10.2136/sssaj1987.03615995005100050012x

Neuhierl, B., and Boeck, A. (1996). On the mechanism of selenium tolerance in selenium accumulating plants: purification and characterization of a specific selenocysteine methyltransferase from cultured cells of *Astragalus bisulcatus*. *Eur. J. Biochem.* 239, 235–238. doi: 10.1111/j.1432-1033.1996.0235u.x

Ng, B. H., and Anderson, J. W. (1978). Synthesis of selenocysteine by cysteine synthases from selenium accumulator and non-accumulator plants. *Phytochemistry* 17, 2069–2074. doi: 10.1016/S0031-9422(00)89282-1

O'Neill, S. D. (1997). Pollination regulation of flower development. *Annu. Rev. Plant Physiol. Plant Mol. Biol.* 48, 547–574. doi: 10.1146/annurev.arplant.48.1.547

Pattyn, J., Vaughan−Hirsch, J., and Van de Poel, B. (2020). The regulation of ethylene biosynthesis: a complex multilevel control circuitry. *New Phytol.* doi: 10.1111/nph.16873 [Epub ahead of print].

Pezzarossa, B., Remorini, D., and Gentile, M. L. (2012). Effects of foliar and fruit addition of sodium selenate on selenium accumulation and fruit quality. *J. Sci. Food Agric.* 92, 781–786. doi: 10.1002/jsfa.4644

Pezzarossa, B., Rosellini, I., Borghesi, E., Tonutti, P., and Malorgio, F. (2014). Effects of Se-enrichment on yield, fruit composition and ripening of tomato (*Solanum lycopersicum*) plants grown in hydroponics. *Sci. Hortic.* 65, 106–110. doi: 10.1016/j.scienta.2013.10.029

Pilon-Smits, E. A. H., and Quinn, C. F. (2010). "Selenium metabolism in plants," in *Cell Biology of Metals and Nutrients. Plant Cell Monographs*, eds R. Hell and R. R. Mendel (Berlin: Springer), 225–241.

Quinn, C. F., Prins, C. N., Freeman, J. L., Gross, A. M., Hantzis, L. J., Reynolds, R. J. B., et al. (2011). Selenium accumulation in flowers and its effects on pollination. *New Phytol.* 192, 727–737. doi: 10.1111/j.1469-8137.2011.03832.x

Rayman, M. P. (2002). The argument for increasing selenium intake. *Proc. Nutr. Soc.* 2, 203–215. doi: 10.1079/PNS2002153

Reid, M. S., and Wu, M. J. (1992). Ethylene and flower senescence. *Plant Growth Regul.* 11, 37–43.

Ren, P. J., Jin, X., Liao, W. B., Wang, M., Niu, L. J., Li, X. P., et al. (2017). Effect of hydrogen-rich water on vase life and quality in cut lily and rose flowers. *Hortic. Environ. Biotechnol.* 58, 576–584. doi: 10.1007/s13580-017-0043-2

Ribeiro, D. M., Silva Júnior, D. D., Cardoso, F. B., Martins, A. O., Silva, W. A., Nascimento, V. L., et al. (2016). Growth inhibition by selenium is associated with changes inprimary metabolism and nutrient levels in *Arabidopsis thaliana*. *Plant Cell Environ.* 39, 2235–2246. doi: 10.1111/pce.12783

Ribeiro, R. P., Costa, L. C., Medina, E. F., Araújo, W. L., Zsögön, A., and Ribeiro, D. M. (2018). Ethylene coordinates seed germination behavior in response to low soil pH in *Stylosanthes humilis*. *Plant Soil.* 425, 87–100. doi: 10.1007/s11104-018-3572-2

Rogers, H., and Munné-Bosch, S. (2016). Production and scavenging of reactive oxygen species and redox signaling during leaf and flower senescence: similar but different. *Plant Physiol.* 171, 1560–1568. doi: 10.1104/pp.16.00163

Saidi, I., Chtourou, Y., and Djebali, W. (2014). Selenium alleviates cadmium toxicity by preven-ting oxidative stress in sunflower (*Helianthus annuus*) seedlings. *J. Plant Physiol.* 171, 85–91. doi: 10.1016/j.jplph.2013.09.024

Salman-Minkov, A., Levi, A., Wolf, S., and Trebitsh, T. (2008). ACC synthase genes are polymorphic in watermelon (Citrullus spp.) and differentially expressed in

flowers and in response to auxin and gibberellin. *Plant Cell Physiol.* 49, 740–750. doi: 10.1093/pcp/pcn045

Sattar, A., Cheema, M. A., Sher, A., Ijaz, M., Ul-Allah, S., Nawaz, A., et al. (2019). Physiological and biochemical attributes of bread wheat (*Triticum aestivum* L.) seedlings are influenced by foliar application of silicon and selenium under water deficit. *Acta Physiol. Plant* 41:146. doi: 10.1007/s11738-019-2938-2

Savada, R. P., Ozga, J. A., Jayasinghege, C. P. A., Waduthanthri, K. D., and Reinecke, D. M. (2017). Heat stress differentially modifies ethylene biosynthesis and signaling in pea floral and fruit tissues. *Plant Mol. Biol.* 95, 313–331. doi: 10.1007/s11103-017-0653-1

Scariot, V., Paradiso, R., Rogers, H., and De Pascale, S. (2014). Ethylene control in cut flowers: classical and innovative approaches. *Postharvest Biol. Technol.* 97, 83–92. doi: 10.1016/j.postharvbio.2014.06.010

Serek, M., and Andersen, A. S. (1993). AOA and BA influence on floral development and longevity of potted 'Victory Parade' miniature rose. *HortScience* 28, 1039–1040. doi: 10.21273/HORTSCI.28.10.1039

Serek, M., Sisler, E. C., Frello, S., and Sriskandarajah, S. (2006b). Postharvest technologies for extending the shelf life of ornamental crops. *Int. J. Postharvest Technol. Inn.* 1, 69–75. doi: 10.1504/IJPTI.2006.009184

Serek, M., Sisler, E. C., and Reid, M. S. (1994). Novel gaseous ethylene binding inhibitor prevents ethylene effects in potted flowering plants. *J. Am. Hort. Sci.* 119, 1230–1233. doi: 10.21273/JASHS.119.6.1230

Serek, M., Sisler, E. C., and Reid, M. S. (1995). 1-Methylcyclopropene, a novel gaseous inhibitor of ethylene action, improves the vase life of fruits, cut flowers and potted plants. *Acta Hort.* 394, 337–346. doi: 10.17660/ActaHortic.1995.394.37

Serek, M., Woltering, E. J., Sisler, E. C., Frello, S., and Sriskandarajah, S. (2006a). Controlling ethylene responses in flowers at the receptor level. *Biotechnol. Adv.* 24, 368–381. doi: 10.1016/j.biotechadv.2006.01.007

Shahverdi, M. A., Omidi, H., and Damalas, C. A. (2020). Foliar fertilization with micronutrients improves Stevia rebaudiana tolerance to salinity stress by improving root characteristics. *Braz. J. Bot.* 43, 55–65. doi: 10.1007/s40415-020-00588-6

Shaw, W. H., and Anderson, I. W. (1972). Purification, properties, and substrate specificities of ATP sulfurylase from spinach leaf tissue. *Biochem. J.* 127, 237–247. doi: 10.1042/bj1270237

Shibuya, K., Yamada, T., and Ichimura, K. (2016). Morphological changes in senescing petal cells and the regulatory mechanism of petal senescence. *J. Exp. Bot.* 67, 5909–5918. doi: 10.1093/jxb/erw337

Silva, N. C. Q., de Souza, G. A., Pimenta, T. M., Brito, F. A. L., Picoli, E. A. T., Zsögön, A., et al. (2018). Salt stress inhibits germination of Stylosanthes humilis seeds through abscisic acid accumulation and associated changes in ethylene production. *Plant Physiol. Biochem.* 130, 399–407. doi: 10.1016/j.plaphy.2018.07.025

Sisler, E. C., Blankenship, S. M., Fearn, J. C., and Haynes, R. (1993). "Effect of diazocyclopen-tadiene (DACP) on cut carnations," in *Cellular and Molecular Aspects of the Plant Hormone Ethylene*, Vol. 16, eds J. C. Pech, A. Latche, and C. Balague (Dordrecht: Springer), 182–187.

Sisler, E. C., Blankenship, S. M., and Guest, M. (1990). Competition of cyclooctenes and cyclooctadienes for ethylene binding and activity in plants. *Plant Growth Regul.* 9, 157–164. doi: 10.1007/BF00027443

Sisler, E. C., and Serek, M. (1997). Inhibitors of ethylene responses in plants at the receptor level: recent developments. *Physiol. Plant* 100, 577–582. doi: 10.1111/j.1399-3054.1997.tb03063.x

Sisler, E. C., Serek, M., Dupille, E., and Goren, R. (1999). Inhibition of ethylene responses by 1-methylcyclopropene and 3-methylcyclopropene. *Plant Growth Regul.* 27, 105–111. doi: 10.1023/A:1006153016409

Sisler, E. C., and Yang, S. F. (1984). Anti-ethylene effects of cis-2-butene and cyclic olefins. *Phytochemistry* 23, 2765–2768. doi: 10.1016/0031-9422(84)83011-3

Sors, T. G., Ellis, D. R., Na, G. N., Lahner, B., Lee, S., Leustek, T., et al. (2005). Analysis of sulfur and selenium assimilation in *Astragalus* plants with varying capacities to accumulate selenium. *Plant J.* 42, 785–797. doi: 10.1111/j.1365-313x.2005.02413.x

Steffens, B. (2014). The role of ethylene and ROS in salinity, heavy metal, and flooding responses in rice. *Front. Plant Sci.* 5:685. doi: 10.3389/fpls.2014.00685

Su, J., Nie, Y., Zhao, G., Cheng, D., Wang, R., Chen, J., et al. (2019). Endogenous hydrogen gas delays petal senescence and extends the vase life of lisianthus cut flowers. *Postharvest Biol. Tecnol.* 147, 148–155. doi: 10.1016/j.postharvbio.2018.09.018

Tagmount, A., Berken, A., and Terry, N. (2002). An essential role of S-adenosyl-L-methionine:L-methionine S-methyltransferase in selenium volatilization by plants. Methylation of selenomethionine to selenium-methyl-L-selenium methionine, the precursor of volatile selenium. *Plant Physiol.* 130, 847–856. doi: 10.1104/pp.001693

Terry, N., Zayed, A. M., de Souza, M. P., and Tarun, A. S. (2000). Selenium in higher plants. *Annu. Rev. Plant Physiol. Plant Mol. Biol.* 51, 401–432. doi: 10.1146/annurev.arplant.51.1.401

Thao, N. P., Khan, M. I. R., Thu, N. B. A., Hoang, X. L. T., Asgher, M., Khan, N. A., et al. (2015). Role of ethylene and its cross talk with other signaling molecules in plant responses to heavy metal stress. *Plant Physiol.* 169, 73–84. doi: 10.1104/pp.15.00663

Tognon, G. B., Sanmartin, C., Alcolea, V., Cuquel, F. L., and Goicoechea, N. (2016). Mycorrhizal inoculation and/or selenium application affect post-harvest performance of snapdragon flowers. *Plant Growth Regul.* 78, 389–400. doi: 10.1007/s10725-015-0100-8

Ueda, H., and Kusaba, M. (2015). Strigolactone regulates leaf senescence in concert with ethylene in *Arabidopsis*. *Plant Physiol.* 169, 138–147. doi: 10.1104/pp.15.00325

Van Doorn, W. G. (2001). Categories of petal senescence and abscission: a re-evaluation. *Ann. Bot.* 87, 447–456. doi: 10.1006/anbo.2000.1357

Van Doorn, W. G. (2002). Effect of ethylene on flower abscission: a survey. *Ann. Bot.* 89, 689–693. doi: 10.1093/aob/mcf124

Van Meeteren, U., and Aliniaeifard, S. (2016). "Stomata and postharvest physiology," in *Postharvest Ripening Physiology of Crops*, ed. S. Pareek (Boca Raton, FL: CRC Press), 157–216.

Veen, H. (1979). Effects of silver on ethylene synthesis and action in cut carnations. *Planta* 145, 467–470. doi: 10.1007/BF00380101

Wallenberg, M., Olm, E., Hebert, C., Björnstedt, M., and Fernandes, A. P. (2010). Selenium compounds are substrates for glutaredoxins: a novel pathway for selenium metabolism and a potential mechanism for selenium-mediated cytotoxicity. *Biochem. J.* 429, 85–93. doi: 10.1042/BJ20100368

Wang, C. Y., Baker, J. E., Hardenburg, R., and Lieberman, M. (1977). Effects of two analogs of rhizobitoxine sodium benzoate on senescence of snapdragons. *J. Am. Soc. Hortic. Sci.* 102, 517–520.

Wang, H., and Woodson, W. R. (1989). Reversible inhibition of ethylene action and interruption of petal senescence in carnation flowers by norbornadiene. *Plant Physiol.* 89, 434–438. doi: 10.1104/pp.89.2.434

Wang, K. L. C., Li, H., and Ecker, J. R. (2002). Ethylene biosynthesis and signalling networks. *Plant Cell* 14, 131–151. doi: 10.1105/tpc.001768

Wang, Y., Liu, C., Li, K., Sum, F., Hu, Z., Li, X., et al. (2007). Arabidopsis EIN2 modulates stress response through abscisic acid response pathway. *Plant Mol. Biol.* 64, 633–644. doi: 10.1007/s11103-007-9182-7

Wang, Y., Zhao, H., Liu, C., Cui, G., Qu, L., Bao, M., et al. (2020). Integrating physiological and metabolites analysis to identify ethylene involvement in petal senescence in Tulipa gesneriana. *Plant Physiol. Biochem.* 149, 121–131. doi: 10.1016/j.plaphy.2020.02.001

White, P. J., Bowen, H. C., Parmaguru, P., Fritz, M., Spracklen, W. P., Spiby, R. E., et al. (2004). Interactions between selenium and sulphur nutrition in *Arabidopsis thaliana*. *J. Exp. Bot.* 55, 1927–1937. doi: 10.1093/jxb/erh192

Wilson, R. L., Kim, H., Bakshi, A., and Binder, B. M. (2014). The ethylene receptors ETHYLENE RESPONSE1 and ETHYLENE RESPONSE2 have contrasting roles in seed germination of *Arabidopsis* during salt stress. *Plant Physiol.* 165, 1353–1366. doi: 10.1104/pp.114.241695

Wu, F., Zhang, C., Wang, X., Guo, J., and Dong, L. (2017). Ethylene-influenced development of tree peony cut flowers and characterization of genes involved in ethylene biosynthesis and perception. *Postharvest Biol. Tecnol.* 125, 150–160. doi: 10.1016/j.postharvbio.2016.11.014

Wuriyanghan, H., Zhang, B., Cao, W.-H., Ma, B., Lei, G., Liu, Y.-F., et al. (2009). The ethylene receptor ETR2 delays floral transition and affects starch accumulation in rice. *Plant Cell* 21, 1473–1494. doi: 10.1105/tpc.108.065391

Xue, J., Huang, Z., Wang, S., Xue, Y., Ren, X., Zeng, X., et al. (2020). Dry storage improves the vase quality of cut peony by increasing water uptake efficiency through aquaporins regulation. *Plant Physiol. Biochem.* 148, 63–69. doi: 10.1016/j.plaphy.2020.01.007

Yamasaki, S., Fujii, N., Matsuura, S., Mizusawa, H., and Takahashi, H. (2001). The M locus and ethylene-controlled sex determination in andromonoecious cucumber plants. *Plant Cell Physiol.* 42, 608–619. doi: 10.1093/pcp/pce076

Yang, S., and Hoffman, F. (1984). Ethylene biosynthesis and its regulation in higher plants. *Annu. Rev. Physiol.* 35, 155–189. doi: 10.1146/annurev.pp.35.060184.001103

Zeng, Z., Jiang, H., Zhang, H., and Jiang, Z. (2012). The synthesis of novel oxime ethers and their effects on the senescence of cut carnation flowers. *Res. Chem. Intermed.* 38, 463–470. doi: 10.1007/s11164-011-0363-2

Zhang, M., Smith, J. A. C., Harberd, N. P., and Jiang, C. (2016). The regulatory roles of ethylene and reactive oxygen species (ROS) in plant salt stress responses. *Plant Mol. Biol.* 91, 651–659. doi: 10.1007/s11103-016-0488-1

Zhu, Z., Chen, Y., Shi, G., and Zhang, X. (2017). Selenium delays tomato fruit ripening by inhibiting ethylene biosynthesis and enhancing the antioxidant defense system. *Food Chem.* 219, 179–184. doi: 10.1016/j.foodchem.2016.09.138

Conflict of Interest: The authors declare that the research was conducted in the absence of any commercial or financial relationships that could be construed as a potential conflict of interest.

frontiers in Plant Science

ORIGINAL RESEARCH
published: 18 December 2020
doi: 10.3389/fpls.2020.614871

Interspecific Hybrids Between *Pelargonium* × *hortorum* and Species From *P.* Section *Ciconium* Reveal Biparental Plastid Inheritance and Multi-Locus Cyto-Nuclear Incompatibility

Floris C. Breman[1†], Ronald C. Snijder[2], Joost W. Korver[1], Sieme Pelzer[1], Mireia Sancho-Such[2], M. Eric Schranz[1] and Freek T. Bakker[1†]*

[1] Biosystematics Group, Wageningen University and Research, Wageningen, Netherlands, [2] Syngenta Seeds BV, Andijk, Netherlands

OPEN ACCESS

Edited by:
Patrícia Duarte De Oliveira Paiva, Federal University of Lavras, Brazil

Reviewed by:
Flávia Botelho, Universidade Federal de Lavras, Brazil
Henrik Lütken, University of Copenhagen, Denmark

***Correspondence:**
Freek T. Bakker
freek.bakker@wur.nl

†ORCID:
Floris C. Breman
orcid.org/0000-0002-9722-7564
Freek T. Bakker
orcid.org/0000-0003-0227-6687

Specialty section:
This article was submitted to Crop and Product Physiology, a section of the journal Frontiers in Plant Science

Received: 07 October 2020
Accepted: 23 November 2020
Published: 18 December 2020

Citation:
Breman FC, Snijder RC, Korver JW, Pelzer S, Sancho-Such M, Schranz ME and Bakker FT (2020) Interspecific Hybrids Between Pelargonium × hortorum and Species From P. Section Ciconium Reveal Biparental Plastid Inheritance and Multi-Locus Cyto-Nuclear Incompatibility. Front. Plant Sci. 11:614871. doi: 10.3389/fpls.2020.614871

The genetics underlying Cyto-Nuclear Incompatibility (CNI) was studied in *Pelargonium* interspecific hybrids. We created hybrids of 12 closely related crop wild relatives (CWR) with the ornamental *P.* × *hortorum*. Ten of the resulting 12 (F_1) interspecific hybrids segregate for chlorosis suggesting biparental plastid inheritance. The segregation ratios of the interspecific F_2 populations show nuclear interactions of one, two, or three nuclear genes regulating plastid function dependent on the parents. We further validated that biparental inheritance of plastids is common in section *Ciconium,* using diagnostic PCR primers. Our results pave the way for using the diverse species from section *Ciconium*, each with its own set of characteristics, as novel sources of desired breeding traits for *P.* × *hortorum* cultivars.

Keywords: *Pelargonium*, cyto-nuclear incompatibility, interspecific hybridization, biparental inheritance, plastid

INTRODUCTION

Several closely related species from *Pelargonium* sect. *Ciconium* have been used for producing hybrids that are sold world-wide, commonly known as "garden geraniums," that are some of the most popular and iconic ornamentals. However, there are genetic barriers to establishing crosses and making new hybrids, including Cyto-Nuclear Incompatibility (CNI) that can cause cytoplasmic male sterility (CMS), dwarf growth (DG) and chlorosis in hybrid offspring (Greiner et al., 2015; Postel and Touzet, 2020). Nearly all angiosperms have uniparental maternal organelle inheritance. Unusually, *Pelargonium* × *hortorum* as well as the species *P. zonale* display biparental inheritance of their organelles (Baur, 1909; Tilney-Bassett et al., 1992; Weihe et al., 2009). Inheritance of organelles in plants with biparental transmission was found to be non-Mendelian

in these studies, even though the expression of organelles is managed by the nuclear genome (Barkan and Small, 2014; Börner et al., 2015; Zhang and Lu, 2019). Phenotypic effects of plastid types in otherwise equal nuclear genomic backgrounds were recently demonstrated in *Arabidopsis* (Flood et al., 2020), but other such studies are so far rare.

Pelargonium species are an attractive model system to study CNI as different organellar effects can be evaluated in offspring with equal nuclear-genomic backgrounds, using established crossing techniques. There is a long history of observations of CNI in *Pelargonium* starting in the twentieth century when the foundations were laid for some of the cultivars we have today (e.g., Sweet 1820, 1822). Subsequently, more detailed studies of CNI, especially plastid-induced, were carried out in *Pelargonium* (Baur, 1909; Tilney-Bassett, 1973, 1974, 1975), which, based on segregation ratios, ultimately found support for a two-gene model of complementary nuclear genomic alleles that control the inheritance of organelles in *Pelargonium* (Tilney-Bassett, 1976, 1984, 1988; Tilney-Bassett and Birky, 1981; Tilney-Bassett and Abdel-Wahab, 1982; Tilney-Bassett et al., 1989b).

To further advance our knowledge of CNI in *Pelargonium*, we have performed a section-wide survey of most of the crop wild relatives (CWR) of *P.* × *hortorum* and its supposed ancestors *P. inquinans* and *P. zonale* (James et al., 2004) to investigate the inheritance of organelles in general and plastids in particular. There are currently 17 species recognized in *Pelargonium* section *Ciconium* (van der Walt and Vorster, 1988; Röschenbleck et al., 2014) which are all considered the CWR of *P* × *hortorum*. Phylogenetic relationships among these species have recently been reconstructed based on 76 plastome exon sequences (van de Kerke et al., 2019 and references therein). We further investigated if chlorosis in the hybrid offspring can be correlated with a particular plastid type (e.g., the combined plastid proteome, metabolome, and transcriptome inherited from one parent). Given the ubiquitous occurrence of chlorosis in crosses between species of *P.* sect. *Ciconium* and in other sections in the genus (Sweet 1820–1822, Horn, 1994; Breman pers. obs.), we expect that biparental inheritance of organelles is more common than is currently reported in the published literature.

Finally, based on segregation ratios over one of the crossing series, we deduced the underlying model of interacting genes which can explain the occurrence of chlorotic phenotypes in these crosses, and hence CNI. We did this by disentangling the effects of each possible plastome type on chlorosis in the F1 species hybrids.

MATERIALS AND METHODS

We established novel interspecific crossings between twelve related diploid species of *P.* section *Ciconium* and *P.* × *hortorum* (species and acronyms mentioned in **Table 1**). We verified the hybrid status of the offspring using phenotyping, especially by evaluating leaf morphology, as well as flower color and shape (for an example see **Figure 1** for all others see **Supplementary Figure 4**). In addition, hybrid status and ploidy level of obtained F_1 hybrids were verified by flow-cytometry using *P.* × *hortorum* as internal reference. Flow-cytometry was performed by Iribov bv (Heerhugowaard, Netherlands) on freshly collected leaf material using a Partec CA-II flowcytometer according to De Laat et al. (1987). Nuclei were stained with a High-Resolution Kit (Partec).

Interspecific F_1 Hybrids

The F_1 hybrids generated in this study were produced from the diploid HORT cultivar "Pinto White" (PW) crossed with the species outlined above (listed in **Table 1** and **Figure 2**). In addition, we attempted one interspecific cross at the tetraploid level using HORT "Tango White" (TW) and *P. articulatum* (ARTI). For all crosses, plants were moved to a pre-cleaned greenhouse and manually pollinated by using dedicated small paint brushes, made of animal hair, at 1-day intervals from the moment of flowering, dependent on the species. When seed development did not take place or was impaired, embryo rescue (**Table 2**) was performed as follows: at 2–3 weeks after pollination, embryos were collected, dissected and put on tissue culture in dedicated cabinets using an approach similar to Kamlah et al. (2019).

Interspecific F_2 Populations

In order to evaluate the nuclear background of CNI, we created F_2 progeny of particular F_1 individuals (**Table 3**). We selected F_1 plants which we assume to contain either one, or both parental cytotypes based on overall leaf coloration. We hypothesized that green and chlorotic plants contained one parental type (at that point unknown which one) and that variegated plants contained both (biparental). We selected from these a number of individuals

TABLE 1 | Plant materials used in this study.

Species	Herbarium voucher	Species acronym used in the text	Institute[a]
P. acetosum	1243	ACET	NHM
P. acraeum	1975	ACRA	STEU
P. alchemilloides	1885	ALCH	STEU
P. articulatum	S1026	ARTI	SYN
P. barklyi	S1027	BARK	SYN
P. frutetorum	S1087	FRUT	SYN
P. inquinans	0682	INQU	STEU
P. multibracteatum	2902	MULT	STEU
P. peltatum	1890	PELT	STEU
P. quinquelobatum	S1044	QUIN	SYN
P. ranunculophyllum	A3651	RANU	MSUN(*)
P. tongaense	3074	TONG	STEU
P. zonale	1896	ZONA	STEU
P. elongatum	0854	ELON	STEU
P. aridum	S1088	ARID	SYN
P. × *hortorum* "Pinto white" (PW)	PEZ-BD8517	HORT	SYN
P. × *hortorum* "Tango White" (TW)	NA	HORT	NA

Herbarium voucher information. [a]STEU, Stellenbosch University, RSA; AL, Albers/MSUN, Münster Germany; SYN, Syngenta collection number; NHM, Natural History Museum London UK.

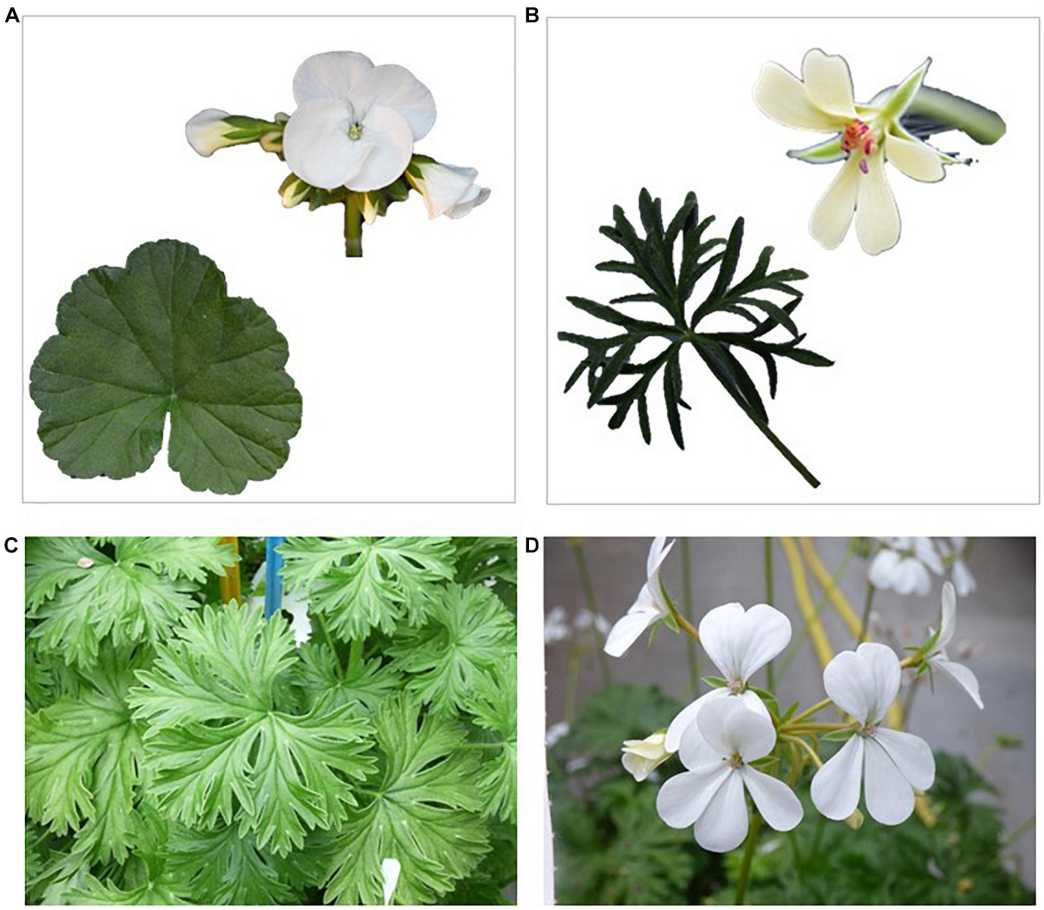

FIGURE 1 | Example of the phenotype of an F1 hybrid generated from the HORT × ARID cross. **(A)** Shows the leaf and flower phenotypes of *P.* × *hortorum*; **(B)** shows the leaf and flower phenotypes of *P. aridum*; **(C)** shows the leaf phenotype of F_1 HORT × ARID; **(D)** shows the flower phenotype of F1 HORT × ARID.

for subsequent self-pollination to generate the F_2 populations: six plants in total representing three phenotypes encountered in the HORT × ZONA F_1 which includes 2 green (denoted as: HORT × ZONA^G'), 2 variegated (denoted as: "HORT × ZONA^V") and 2 chlorotic (denoted as: "HORT × ZONA^C") plants (see **Figures 3**, **5**). In addition, we included one cross (three green plants, the only surviving phenotype) involving *P. acetosum* (*ACET*). We also selected plants from a crossing involving *P. frutetorum* (*FRUT*) and *P. inquinans* (*INQU*) as positive controls for the evaluation. This is because *Pinto White* contains a plastid that is considered to have originated from the *P. inquinans* ancestor (James et al., 2004) and the plastid of *P. frutetorum* is indistinguishable from that of *PW* and *P. inquinans* (Breman et al., in prep). Therefore, we expected these crosses not to display chlorosis in the F_2.

We also evaluated a subset of plants for evaluation of segregation for CNI phenotype patterns that are expressed during the pre-seedling phase. We selected three F_1 parents of HORT × ACET^G, four HORT × ZONA^G and one parent each of HORT × FRUT^G and HORT × ACRA^G. Because fruit-set was low this season for HORT × ZONA we pooled these to enable Chi^2 testing. We feel pooling was justified, because these plants share parentage, and have the same phenotype and plastid.

Plant Rearing

Plants were grown in a greenhouse from seeds and leaf material was collected from the first primary leaves for DNA extraction. See **Table 1** for the full list of plant material used with Herbarium accession numbers and see **Supplementary Figures 6A–K** for representative phenotypes of each F1 plant.

DNA Extraction, Primer Design, and Genotyping

Genomic DNA was extracted from leaf material using a modified CTAB protocol (Bakker et al., 1998) followed by RNAse treatment. We designed specific primers for plastome-typing parents and F1 offspring We used the Long Single Copy region (LSC) of assembled plastomes (Breman et al., in prep) for *Pelargonium* section *Ciconium* species. LSC has been shown to contain numerous indels (Chumley et al., 2006; Guisinger et al., 2008, 2011; Weng et al., 2017; Breman et al., in prep) which can be used to create genotype-specific primer sites. Visual inspection of sequence alignments, combined with parsimony analysis and using the "Apomorphy list" command

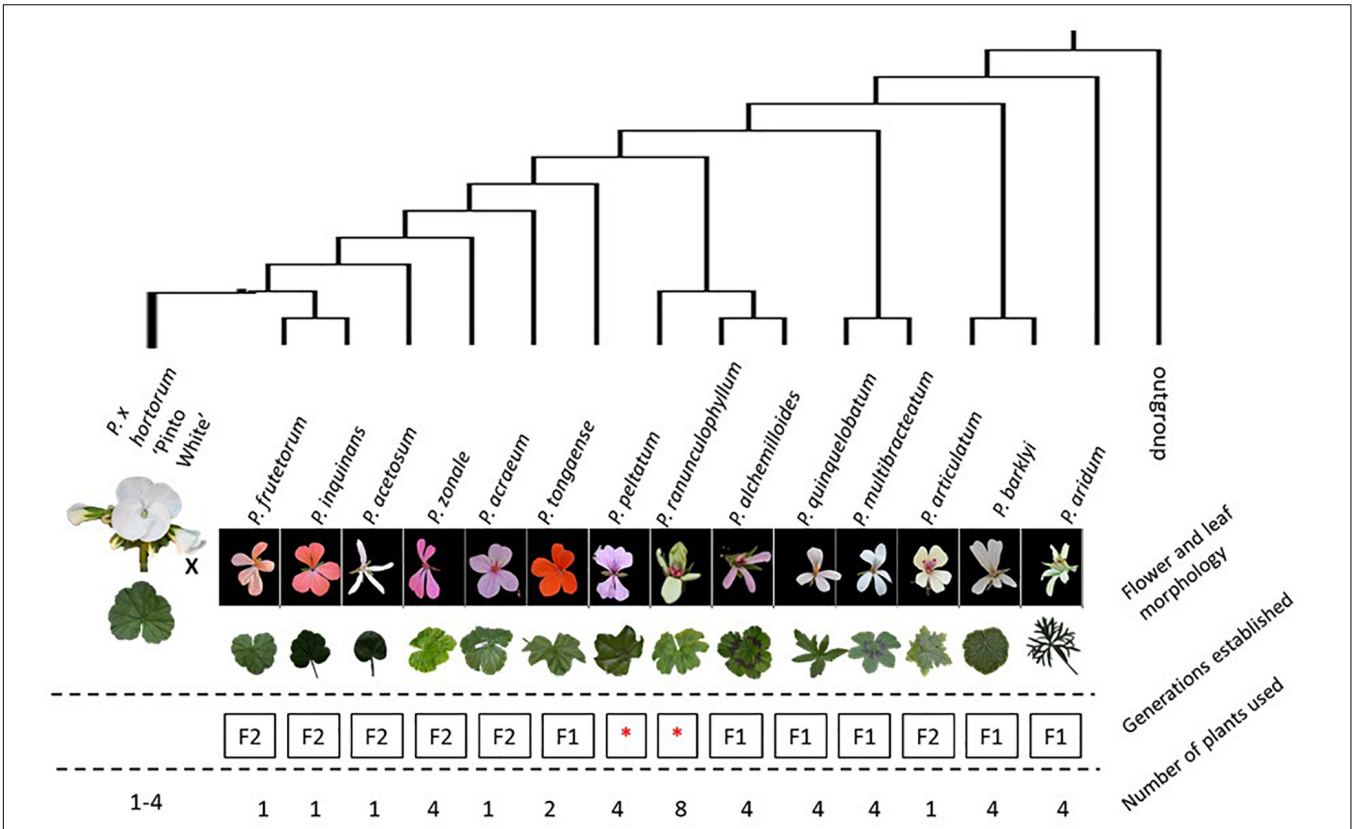

FIGURE 2 | Schematic overview of the experimental setup for the F_1 crosses put in a phylogenetic context. The tree displayed tree is based on van de Kerke et al. (2019). The position of *P. ranunculophyllum* is inferred from our plastome assembly data (Breman et al. in prep), combined with those of van de Kerke et al. (2019) and Breman et al. (in prep). On the top row are all accessions used, represented by their respective floral and leaf phenotypes and structured by their presumed phylogenetic distance to "HORT" (van de Kerke et al., 2019); "Generations established" indicates results obtained with "F_1" indicating only F_1 plants were obtained, no F_2 could be generated; "F_2" meaning the plants were fertile and could produce F_2 offspring; red asterisks denote crosses that failed for reasons explained in the text. The bottom row indicates the number of plants used across the seasons.

in PAUP*4b10 for windows (Swofford, 2002), was performed to find suitable primer sites and to check for unique autapomorphies therein. We specifically scanned for regions with a unique indel or multiple unique substitutions, allowing for genotype-specific primers. Amplicon sizes were designed to be < 500 bp, allowing for shorter PCR thermo-profiles. Candidate primer pairs were evaluated using Oligocalc (Kibbe, 2007)[1] checking for differences between melting temperatures (ΔTm), self-priming and hairpin formation. Primers were accepted when ΔTm between forward and reverse primers was < 3°C and with only one hairpin and/or one self-priming was predicted. Further, we required a primer site to have a minimum Illumina read coverage of 20. A GC content of 40–50% was preferred, but this was not always possible. A GC content of 40–50% is considered best for ensuring stable binding during annealing and increase the primer pairs efficiency. Finally, we submitted the primers to a BLAST search (set for analyzing short sequences) to compare to all available *Pelargonium* sequences to verify target-specificity. Occasionally a single primer would have a significant hit to *Pelargonium* species outside section *Ciconium*, but this never occurred for both primers of a pair.

Primers were tested *in vitro*, using a panel of 16 section *Ciconium* species representing the range of parental plastid variation we would encounter in our offspring. Primer candidates were evaluated using the target accession and an annealing temperature gradient ranging from 49 to 60°C. Primers that amplified were subsequently tested against the panel of accessions at the highest possible temperature for which it showed amplification of the target. For PCR profiles and reaction conditions see **Supplementary Figure 3**.

Phenotyping of F_1 and F_2 Plants

Leaf color phenotyping was performed at the seedling stage (**Figures 4A,B**). In order to consistently compare phenotypes across populations per cross, we took photos of seedlings at 2-week intervals during the seedling stage until the development of the first two primary leaves (**Figure 4**). We used the following four leaf-phenotyping categories based on a visual assessment of the phenotypes: (1) "Green": leaf phenotype comparable to parents; (2) "Chlorotic," plants are lighter green than either parent or even yellow; (3)

[1]http://biotools.nubic.northwestern.edu/OligoCalc.html

"White," plants germinate, but die within 2 weeks. Seeds that failed to germinate are added to this category; (4) "Variegated," plants display more than one chlorotic phenotype in the same individual, presumably due to heteroplasmy (see **Figures 4B,C**, **5**).

Ratios of the four phenotypes for each tested F_2 population were compared and fitted to a one-, two- and three-gene model of inheritance of nuclear genomic alleles (calculated using the spreadsheet from Montoliu, 2012). We assumed four phenotypes and combined these according to five different scenarios, each representing assumptions on expected phenotypic ratios and their expression. The first scenario tested considers four phenotypes (i.e., "not affected," "mildly," "severely," and "lethal"). The second and third scenarios consider there to be three phenotypes ("not affected," "affected," and "lethally affected"). Finally, the fourth and fifth scenarios consider only two phenotypes ("affected" vs. "not affected"). We then evaluated these five different scenarios by binning individuals differently. E.g., under scenarios two and three only green plants are considered to be unaffected but the lethal category consisted either of only the white or the white and severely affected plants (**Table 4A**). Thereby we further assumed different parental genotypes and their expected phenotypic ratios leading to eight testable phenotypic ratios representing models of one, two, or three loci involved (**Table 4B**).

TABLE 2 | F_1 offspring overview.

Hybrid	Origins of plastid	Phenotype	# offspring obtained
HORT × ZONA	Maternal	Chlorotic	144
HORT × ZONA	Paternal	Mostly Green	
HORT × ZONA	Biparental	Variegated	
HORT × ACET	Paternal	Green Vir	7
HORT × ACET	Maternal	Lethal	
HORT × FRUT	NP	Green	72
HORT × INQU	NP	Green	2
HORT × ACRA	Paternal	Green	24
HORT × QUIN	Maternal	Lethal	12
HORT × QUIN	Paternal	Chlorotic Vir	
HORT × QUIN	Biparental	Variegated	
HORT × MULT	Paternal	Chlorotic Vir	21
HORT × ALCH	Paternal	Chlorotic Vir	8
HORT × TONG	Paternal	Chlorotic	36
HORT × ARID	Paternal	Chlorotic	10
HORT × ARID	Maternal	Lethal	
HORT × PELT	*	–	–
HORT × RANU	*	–	–
HORT × BARK	Paternal	Lethal	2
$HORT^4$ × ARTI	Either	Green	–
$HORT^4$ × ARTI	Eihter	Chlorotic	
$HORT^4$ × ARTI	Either	Lethal	

*Vir indicates plants were virescent. *Crosses failed either because (paternal) plants would not flower or no fruit was ever observed.* ***HORT****^{4} refers to a tetraploid cultivar from HORT called "Tango White" All other HORT refer to the diploid "Pinto White" cultivar.*

For evaluating seed phenotypes, we used a similar approach, distinguishing four phenotypes: (1) "normal," not affected by CNI, 2); "bleached," seed contains endosperm that is still filled, but the seed is bleached; (3) "watery," in this case the endosperm

TABLE 3 | Genotypes detected in F1 and F2 offspring, using diagnostic PCR, for the HORT × ZONA cross.

Pedigree	Plant/cross	Phenotype	Origin of plastid
F0	Hortorum	G	Wild-type M
	Zonale	G	Wild-type P
F1	8542	G	P
	8542	C	M
	8552	G	P
	8552	V	M
	8570	C	M
	8570	G	P
	8570	C	P
	8570	V	M
PEZ-BD8542	8618	C	G-P
	8618	G	G-P
	8618	C	NA
	8619	G	G-P
	8619	C	G-P
	8620	C	G-M
	8620	C	G-M
	8620	C	G-M
	8620	C	G-M
	8627	C	G-P
	8627	G	G-P
	8628	C	G-M
	8628	V	biparental
	8628	G	G-P
	8628	C	G-M
	8629	C	G-M
PEZ-BD85552	8621	C	NA
	8621	G	G-P
	8623	C	G-M
	8623	G	G-M
	8630	C	G-P
	8630	G	G-P
	8631	C	G-M
	8631	G	G-M
	8632	Lethal	G-M
	8632	C	G-M
PEZ-BD8570	8624	C	G-M
	8625	C	G-M
	8625	C	G-M
	8625	G	G-M
	8626	G	G-P
	8626	C	G-P
	8634	Lethal	G-M
	8634	G	G-P
	8634	C	G-M

Structured by cross. (G)-P and (G)-M denotes (grand) paternally-and maternally inherited plastids.

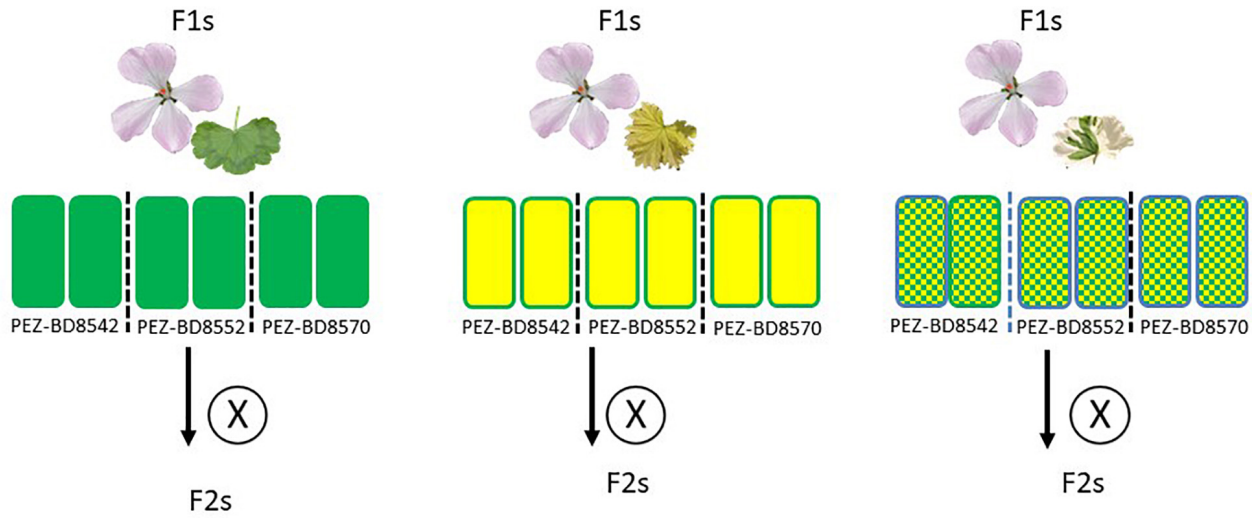

FIGURE 3 | Experimental setup for obtaining F_2 crosses of F_1 parents with different phenotypes.

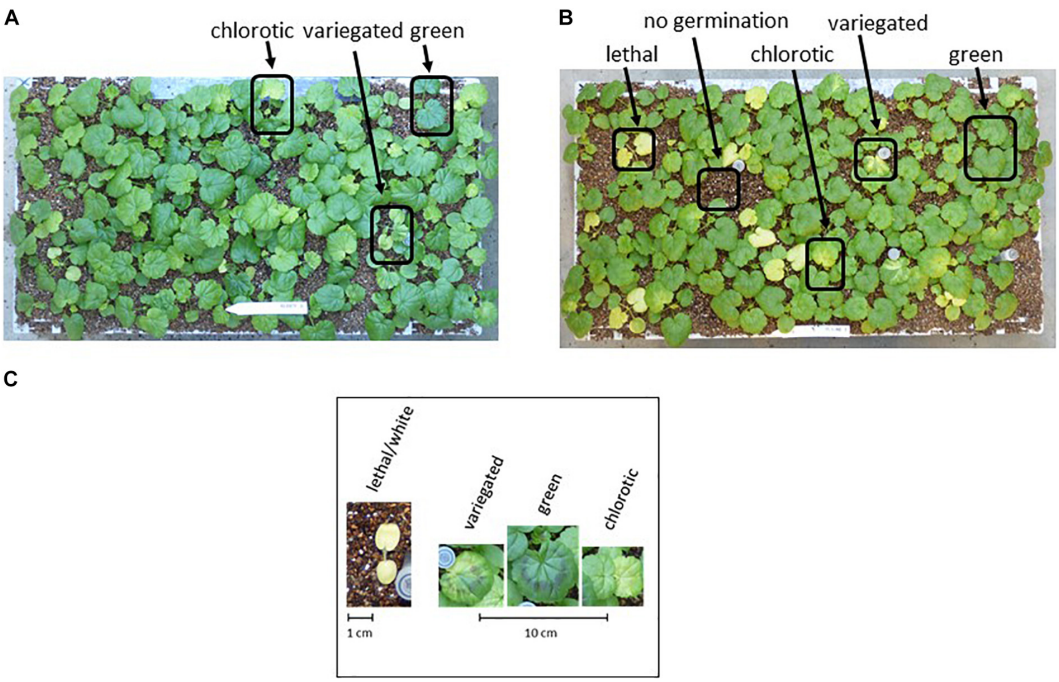

FIGURE 4 | Chlorosis phenotypes. **(A)** Segregation for chlorosis among progeny in the F_2 HORT × FRUT. **(B)** Segregation for chlorosis in F_1 HORT × ZONA. Examples of "green," "chlorotic" and "variegated" plants are indicated, as well as "lethal" phenotypes and seeds that failed to germinate. **(C)** Scaled close-up of examples of phenotypes.

is bleached and not properly filled; (4) "lethal," seeds with this phenotype displayed early aborted or undeveloped embryos. For examples see **Figure 6**.

As for leaf phenotypes, for seed phenotyping we evaluated five scenarios as well. We assumed four ("normal," "bleached," "empty," "lethal," scenario 1), three ("not affected," "affected," and "lethally affected," scenarios 2 and 3) and two ("affected" vs. "not affected," scenarios 4 and 5) phenotypes.

Genotyping F_1 Plants and F_2 Populations

We plastome-typed F_1 plants using our diagnostic primers described above (**Table 3**). In those cases where the F_1 population segregated for chlorosis, we tested accessions representing each phenotype. We then typed F_2 plants from each population, and plastome types were then associated with the measured leaf phenotypes to establish the correlation, and thus effect, of each plastid type in the segregating offspring.

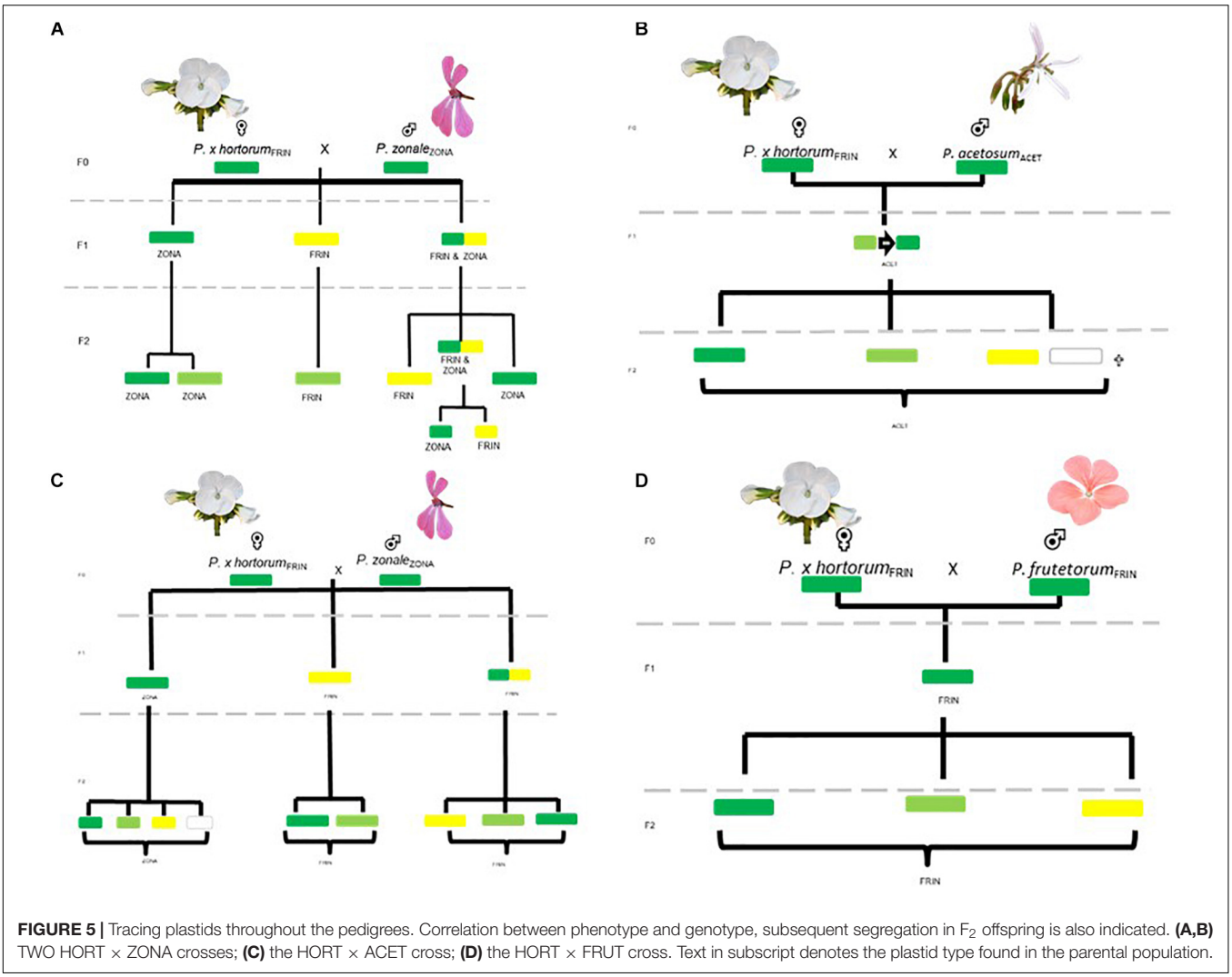

FIGURE 5 | Tracing plastids throughout the pedigrees. Correlation between phenotype and genotype, subsequent segregation in F_2 offspring is also indicated. **(A,B)** TWO HORT × ZONA crosses; **(C)** the HORT × ACET cross; **(D)** the HORT × FRUT cross. Text in subscript denotes the plastid type found in the parental population.

RESULTS

Crossing Results

Interspecific F_1 Hybrids

From thousands of pollination attempts we created a total of 314 F_1 hybrid plants from crossing our species panel to the ornamental cultivar *P.* × *hortorum* PW (see **Table 2**). Twelve interspecific crosses were successful in producing F_1 plants (**Table 2**). For three crosses embryo rescue (ER) was needed In order to produce scorable progeny, whereas three attempted crossings failed. Attempts to cross HORT with *P. elongatum (*ELON*)* failed, but this was expected given the difference in basic chromosome numbers between the two accessions (HORT × = 9, *P. elongatum* × = 4 (Gibby and Westfold, 1986; Gibby et al., 1990). The other two failed due to a lack of flowering HORT with *P. peltatum* (HORT × PELT) or poor greenhouse conditions (such as too high humidity or temperature) for the paternal source HORT with *P. ranuncluophyllum* (HORT × RANU). Except for HORT × ZONA (Baur, 1909 and many others since), HORT × ACET and HORT × QUIN (Hondo et al., 2014, 2015), these crosses are novel and were never reported in literature before. Remarkably, in 10 cases the F_1 offspring displayed segregation for leaf color phenotype (e.g., chlorosis). When segregation did occur, it ranged from varying levels of chlorosis to nearly green for some crosses to spanning the full range of possible phenotypes from lethal white plantlets to nearly fully green plants (**Figure 4**).

Establishment of the F_2 Populations

For all F_1 crosses we were able to obtain an F_2 generation (**Figure 3**) with varying degrees of success, e.g., the green F_1 "HORT × ZONA" cross used to produce the F_2 yielded significantly more offspring as well as a slightly higher germination success than the variegated or chlorotic parents did (**Table 5**). The seed phenotypes for F2 crosses which were used in this study are shown in **Figure 6**.

Primer Design and PCR Verification

We designed 11 primer-pairs targeting single accessions (e.g., genotype-specific primers) or a group of accessions (**Table 6**). All primer-pairs performed as expected, except

Table 4A | Crosses matching genetic models of inheritance.

		One gene model			Two gene model			Three gene model		Observed ratios
Scenarios	**Crosses meeting criteria**	**a**	**b**	**c**	**d**	**e**	**f**	**g**	**h**	
Scenario 1	F2_hort_x_zona^{V}	M***	–	–	–	–	M***	–	M***	∼4:5:1:3
Scenario 2	F2_hort_x_zona^{G}	–	–	M***	–	–	–	–	–	∼7:7:1
	F2_hort_x_zona^{V}	M***	M***	–	–	–	M***	–	M***	∼1:2:1
	F2_hort_x_frut	–	M***	–	–	–	M***	–	M***	∼1:3:0
Scenario 3	None	–	–	–	–	–	–	–	–	–
Scenario 4	None	–	–	–	–	–	–	–	–	–
Scenario 5	F2_hort_x_zona^{G}	–	–	M***	–	–	–	–	–	∼1:1!$^{50:50}$
	F2_hort_x_zona^{V}	M***	M***	–	–	–	M***	–	M***	∼1:2!$^{75:25}$
	F2_hort_x_frut	–	M***	–	–	–	M***	–	M***	∼1:3!$^{75:25}$
				Fruit/seed phase						
Scenario 1	None	–	–	–	–	–	–	–	–	–
Scenario 2	None	–	–	–	–	–	–	–	–	–
Scenario 3	None	–	–	–	–	–	–	–	–	–
Scenario 4	F2_hort_x_frut	–	–	M***	–	–	–	–	–	1:1!$^{\mathbf{50:50}}$
	F2_hort_x_zona^{G}	—-	M***	–	–	–	M***	–	M***	∼1:3!$^{\mathbf{25:75}}$
	F2_hort_x_acet	–	M***		–	–	M***	–	M***	∼1:3!$^{\mathbf{25:75}}$
Scenario 5	F2_hort_x_frut	–	M***		–	–	M***	–	–	∼1:4
	F2_hort_x_acra	–	–	M***	–	–	–	–	–	∼1:1.5
	F2_hort_x_zona^{G}	–	M***	–	–	–	M***	–	–	∼1:1.3

*M: mendelian model applies, ***P < 0.001 under the χ^2-test! indicates ratios matching particular model. For all observed ratios and counts of phenotypes under each scenario please see* ***Supplementary Material 5****.*

Table 4B | Possible parental genotype and expected phenotypic ratios.

Lettercode	Genetic model and expected ratios
a	F1xF1 = AaxAa 25:50:25
b	F1xF1 = AaxAa 25:75
c	F1xF1 = AaxAA 50:50
d	F1xF1 = AaBbxAaBb 6.25:18.75:18.75:56.25
e	F1xF1 = AABbxAaBB 25:25:25:25
f	F1xF1 = AABbxAaBB 25:75
g	F1xF1 = AaBbCcxAaBbCC 6.25:18.75:56.25:18.75
h	F1xF1 = AaBbCcxAaBbCC 25:75

BART, which amplified ARTI but not BARK. We therefore used this primer only for detecting ARTI. For gel photo documentation accompanying the primer pair evaluations we refer to **Supplementary Figures 2**, **3**. All primers worked across a range of template DNA concentrations (0.1 ng/μl up to > 5 ng/μl). A 1/10th dilution of the extracts generally increased PCR performance.

Phenotyping and Genotyping the F_1 and F_2 Population for HORT × ZONA and HORT × ACET

For a full overview of the tests for all scenarios under all eight genetic models (**Tables 4A,B**) we refer to **Supplementary Figure 5**. We discuss here those crosses that demonstrated Mendelian patterns of segregation as well as the models under which this applies. We found that the F_1 plants segregate for chlorosis, with no obvious Mendelian patterns of segregation (**Table 4A** and **Supplementary Figure 5**), but that they are otherwise phenotypically homozygous, i.e., non-segregating. When genotyping the F_1 plants, we found that green individuals contained the *P. zonale* type plastid (ZONA), whereas chlorotic individuals contained that of *P. frutetorum/P. inquinans* (FRIN) (**Tables 2**, **3** plastids of "maternal origin"). A small minority (< 5%) of the plants displayed (partial) variegation and this percentage reduced, for most, as the plant aged with most settling into a single phenotype. From these we detected either the FRIN or the ZONA plastids, but as we recovered both from the F_2 offspring (see below) they must actually have contained both. We have evaluated plastid types in all phenotypes of F_2 offspring (structured per F_1 cross, **Figure 5**) for the HORT × ZONA cross series. We found FRIN and ZONA plastid types in the F_2 (**Table 3**) and, in general, F_2 offspring always contained the same plastid as was detected in the F_1 plant (for example, see **Figure 5**), except for the variegated plants. In the F_1 HORT × ZONA variegated plants we found only one of the plastids, either FRIN or ZONA, but in the F_2 we detected both, even once in one variegated individual (**Figure 5A**). We analyzed the bleached and green tissue from this plant and found that white tissue predominantly contained the FRIN type and green contained the ZONA type (**Figure 5A**).

When pooling the green and light green plants and treating these as one (scenarios 4 and 5) phenotype, subsequent testing for Mendelian patterns of segregation did not yield a clear pattern (**Supplementary Figure 5**), as was the case for three phenotypic categories. When we categorized the phenotype ratios as "affected" or "not affected," we saw that they matched those expected under either a one- or two-gene model for all

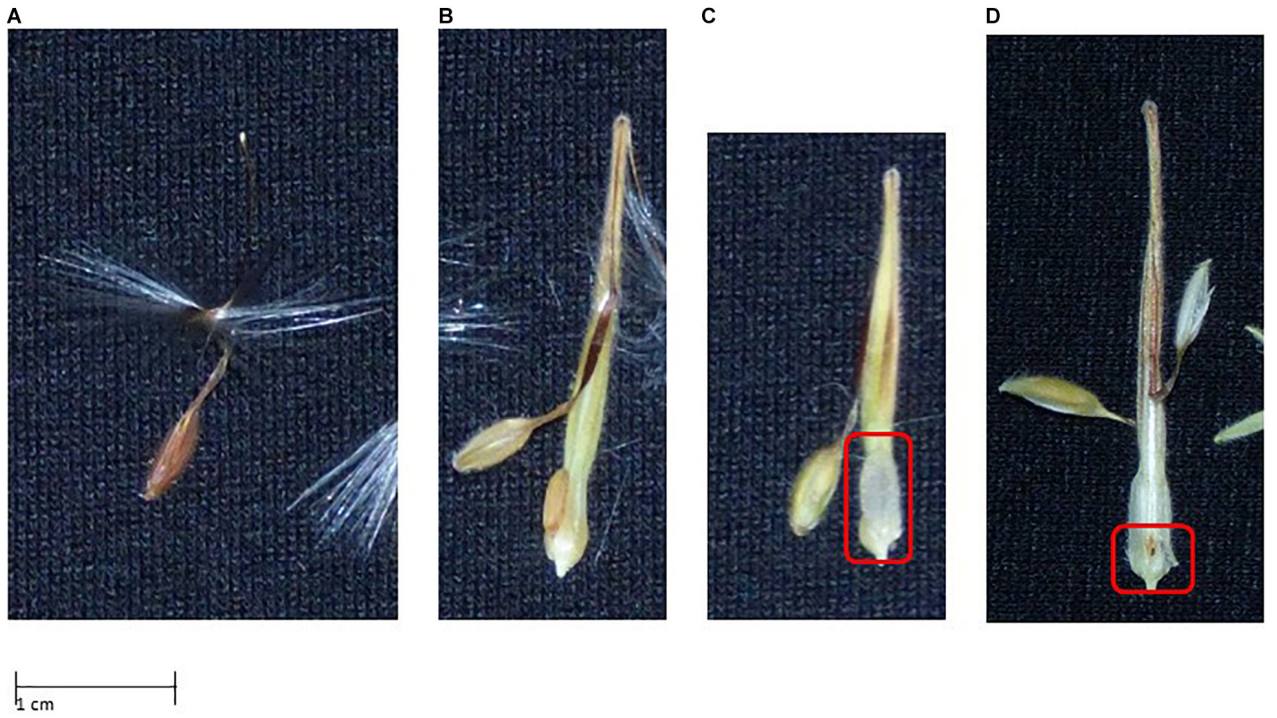

FIGURE 6 | Seed phenotypes displaying signs of Cyto-nuclear incompatibility (see text for further explanation). **(A)** Normal seed phenotype; **(B)** bleached seed phenotype; **(C)** seed containing no or watery endosperm; **(D)** no embryo development.

Table 5 | F_2 material obtained using selection of plants from **Table 1**.

Cross	G	V	C	Lethal*	# seeds	Sum	Germination %	Marker(s) found	Ratio
F_2_hort_x_zona^C	8	1	51	34	125	94	0.78	5 FRIN, 1 ZONA	∼1:6:4
F_2_hort_x_zona^G	139	3	138	20	332	300	0.84	1 FRIN, 5 ZONA	∼7:7:1
F_2_hort_x_zona^V	52	4	79	48	230	183	0.76	2 FRIN, 1 ZONA, 2 FRIN, and ZONA	∼1:2:1
F_2_hort_x_acet^C	33	2	49	28	116	112	0.95	ACET	1
F_2_hort_x_frut^G	24	3	63	0	90	90	1.00	FRIN	1
F_2_hort_x_inqu^G	144	0	0	0	144	144	1.00	FRIN	1

*Chlorosis phenotypes of F_1 parents and plant counts are given. "**G**" denotes a green plant, "**C**" a chlorotic one and "**V**" a variegated plant. For the description of the chlorosis categories see the text. *Lethal plants are counted without the seeds that failed to germinate.*

crosses assuming lethal interactions are also possible between alleles. The populations where the ratios conformed to the one gene model are F_2 HORT × ZONA^V and F_2 HORT × ZONA^C. The segregation ratios in this "affected vs. not-affected" analysis pointed to one lethal combination of alleles and two combinations that yield viable or affected plants. When pooling light green and yellow plants and subsequently testing for Mendelian patterns of segregation, a pattern emerges for the F_2 HORT × ZONA^V and the F_2 HORT × ZONA^G populations (scenario 2). In contrast, when analyzing the observations for the F_2 HORT × ZONA^C plants there did not appear to be a pattern. The patterns for the F_2 HORT × ZONA^V and the F_2 HORT × ZONA^G populations did point to a genetic difference in the F_1 population (and therefore also in the F_0 populations). With the green populations following the one gene model whereby the F_1 was Aa × AA.

The ratios for the plants phenotyped for F_2 seeds and their corresponding possible underlying genetic models are listed in **Table 4A**. We deduced that there were likely one (in HORT × FRUT and in HORT × ZONA) and two loci (in HORT × ACET) interacting in this phase of plant development. Given that the phenotypic ratios under scenarios 1–4 did are similar to, but not exactly what would expected when of one, two, or three genes interact. We suspect that more complex interactions, possibly involving more than two or even three genes, played are role or that the loci involved are linked in some cases with aggravating or moderating effects of linked loci. This appears especially to be the case for HORT × ACRA where ratios under scenarios 1–4 are: ∼2:1:2:20 (3 loci); ∼2:1:2 (2 loci); ∼1:1:10 (3 loci), and ∼1:12 (3 loci), respectively (see **Supplementary Figure 5** for more details).

Table 6 | Primer pair details.

Primer pair name	Target(s)	Sequence 5′–>3′	Plastome region
FRIN	*P. inquinans, frutetorum and* × *hortorum*	AAAGGCCAGATTGGGCGGC	F: IGS and R; 5′ of rna polymerase beta subunit 2 exon
		GACGAATTCGGTCCGATTCAACAC	
ZONA	*P. zonale*	GAATTGTAATGCGGAGCTGC	F and R: IGS
		AAGAAAGAGGATATAGCCGGAC	
ACET	*P. acetosum*	GAATCCCCACCTACACTACAC	F and R: MATK exon, 3′end
		CCTTGACTAAAGCGCAATTTTG	
ACRA	*P. acraeum*	GACCCTATCTCTCTGTATTC	F and R: IGS
		TTTGGTCTCCGAAAAGAAAAGG	
ALRA	*P. alchemilloides* and *ranunculophyllum*	GGATCTTATCTATTCTCTATTC	F and R: IGS just downstream of trnK-UUU small exon
		CGATCTAGATCTAATTGTAC	
MUQU	*P. multibracteatum* and *quinquelobatum*	GGTTTCGCGTCAATTGC	F and R in flanking IGS's of atpH, atpH exon is entirely covered by fragment
		CTGAATTTAGCTATGATTTCG	
ARID	*P. aridum*	CTGAACTGAACTCAAATGGA	F and R: in IGS, fragment contains trnH-IS and trnI-LE
		ATTGCGAGGATCCTACTTTG	
BARK	*p. barklyi*	GAAAGATCTATTCGAGTCGAG	F: in IGS, R: in intron between tnrL-UAA exons
		GGGGCCTCATTACATTAATC	
PELT	*P. peltatum*	CTCAAAAGAAGGGTAGAAGGG	F and R: in IGS's surrounding trnS-GGA
		CCCTGTCTGCTCTTTCCAA	
TONG	*P. tongaense*	GATCTCAAAGCAAAGAGAGC	F: IGS, R: in ndhJ exon
		CTTGGCTAGTGTATACCATTTG	
BART	*P. articulatum* and *P. barklyi*	GAATCCAAAAGAAATGAAATG	F and R: IGS between atpB and rbcL
		AAAAGGAATAGGTTTTGTAG	

Plastome regions were identified using genbank ID: DQ897681.1 (P. × *hortorum, Chumley et al., 2006). F refers to forward, R refers to reverse.*

Positive Controls

Our positive controls HORT × INQU and HORT × FRUT yielded 100% green plants in the F2. In the F_2 this was maintained for HORT × INQU for both plant and seed phenotypes, but surprisingly, the F_2 of HORT × FRUT displayed segregation for chlorosis and seed phenotypes (**Figures 4A** and **6**) indicative of the one gene model of segregation with a heterozygous parent with possible lethal combinations expressed in the pre-seedling phase as well (**Table 4A** and **Figure 6**).

Genotyping Phylogenetically More Distant F_1 Hybrids

We recovered two plastid types in the offspring of F_1 of HORT × QUIN (**Table 2**). We found segregation for chlorosis and detected both the FRIN type as well as the MUQU type plastids in the offspring. None of these plants were fully green. In the F_1 HORT with *P. aridum* (HORT × ARID) we found segregation for chlorosis, with the majority of offspring lethal and one plant surviving a full season. For F_1 HORT × ARID We detected FRIN and ARID plastids in the offspring. In the F_1 HORT × ALCH, F_1 HORT × TONG, F_1 HORT × ACRA, F_1 HORT × MULT and HORT × BARK, we detected only the paternal plastids (**Supplementary Figure 2**). This is similar to the F_1 HORT × ACET cross in that we detected only one type in the offspring suggesting lethal interactions with the FRIN type plastid. In the F_1 HORT × ARTI cross we find segregation for chlorosis and no correlation between phenotype and genotype, we detected both the FRIN and ARTI type plastids. For an overview of all the results (see **Table 2**).

DISCUSSION

We show that biparental inheritance occurs throughout the section and that hybridization is relatively easy, both observations have important implications for interpreting current concepts of *Pelargonium* section *Ciconium* evolution. This study further demonstrates that using multiple interspecific crosses can be used to gain insight into the genetics underlying organelle management and expression, potentially uncovering drivers of speciation. Our studies expand on the two-interacting gene model found to regulate plastid inheritance in *Ciconium* which was inferred 50 years ago by Tilney-Bassett et al. (1989b, 1992). While a limited number of crosses between *P.* × *hortorum* and section *Ciconium* have been previously reported (e.g., Hondo et al., 2014, 2015), we have greatly expanded on this by covering nearly all of the CWR in the section including those that are phylogenetically more distantly related.

Biparental Inheritance of Plastids and Evolutionary Implications

We have found maternal (*P. frutetorum/inquinans*; FRIN) and paternal (other *Ciconium* plastid types) inheritance in nearly all

our offspring indicating that the ability to inherit and express more than one plastid is the rule rather than the exception in *Pelargonium* section *Ciconium*. Even though it was demonstrated before on a limited scale (Baur, 1909; Tilney-Bassett et al., 1992; Weihe et al., 2009), it was never demonstrated to be so ubiquitous. This has important implications for the study of *Ciconium* speciation as bi-parental inheritance may provide an escape from the acquisition of deleterious plastid mutations (Mullers ratchet), because there is the possibility for an additional plastome types to occur in the individual plant. Also, it may allow to occupy new niches quicker and perhaps even allow populations that have become separate in space and time to reconnect (Greiner et al., 2011; Apitz et al., 2013; Greiner and Bock, 2013; Greiner et al., 2015; Barnard-Kubow et al., 2016, 2017; Sobanski et al., 2019).

Plastid Effects

We have found evidence that in our crosses the FRIN plastid caused bleaching in the HORT × ZONA crosses and that it was possibly lethal for the HORT × ACET cross given the absence of any offspring containing FRIN. The observation that ZONA plastids caused less chlorosis than FRIN in these types of crosses is not new in itself and this study confirms what was already hinted at by Tilney-Bassett and Almouslem (1989a) and more recently confirmed by Weihe et al., 2009 who observed that the "inquinans plastid" caused bleaching. The F_1 HORT × ZONA plants were, in some cases viable when containing the FRIN plastid allowing us to evaluate the effects of both plastid types in subsequent generations. As to which part of the plastome is the root cause we can only speculate, but a number of genes have been demonstrated to be under selection in the Geraniaceae plastomes (Shikanai et al., 2001; Blazier et al., 2016a,b; Ruhlman et al., 2017; Weng et al., 2017; Ruhlman and Jansen, 2018). More surprising was the find that the F_2 HORT × FRUT showed a segregation for chlorosis, even though the F_1 did not. This hints at a slight incompatibility between the FRIN type plastid and either the HORT or FRUT parent. This is surprising given that we cannot distinguish the plastids. Therefore, given the segregation ratios (**Table 4A**), one nuclear gene, either originating from HORT or FRUT, must be slightly divergent and must be responsible for this effect. Given that this segregation was not the case for The HORT × INQU F_2 population and no segregation occurs when selfing HORT, we deduce that one of the alleles originating from FRUT was responsible.

F_2 Segregation Pointing to Two or Three Epistatically Interacting Genes

We demonstrate, in a second generation series of plants that, irrespective of plastid type, there was segregation for chlorosis. Chlorotic phenotypes of the F_2 did not appear to show Mendelian inheritance patterns under a one or two allele model in all cases. However, nuclear alleles must be involved because the plastid backgrounds are the same for each plant (Stubbe, 1958, 1959, 1989; Amoatey and Tilney-Basset, 1994; Barr and Fishman, 2010; Li et al., 2013). For the F_2 HORT × $ZONA^V$ population both the one gene model and the two gene model did seem to be equally good at explaining the results. The observed numbers conformed well to the F_1 HORT × $ZONA^V$ population being heterozygous. As outlined above, ratios for the three phenotypic categories do not shed much light on the underlying genetics, but when we categorize the phenotype ratios in a binary way, "affected or not affected," we see the ratios for all crosses matching or approaching ratios for phenotypes that resemble the situation where one combination is lethal and two combinations of alleles are not. For the HORT × $ZONA^C$ population the ratio is more akin (10:1 under the two phenotypes scenario 5, **Supplementary Figure 5A**) to the ratio's expected (9:1 under the two phenotypes scenario 4, **Supplementary Figure 5A**) under a two gene interaction model whereby heterozygous combinations are lethal and the homozygous combinations of at least one allele are not. The ratios for the HORT × ACET cross hint at a possible trihybrid segregation, whereby two alleles interact in a lethal way, because of the following reasoning: If segregation was perfect we would expect the following phenotypic ratio's under the three gene model; 27:9:9:9:3:3:3:1 but we observe 25:9:1:5 under the four phenotypes scenario 1 (**Supplementary Figure 5A**). For this pattern to occur we would have to assume there are two alleles that interact in a lethal way, causing the deviation from the expected ratio's, but also that there is a third allele which in turn moderates some of these effects or may cause extra lethality.

The ratios of CNI phenotypes observed in the seeds points to a similar type of interactions further explaining why we observe sometimes skewed segregation ratios. In the case of the HORT × ACET cross we observe mendelian segregation of under gene models b, f, h (25:75 phenotype ratios under the one, two, and three gene models) with the majority of the individuals being lethal. When we view the ratios of all phenotypes for HORT × ACET and HORT × ACRA (10:3:2:1 and 20:2:1:2, respectively, **Supplementary Figure 5B**) these, similarly as for the seedlings evaluated, reminiscent of ratios for the two gene model whereby heterozygous combinations are lethal and the homozygous combinations of at least one allele are not. Thus, combining the observations of both seed and seedling phase of plant development, would yield for the HORT × ACET cross a series of at least five loci involved in development and expression of organelles. For the HORT × FRUT at least two loci would be required to explain the observations, one acting in each stage of development we studied.

Model of > 3 Interacting Nuclear Genes

The observation that the HORT × ACET cross needs two and a three gene model to explain the observed patterns may indicate that those crosses which consist of combination that are phylogenetically further removed from HORT may be subject to the effects of more than three genes. As mentioned above CNI plays a role in embryo and fruit development as well. This in turn could point to a more complex model of genetic interactions involving more loci than we thus far proposed. The machinery for synthesis and management of organelles consists of numerous PPR genes that each act during a different step of these processes (Barkan and Small, 2014; Börner et al., 2015; Zhang and Lu, 2019). These can perhaps be viewed as a genetic "block chain" whereby no mismatch of combinations is allowed in order to result in a viable, green and self-sustaining plant. In our interspecific crosses there were ample opportunities for these mismatches to occur. While we have no hard evidence for this we

do see from the numbers of plants recovered from our crossing attempts decreases with increased phylogenetic distance. In other words for the plants from the crosses of e.g., HORT × ARID we obtained one plant only using the same effort as was invested in the other crosses. This one plant may represent the rare, fortunate gene combination that allows the individual to survive under ideal conditions, while all other combinations are lethal. Given that phylogenetically close crosses (HORT × FRUT, HORT × ZONA, HORT × ACET) require the one, two, or three gene model with the assumption of lethality to explain the phenotypic ratios for both the seedling and seed phase we evaluated, we may just be viewing the tip of the iceberg for the phylogenetically more distant crosses. Generally, genes thought to be involved in chloroplast management and expression are Whirly genes (Maréchal et al., 2009; Isemer et al., 2012; Krupinska et al., 2014, 2019), involved in importing proteins into chloroplasts (Krausea et al., 2005; Chateigner-Boutin et al., 2008; Mackenzie and Kundariya, 2019), and PPR genes, acting at the level of RNA editing (Takenaka et al., 2013; Wang et al., 2016a,b; Rojas et al., 2019; Small et al., 2020). These genes are good candidates to study in *Pelargonium* and a closer study of the proteins they encode for as well as the type of RNA editing taking place, may explain both biparental inheritance as well as early stage processes of speciation.

Data Quality

Our approach to phenotyping contains a number of potential sources of error possibly obscuring more nuanced phenotypic differences. We evaluated the seedlings at two points in time to correct for differences in development phase and possible environmental effects on the stability of the phenotypes. Differences in ambient temperature at each point can, potentially severely, affect the expression of chlorosis (pers. observations all authors). Furthermore, the interpretation of the photos, while allowing for reviewing the phenotyping afterward is subject to interpretation. Defining a plant as "affected" or not is sometimes context dependent. In the initial germination phase seedlings were germinated under controlled conditions and all at the same time to insure that we were comparing plants in equal phases of development. Great care was taken to make sure the photos of each set were taken at the same day to reduce chance of observing changed phenotypes when environmental conditions change. A further reduction of errors in interpretation can, in the future, be achieved by germinating seeds under even more controlled conditions and using automated imaging software, for interpretation of chlorotic phenotypes (see for an example of this approach Flood et al., 2020).

Seed phenotypes in *Pelargonium* related to CNI have not been studied before. We have chosen very clear-cut categories and in doing so may have underestimated the actual level of CNI. Nevertheless, our phenotypes are reminiscent of what is regularly encountered in relation to mutated organelle expressing PPR genes in *Arabidopsis thaliana* (Chi et al., 2008; Du et al., 2017; Zhang et al., 2017). Finally, in some cases we found a discrepancy in plastid types detected, between parents and the offspring of the variegated plants. Probably, variegated plants are able to manage and express both plastids and subsequently one type is outcompeted but not completely removed. This competition was demonstrated in *Oenothera* and occurs at a cellular level (Sobanski et al., 2019).

Crossings

In our study we have obtained at least one individual F_1 hybrid plants for the majority of interspecific crosses attempted (except for *P. ranunculophyllum*). Most were obtainable from seed showing high compatibility of the genomes and plastids. We attribute the two unsuccessful crosses to suboptimal greenhouse climate conditions as we observed that for a pollination to be successful abiotic factors such as climate and humidity are important (reviewed by Lohani et al., 2020). The chance to obtain a (viable) F_1 plant further roughly correlates with previously published plastome based phylogenetic distances (**Figure 1**).

Our approach in this study is reminiscent of the study recently published by Flood et al. (2020) who used cybrids to study the effects of different plastids types in equal nuclear genomic backgrounds. We have used F_1 generation crosses which, though different from the cybrids in the sense that the nuclear genome is hybrid, is still uniform and allows us to study the effects of different types of organelles. Our approach is different that this study focuses more on an evolutionary, rather than at the population level as was the case in Flood et al. (2020).

CONCLUSION AND FUTURE APPLICATIONS

The insight from this study further open up possibilities for breeding of currently available *Pelargonium* cultivars with their crop wild relatives. Now we could conceivably start breeding in plastids that, for instance, perform better in warmer/colder/dryer climates allowing for the adjustment of cultivars to different climates (Deng et al., 2004; Cortés and Blair, 2018; Westerbergh et al., 2018) and other abiotic factors (Mezghani et al., 2019; Wang et al., 2019; Ribera et al., 2020; Singh et al., 2020). Especially, photosynthesis would be an interesting trait to focus on as differences between the species are, likely, more dramatic than those observed between the different populations of *A. thaliana* which has been the focus so far when studying the effects of plastid types and photosynthetic efficiency (Flood et al., 2011; Cruz et al., 2016; Flood et al., 2020). The fact that different types of plastids have a different effect in a similar nuclear background means that breeding efforts that wish to incorporate crop wild relatives to increase genetic diversity or introduce new traits should consider the organellar background of the material as well. Knowing the effects can aid in making more informed decisions as to which species to attempt a cross with and which not. This then can lead to more focused and mores successful breeding attempts.

DATA AVAILABILITY STATEMENT

The original contributions presented in the study are included in the article/**Supplementary Material**, further inquiries can be directed to the corresponding author.

AUTHOR CONTRIBUTIONS

FCB, FTB, RCS, and MES conceived the study. FCB carried out the analysis. FCB and FTB wrote the manuscript. FCB, SP, and JWK did the laboratory work PCR. MS-S did laboratory work embryo rescue. All authors read the draft and gave feedback.

FUNDING

This research was funded by the Dutch Foundations for applied scientific research (TTW). Grant number: 14531 "*Pelargonium* genomics for overcoming cytonuclear incompatibility and bridging species barriers" of the Green Genetics program.

ACKNOWLEDGMENTS

We thank Frank Becker for his assistance with testing primers, Toni Lockers for her work on the countless pollinations, Dennis Reus Harald Gorter for the greenhouse management and Ewa Schoutsen and Anja Kolk for performing embryo rescue. Finally we thank the two reviewers who's comments improved this manuscript.

SUPPLEMENTARY MATERIAL

The Supplementary Material for this article can be found online at: https://www.frontiersin.org/articles/10.3389/fpls.2020.614871/full#supplementary-material

Supplementary Figure 1 | Diagnostic PCR targeted on HORT × ZONA and HORT × ACET.

Supplementary Figure 2 | Gel images other HORT × *Ciconium* F_1 crosses displaying plastid types as identified using PCR.

Supplementary Figure 3 | PCR mastermix and thermo profile.

Supplementary Figure 4 | Overview of representative hybrid plants of F1 plants obtained in this study.

Supplementary Figure 5 | Full overview of all scenarios and gene models tested.

Supplementary Figure 6 | (A–K) Representative phenotypes for all F1 plants created in the course of this study.

REFERENCES

Amoatey, H. M., and Tilney-Basset, R. A. E. (1994). A test of the complementary gene model for the control of biparental plastid inheritance in zonal Pelargoniums. *Heredity* 72, 69–77. doi: 10.1038/hdy.1994.8

Apitz, J., Weihe, A., Pohlheim, F., and Börner, T. (2013). Biparental inheritance of organelles in *Pelargonium*: evidence for intergenomic recombination of mitochondrial DNA. *Planta* 237, 509–515. doi: 10.1007/s00425-012-1768-x

Bakker, F. T., Hellbrügge, D., Culjam, A., and Gibby, M. (1998). Phylogenetic relationships within *Pelargonium* sect. Peristera (Geraniaceae) inferred from nrDNA and cpDNA sequence comparisons. *Syst. Evol.* 211, 273–287. doi: 10.1007/bf00985364

Barkan, A., and Small, I. (2014). Pentatricopeptide repeat proteins in plants. *Annu. Rev. Plant Biol.* 65, 415–442.

Barnard-Kubow, K. B., McCoy, M. A., and Galloway, L. F. (2017). Biparental chloroplast inheritance leads to rescue from cytonuclear incompatibility. *New Phytol.* 213, 1466–1476. doi: 10.1111/nph.14222

Barnard-Kubow, K. B., So, N., and Galloway, L. F. (2016). Cytonuclear incompatibility contributes to the early stages of speciation. *Evolution* 70, 2752–2766. doi: 10.1111/evo.13075

Barr, C. M., and Fishman, L. (2010). The nuclear component of a cytonuclear hybrid incompatibility in Mimulus maps to a cluster of pentatricopeptide repeat genes. *Genetics* 184, 455–465. doi: 10.1534/genetics.109.108175

Baur, E. (1909). Das Wesen und die Earblichkeitsverhältnisse der 'arietates albomarginatae hort' von *Pelargonium zonale*. *Z. Indukt. Abstammungs-Vererbungsl* 1, 330–351. doi: 10.1007/bf01990603

Blazier, J. C., Jansen, R. K., Mower, J. P., Govindu, M., Zhang, J., Weng, M.-L., et al. (2016a). Variable presence of the inverted repeat and plastome stability in *Erodium*. *Ann. Bot.* 117, 1209–1220. doi: 10.1093/aob/mcw065

Blazier, J. C., Ruhlman, T. A., Wenig, M.-L., Rehman, S. K., Sabir, J. S. M., and Jansen, R. K. (2016b). Divergence of RNA polymerase a subunits in angiosperm plastid genomes is mediated by genomic rearrangement. *Sci. Rep.* 6:24595. doi: 10.1038/srep24595

Börner, T., Aleynikova, A. Y., Zubo, Y. O., and Kusnetsov, V. V. (2015). Chloroplast RNA polymerases: role in chloroplast biogenesis. *Biochim. Biophys. Acta* 1847, 761–769. doi: 10.1016/j.bbabio.2015.02.004

Chateigner-Boutin, A. L., Ramos-Vega, M., Guevara-Garcia, A., Andres, C., de la Luz Gutiérrez-Nava, M., Cantero, A., et al. (2008). CLB19, a pentatricopeptide repeat protein required for editing of rpoA and clpP chloroplast transcripts. *Plant J.* 56, 590–602. doi: 10.1111/j.1365-313X.2008.03634.x

Chi, W., Ma, J., Zhang, D., Guo, J., Chen, F., Lu, C., et al. (2008). The Pentratricopeptide Repeat Protein DELAYED GREENING1 Is involved in the regulation of early chloroplast development and chloroplast gene expression in *Arabidopsis*. *Plant Physiol.* 147, 573–584. doi: 10.1104/pp.108.116194

Chumley, T. W., Palmer, J. D., Mower, J. P., Fourcade, M. H., Calie, P. J., Boore, J. L., et al. (2006). The complete chloroplast genome sequence of *Pelargonium* x *hortorum*: organization and evolution of the largest and most highly rearranged chloroplast genome of land plants. *Mol. Biol. Evol.* 23, 2175–2190. doi: 10.1093/molbev/msl089

Cortés, A. J., and Blair, M. W. (2018). Genotyping by sequencing and genome–environment associations in wild common bean predict widespread divergent adaptation to drought. *Front. Plant Sci.* 9:128. doi: 10.3389/fpls.2018.00128

Cruz, J. A., Savage, L. J., Zegarac, R., Hall, C. C., Satoh-Cruz, M., Davis, G. A., et al. (2016). Dynamic environmental photosynthetic imaging reveals emergent phenotypes. *Cell Syst.* 2, 365–377. doi: 10.1016/j.cels.2016.06.001

De Laat, A., Godhe, W., and Vogelzang, M. (1987). Determination of ploidy of single plants and populations by flow cytometry. *Plant Breed.* 99, 303–307. doi: 10.1111/j.1439-0523.1987.tb01186.x

Deng, J., Hondo, K., Kakihara, F., and Masahira, K. (2004). Seasonal variation of flowering characteristics and high-temperature stress tolerance in Geraniums. *J. High Technol. Agric.* 16, 173–182. doi: 10.2525/jshita.16.173

Du, L., Zhang, J., Qu, S., Zhao, Y., Su, B., Lv, X., et al. (2017). The pentatricopeptide repeat protein pigment-defective mutant2 is Involved in the regulation of chloroplast development and chloroplast gene expression in *Arabidopsis*. *Plant Cell Physiol.* 58, 747–759. doi: 10.1093/pcp/pcx004

Flood, P. J., Harbinson, J., and Aarts, M. G. M. (2011). Natural genetic variation in plant photosynthesis. *Trends Plant Sci.* 16, 327–335. doi: 10.1016/j.tplants.2011.02.005

Flood, P. J., Theeuwen, T. P. J. M., Schneeberger, K., Keizer, P., Kruijer, W., Severing, E., et al. (2020). Reciprocal cybrids reveal how organellar genomes affect plant phenotypes. *Nat. Plants* 6, 13–21. doi: 10.1038/s41477-019-0575-9

Gibby, M., Albers, F., and Prinsloo, B. (1990). Karyological studies in *Pelargonium* sects. Ciconium, Dibrachya, and *Jenkinsonia* (Geraniaceae). *Plant Syst. Evol.* 170, 151–159. doi: 10.1007/BF00937700

Gibby, M., and Westfold, J. (1986). A cytological study of *Pelargonium* sect. *Eumorpha*. *Syst. Evol.* 153, 205–222. doi: 10.1007/BF00983688

Greiner, S., Rauwolf, U., Meurer, J., and Hermann, R. G. (2011). The role of plastids in plant speciation. *Mol. Ecol.* 20, 671–691. doi: 10.1111/j.1365-294X.2010.04984.x

Greiner, S., and Bock, R. (2013). Tuning a ménage à trois: co-evolution and co-adaptation of nuclear and organellar genomes in plants. *Bioessays* 35, 354–365. doi: 10.1002/bies.201200137

Greiner, S., Sobanski, J., and Bock, R. (2015). Why are most organelle genomes transmitted maternally? *Bioessays* 37, 80–94. doi: 10.1002/bies.201400110

Guisinger, M. M., Kuehl, J. V., Boore, J. L., and Jansen, R. K. (2008). Genome-wide analyses of Geraniaceae plastid DNA reveal unprecedented patterns of increased nucleotide substitutions. *Proc. Natl. Acad. Sci. U. S. A.* 105, 18424–18429. doi: 10.1073/pnas.0806759105

Guisinger, M. M., Kuehl, J. V., Boore, J. L., and Jansen, R. K. (2011). Extreme reconfiguration of plastid genomes in the angiosperm family Geraniaceae: rearrangements, repeats, and codon usage. *Mol. Biol. Evol.* 28, 583–600. doi: 10.1093/molbev/msq229

Hondo, K., Iwasaki, C., and Kakihara, F. (2014). Characteristics of progeny obtained from the cross between Geraniums (*Pelargonium* x *hortorum*) and wild species in section *Ciconium*, Including heat tolerance and odor of leaves. *Environ. Control Biol.* 52, 37–43. doi: 10.2525/ecb.52.37

Hondo, K., Sukhumpinij, P., and Kakihara, F. (2015). Flower color and pigments in yellow-flowered hybrid progeny raised from the interspecific cross *Pelargonium quinquelobatum* × white-flowered geraniums. *Sci. Hortic.* 195, 145–153. doi: 10.1016/j.scienta.2015.09.014

Horn, W. (1994). Interspecific crossability and inheritance in *Pelargonium*. *Plant Breed.* 113, 3–17. doi: 10.1111/j.1439-0523.1994.tb00696.x

Isemer, R., Mulisch, M., Schäfer, A., Kirchner, S., Koop, H.-U., and Krupinska, K. (2012). Recombinant Whirly1 translocates from transplastomic chloroplasts to the nucleus. *FEBS Lett.* 586, 85–88. doi: 10.1016/j.febslet.2011.11.029

James, C. M., Gibby, M., and Barrett, J. A. (2004). Molecular studies in *Pelargonium* (Geraniaceae). A taxonomic appraisal of section Ciconium and the origin of the "Zonal" and "Ivy-leaved" cultivars. *Plant Syst. Evol.* 243, 131–146. doi: 10.1007/s00606-003-0074-2

Kamlah, R., Pinker, I., Plaschil, S., and Olbricht, K. (2019). Hybridization between *Pelargonium acetosum* L'Hér. and *Pelargonium*× *peltatum*. *J. Appl. Bot. Food Qual.* 92, 49–56. doi: 10.5073/JABFQ.2019.092.007

Kibbe, (2007). OligoCalc: an online oligonucleotide properties calculator. *Nucleic Acids Res.* 35, W43–W46. doi: 10.1093/nar/gkm234

Krausea, K., Kilbienski, I., Mulisch, M., Rödiger, A., Schäfer, A., and Krupinska, K. (2005). DNA-binding proteins of the Whirly family in *Arabidopsis thaliana* are targeted to the organelles. *FEBS Lett.* 579, 3707–3712. doi: 10.1016/j.febslet.2005.05.059

Krupinska, K., Braun, S., Nia, M. S., Schäfer, A., Hensel, G., and Bilger, W. (2019). The nucleoid-associated protein WHIRLY1 is required for the coordinate assembly of plastid and nucleus-encoded proteins during chloroplast development. *Planta* 249, 1337–1347. doi: 10.1007/s00425-018-03085-z

Krupinska, K., Oetke, S., Desel, C., Mulisch, M., Schäfer, A., Hollmann, J., et al. (2014). WHIRLY1 is a major organizer of chloroplast nucleoids. *Front. Plant Sci.* 5:432. doi: 10.3389/fpls.2014.00432

Li, D., Qi, X., Li, X., Li, L., Zhong, C., and Huang, H. (2013). Maternal inheritance of mitochondrial genomes and complex inheritance of chloroplast genomes in *Actinidia* Lind.: evidences from interspecific crosses. *Mol. Genet. Genomics.* 288, 101–110. doi: 10.1007/s00438-012-0732-6

Lohani, N., Singh, M. B., and Bhalla, P. L. (2020). High temperature susceptibility of sexual reproduction in crop plants. *J. Exp. Bot.* 71, 555–568. doi: 10.1093/jxb/erz426

Mackenzie, S. A., and Kundariya, H. (2019). Organellar protein multi-functionality and phenotypic plasticity in plants. *Phil. Trans. R. Soc. B* 375:20190182. doi: 10.1098/rstb.2019.0182

Maréchal, A., Parent, J.-S., Véronneau-Lafortune, F., Joyeux, A., Lang, B. F., and Brisson, B. (2009). Whirly proteins maintain plastid genome stability in *Arabidopsis*. *PNAS* 106, 14693–14698. doi: 10.1073/pnas.0901710106

Mezghani, N., Khoury, C.-K., Carver, D., Achicanoy, H. A., Simon, P., Flores, F. M., et al. (2019). Distributions and conservation status of carrot wild relatives in Tunisia: a case study in the western Mediterranean basin. *Crop Sci.* 59, 2317–2328. doi: 10.2135/cropsci2019.05.0333

Montoliu, L. (2012). Mendel: a simple excel workbook to compare the observed and expected distributions of genotypes/phenotypes in transgenic and knockout mouse crosses involving up to three unlinked loci by means of a $\chi 2$ test. *Transgenic Res.* 21, 677–681. doi: 10.1007/s11248-011-9544-4

Postel, Z., and Touzet, P. (2020). Cytonuclear genetic incompatibilities in plant speciation. *Plants* 9:487. doi: 10.3390/plants9040487

Ribera, A., Bai, Y., Wolters, A.-M. A., van Treuren, R., and Kik, C. (2020). A review on the genetic resources, domestication and breeding history of spinach (*Spinacia oleracea* L.). *Euphytica* 216:48. doi: 10.1007/s10681-020-02585-y

Rojas, M., Yu, Q., Williams-Carrier, R., Maliga, P., and Barkan, A. (2019). Engineered PPR proteins as inducible switches to activate the expression of chloroplast transgenes. *Nat. Plants* 5, 505–511. doi: 10.1038/s41477-019-0412-1

Röschenbleck, J., Albers, F., Müller, K., Weinl, S., and Kudla, J. (2014). Phylogenetics, character evolution and a subgeneric revision of the genus *Pelargonium* (Geraniaceae). *Phytotaxa* 159, 31–76. doi: 10.11646/phytotaxa.159.2.1

Ruhlman, T. A., and Jansen, R. K. (2018). "Aberration or analogy? The atypical plastomes of Geraniaceae," in *Advances in Botanical Research 85: Plastid Genome Evolution*, eds S.-M. Chaw and R. K. Jansen (Amsterdam, NL: Elsevier), 223–262. doi: 10.1016/bs.abr.2017.11.017

Ruhlman, T. A., Zhang, Z., Blazier, J. C., Sabir, J. M. S., Jansen, R. K., et al. (2017). Recombination-dependent replication and gene conversion homogenize repeat sequences and diversify plastid genome structure. *Am. J. Bot.* 104, 559–572. doi: 10.3732/ajb.1600453

Shikanai, T., Shimizu, K., Ueda, K., Nishimura, Y., Kuroiwa, T., and Hashimoto, T. (2001). The chloroplast clpP gene, encoding a proteolytic subunit of ATP-dependent protease, is indispensable for chloroplast development in Tobacco. *Plant Cell Physiol.* 42, 264–273. doi: 10.1093/pcp/pce031

Singh, M., Kumar, S., Basandrai, A. K., Basandrai, D., Malhotra, N., Saxena, D. R., et al. (2020). Evaluation and identification of wild lentil accessions for enhancing genetic gains of cultivated varieties. *PLoS One* 15:e0229554. doi: 10.1371/journal.pone.0229554

Small, I. D., Schallenberg-Rüdinger, M., Takenaka, M., Mireau, H., and Ostersetzer-Biran, O. (2020). Plant organellar RNA editing: what 30 years of research has revealed. *Plant J.* 101, 1040–1056. doi: 10.1111/tpj.14578

Sobanski, J., Giavalisco, P., Fischer, A., Kreiner, J. M., Walther, D., Schöttler, M. A., et al. (2019). Chloroplast competition is controlled by lipid biosynthesis in evening primroses. *PNAS* 116, 5665–5674. doi: 10.1073/pnas.1811661116

Stubbe, W. (1958). Dreifarbenpanschierung bei *Oenothera*: II. Wechselwirkungen zwischen Geweben mit zweierblich verschiedenen Plastidensorten. *Z. für Vererbungslehre* 89, 189–203. doi: 10.1007/bf00890107

Stubbe, W. (1959). Genetische analyse des zusammenwirkens von genom und plastom bei *Oenothera*. *Z. für Vererbungslehre* 90, 288–298. doi: 10.1007/bf00888761

Stubbe, W. (1989). *Oenothera*—An ideal system for studying the interaction of genome and plastome. *Plant Mol. Biol. Rep.* 7, 245–257. doi: 10.1007/BF02668633

Swofford, D. L. (2002). PAUP*: Phylogenetic analysis using parsimony (*and other methods), version 4. doi: 10.1007/bf02668633

Tilney-Bassett, R. A. E. (1973). The control of plastid inheritance in *Pelargonium* II. *Heredity* 30, 1–13. doi: 10.1038/hdy.1973.1

Tilney-Bassett, R. A. E. (1974). The control of plastid inheritance in *Pelargonium* III. *Heredity* 33, 353–360. doi: 10.1038/hdy.1974.102

Tilney-Bassett, R. A. E. (1975). "Genetics of variegated plants," in *Genetics and biogenesis of mitochondria and chloroplasts*. eds C. W.Birky P. S Perlman, and T. J Byers (Columbus: Ohio State University Press), 268–308.

Tilney-Bassett, R. A. E. (1976). The control of plastid inheritance in *Pelargonium* IV. *Heredity* 37, 95–107. doi: 10.1038/hdy.1976.68

Tilney-Bassett, R. A. E. (1984). "The genetic evidence for nuclear control of chloroplast biogenesis in higher plants," in *Chloroplast biogenesis. Society for Experimental Biology Seminar Series 21*, ed. R. J. Ellis (Cambridge: Cambridge University Press), 13–50.

Tilney-Bassett, R. A. E. (1988). "Inheritance of plastids in *Pelargonium*," in *The Division and Segregation of Organelles. Society for Experimental Biology Seminar Series 35*, eds S. A. Boffey and D. Lloyd (Cambridge: Cambridge University Press), 115–129.

Tilney-Bassett, R. A. E., and Abdel-Wahab, O. A. L. (1982). Irregular segregation at the Pr locus controlling plastid inheritance in *Pelargonium*: gametophytic lethal or incompatibility system? *Theor. Appl. Genet.* 62, 185–191. doi: 10.1007/BF00293357

Tilney-Bassett, R. A. E., and Almouslem, A. B. (1989a). Variation in plastid inheritance between *Pelargonium* cultivars and their hybrids. *Heredity* 63, 145–153. doi: 10.1038/hdy.1989.86

Tilney-Bassett, R. A. E., Almouslem, A. B., and Amoate, H. M. (1992). Complementary genes control biparental plastid inheritance in *Pelargonium*. *Theor. Appl. Genet.* 85, 317–324. doi: 10.1007/BF00222876

Tilney-Bassett, R. A. E., Almouslem, A. B., and Amoatey, H. M. (1989b). "The complementary gene model for biparental plastid inheritance," in *Physiology, Biochemistry, and Genetics of Non Green Plastids*, eds C. D. Boyer, J. C. Shannon, and R. C. Hardison (Rockville, MD: The American Society of Plant Physiologists), 265–266.

Tilney-Bassett, R. A. E., and Birky, C. W. Jr. (1981). The mechanism of the mixed inheritance of chloroplast genes in *Pelargonium*: evidence from gene frequency distributions among the progeny of crosses. *Theor. Appl. Genet.* 60, 43–53. doi: 10.1007/BF00275177

van de Kerke, S. J., Shrestha, B., Ruhlman, T. A., Weng, M.-L., Jansen, R. K., Jones, C. S., et al. (2019). Plastome based phylogenetics and younger crown node age in *Pelargonium*. *Mol. Phylogenet. Evol.* 137, 33–43. doi: 10.1016/j.ympev.2019.03.021

van der Walt, J. J. A., and Vorster, P. J. (1988). *Pelargoniums* of Southern Africa. Volumes I-III. Annals of Kirstenbosch botanic gardens. Pretoria: National Botanic Gardens of South Africa.

Wang, D., Liu, H., Zhai, G., Wang, L., Shao, J., and Tao, Y. (2016b). *OspTAC2* encodes a pentatricopeptide repeat protein and regulates rice chloroplast development. *J.Genet. Genomics* 43, 601–608. doi: 10.1016/j.jgg.2016.09.002

Wang, J., Li, Y., Li, C., Yan, C., Zhao, X., Yuan, C., et al. (2019). Twelve complete chloroplast genomes of wild peanuts: great genetic resources and a better understanding of *Arachis* phylogeny. *BMC Plant Biol.* 19:504. doi: 10.1186/s12870-019-2121-3

Wang, W., Wu, Y., and Messing, J. (2016a). Genome-wide analysis of pentatricopeptide-repeat proteins of an aquatic plant. *Planta* 244, 893–899. doi: 10.1007/s00425-016-2555-x

Weihe, A., Apitz, J., Salinas, A., Pohlheim, F., and Börner, T. (2009). Biparental inheritance of plastidial and mitochondrial DNA and hybrid variegation in *Pelargonium*. *Mol. Genet. Genomics* 282, 587–593. doi: 10.1007/s00438-009-0488-9

Weng, M.-L., Ruhlman, T. A., and Jansen, R. K. (2017). Expansion of inverted repeat does not decrease substitution rates in *Pelargonium* plastid genomes. *New Phytol.* 214, 842–851. doi: 10.1111/nph.14375

Westerbergh, A., Lerceteau-Köhler, E., Sameri, M., Bedada, G., and Lundquist, P.-O. (2018). Towards the development of perennial barley for cold temperate climates—evaluation of wild barley relatives as genetic resources. *Sustainability* 10:1969. doi: 10.3390/su10061969

Zhang, J., Xiao, J., Li, Y., Su, B., Xu, H., Shan, X., et al. (2017). PDM3, a pentatricopeptide repeat-containing protein, affects chloroplast development. *J. Exp. Bot.* 68, 5615–5627. doi: 10.1093/jxb/erx360

Zhang, Y., and Lu, C. (2019). The enigmatic roles of PPR-SMR proteins in plants. *Adv. Sci.* 6:1900361. doi: 10.1002/advs.201900361

Conflict of Interest: RCS and MS-S were employed by the Syngenta Seeds BV, Netherlands.

The remaining authors declare that the research was conducted in the absence of any commercial or financial relationships that could be construed as a potential conflict of interest.

frontiers in Plant Science

OPINION
published: 21 December 2020
doi: 10.3389/fpls.2020.573490

Use of Light Stimuli as a Postharvest Technology for Cut Flowers

*Takanori Horibe**

College of Bioscience and Biotechnology, Chubu University, Kasugai, Japan

Keywords: circadian rhythm, flower opening, flower quality, petal growth, photoperiod

INTRODUCTION

Cut flowers are a unique aspect of the flora industry, and they are globally recognized as one of the most commercially produced ornamentals. Thus, it is necessary to increase their quality for consumers' satisfaction over a long period. The quality of a cut flower depends on its external characteristics such as color, length, volume, freshness, and fragrance as well as its perishability, which is determined by the duration of these external characteristics. Recent researches have shown that external light emission significantly affects several aspects of cut flower traits, such as; the vase life, petal color, and volatile compounds emission. Clarifying the relationship between these flower traits and light stimuli, which can increase the understanding of the mechanisms of these traits, can help to improve the quality of cut flower through light environmental control. This study proposes that the external light stimuli is an effective tool for improving the quality of cut flowers, and also highlights the several issues related to this proposal.

POSTHARVEST TECHNOLOGY FOR CUT FLOWERS

The vase life is a critical factor in determining the market value of cut flowers. However, since it takes some days to sell cut flowers from farmers via retailers to general consumers, the quality of the cut flowers could depreciate during this process. For this reason, most cut flowers lose their ornamental value within 1 week after being purchased by consumers, to the dissatisfaction of the customers. The quality of cut flower and its vase life are affected by several factors. These include the aging, detachment, and withering of tissues by ethylene generation, deficiency in saccharides that act as osmoregulators and respiratory substrates, obstruction of vessels due to bacterial propagation, and generation of air embolism in stem (poor water absorption) (Burdett, 1970; Durkin, 1979; De Stigter, 1980; Reid et al., 1989; van Doorn, 1997; Macnish et al., 2010).

Continuous efforts have been made to improve the quality of cut flowers and prolong their vase life, which has led to the development of numerous agents to preserve flower quality (van Doorn and Woltering, 2008). Ethylene inhibitors, such as silver thiosulfate complex (STS) and 1-methylcyclopropene (1-MCP) are widely used as quality retention agent because ethylene is a major factor in the aging of many cut flowers (Veen, 1979; Mor et al., 1983; Ichimura et al., 2002). Quality preservatives include ethylene production/action inhibitors, sugars, antibacterial agents, plant growth regulators, surfactants, and inorganic salts (van Doorn and Woltering, 2008; Ichimura, 2018). Commercially available preservatives consist of a mixture of these various agents, but the detailed composition of the ingredients is usually concealed. However, some quality preservatives, such as STS causes environmental damage, and many countries prohibit using them in order to sustain environmental protection (Tacuri et al., 2016). The negative effect of STS in the environment is mainly due to the residual effects of the inherent metal it deposits into the soil and groundwater for long period and its potential migration to drinking water systems (Tacuri et al., 2016).

OPEN ACCESS

Edited by:
Antonio Ferrante, University of Milan, Italy

Reviewed by:
Paulo Eduardo Ribeiro Marchiori, Universidade Federal de Lavras, Brazil
Morteza Soleimani Aghdam, Imam Khomeini International University, Iran
Julita Rabiza-Świder, Warsaw University of Life Sciences, Poland
Sasan Aliniaeifard, University of Tehran, Iran

***Correspondence:**
Takanori Horibe
t-horibe@isc.chubu.ac.jp

Specialty section:
This article was submitted to Crop and Product Physiology, a section of the journal Frontiers in Plant Science

Received: *17 June 2020*
Accepted: *02 December 2020*
Published: *21 December 2020*

Citation:
Horibe T (2020) Use of Light Stimuli as a Postharvest Technology for Cut Flowers. Front. Plant Sci. 11:573490. doi: 10.3389/fpls.2020.573490

It has also been found that high temperatures during transport or storage significantly reduce the vase life and quality of cut flowers, and make ethylene-sensitive species more susceptible to ethylene (Halevy and Mayak, 1973; Rudnicki et al., 1991; Leonard et al., 2011). For example, a previous study showed that exposing flowers to 20°C for 8 h early in the marketing chain accelerated the opening of the *Aster* spp., *Chrysanthemum* spp., *Dianthus* spp., and *Gypsophila* spp. compared to continuous exposure of 8°C (van Gorsel and Ravesloot, 1994). The effect of the higher temperature became more apparent later in the marketing chain. However, the mean interruption temperatures showed that 1 day delay in the marketing chain resulted in 1 day (*Aster* spp. and *Gypsophila* spp.) to 3 days (*Dianthus* spp. and *Chrysanthemum* spp.) decrease in vase life (van Gorsel and Ravesloot, 1994). Thus, there has been a considerable emphasis and discussion within the floral industry regarding the need of cold-chain, which is a type of supply chain that is temperature-controlled from the point of production, to the transportation stages, storage, distribution processes and finally delivery to the end-user (van der Hulst, 2004; Reid and Jiang, 2005; Leonard et al., 2011). Although automatic machines have been invented to improve the efficiency of the fresh flower logistics, a large part of the logistics process is handled manually because various types of fresh flowers are difficult to control by only machines (Babalola and Sundarakani, 2011). Thus, there is often a lack of cold-chain during logistics, leading to the exposition of flowers to high and fluctuating temperatures. Furthermore, establishing perfect cold-chain needs a lot of initial investment and running costs (e.g., fuel and energy).

Thus, it is desirable to introduce a new technology that is inexpensive, of low environmental load, and can improve the quality of cut flowers.

USE OF LIGHT FOR IMPROVING CUT FLOWER QUALITY

Light acts as an environmental signal and also drives photosynthesis in plants. Plants respond to the intensity, wavelength, duration, and direction of light (Zheng and Labeke, 2018), and the use of various light sources such as light-emitting diodes (LED) has been experimented in agricultural science. For example, long-day treatment (night interruption) using incandescent and fluorescent lamps during the short day, which effectively accelerate the flowering of long-day plants and allowed earlier marketing or seed production, has been applied to numerous long-day plants in Japan, including *Ammi majus* L. (Tsuchiya, 1991), *Bupleurum griffithii* L. (Hara and Katsutani, 1993), *Campanula* spp. (Moe et al., 1991).

Recent researches have shown that the light environment also affects diverse aspects of cut flower qualities. For example, on the effects of light environment on flower opening in cut rose (*Rosa hybrida* L.) revealed that red light suppressed flower opening and wilting, resulting in longer vase life compared with other treatments; blue light, white fluorescent light, and constant darkness condition (Horibe et al., 2020). On the other hand, the red light was shown to promote flower opening, but its effect was reversed by subsequent exposure to far-red light in *Ipomoea nil* L. (Kaihara and Takimoto, 1980, 1981). It has also been observed that high light intensity extends vase life in *Anthurium andraeanum* H, *Chrysanthemum* spp., *Delphinium* spp. and *Dianthus caryophyllus* L. (Pun and Ichimura, 2003; Evelyn et al., 2020). Flower color is also an important factor affecting cut flower quality, and light spectra such as ultraviolet (UV) and blue light is involved in anthocyanin biosynthesis of flowers. For example, UV and blue light irradiation increase anthocyanin biosynthesis in petals of cherry blossom (*Prunus* × *yedoensis* "Somei-yoshino"), *Gerbera hybrida* H., *Malus domestica* L. and *Rosa hybrida* L. (Maekawa et al., 1980; Dong et al., 1998; Meng et al., 2004; An et al., 2020). Furthermore, light stimuli are closely related to floral scent emission. Studies have shown that several scent components are under the control of the circadian clock, and plants can quickly entrain their scent emission to the new light/dark cycles after shifting the photoperiod (Hendel-Rahmanim et al., 2007; Fenske and Imaizumi, 2016). Blue light has also been shown to suppress the development of blue mold (*Penicillium italicum*) in *Citrus unshiu* M. and gray mold (*Botrytis cinerea*) in *Solanum lycopersicum* L., and at least, these effects could be partially related with the enhanced proline accumulation and antioxidative processes (Kim et al., 2013; Yamaga et al., 2015). Since gray mold caused by *Botrytis cinerea* is one of the most important diseases of several ornamental flowers including *Chrysanthemum* spp., *Begonia* spp., *Dahlia* spp., *Geranium* spp., *Gerbera* spp., *Tulipa* spp., *Rosa hybrida* L., and *Viola* spp. (Marrois et al., 1988; Terry and Joyce, 2004; Araújo et al., 2015), blue light irradiation may become an effective way to suppress pathogenic development in cut flowers. Furthermore, several studies have revealed that flowers are the site of photoperception and synchronize their growth to photoperiods (Saito and Yamaki, 1967; Kaihara and Takimoto, 1980, 1981). In *Calendula arvensis* L., the opening and closing rhythm of flowers followed the light/dark cycle to which flowers had been exposed when the leaves were subjected to a different cycle from the flowers (van Doorn and van Meeteren, 2003). Horibe and Yamada (2014) reported that even a petal removed from a rose flower showed rhythmic growth when exposed to a 12 h light/12 h dark photoperiod, indicating that petals could perceive light and synchronize their growth to the photoperiod. These results have shown that light affects various important traits of cut flower quality including vase life, petal color, fragrance, and perishability. Therefore, we think light environment control can be a remarkable quality preservation technique, despite that its commercial use is still inadequate compared to existing technologies such as the use of preservatives and cold-chain.

Then, what kind of mechanisms underlie the responses of cut flowers to light stimuli? Cut flower reactions toward light stimuli including rhythmic growth, volatile compound emission, pigment synthesis, and disease resistance should be regulated through the interaction between plant photoreceptors sensitive to a particular wavelength and their downstream signaling pathways. In cut carnation (*Dianthus caryophyllus* L.), blue light delayed the petal senescence through down-regulation of ethylene biosynthetic genes and up-regulation of antioxidant enzymes (Aalifar et al., 2020a,b). It is well-recognized that adverse

water relation caused by water loss from stomata and cuticular can lead to problems in flower opening, such as premature petal wilting and bending of pedicel, resulting in short vase life (van Meeteren and Aliniaeifard, 2016; Aliniaeifard and van Meeteren, 2018). In these experiments, blue light also promoted stomata opening and water uptake (Aalifar et al., 2020a,b). Elevated water uptake and higher transpiration rates are reported to be beneficial for cut flowers placed in water (Elibox and Umaharan, 2010; Lu et al., 2010). Aalifar et al. (2020a,b) reported that blue light might increase water transport efficiency by increasing transpiration rate and water uptake. However, petal growth and vase life of cut roses changed when exposed to different light environments even without leaves (Horibe et al., 2020), indicating that responses of cut flowers to light stimuli cannot be explained only by the function of leaves. In addition, blue light resulted in shorter vase life in cut anthurium (*Anthurium andraeanum*) under cold storage and the negative effect of blue light was attributed to its effect on increased water loss and oxidative stress (Aliniaeifard et al., 2020). There are still many unsolved questions between light stimuli and flower responses. What is the source of discrepancy in the reports on the effects of light on cut flower postharvest quality? Why different cut flowers respond differently to the light quality or intensity? Can light environment control prevent postharvest disease outbreak and infections? However, most of the details are still unknown. Further research is needed to explain the above phenomenon, and these would be an interesting topic from a viewpoint of plant physiology.

Challenges for the use of light environment control as postharvest technology are its initial and running costs. However, with the use of LED, which has low power consumption, low heat generation, and adjustable wavelength, the costs would be minimized compared with other light sources (Hong et al., 2011). Initial and running costs would not be high when compared to the establishment of cold-chains, since light environmental control can be possible with only lighting devices. Besides, it is relatively easy to use and does not require much labor. Furthermore, it can be used in combination with the conventional quality retention technology such as use of quality preservatives and temperature control (cold-chain). Therefore, we believe that the light environment control including wavelength and photoperiod can be a promising tool for improving the quality of cut flowers during transportation and storage.

FINAL REMARKS

As indicated above, light environment control could be a powerful tool for improving postharvest quality of ornamental cut flowers. Recently, there is an urgent need for sustainability and food security that should lead to advancement in horticulture market such as increased production of fruit and flowers. In this context, efforts have been made to reduce the use of inorganic pesticides and natural substance to prevent the harmful effects of chemical compounds that threaten both the environment and human health. Compared to the existing technology, such as the application of quality retention agents to vase water, light environment control has little negative effect on environment and is well-suited with an environmentally-friendly market. Further research is needed to determine the reaction of cut flowers toward light among species and cultivars, and investigate how light stimuli affect several features of cut flowers. To apply light environment control into the floral industry for the improvement of several cut flower qualities, more practical attention should be given to this strategy.

AUTHOR CONTRIBUTIONS

TH wrote the article.

REFERENCES

Aalifar, M., Aliniaeifard, S., Arab, M., Mehrjerdi, M. Z., and Serek, M. (2020b). Blue light postpones senescence of carnation flowers through regulation of ethylene and abscisic acid pathway-related genes. *Plant Physiol. Biochem.* 151, 103–112. doi: 10.1016/j.plaphy.2020.03.018

Aalifar, M., Aliniaeifard, S., Arab, M., Zare, M. M., Dianati, D. S., Serek, M., et al. (2020a). Blue light improves vase life of carnation cut flowers through its effect on the antioxidant defense system. *Front. Plant Sci.* 26:511. doi: 10.3389/fpls.2020.00511

Aliniaeifard, S., Falahi, Z., Dianati, D. S., Li, T., and Woltering, E. (2020). Postharvest spectral light composition affects chilling injury in anthurium cut flowers. *Front. Plant Sci.* 12:846. doi: 10.3389/fpls.2020.00846

Aliniaeifard, S., and van Meeteren, U. (2018). Greenhouse vapour pressure deficit and lighting conditions during growth can influence postharvest quality through the functioning of stomata. *Acta Horticulturae* 1227, 677–684. doi: 10.17660/ActaHortic.2018.1227.86

An, S., Arakawa, O., Tanaka, N., Zhang, S., and Kobayashi, M. (2020). Effects of blue and red light irradiations on flower colouration in cherry blossom (*Prunus* × *yedoensis* 'Somei-yoshino'). *Sci. Horticult.* 263:109093. doi: 10.1016/j.scienta.2019.109093

Araújo, A. E., Maffia, L. A., Guy de Capdeville, G., and Mizubuti, E. S. G. (2015). Infection of rose flowers by *Botrytis cinerea* under different temperatures and petal wetness. *Afr. J. Agric. Res.* 10, 845–849. doi: 10.5897/AJAR2014.8653

Babalola, A. O., and Sundarakani, B. (2011). Cold chain logistics in the floral industry. *Int. J. Enterprise Netw. Manage.* 4, 400–413. doi: 10.1504/IJENM.2011.043801

Burdett, A. N. (1970). The cause of bent neck in cut roses. *J. Amer. Soc. Hort. Sci.* 95, 427–431.

De Stigter, H. C. M. (1980). Water balance of cut and intact Sonia rose plants. *Z. Pflanzenphysiol.* 99:131140. doi: 10.1016/S0044-328X(80)80122-X

Dong, Y. H., Lesley, B., Kevin, D., Deepali, M., Bret, M., and Arend, K. (1998). Expression of pigmentation genes and photo-regulation of anthocyanin biosynthesis in developing Royal Gala apple flowers. *Aust. J. Plant Physiol.* 25, 245–252. doi: 10.1071/PP97108

Durkin, D. J. (1979). Effect of Millipore filtration, citric acid, and sucrose on peduncle water potential of cut rose flower. *J. Amer. Soc. Hort. Sci.* 104, 860–863.

Elibox, W., and Umaharan, P. (2010). Cultivar differences in the deterioration of vase-life in cut-flowers of *Anthurium andraeanum* is determined by mechanisms that regulate water uptake. *Sci. Hortic.* 124, 102–108. doi: 10.1016/j.scienta.2009.12.005

Evelyn, S., Farrella, A. D., Eliboxa, W., Abreua, K. D., and Umaharana, P. (2020). The impact of light on vase life in (*Anthurium andraeanum* Hort.) cut flower. *PBT* 159:110984. doi: 10.1016/j.postharvbio.2019.110984

Fenske, M. P., and Imaizumi, T. (2016). Circadian rhythms in floral scent emission. *Front. Plant Sci*. 13:462. doi: 10.3389/fpls.2016.00462

Halevy, A. H., and Mayak, S. (1973). Transport and conditioning of cut flowers. *Acta Hort*. 43, 291–306. doi: 10.17660/ActaHortic.1974.43.32

Hara, H., and Katsutani, N. (1993). Effect of daylength on growth and flowering of *Bupleurum griffithii*. *J. Jpn. Soc. Hort. Sci.* 62:703.

Hendel-Rahmanim, K., Masci, T., Vainstein, A., and Weiss, D. (2007). Diurnal regulation of scent emission in rose flowers. *Planta* 226, 1491–1499. doi: 10.1007/s00425-007-0582-3

Hong, P. H., Kwon, O. H., Lee, D. I., Park, J. R., Ha, J. M., Jeong, D. U., et al. (2011). Effects of LED light and temperature on lettuce growth. *Agribusiness Information Manage.* 3, 67–74. Available online at: www.koreascience.or.kr/article/JAKO201107559763151

Horibe, T., Horie, K., Kawai, M., Kurachi, Y., Watanabe, Y., and Makita, M. (2020). Effect of light environment on flower opening and water balance in cut rose. *Environ. Control in Biol*. 58, 15–20. doi: 10.2525/ecb.58.15

Horibe, T., and Yamada, K. (2014). Petals of cut rose flower show diurnal rhythmic growth. *J. Jpn. Soc. Hort. Sci*. 83, 302–307. doi: 10.2503/jjshs1.CH-101

Ichimura, K. (2018). Postharvest physiology and technology for cut flowers: recent progress and future aspects. *Hort. Res.* 17, 279–292. doi: 10.2503/hrj.17.279

Ichimura, K., Shimizu, H., and Hiraya, T. (2002). Effect of 1-methylcyclo- propene (1-MCP) on the vase life of cut carnation, Delphinium and sweet pea flowers. *Bull. Natl. Inst. Flor. Sci*. 2, 1–8. Available online at: www.naro.affrc.go.jp/publicity_report/publication/archive/files/naro-se/NIFS02-01

Kaihara, S., and Takimoto, A. (1980). Studies on the light controlling the time of flower-opening in *Pharbitis nil*. *Plant Cell Physiol*. 21, 21–26.

Kaihara, S., and Takimoto, A. (1981). Effects of light and temperature on flower-opening in *Pharbitis nil*. *Plant Cell Physiol*. 22, 215–221.

Kim, K., Kook, H., Jang, Y., Lee, W., Kamala-Kannan, S., Chae, J., et al. (2013). The effect of blue-light-emitting diodes on antioxidant properties and resistance to *Botrytis cinerea* in tomato. *J. Plant Pathol. Microb*. 4:203. doi: 10.4172/2157-7471.1000203

Leonard, R. T., Alexander, A. M., and Nell, T. A. (2011). Postharvest performance of selected Colombian cut flowers after three transport systems to the United States. *HortTechnology* 21, 435–442. doi: 10.21273/HORTTECH.21.4.435

Lu, P., Cao, J., He, S., Liu, J., Li, H., Cheng, G., et al. (2010). Nano-silver pulse treatments improve water relations of cut rose cv. Movie Star flowers. *Postharvest Biol. Technol*. 57, 196–202. doi: 10.1016/j.postharvbio.2010.04.003

Macnish, A. J., Leonard, R. T., Borda, A. M., and Nell, T. A. (2010). Genetic variation in the postharvest performance and ethylene sensitivity of cut rose flowers. *Hort. Sci*. 45, 790–796. doi: 10.21273/HORTSCI.45.5.790

Maekawa, S., Terabun, M., and Nakamura, N. (1980). Studies on flower coloration in flowering trees and shrubs during forcing period. II: Effects of light intensity and light quality on pigmentation of flowering quince and cherry flowers. *Sci. Rep. Faculty Agric*. 14, 51–55.

Marrois, J. J., Redmond, J. C., and McDonald, J. D. (1988). Quantification of the impact of environment on the susceptibility of *Rosa hybrida* flowers to *Botrytis cinerea*. *J. Amer. Soc. Hort. Sci*. 113, 842–845.

Meng, X. C., Xing, T., and Wang, X. J. (2004). The role of light in the regulation of anthocyanin accumulation in *Gerbera hybrida*. *Plant Growth Reg*. 44, 243–250. doi: 10.1007/s10725-004-4454-6

Moe, R., Heins, R. D., and Erwin, J. (1991). Stem elongation and flowering of the long-day plant *Campanula isophylla* Moretti in response to day and night temperature alternations and light quality. *Sci. Hort*. 48, 141–151. doi: 10.1016/0304-4238(91)90161-Q

Mor, Y., Spiegelstein, H., and Halevy, A. H. (1983). Inhibition of ethylene biosynthesis in carnation petals by cytokinin. *Plant Physiol*. 71, 541–546. doi: 10.1104/pp.71.3.541

Pun, U. K., and Ichimura, K. (2003). Review- role of sugars in senescence and biosynthesis of ethylene in cut flowers. *JARQ* 37, 219–224. doi: 10.6090/jarq.37.219

Reid, M. S., Evans, R. Y., Dodge, L. L., and Mor, Y. (1989). Ethylene and silver thiosulfate influence opening of cut rose flowers. *J. Amer. Soc. Hort. Sci*. 114, 436–440.

Reid, M. S., and Jiang, C. Z. (2005). New strategies in transportation for floricultural crops. *Acta Hort*. 682, 1667–1673. doi: 10.17660/ActaHortic.2005.682.222

Rudnicki, R. M., Nowak, J., and Goszczynska, D. M. (1991). Cold storage and transportation conditions for cut flowers cuttings and potted plants. *Acta Hort*. 298, 225–236. doi: 10.17660/ActaHortic.1991.298.27

Saito, M., and Yamaki, T. (1967). Retardation of flower opening in *Oenothera lamarckina* caused by blue and green light. *Nature* 214:1027. doi: 10.1038/2141027a0

Tacuri, M., Flores, D., Anrango, M. J., Koch, A., Naranjo, B., and Cumbal, L. (2016). Novel technique for degradation of silver thiosulfate present in wastewater of the post- harvest treatment of ethylene-sensitive flowers. *Biol. Med*. 8:3. doi: 10.4172/0974-8369.1000278

Terry, L. A., and Joyce, D. C. (2004). Elicitors of induced disease resistance in postharvest horticultural crops. A brief review. *PBT* 32, 1–13. doi: 10.1016/j.postharvbio.2003.09.016

Tsuchiya, S. (1991). Effects of daylength on the growth and flowering of *Ammi majus* L. *J. Japan. Soc. Hort. Sci*. 60:644.

van der Hulst, J. (2004). Cool chain management for cut flowers. *FlowerTECH* 7, 49–51.

van Doorn, W. G. (1997). Water relations of cut flowers. *Hort. Rev*. 18, 1–85. doi: 10.1002/9780470650608.ch1

van Doorn, W. G., and van Meeteren, U. (2003). Flower opening and closure: a review. *J. Exp. Bot*. 54, 1801–1812. doi: 10.1093/jxb/erg213

van Doorn, W. G., and Woltering, E. J. (2008). Physiology and molecular biology of petal senescence. *J. Exp. Bot*. 59, 453–480. doi: 10.1093/jxb/erm356

van Gorsel, R., and Ravesloot, M. (1994). Short interruptions of the cold chain reduce the vase life of Aster ericoides, chrysanthemum, dianthus, and gypsophila cut flowers. *HortScience* 29:554. doi: 10.21273/HORTSCI.29.5.554f

van Meeteren, U., and Aliniaeifard, S. (2016). "Stomata and postharvest physiology," in *Postharvest Ripening. Physiology of Crops*, ed S. Pareek (Boca Raton, FL: CRC Press), 157–216.

Veen, H. (1979). Effects of silver on ethylene synthesis and action in cut carnations. *Planta* 145, 467–470. doi: 10.1007/BF00380101

Yamaga, I., Takahashi, T., Ishii, K., Kato, M., and Kobayashi, Y. (2015). Suppression of blue mold symptom development in satsuma mandarin fruits treated by low-intensity blue LED irradiation. *Food Sci. Technol. Res*, 21, 347–351. doi: 10.3136/fstr.21.347

Zheng, L., and Labeke, M. (2018). Effects of different irradiation levels of light quality on chrysanthemum. *Sci. Hortic*. 233, 124–131. doi: 10.1016/j.scienta.2018.01.033

Conflict of Interest: The author declares that the research was conducted in the absence of any commercial or financial relationships that could be construed as a potential conflict of interest.

frontiers in Plant Science

ORIGINAL RESEARCH
published: 07 January 2021
doi: 10.3389/fpls.2020.540821

The Effect of Post-harvest Conditions in *Narcissus* sp. Cut Flowers Scent Profile

*Marta I. Terry[1], Victoria Ruiz-Hernández[2], Diego J. Águila[3], Julia Weiss[1] and Marcos Egea-Cortines[1]**

[1] Genética Molecular, Instituto de Biotecnología Vegetal, Universidad Politécnica de Cartagena, Cartagena, Spain, [2] Department of Biosciences, University of Salzburg, Salzburg, Austria, [3] Las Cabezuelas Sociedad Cooperativa, Alhama de Murcia, Spain

OPEN ACCESS

Edited by:
Julian C. Verdonk, Wageningen University & Research, Netherlands

Reviewed by:
Jonas Kuppler, University of Ulm, Germany
Adinpunya Mitra, Indian Institute of Technology Kharagpur, India

***Correspondence:**
Marcos Egea-Cortines
marcos.egea@upct.es

Specialty section:
This article was submitted to Crop and Product Physiology, a section of the journal Frontiers in Plant Science

Received: *06 March 2020*
Accepted: *08 December 2020*
Published: *07 January 2021*

Citation:
Terry MI, Ruiz-Hernández V, Águila DJ, Weiss J and Egea-Cortines M (2021) The Effect of Post-harvest Conditions in Narcissus sp. Cut Flowers Scent Profile. Front. Plant Sci. 11:540821. doi: 10.3389/fpls.2020.540821

Narcissus flowers are used as cut flowers and to obtain high quality essential oils for the perfume industry. As a winter crop in the Mediterranean area, it flowers at temperatures ranging between 10 and 15°C during the day and 3–10°C during the night. Here we tested the impact of different light and temperature conditions on scent quality during post-harvest. These two types of thermoperiod and photoperiod. We also used constant darkness and constant temperatures. We found that under conditions of 12:12 Light Dark and 15-5°C, *Narcissus* emitted monoterpenes and phenylpropanoids. Increasing the temperature to 20°-10°C in a 12:12 LD cycle caused the loss of cinnamyl acetate and emission of indole. Under constant dark, there was a loss of scent complexity. Constant temperatures of 20°C caused a decrease of scent complexity that was more dramatic at 5°C, when the total number of compounds emitted decreased from thirteen to six. Distance analysis confirmed that 20°C constant temperature causes the most divergent scent profile. We found a set of four volatiles, benzyl acetate, eucalyptol, linalool, and ocimene that display a robust production under differing environmental conditions, while others were consistently dependent on light or thermoperiod. Scent emission changed significantly during the day and between different light and temperature treatments. Under a light:dark cycle and 15-5°C the maximum was detected during the light phase but this peak shifted toward night under 20-10°C. Moreover, under constant darkness the peak occurred at midnight and under constant temperature, at the end of night. Using Machine Learning we found that indole was the volatile with a highest ranking of discrimination followed by D-limonene. Our results indicate that light and temperature regimes play a critical role in scent quality. The richest scent profile is obtained by keeping flowers at 15°-5°C thermoperiod and a 12:12 Light Dark photoperiod.

Keywords: circadian rhythm, constitutive volatiles, floral scent, gcProfileMakeR, machine learning, non-constitutive volatile, Random Forest

INTRODUCTION

Plants are able to produce and emit a high variety of volatile organic compounds (VOCs). Plant volatiles play several and complex roles in stress response and chemical communication, including pest repellence, herbivore deterrence, pollinator attraction, and plant-plant interaction (Jürgens et al., 2000; Matsui, 2006; Niinemets et al., 2013; van Dam and Bouwmeester, 2016). Principal volatile compound classes include fatty acid derivatives, terpenoids, and benzenoids/phenylpropanoids, synthesized in four major pathways: methylerythritol phosphate, mevalonic acid, lipoxygenase, and shikimate/phenylalanine (Dudareva et al., 2013; Muhlemann et al., 2014; Nagegowda, 2018).

Interestingly, plants emits a mix of compounds and their respective amount determines a particular aroma blend (Füssel et al., 2007; Weiss et al., 2016). Moreover, scent profiles differ between plant organs and tissues, such as leaves and petals, but also among species, genotypes and even life span (Jürgens et al., 2002; Dötterl et al., 2005; Majetic et al., 2014). In addition, the synthesis and emission of volatile compounds rely on biotic and abiotic factors (Peñuelas and Llusià, 2001; Loreto and Schnitzler, 2010). Temperature affects floral scent emission in a variety of species such as Petunia, *Osmanthus* or *Lilium* (Sagae et al., 2008; Hu et al., 2013; Fu et al., 2017). This indicates that both growing conditions and managing temperatures during post-harvest may affect the actual scent profile. Light intensity and light quality or spectral distribution also play a role in coordinating scent emission (Hu et al., 2013; Chuang et al., 2017). The number of released terpenoids, alcohols or aromatic compounds increases with light intensity in corn plants and *Lilium* "Siberia" (Gouinguené and Turlings, 2002; Hu et al., 2013). Compared with white light, red, and far red lighting cause increased release of phenylpropanoids/benzenoids compounds in petunia flowers (Colquhoun et al., 2013).

Sensorial quality of fruits and cut flowers such as aroma and flavor, is important to consumers. Both aroma and flavor depend on genotype, crop management, culture practices, maturity but also post-harvest management. Several methods can modify and improve the scent quality and the content in sugars and phenolic compounds. Post-harvest handling include controlled atmospheres (Lopez et al., 2000), UV-B irradiation (Hagen et al., 2007) and storage temperature, which has been widely studied in fruits and vegetables. Tomato and pineapple fruit for example, show a higher accumulation of aromatic compounds as esters and ketones under elevated temperatures (Maul et al., 2000; Liu and Liu, 2014). Moreover, a high temperature is not optimal for long distance shipping or long storage, which typically require low temperatures and is carried out in darkness. Low temperature prevents fruit ripening and pathogen proliferation but it may result in chilling injuries and loss of flavor and aroma quality (Imahori et al., 2008; Weiss and Egea-Cortines, 2009; Tietel et al., 2012).

Cut flowers are also shipped and stored in modified atmospheres and/or low temperatures. As described in fruits and vegetables, low temperature tolerance vary among species (Redman et al., 2002). Low temperature has undesired effects as chilling injury symptoms including loss of coloration and flower malformation (Joyce et al., 2000; Bunya-atichart et al., 2004). In addition to this, inadequate post-harvest handling may alter enzymatic activity and secondary metabolism, affecting aroma volatile composition.

Floral volatiles and their distilled oils from *Narcissus* sp. are important in the perfume and chemical industry (Remy, 2004). The flowering of narcissi like other geophytes is activated by cold and flowers in winter in Mediterranean environments (Rees and Wallis, 1970; Rees and Hanks, 1984; González et al., 1998). A correct post-harvest technical knowledge is key to preserve the quality of cut flowers. Pre-harvest management also has an impact in essential oil yield and composition (Perry et al., 1999; Angioni et al., 2006). In the last years, several researchers have analyzed the relationship between environment and volatiles quality and quantity. Terpenes, an abundant group of VOCs, show a positive correlation between emitted amount and temperature and light (Staudt and Lhoutellier, 2011; Chen et al., 2020). Another important aspect is scent composition, which changes in response to high temperature and drought stress (Haberstroh et al., 2018). In relation to environmental factors, several studies address climate change and its possible impact on plant volatiles (Yuan et al., 2009). The effect of climate warming seemed to differ in terms of emitted amount, but has a noticeable effect on scent composition (Faubert et al., 2012; Schollert et al., 2015). Changes in aroma blend may alter several biological functions as pollinator attraction, plant defense or plant-plant communication (Farré-Armengol et al., 2013). Therefore, environmental conditions, both in pre-harvest and post-harvest conditions, play a critical role on the synthesis and emission of volatiles.

While metabolomic studies of fruits often include complete metabolite profiles, the number of studies describing the environmental effects on complete metabolomes of flowers has been performed in very few species (Verdonk et al., 2003; Cheng et al., 2016). The aim of the present work was to define the effect of environmental conditions during post-harvest on the quantity and composition of *Narcissus* sp. (Amaryllidaceae) scent. Our results indicate a significant effect of light regimes, and specially temperature, on scent quantity and profiles.

MATERIALS AND METHODS

Plant Material and Experimental Design

Narcissus (Amaryllidaceae) is a group of perennial bulbiferous widely distributed in the Mediterranean basin. The number of species is still unclear. The presence of several hybrids makes it difficult to identify narcissi species as well as define their distribution (Santos-Gally et al., 2012; Marques et al., 2017). In Spain, at least 25 species have been described as well as different hybrids (Aedo and Herrero, 2005). We used a local *Narcissus* cultivar variety called "double flower" owned by Cooperativa las Cabezuelas (**Figure 1A**). The variety was originally isolated by Matías Águila Noguera in 1960, founder of Las Cabezuelas, and has been reproduced by bulbs ever since (DÁ, unpublished observation). Plants grew as intercrop

FIGURE 1 | Flowers of *Narcissus* sp. "Double flower" used in the study. **(A)** Close up of double flower. **(B)** Plants at harvesting point. **(C)** Overview of Narcissus growing as intercrop between organic grape vines.

between organic grapevines in Las Cabezuelas (**Figures 1B,C**), located in Alhama de Murcia (Spain) as described before (Ruíz-Ramón et al., 2014). Narcissi were harvested at flower opening, coinciding with anthesis, and cut flowers were brought to the lab maintained with the stalks in water until volatile sampling. As narcissi flowers have a short lifespan, we performed the volatile sampling in the first 24–36 h after harvesting. Harvesting was the moment of cutting in the field roughly at 0830. Floral stalks were kept on water glasses and brought to the lab at 1800. Sampling was performed during the winter of 2015 and 2016. We selected flowers without any visual damage. Each flower was weighted before sampling and placed into a growth chamber. Flowers were kept in the chamber in the initial conditions 1 h before the first twister was introduced. We collected volatiles under six different conditions: four assays were conducted under light:dark conditions and two under constant darkness (see below). Constant darkness simulated storage and/or shipping conditions. In Alhama de Murcia in winter (December-February), average temperature is 11.1 ± 5.2°C, with minimum of 4 and maximum of 15.7°C. We decided to study the aroma emission under a range of temperature similar to field conditions (15-5°C) and simulate a hypothetical warm winter day (20-10°C). Furthermore, we also analyzed the effect of constant temperature, typical of post-harvest conditions on scent emission and aroma profile. Then, experimental conditions were defined as follow, comparing three pairs of treatments: First, we analyzed the scent emission under a 12 h light and 12 h dark cycle (12LD) and two different temperature regimens: 20-10°C and 15-5°C. The highest temperature coincided with the light period whereas the lowest temperature, corresponded to the dark phase. We defined the 12LD and 15-5°C group as control conditions. The second experiment consisted in continuous darkness (12DD) and two thermoperiods, 20-10°C and 15-5°C. Finally, in the last experiment flowers were sampled under a 12LD cycle with constant temperature of 20°C and 5°C, respectively. For light:dark experiments, we defined *zeitgeber* time 0 (ZT0) as the time when lights turned on. For constant darkness experiments, we defined ZT0 as the time when high temperature cycle started.

Analysis of Volatile Compounds

We used five narcissi cut flowers for each experiment. We introduced one cut flower during 24 h into a beaker containing a 4% sucrose solution, which was located into a 2l desiccator. Each desiccator consisted in a glass container, which we cleaned before and after sampling with 100% ethanol. Volatiles were collected by SBSE magnetic stir bar sorptive extraction, GERSTEL, coated with polydimethylsiloxane (PDMS) Twister, as they absorb volatile non-polar compounds optimally (Bicchi et al., 2005). Twisters were previously conditioned, by incubating at 40°C and ramping to 300°C at 25°C/min and maintaining at 300°C for 20 min. In each container, we introduced a paper clip in order to attach a stir bar. We used empty desiccators (without cut flowers) as negative controls.

We analyzed volatile emission at different time points during the light and dark period or subjective day and night. Two time points corresponded to the subjective day and two to the subjective night, ZT0, ZT4, ZT16, and ZT22 for constant darkness and constant temperature groups, and ZT4, ZT16, ZT22, and ZT24 for light;dark and cycling temperature. Twisters were left inside the desiccators for a period of 2 h.

Volatiles were separated and identified as described by Manchado-Rojo et al. (2012). Briefly, we used a 6890 gas chromatograph coupled to a 5975 inert XL mass selective detector (Agilent Technologies) with a thermal desorption unit, a cooled injector system and a multi-purpose sampler (MPS2, GERSTEL). We used a HP-5MS capillary column (30 m length, 0.25 mm internal diameter and 0.25 m film) in constant pressure, using helium as carrier gas. The temperature was increased from 50 to 70°C (5°C per min) held 1 min and then increased to 240°C (10°C per min) and held 15 min. Twister bars were desorbed using an initial temperature of 40°C ramping to 150°C (100 C per min) and a holding time of 5 min. The transfer temperature was 300°C. The desorbed compounds were cryo-focused in the cooled injector system inlet at -100 C. Finally, volatiles were transferred into the column by heating the CIS4 inlet at a rate of 10°C sec^{-1} to 150°C with a holding time of 3 min.

In those cases when we did not have commercial standards to identify properly VOCs, we tentatively identified compounds using Willey10th-NIST11b (Agilent Technologies, Wilmington, United States). The integrated peak area of every identified volatile was normalized by dividing it by the flower fresh weight (Ruiz-Hernández et al., 2018).

Data Analysis

We considered that compounds that appeared in more than 70% of the replicates, with an average quality match with

mass-spectra library over 80%, could be considered as part of the constitutive scent emission of narcissi flowers under each treatment. We obtained the scent profiles by using the R library "gcProfileMakeR" version 2.2.2 (Pérez-Sanz et al., 2020). We set the parameters pFreqCutoff (minimum frequency cutoff, percentage of samples that emit a volatile) to 0.70 and qcutoff (compound quality, expressed as percentage) to 80. We also applied an initial filter to remove compounds by their CAS number, as siloxanes that may derive from stir bars (Montero et al., 2005; **Supplementary Table 1**). In order to visualize the data, we classified the selected compounds based on their contribution to the scent profile, in two groups. Major volatiles contributed to the scent profile above 2% and remained compounds comprised the minor volatile group (see section "Results").

The study of biogenic volatiles can generate large amounts of data. Tools such as the R library gcProfileMakeR determines the core profile and non-constitutive profile of a set of samples (Pérez-Sanz et al., 2020). These profiles can be analyzed with Machine Learning methods. They are useful to identify volatile signatures, which allow recognizing different organisms (Ranganathan and Borges, 2010). Algorithms such as Random Forest (Breiman, 2001) can identify the compounds that can be used for classifying between different sets of samples.

We used the Random Forest algorithm to identify those volatiles that can be used for classifying the different treatments of photoperiod and thermoperiod (Breiman, 2001). This analysis was performed by the R package "randomForest" (Liaw and Wiener, 2002). We merged all sampling time points per replicate, photoperiod and thermoperiod conditions.

To analyze the effects of experimental conditions and sampling time points on scent quantities, we performed a Kruskall–Wallis test followed by a Dunn test as *post hoc* analysis, implemented in stats and dunn.test packages (R version 3.6.1) (Dinno, 2017).

We used a principal component analysis (PCA) to explore differences across experimental treatments. The complete set of volatiles for each replica point was used as input. The analysis was performed in R using the prcomp function of the stats package, and plotted with ggfortify (Tang et al., 2016).

RESULTS

Scent Profiles Are Affected by Photoperiod and Thermoperiod

Narcissi cut flowers showed a complex profile. The number of identified compounds by GC-MS varied among conditions and daytime. We identified in total 73 compounds with a quality higher than 80% (**Supplementary Figure 1** and **Table 1**). For every experimental group, we filtered the list of volatiles using the R library "gcProfileMakeR" (Pérez-Sanz et al., 2020). We selected the volatiles emitted by more than 70% of the samples with a minimum quality of 80% for every experimental condition labeling them as constitutive volatiles. We obtained a list of 68 volatiles present in the six different experimental conditions. They were divided in constitutive where we found 14 VOCs and non-constitutive comprising 64 VOCs (**Figure 2** and **Supplementary Figure 1**). The minimum quality was 87% for myrcene. These compounds comprised mainly monoterpenes and phenylpropanoids (**Table 1**). The rest of volatiles found were non-constitutive and were found in less than 70% of the samples for a given environmental condition (**Supplementary Figure 1**). We defined the group of cut flowers sampled under 12h light: 12h dark (12LD) and 15-5°C as the control group. These are the typical day/night temperatures found in the field during December/January when they flower (Viti et al., 2010).

We found 13 different compounds under 12LD and 15-5°C thermoperiod (**Figure 2**). When we mimicked the situation of a warm winter, with 12LD and 20-10°C, we found indole, not present in the control conditions, while cinnamyl acetate became a non-constitutive component of the profile (**Figure 2** and **Supplementary Figure 1**). Plants under constant darkness (12DD) with thermocycle emitted 10 VOCs at 20-10°C and 8 volatiles at 15-5°C. In contrast, flowers under a 12LD and constant temperature showed a lower complexity. We only detected 8 and 6 volatiles at 20 and 5°C, respectively. We found the highest complexity, defined as number of detected VOCs, under cycling light and thermoperiodic conditions.

As the number of detected compounds varied among experimental conditions, we defined four groups. The first group comprised four robustly emitted compounds that were detected regardless of light or temperature conditions. These were the monoterpenes eucalyptol, linalool and ocimene, and the benzenoid benzyl acetate. Thus, these compounds can be considered the common chemical scent profile of this *Narcissus* variety. A second group contained 3,4-dimethyl-2,4,6 octatriene, pinene, and benzenepropanol, that were only detected under cycling conditions of light and temperature. The monoterpenes myrcene and limonene were not detected under a constant temperature of 5°C or 20°C (**Figure 2**). The remaining compounds, indole, phenethyl acetate, and prenyl acetate, were variable. Although many compounds appeared under several conditions, their amount or contribution varied (**Figure 2**, see below). We can conclude that the scent profile in Narcissus comprises a set of volatiles robustly produced under different environmental conditions, a second set that requires light cycling conditions, a third set that depends on thermoperiod, and a last one with variable behavior.

We explored the differences in qualitative changes through the sampling periods to identify possible clusters. We used PCA at different time points and comparing three pairs of treatments (**Figure 3**). The two first principal components, PC1 and PC2, explained the 68.57% of the variation (ZT0), 60.51% (ZT4), 57.98% (ZT16), 74.29% (ZT22), and 84.05% (ZT24) (**Figure 3** and **Supplementary Table 2**). Groups sampled under 12LD/15-5°C, 12DD/15-5°C, and 12LD/5°C showed a similar pattern and clustered together. In contrast, the aroma blend of narcissi sampled under 12LD and constant 20°C differed from other narcissi groups. We also observed variations across time and conditions. At ZT0, 12DD/15-5°C and 12LD/5°C patterns were similar and clustered together whereas 12DD/20-10°C and 12LD/20°C differed. At ZT4, narcissi under 12LD/15-5°C and 12LD/20-10°C, constant darkness and constant temperature

TABLE 1 | Selected volatile organic compounds from Narcissus cut flowers.

CAS	RT	Quality	Volatile	Class
000120-72-9	11.982	96.9	Indole	Amine
000140-11-4	9.42	97.3	Benzyl acetate	Benzenoid
007785-26-4	5.011	95.8	α-Pinene	Monoterpene
000123-35-3	6.311	95.1	β-Myrcene	
005989-27-5	7.134	97.3	D-Limonene	
000470-82-6	6.858	98.3	Eucalyptol	
003779-61-1	7.577	98.0	Ocimene	
000078-70-6	8.592	96.0	Linalool	
057396-75-5	9.158	96.2	3,4-Dimethyl-2,4,6-octatriene	
000103-45-7	11.22	89.5	β-Phenethyl acetate	Phenylpropanoid
000122-97-4	10.973	95.9	Benzenepropanol	
000122-72-5	13.134	90.1	Benzenepropyl acetate	
000103-54-8	14.196	96.7	Cinnamyl acetate	
001191-16-8	4.744	93.7	Prenyl acetate	Terpene

We detected these compounds in at least the 70% of the samples, in one or more experimental groups, with a minimum quality of 80%. CAS chemical abstracts service registry number, RT retention time expressed in minutes, Quality average match quality expressed as a percentage.

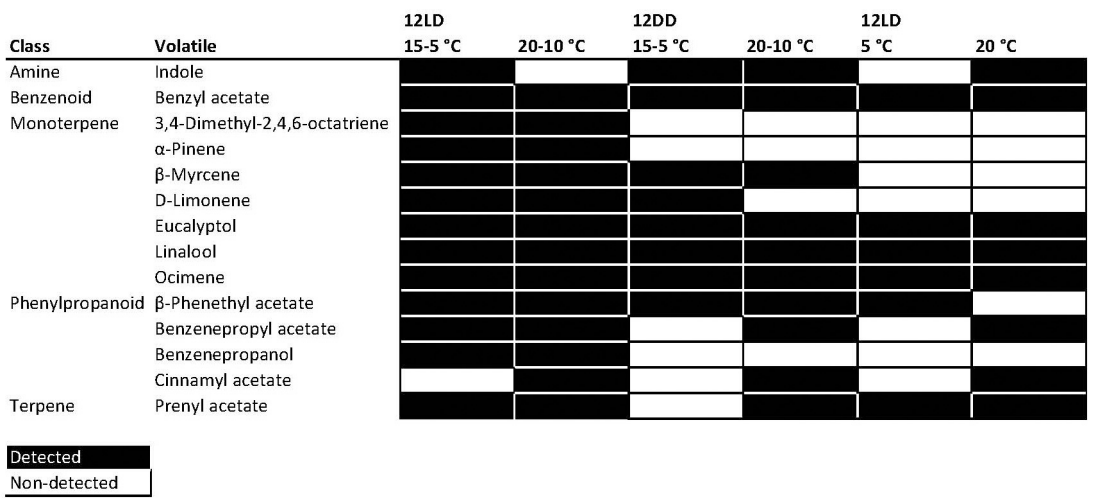

FIGURE 2 | Heat map of volatiles emitted by Narcissus across experimental conditions. First column shows the chemical abstract service (CAS) number of the volatiles. 12LD indicates a 12-h light:dark cycle and 12DD constant darkness. Black indicates a detected compound and white an undetected compound.

showed a similar distribution. The 5°C constant temperature treatment caused an extremely compact cluster. It was centered with most profiles, as it comprises the four constitutive volatiles found under all conditions. As mentioned previously, at ZT16 and ZT22, all experimental conditions showed a similar pattern except those narcissi that were sampled under 12LD and 20°C. Finally, at ZT0 12LD/15-5°C and 12LD/20-10°C aroma patterns were different (**Figure 3**).

We found that the importance of each volatile (expressed as loading factors) to the narcissi aroma changed along the day (**Supplementary Table 2**).

The first principal component revealed that the most important volatiles were ocimene at ZT0, ZT4, benzyl acetate at ZT16 and ZT22, and pinene at ZT24. The volatiles limonene at ZT0 and ZT4, ocimene at ZT16 and ZT24 and phenethyl acetate at ZT22 contributed positively to the PC2 (**Supplementary Table 2**). Two of these volatiles, benzyl acetate and ocimene, were constitutively emitted. In contrast, pinene was absent in narcissi sampled under constant darkness and constant temperature, phenethyl acetate was not detected at constant 5°C and pinene emission was variable and detected under 12LD/15-5°C, 12LD/20-10°C, and 12DD/20-10°C (**Figure 2**). All these results suggested that temperature, light and daytime determined the aroma blend of narcissi cut flowers as well as its emission pattern.

Effect of Thermoperiod and Photoperiod on Quantitative Changes in Scent Profiles

The contribution of every volatile to the floral aroma determines a specific aroma blend. A previous study characterized the floral

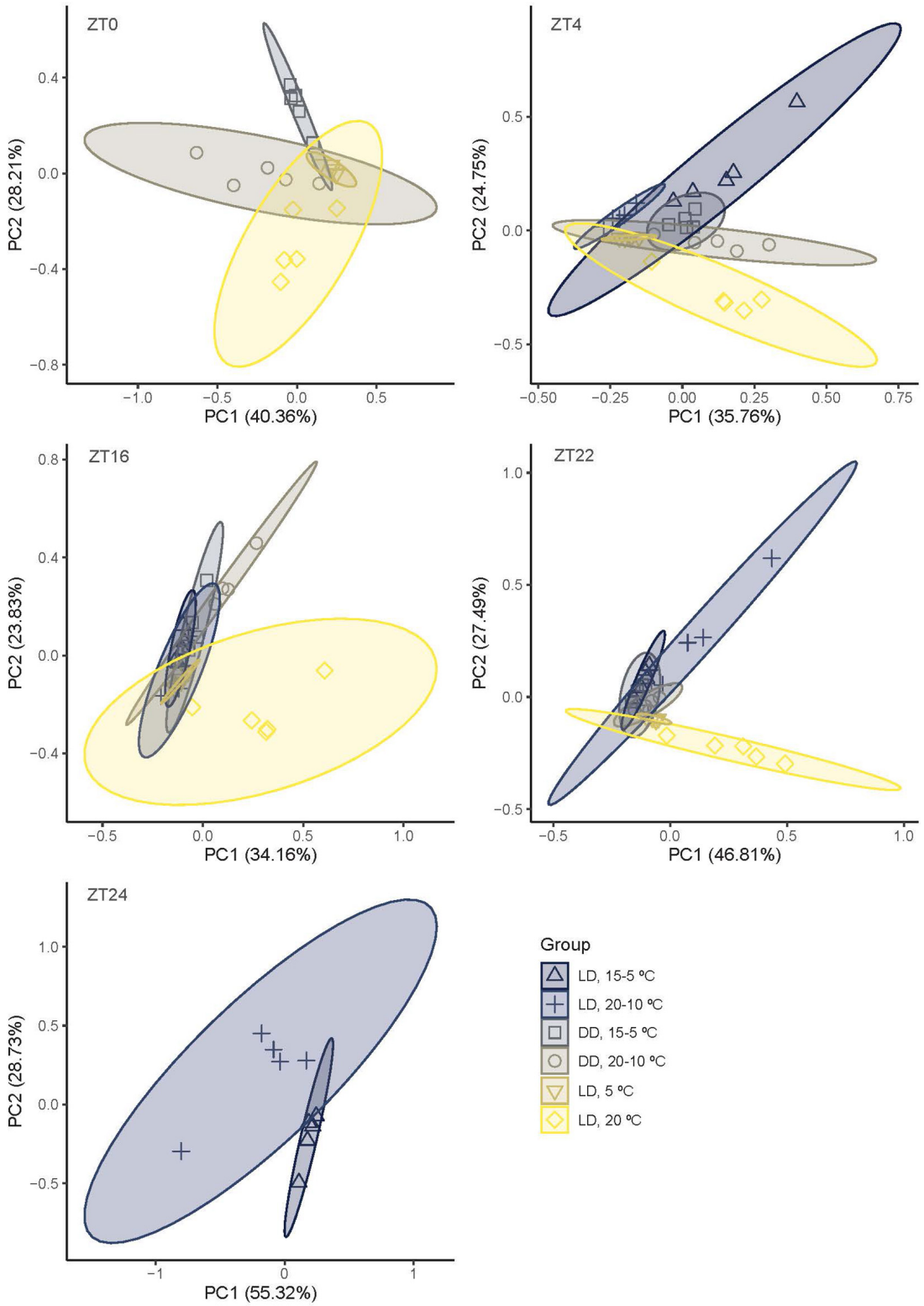

FIGURE 3 | Principal component analysis (PCA) based on narcissi emitted volatiles at five time points (ZT, *zeitgeber* time) under six different light:dark and temperature conditions. LD, light:dark; DD, constant darkness; PC, principal component.

aroma of several *Narcissus* species (Dobson et al., 1997). The scent profile obtained in the present work was dominated by monoterpenes and phenylpropanoids. However, amines and a benzenoid were also detected (**Figure 2** and **Supplementary Figure 1**; Ruíz-Ramón et al., 2014). We divided narcissi in three experimental groups and each group consisted in two different light:dark and temperature conditions, sampling volatiles at four time points. As we expected to observe changes along time but also among experimental treatments, we performed two different analysis. First, we analyzed each group and each pair in order to determine if the release of volatiles increased or decreased at different times of the day/night period (**Figures 4A–F** and **Table 2**). This data was log-transformed.

The time series analysis revealed different scent emission patterns (**Figures 4A–F** and **Table 2**). Under control conditions, 12LD and 15-5°C, the maximum scent release occurred during the light period at ZT4 and decreased significantly at night (Dunn's test $p < 0.05$, **Figure 4A**). In contrast, under 12LD and 20-10°C, the scent emission increased progressively and significantly along the light-dark period, showing opposite (**Figure 4B**). Under constant darkness, and irrespective of temperature regimes, the emission displayed a delayed pattern compared to control (**Figures 4C,D**). Indeed, the control maximal emission occurred at ZT4 while constant dark peaked at ZT16 and declined significantly thereafter (Dunn's test $p < 0.05$, **Table 2** and **Figures 4C,D**). Narcissi floral emission sampled under constant 5°C decreased at midnight (ZT16), whereas under constant 20°C revealed a somewhat stable emission (**Figures 4E,F**).

In order to assess the effects of light and temperature on overall scent emission we compared the emitted amount at each time point (**Figure 4G** and **Table 3**). We analyzed each pair of experimental conditions, e.g., constant 5 and 20°C, and we compared all groups among them. At ZT0 we did not observe differences among narcissi pairs ($p > 0.05$). Moreover, the emitted amount under constant darkness and constant temperature differed and we observed the lowest emission under constant 5°C (**Figure 4G** and **Table 3**). At ZT4, the emitted amount differed between two experimental pairs: 12LD/15-5°C and 12LD/20-10°C and constant 5 and 20°C ($p < 0.05$). Comparing all groups we observed that flowers under 12LD/20-10°C and 12LD/5°C displayed the lowest emission (**Figure 4G**). We observed a similar pattern at ZT16. The two groups of narcissi sampled under constant temperature showed a significant difference in emitted amounts ($p < 0.05$) whereas remaining pairs did not change. When we compared all groups, we found that the lowest emission corresponded to 12LD/20-10°C and 12LD/5°C, as observed at ZT4 (**Figure 4G** and **Table 3**). At ZT22, we only observed difference in the pair 12LD/15-5°C and 12LD/20-10°C ($p < 0.05$, **Figure 4**). Furthermore, the emission under 12LD/20-10°C and 12LD/20°C was higher compared with other groups (**Figure 4G** and **Table 3**). Finally, at ZT24 the pair sampled under LD and cycling temperature displayed a significant difference between 15-5°C and 20-10°C, with a highest emission under 20-10°C (**Figure 4G** and **Table 3**).

Although emission patterns changed among groups (**Figures 4A–F**, see above), narcissi sampled under constant temperatures showed important differences, except at ZT0. Narcissi scent emission under constant 20°C was higher than at 5°C (**Figure 4G** and **Table 3**).

We can conclude that floral scent emission is strongly affected by temperature regimes in *Narcissus*, while light plays a lesser role.

Effect of Thermoperiod and Photoperiod on Qualitative Changes in Scent Profiles

The observed changes in scent emission among narcissi groups (**Figure 4G** and **Table 3**) could be the result of different emission patterns (**Figures 4A–F** and **Table 2**), the effect of temperature on enzymatic activity, storage, and/or release of VOC but also may be related to the absence of certain volatiles (**Figure 1**). We examined the emission of every volatile and its contribution to the narcissi scent (**Figure 5**).

Under cycling light and both temperature cycles, 15-5°C and 20-10°C, we found a first group of volatiles with maximum emissions during the light period. These included 3,4-dimethyl 2,4,6-octatriene, eucalyptol, and limonene. In contrast, a second group reached their maximum quantity at night. It comprised benzenpropyl acetate, benzenepropanol, myrcene, and prenyl acetate. Other compounds such as ocimene, did not follow a clear pattern. Under a 15-5°C cycle, the highest emission of ocimene occurred during the light period whereas under 20-10°C, this volatile displayed its maximum amount at night (**Figure 5**).

Flowers sampled in constant darkness with cycling temperature, 15-5°C and 20-10°C showed two patterns. The highest amount of indole, benzyl acetate, benzenepropyl acetate, linalool, and phenethyl acetate were found at ZT4. In contrast, we found the highest amount of eucalyptol, limonene, myrcene, ocimene, cinnamyl acetate, and prenyl acetate during the subjective night, at ZT16 and ZT22 (**Figure 5**).

As mentioned above, we detected the highest quantity of volatiles under a light:dark cycle and a constant temperature of 20°C (**Figure 4**). Interestingly, the maximum amounts of all volatiles appeared during the dark period, at ZT16 or ZT22. This pattern was similar under a light:dark cycle with constant temperature of 5 C. Indeed, the emitted amount of eucalyptol, linalool, ocimene, and prenyl acetate increased during the dark period (**Figure 5**). In contrast, benzyl acetate and phenethyl acetate showed their maximum emission during the light period. Altogether, these results revealed that the maximum levels of a volatile depended on time of the day, light and temperature conditions. Furthermore, narcissi sampled at constant 5° and 20°C revealed a lower number of volatiles, compared to control group (**Figure 2**). In this case seemed that temperature but not the number of emitted compounds determine the scent intensity (**Figures 4**, **5**).

Random Forest Classification

The scent profiles obtained appeared to be highly divergent between the different temperature and light regimes. We investigated if the diverging profiles could be classified as different using Machine Learning algorithms. In order to identify the volatiles, among the 14 selected compounds, which can be

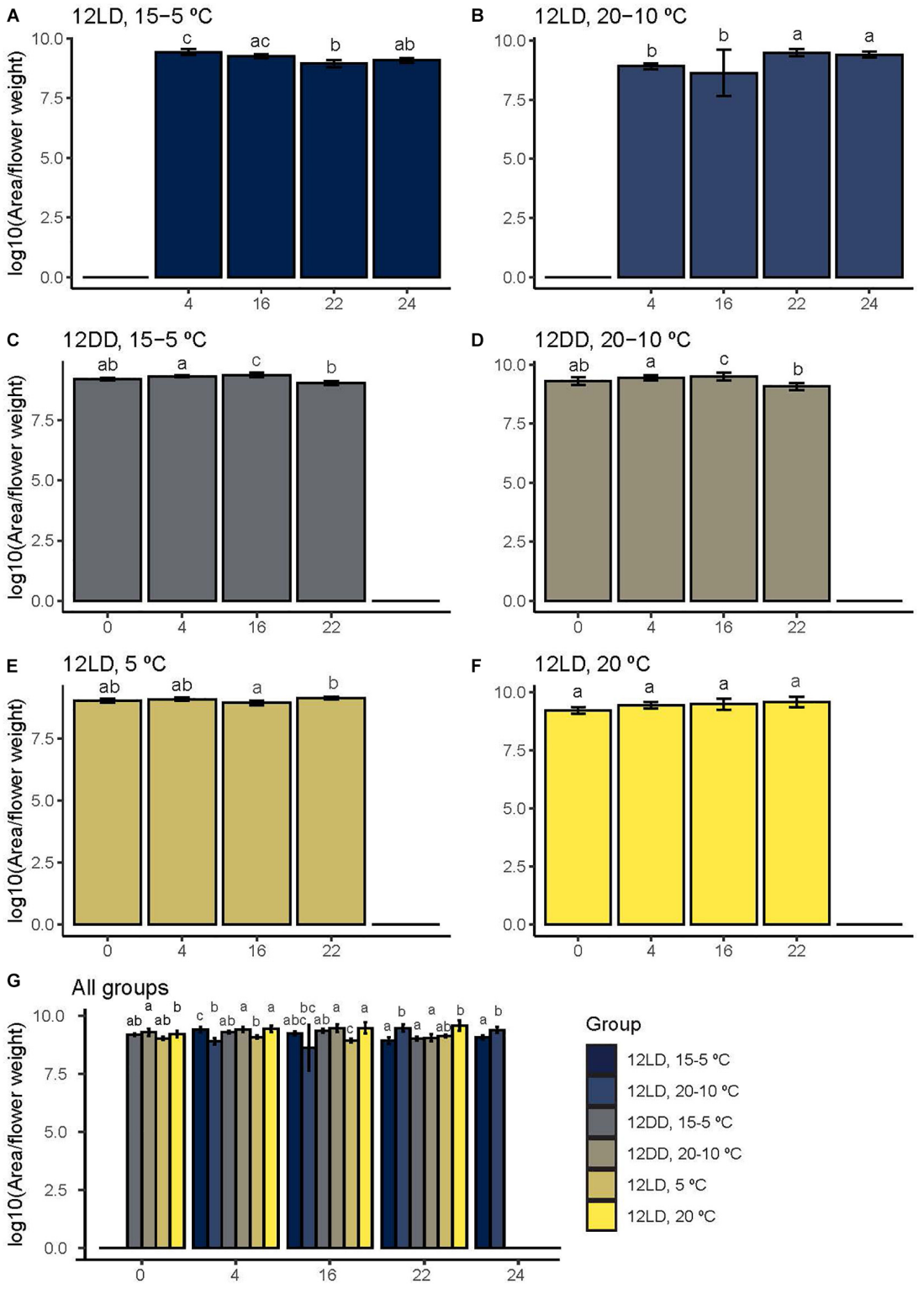

FIGURE 4 | Narcissi flower total scent emission under six different light:dark and temperature conditions. Volatiles were sampled at four time points (ZT). To detect scent emission patterns, we analyzed each group along time **(A–F)**. We also compared the emitted amount under six experimental conditions at each time point **(G)**. Each bar represents the average ± standard deviation of five flowers. Letters over bars indicate differences among time points **(A–F)** and groups **(G)** (Dunn's test, see **Tables 2**, **3**), LD, light:dark; DD, continuous dark; fw, fresh weight.

TABLE 2 | Analysis of narcissi volatile emission at four time points under different light and temperature conditions.

Group	Comparison (ZT)								
	0–4	**0–16**	**0–22**	**4–16**	**4–22**	**4–24**	**16–22**	**16–24**	**22–24**
12LD, 15-5°C	–	–	–	0.372	0.003	0.026	0.024	0.163	0.364
12LD, 20-10°C	–	–	–	0.021	0.708	0.043	0.010	0.668	0.016
12DD, 15-5°C	0.021	0.043	0.668	0.708	0.010	–	0.016	–	–
12DD, 20-10°C	0.342	0.223	0.242	0.708	0.026	–	0.017	–	–
12LD, 5°C	0.403	0.299	0.174	0.074	0.454	–	0.017	–	–
12LD, 20°C	N.S.	N.S.	N.S.	N.S.	N.S.	–	N.S.	–	–

For each group, all pairwise multiple comparison were calculated using a Dunn's test. 12LD, 12h light:12h dark; 12DD, constant darkness; ZT, zeitgeber time; N.S., no significant differences.

TABLE 3 | Analysis of narcissi volatile emission under different light and temperature conditions.

Comparison		ZT0	ZT4	ZT16	ZT22	ZT24
12LD, 15-5°C	12LD, 20-10°C	–	0.005	0.214	0.214	0.020
	12DD, 15-5°C	–	0.406	0.598	0.598	–
	12DD, 20-10°C	–	0.971	0.258	0.258	–
	12LD, 5°C	–	0.027	0.103	0.103	–
	12LD, 20°C	–	1	0.251	0.251	–
12LD, 20-10°C	12DD, 15-5°C	–	0.051	0.065	0.065	–
	12DD, 20-10°C	–	0.006	0.012	0.012	–
	12LD, 5°C	–	0.563	0.742	0.742	–
	12LD, 20°C	–	0.011	0.013	0.013	–
12DD, 15-5°C	12DD, 20-10°C	0.453	0.422	0.591	0.591	–
	12LD, 5°C	0.196	0.246	0.026	0.026	–
	12LD, 20°C	0.641	0.442	0.586	0.586	–
12DD, 20-10°C	12LD, 5°C	0.039	0.029	0.006	0.006	–
	12LD, 20°C	0.659	1	0.943	0.943	–
12LD, 5°C	12LD, 20°C	0.117	0.033	0.010	0.010	–

For each time point, all pairwise multiple comparison were calculated using a Dunn's test. 12LD, 12h light-12h dark; 12DD, constant darkness; ZT, zeitgeber time.

useful for classification, we used the Random Forest algorithm. The model classified correctly all the samples except one of LD continuous temperature of 20°C that was classified as continuous 5°C (**Table 4**). The obtained out-of-bag error (OOB) was 3.33%. This analysis ranked the volatiles based on mean decreasing accuracy (MDA) (**Table 5**). The five most important volatiles to classify between light:dark and temperature conditions were indole, limonene, cinnamyl acetate, myrcene, and benzenepropyl acetate (**Table 5**). These results confirmed that the scent profile was different among analyzed conditions. However, and as mentioned above, constant temperatures, typical of post-harvest conditions, caused the most drastic changes in scent profiles.

DISCUSSION

The absolute emitted amounts and specific composition of fragrances are two factors, both for the industry and at the ecological level. Indeed, industrial quality of essential oils is based on the specific composition in both qualitative and quantitative terms (Nejad Ebrahimi et al., 2008; Nabiha et al., 2009). Scent composition is an important component of breeding in ornamentals such as *Chrysanthemum* or *Iris* (Sun et al., 2015; Yuan et al., 2019). As ambient conditions may affect scent emission at the metabolic level and/or aroma accumulation and vaporization (Hu et al., 2013; Farré-Armengol et al., 2014; Cna'ani et al., 2015), we have studied the effect of light and temperature on *Narcissus* scent.

Scent emission is also related to flower development, and stops rapidly upon floral senescence (Dudareva et al., 2000; Weiss et al., 2016). As the *Narcissus* variety used in this study showed a very short life, we had to do single day tests. The mistletoe flower scent complexity decreases along its lifetime, volatiles such as nonanal and farnesene were not present in all flower stages. At the same time, the emitted amount of ocimene increases during the lifespan of flowers (Quintana-Rodríguez et al., 2018). These modifications of aroma occur within days, suggesting changes in volatile biosynthesis, accumulation and release, and may be considered in post-harvest handling. Experiments in snapdragon and wild relatives have shown a stable scent profile within a span of 3 to 5 days, indicating that there is a genetic component defining floral lifespan (Weiss et al., 2016). This may also play an important role in scent emission and stability.

Several flowering species including rose, snapdragon or tobacco display a robust circadian pattern (Kolosova et al., 2001;

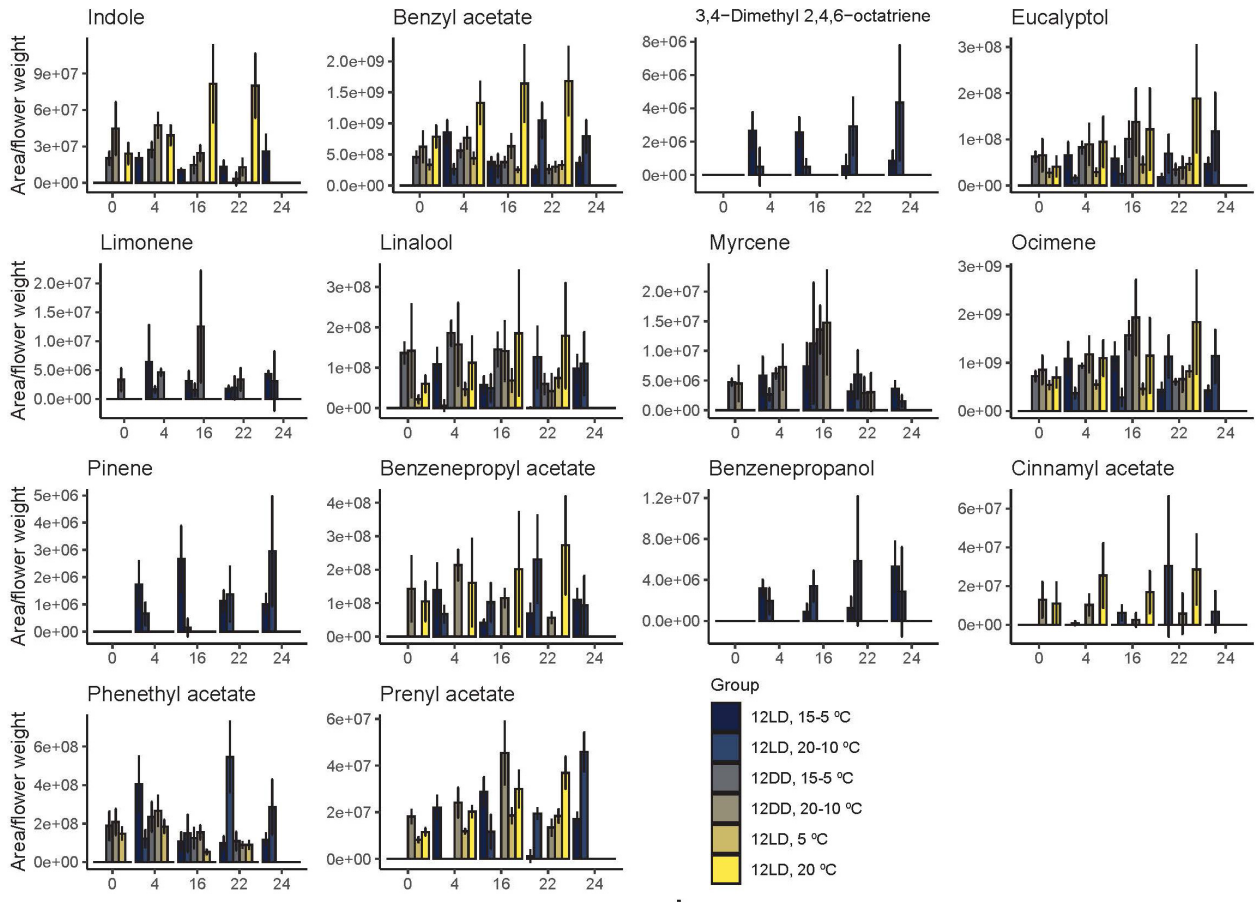

FIGURE 5 | Daily emission of narcissi volatiles. Each bar represents the average emission ± standard deviation of five flowers at four different time points (*zeitgeber* time, ZT).

TABLE 4 | Random forest confusion matrix showing the observed and the predicted groups among light:dark and temperature cycles.

Observed	Predicted						Error
	DD, 15-5°C	DD, 20-10°C	LD, 15-5°C	LD, 20-10°C	LD, 20°C	LD, 5°C	
DD, 15-5°C	5	0	0	0	0	0	0
DD, 20-10°C	0	5	0	0	0	0	0
LD, 15-5°C	0	0	5	0	0	0	0
LD, 20-10°C	0	0	0	5	0	0	0
LD, 20°C	0	0	0	0	4	1	0.2
LD, 5°C	0	0	0	0	0	5	0

Every group consisted in five replicates. LD, light:dark; DD, constant darkness.

Raguso et al., 2003; Picone et al., 2004). The robust circadian scent oscillation is maintained by *PhLHY, NaZTL, PhCHL, AmLHY*, and *PhGI1* (Fenske et al., 2015; Yon et al., 2015; Terry et al., 2019a,b; Brandoli et al., 2020). As coordination of circadian scent emission can be considered a downstream process of the clock, it is important to determine if daily changes in scent emission respond to drastic modifications in environmental conditions such as those used in post-harvest, or as a result in natural changes in growing temperatures.

The daily changes in emission patterns and volatile quantities produces floral scent variation along the day (Barman and Mitra, 2019; Terry et al., 2019a,b). The aroma blend plays a role in pollinator attraction, plant defense and plant-plant interaction, among other (Heil and Ton, 2008; Schiestl, 2010; Ueda et al., 2012), and changes in the aroma can alter these functions. As previously reported, narcissi aroma consisted in monoterpenes, but also benzenoids and phenylpropanoids (Dobson et al., 1997; Ruíz-Ramón et al., 2014). Our results

TABLE 5 | Importance ranking of volatile organic compounds (VOCs) for classifying narcissi by random forest algorithm, based on mean decreasing accuracy (MDA).

Rank	VOCs	Class	MDA
1	Indole	Amine	14.56
2	D-Limonene	Monoterpene	13.52
3	Cinnamyl acetate	Phenylpropanoid	12.81
4	β-myrcene	Monoterpene	12.65
5	Benzenepropyl acetate	Phenylpropanoid	12.57
6	Benzyl acetate	Benzenoid	11.33
7	Prenyl acetate	Terpene	11
8	β-Phenethyl acetate	Phenylpropanoid	10.92
9	Benzenepropanol	Phenylpropanoid	10.35
10	3,4-Dimethyl 2,4,6-octatriene	Monoterpene	10.25
11	α-Pinene	Monoterpene	10.04
12	Ocimene	Monoterpene	3.72
13	Linalool	Monoterpene	3.53
14	Eucalyptol	Monoterpene	0.83

revealed that a modification in light:dark and temperature conditions can drastically alter the fragrance blend. We identified 14 volatiles organic compounds and four of them, benzyl acetate, eucalyptol, linalool, and ocimene, were constitutively emitted. Narcissi cut flowers also emitted phenylpropanoid and benzenoid volatiles. We can conclude that both benzenoid and monoterpene production is resilient to changes in environmental conditions, however, not all monoterpenes were robustly produced. Indeed, 3,4-dimethyl-2,4,6-octatriene, pinene, myrcene, and limonene emissions were controlled by light or temperature. As observed in monoterpene compounds, benzyl acetate was constitutive while all phenylpropanoids varied with environmental conditions. As the synthesis pathways of monoterpenes are shared (Dudareva et al., 2003; Byers et al., 2014), and benzenoids and phenylpropanoids are synthesized from phenylalanine (Boatright et al., 2004), an emerging hypothesis is that transport and/or synthesis maybe affected at specific biosynthetic steps. The effect of temperature in scent emission in *Narcissus* appears to be a common response in other geophytes.

Similar to stored terpenes in leaves, flowers can accumulate several volatile compounds, as petunia, that accumulates glycosylated phenylpropanoids, that are metabolized during the emission (Cna'ani et al., 2017). The metabolism of phenylpropanoids as well as its possible accumulation in narcissi flowers may explain the differences in emitted levels under different light and temperature conditions. Our results agree with those found in petunia, except under a constant temperature of 20°C. As terpenoids and phenylpropanoids show diverging patterns, we conclude that their synthesis or emission may have distinct genetic coordination.

The group comparison of temperature and light treatments suggested that the major differences found were imputable to constant temperatures. Indeed, emission maxima changed from day to night when comparing 15-5 to 20-10°C indicating a major impact of day night temperatures on overall scent emissions. The fact that continuous dark does not change the maximum emissions and constant temperatures caused a somewhat flat curve indicates that overall temperature has the highest impact in *Narcissus*. Changes in temperature have been shown to affect the quantity of emitted compounds in plants such as *Quercus ilex*, *Sonchus tenerrimus*, and *Lilium* sp. (Hu et al., 2013; Farré-Armengol et al., 2014). This pattern was especially remarkable under a constant temperature of 20°C, whereas the lowest amount of emitted VOCs was found under a constant temperature of 5°C (**Figure 4**). The timing of maximum emission under 12LD and 15-5°C occurred during the light phase but it was delayed to midnight under 20-10°C. Constant darkness shifted maximum emission to the end of the dark period and under constant temperature, narcissi scent emission tended to reach at the dark phase. These changes suggest that post-harvest conditions determine the emission pattern, indicating that light and temperature also control volatile accumulation and probably other secondary metabolites. As industrial post-harvest conditions tend to have fixed regimes of light and temperature, this aspect may be address in order to improve essential oil extraction.

As pre-harvest conditions are important in flower scent and essential oil quality and quantity (Angioni et al., 2006; Chen et al., 2020), growth under warm climate conditions may alter these properties. Some studies suggest that temperature is positively related with volatile emission (Faubert et al., 2010) including alteration of scent profiles (Faubert et al., 2012). However, some species appear to have stable emissions under changing environments such as the artic shrubs *Empetrum hermaphroditum* and *Cassiope tetragona* (Schollert et al., 2015). Temperature may regulate at different levels including metabolism, availability of substrates, enzyme activity and/or accumulation and release mechanisms (Oyama-Okubo et al., 2005; Farré-Armengol et al., 2013; Barman and Mitra, 2019). This may also depend on species, tissues and organs (Schollert et al., 2015; Jamieson et al., 2017).

Due to the complexity of plant volatilomes, classification methods such as principal component analysis, or machine learning algorithms as random forest are useful to identify patterns and to reduce the number of compounds that

can be used to discriminate related species or varieties, among other procedures (Ranganathan and Borges, 2010; Dos-Santos et al., 2013; Brückner and Heethoff, 2017). In this study, narcissi under control conditions revealed more than 50 different identified compounds with a quality higher than 80% (**Supplementary Figure 1**). We used the R package "gcProfileMakeR" to reduce the number of compounds (Pérez-Sanz et al., 2020), based on their frequency, and we applied the random forest classification algorithm. Random forest showed a very low error rate. Only one sample was misclassified, suggesting that differences in floral fragrance among treatments were significant from a mathematical perspective.

The four VOCs found with a higher level of MDA were indole, D-limonene, cinnamyl acetate, and β-myrcene. These compounds were differentially emitted as indole was found only in four out of six conditions, cinnamyl acetate was found in 20-10°C or 20°C while β-myrcene disappeared at constant temperatures. This indicates a possibility to enrich or decrease a single component of a scent profile via changes in growth and/or storage conditions.

Our study showed that the temperature regimens modified scent emission at several levels, including rhythmic emission, emitted quantity, and fragrance composition. Altogether, these modifications resulted in new aroma blends, which can be useful in ornamental and perfume industry. Future perspectives should consider analyzing the internal pool of volatiles as well as the activity of involved enzymes and vaporization mechanisms.

Insights provided reveal that post-harvest conditions affect the scent composition and quantity emitted by narcissi flowers. In addition, floral bouquets composition also changes along the day. These results might be of interest to the perfume and ornamentals industries. Our results show that keeping both a thermoperiod and photoperiod are more appropriate to keep a high-quality scent profile. It is remarkable that the 15°-5°C with 12:12 LD photoperiod resembling the natural winter growing conditions could be considered the best environmental treatment for post-harvest of Narcissus flowers in terms of scent profile.

DATA AVAILABILITY STATEMENT

The datasets generated for this study are available on request to the corresponding author.

AUTHOR CONTRIBUTIONS

MT, VR-H, DÁ, JW, and ME-C conceived and designed the experiments, and corrected the manuscript. DÁ provided the plant material. MT and VR-H sampled and obtained data. MT, VR-H, and DÁ analyzed the data. MT, JW, and ME-C wrote the manuscript. JW and ME-C wrote project and obtained funding. All authors contributed to the article and approved the submitted version.

FUNDING

This wok was funded by MICINN-FEDER-BFU-2017-88300-C2-1-R to JW and ME-C.

SUPPLEMENTARY MATERIAL

The Supplementary Material for this article can be found online at: https://www.frontiersin.org/articles/10.3389/fpls.2020.540821/full#supplementary-material

REFERENCES

Aedo, C., and Herrero, A. (2005). *Flora Iberica. Plantas Vasculares de la Península Ibérica e Islas Baleares.* Available online at: http://www.floraiberica.es/floraiberica/texto/imprenta/tomoXX/20_184_05_Narcissus.pdf (accessed November 1, 2020).

Angioni, A., Barra, A., Coroneo, V., Dessi, S., and Cabras, P. (2006). Chemical composition, seasonal variability, and antifungal activity of *Lavandula stoechas* L. ssp. stoechas essential oils from stem/leaves and flowers. *J. Agric. Food Chem.* 54, 4364–4370. doi: 10.1021/jf0603329

Barman, M., and Mitra, A. (2019). Temporal relationship between emitted and endogenous floral scent volatiles in summer- and winter-blooming Jasminum species. *Physiol. Plant.* 166, 946–959. doi: 10.1111/ppl.12849

Bicchi, C., Cordero, C., Liberto, E., Rubiolo, P., Sgorbini, B., David, F., et al. (2005). Dual-phase twisters: a new approach to headspace sorptive extraction and stir bar sorptive extraction. *J. Chromatogr. A* 1094, 9–16. doi: 10.1016/j.chroma.2005.07.099

Boatright, J., Negre, F., Chen, X., Kish, C. M., Wood, B., Peel, G., et al. (2004). Understanding in vivo benzenoid metabolism in petunia petal tissue. *Plant Physiol.* 135, 1993–2011. doi: 10.1104/pp.104.045468

Brandoli, C., Petri, C., Egea-Cortines, M., and Weiss, J. (2020). The clock gene Gigantea 1 from Petunia hybrida coordinates vegetative growth and inflorescence architecture. *Sci. Rep.* 10, 1–17. doi: 10.1038/s41598-019-57145-9

Breiman, L. (2001). Random forests. *Mach. Learn.* 45, 5–32. doi: 10.1023/A:1010933404324

Brückner, A., and Heethoff, M. (2017). A chemo-ecologists' practical guide to compositional data analysis. *Chemoecology* 27, 33–46. doi: 10.1007/s00049-016-0227-8

Bunya-atichart, K., Ketsa, S., and van Doorn, W. G. (2004). Postharvest physiology of *Curcuma alismatifolia* flowers. *Postharvest Biol. Technol.* 34, 219–226. doi: 10.1016/j.postharvbio.2004.05.009

Byers, K. J. R. P., Vela, J. P., Peng, F., Riffell, J. A., and Bradshaw, H. D. (2014). Floral volatile alleles can contribute to pollinator-mediated reproductive isolation in *monkeyflowers* (*Mimulus*). *Plant J.* 80, 1031–1042. doi: 10.1111/tpj.12702

Chen, J., Tang, J., and Yu, X. (2020). Environmental and physiological controls on diurnal and seasonal patterns of biogenic volatile organic compound emissions from five dominant woody species under field conditions. *Environ. Pollut.* 259:113955. doi: 10.1016/j.envpol.2020.113955

Cheng, S., Fu, X., Mei, X., Zhou, Y., Du, B., Watanabe, N., et al. (2016). Regulation of biosynthesis and emission of volatile phenylpropanoids/benzenoids in petunia× hybrida flowers by multi-factors of circadian clock, light, and temperature. *Plant Physiol. Biochem.* 107, 1–8. doi: 10.1016/j.plaphy.2016.05.026

Chuang, Y.-C., Lee, M.-C., Chang, Y.-L., Chen, W.-H., and Chen, H.-H. (2017). Diurnal regulation of the floral scent emission by light and circadian rhythm in the *Phalaenopsis orchids*. *Bot. Stud.* 58:50. doi: 10.1186/s40529-017-0204-8

Cna'ani, A., Mühlemann, J. K., Ravid, J., Masci, T., Klempien, A., Nguyen, T. T. H., et al. (2015). Petunia × hybrida floral scent production is negatively affected

by high-temperature growth conditions. *Plant Cell Environ.* 38, 1333–1346. doi: 10.1111/pce.12486

Cna'ani, A., Shavit, R., Ravid, J., Aravena-Calvo, J., Skaliter, O., Masci, T., et al. (2017). Phenylpropanoid scent compounds in petunia x hybrida are glycosylated and accumulate in vacuoles. *Front. Plant Sci.* 8:1898. doi: 10.3389/fpls.2017.01898

Colquhoun, T. A., Schwieterman, M. L., Gilbert, J. L., Jaworski, E. A., Langer, K. M., Jones, C. R., et al. (2013). Light modulation of volatile organic compounds from petunia flowers and select fruits. *Postharvest Biol. Technol.* 86, 37–44. doi: 10.1016/j.postharvbio.2013.06.013

Dinno, A. (2017). *dunn.test: Dunn's Test of Multiple Comparisons Using Rank Sums*. Available online at: https://CRAN.R-project.org/package=dunn.test (accessed May 24, 2020).

Dobson, H. E. M., Arroyo, J., Bergström, G., and Groth, I. (1997). Interspecific variation in floral fragrances within the genus *Narcissus* (Amaryllidaceae). *Biochem. Syst. Ecol.* 25, 685–706. doi: 10.1016/S0305-1978(97)00059-8

Dos-Santos, N., Bueso, M. C., and Fernández-Trujillo, J. P. (2013). Aroma volatiles as biomarkers of textural differences at harvest in non-climacteric near-isogenic lines of melon. *Food Res. Int.* 54, 1801–1812. doi: 10.1016/j.foodres.2013.09.031

Dötterl, S., Wolfe, L. M., and Jürgens, A. (2005). Qualitative and quantitative analyses of flower scent in *Silene latifolia*. *Phytochemistry* 66, 203–213. doi: 10.1016/j.phytochem.2004.12.002

Dudareva, N., Klempien, A., Muhlemann, J. K., and Kaplan, I. (2013). Biosynthesis, function and metabolic engineering of plant volatile organic compounds. *New Phytol.* 198, 16–32. doi: 10.1111/nph.12145

Dudareva, N., Martin, D., Kish, C. M., Kolosova, N., Gorenstein, N., Fäldt, J., et al. (2003). (E)-β-ocimene and myrcene synthase genes of floral scent biosynthesis in snapdragon. *Plant Cell* 15, 1227–1241. doi: 10.1105/tpc.011015

Dudareva, N., Murfitt, L. M., Mann, C. J., Gorenstein, N., Kolosova, N., Kish, C. M., et al. (2000). Developmental regulation of methyl benzoate biosynthesis and emission in snapdragon flowers. *The Plant Cell* 12, 949–961. doi: 10.1105/tpc.12.6.949

Farré-Armengol, G., Filella, I., Llusia, J., and Peñuelas, J. (2013). Floral volatile organic compounds: between attraction and deterrence of visitors under global change. *Perspect. Plant Ecol. Evol. Syst.* 15, 56–67. doi: 10.1016/j.ppees.2012.12.002

Farré-Armengol, G., Filella, I., Llusià, J., Niinemets, Ü, and Peñuelas, J. (2014). Changes in floral bouquets from compound-specific responses to increasing temperatures. *Global Change Biol.* 20, 3660–3669. doi: 10.1111/gcb.12628

Faubert, P., Tiiva, P., Michelsen, A., Rinnan, Å, Ro-Poulsen, H., and Rinnan, R. (2012). The shift in plant species composition in a subarctic mountain birch forest floor due to climate change would modify the biogenic volatile organic compound emission profile. *Plant Soil* 352, 199–215. doi: 10.1007/s11104-011-0989-2

Faubert, P., Tiiva, P., Rinnan, Å, Michelsen, A., Holopainen, J. K., and Rinnan, R. (2010). Doubled volatile organic compound emissions from subarctic tundra under simulated climate warming. *New Phytol.* 187, 199–208. doi: 10.1111/j.1469-8137.2010.03270.x

Fenske, M. P., Hazelton, K. D. H., Hempton, A. K., Shim, J. S., Yamamoto, B. M., Riffell, J. A., et al. (2015). Circadian clock gene LATE ELONGATED HYPOCOTYL directly regulates the timing of floral scent emission in *Petunia*. *Proc. Natl. Acad. Sci. U.S.A.* 112, 9775–9780. doi: 10.1073/pnas.1422875112

Fu, J., Hou, D., Zhang, C., Bao, Z., Zhao, H., and Hu, S. (2017). The emission of the floral scent of four *Osmanthus fragrans* cultivars in response to different temperatures. *Molecules* 22:430. doi: 10.3390/molecules22030430

Füssel, U., Dötterl, S., Jürgens, A., and Aas, G. (2007). Inter- and intraspecific variation in floral scent in the genus *Salix* and its implication for pollination. *J. Chem. Ecol.* 33, 749–765. doi: 10.1007/s10886-007-9257-6

González, A., Bañón, S., Fernández, J. A., Franco, J. A., Casas, J. L., and Ochoa, J. (1998). Flowering responses of *Gladiolus tristis* (L.) after exposing corms to cold treatment. *Sci. Hortic.* 74, 279–284. doi: 10.1016/S0304-4238(98)00092-2

Gouinguené, S. P., and Turlings, T. C. J. (2002). The effects of abiotic factors on induced volatile emissions in corn plants. *Plant Physiol.* 129, 1296–1307. doi: 10.1104/pp.001941

Haberstroh, S., Kreuzwieser, J., Lobo-do-Vale, R., Caldeira, M. C., Dubbert, M., and Werner, C. (2018). Terpenoid emissions of two mediterranean woody species in response to drought stress. *Front. Plant Sci.* 9:1071. doi: 10.3389/fpls.2018.01071

Hagen, S. F., Borge, G. I. A., Bengtsson, G. B., Bilger, W., Berge, A., Haffner, K., et al. (2007). Phenolic contents and other health and sensory related properties of apple fruit (*Malus domestica* Borkh., cv. Aroma): effect of postharvest UV-B irradiation. *Postharvest Biol. Technol.* 45, 1–10. doi: 10.1016/j.postharvbio.2007.02.002

Heil, M., and Ton, J. (2008). Long-distance signalling in plant defence. *Trends Plant Sci.* 13, 264–272. doi: 10.1016/j.tplants.2008.03.005

Hu, Z., Zhang, H., Leng, P., Zhao, J., Wang, W., and Wang, S. (2013). The emission of floral scent from Lilium 'siberia' in response to light intensity and temperature. *Acta Physiol. Plant* 35, 1691–1700. doi: 10.1007/s11738-012-1211-8

Imahori, Y., Takemura, M., and Bai, J. (2008). Chilling-induced oxidative stress and antioxidant responses in mume (*Prunus mume*) fruit during low temperature storage. *Postharvest Biol. Technol.* 49, 54–60. doi: 10.1016/j.postharvbio.2007.10.017

Jamieson, M. A., Burkle, L. A., Manson, J. S., Runyon, J. B., Trowbridge, A. M., and Zientek, J. (2017). Global change effects on plant–insect interactions: the role of phytochemistry. *Curr. Opin. Insect Sci.* 23, 70–80. doi: 10.1016/j.cois.2017.07.009

Joyce, D. C., Meara, S. A., Hetherington, S. E., and Jones, P. (2000). Effects of cold storage on cut *Grevillea* 'Sylvia' inflorescences. *Postharvest Biol. Technol.* 18, 49–56. doi: 10.1016/S0925-5214(99)00059-9

Jürgens, A., Webber, A. C., and Gottsberger, G. (2000). Floral scent compounds of Amazonian Annonaceae species pollinated by small beetles and thrips. *Phytochemistry* 55, 551–558. doi: 10.1016/S0031-9422(00)00241-7

Jürgens, A., Witt, T., and Gottsberger, G. (2002). Flower scent composition in night-flowering Silene species (Caryophyllaceae). *Biochem. Syst. Ecol.* 30, 383–397. doi: 10.1016/S0305-1978(01)00106-5

Kolosova, N., Gorenstein, N., Kish, C. M., and Dudareva, N. (2001). Regulation of circadian methyl benzoate emission in diurnally and nocturnally emitting plants. *Plant Cell* 13, 2333–2347. doi: 10.1105/tpc.010162

Liaw, A., and Wiener, M. (2002). Classification and regression by randomForest. *R News* 2, 18–22.

Liu, C., and Liu, Y. (2014). Effects of elevated temperature postharvest on color aspect, physiochemical characteristics, and aroma components of pineapple fruits. *J. Food Sci.* 79, C2409–C2414. doi: 10.1111/1750-3841.12688

Lopez, M. L., Lavilla, M. T., Recasens, I., Graell, J., and Vendrell, M. (2000). Changes in aroma quality of 'Golden Delicious' apples after storage at different oxygen and carbon dioxide concentrations. *J. Sci. Food Agric.* 80, 311–324. doi: 10.1002/1097-0010(200002)80:3<311::aid-jsfa519>3.0.co;2-f

Loreto, F., and Schnitzler, J.-P. (2010). Abiotic stresses and induced BVOCs. *Trends Plant Sci.* 15, 154–166. doi: 10.1016/j.tplants.2009.12.006

Majetic, C. J., Levin, D. A., and Raguso, R. A. (2014). Divergence in floral scent profiles among and within cultivated species of Phlox. *Sci. Hortic.* 172, 285–291. doi: 10.1016/j.scienta.2014.04.024

Manchado-Rojo, M., Delgado−Benarroch, L., Roca, M. J., Weiss, J., and Egea-Cortines, M. (2012). Quantitative levels of Deficiens and Globosa during late petal development show a complex transcriptional network topology of B function. *Plant J.* 72, 294–307. doi: 10.1111/j.1365-313X.2012.05080.x

Marques, I., Aguilar, J. F., Martins-Louçao, M. A., Moharrek, F., and Feliner, G. N. (2017). A three-genome five-gene comprehensive phylogeny of the bulbous genus *Narcissus* (Amaryllidaceae) challenges current classifications and reveals multiple hybridization events. *TAXON* 66, 832–854. doi: 10.12705/664.3

Matsui, K. (2006). Green leaf volatiles: hydroperoxide lyase pathway of oxylipin metabolism. *Curr. Opin. Plant Biol.* 9, 274–280. doi: 10.1016/j.pbi.2006.03.002

Maul, F., Sargent, S. A., Sims, C. A., Baldwin, E. A., Balaban, M. O., and Huber, D. J. (2000). Tomato flavor and aroma quality as affected by storage temperature. *J. Food Sci.* 65, 1228–1237. doi: 10.1111/j.1365-2621.2000.tb10270.x

Montero, L., Conradi, S., Weiss, H., and Popp, P. (2005). Determination of phenols in lake and ground water samples by stir bar sorptive extraction–thermal desorption–gas chromatography–mass spectrometry. *J. Chromatogr. A* 1071, 163–169. doi: 10.1016/j.chroma.2005.01.097

Muhlemann, J. K., Klempien, A., and Dudareva, N. (2014). Floral volatiles: from biosynthesis to function. *Plant Cell Environ.* 37, 1936–1949. doi: 10.1111/pce.12314

Nabiha, B., Abdelfateh, E. O., Faten, K., Paul, W. J., Michel, M., and Moncef, C. M. (2009). Chemical composition and antioxidant activity of *Laurus nobilis* floral buds essential oil. *J. Essent. Oil Bearing Plants* 12, 694–702. doi: 10.1080/0972060X.2009.10643777

Nagegowda, D. A. (2018). Plant volatile terpenoid metabolism: biosynthetic genes, transcriptional regulation and subcellular compartmentation. *FEBS Lett.* 584, 2965–2973. doi: 10.1016/j.febslet.2010.05.045

Nejad Ebrahimi, S., Hadian, J., Mirjalili, M. H., Sonboli, A., and Yousefzadi, M. (2008). Essential oil composition and antibacterial activity of *Thymus caramanicus* at different phenological stages. *Food Chem.* 110, 927–931. doi: 10.1016/j.foodchem.2008.02.083

Niinemets, Ü, Kännaste, A., and Copolovici, L. (2013). Quantitative patterns between plant volatile emissions induced by biotic stresses and the degree of damage. *Front. Plant Sci.* 4:262. doi: 10.3389/fpls.2013.00262

Oyama-Okubo, N., Ando, T., Watanabe, N., Marchesi, E., Uchida, K., and Nakayama, M. (2005). Emission mechanism of floral scent in *Petunia axillaris*. *Biosci. Biotechnol. Biochem.* 69, 773–777. doi: 10.1271/bbb.69.773

Peñuelas, J., and Llusià, J. (2001). The complexity of factors driving volatile organic compound emissions by plants. *Biol. Plant.* 44, 481–487. doi: 10.1023/A:1013797129428

Pérez-Sanz, F., Ruiz-Hernández, V., Terry, M. I., Arce-Gallego, S., Weiss, J., Navarro, P. J., et al. (2020). Automatic classification of constitutive and non-constitutive metabolites with gcProfileMakeR. *bioRxiv* [Preprint]. doi: 10.1101/2020.02.24.963058

Perry, N. B., Anderson, R. E., Brennan, N. J., Douglas, M. H., Heaney, A. J., McGimpsey, J. A., et al. (1999). Essential oils from dalmatian sage (*Salvia officinalis* L.): variations among individuals, plant parts, seasons, and sites. *J. Agric. Food Chem.* 47, 2048–2054. doi: 10.1021/jf981170m

Picone, J. M., Clery, R. A., Watanabe, N., MacTavish, H. S., and Turnbull, C. G. N. (2004). Rhythmic emission of floral volatiles from *Rosa damascena* semperflorens cv. 'Quatre Saisons.'. *Planta* 219, 468–478. doi: 10.1007/s00425-004-1250-5

Quintana-Rodríguez, E., Ramírez-Rodríguez, A. G., Ramírez-Chávez, E., Molina-Torres, J., Camacho-Coronel, X., Esparza-Claudio, J., et al. (2018). Biochemical traits in the flower lifetime of a mexican mistletoe parasitizing mesquite biomass. *Front. Plant Sci.* 9:1031. doi: 10.3389/fpls.2018.01031

Raguso, R. A., Levin, R. A., Foose, S. E., Holmberg, M. W., and McDade, L. A. (2003). Fragrance chemistry, nocturnal rhythms and pollination "syndromes" in *Nicotiana*. *Phytochemistry* 63, 265–284. doi: 10.1016/S0031-9422(03)00113-4

Ranganathan, Y., and Borges, R. M. (2010). Reducing the babel in plant volatile communication: using the forest to see the trees. *Plant Biol.* 12, 735–742. doi: 10.1111/j.1438-8677.2009.00278.x

Redman, P. B., Dole, J. M., Maness, N. O., and Anderson, J. A. (2002). Postharvest handling of nine specialty cut flower species. *Sci. Hortic.* 92, 293–303. doi: 10.1016/S0304-4238(01)00294-1

Rees, A. R., and Hanks, G. R. (1984). Storage treatments for very early forcing of narcissus. *J. Hortic. Sci.* 59, 229–239. doi: 10.1080/00221589.1984.11515192

Rees, A. R., and Wallis, L. W. (1970). *Pre-Cooling of Narcissus Bulbs for Early Flowering in the Field*. Available online at: https://www.cabdirect.org/cabdirect/abstract/19710301814 (accessed March 5, 2020)

Remy, C. (2004). "Narcissus in perfumery," in *Narcissus and Daffodil: The Genus Narcissus*, ed. G. H. Hanks (London: Taylor and Francis e-library), 452–452.

Ruiz-Hernández, V., Roca, M. J., Egea-Cortines, M., and Weiss, J. (2018). A comparison of semi-quantitative methods suitable for establishing volatile profiles. *Plant Methods* 14:67. doi: 10.1186/s13007-018-0335-2

Ruíz-Ramón, F., Águila, D. J., Egea-Cortines, M., and Weiss, J. (2014). Optimization of fragrance extraction: daytime and flower age affect scent emission in simple and double narcissi. *Ind. Crops Products* 52, 671–678. doi: 10.1016/j.indcrop.2013.11.034

Sagae, M., Oyama-Okubo, N., Ando, T., Marchesi, E., and Nakayama, M. (2008). Effect of temperature on the floral scent emission and endogenous volatile profile of *Petunia axillaris*. *Biosci. Biotechnol. Biochem.* 72, 110–115. doi: 10.1271/bbb.70490

Santos-Gally, R., Vargas, P., and Arroyo, J. (2012). Insights into Neogene Mediterranean biogeography based on phylogenetic relationships of mountain and lowland lineages of *Narcissus* (Amaryllidaceae). *J. Biogeogr.* 39, 782–798. doi: 10.1111/j.1365-2699.2011.02526.x

Schiestl, F. P. (2010). The evolution of floral scent and insect chemical communication. *Ecol. Lett.* 13, 643–656. doi: 10.1111/j.1461-0248.2010.01451.x

Schollert, M., Kivimäenpää, M., Valolahti, H. M., and Rinnan, R. (2015). Climate change alters leaf anatomy, but has no effects on volatile emissions from arctic plants. *Plant Cell Environ.* 38, 2048–2060. doi: 10.1111/pce.12530

Staudt, M., and Lhoutellier, L. (2011). Monoterpene and sesquiterpene emissions from *Quercus coccifera* exhibit interacting responses to light and temperature. *Biogeosciences* 8, 2757–2771. doi: 10.5194/bg-8-2757-2011

Sun, H., Zhang, T., Fan, Q., Qi, X., Zhang, F., Fang, W., et al. (2015). Identification of floral scent in *chrysanthemum* cultivars and wild relatives by gas chromatography-mass spectrometry. *Molecules* 20, 5346–5359. doi: 10.3390/molecules20045346

Tang, Y., Horikoshi, M., and Li, W. (2016). ggfortify: unified interface to visualize statistical results of popular R packages. *R J.* 8:474. doi: 10.32614/RJ-2016-060

Terry, M. I., Pérez-Sanz, F., Díaz-Galián, M. V., Pérez de los Cobos, F., Navarro, P. J., Egea-Cortines, M., et al. (2019a). The *Petunia* CHANEL gene is a ZEITLUPE ortholog coordinating growth and scent profiles. *Cells* 8:343. doi: 10.3390/cells8040343

Terry, M. I., Pérez-Sanz, F., Navarro, P. J., Weiss, J., and Egea-Cortines, M. (2019b). The snapdragon LATE ELONGATED HYPOCOTYL plays a dual role in activating floral growth and scent emission. *Cells* 8:920. doi: 10.3390/cells8080920

Tietel, Z., Lewinsohn, E., Fallik, E., and Porat, R. (2012). Importance of storage temperatures in maintaining flavor and quality of mandarins. *Postharvest Biol. Technol.* 64, 175–182. doi: 10.1016/j.postharvbio.2011.07.009

Ueda, H., Kikuta, Y., and Matsuda, K. (2012). Plant communication. *Plant Signal. Behav.* 7, 222–226. doi: 10.4161/psb.18765

van Dam, N. M., and Bouwmeester, H. J. (2016). Metabolomics in the rhizosphere: tapping into belowground chemical communication. *Trends Plant Sci.* 21, 256–265. doi: 10.1016/j.tplants.2016.01.008

Verdonk, J. C., Ric de Vos, C. H., Verhoeven, H. A., Haring, M. A., van Tunen, A. J., and Schuurink, R. C. (2003). Regulation of floral scent production in petunia revealed by targeted metabolomics. *Phytochemistry* 62, 997–1008. doi: 10.1016/S0031-9422(02)00707-0

Viti, R., Andreini, L., Ruiz, D., Egea, J., Bartolini, S., Iacona, C., et al. (2010). Effect of climatic conditions on the overcoming of dormancy in apricot flower buds in two Mediterranean areas: Murcia (Spain) and Tuscany (Italy). *Sci. Hortic.* 124, 217–224. doi: 10.1016/j.scienta.2010.01.001

Weiss, J., and Egea-Cortines, M. (2009). Transcriptomic analysis of cold response in tomato fruits identifies dehydrin as a marker of cold stress. *J. Appl. Genet.* 50, 311–319. doi: 10.1007/BF03195689

Weiss, J., Mühlemann, J. K., Ruiz-Hernández, V., Dudareva, N., and Egea-Cortines, M. (2016). Phenotypic space and variation of floral scent profiles during late flower development in *Antirrhinum*. *Front. Plant Sci.* 7:1903. doi: 10.3389/fpls.2016.01903

Yon, F., Joo, Y., Cort, L., Rothe, E., Baldwin, I. T., Kim, S., et al. (2015). Silencing *Nicotiana attenuata* LHY and ZTL alters circadian rhythms in flowers. *New Phytol.* 209, 1058–1066. doi: 10.1111/nph.13681

Yuan, J. S., Himanen, S. J., Holopainen, J. K., Chen, F., and Stewart, C. N. (2009). Smelling global climate change: mitigation of function for plant volatile organic compounds. *Trends Ecol. Evol.* 24, 323–331. doi: 10.1016/j.tree.2009.01.012

Yuan, Y., Sun, Y., Zhao, Y., Liu, C., Chen, X., Li, F., et al. (2019). Identification of floral scent profiles in bearded irises. *Molecules* 24:1773. doi: 10.3390/molecules24091773

Conflict of Interest: DÁ is co-owner of the Las Cabezuelas Sociedad Cooperativa. Samples were provided by the company. The results obtained in the current paper were not influenced by any commercial interest.

The remaining authors declare that the research was conducted in the absence of any commercial or financial relationships that could be construed as a potential conflict of interest.

frontiers in Plant Science

ORIGINAL RESEARCH
published: 12 March 2021
doi: 10.3389/fpls.2021.541171

In vitro Regeneration of Clematis Plants in the Nikita Botanical Garden via Somatic Embryogenesis and Organogenesis

Irina Mitrofanova[1], Natalia Ivanova[1], Tatyana Kuzmina[2], Olga Mitrofanova[1] and Natalya Zubkova[3]*

[1] Plant Biotechnology and Virology Laboratory, Plant Developmental Biology, Biotechnology and Biosafety Department, FSFIS "The Nikita Botanical Gardens – National Scientific Center of the RAS," Yalta, Russia, [2] Structural Botany and Plant Reproductive Biology Section, FSFIS "The Nikita Botanical Gardens – National Scientific Center of the RAS," Yalta, Russia, [3] Floriculture Laboratory, FSFIS "The Nikita Botanical Gardens – National Scientific Center of the RAS," Yalta, Russia

The effects of growth regulators, namely, 6-benzylaminopurine (BAP) and thidiazuron (TDZ), on the morphogenic capacity of 13 cultivars of clematis plants, in terms of their morphological structure formation, shoot regeneration, and somatic embryo development, are presented. The clematis cultivars 'Alpinist,' 'Ay-Nor,' 'Bal Tsvetov,' 'Crimson Star,' 'Crystal Fountain,' 'Kosmicheskaya Melodiya,' 'Lesnaya Opera,' 'Madame Julia Correvon,' 'Nevesta,' 'Nikitsky Rosovyi,' 'Nikolay Rubtsov,' 'Serenada Kryma,' and 'Vechniy Zov' were taken in collection plots of the Nikita Botanical Gardens for use in study. After explant sterilization with 70% ethanol (1 min), 0.3–0.4% Cl_2 (15 min), and 1% thimerosal (10 min), 1-cm long segments with a single node were introduced to an *in vitro* culture. The explants were established on the basal MS medium supplemented with BAP (2.20–8.90 μM) and 0.049 μM NAA, or TDZ (3.0; 6.0, and 9.0 μM) with 30 g/L sucrose and 9 g/L agar. The medium with 0.89 μM BAP served as the control. Culture vessels and test tubes with the explants were maintained in plant growth chamber-controlled conditions: with a 16-h photoperiod, under cool-white light fluorescent lamps with a light intensity of 37.5 μmol m^{-2} s^{-1}, at a temperature of 24 ± 1°C. Histological analysis demonstrated that adventitious bud and somatic embryo formation in studied clematis cultivars occurred at numerous areas of active meristematic cell zones. The main role of plant growth regulators and its concentrations were demonstrated. It was determined that maximum adventitious microshoot regeneration without any morphological abnormalities formed on the media supplemented with BAP or TDZ. 4.40 μM BAP, or 6.0 μM TDZ were optimal cytokinin concentrations for micropropagation. The explants of 'Alpinist,' 'Ay-Nor,' 'Crimson Star,' 'Crystal Fountain,' 'Nevesta,' and 'Serenada Kryma' cultivars displayed high morphogenetic capacity under *in vitro* culturing. During indirect somatic embryogenesis, light intensity 37.5 μmol m^{-2} s^{-1} stimulated a higher-number somatic embryo formation and a temperature of 26°C affected somatic embryo development. Active formation of primary and secondary somatic embryos was also demonstrated. 2.20 μM BAP with 0.09 μM IBA affected the high-number somatic embryo formation for eight cultivars. Secondary somatic embryogenesis by the same concentration of BAP was induced.

OPEN ACCESS

Edited by:
Renato Paiva, Universidade Federal de Lavras, Brazil

Reviewed by:
Giancarlo Fascella, Council for Agricultural and Economics Research (CREA), Italy
Diego Rocha, Federal University of Goiás, Brazil
Wagner Campos Otoni, Universidade Federal de Viçosa, Brazil
Anwar Shahzad, Aligarh Muslim University, India

***Correspondence:**
Irina Mitrofanova
irimitrofanova@yandex.ru

Specialty section:
This article was submitted to Crop and Product Physiology, a section of the journal Frontiers in Plant Science

Received: *07 March 2020*
Accepted: *09 February 2021*
Published: *12 March 2021*

Citation:
Mitrofanova I, Ivanova N, Kuzmina T, Mitrofanova O and Zubkova N (2021) In vitro Regeneration of Clematis Plants in the Nikita Botanical Garden via Somatic Embryogenesis and Organogenesis. Front. Plant Sci. 12:541171. doi: 10.3389/fpls.2021.541171

The frequency of secondary somatic embryogenesis was higher in 'Crystal Fountain' (100%), 'Crimson Star' (100%), 'Nevesta' (97%), and 'Ay-Nor' (92%) cultivars. Based on these results, the methodology for direct somatic embryogenesis and organogenesis of studied clematis cultivars has been developed.

Keywords: somatic embryo, shoots regeneration, morphogenic capacity, plantlets, clematis

INTRODUCTION

The genus *Clematis* L. belongs to the buttercup family (Ranunculaceae Juss.) and includes ca. 300 species and over 3000 cultivars (Surhone et al., 2011; Zubkova, 2015) of this mainly perennial flowering liana. Clematis plants are widely used in ornamental gardening, but many species are also of great economic importance, since they contain essential oils, tannins, vitamin C, and volatiles, and some may have fungicidal effects that inhibit the development of molds. Accordingly, certain clematis species are used in Tibetan, Chinese, and Mongolian medicine (Lloyd, 1989; Toomey and Leeds, 2001; Zubkova, 2015).

In the Nikita Botanical Gardens—National Scientific Center of the Russian Academy of Sciences (NBG-NSC), a collection of clematis plants has been created that includes 24 species and 236 cultivars of native and foreign origin (Zubkova, 2015). This valuable collection helps to conserve clematis species, yet also provides a variety of biomorphological features in one place for investigation, in addition to research into the breeding stages of these plants. The large-flowered clematis plants are propagated vegetatively because most hybrid cultivars lack viable seed progeny. Furthermore, many of the cultivated seedlings are often not decorative enough and fail to preserve the aesthetic features of the mother plant. Adding to this, clematis plants are significantly affected by viral, fungal, and bacterial diseases, which not only reduce their decorativeness but also limit their mass propagation. Over the past few years, a number of viral pathogens that cause various disease symptoms on the leaves and flowers of tested plants have been found in the NBG-NSC collection (Zakubanskiy et al., 2018a,b).

Conventional propagation methods are inefficient for obtaining sufficient amounts of both planting and raw material to meet the demand of the food and medical industries. Modern biotechnological methods, using such plant cell properties as totipotency, can ensure the successful multiplication of rare and single plants, as well as new cultivars and breeding forms. Depending on the species and cultivar used, however, morphogenetic capacity in plants can be realized in various ways. One of these is organogenesis, which is the process of *de novo* formation of adventitious shoots and roots from an unorganized growing callus mass (i.e., indirect regeneration) and directly from leaf, stem, germ, or flower cells (i.e., direct regeneration) (Pati et al., 2004; Pipino et al., 2008, 2010; Deepika and Kanwar, 2010). Another mode of plant regeneration is somatic embryogenesis, which is the process of asexual development of embryogenic structures from reproductive and somatic tissues in a way similar to zygotic embryogenesis (Mitrofanova, 2011; Nic-Can et al., 2015; Germanà and Lambardi, 2016; Martins et al., 2016; Loyola-Vargas and Ochoa-Alejo, 2018). In studying the plant regeneration features of *Clematis integrifolia* × *C. viticella*, no genetic changes in plants were obtained via somatic embryogenesis (Mandegaran and Sieber, 2000). Genome variability was established in regenerated clematis plants of the cultivar 'Serenada Kryma,' but this was dependent on direct and indirect somatic embryogenesis or organogenesis (Mitrofanova et al., 2003). Using ISSR primers, 105 amplicons were found of which six were polymorphic, with the heterogeneity of clematis plants averaging 5.7%, and this detected variability due to indirect organogenesis. In later work, a comparative study of morphogenetic capacity realization via direct somatic embryogenesis was carried out in eight clematis cultivars; this established the effects of biotic and abiotic factors upon somatic embryo formation and plant regeneration during cultivation (Mitrofanova et al., 2007; Mitrofanova, 2011). Indirect somatic embryogenesis has been described in the clematis cultivar 'Multi-Blue,' for which histological analysis confirmed the formation of embryogenic structures in its callus (Zhang et al., 2011). Earlier, anatomical research had confirmed the formation of morphogenic structures and adventitious roots as a result of organogenesis in the same cultivar (Zhang et al., 2010). Among clematis hybrids, a comparative histological study of embryogenic structures and zygotic embryos revealed differences in their *in vitro* development (Arene et al., 2006). Chlorophyll and anthocyanin content of microshoots in *C. pitcheri* Torr. & A. Gray was changed during its cultivation on culture media having different concentrations of nitrogen and sucrose under variable temperature conditions (Kawa-Miszczak et al., 2009). More recently, the biochemical and physiological characteristics of some clematis cultivars grown in the NBG-NSC open-field collection and cultured *in vitro* have been presented (Brailko et al., 2018), and the effect of ribavirin on clematis plant improvement was reported in Ivanova et al. (2018). The medicinal plants *C. gouriana* Roxb. and *C. heynei* M.A. Rau were successfully regenerated by direct and indirect organogenesis, with the resulting plants then planted for *ex vitro* acclimatization (Naika and Krishna, 2008; Chavan et al., 2012). Finally, the effects of various substrates on microshoots and softwood stem cuttings' rooting were studied in five clematis cultivars from the *Atragene* section (Kreen et al., 2002).

In sum, as evinced by the foregoing, the morphogenetic capacity of certain clematis cultivars and species has been mainly studied, albeit to various extents. However, we still lack a thorough and robust evaluation of the regenerative capacity of clematis plants cultured *in vitro* under the combined influences from multiple factors, namely, genotype, plant growth regulators, light intensity, and temperature (among others). Therefore, this study's main objective was to assess the morphogenetic potential

of explants from 13 clematis cultivars, under the influence of various culture factors, at stages of formation induction of morphogenic structures and plant regeneration. The obtained results could be used for the subsequent propagation of healthy plants and the creation of an *in vitro* gene bank.

MATERIALS AND METHODS

Plant Material and Culture Establishment

The mother plants of 13 clematis cultivars—'Alpinist,' 'Ay-Nor,' 'Bal Tsvetov,' 'Crimson Star,' 'Crystal Fountain,' 'Kosmicheskaya Melodiya,' 'Lesnaya Opera,' 'Madame Julia Correvon,' 'Nevesta,' 'Nikitsky Rosovyi,' 'Nikolay Rubtsov,' 'Serenada Kryma,' and 'Vechniy Zov'—grown at the collection plot of ornamental plants in the Nikita Botanical Gardens (Yalta, Russian Federation) were used as explant sources (**Table 1**).

The investigations were carried out in the Laboratory of Plant Biotechnology and Virology of the Plant Developmental Biology, Biotechnology and Biosafety Department, Federal State Funded Institution of Science "The Nikita Botanical Gardens—National Scientific Center of the RAS." To obtain an aseptic culture, plant material isolated in January–February 2017–2019 underwent sequential sterilization in this way: 1 min in 70% ethanol, followed by 15 min in 0.3–0.4% chlorine-containing solution (Dez Tab, China) and 10 min in 1% thimerosal solution (Sigma, United States) with 1–2 drops of Tween 20. After adding each reagent, the shoot segments 3 cm long were washed three times in sterile distilled water. After shoot segments had been surface-sterilized with a contamination frequency not greater than 10%, the nodal explants 1 cm long with axillary buds were established in test tubes on the MS (Murashige and Skoog, 1962) induction culture medium supplemented with 0.89 μM 6-benzylaminopurine (BAP, Sigma, United States), 30 g/L sucrose, and 9 g/L of agar (PanReac, Spain). For the elimination of viral infection, 10 mg/L virocid ribavirin (Virazole, 1-β-D-ribofuranosyl-1,2,4-triazole-3-carboxamide, Duchefa Biochemie, Holland) was added to the medium at the explant introduction stage. Subculturing was carried out at 2 week intervals. All plant handling and treatment were done under aseptic conditions in the SC2 laminar flow cabinet (ESCO, Singapore).

Organogenesis Induction and Plant Regeneration

To induce organogenesis and plant regeneration, 1 cm long microshoots and microcuttings of 13 cultivars were used. Explants were placed on the MS culture medium with MS vitamins and various concentrations of plant growth regulators, 2.20–8.90 μM BAP in combination with 0.049 μM α-naphthylacetic acid (NAA, Duchefa Biochemie, Holland) or 3.0–9.0 μM thidiazuron (TDZ, Duchefa Biochemie, Holland), supplemented with 100 mg/L myo-inositol (Duchefa Biochemie, Holland), 30 g/L sucrose, and 9 g/L of agar. As the control, the MS medium with 0.89 μM BAP was used. Medium pH was 5.7–5.8 for all culture media, which were autoclaved at 120°C for 7–12 min in a LAC 5060S sterilizer (Daihan Labtech, South Korea). Plant growth regulators and vitamins were first sterilized by cold filtration through MILLEX® GP filters (0.22 μm) and then added to the media after the autoclaving. Culture vessels (100 or 250 ml jars) with explants were maintained in "BIOTRON" growth chambers and in a plant growth chamber (MLR-352-PE, Panasonic, Japan) at 24 ± 1°C, with a 16-h photoperiod under cool-white light fluorescent lamps (Philips TL, 40 W: light intensity of 37.5 μmol m^{-2} s^{-1}). Subculturing of each cultivar was carried out at 3–4 week intervals.

Somatic Embryogenesis Induction and Plant Regeneration

For the induction experiments of indirect somatic embryogenesis, clematis microshoots or microcuttings with one or two internodes of 13 cultivars were cultured on a solidified MS medium with MS vitamins, 100 mg/L of myo-inositol, and different plant growth regulators. Firstly, microcuttings of 13 cultivars with one or two internodes were placed on an MS culture medium supplemented with 1.8 μM zeatin and 0.04 μM indole-3-butyric acid (IBA, Duchefa Biochemie, Holland) to induce callus formation. To induce embryogenic callus formation, 0.9–6.8 μM zeatin (Sigma, United States) or 0.9–6.8 μM 2,4-D (2,4-dichlorophenoxyacetic acid; Sigma, United States) was used. Callus was placed on an MS medium with 0.4–4.6 μM zeatin in order to induced indirect somatic embryogenesis. To induce the secondary somatic embryo formation, primary somatic embryos derived from callus were transferred to media with 0.4–4.6 μM IBA and 1.8 μM zeatin. All culture media were supplemented with 30 g/L sucrose, and the media were solidified with 9 g/L agar. The plant growth regulator-free medium served as the control. Culture vessels (100 or 250 ml jars) with microshoots, microcuttings, and somatic embryos were maintained at 24 ± 1°C, with a 16-h photoperiod under cool-white light fluorescent lamps (Philips TL, 40 W: 37.5 μmol m^{-2} s^{-1} light intensity). In an experiment with somatic embryogenesis induction, the culture vessels with calli were placed in growth chambers with temperature (20–30°C) and light intensity (5–60 μmol m^{-2} s^{-1}) regulated under a 16-h photoperiod. Subculturing of each cultivar was carried out at 3–4 week intervals.

For the direct somatic embryogenesis induction experiments, firstly, vegetative buds of 13 clematis cultivars were cultured on an MS medium with 0.44–8.9 μM BAP and 0.09 μM IBA. The plant growth regulator-free medium served as the control. Due to the low rate of direct somatic embryogenesis induction in five cultivars, the main experiments with 'Ay-Nor,' 'Crimson Star,' 'Crystal Fountain,' 'Kosmicheskaya Melodiya,' 'Lesnaya Opera,' 'Nevesta,' 'Serenada Kryma,' and 'Vechniy Zov' cultivars were followed. For the secondary somatic embryogenesis induction, the primary somatic embryos were cultured on an MS medium with 0.89 or 2.22 μM BAP. All culture media were supplemented with 30 g/L sucrose and media solidified with 9 g/L agar. Cultures were incubated at 24 ± 1°C, 16-h photoperiod under cool-white light fluorescent lamps (Philips TL, 40 W: 37.5 μmol m^{-2} s^{-1} light intensity). Subculturing of each cultivar was carried out at 3–4 week intervals.

Histological Analysis of Morphogenic Structures

The morphogenic structures that formed during organogenesis and somatic embryogenesis of clematis cultivars were subjected to histological analysis. Four cultivars with six regenerating structures from each (a total of 24 samples) were analyzed: 'Alpinist' and 'Madame Julia Correvon'—bud conglomerates, 'Crystal Fountain'—callus with somatic embryos, and 'Nevesta' and 'Crystal Fountain'—somatic embryos on different stages. Slides for this analysis were prepared according to the commonly used methods (refer to Zhinkina and Voronova, 2000). Briefly, callus and somatic embryo conglomerates were fixed in formalin-aceto-alcohol (FAA) solution; after fixation, the material was transferred to a 70% ethyl alcohol solution. For material dehydration, isopropyl alcohol was used. Then, the material was maintained in two xylene solutions, for 2 h in each, and then embedded in paraffin. Infiltration with paraffin was performed over a 7 day period. Serial sections of callus and somatic embryo conglomerates were cut into the slides 10 μm thick with a rotary semiautomatic microtome RMD-3000 (MedTehnikaPoint, Russia) and affixed to permanent slides stained with methyl green–pyronin and alcian blue, as well as hematoxylin and alcian blue. The slides were analyzed under a light microscope (AxioScope A.1, Zeiss, Germany) using the bright-field method and polarized light observations. Microphotographs were taken with an AxioCam ERc 5s unit (Zeiss, Germany) and an IXUS 265HS digital camera (Canon Inc., Japan). To analyze the obtained images, AxioVisionRel v4.8.2 software (Zeiss, GmbH, Germany) was used.

Statistical Analyses

Each treatment consisted of five glass vessels with four explants of each clematis cultivar (microshoots, microcuttings, callus, somatic embryos), repeated in triplicate. The number of vegetative buds regenerating the callus or somatic embryos was recorded after 2–4 weeks of culturing. The frequency of this regeneration was calculated as the average percentage of buds or calli which formed morphogenic structures. The number of

TABLE 1 | List of investigated clematis cultivars.

Cultivar	Garden group	Originator and main characteristics
Alpinist	Lanuginosa	M.A. Beskaravaynaya, 1974. Shrubby climber up to 2.5–3.5 m long. Leaves are compound, with 5 leaflets, green and light green. Flowers are lilac white, 10.0–14.0 cm in diameter; anthers are yellow. Remontant cultivar of late flowering (II decade of July). Pruning group #2.
Ay-Nor	Viticella	M.A. Beskaravaynaya, 1972. Shrubby climber up to 2.0 m long. Leaves are compound, ternate, rarely simple, dark green. Flowers are pink, with a blue-purple tinge at the base, 12.0–14.0 cm in diameter; anthers are yellow. Remontant cultivar with the middle terms flowering (III decade of May). Pruning group #3.
Bal Tsvetov	Lanuginosa	M.A. Beskaravaynaya, 1972. Shrubby climber up to 2.0 m long. Leaves are compound, ternate, dark green. Flowers are violet-blue with a violet-purple stripe in the center of the sepals, 15.0–18.0 cm in diameter; anthers are brown. Remontant cultivar of early flowering (II decade of May). Pruning group #2.
Crimson Star	Lanuginosa	Shrubby climber up to 2.0–2.5 m long. Leaves are ternate, green. Flowers are crimson red, 10.0–12.0 cm in diameter; anthers are yellow. Remontant cultivar of early flowering (II decade of May). Pruning group #2.
Crystal Fountain [syn. 'Fairy Blue']	Florida	H. Hayakawa, 1994. Shrubby climber up to 2.0 m long. Leaves are ternate, green. Flowers are purple-blue, pale blue in the center, double, 10.5–12.0 cm in diameter. Remontant cultivar of early flowering (II decade of May). Pruning group #2.
Kosmicheskaya Melodiya	Jackmanii	A.N. Volosenko-Valenis, M.A. Beskaravaynaya, 1965. Shrubby climber up to 3.0 m long. Leaves are compound, with 3–5 leaflets. Purple flowers, 10.0–14.0 cm. in diameter; anthers are of dark cherry color. Profusely and long blooming cultivar with the middle terms of flowering (III decade of May). Pruning group #3.
Lesnaya Opera	Viticella	M.A. Beskaravaynaya, 1972. Shrubby climber up to 2.5–2.8 m long. Leaves are compound, consisting of three green leaves. Flowers are white, 10.0–14.0 cm in diameter; anthers are yellow. Remontant cultivar with the middle terms of flowering (III decade of May). Pruning group #3.
Madame Julia Correvon	Viticella	F. Morel, 1900. Shrubby climber up to 2.2–3.0 m long. Leaves are unequally pinnate, the lower ones are often ternate, green. Flowers are red-purple, 10.5–12.5 cm in diameter; anthers are yellow. Profusely blooming remontant cultivar with the middle terms of flowering (III decade of May). Pruning group #3.
Nevesta	Lanuginosa	M.A. Beskaravaynaya, E.A. Donyushkina, 1979. Shrubby climber up to 3.0 m long. Leaves are simple and compound, consist of 1–3–5–7 green and light green leaves that burn in the sun. Flowers are grayish-white 13.0–15.0 cm in diameter; anthers are yellow. Remontant cultivar with the middle terms of flowering (I decade of June). Pruning group #2.
Nikitsky Rozovyi	Viticella	A.N. Volosenko-Valenis, M.A. Beskaravaynaya, 1965. Shrubby climber up to 2.1–2.8 m long. Leaves are ternate, green and dark green, not burn in the sun. Flowers are pink, 12.0–14.0 cm in diameter; anthers are light yellow. Remontant cultivar with the middle terms of flowering (II decade of June). Pruning group #3.
Nikolay Rubtsov	Jackmanii	A.N. Volosenko-Valenis, M.A. Beskaravaynaya, 1967. Shrubby climber up to 2.5 m long. Leaves are compound, with 3–5 leaflets, green. Pink flowers are lighter toward the center, 10.0–17.0 cm in diameter; anthers are light yellow. Remontant cultivar of early flowering (II decade of May). Pruning group #3.
Serenada Kryma	Lanuginosa	M.A. Beskaravaynaya, 1978. Shrubby climber up to 3.5 m long. Ternate leaves of dark green color. Flowers are violet-blue, with carmine veins and a light middle, 13.5–17.0 cm in diameter; anthers are brownish. Remontant cultivar of early flowering (II decade of May). Pruning group #2.
Vechniy Zov	Jackmanii	M.A. Beskaravaynaya, E.A. Donyushkina, 2003. Shrubby climber up to 2.5–3.0 m long. Leaves are compound, with 3–5 leaflets, green, and light green. Flowers are crimson-pink, 0.9–10.0 cm in diameter; anthers are light yellow. Remontant cultivar with the middle terms of flowering (III decade of May). Pruning group #3.

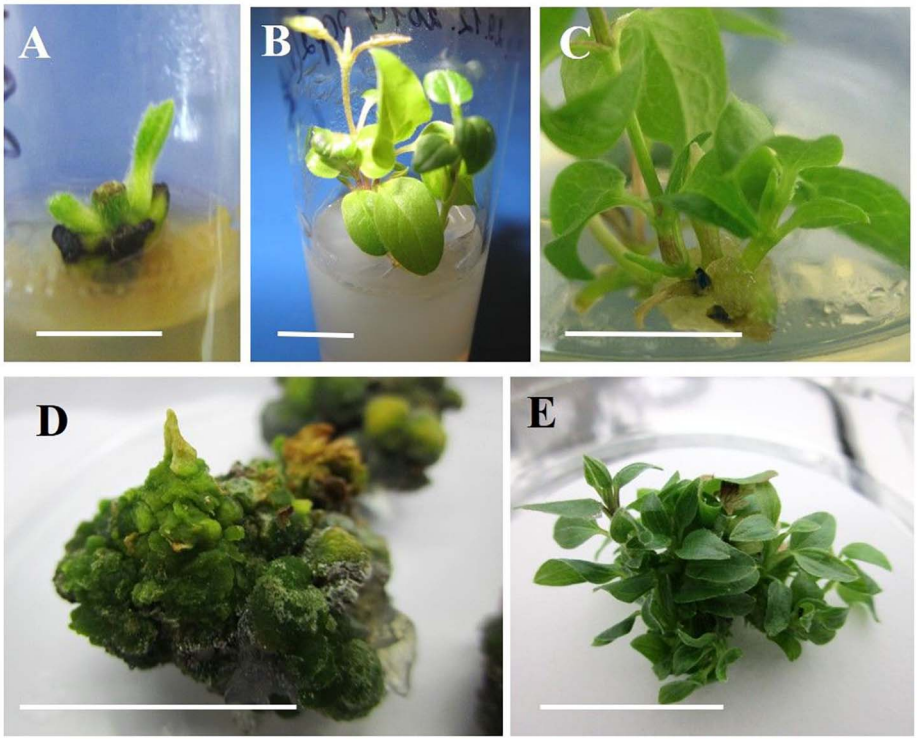

FIGURE 1 | Indirect organogenesis in vegetative buds of clematis plant cultivars. **(A)** Vegetative bud development in the cultivar 'Alpinist' on the MS medium supplemented with 0.89 μM BAP and 10 mg/L ribavirin at the 1st week of culturing. **(B)** Single microshoots of the cultivar 'Alpinist' obtained on the same culture medium at 2–3 weeks after establishing the culture. **(C)** Callus formation on the base of a microshoot of the cultivar 'Serenada Kryma' on the medium with 4.40 μM BAP and 0.049 μM. **(D)** Compact morphogenic callus of cultivar 'Crystal Fountain' on the culture medium with 6 μM TDZ. **(E)** Conglomerate of the regenerated microshoots of cultivar 'Crystal Fountain' after 3–4 weeks of callus culturing with 6 μM TDZ. Scale bars correspond to 1 cm **(A–E)**.

TABLE 2 | Regeneration responses of different clematis cultivars that were cultured on the MS medium with 6-benzylaminopurine (BAP) and 0.049 μM NAA, or thidiazuron (TDZ).

Cultivar*	Average number of regenerated microshoots per explant						
	BAP (μM)				TDZ (μM)		
	0.89**	2.2	4.4	8.9	3.0	6.0	9.0
A	0.7 ± 0.3^{ab}	1.5 ± 0.9^{a}	2.5 ± 1.1^{a}	3.0 ± 1.2^{a}	5.0 ± 1.4^{a}	7.0 ± 1.6^{a}	11.0 ± 1.9^{a}
A-N	0.4 ± 0.1^{de}	1.1 ± 0.2^{ef}	1.9 ± 0.8^{de}	2.3 ± 0.7^{c}	2.4 ± 0.8^{bc}	4.0 ± 1.8^{bc}	5.0 ± 1.0^{ef}
BT	0.4 ± 0.1^{de}	1.2 ± 0.4^{cd}	2.3 ± 1.2^{ab}	2.7 ± 1.2^{b}	2.3 ± 1.3^{c}	4.2 ± 1.7^{b}	6.0 ± 0.8^{bc}
CS	0.6 ± 0.4^{bc}	1.4 ± 0.6^{ab}	2.3 ± 1.2^{ab}	2.3 ± 1.1^{c}	4.1 ± 1.7^{a}	7.2 ± 1.6^{a}	8.6 ± 1.2^{ab}
CF	0.7 ± 0.2^{b}	1.3 ± 0.9^{bc}	2.4 ± 1.1^{a}	2.8 ± 1.2^{a}	5.0 ± 1.6^{a}	7.0 ± 1.9^{a}	9.0 ± 2.0^{a}
KM	0.3 ± 0.1^{f}	0.9 ± 0.6^{gh}	1.4 ± 0.8^{h}	2.1 ± 0.9^{e}	1.8 ± 0.6^{tf}	3.0 ± 1.8^{fg}	4.4 ± 1.8^{gh}
LO	0.4 ± 0.1^{de}	0.7 ± 0.6^{h}	1.2 ± 0.6^{i}	2.2 ± 0.4^{d}	1.6 ± 0.2^{gh}	3.0 ± 1.8^{fg}	4.4 ± 1.8^{gh}
MJC	0.6 ± 0.3^{cd}	1.4 ± 0.7^{ab}	2.3 ± 1.3^{ab}	2.7 ± 1.4^{ab}	3.0 ± 1.3^{ab}	4.0 ± 1.8^{bc}	6.0 ± 1.0^{bc}
N	0.4 ± 0.1^{de}	1.4 ± 0.3^{b}	2.1 ± 1.2^{bc}	3.0 ± 1.2^{a}	2.3 ± 1.3^{c}	3.7 ± 1.3^{de}	6.0 ± 0.8^{bc}
NRo	0.6 ± 0.3^{cd}	1.3 ± 0.9^{bc}	2.2 ± 1.3^{ab}	2.7 ± 1.2^{b}	3.0 ± 1.3^{ab}	4.0 ± 1.8^{bc}	6.0 ± 1.0^{bc}
NRu	0.4 ± 0.1^{de}	1.6 ± 0.8^{a}	2.2 ± 1.1^{bc}	2.8 ± 0.9^{a}	2.0 ± 0.6^{d}	3.8 ± 0.9^{cd}	8.6 ± 1.4^{ab}
SK	0.7 ± 0.3^{b}	1.4 ± 0.6^{ab}	2.2 ± 1.1^{bc}	2.6 ± 1.2^{b}	2.8 ± 1.1^{ab}	4.4 ± 1.8^{ab}	6.7 ± 1.3^{b}
VZ	0.8 ± 0.1^{a}	1.1 ± 0.2^{ef}	1.7 ± 0.3^{h}	2.2 ± 0.4^{d}	2.6 ± 1.2^{b}	4.0 ± 1.8^{bc}	5.8 ± 1.1^{d}

**A, 'Alpinist'; A-N, 'Ay-Nor'; BT, 'Bal Tsvetov'; CS, 'Crimson Star'; CF, 'Crystal Fountain'; KM, 'Kosmicheskaya Melodiya'; LO, 'Lesnaya Opera'; MJC, 'Madame Julia Correvon'; N, 'Nevesta'; NRo, 'Nikitsky Rosovyi'; NRu, 'Nikolay Rubtsov'; SK, 'Serenada Kryma'; VZ, 'Vechniy Zov.' **Control culture medium. Different lowercase letters in the same column indicated the significant difference at $P \leq 0.05$ (Duncan's multiple-range test).*

TABLE 3 | Morphometric characteristics (means ± SE) of adventitious microshoots in 13 clematis cultivars cultured on the MS medium with different concentrations of thidiazuron (TDZ) and 6-benzylaminopurine (BAP) with 0.049 μM NAA.

Cultivar	TDZ (μM)					
	3.0		6.0		9.0	
	Length of explant (cm)	Number of internodes	Length of explant (cm)	Number of internodes	Length of explant (cm)	Number of internodes
Alpinist	1.1 ± 0.01^{a}	3.0^{a}	1.5 ± 0.04^{a}	4.0^{a}	1.9 ± 0.04^{a}	4.6 ± 0.2^{a}
Ay-Nor	1.0 ± 0.01^{ab}	2.0^{b}	1.2 ± 0.01^{bc}	3.0^{bc}	1.6 ± 0.03^{bc}	4.0^{bc}
Bal Tsvetov	1.0 ± 0.03^{ab}	3.0^{a}	1.3 ± 0.04^{b}	3.2 ± 0.3^{ab}	1.8 ± 0.03^{ab}	4.4 ± 0.4^{ab}
Crimson Star'	0.9 ± 0.01^{b}	2.0^{b}	1.2 ± 0.01^{bc}	3.0^{bc}	1.6 ± 0.03^{bc}	4.0^{bc}
Crystal Fountain	1.1 ± 0.03^{a}	3.0^{a}	1.5 ± 0.04^{a}	4.0^{a}	1.8 ± 0.03^{ab}	4.4 ± 0.4^{ab}
Kosmicheskaya Melodiya	0.9 ± 0.01^{b}	2.0^{b}	1.2 ± 0.01^{bc}	3.0^{bc}	1.6 ± 0.03^{bc}	4.0^{bc}
Lesnaya Opera	1.0 ± 0.02^{ab}	2.0^{b}	1.2 ± 0.01^{bc}	3.0^{bc}	1.6 ± 0.03^{bc}	4.0^{bc}
Madame Julia Correvon	1.0 ± 0.02^{ab}	3.0^{a}	1.4 ± 0.03^{ab}	3.2 ± 0.3^{ab}	1.7 ± 0.04^{b}	4.0^{bc}
Nevesta	0.9 ± 0.01^{b}	2.0^{b}	1.2 ± 0.01^{bc}	3.0^{bc}	1.6 ± 0.03^{bc}	4.0^{bc}
Nikitsky Rosovyi	1.0 ± 0.04^{ab}	3.0^{a}	1.4 ± 0.02^{ab}	3.2 ± 0.3^{ab}	1.8 ± 0.04^{ab}	4.0^{bc}
Nikolay Rubtsov	0.8 ± 0.01^{c}	2.0^{b}	1.1 ± 0.01^{de}	3.0^{bc}	1.4 ± 0.02^{de}	3.6 ± 0.2^{cd}
Serenada Kryma	0.9 ± 0.01^{b}	2.0^{b}	1.2 ± 0.01^{bc}	3.0^{bc}	1.6 ± 0.03^{bc}	4.0^{bc}
Vechniy Zov	0.9 ± 0.01^{b}	2.0^{b}	1.2 ± 0.01^{bc}	3.0^{bc}	1.6 ± 0.03^{bc}	4.0^{bc}
	BAP (μM)					
	2.2		4.4		8.9	
Alpinist	1.08 ± 0.04^{ab}	3.0^{ab}	1.4 ± 0.03^{a}	3.2 ± 0.2^{a}	2.0 ± 0.04^{a}	3.4 ± 0.2^{ab}
Ay-Nor	0.86 ± 0.01^{d}	2.0^{bc}	1.0 ± 0.01^{cd}	3.0^{a}	1.4 ± 0.02^{cd}	3.0^{c}
Bal Tsvetov	1.20 ± 0.03^{a}	3.0^{ab}	1.2 ± 0.04^{ab}	3.0^{a}	1.9 ± 0.02^{ab}	3.4 ± 0.1^{ab}
Crimson Star'	0.90 ± 0.02^{bc}	2.0^{bc}	1.0 ± 0.01^{cd}	3.0^{a}	1.6 ± 0.02^{bc}	4.0^{a}
Crystal Fountain	1.10 ± 0.03^{a}	3.0^{ab}	1.3 ± 0.02^{ab}	3.0^{a}	1.7 ± 0.04^{b}	3.0^{c}
Kosmicheskaya Melodiya	0.96 ± 0.02^{ab}	2.0^{bc}	1.0 ± 0.01^{cd}	3.0^{a}	1.4 ± 0.02^{cd}	3.0^{c}
Lesnaya Opera	0.90 ± 0.02^{bc}	2.0^{bc}	1.2 ± 0.01^{ab}	3.0^{a}	1.7 ± 0.04^{b}	4.0^{a}
Madame Julia Correvon	0.98 ± 0.02^{ab}	3.0^{ab}	1.3 ± 0.03^{ab}	3.0^{a}	1.7 ± 0.04^{b}	3.0^{c}
Nevesta	0.96 ± 0.02^{ab}	2.0^{bc}	1.2 ± 0.01^{ab}	3.0^{a}	1.6 ± 0.02^{bc}	3.0^{c}
Nikitsky Rosovyi	1.06 ± 0.04^{ab}	3.2 ± 0.2^{a}	1.3 ± 0.02^{ab}	3.0^{a}	1.8 ± 0.04^{ab}	3.2 ± 0.3^{b}
Nikolay Rubtsov	0.90 ± 0.02^{bc}	2.0^{bc}	1.1 ± 0.01^{bc}	3.0^{a}	1.7 ± 0.04^{b}	4.0^{a}
Serenada Kryma	0.88 ± 0.01^{c}	2.0^{bc}	1.0 ± 0.01^{cd}	3.0^{a}	1.9 ± 0.02^{ab}	4.0^{a}
Vechniy Zov	0.98 ± 0.02^{ab}	2.0^{bc}	1.2 ± 0.01^{ab}	3.0^{a}	1.8 ± 0.04^{ab}	4.0^{a}

Control medium—with 0.89 μM BAP: for all cultivars, the length of microshoots was 0.6 cm with a single internode. Different lowercase letters in the same column indicated the significant difference at $P \leq 0.05$ (Duncan's multiple-range test).

microshoots per explant was determined on a monthly basis. All of the obtained data were processed in the Statistica for Windows program v10.0 (StatSoft, Inc., United States). The data of amount of regenerated microshoots per explant, length of explant, and number of internodes were analyzed, statistically averaging analysis of the variance (ANOVA) and standard deviation to find the variability between the different treatments. To see which means differed from each other and to indicate the significant difference during the analysis of percentage and number of investigated explants, Duncan's multiple-range test was used (at $P < 0.05$).

RESULTS

Organogenesis Induction and Plant Regeneration

The factors inducing explant development during *in vitro* culturing were the type and concentration of plant growth regulators in the culture medium. The initiation of vegetative bud development on the MS medium supplemented with 0.89 μM BAP and 10 mg/L ribavirin was observed within the 1st week of culturing in all 13 investigated cultivars (**Figure 1A**). Single microshoot formations were observed in the 2nd week of culturing, but at the base of these microshoots, the callus was poorly formed (**Figures 1B,C**). Both the obtained microshoots and calli were segmented after culturing on the MS medium with 2.20–4.40 μM BAP and 0.049 μM NAA, or the medium with 3.0–9.0 μM TDZ. In the case of BAP, it marginally increased the number of adventitious buds and microshoot regeneration. After 3–4 weeks of culturing, the best response in terms of the amount of morphogenic callus, adventitious buds, and microshoot formation was observed on the medium with TDZ (**Figures 1D,E**). A high number of regenerated shoots per explant on culture media supplemented with 6 and 9 μM TDZ were obtained (**Table 2**). Among the tested genotypes on the medium with 6 μM of TDZ, the cultivars 'Alpinist,' 'Crystal Fountain' and 'Crimson Star' regenerated seven microshoots per

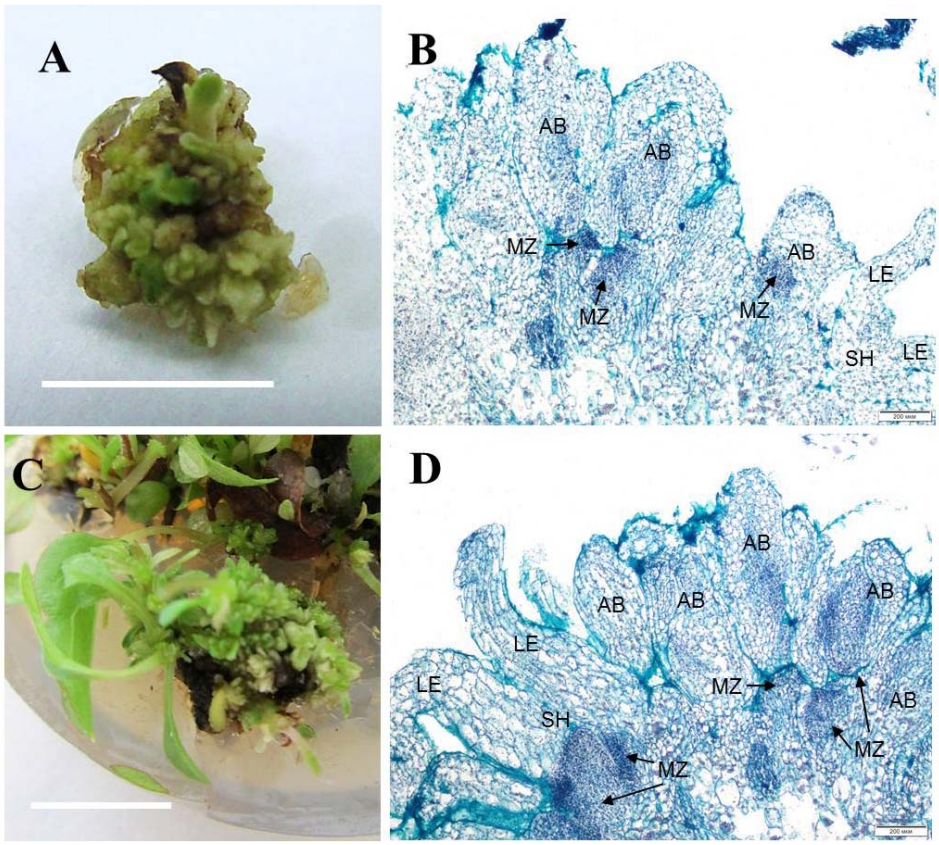

FIGURE 2 | Adventitious vegetative bud regeneration via direct organogenesis of clematis plant cultivars. **(A)** Adventitious bud formation in the cultivar 'Alpinist' on the culture medium with 6 μM TDZ. **(B)** Meristematic tombs that developed on the surface of explants of the cultivar 'Alpinist' from active meristematic zones on the medium with 6 μM TDZ. Bright field. Hematoxylin and alcian blue straining. MZ—meristematic zone, AB—adventitious bud, two-leaf-stage shoot (SH—shoot, LE—leaf). **(C)** Adventitious bud and microshoot regeneration from a gemmiferous callus of the cultivar 'Madam Julia Correvon' on the culture medium with 6 μM TDZ. **(D)** Mass regeneration of adventitious buds and primordial leaves that developed directly on the explant surface in the cultivar 'Madam Julia Correvon' on the medium with 6 μM TDZ. Bright field. The section was stained with hematoxylin and alcian blue. MZ—meristematic zone, AB—adventitious bud, two-leaf-stage shoot (SH—shoot, LE—leaf). Scale bars correspond to 1 cm **(A)**, 200 μm **(B,D)**, and 0.5 cm **(C)**.

explant, while 'Bal Tsvetov,' Madame Julia Correvon,' 'Nikitsky Rosovyi,' 'Serenada Kryma,' 'Vechniy Zov' developed more than four microshoots per explant. On the medium with 9 μM TDZ, in some cultivars, their number of adventitious microshoots increased to 11 per explant; however, some of these were hydrated. Therefore, for further micropropagation, 6 μM TDZ was used, which provided more adventitious microshoot regeneration. Using 4.40 μM BAP with 0.049 μM NAA in the experiments also promoted adventitious shoot formation in all the studied clematis cultivars. For example, 2.5 microshoots per explant were obtained for the cultivar 'Alpinist,' and likewise 2.4 microshoots per explant for 'Crystal Fountain' and 2.3 microshoots per explant for both 'Nikitsky Rosovyi' and 'Madame Julia Correvon' (**Table 2**).

On the culture medium with 6 μM TDZ, the average length of each microshoot was 1.5 cm for the cultivars 'Alpinist' and 'Crystal Fountain,' 1.4 cm for 'Nikitsky Rosovyi' and 'Madame Julia Correvon,' and 1.3 cm for 'Bal Tsvetov' (**Table 3**). Correspondingly, on the culture medium supplemented with 9 μM TDZ, the number of internodes was 3.6–4.6 per microshoot; these microshoots were all well-formed, were compact, have shortened internodes, and have a bright-green color. Further subculturing increased the number of adventitious shoots. Thus, in clematis cultivars 'Alpinist,' 'Crystal Fountain,' 'Madame Julia Correvon,' and 'Crimson Star,' the number of shoots had reached 10–15 per explant after 4 weeks of culturing. The average number of internodes on culture media, supplemented with 2.20–8.90 μM BAP and 0.049 μM NAA, was 3.0–3.4 per microshoot. At the same time, some elongated internodes were noted, as well as the formation of single, disproportionately large leaves. The data presented in **Table 3** demonstrates that adventitious microshoots of maximum length developed on the culture medium supplemented with 8.90 μM BAP and 0.049 μM NAA. Yet, higher BAP concentration stimulated the appearance of numerous morphological changes: the formation of strained shoots, hydration, twisting of leaves, the presence of a yellow-green color, and the formation of loose callus at the base of explants, all of which hindered their development and its pace.

TABLE 4 | Callogenesis induction (means ± SE) in investigated clematis cultivars on culture medium with 2,4-dichlorophenoxyacetic acid (2,4-D) and zeatin.

Concentration of plant growth regulators (μM)	Number of explants with the callus formed (%)	Callus type (%)		
		E	NE	*M*
Control (0)	0^{h}	0^{f}	0^{e}	0^{d}
2,4-D				
0.9	0^{h}	0^{f}	0^{e}	0^{d}
1.8	0^{h}	0^{f}	0^{e}	0^{d}
2.3	0^{h}	0^{f}	0^{e}	0^{d}
4.6	56 ± 2.3^{bc}	0^{f}	100^{a}	0^{d}
6.8	50 ± 2.1^{de}	0^{f}	100^{a}	0^{d}
Zeatin				
0.9	20 ± 2.2^{fg}	20 ± 2.6^{de}	56 ± 3.3^{b}	14 ± 1.2^{ab}
1.8	100^{a}	100^{a}	0^{e}	0^{d}
2.3	100^{a}	83 ± 6.3^{ab}	6 ± 0.1^{cd}	11 ± 0.7^{ab}
4.6	80 ± 6.1^{ab}	56 ± 3.9^{ab}	14 ± 1.3^{bc}	30 ± 4.6^{a}
6.8	70 ± 7.2^{ab}	23 ± 1.2^{bc}	70 ± 4.2^{ab}	7 ± 0.9^{bc}

E, embryogenic; NE, non-embryogenic; M, mixed; 0, no callus formed. Different lowercase letters in the same column indicated the significant difference at $P \leq 0.05$ (Duncan's multiple-range test).

Zones of meristematic activity were mainly noted at the base of adventitious buds and microshoots, where a small amount of callus formed. Some adventitious buds regenerated directly from the determinate cells on the surface of microshoot segments. For the cultivar 'Alpinist,' histological analysis of the callus structure showed that it was produced by parenchymal cells, containing some inclusions, had anisotropic features, and glowed in polarized light, which is typical of starch and other polysaccharides (**Figures 2A,B**). Meristematically active cells were characterized by a dense cytoplasm and being large in size relative to the cell and nucleus (high nucleus/cytoplasm ratio); it was these areas that gave rise to meristems with primordial leaves. Subsequently, the development of meristems resulted in the formation of microshoots accompanied by the differentiated vascular elements connecting the apical zone of the microshoot and leaf-like structures to the main parenchymal tissue of the callus. On the periphery of the gemmiferous callus structures, small meristematic cells were evident. The callus of the cultivar 'Madam Julia Correvon' was produced by parenchymal tissue, the cells of which contained anisotropic inclusions. This cultivar was characterized by secondary cytodifferentiation of cells into the vascular elements that formed numerous centers of the vascular system. In the area of parenchymal cells, we also noted the presence of meristematic zones and the development of adventitious buds and microshoots (**Figures 2C,D**).

Somatic Embryogenesis Induction and Plant Regeneration

Indirect Somatic Embryogenesis

During the microcutting of 13 cultivars with one or two internodes culturing on the MS culture medium supplemented with 1.8 μM zeatin and 0.04 μM IBA, a compact callus of light-green color formed at the base of those explants. The obtained callus was first separated from the base of the microshoots and microcuttings, then divided into segments, and transferred onto a culture medium supplemented with 2,4-D or zeatin. **Table 4** reports the effects of various 2,4-D and zeatin concentrations on the induction of the embryogenic callus formation in the clematis cultivars. The presence of 2,4-D in a culture medium at the concentrations of either 4.6 μM or 6.8 μM stimulated the formation of a loosened non-embryogenic white-colored callus. In the course of this experiment, we noted that on the medium containing 1.8 μM of zeatin, cultured callus cells actively divided and, accordingly, the resulting callus had a dense structure. Embryogenic calli also formed on the media supplemented with 2.3 μM and 4.6 μM zeatin (**Figure 3A**). Mixed callus formation was seen to occur on the culture media containing 0.9 μM, 2.3 μM, 4.6 μM, or 6.9 μM zeatin. We should note that the appearance of meristematic zones and meristematic tubercles happened within a month's time in this experimental work. These formations differed from the cell mass in having a bright-green color. Histological analysis revealed that two types of cells were present in the embryogenic mass: in the first, cells had a relatively dense cytoplasm, fairly thin cell walls, and very small vacuoles (embryogenic cells); the second was characterized by cells with a turbid cytoplasm and large vacuoles (non-embryogenic cells). On the 3 day of culturing, the processes of mitotic and meristematic activity in the embryogenic cell mass had become activated. Proembryo development was initiated, with asymmetric cell division occurring most often directly inside the callus (**Figure 3B**). Only after 12–14 days of culturing, the formation of somatic embryos from induced embryogenic determinate cells in the clematis callus was observed. Nonetheless, only during days 27–30 of culture was the embryo itself clearly visible. The presence of zeatin in the medium induced the formation of bipolar structures on the surface and inside the callus. It was possible to observe the appearance of somatic embryos on the callus surface only after 5–7 days of their formation in the callus itself (**Figure 3C**). All new non-zygotic embryos were light green in color and tightly connected to the maternal callus. During the cultivation of this callus structure, a part of the embryoids did separate easily, but due to the callus formed on their surface, this impeded their further development (**Figure 3D**).

Table 5 presents the results of somatic embryo formation as affected by various zeatin concentrations tested. The most embryoids per explant (25) were obtained on an MS medium supplemented with 1.8 μM zeatin after 4 weeks of culture. Some primary clematis explants formed spherical structures with a diameter of 0.1–0.5 mm, yet these did not develop into full-fledged plants. Germination of somatic embryos occurred during a rather long period of cultivation (30–40 days); at first, some root growth was noted, and in the next stage, the hypocotyl had emerged and was colored green. During the somatic embryo culturing, the simultaneous germination of the shoot and root was most often observed. A typical feature of clematis seedlings was the formation and growth of two roots apparently lacking root hairs. Somatic embryoids

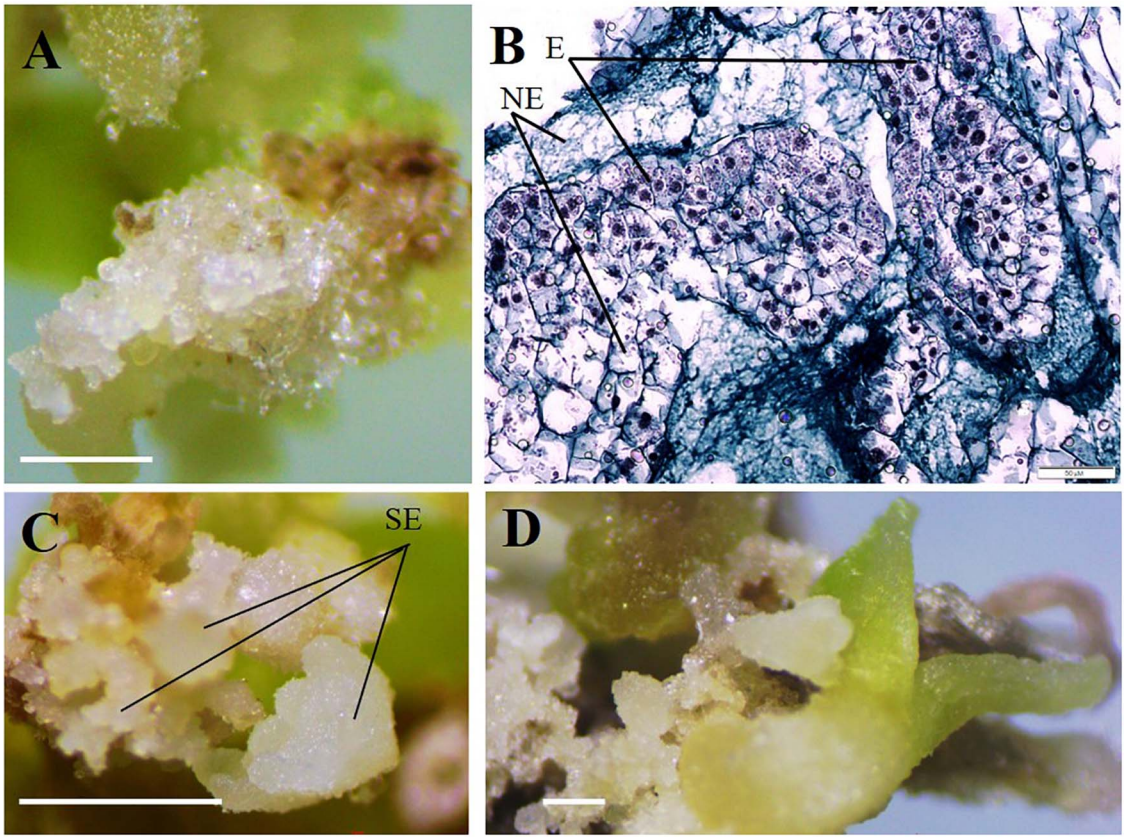

FIGURE 3 | Indirect somatic embryogenesis in calli of clematis plant cultivars. **(A)** Embryogenic callus formation on the surface of vegetative buds and microshoot segments in the cultivar 'Serenada Kryma' on the MS medium with 2.3 μM or 4.6 μM zeatin. **(B)** Non-embryogenic (NE) and embryogenic (E) cells in the callus of the cultivar 'Crystal Fountain,' periclinal cell division, and somatic embryoid realization. Bright field. Methyl green–pyronin and alcian blue. **(C)** Somatic embryoids (SE) of the cultivar 'Crystal Fountain' at different stages of development on the medium with 1.8 μM zeatin. **(D)** Growth of somatic embryoids and the callus formed on surfaces of primary embryoids. Scale bars correspond to 1 mm **(A,C,D)** and 50 μm **(B)**.

on the culture medium with a zeatin concentration higher than 1.8 μM were not occurred. Subsequent subcultures of somatic embryos put on media with 1.8 μM zeatin combined with various concentrations of IBA led to secondary embryoids forming on the surface of already formed and developing somatic embryos (**Table 6**). During this experiment, it was found that, in the course of indirect somatic embryogenesis, the frequency of secondary embryogenesis depended on the IBA concentration in the culture medium. The optimal IBA concentration was 0.9 μM, in that under this condition the average number of embryoids per explant was 30, for which the average embryo size was up to 1.5 mm at the onset of the cotyledon stage. With 30 days of light exposure, the size of these cotyledons increased, to 4–5 mm. The resulting secondary embryoids easily separated from each other: their culturing showed that if the embryoid was placed in a culture vessel, it actively developed and grew, reaching 9–10 mm after 30–45 days. Nevertheless, high concentrations of IBA inhibited the embryoids' growth and significantly reduced the frequency of secondary embryogenesis in the clematis cultivars. Further, additional somatic embryos formed, in the zone between the hypocotyl and epicotyl, on the seedlings that had developed from the primary embryoids.

Our research also uncovered the effects of physical factors upon the development of somatic embryos in the calli of clematis. In this case, a drop or rise in temperature significantly influenced the number of developed somatic embryoids (**Figure 4A**), with the best results for development somatic embryoid obtained at 26°C, when its numbers reached 30 units per explant. Among the embryos, however, embryoids at different stages of their development could be observed, spanning the globular to cotyledon phase.

Unlike temperature, light intensity did have a significant effect upon the number of formed somatic embryoids. Reducing the light level to 12.5 μmol m^{-2} s^{-1} strongly reduced the number of somatic embryos formation (**Figure 4B**). Optimal light intensity was determined to be 37.5 μmol m^{-2} s^{-1}. Under this condition, the number of formed embryoids reached 25–30 per explant. All the somatic embryos were bright green in color. Additionally, 80% of explants cultured at this light intensity level had competent cells; that is, they were capable of forming non-zygotic embryos.

TABLE 5 | Clematis somatic embryos' formation (means ± SE) on the MS medium with zeatin.

Cultivar*	Number of explants with formed embryoids (%)		
	Zeatin concentration (μM)		
	0.4	0.9	1.8
A	24 ± 0.63^{ab}	31 ± 0.87^{ab}	89 ± 1.0^{ab}
A-N	18 ± 0.54^{cd}	21 ± 0.80^{ef}	73 ± 0.77^{ef}
BT	22 ± 0.52^{c}	28 ± 0.82^{bc}	86 ± 1.02^{cd}
CS	23 ± 0.47^{ab}	29 ± 0.92^{bc}	89 ± 0.87
CF	23 ± 0.52^{ab}	30 ± 1.21^{ab}	86 ± 1.37^{cd}
KM	16 ± 0.58^{fg}	20 ± 0.88^{gh}	72 ± 0.87^{g}
LO	17 ± 0.70^{ef}	21 ± 0.94^{ef}	72 ± 0.86^{g}
MJC	16 ± 0.67^{fg}	19 ± 0.92^{i}	71 ± 1.20^{gh}
N	26 ± 0.89^{a}	35 ± 0.82^{a}	92 ± 0.95^{a}
NRo	15 ± 0.87^{hi}	19 ± 0.77^{i}	72 ± 0.95^{g}
NRu	18 ± 0.61^{cd}	22 ± 0.80^{cd}	75 ± 1.03^{de}
SK	25 ± 0.87^{a}	30 ± 0.92^{ab}	90 ± 1.04^{ab}
VZ	17 ± 0.86^{ef}	20 ± 1.32^{gh}	73 ± 1.15^{ef}

Cultivar	Number of formed somatic embryos per explant					
	2 weeks	4 weeks	2 weeks	4 weeks	2 weeks	4 weeks
A	0	4 ± 0.47^{ab}	3 ± 0.37^{a}	8 ± 0.39^{a}	13 ± 0.71^{a}	28 ± 0.87^{a}
A-N	0	4 ± 0.37^{ab}	2 ± 0.37^{ab}	7 ± 0.37^{ab}	10 ± 0.58^{b}	24 ± 1.17^{bc}
BT	0	4 ± 0.37^{ab}	2 ± 0.26^{ab}	7 ± 0.49^{ab}	10 ± 0.47^{b}	26 ± 0.70^{ab}
CS	0	4 ± 0.47^{ab}	3 ± 0.33^{a}	7 ± 0.63^{ab}	11 ± 0.42^{ab}	26 ± 1.03^{ab}
CF	0	4 ± 0.63^{ab}	2 ± 0.30^{ab}	7 ± 0.37^{ab}	9 ± 0.39^{bc}	27 ± 0.70^{ab}
KM	0	4 ± 0.45^{ab}	2 ± 0.37^{ab}	6 ± 0.33^{bc}	8 ± 0.76^{d}	22 ± 0.67^{cd}
LO	0	4 ± 0.56^{ab}	1 ± 0.21^{bc}	7 ± 0.54^{ab}	9 ± 0.56^{bc}	22 ± 0.87^{cd}
MJC	0	3 ± 0.58^{bc}	1 ± 0.15^{bc}	6 ± 0.42^{bc}	9 ± 0.58^{bc}	23 ± 1.04^{bc}
N	0	5 ± 0.39^{a}	3 ± 0.37^{a}	8 ± 0.39^{a}	13 ± 0.87^{a}	29 ± 0.98^{a}
NRo	0	4 ± 0.52^{ab}	1 ± 0.30^{bc}	7 ± 0.56^{ab}	9 ± 0.37^{bc}	24 ± 1.26^{bc}
NRu	0	4 ± 0.52^{ab}	2 ± 0.30^{ab}	6 ± 0.45^{bc}	9 ± 0.52^{bc}	24 ± 0.93^{bc}
SK	0	5 ± 0.76^{a}	2 ± 0.30^{ab}	8 ± 0.37^{a}	12 ± 0.63^{ab}	27 ± 0.61^{ab}
VZ	0	3 ± 0.60^{bc}	2 ± 0.30^{ab}	7 ± 0.37^{ab}	8 ± 0.67^{d}	23 ± 0.52^{bc}

**A, 'Alpinist'; A-N, 'Ay-Nor'; BT, 'Bal Tsvetov'; CS, 'Crimson Star'; CF, 'Crystal Fountain'; KM, 'Kosmicheskaya Melodiya'; LO, 'Lesnaya Opera'; MJC, 'Madame Julia Correvon'; N, 'Nevesta'; NRo, 'Nikitsky Rosovyi'; NRu, 'Nikolay Rubtsov'; SK, 'Serenada Kryma'; VZ, 'Vechniy Zov.' Control medium—free plant growth regulator medium. Different lowercase letters in the same column indicated the significant difference at P ≤ 0.05 (Duncan's multiple-range test).*

Direct Somatic Embryogenesis

For the induction of direct somatic embryogenesis, BAP was used in various concentrations (0.44–8.9 μM) in the combination with a fixed IBA concentration (0.09 μM). Through this experimental work, firstly, we were able to induce direct somatic embryogenesis in all 13 studied clematis cultivars, but a genotypic influence was discernable: at 30 days since the buds were placed on media for culturing, the number of somatic embryos formed was different for each cultivar *in vitro*. At the base of the buds in 'Alpinist,' 'Bal Tsvetov,' 'Madame Julia Correvon,' 'Nikitsky Rosovyi,' and 'Serenada Kryma' cultivars, only single somatic embryos were formed. Secondly, we found that the ability of explants to form embryoids depended on the BAP concentrations. The optimal BAP concentration was 2.20 μM, in that this promoted the induction of somatic embryogenesis and the formation of the maximum number of embryos in 'Ay-Nor,' 'Crimson Star,' 'Crystal Fountain,' 'Kosmicheskaya Melodiya,' 'Lesnaya Opera,' 'Nevesta,' 'Serenada Kryma,' and 'Vechniy Zov' cultivars (**Figure 5**). In the control medium lacking any plant growth regulators, the development of microshoots was observed occasionally in some cultivars ('Crystal Fountain,' 'Crimson Star,' 'Kosmicheskaya Melodiya,' 'Lesnaya Opera'). Increasing the BAP concentration to 4.40 μM also promoted shoot formation, rather than the formation of embryoids; however, far fewer microshoots emerged than when cultured on a medium supplemented with 2.20 μM of BAP. Moreover, we noted that the buds of clematis cultivars from the groups Lanuginosa and Florida displayed a higher morphogenetic capacity. The number of somatic embryos in 'Nevesta' cultivar was ca. 40 per explant. The formation of somatic embryos always took place directly on the surface of vegetative buds, most often in the zone of apex meristematic cells (**Figure 6A**). After 20 days of culturing, the formation of

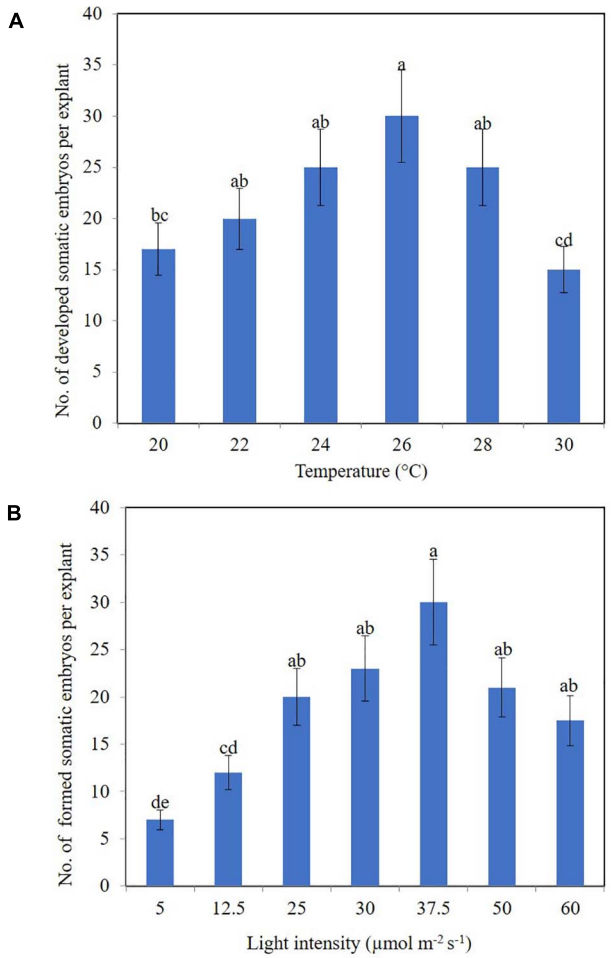

FIGURE 4 | Somatic embryoids' regeneration of clematis plant cultivars on the medium with 1.8 μM zeatin under different culturing conditions: temperature **(A)** and light intensity **(B)**. Bars represent the mean ± SE (n = 3). Bars marked with different letters indicate statistically different values between the realized morphogenic capacity of explants via somatic embryogenesis, at different temperatures and light intensities, according to Duncan's test ($P \leq 0.05$). The experiments were performed three times.

multiple globular structures was evident; they were absolutely smooth, round, or slightly oblong in shape, and light green and yellow in color. Initially, these structures lay very close to each other (**Figures 6B,C**). In this form, at the same time they could be up to the heart, torpedo, or cotyledon stages. After 30–40 days of culturing, the embryoids began to separate from each other somewhat easily (**Figure 6D**), but the extent to which this process occurred depended on the clematis cultivar. The somatic embryos of 'Crystal Fountain,' 'Nevesta,' 'Crimson Star,' and 'Ay-Nor' were those that best separated from each other. A typical feature of embryoids during this period was root germination, after which regeneration of the microshoot began (**Figures 6C,D**). The average root and shoot length after 14 days of germination did not significantly differ among the cultivars. After germination and 21 days of culturing, the roots became actively developed in the cultivars 'Nevesta,' 'Crimson Star,' 'Vechniy Zov,' and 'Ay-Nor,' whose average lengths were 4.8, 4.5, 4.2, and 3.9 cm, respectively. Further, seedlings of the cultivars 'Nevesta,' 'Crimson Star,' and 'Ay-Nor' formed between 2.1 and 2.5 roots per explant.

The frequency of secondary embryogenesis varied across the studied cultivars. A high embryogenesis rate, upward of 65%–100%, was observed in the cultivars 'Nevesta,' 'Crimson Star,' 'Serenada Kryma,' 'Crystal Fountain,' and 'Ay-Nor' when cultured on the medium with 2.20 μM of BAP and 0.09 μM of IBA (**Table 7**). The three other cultivars showed a low frequency of secondary embryogenesis, which did not exceed 30%–50%. Induction of embryoid formation, development, and plant regeneration occurred on the same culture medium. When somatic embryos selected from the globular, heart, and torpedo stages were placed on media with a reduced BAP content or free of cytokinin, the embryoid's development halted and could go 2–3 weeks without any signs of growth. Thus, these embryos could be grouped by size and stage of development, for later propagation in a biotechnological system, if necessary.

Secondary embryos most often formed along the edges of the somatic embryoids' cotyledons. Nonetheless, embryo formation directly from the apical zone of embryoids was also noted. Initially, the formation of transparent round structures was observed, but then they became white and increased in size (**Figure 6E**). Since this process occurred in light, globular embryoids were stained green and had a smooth shiny surface. Though the embryos were positioned tightly adjacent to each other, they could easily be divided among themselves. The ensuing plantlets developed and formed the cultivar-specific plants (**Figure 6F**), whose overall frequency was 80%–95%, on average.

DISCUSSION

Organogenesis and Somatic Embryogenesis Are the Main Plant Regeneration Modes of Clematis

The widespread use of biotechnological research in the introduction, breeding, and propagation of plants has enabled us to significantly advance our knowledge of plant biology and actively use them in studying morphogenesis via somatic embryogenesis and organogenesis. It is well known that exogenous factors significantly affect the realized morphogenetic capacity of plant tissues and organs; hence, only by combining the results from multiple experiments can an efficient system of somatic embryogenesis and organogenesis for a specific crop be developed that would work in most plant species and cultivars. Most of the clematis plants that housed the NBG-NSC open-field collection are old-aged (more than 170 years old). Studies of the morphogenetic capacity of tissues and organs in mature plants *in vitro* are of great scientific and practical interest. Firstly, this is because using mature plant tissue as a primary explant allows one to obtain plant material with economically valuable features. Yet working with mature plant tissues is hampered by the fact that as the plant ages, the processes that result in growth

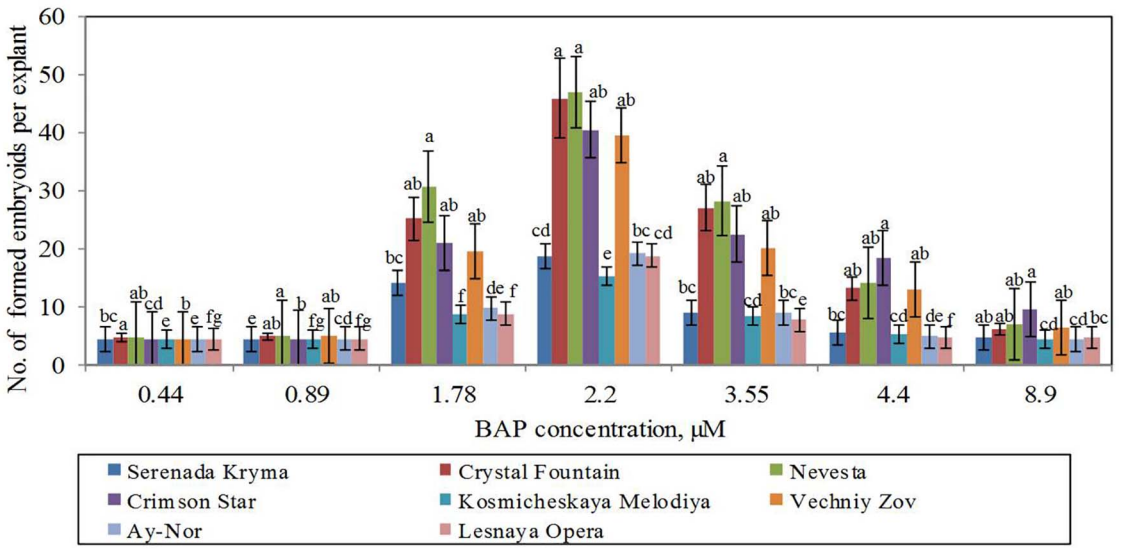

FIGURE 5 | Somatic embryoids' formation in eight cultivars of clematis plants on the MS culture medium containing different BAP concentrations with 0.09 μM IBA. Bars represent the mean ± SE (n = 3), for which different letters represent a significant difference, according to Duncan's test ($P \leq 0.05$).

inhibition and reduced regenerative ability also occur in the plant tissues and organs. Microshoots obtained via regeneration are thus characterized by slow growth and weak rooting ability.

Despite this obstacle, plant scientists all over the world continue to work on this problem, pursuing their research programs and developing more and more biotechnologies applicable to specific crop (Geneve and Preece, 1997; Jain and Ishii, 2003; Preil, 2003; Rout and Jain, 2004; Rout et al., 2006; Mitrofanova, 2011; Germanà and Lambardi, 2016; Mitrofanova et al., 2019; Narvaez et al., 2019). For our study here, we selected 13 cultivars from the main clematis groups that demonstrated different morphogenetic capacities.

It is known that plant growth regulators play an essential role in the interaction of plant cells, tissues, and organs. Low concentrations of these substances are necessary for the induction and regulation of key physiological and morphogenic processes. For each plant species and cultivar, the optimal concentrations and combinations of plant growth regulators in the culture medium could be experimentally deduced. Thus, cytokinins, in addition to enhancing cell division and growth processes, stimulate cell differentiation, histogenesis, and shoot formation; they also affect callus differentiation and induce the development of axillary buds, the growth of lateral shoots, adventitious bud formation, and subsequent regeneration of plants (Kalinin et al., 1992; Kunah, 2005; Mitrofanova, 2011; Loyola-Vargas and Ochoa-Alejo, 2018). In our present work, zeatin, BAP, and TDZ were used as the main cytokinins in tissue and organ culturing of clematis plants. Along with them, the auxins 2,4-D, NAA, and IBA were used to induce the processes of organogenesis and somatic embryogenesis. Each of them performed its function as expected. Auxins, activating the process of cell division and stretching, are required for the formation of vascular and root systems in plants (Horvath et al., 2006; Novikova et al., 2013; Kuluev et al., 2015). Auxin-saturated tissues have an attracting effect, that is, the ability to attract nutrients, which are then deposited as reserves in seeds, fruits, tubers, and root crops or are instead actively used during the growth and development of the meristem. Auxins play a crucial role in cell differentiation. For example, the induction of division in resting vacuolated parenchymal cells from an auxin application is dedifferentiation. Almost immediately, auxin causes the phenomenon of apical dominance by inhibition of axillary soot growth by the continued meristematic activity in shoot apex. The auxin–cytokinin interaction regulates the coordination of the main and lateral shoot formation and growth (Bari and Jones, 2009; Davies, 2010; Fatima and Anis, 2012; Rademacher, 2015; Bhatla, 2018; Yegorova et al., 2019).

Theoretical studies in the field of somatic embryogenesis have shown that the whole embryogenic cell mass is determined by the process of embryoid formation, but this is not entirely true. Only some cells are capable of forming a somatic embryo. Observations of clover and pistachios support the hypothesis that growth regulators initiate asymmetric division and lead to a change in cell polarity (Maheswaran and Williams, 1985; Onay, 2000). It is likely that exogenous plant growth regulators directly change the polarity of the cells by interfering with the pH gradient or the electric field around the cells (Mitrofanova, 2011; Germanà and Lambardi, 2016). In our previously histological analysis of clematis cultivars, we noted the appearance of two distinct cell types: deterministic and non-deterministic (Mitrofanova, 2011). Observations during this experiments revealed no less than seven morphological types of new somatic embryos capable of forming in clematis plants: (1) monocotyledonous, in which the embryoid is formed from one cotyledon, and the second, most often, is underdeveloped or completely reduced; (2) dicotyledonous, which resembles a zygotic embryo in clematis;

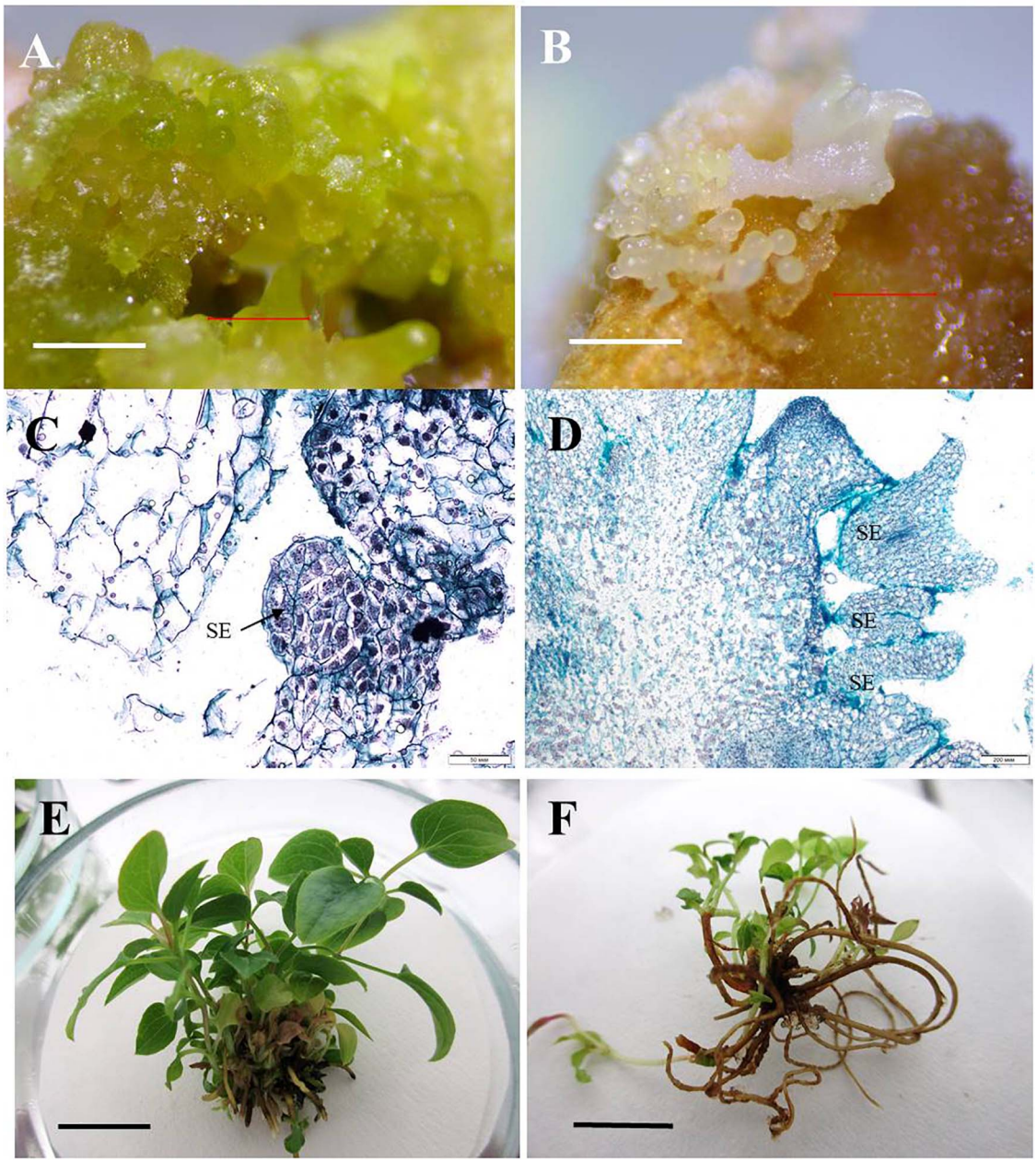

FIGURE 6 | Direct somatic embryogenesis in clematis plant cultivars. **(A)** Globular structures on the surface of a vegetative bud in the cultivar 'Nevesta' on the MS culture medium, with 2.2 μM BAP and 0.09 μM IBA, after 20 days of somatic embryogenesis induction. **(B)** Embryoids on the globular and torpedo growth stages of the cultivar 'Crystal Fountain' on the medium with 2.2 μM BAP and 0.09 μM IBA. **(C)** Meristematic active zone and globular embryoid formation in the cultivar 'Nevesta.' Bright field. Methyl green–pyronin and alcian blue. SE—somatic embryo. **(D)** Somatic embryoids of the cultivar 'Crystal Fountain' at different stages of its development. Bright field. The section was stained with hematoxylin and alcian blue. SE—somatic embryo. **(E)** Plantlets' development from somatic embryoids of the cultivar 'Nevesta.' **(F)** Developed plantlets from somatic embryoids of the cultivar 'Crystal Fountain.' Scale bars correspond to 1 mm **(A,B)**, 50 μm **(C)**, 200 μm **(D)**, and 1 cm **(E,F)**.

(3) polycotyledonous, meaning a newly developing embryoid having three or more cotyledons; (4) tube-like, in which the embryoid cotyledons inosculate in the form of a tube; (5) an embryoid with an elongated hypocotyl and almost reduced cotyledons (the cotyledons of the embryo are very narrow and the apex is not clear in the epicotyl zone); (6) an embryoid similar to a zygotic embryo, thus resembling a zygotic embryo, yet in which development stops at the stage of cotyledon opening, after which the embryoid dies; and (7) an embryoid in the form of an open terry bud, the cotyledons of which grow vigorously and deformed. During the subsequent culturing of all types of somatic embryos and embryo-like structures, we found that only the first

TABLE 6 | Indole-3-butyric acid (IBA) concentration influence on the frequency of secondary embryogenesis (means ± SE) in investigated clematis cultivars cultured on the MS medium with 1.8 μM zeatin.

Cultivar*	Number of explants with secondary embryoids formed (%)			
	IBA concentration (μM)			
	0.4	0.9	1.8	4.6
A	36 ± 0.94^{ab}	99 ± 0.42^{ab}	30 ± 0.88^{ab}	10 ± 0.52^{b}
A-N	26 ± 0.79^{cd}	90 ± 0.83^{e}	28 ± 0.87^{bc}	8 ± 0.49^{c}
BT	36 ± 0.92^{ab}	98 ± 0.52^{ab}	30 ± 1.01^{ab}	10 ± 0.52^{b}
CS	43 ± 0.73^{ab}	100^{a}	32 ± 0.77^{a}	11 ± 0.63^{ab}
CF	33 ± 0.99^{ab}	98 ± 0.84^{ab}	32 ± 0.95^{a}	11 ± 0.71^{ab}
KM	28 ± 1.12^{bc}	92 ± 1.05^{bc}	27 ± 0.65^{cd}	7 ± 0.58^{de}
LO	29 ± 0.89^{b}	90 ± 0.97^{e}	25 ± 0.68	7 ± 0.37^{de}
MJC	25 ± 1.0^{ef}	92 ± 0.91^{bc}	27 ± 0.83^{cd}	8 ± 0.39^{c}
N	46 ± 1.15^{a}	100^{a}	32 ± 0.58^{a}	13 ± 0.77^{a}
NRo	23 ± 0.99^{gh}	91 ± 0.82^{cd}	28 ± 0.82^{bc}	9 ± 0.58^{bc}
NRu	30 ± 1.17^{ab}	92 ± 1.32^{bc}	29 ± 0.98^{ab}	9 ± 0.73^{bc}
SK	46 ± 1.04^{a}	100^{a}	30 ± 0.86^{ab}	12 ± 0.67^{ab}
VZ	27 ± 1.28^{c}	93 ± 1.31^{b}	27 ± 0.58^{cd}	9 ± 0.52^{bc}

Cultivar	Number of secondary embryoids per explant							
	2 weeks	4 weeks	2 weeks	4 weeks	2 weeks	4 weeks	2 weeks	4 weeks
A	3 ± 0.39^{c}	14 ± 0.63^{ab}	18 ± 0.82^{a}	30 ± 0.77^{ab}	2 ± 0.33^{bc}	5 ± 0.33^{b}	0	3 ± 0.30^{ab}
A-N	2 ± 0.33^{de}	9 ± 0.52^{de}	13 ± 0.56^{cd}	33 ± 0.73^{ab}	4 ± 0.52^{a}	6 ± 0.37^{ab}	0	2 ± 0.21^{b}
BT	3 ± 0.26^{c}	13 ± 0.54^{ab}	17 ± 0.83^{ab}	34 ± 0.88^{ab}	2 ± 0.42^{bc}	5 ± 0.63^{b}	0	2 ± 0.21^{b}
CS	4 ± 0.54^{b}	14 ± 0.60^{ab}	17 ± 0.37^{ab}	33 ± 0.84^{ab}	3 ± 0.45^{ab}	5 ± 0.37^{b}	0	2 ± 0.42^{b}
CF	4 ± 0.37^{b}	14 ± 0.73^{ab}	18 ± 0.68^{a}	34 ± 0.63^{ab}	4 ± 0.52^{a}	6 ± 0.52^{ab}	0	4 ± 0.52^{a}
KM	2 ± 0.39^{de}	9 ± 0.63^{de}	12 ± 0.98^{ef}	28 ± 0.70^{bc}	2 ± 0.33^{bc}	5 ± 0.37^{b}	0	2 ± 0.33^{b}
LO	2 ± 0.45^{de}	9 ± 0.61^{de}	13 ± 0.88^{cd}	25 ± 0.83^{ef}	0^{d}	4 ± 0.33^{cd}	0	2 ± 0.37^{b}
MJC	2 ± 0.37^{de}	11 ± 0.58^{bc}	12 ± 0.82^{ef}	26 ± 0.58^{d}	0^{d}	4 ± 0.42^{cd}	0	0^{c}
N	6 ± 0.52^{a}	18 ± 0.65^{a}	18 ± 0.58^{a}	36 ± 0.73^{a}	4 ± 0.47^{a}	7 ± 0.37a	0	4 ± 0.30^{a}
NRo	2 ± 0.39^{de}	11 ± 0.60^{bc}	13 ± 0.76^{cd}	26 ± 0.49^{d}	0^{d}	4 ± 0.37^{cd}	0	0^{c}
NRu	2 ± 0.26^{de}	11 ± 0.54^{bc}	14 ± 0.70^{cd}	27 ± 0.61^{c}	2 ± 0.37^{bc}	4 ± 0.21^{cd}	0	0^{c}
SK	5 ± 0.49^{ab}	12 ± 0.67^{b}	17 ± 0.63^{ab}	33 ± 0.75^{ab}	3 ± 0.37^{ab}	6 ± 0.37^{ab}	0	3 ± 0.33^{ab}
VZ	2 ± 0.30^{de}	9 ± 0.42^{de}	13 ± 0.89^{cd}	25 ± 0.47^{ef}	0^{d}	4 ± 0.42^{cd}	0	2 ± 0.37^{b}

**A, 'Alpinist'; A-N, 'Ay-Nor'; BT, 'Bal Tsvetov'; CS, 'Crimson Star'; CF, 'Crystal Fountain'; KM, 'Kosmicheskaya Melodiya'; LO, 'Lesnaya Opera'; MJC, 'Madame Julia Correvon'; N, 'Nevesta'; NRo, 'Nikitsky Rosovyi'; NRu, 'Nikolay Rubtsov'; SK, 'Serenada Kryma'; VZ, 'Vechniy Zov.' Control medium—culture medium with 1.8 μM zeatin. Different lowercase letters in the same column indicated the significant difference at $P \leq 0.05$ (Duncan's multiple-range test).*

four morphological types of embryoid featured the capacity to regenerate plants (Mitrofanova, 2011).

There is a close correlation between the effect of light quality on a plant and the accumulation of certain hormones and growth inhibitors in it. We also know that the optimum temperature for culturing somatic embryos of most plant species is in the range of 21–25°C (Merkle, 1997; Han and Park, 1999; Jain and Ishii, 2003; Jain and Gupta, 2018). A temperature of 28°C stimulated the induction of somatic embryogenesis in *Pinus halepensis* Miller (Pereira et al., 2016), whereas we detected a high number of developed somatic embryos in clematis cultivars at a lower temperature of 26°C. Our results for how light intensity influenced the production of clematis somatic embryos differ markedly from those obtained in other crops, since those embryoids are usually formed in the dark (Oliveira and Pais, 1992; Mitrofanova et al., 1997; Dal Vesco and Guerra, 2001; Germanà and Lambardi, 2016; Corredoira et al., 2019). This once again confirms the need for thorough studies of the regeneration features and selection of suitable culture conditions for each new species or plant cultivar.

Direct somatic embryogenesis is the process of somatic embryoid formation directly from cells of somatic explant tissues *in vitro* and is thus more similar to the formation of zygotic embryos. This plant regeneration pathway was first described 40 years ago (Sharp et al., 1980). The somatic development of the embryos is very flexible, as it is influenced by both the plant genotype itself and the culture conditions applied to it. Since then, the main parameters determining somatic embryogenesis have been elucidated, namely, being the type of explant, the stage of the explant's development, and interactions between the culturing conditions and the explant (Souter and Lindsey, 2000; Hamama et al., 2001; Nanda and Rout, 2003; Correia et al., 2011;

Zhang et al., 2011; Nic-Can et al., 2015; Germanà and Lambardi, 2016; Jain and Gupta, 2018; Loyola-Vargas and Ochoa-Alejo, 2018; Corredoira et al., 2019; Mitrofanova et al., 2019).

We had noted that there was a zone of activation of somatic embryo formation; that is, a particular clematis explant of eight cultivars ('Ay-Nor,' 'Crimson Star,' 'Crystal Fountain,' 'Kosmicheskaya Melodiya,' 'Lesnaya Opera,' 'Nevesta,' 'Serenada Kryma,' 'Vechniy Zov') was able to induce somatic embryogenesis, both primary and secondary. This zone of somatic embryogenesis induction ("inducer") in culture vessels could be one or a group of somatic embryos. Perhaps, this driver is the center of *in vitro* plant embryogenesis. It is known that in animals, the reacting system, which undergoes differentiation under the influence of an "inductor," often becomes an inducer for new organs and tissues, and the entire development of the embryo can thus be viewed as a chain of successive induction interactions (Souter and Lindsey, 2000; Fehér and Magyar, 2015). A similar process was observed here in the studied clematis plants. It may be surmised that the "inducer's" effect on neighboring explants manifests via the culture medium into which inducing substances (metabolites and hormones, among others) are released, or, perhaps, this effect comes from the altered electric fields transmitted directly from the explant to the explant within the culture vessel. In our experiments, using the medium on which the "inducer" was cultured to activate the somatic embryogenesis in clematis was not successful. Accordingly, we could rule out the influence from the "inducer" through the culture medium *per se*. Possibly, the action through the medium is short-term in nature and we were not able to fixate this moment. Furthermore, to implement this induction, it is necessary that the cells exposed to the "inducer" have the appropriate competence. When it comes to a biotechnological *in vitro* propagation system, only competent cells are involved in the plant regeneration. In addition, the determination of induced clematis cells occurred after 7–8 days of culturing. Published data on the prevalence of embryogenic capacity in cultured plant cells indicates that, among 10^3–10^4 cells, just one will have the ability to form a somatic embryo (Hari, 1980). On a suspension culture of carrots, an original method was applied, involving the fractionation of the initial cell suspensions and isolation of cell fractions that was characterized by high embryogenic capacity (Fujimura and Komanima, 1979). It is known that applying fractionation methods makes it possible to obtain fractions of single globular, heart-shaped, and torpedo-shaped embryoids and plantlets in preparative amounts (Moiseeva, 1991). In our experiments, the effect of the "inducer" on somatic embryogenesis, expressed in the active formation of adventitious embryos on explants placed on a culture medium, was observed in almost all the clematis cultivars except for 'Kosmicheskaya Melodiya.' For this cultivar, perhaps we were unable to identify such an activation zone for its embryogenic processes. Removal of the "inducer" from the culture vessel significantly reduced the frequency of embryogenesis, or regeneration did not occur at all. Further, it was evident that the "inducer" can operate for a sufficiently long period of time. In some cultivars—'Crystal Fountain,' 'Nevesta,' and 'Crimson Star'—this phenomenon was observed for 2–3 years (unpublished data). Thus, for both primary and secondary somatic embryogenesis, the biotechnological system was the most effective in the clematis groups Lanuginosa and Florida.

TABLE 7 | Secondary embryogenesis (means ± SE) in eight cultivars of clematis during primary somatic embryos culture on the MS medium with 6-benzylaminopurine (BAP) with 0.09 μM IBA.

Cultivar	Frequency of secondary embryogenesis (%)	
	BAP concentration (μM)	
	0.89	2.22
Serenada Kryma	15 ± 1.3^{bc}	65 ± 4.5^{b}
Crystal Fountain	53 ± 3.4^{a}	100^{a}
Nevesta	26 ± 2.2^{ab}	97 ± 4.3^{a}
Crimson Star	21 ± 1.6^{ab}	100^{a}
Kosmicheskaya Melodiya	0^{d}	35 ± 3.1^{de}
Vechniy Zov	0^{d}	57 ± 3.9^{bc}
Ay-Nor	26 ± 3.3^{ab}	92 ± 4.2^{ab}
Lesnaya Opera	0^{d}	32 ± 1.5^{e}

Control medium—free plant growth regulator medium. Different lowercase letters in the same column indicated the significant difference at $P \leq 0.05$ (Duncan's multiple-range test).

Despite available reports on the critical period in the process of *in vitro* plant regeneration and the need to change culture media at various stages of morphogenesis (Merkle, 1997; Zhang et al., 2011; Germanà and Lambardi, 2016; Jain and Gupta, 2018; Loyola-Vargas and Ochoa-Alejo, 2018; Tomiczak et al., 2019), in the studied clematis cultivars we found no evidence of cell addiction to exogenous plant growth regulators and a delayed somatic embryogenesis process. In our opinion, the somatic embryo or group of somatic embryos, temperature, and light intensity are the critical factors for stimulating or inhibiting the process of proembryo formation.

In conclusion, based on our study's results, we were able to reveal that further development of somatic embryoids and obtaining full-fledged regenerated plantlets of clematis cultivars were successful under the same conditions as the induction of somatic embryogenesis. Unlike many other plant species, in whose propagation via somatic embryogenesis two or three culture media are sequentially used (Correia et al., 2011; Corredoira et al., 2015; Jain and Gupta, 2018), our clematis somatic embryos and regenerants from them were obtained on the same medium. An interesting fact was that BAP was used effectively as an exogenous cytokinin to induce the direct regeneration of somatic embryos. It is known that in most plants cultured *in vitro*, the auxin 2.4-D is typically used for this goal (Raghavan, 2004; Mitrofanova, 2011; Correia et al., 2012; de Alcantara et al., 2014; Germanà and Lambardi, 2016; Jain and Gupta, 2018). The next stage of investigation is to discover the molecular mechanisms underpinning the realization of morphogenetic potential, especially the induction of somatic embryogenesis, the development and death of somatic embryos, and plant formation (Smertenko and Bozhkov, 2014; Fehér, 2019; Méndez-Hernández et al., 2019).

CONCLUSION

In this comprehensive study, both organogenesis and somatic embryogenesis were induced from the base of clematis vegetative buds and microshoots. An increase in regenerative capacity by adventitious shoot formation for 13 cultivars due to TDZ in the culture medium was demonstrated. The main factors affecting the process of somatic embryo regeneration were established: these were mother plant genotype, plant growth regulators (BAP and IBA), a temperature of 26°C, and a light intensity of 37.5 μmol m^{-2} s^{-1}. In the case of indirect somatic embryogenesis as well as its direct one, secondary embryogenesis was always observed, which significantly increased the frequency of somatic embryo formation and plant regeneration for eight cultivars. As far as we know, this is the first time that the studied clematis cultivars have been shown to possess high morphogenic capacity due to a combination of methods applied during their plant micropropagation. In so doing, this work paves the way for the letting use biotechnology tools, such as cryobank creation, genomic investigation, and genetic transformation (among others). The presented system of somatic embryogenesis allows not only for the propagation of clematis species and cultivars but also to save plant material in the form of slow-growing *in vitro* collections which could be used to replenish collections of other botanical gardens.

DATA AVAILABILITY STATEMENT

The raw data supporting the conclusions of this article will be made available by the authors, without undue reservation.

AUTHOR CONTRIBUTIONS

NZ provided the clematis cultivars for the experiments and assigned them to groups. NI and OM were responsible for the *in vitro* experiments. TK prepared the permanent slides for microscopy, and TK and IM described and analyzed them. IM and OM checked and corrected the manuscript. IM planned this research and its experiments and wrote the manuscript. All coauthors agreed with the content of the manuscript and support its conclusions.

FUNDING

Investigation of clematis plants' organogenesis and induction of somatic embryo formation was funded by the Russian Science Foundation (Grant No. 14-50-00079), while the studies of different factors' influence on clematis somatic embryogenesis were supported by the Ministry of Science and Higher Education of the Russian Federation (ST No. 0829-2019-0038 of the FSFIS "NBG-NSC").

SUPPLEMENTARY MATERIAL

The Supplementary Material for this article can be found online at: https://www.frontiersin.org/articles/10.3389/fpls.2021.541171/full#supplementary-material

REFERENCES

Arene, L., Chevalier, M., Cognee, N., Tellier, M., and Cadic, A. (2006). A comparative histological study between embryogenic structures and zygotic embryos of *Clematis hybrids* cultivated in vitro. *Acta Hort.* 725, 227–229. doi: 10.17660/actahortic.2006.725.28

Bari, R., and Jones, J. D. (2009). Role of plant hormones in plant defence responses. *Plant Mol. Biol.* 69, 473–488. doi: 10.1007/s11103-008-9435-0

Bhatla, S. C. (2018). "Auxins," in *Plant Physiology, Development and Metabolism*, eds S. C. Bhatla, and M. A. Lal, (Singapore: Springer), 569–601.

Brailko, V., Grebennikova, O., Paliy, A., Ivanova, N., Zubkova, N., and Mitrofanova, I. (2018). Physiological and biochemical characteristics of some clematis cultivars cultured ex situ and in vitro. *In Vitro Cell Dev. Biol. Plant* 58, 9–10.

Chavan, J. J., Kshirsagar, P. R., and Gaikwad, N. B. (2012). Rapid in vitro propagation of *Clematis heynei* M. A. Rau: an important medicinal plant. *Emir. J. Food Agric.* 24, 79–84. doi: 10.9755/ejfa.v24i1.10601

Corredoira, E., Ballester, A., Ibarra, M., and Vieitez, A. M. (2015). Induction of somatic embryogenesis in explants of shoot cultures established from adult *Eucalyptus globulus* and E. saligna × E. maidenii trees. *Tree Physiol.* 35, 678–690. doi: 10.1093/treephys/tpv028

Corredoira, E., Merkle, S. A., Martínez, M. T., Toribio, M., Canhoto, J. M., Correia, S. I., et al. (2019). Non-Zygotic embryogenesis in hardwood species. *Crit. Rev. Plant Sci.* 38, 29–97. doi: 10.1080/07352689.2018.1551122

Correia, S., Cunha, A. E., Salgueiro, L., and Canhoto, J. M. (2012). Somatic embryogenesis in tamarillo (*Cyphomandra betacea*): approaches to increase efficiency of embryo formation and plant development. *Plant Cell Tiss. Organ Cult.* 109, 143–152. doi: 10.1007/s11240-011-0082-9

Correia, S., Lopes, M. L., and Canhoto, J. M. (2011). Somatic embryogenesis induction system for cloning an adult *Cyphomandra betacea* (Cav.) Sendt. (tamarillo). *Trees* 25, 1009–1020. doi: 10.1007/s00468-011-0575-5

Dal Vesco, L. L., and Guerra, M. P. (2001). The effectiveness of nitrogen sources in Feijoa somatic embryogenesis. *Plant Cell Tissue Organ Cult.* 64, 19–25.

Davies, P. J. (2010). "The plant hormones: their nature, occurrence, and functions," in *Plant Hormones*, ed. P. J. Davies, (Dordrecht: Springer), 1–15. doi: 10.1007/978-94-011-0473-9_1

de Alcantara, G. B., Dibax, R., de Oliveira, R. A., Bespalhok Filho, J. C., and Daros, E. (2014). Plant regeneration and histological study of the somatic embryogenesis of sugarcane (*Saccharum* spp.) cultivars RB855156 and RB72454. *Acta Sci. Agron.* 36, 63–72. doi: 10.4025/actasciagron.v36i1.16342

Deepika, R., and Kanwar, K. (2010). In vitro regeneration of *Punica granatum* L. plants from different juvenile explants. *J. Fruit Ornamental. Plant Res.* 18, 5–22.

Fatima, N., and Anis, M. (2012). Role of growth regulators on in vitro regeneration and histological analysis in Indian ginseng (*Withania somnifera* L.) Dunal. *Physiol. Mol. Biol. Plants* 18, 59–67. doi: 10.1007/s12298-011-0099-x

Fehér, A. (2019). Callus, dedifferentiation, totipotency, somatic embryogenesis: what these terms mean in the era of molecular plant biology? *Front. Plant Sci.* 10:536.

Fehér, A., and Magyar, Z. (2015). Coordination of cell division and differentiation in plants in comparison to animals. *Acta Biol. Szegediensis* 59, 275–289.

Fujimura, T., and Komanima, A. (1979). Synchronization of somatic embryogenesis in carrot cell suspension culture. *Plant Physiol.* 64, 162–164. doi: 10.1104/pp.64.1.162

Geneve, J. E., and Preece, S. A. (1997). *Biotechnology of Ornamental Plants*. Wallington: CAB International.

Germanà, M. A., and Lambardi, M. (2016). *In Vitro Embryogenesis in Higher Plants*. New York: Humana Press.

Hamama, L., Baaziz, M., and Letouze, R. (2001). Somatic embryogenesis and plant regeneration from leaf tissue of jojoba. *Plant Cell Tissue Organ Cult.* 65, 109–113.

Han, K. H., and Park, Y. G. (1999). "Somatic embryogenesis in black locust (*Robinia pseudoacacia* L," in *Somatic Embryogenesis in Woody Plants*, eds S. M. Jain, P. K. Gupta, and R. J. Newton, (Dordrecht: Kluwer Acad. Publishers), 149–161. doi: 10.1007/978-94-011-4774-3_10

Hari, V. (1980). Effect of cell density changes and conditioned media on carrot cell embryogenesis. *J. Plant Physiol.* 96, 227–233. doi: 10.1016/s0044-328x(80)80039-0

Horvath, B. M., Magyar, Z., Zhang, Y., Hamburger, A. W., Bako, L., Visser, R. G., et al. (2006). EBP1 regulates organ size through cell growth and proliferation in plants. *EMBO J.* 25, 4909–4920. doi: 10.1038/sj.emboj.7601362

Ivanova, N., Mitrofanova, O., Lesnikova-Sedoshenko, N., Chirkov, S., and Mitrofanova, I. (2018). The effect of ribavirin on the regeneration capacity in vitro in some horticultural plants. *In Vitro Cell Dev. Biol. Plant* 58, 44–45.

Jain, S. M., and Gupta, P. (2018). *Step Wise Protocols for Somatic Embryogenesis of Important Woody Plants. II*. Switzerland: Springer.

Jain, S. M., and Ishii, K. (2003). *Micropropagation of Woody Trees and Fruits*. Dordrecht: Kluwer Acad. Publishers.

Kalinin, F. L., Kushnir, G. P., and Sarnatskaya, V. V. (1992). *Tehnologia Mikroklonal'nogo Razmnozhenia Rastenii (Techniques of Plant Microclonal Propagation, in Russian)*. Kiev: Naukova Dumka.

Kawa-Miszczak, L., Wegrzynowicz-Lesiak, E., Gabryszewska, E., and Saniewski, M. (2009). Effect of different sucrose and nitrogen levels in the medium on chlorophyll and anthocyanin content in *Clematis pitcheri* shoots cultured in vitro at different temperatures. *J. Fruit Ornam. Plant Res.* 17, 113–121.

Kreen, S., Svensson, M., and Rumpunen, K. (2002). Rooting of clematis microshoots and stem cuttings in different substrates. *Sci. Hort.* 96, 351–357. doi: 10.1016/s0304-4238(02)00126-7

Kuluev, B. R., Avalbaev, A. M., Nurgaleeva, E. Z., Knyazev, A. V., Nikonorov, Y. M., and Chemeris, A. V. (2015). Role of Aintegumenta-like gene NtANTL in the regulation of tobacco organ growth. *J. Plant Physiol.* 189, 11–23. doi: 10.1016/j.jplph.2015.08.009

Kunah, V. A. (2005). *Biotechnology of Medical Plants. Genetically and Physiology-Biochemical Bases (in Ukrainian)*. Kiev: Logos.

Lloyd, C. H. (1989). *Clematis*, 2nd Edn. London: Collins.

Loyola-Vargas, V. M., and Ochoa-Alejo, N. (2018). *Somatic Embryogenesis: Fundamental Aspects and Applications*. Switzerland: Springer.

Maheswaran, G., and Williams, E. G. (1985). Origin and development of somatic embryos formed directly on immature embryos of *Trifolium repens* in vitro. *Ann. Bot.* 56, 619–630. doi: 10.1093/oxfordjournals.aob.a087052

Mandegaran, Z., and Sieber, V. K. (2000). Somatic embryogenesis in *Clematis integrifolia* × C. *viticella*. *Plant Cell Tissue Organ Cult.* 62, 163–165.

Martins, J. F., Correia, S. I., and Canhoto, J. M. (2016). "Somatic embryogenesis induction and plant regeneration in strawberry tree (*Arbutus unedo* L.)," in *In Vitro Embryogenesis in Higher Plants. Methods in Molecular Biology*, eds M. Germana, and M. Lambardi, (New York: Humana Press), 329–339. doi: 10.1007/978-1-4939-3061-6_14

Méndez-Hernández, H. A., Ledezma-Rodríguez, M., Avilez-Montalvo, R. N., Juárez-Gómez, Y. L., Skeete, A., Avilez-Montalvo, J., et al. (2019). Signaling overview of plant somatic embryogenesis. *Front. Plant Sci.* 10:77.

Merkle, S. A. (1997). "Somatic embryogenesis in ornamentals," in *Biotechnology of Ornamental Plants*, eds R. L. Geneve, J. E. Preece, and S. A. Merkle, (Wallingford: CAB International), 13–33.

Mitrofanova, I. V. (2011). *Somatic Embryogenesis and Organogenesis as a Base of Biotechnology Perennial Horticultural Plants Obtaining and Conservation (in Russian)*. Kiev: Agrarna nauka.

Mitrofanova, I. V., Galaev, A. V., and Sivolap, Y. M. (2003). Investigation of molecular-genetic heterogeneity of clematis plants (*Clematis* L.) obtained by organogenesis and somatic embryogenesis in vitro. *Tsitologiya i Genetica.* 37, 12–26.

Mitrofanova, I. V., Lesnikova-Sedoshenko, N. P., Brailko, V. A., Kuzmina, T. N., Chelombit, S. V., Shishkina, E. L., et al. (2019). Realization of Ficus carica L. morphogenic capacity via organogenesis and somatic embryogenesis in vitro. *Acta Hort.* 1255, 69–76. doi: 10.17660/actahortic.2019.1255.12

Mitrofanova, I. V., Mitrofanova, O. V., and Pandei, D. K. (1997). Somatic embryogenesis and plant regeneration in *Zizyphus jujuba* Mill. in vitro. *Russ. J. Plant Physiol.* 44, 94–99.

Mitrofanova, I. V., Zubkova, N. V., and Sokolova, M. K. (2007). Comparative study of features of direct somatic embryogenesis in 8 cultivars of Clematis sp. *Works State Nikitskiy Botanical Gardens* 128, 12–24.

Moiseeva, N. A. (1991). "Molecular and cell mechanisms of morphogenesis in plant cell and tissue culture," in *Biology of Cultured Cells and Biotechnology*, ed. R. G. Butenko, (Moscow: Nauka), 166–185.

Murashige, T, and Skoog, F. (1962). A revised medium for rapid growth and bioassays with tobacco tissue culture. *Physiol. Plant* 15, 473–497. doi: 10.1111/j.1399-3054.1962.tb08052.x

Naika, H. R., and Krishna, V. (2008). Plant regeneration from callus culture of *Clematis gouriana* Roxb. *Turk. J. Biol.* 32, 99–103.

Nanda, R., and Rout, G. R. (2003). In vitro somatic embryogenesis and plant regeneration in *Acacia arabica*. *Plant Cell Tissue Organ Cult.* 73, 131–135.

Narvaez, I., Martin, C., Jimenez-Diaz, R. M., Mercado, J. A., and Pliego-Alfaro, F. (2019). Plant regeneration via somatic embryogenesis in mature wild olive genotypes resistant to the defoliating pathotype of *Verticillium dahlia*. *Front. Plant Sci.* 10:1471.

Nic-Can, G. I., Galaz-Ávalos, R. M., De-la-Peña, C., AlcazarMagaña, A., Wrobel, K., and Loyola-Vargas, V. M. (2015). Somatic embryogenesis: identified factors that lead to embryogenic repression. a case of species of the same genus. *PLoS One* 10:e0126414. doi: 10.1371/journal.pone.0126414

Novikova, G. V., Nosov, A. V., Stepanchenko, N. S., Fomenkov, A. A., Mamaeva, A. S., and Moshkov, I. E. (2013). Plant cell proliferation and its regulators. *Russ. J. Plant Physiol.* 60, 500–506. doi: 10.1134/s1021443713040109

Oliveira, M. M., and Pais, M. S. S. (1992). Somatic embryogenesis in leaves and leaf-derived protoplasts of *Actinidia deliciosa* var. deliciosa cv. Hayward (kiwifruit). *Plant Cell Rep.* 11, 314–317.

Onay, A. (2000). Histology of somatic embryogenesis in cultured leaf explants of pistachio (*Pistacia vera* L.). *Turk. J. Bot.* 24, 91–96.

Pati, P. K., Sharma, M., Sood, A., and Ahuja, P. S. (2004). Direct shoot regeneration from leaf explants of *Rosa damascena* Mill. *In Vitro Cell. Dev. Biol.Plant* 40, 192–195. doi: 10.1079/ivp2003503

Pereira, C., Montalbán, I. A., García-Mendiguren, O., Goicoa, T., Ugarte, D., Correia, S., et al. (2016). Pinus halepensis somatic embryogenesis is affected by the physical and chemical conditions at the initial stages of the process. *J. For. Res.* 21, 143–150. doi: 10.1007/s10310-016-0524-7

Pipino, L., Braglia, L., Giovannini, A., Fascella, G., and Mercuri, A. (2008). In vitro regeneration of Passiflora species with ornamental value. *Prop. Ornam. Plants* 8, 47–49. doi: 10.17660/actahortic.2010.855.5

Pipino, L., Braglia, L., Giovannini, A., Fascella, G., and Mercuri, A. (2010). in *Protocols for in Vitro Propagation of Ornamental Plants, Methods in Molecular Biology Ser., 589*, eds S. Mohan Jain, and S. J. Ochatt, (New York: Springer-Humana Press), 153–162.

Preil, W. (2003). "Micropropagation of ornamental plants," in *Plant Tissue Culture*, eds M. Laimer, and W. Rücker, (Vienna: Springer), 115–133. doi: 10.1007/978-3-7091-6040-4_7

Rademacher, W. (2015). Plant growth regulators: backgrounds and uses in plant production. *J. Plant Growth Regul.* 34, 845–872. doi: 10.1007/s00344-015-9541-6

Raghavan, V. (2004). Role of 2,4-dichlorophenoxyacetic acid (2,4-D) in somatic embryogenesis on cultured zygotic embryos of *Arabidopsis*: cell expansion, cell cycling, and morphogenesis during continuous exposure of embryos to 2,4-D. *Am. J. Bot.* 91, 1743–1756. doi: 10.3732/ajb.91.11.1743

Rout, G. R., and Jain, S. M. (2004). Micropropagation of ornamental plants – cut flowers. *Prop. Ornam. Plants* 4, 3–28.

Rout, G. R., Mohapatra, A., and Jain, S. M. (2006). Tissue culture of ornamental pot plant: a critical review on present scenario and future prospects. *Biotechnol. Adv.* 24, 531–560. doi: 10.1016/j.biotechadv.2006.05.001

Sharp, W. R., Sondahl, M. R., Caldas, L. S., and Marraffa, S. B. (1980). The physiology of in vitro asexual embryogenesis. *Hort. Rev.* 2, 268–310. doi: 10.1002/9781118060759.ch6

Smertenko, A., and Bozhkov, P. V. (2014). Somatic embryogenesis: life and death processes during apical–basal patterning. *J. Exp. Bot.* 65, 1343–1360. doi: 10.1093/jxb/eru005

Souter, M., and Lindsey, K. (2000). Polarity and signaling in plant embryogenesis. *J. Exp. Bot.* 51, 971–983. doi: 10.1093/jexbot/51.347.971

Surhone, L. M., Tennoe, M. T., and Henssonow, S. F. (2011). *Clematis*. Saarbrücken: Betascript Publishing

Tomiczak, K., Mikuła, A., Niedziela, A., Wójcik-Lewandowska, A., Domżalska, L., and Rybczyński, J. J. (2019). Somatic embryogenesis in the family gentianaceae and its biotechnological application. *Front. Plant Sci.* 10:762.

Toomey, M., and Leeds, E. (2001). *An Illustrated Encyclopedia of Clematis*. Portland: Timber Press.

Yegorova, N. A., Mitrofanova, I. V., Brailko, V. A., Grebennikova, O. A., Paliy, A. E., and Stavtseva, I. V. (2019). Morphogenetic, physiological, and biochemical features of *Lavandula angustifolia* at long-term micropropagation in vitro. *Russ. J. Plant Physiol.* 66, 326–334. doi: 10.1134/s1021443719010060

Zakubanskiy, A., Mitrofanova, I., and Chirkov, S. (2018a). First report of clematis mottle virus on clematis in Russia. *J. Plant Pathol.* 100:605. doi: 10.1007/s42161-018-0112-0

Zakubanskiy, A., Mitrofanova, I., and Chirkov, S. (2018b). First report of moroccan pepper virus on clematis in russia and worldwide. *Plant Dis.* 102:1469. doi: 10.1094/pdis-10-17-1646-pdn

Zhang, Q. X., Hu, H. K., and Fang, Y. M. (2010). Induction culture and anatomical observation of organogenesis of adventitious root of *Clematis* 'Multi-Blue'. *J. Plant Resour. Environm.* 19, 80–85.

Zhang, Q. X., Hu, H. K., Wang, A. X., and Fang, Y. M. (2011). Somatic embryogenesis and plant regeneration of *Clematis* 'Multi-Blue'. *Prop. Ornam. Plants* 11, 21–27.

Zhinkina, N. A., and Voronova, O. N. (2000). About the technique of embryological sections staining. *Botan. Zhurnal.* 85, 168–171.

Zubkova, N. V. (2015). "Promising *Clematis* L. cultivars for the southern coast of the crimea," in *Introduction and Breeding of Ornamental and Decorative Plants in NBG (Actual State, Development Prospects and use in Landscape Architecture)*, ed. Y. V. Plugatar, (Simferopol: IT ARIAL), 109–117.

Conflict of Interest: The authors declare that the research was conducted in the absence of any commercial or financial relationships that could be construed as a potential conflict of interest.

frontiers in Plant Science

ORIGINAL RESEARCH
published: 07 May 2021
doi: 10.3389/fpls.2021.672023

Transgenic *Kalanchoë blossfeldiana*, Containing Individual *rol* Genes and Open Reading Frames Under *35S* Promoter, Exhibit Compact Habit, Reduced Plant Growth, and Altered Ethylene Tolerance in Flowers

Bruno Trevenzoli Favero[1], Yi Tan[1], Yan Lin[1], Hanne Bøge Hansen[1], Nasim Shadmani[1], Jiaming Xu[1], Junou He[1], Renate Müller[1], Aldo Almeida[2] and Henrik Lütken[1]*

[1]Section for Crop Sciences, Department of Plant and Environmental Sciences, Faculty of Science, University of Copenhagen, Taastrup, Denmark, [2]Section for Plant Biochemistry, Department of Plant and Environmental Sciences, Faculty of Science, University of Copenhagen, Frederiksberg, Denmark

OPEN ACCESS

Edited by:
Patrícia Duarte De Oliveira Paiva, Federal University of Lavras, Brazil

Reviewed by:
Pejman Azadi, Agricultural Biotechnology Research Institute of Iran, Iran
Cristian Silvestri, University of Tuscia, Italy

***Correspondence:**
Bruno Trevenzoli Favero
btf@plen.ku.dk

Specialty section:
This article was submitted to Crop and Product Physiology, a section of the journal Frontiers in Plant Science

Received: *25 February 2021*
Accepted: *14 April 2021*
Published: *07 May 2021*

Citation:
Favero BT, Tan Y, Lin Y, Hansen HB, Shadmani N, Xu J, He J, Müller R, Almeida A and Lütken H (2021) Transgenic Kalanchoë blossfeldiana, Containing Individual rol Genes and Open Reading Frames Under 35S Promoter, Exhibit Compact Habit, Reduced Plant Growth, and Altered Ethylene Tolerance in Flowers. Front. Plant Sci. 12:672023. doi: 10.3389/fpls.2021.672023

Reduced growth habit is a desirable trait for ornamental potted plants and can successfully be obtained through *Rhizobium rhizogenes* transformation in a stable and heritable manner. Additionally, it can also be obtained by transformation with *Agrobacterium tumefaciens* harboring specific genes from *R. rhizogenes*. The bacterial T-DNA harbors four *root oncogenic loci* (*rol*) genes and 14 less known open reading frames (ORFs). The four *rol* genes, i.e., *rol*A, *rol*B, *rol*C, and *rol*D, are conceived as the common denominator for the compact phenotype and the other less characterized ORFs seem auxiliary but present a potential breeding target for less aberrant and/or more tailored phenotypes. In this study, *Kalanchoë blossfeldiana* 'Molly' was transformed with individual *rol* genes and selected ORFs in *35S* overexpressing cassettes to comprehensively characterize growth traits, gene copy and expression, and ethylene tolerance of the flowers. An association of reduced growth habit, e.g. height and diameter, was observed for *rol*B2 and ORF14-2 when a transgene single copy and high gene expression were detected. Chlorophyll content was reduced in overexpressing lines compared to wild type (WT), except for one ΔORF13a (a truncated ORF13a, where SPXX DNA-binding motif is absent). The flower number severely decreased in the overexpressing lines compared to WT. The anthesis timing showed that WT opened the first flower at 68.9 ± 0.9 days and the overexpressing lines showed similar or up to 24 days delay in flowering. In general, a single or low relative gene copy insertion was correlated to higher gene expression, ca. 3 to 5-fold, in *rol*B and ΔORF13a lines, while in ORF14 such relation was not directly linked. The increased gene expression observed in *rol*B2 and ΔORF13a-2 contributed to reducing plant growth and a more compact habit.

Tolerance of detached flowers to 0.5 μl L^{-1} ethylene was markedly higher for ORF14 with 66% less flower closure at day 3 compared to WT. The subcellular localization of *rol*C and ΔORF13a was investigated by transient expression in *Nicotiana benthamiana* and confocal images showed that *rol*C and ΔORF13a are soluble and localize in the cytoplasm being able to enter the nucleus.

Keywords: *Agrobacterium rhizogenes*, cellular localization, compact plant, flower longevity, postharvest performance, root oncogenic loci, ΔORF13a, ORF14

INTRODUCTION

Rhizobium rhizogenes-mediated plant transformation has for the last 4 decades been intensively applied in many studies with the pursuit of introducing compact habit and reduced plant growth traits in plants, primarily ornamentals (Christensen et al., 2008; Pérez de la Torre et al., 2018). The rationale has often been to develop genetically stable compact plants as a bio-sustainable alternative to chemical growth retardants. Several places, e.g., Europe, the application of chemical growth retardants is increasingly restricted by legislation and as a result many of the most effective regulators have already been banned and further restrictions are expected (Rademacher, 2016). These restrictions have been implemented as several of those compounds exhibit potential detrimental effects on both the environment and human health (Rademacher, 2000, 2016; De Castro et al., 2004). However, numerous abiotic bio-friendly alternatives have been developed and are commonly applied in ornamental plant production, e.g., brushing and shaking of plants, cold-morning treatment, and light control (McMahon, 1999; Clifford et al., 2004; Bergstrand, 2017). Unfortunately, these methods do not completely fulfill the desired requirements for compact habit and reduced plant growth as the treatment effect ceases to work once the plant is out of the production site. Moreover, several efficient genetic engineering approaches exist to create stable compact phenotypes. These approaches have been pursued in several ornamental plants, e.g., *Calibrachoa* (Gennarelli et al., 2009), *Kalanchoë* (Christensen et al., 2008), *Mecardonia* (Pérez de la Torre et al., 2018), *Petunia* (Mishiba et al., 2006), and poinsettia (Islam et al., 2013). Some of these strategies target alteration of gibberellic acid (GA) metabolism; GA_{20} oxidases have silenced (Topp et al., 2008), GA_2 oxidases have been over-expressed (Gargul et al., 2013), the *Arabidopsis thaliana Short Internodes* gene has been overexpressed (Lütken et al., 2010; Islam et al., 2013), and knotted homeobox genes have been modulated (Lütken et al., 2011). Although being successful, these strategies unfortunately all fall under the EU GMO regulation (European Union, 2001) and are, due to legislation and low public acceptance, presently not applicable for the horticultural market in e.g., Europe. In this respect, transformation with unmodified bacterial strains of e.g., *R. rhizogenes* without the use of recombinant DNA technologies and the plants derived from this approach are not classified as GMO according to the current European GMO legislation (European Union, 2001). The terminology of "natural transformation" has been used as a label for these strategies and it presents a very promising beacon for generating compact habit and reduced plant growth (as reviewed by Lütken et al., 2012a; Desmet et al., 2019).

Understanding how *R. rhizogenes* confers compact habit and reduced growth traits in plants is highly relevant given the potential to reduce the use of chemical growth retardants. When plants are infected with *R. rhizogenes*, T-DNA from the root inducing (Ri)-plasmid is inserted and integrated in the plant host DNA (Chilton et al., 1982) leading to the development of the Ri-phenotype, in which hairy roots protrude from the site of infection (Tepfer, 1990). The Ri-plasmid of agropine strains is a split T-DNA plasmid, harboring two regions designated as the left T-DNA (T_L-DNA) and right T-DNA (T_R-DNA), which are separated by about 15–20 kb of non-transferred DNA (White et al., 1985). Numerous genes and open reading frames (ORFs) are present on the T_L-DNA. The most well-known and characterized genes known to be involved in the compact habit and reduced plant growth, are the *root oncogenic loci* (*rol*) genes; *rol*A, *rol*B, *rol*C, and *rol*D, which correspond to ORFs 10, 11, 12, and 15, respectively (White et al., 1985; Slightom et al., 1986; reviewed by Rangslang et al., 2018; De Paolis et al., 2019). In comparison, the T_R-DNA harbors *aux1* and *aux2* genes (*iaaM* and *iaaH*, respectively; Camilleri and Jouanin, 1991) involved in auxin biosynthesis (Mashiguchi et al., 2019) as well as a homolog of the *rol*B gene, termed *rol*BTr (Bouchez and Camilleri, 1990). Plants can be regenerated from the hairy roots following treatment with various, often high, and ratios of cytokinins:auxins (Hegelund et al., 2017; Mandal et al., 2020; Neumann et al., 2020). Regenerated plants exhibit, among other features, compact habit, reduced plant growth, and frequently thicker leaves that are often reduced in size (as reviewed by Lütken et al., 2012a; Rangslang et al., 2018).

In attempts to unravel the effect of the individual *rol* genes, several genetic constructs with individual as well as multiple *rol* genes/ORFs delivered using *Agrobacterium tumefaciens* have been investigated in a range of plant species. Analysis of especially *rol*A–D, but also some of the other ORFs has indicated that several of these genes/ORFs influence plant morphology and hormone sensitivity specifically as well as differently (Casanova et al., 2005). Presence of *rol*A typically leads to wrinkled leaves (Sinkar et al., 1988; Bettini et al., 2016b). It has been demonstrated that *rol*B has a crucial role in hairy root formation. In tobacco, its expression alone is sufficient to produce roots that are often fast growing, highly branched, and ageotropic (Cardarelli et al., 1987). Additionally, *rol*B plants display necrosis in leaves and altered shoot

morphology, including increased flower size and change in leaf shape (Schmulling et al., 1989; Kodahl et al., 2016). Plants transformed with *rol*C under its endogenous promoter display dwarf phenotypes with reduced apical dominance, lanceolate leaves, early inflorescence, and smaller flowers (Schmülling et al., 1988). It has been speculated that *rol*C increases the levels of active cytokinins, based on the findings that its encoded protein has beta-glucosidase activity which enables the release of free active cytokinins from their active conjugates; observed *in vitro* (Estruch et al., 1991a). Although being the least studied *rol*-gene, *rol*D is the only gene where the protein function is elucidated; it encodes an ornithine cyclodeaminase (Trovato et al., 2001). In respect to the ORFs, e.g., ORF13, ORF13a, and ORF14, less information is available. In transgenic tobacco plants harboring ORF13, phenotypic alterations were detected, such as dwarfing, wrinkled leaves, and shortened internodes (Lemcke and Schmülling, 1998). Interestingly, it was recently found that ORF13 confers a major role in the compact habit phenotype when overexpressed in *Arabidopsis* (Kodahl et al., 2016). The ORF located on the lagging strand of the Ri plasmid between ORF13 and ORF14 was termed ORF13a (Hansen et al., 1991) and is speculated to encode a regulatory protein (Hansen et al., 1994). Overexpression of ORF13a in *Nicotiana tabacum* did not exhibit phenotypic effects in the regenerated F1 populations (Lemcke and Schmülling, 1998). For ORF14, it was found that overexpression has no changes in the transgenic plant's morphology (Lemcke and Schmülling, 1998). It has been suggested that ORF13 and ORF14 co-act in synergy with the other *rol* genes, improving root induction in *N. tabacum* and *Daucus carota* (Capone et al., 1989; Aoki and Syono, 1999a).

In the economically important *Kalanchoë*, many studies have been made to investigate the effects of the inserted T-DNA of *R. rhizogenes* (Lütken et al., 2012a), and several transformants exhibited large variations in plant diameter, number of branches, flower diameter, time to first open flower, and duration of flowering compared to control plants (Christensen et al., 2010). Advanced knowledge on the specific phenotype effects of the individual *rol* genes and ORFs transferred *via A. tumefaciens* will be beneficial to guide back-crossing approaches to confer compactness from naturally *R. rhizogenes* transformed plants. Moreover, detailed molecular data and more specifically the protein sub-cellular localization using transient expression *via A. tumefaciens* could prove beneficial in future characterization of encoded proteins of *rol* genes/ORFs.

This study aimed to investigate the phenotypic effects of individual *rol* genes/ORFs on regenerated plants of *Kalanchoë blossfeldiana*. This was obtained by producing and characterizing transgenic lines with 35S driven overexpressing cassettes separately containing *rol*B, *rol*C, ΔORF13a, and ORF14 with special focus on postharvest aspects such as ethylene tolerance in detached flowers. Moreover, relative copy number and gene expression data were obtained. In addition, due to the strong phenotypes observed for *rol*C and ΔORF13a transformed lines, we investigated the subcellular localization of their encoded proteins to provide deeper molecular understanding of *rol* genes/ORFs.

MATERIALS AND METHODS

Annotation of ORF13a From pRiA4 and Gene Cloning

The reported sequence for the T_L-DNA (Genbank accession: K03313) of the Ri plasmid of *R. rhizogenes* A4 strain (ATCC43057) was annotated using the FgenesH tool (Solovyev et al., 2006). Subsequently, a previously annotated sequence of ORF13a from pRi8196 (Genbank accession: AAA22098; Hansen et al., 1991) was used to search for the corresponding homologous ORF13a from the predicted ORFs by FgenesH. Sequences were compared by using BLASTp. Primers for cloning a truncated ORF13a (ΔORF13a) sequence from *R. rhizogenes* A4 strain were specifically designed to exclude the putative regulatory region with the SPXX motif repeats (**Supplementary Table S1**).

Selected genes and ORFs from *R. rhizogenes* A4, i.e., *rol*B, *rol*C (Genbank accession number: MT514512), ΔORF13a (Genbank accession: MT514511), and ORF14, were previously available in pDONR™221 and recombined into the destination vector pK2GW7 (Karimi et al., 2002) using the Gateway™ LR Clonase™ II Enzyme mix (Invitrogen, Carlsbad, CA, United States), according to Kodahl et al. (2016). The destination vector includes selection markers streptomycin/spectinomycin and kanamycin for bacteria and plants, respectively, as well as the constitutive plant promoter *35S* derived from *Cauliflower mosaic* virus. All PCR-based constructs were verified by Sanger sequencing (Mix2Seq kit, Eurofins Genomics, Ebersberg, Germany; **Supplementary Tables S1**, **S2**). The sequencing verified vectors were transformed by electroporation (MicroPulser Electroporator, Bio-Rad) into rifampicin resistant and competent *A. tumefaciens* C58C1 (pGV3850). Colony selection was performed in *Agrobacterium* growth media supplemented with 10 g L^{-1} agar (Duchefa Biochemie B.V., Haarlem, The Netherlands), followed by single-colony inoculated liquid culture maintained in *Agrobacterium* growth media (**Supplementary Table S3**). Additionally, successful *A. tumefaciens* transformation was verified by plasmid purification (GenElute™ Plasmid Miniprep Kit, Sigma-Aldrich, St. Louis, MO, United States) followed by PCR detection of the inserted target gene using full-length gene specific primers (Kodahl et al., 2016).

Plant Material

Vegetatively propagated *K. blossfeldiana* 'Molly' plants were grown in 10 cm diameter pots with sand, vermiculite, and Pindstrup peat substrate in a 1:1:1 ratio (Substrate no. 1, PindstrupMosebrug A/S, Ryomgard, Denmark), saturated with a solution of 1 ml L^{-1} Gnatrol® (Valent BioSciences, Libertyville, IL, United States), and kept in long day greenhouse conditions (**Supplementary Table S4**). The watering was based on substrate drying assessment, i.e., approximately 2–3 per week, utilizing ebb/flow irrigation. The fertilized water contained nitrogen, phosphorus, and potassium supplemented with magnesium (1 g L^{-1} of Pioner NPK Makro Blå 14-3-23+[3]Mg, Azelis Denmark A/S, Kgs Lyngby, Denmark) and micronutrients (0.1 ml L^{-1} of Pioner Mikro med Jern, Azelis Denmark A/S), adjusted to pH 6.0 and with electrical conductance of 2.0 μS cm^{-1}.

Leaf material was selected for transformation from up to 3-month old plants, collected, and surface-sterilized using 70% ethanol (VWR chemicals, Søborg, Denmark) for 1 min, followed by 90 g L^{-1} $Ca(ClO)_2$ (ACROS Organics, Geel, Belgium) and 0.03% Tween® 20 (Sigma-Aldrich) for 20 min and rinsed three times in sterile deionized water. Additionally, the leaves were cut into 1 cm^2 pieces, excluding the leaf margins and central vein, and the generated explants were placed in sterile deionized water until inoculation according to Lütken et al. (2010).

Kalanchoë blossfeldiana Transformation and *de novo* Organogenesis

Pre-inoculum liquid cultures of *A. tumefaciens* were initiated by adding 1 ml glycerol stock for each construct to 10 ml *Agrobacterium* growth media (**Supplementary Table S3**) and cultured O/N at 28°C and 200 rpm (Topp et al., 2008). The inoculum was prepared by increasing the liquid culture volume to 200 ml with *Agrobacterium* growth media and subsequently, adjusting the optical density (OD) to 0.2 using the inoculation media (**Supplementary Table S3**) as diluent and cultured for 2–4 h at 28°C and 200 rpm. Prior to inoculation, the OD was measured again and adjusted to 0.4–0.6 with inoculation media. *Kalanchoë* leaf explants were inoculated with the adjusted *A. tumefaciens* liquid cultures according to Lütken et al. (2010). The experimental control included plant material submerged in inoculation media without bacteria following the same criteria. Succeeding the co-cultivation period, the explants were immersed in washing media (**Supplementary Table S3**) containing antibiotics for 30 min under 50 rpm agitation, blotted, and transferred to *de novo* organogenesis media (**Supplementary Table S3**). *Kalanchoë* explants on *de novo* organogenesis media were placed at long day tissue culture growth conditions (**Supplementary Table S4**) for 4–6 months and sub-cultured to fresh media every 3–4 weeks until the appearance of shoots. Unrooted *Kalanchoë* shoots were excised from the callus material, transferred to rooting media (**Supplementary Table S3**) until the formation of roots, and placed at the same growth conditions and sub-culturing frequency. Upon significant rooting, e.g., >5 mm long roots, the plantlets were transferred to 10 cm diameter pots with Pindstrup peat substrate (Substrate no. 1, PindstrupMosebrug A/S) and saturated with a solution of Gnatrol® (Valent BioSciences). The pots were placed in the long day climate chamber (PGV56, Conviron, Winnipeg, MB, Canada) growth condition (**Supplementary Table S4**) for 4–6 weeks, i.e., intermediary between tissue culture and greenhouse conditions. The plantlets were covered with a plastic lid during the initial week to accommodate acclimation. The initial shoots and later plantlets remained green after successive tissue culture sub-cultivation rounds on media containing kanamycin, as well as showed stable phenotypes after at least three clonal propagations in the pots.

Transgene Verification

Plant material, i.e., leaves, were collected, snap frozen, and pulverized using liquid N_2, followed by −80°C storage. Genomic DNA extraction was proceeded with Plant DNA Isolation Reagent (Takara Bio Inc.) according to the manufacturer's instructions and the concentration and purity assessed using a NanoDrop (ThermoFisher Scientific, Waltham, MA, United States). Genotyping was performed using specific primer sets targeting full-length *rol* genes/ORFs and *Kalanchoë daigremontiana Actin* (*KdActin*, control; **Supplementary Table S1**) were used. Multiple PCRs to amplify these products were performed using Ex Taq® DNA Polymerase (Takara Bio Inc.) as per supplier's instructions and 40–100 ng gDNA added in each 25 µl reaction. The reactions were incubated in a DNA thermal cycler (MyCycler, Bio-Rad) following the programs listed in the **Supplementary Table S2**. The PCR products were mixed with GelRed (Biotium, Hayward, CA, United States), resolved in 1x TAE (ThermoFisher Scientific) 1.5% agarose (VWR chemicals) gel electrophoresis at 100 V for 55 min and visualized under UV-light (GelDoc XR+, Bio-Rad). Positive lines for the respective cassette were further clonally propagated. To attain that the correct gene/ORF sequence was successfully transferred, the selected lines for phenotyping and ethylene experiments were further assessed with a second PCR using the primer set *pK2GW7_35S_Fw1* and *pK2GW7_RB_Rv1* (**Supplementary Table S1**). Upon confirmation of a successful PCR amplification by gel electrophoresis, the purified PCR product (GeneJET PCR Purification Kit, ThermoFisher Scientific) was sent for Sanger sequencing (Mix2Seq kit, Eurofins Genomics) in both forward and reverse direction with the primers *pK2GW7_35S_Fw2* and *pK2GW7_T35S_Rv2* (**Supplementary Table S1**), respectively. An alignment (CLC Main Workbench, Qiagen) with no mismatches from the sequencing results to the expected sequence was assessed as the line being a true positive.

Phenotypical Characterization

To evaluate and analyze the phenotypical differences between the transformed plants and wild type (WT) plants, the available positive lines from each gene construct plus one WT were selected and propagated. About 4–10 cuttings per positive line and eight WT were harvested, made uniform at 2–3 cm height, and planted into new pots filled with Pindstrup peat (Substrate no. 1, Pindstrup Mosebrug A/S) saturated with Gnatrol® solution (Valent BioSciences). Plants were initially grown in long day greenhouse condition (**Supplementary Table S4**) until they had developed three pairs of fully expanded leaves. Plants were then flower induced in short day greenhouse condition (**Supplementary Table S4**) corresponding to the same settings to produce commercial *Kalanchoë* (Lütken et al., 2012b). Irrigation and fertilization were as above mentioned. Data were collected monthly for plants' biometrical characteristics, including plant height, plant diameter, and number of leaves and branches. The experiment was repeated twice displaced in time (4–6 weeks apart), and a total of four monthly measurements were done for each propagation. Data were also collected at the endpoint, consisting of a destructive analysis of the plants, i.e., total number of flowers, flower diameter and shape, leaf area (LI-3100 Area meter, Lincon, NE, United States), fresh and dry weight, and

chlorophyll content (CCM-200, Opti-Science, Hudson, NH, United States) was evaluated on third and fourth-youngest leaf pairs.

Relative Copy Number and Gene Expression of the Transgenic Lines

Relative copy number was determined by real-time quantitative PCR (RT-qPCR) on gDNA, and the reactions were performed on a ICycler instrument (CFX Connect Real-Time PCR Detection System, Bio-Rad) using SsoAdvanced™ Universal SYBR® Green Supermix (Bio-Rad) according to supplier's instructions. Forty nanogram of gDNA was used in each 20 µl reaction. The following fragment primer pairs for *rol*B, *rol*C, ΔORF13a, and ORF14 at 200 nM final concentration were used correspondingly to the transgenic lines analyzed with *K. laxiflora Actin* (*KlActin*) as reference gene (**Supplementary Table S1**). Additionally, gDNA samples from naturally transformed *K. blossfeldiana* lines, namely 306, 324, and 331 were used as reference for known copy number based on Southern blot (Christensen et al., 2008). The following program was used: 98°C for 3 min, 45 cycles of (15 s at 98°C, 30 s at 60°C). Following each run, a melt curve analysis was done in the range 55–95°C with 0.5°C increments in 10 s per step. The threshold cycles (Ct) for these primer pairs were standardized using the corresponding *KlActin* Ct (ΔCt) and line 306 was used as reference for single copy (ΔΔCt). The relative quantification of the target genes, i.e., *rol*B, *rol*C, ORF13a, and ORF14, among different lines was determined as $2^{-\Delta\Delta Cq}$ using the CFX Maestro Software (Bio-Rad). Line 306 was arbitrarily defined as reference for 1-fold, due to one copy in the Southern blot, and relative distribution categories were based on Bartlett et al. (2008) and Lütken et al. (2010). Based on the samples with known copy number and their obtained fold change, the lines were categorized into the following significantly different groups: single copy (fold change < 2), low copy number (2 > fold change < 15), and high copy number (fold change > 15). Values are based on three replicates and were repeated twice.

Total leaf RNA was isolated from a pooled sample of three plants of the same line using RNeasy Plant Mini Kit (Qiagen) and digested with RNAse-free DNAse (Sigma-Aldrich) following the manufacturer's protocol with minor modification. RLC buffer mixed with 30 µl 50% (v/v) PEG 20.000 (Sigma-Aldrich) per extraction was used for the plant cell lysis step. RNA yield and purity were determined by NanoDrop (ThermoFisher Scientific), and integrity was evaluated on 1% agarose (VWR chemicals) 1x TAE (ThermoFisher Scientific) supplemented with 1% sodium hypochlorite (VWR chemicals; Aranda et al., 2012). Deoxyribonuclease I (Sigma-Aldrich) was used to remove residual DNA following the manufacturer's instructions. Reverse transcription synthesis was performed on 0.8 µg DNase treated RNA using iScript cDNA Synthesis Kit (Bio-Rad) according to the manufacturer's recommendations. The RT-qPCR used 400 ng of cDNA per 20 µl reaction as template mixed with SsoAdvanced™ Universal SYBR® Green Supermix (Bio-Rad) according to supplier's instructions and incubated in the ICycler instrument (Bio-Rad). Each transgenic line was assessed with the corresponding above mentioned fragment primer pair and *KlActin* was the reference gene (**Supplementary Table S1**). The following program was used: 95°C for 30 s, 45 cycles of (95°C for 15 s, 60°C for 30s). A melt curve analysis was conducted in the range 55–95°C with 0.5°C increments in 10 s per step after each run. The threshold cycles (Ct) were standardized using the corresponding *KlActin* Ct (ΔCt). The relative quantification of the target genes, i.e., *rol*B, *rol*C, ORF13a, and ORF14, among different lines was determined as $2^{-\Delta Cq}$ using the CFX Maestro Software (Bio-Rad). Values are based on three replicates and were repeated twice.

Tolerance of Detached Flowers to Exogenous Ethylene

Selected overexpressing lines, i.e. *rol*B, ΔORF13a, and ORF14, and WT control were propagated as previously described, being initially kept in long day greenhouse conditions until three pairs of fully opened leaves were reached and then transferred to growth chambers (PGV56, Conviron) programmed to short day conditions for flower induction (**Supplementary Table S4**). Irrigation and fertilization were as above mentioned. It was ensured that all flowers used in the experiment were 1–4 day old by removing all open flowers from the plants accordingly prior to experimental setup. Single open flowers were excised and placed in micro titer plates containing tap water according to Christensen and Müller (2009). The micro titer plates with flowers were transferred to glass tanks that were sealed and exposed to 0.5 µl L^{-1} ethylene (1,000 µl L^{-1} ethylene in N_2, Calgaz, Staffordshire, United Kingdom) or air (control) for 5 days. The glass tanks were kept at ethylene growth chamber conditions (**Supplementary Table S4**). Ethylene tolerance was measured in terms of flower closure by daily recording the flower diameter *via* photographs (Iphone 9 plus, Apple, Cupertino, CA, United States) later analyzed in ImageJ (Rueden et al., 2017), and flower senescence was defined when the petals turned black and the flower was completely closed. Eight replicate flowers obtained from each overexpressing line and WT were considered a repetition. The experiment was repeated four times with flowers derived from two independent propagation rounds. The flower closure was calculated as percentage of the initial diameter of exposed flowers and flower senescence is displayed as percentage from the total assessed flowers.

Sub-Cellular Localization of ΔORF13a and rolC in *Nicotiana benthamiana* Leaves

The preparation of monomeric Red Fluorescent Protein1 (mRFP1) and SbCYP98A1-mRFP1 constructs was conducted as described previously (Laursen et al., 2016). The construction of *rol*C and ΔORF13a fused to enhanced Green Fluorescent Protein (eGFP) at the C or N terminus was done by amplifying the full-length coding sequences with appropriate primers (**Supplementary Table S1**), and the amplicons were inserted in the pCAMBIA1300/UeGFP or pCAMBIA1300/eGFPU vectors, respectively, by the single-insert USER cloning technique (Geu-flores et al., 2007). All PCR-based constructs were verified

by sequencing. Expression constructs were transformed into *A. tumefaciens* strain AGL1. Colonies of *A. tumefaciens* were picked and pre-cultured in 3 ml of LB medium with appropriate antibiotics. Afterward, 10 ml of LB medium containing antibiotics were inoculated with 50 µl of the pre-culture and incubated at 28°C overnight or until reaching an OD_{600} of 1.5. The cultures were centrifuged, the cell pellet was resuspended in infiltration buffer (10 mM $MgCl_2$, 10 mM MES, pH 5.6, and 100 µM acetosyringone), and OD_{600} was adjusted to 0.15. *A. tumefaciens* strains carrying the constructs of interest were co-infiltrated in equal densities with *A. tumefaciens* transformed with a pCAMBIA1300 vector for expression of the viral p19 silencing suppressor protein (Lakatos et al., 2004). Leaf discs from transformed plants were sampled 3 days after infiltration for observation by confocal laser scanning microscopy. An SP5x confocal laser scanning microscopy device equipped with a DM6000 microscope (Leica, Wetzlar, Germany) was used to record images of enzyme subcellular localization with settings described by Laursen et al. (2016).

Statistics

The experiments were conducted in complete randomized design, repeated at least twice over time and ANOVA was performed using the software Sisvar (Ferreira, 2011), considering the lines, i.e., WT, *rol*B1, *rol*B2, *rol*C1, ΔORF13a, and ORF14 as source of variation. The data with $p \leq 0.05$ in the F-test followed the Scott Knott average comparison test ($p \leq 0.05$). Relative gene expression data were compared using Student's *t*-test (Student, 1908). Data are presented as average ± SE (n = 6–32).

RESULTS

Sequences of ORF13a Differs Between Two *Rhizobium rhizogenes* Strains

The ORFs from the T_L-DNA sequence of the pRiA4 (agropine type) reported by Slightom et al. (1986) that would be transcribed in plants were predicted by the FgenesH tool. The sequence of ORF13a was found by using blastn and blastp algorithms with the nucleotide and amino acid sequence of ORF13a from pRi8196 (mannopine type) previously reported by Hansen et al. (1991). The ORF predicted by FgenesH with the highest similarity was ORF10 resulting from the algorithm and was 228 nucleotides long from position 15,012–14,785 in the reverse strand of the pRiA4 and consisted of one exon. The nucleotide sequence for the ΔORF13a of pRiA4 was published in Genbank with the following accession number: MT514511. Comparison of the ORF13a amino acid sequence from the agropine pRiA4 and the mannopine pRi8196 by blastp revealed significant difference in this ORF among the strains. Albeit sequences shared 68% identity and 76% similarity at amino acid level, the ORF13a sequence from pRiA4 is 34 amino acids shorter than that of pRi8196; accordingly, the pRiA4 ORF13a sequence starts at the amino acid 36 of the ORF13a of pRi8196 and the alignment continues to the end of both sequences. Thus, the putative regulatory region with the SPXX motif repeats (which corresponds to four amino acid residues Ser-Pro-X-X) in the ORF13a of pRi8196 is also present in the pRiA4 ORF13a, but with one SPXX motif missing. The region with SPXX motif repeats was excluded for two reasons: (1) although SPXX repeats could function in DNA-binding they could also be under regulation by kinases (Liu et al., 2018) and (2) Lemcke and Schmülling (1998) already overexpressed the full-length ORF13a from pRiA4 in *N. tabacum* and did not observe a distinct phenotype.

Transformation Efficiencies of *K. blossfeldiana* Vary for the Individual *rol* Genes and ORFs

Leaf explants of *K. blossfeldiana* 'Molly' (**Figure 1A**) were successfully transformed with *rol*B, *rol*C, ΔORF13a, and ORF14 cassettes derived from *R. rhizogenes* A4. The kanamycin resistant shoots of each construct were verified by PCR and confirmed by sequencing; the transformation efficiencies ranged between 0.5 and 2.9% (**Table 1**). Kanamycin selection was effective (**Figure 1B**) and *de novo* organogenesis was obtained by media containing high cytokinin:auxin levels of plant growth regulators (see *K. blossfeldiana* Transformation and *de novo* Organogenesis section), which yielded in callus (**Figure 1C**), shoot (**Figure 1D**), and root (**Figure 1E**) formation that enabled the generated plantlets to be transferred to pots (**Figure 1F**). The presence of the T-DNA bearing the overexpressing constructs was confirmed by PCR amplification (**Figures 1G–J**) and followed by sequencing (data not shown).

Compact Habit and Reduced Plant Growth Was Achieved to Different Extent in *K. blossfeldiana* Transformed With *rol* Genes and ORFs

The regenerated lines were clonally propagated in order to perform phenotyping analysis. It was observed that the plant height, diameter, leaf area, and fresh and dry weight of the *rol* genes/ORFs regenerated overexpressing lines were visually (**Figures 2A,B**) and statistically significant (**Figures 3A–F**) lower than the WT line. Height showed inter-line variation, i.e., *rol*B1 was 36% higher than *rol*B2, ΔORF13a-1 was 39% higher than ΔORF13a-2, and ORF14-3 was 33% higher than ORF14-1 and ORF14-2 (**Figure 3A**). Moreover, all these transgenic lines were statistically significant shorter than the WT (18.3 ± 0.4 cm). These inter-line variations were also observed for the other investigated traits, i.e., diameter, number of branches, number of leaves, leaf area, and fresh and dry weight (**Figures 3B–G**). The number of leaves was negatively affected in the *rol* genes/ORFs overexpressing lines compared to WT (54.2 ± 1.9 leaves), the decrease was most pronounced in *rol*C1 (87%) and least in ΔORF13a-1 (43%; **Figure 3D**). Moreover, the leaf area was severely impaired by the presence of the overexpressing *rol* genes/ORFs cassettes in comparison to WT (**Figure 3E**). In contrast to previous observations, plant height and diameter (**Figures 3A,B**), ORF14-2 showed 12% more leaves than ORF14-1; however, the leaf area did

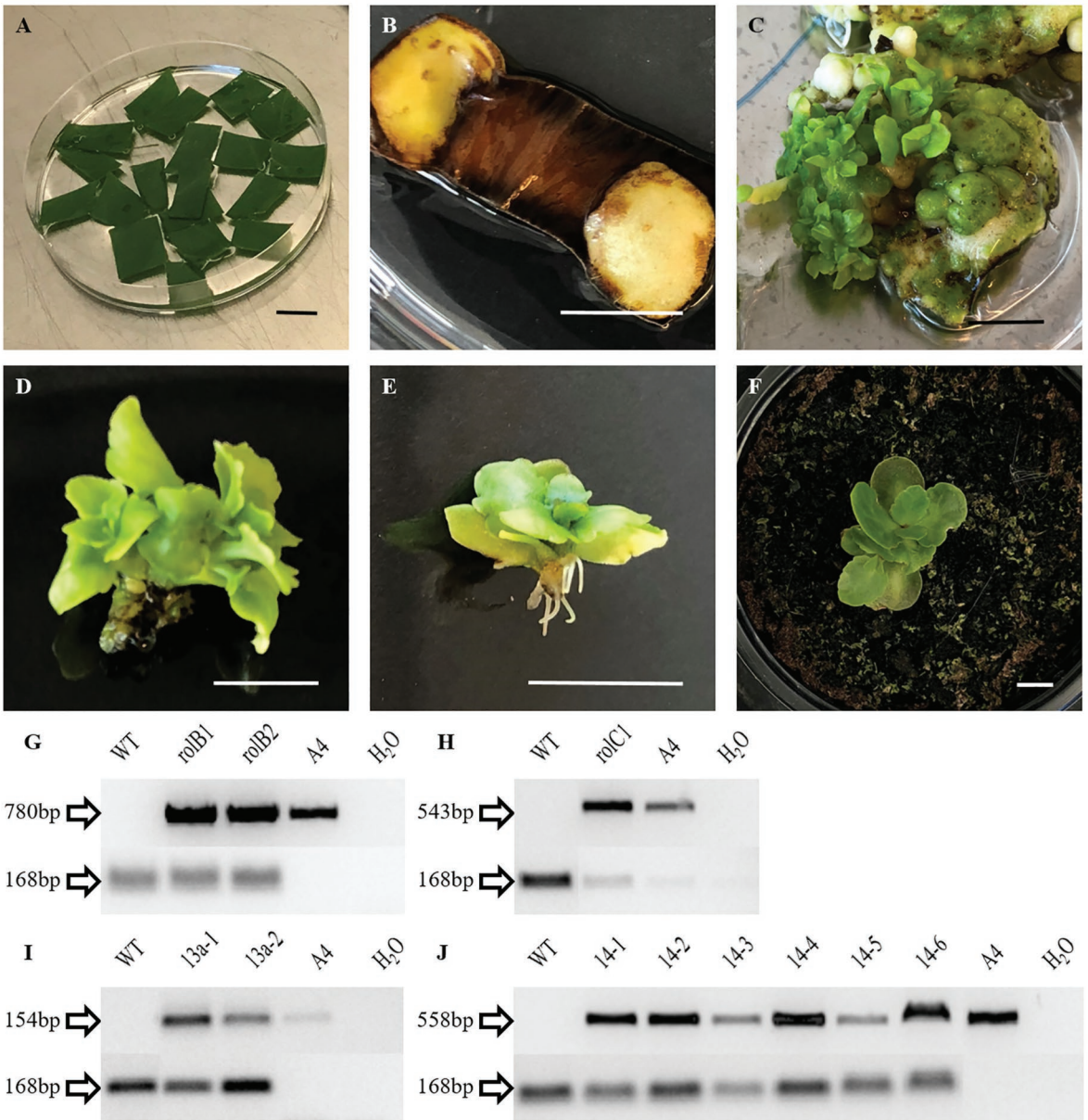

FIGURE 1 | Transformation, regeneration, and molecular characterization for *Kalanchoë blossfeldiana* 'Molly'. *K. blossfeldiana* 'Molly' **(A)** surface sterilized explants ready for inoculation **(B)** senescence associated with kanamycin selection. **(C)** Callus and initial shoots in *K. blossfeldiana* 'Molly' explants **(D)** excised shoot, and **(E)** at a later stage bearing roots. **(F)** *Kalanchoë blossfeldiana* 'Molly' rooted shoots transferred to peat. Genotyping by PCR of regenerated and selected *K. blossfeldiana* 'Molly' lines using full-length primers targeting **(G)** *rol*B (780 bp), **(H)** *rol*C (543 bp), **(I)** ΔORF13a (154 bp), and **(J)** ORF14 (558 bp). *Kalanchoë daigremontiana Actin* (*KdActin*) was the plant reference gene with amplicon of 168 bp, A4 is the unmodified plasmid from *Rhizobium rhizogenes* and positive control for the *rol* genes/open reading frames (ORFs) PCR reactions, and H_2O was the negative control for both plant and *rol* genes/ORFs PCR reactions (see **Supplementary Table S1** for the detailed list of primers). WT, wild type. Bar = 1 cm.

TABLE 1 | Overall *Agrobacterium tumefaciens* transformation data. Number of inoculated explants, kanamycin resistant shoots and confirmed by PCR amplicon sequencing, and transformation efficiency for the investigated constructs.

Construct	No. of explants	No. of kanamycin resistant shoots	No. of PCR-positive shoots	Transformation efficiency (%)
*rol*B	201	3	2	1.0
*rol*C	201	1	1	0.5
ΔORF13a	274	6	3	1.1
ORF14	272	13	8	2.9

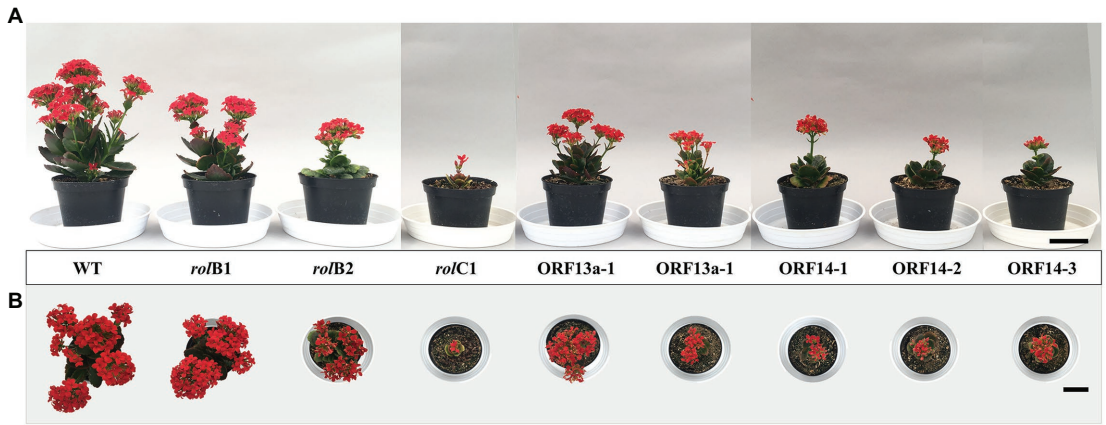

FIGURE 2 | Phenotype of transgenic lines. **(A)** Frontal and **(B)** top view of transgenic lines and wild type (WT) *K. blossfeldiana* 'Molly' plants at 4 months after the flower induction, i.e. short day treatment, was initiated. Bar = 5 cm.

not differ between the two lines (**Figures 3C–E**). In terms of biomass, the fresh and dry weight variation of the overexpressing lines fluctuated negatively in the same order of magnitude for both parameters when compared to WT. The least reduction was observed for *rol*B1 line displaying 49% decrease of leaves in relation to the WT (**Figures 3F,G**). In addition, assessment of the relative chlorophyll content indicated that the chlorophyll accumulation of *rol*B1, *rol*B2, and ORF14-1-3 lines decreased on average 27%, while 91 and 66% in the *rol*C1 and ΔORF13a-2 lines, respectively, when compared to WT (**Figure 3H**). In contrast, chlorophyll accumulation of ΔORF13a-1 was not altered compared to WT (75.6 ± 2.5 SPAD units).

The biometric data for the ornamental features of the *K. blossfeldiana* 'Molly' transgenic lines, i.e., flowers, were collected throughout the period and at the end of the flower induction phase. Parameters regarding developmental, i.e., anthesis and postharvest longevity, and morphological, i.e., flower diameter and petal arrangement, features were assessed. The number of flowers in the WT was 404 ± 32 and severely decreased in the overexpressing lines, varying from 59% less flowers in *rol*B1 to 99% fewer flowers in *rol*C1 (**Figure 4A**). In terms of anthesis, the WT had its first open flower at 68.9 ± 0.9 days after the short-day treatment started with *rol*B1, *rol*B2, ΔORF13a-1, and ORF14-3 showing statistically similar timing, while 12 days later flowering was observed for ΔORF13a-2, ORF14-1, and ORF14-2 (**Figure 4B**). Postharvest longevity, defined as time from first open to first wilted flower, was equal or decreased for the transformed lines compared to WT (18.8 ± 0.9 days, **Figure 4C**). Flower diameter remained unchanged despite the presence of overexpressed *rol* genes/ORFs and alteration in the usual *Kalanchoë* 4-petal configuration was observed in the *rol*C1 line, although not significant due to the low number of observed flowers in this line (**Figures 4D,E**). The *rol*B1 flower (**Figure 4G**) had similar morphology as WT flowers presenting a fused tubular corolla with smooth edged petals (**Figure 4F**). However, morphological alterations were observed; i.e., unfused and fan shaped corolla in *rol*B2, *rol*C1, ΔORF13a-1, ΔORF13a-2, ORF14-1, and ORF14-3 (**Figures 4H–L,N**), irregular petal edges (lobose) in *rol*B2, *rol*C1, ORF14-2, and ORF14-3 (**Figures 4H,L–N**).

Expression of *rol* Gene/ORF Transcripts Depended on the Number of Insertions

In total, two *rol*B, three ΔORF13a, and four ORF14 lines were analyzed for relative gene-copy number by quantitative real-time PCR according to methodology described by Lütken et al. (2010). The presence of the endogenous *KlActin* gene (Wang et al., 2019) was the reference used to normalize the RT-qPCR data, while the relative copy number of *rol* genes/ORFs were standardized using line 306 (Christensen et al., 2008) as reference for single copy, i.e., 1-fold change. Overall, a correlation to Christensen et al. (2008) Southern blot data was found, although in the current study *K. blossfeldiana* 300 lines did not entirely correlate when RT-qPCR was performed using *rol*C primers (**Table 2**). The following lines were attributed to have single copy insertions based on their fold change after RT-qPCR and in relation to the abovementioned categories: *rol*B2, ORF14-2, and ORF14-4; while these were tentatively classified as bearing low copy insertions: *rol*B1, ΔORF13a-1 and ΔORF13a-2, ORF14-1, and ORF14-3 (**Table 2**). The *rol*C1 line was originally verified for gene presence and confirmed by sequencing, but later the gene could not be detected in the mother plant anymore despite the consistent phenotype and was thus discarded from the analysis.

The relative expression of *rol* genes/ORFs was assessed in leaves of transgenic *K. blossfeldiana* lines. RT-qPCR was conducted and the expression levels of the *rol* genes/ORFs lines were correlated to the expression of endogenous *KlActin* and WT plants. The highest relative expression level (correlated within the lines) was found in *rol*B2 (5.0 ± 0.8), ΔORF13a-2 (1.8 ± 0.1), and ORF14-2 (3.7 ± 0.5), all statistically significant. Whereas, the remaining of the lines displayed low relative expression levels. All transgenic lines exhibited expression of *rol* genes/ORFs to various levels (**Table 3**), except the

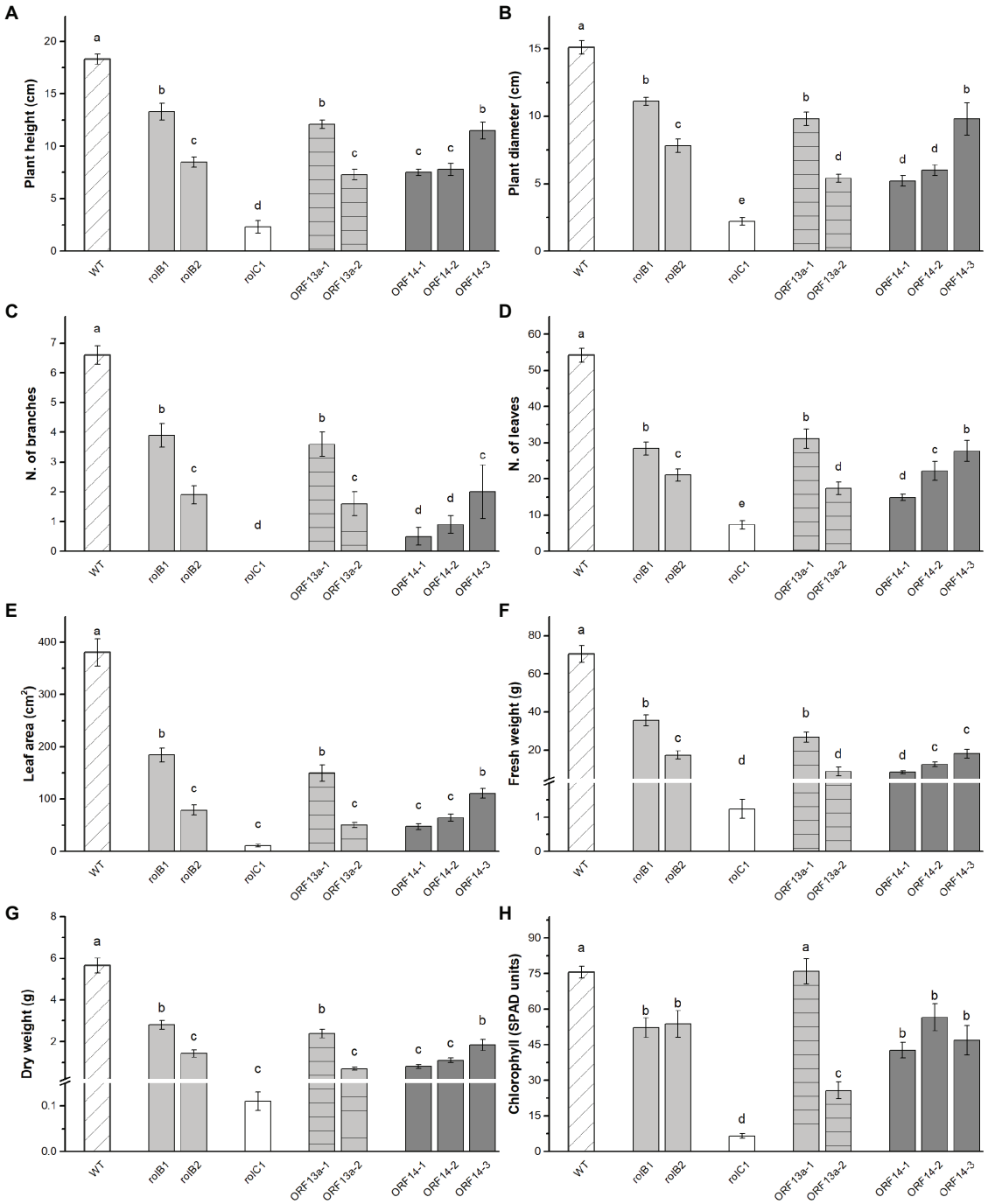

FIGURE 3 | Vegetative biometric data and chlorophyll content in leaves of plants derived from individual transformation events. **(A)** Plant height, **(B)** plant diameter, **(C)** number of branches, **(D)** number of leaves, **(E)** leaf area, **(F)** fresh weight, **(G)** dry weight, and **(H)** chlorophyll of WT *K. blossfeldiana* 'Molly' and overexpressing lines (*rol*B1, *rol*B2, *rol*C1, ΔORF13a-1, ΔORF13a-2, ORF14-1, ORF14-2, and ORF14-3). Data columns represent the average ± SE (n = 6–27) and different lower case letters represent statistical significance using Scott-Knot test ($p \leq 0.05$).

*rol*C1 line, which was originally verified for gene presence and confirmed by sequencing, and displayed a consistently compact habit and reduced plant growth, but could not be further detected in the mother plant thus discarded from this analysis.

Detached Flowers of Line ORF14-3 and ΔORF13a-1 Exhibited Changes in Ethylene Tolerance

The tolerance to exogenous ethylene was measured in detached flowers by assessing flower closure and flower senescence.

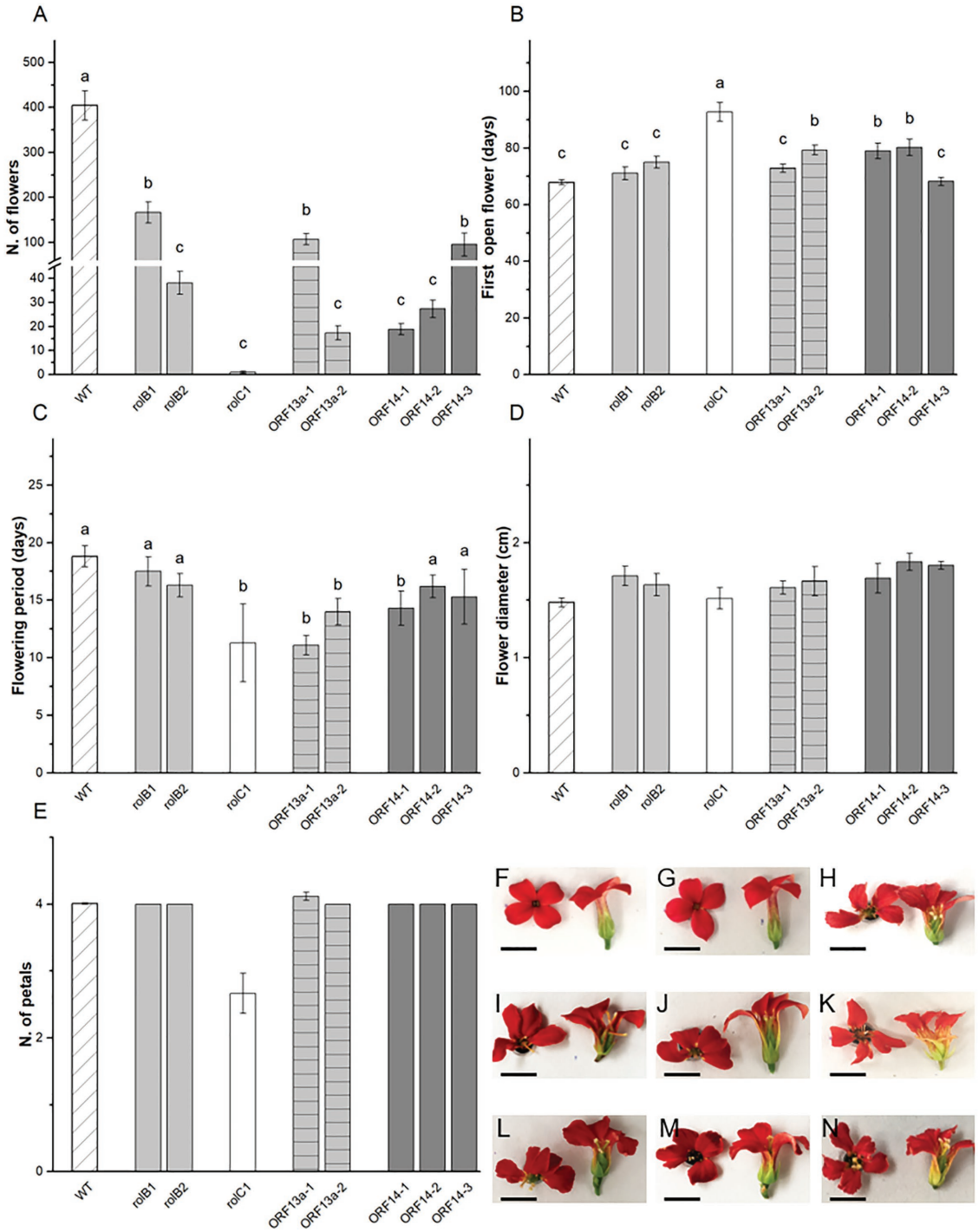

FIGURE 4 | Generative biometric data and flower morphology. **(A)** Number of flowers, **(B)** days to first open flower, **(C)** flowering period, **(D)** flower diameter, and **(E)** number of petals of WT *K. blossfeldiana* 'Molly' and overexpressing lines (*rol*B1, *rol*B2, *rol*C1, ΔORF13a-1, ΔORF13a-2, ORF14-1, ORF14-2, and ORF14-3). Data columns represent the average ± SE (n = 6–27) and different lower case letters represent statistical significance using Scott-Knot test ($p \leq 0.05$). Graphs **(E)** and **(F)** were not statistically significant. Representative flower of **(F)** WT, **(G)** *rol*B1, **(H)** *rol*B2, **(I)** *rol*C1, **(J)** ΔORF13a-1, **(K)** ΔORF13a-2, **(L)** ORF14-1, **(M)** ORF14-2, and **(N)** ORF14-3 illustrating morphological changes between the lines. Bar = 0.5 cm.

Ethylene tolerance of detached flowers was assessed by exposure to 0.5 µl L^{-1} ethylene and the ORF14-3 line was markedly more tolerant to this hormone exhibiting reduced flower closure (**Figure 5A**). Detached flowers of the ORF14-3 line exhibited 66% less closure of individual flowers in the first 3 days after ethylene exposure compared to WT flowers (**Figure 5B**).

TABLE 2 | Relative copy number of the *K. blossfeldiana* transgenic lines.

RT-qPCR target	Genotype	Fold change	Relative no. of copies
*rol*B	*rol*B1	5.9 ± 1.1	low copy
	*rol*B2	1.5 ± 0.2	single copy
	306	1.0 ± 0.1	single (1*)
	331	11.1 ± 1.1	low copy (2*)
	324	21.3 ± 1.2	high copy (9*)
ΔORF13a	ΔORF13a-1	7.0 ± 1.2	low copy
	ΔORF13a-2	4.8 ± 0.7	low copy
	306	1.0 ± 0.1	single (1*)
	331	10.3 ± 0.7	low copy (2*)
	324	19.4 ± 1.6	high copy (9*)
ORF14	ORF14-1	3.7 ± 1.5	low copy
	ORF14-2	1.7 ± 0.6	single copy
	ORF14-3	2.5 ± 0.9	low copy
	ORF14-4	0.4 ± 0.0	single copy
	306	1.0 ± 0.1	single (1*)
	331	14.5 ± 2.4	low copy (2*)
	324	25.0 ± 5.7	high copy (9*)
*rol*C	306	1.0 ± 0.1	single (1*)
	331	8.3 ± 1.0	low copy (2*)
	324	10.3 ± 1.9	low copy (9*)

*The relative rol genes/ORFs copy number inserted into the genome was calculated in terms of fold change ($2^{-\Delta\Delta Ct}$) standardized by K. laxiflora Actin (KlActin) and line 306. Categories were defined based on fold change: single copy (<2), low copy number (2 > and < 15), and high copy number (>15). *Data represent number of bands observed in Southern blot (Christensen et al., 2008). Data represent the average ± SE of three pooled plants for each line and the experiment was repeated twice.*

TABLE 3 | Gene expression of the different *K. blossfeldiana* transgenic lines.

Genotype	Fold change
*rol*B1	0.1 ± 0.1b
*rol*B2	5.0 ± 0.8a
ΔORF13a-1	0.8 ± 0.2b
ΔORF13a-2	1.8 ± 0.1a
ORF14-1	2.5 ± 0.5b
ORF14-2	3.7 ± 0.5a
ORF14-3	2.5 ± 0.2b
ORF14-4	2.6 ± 1.2b

The relative rol genes/ORFs expression was standardized by KlActin and calculated in terms of fold change ($2^{-\Delta Ct}$). Data represent the average ± SE of three pooled plants for each line, the experiment was repeated twice and different lower case letters within the rol gene/ORF represent statistical significance using t-test ($p \leq 0.05$).

The other ORF14 lines, i.e., 1, 2, and 4, and ΔORF13a-1 performed better in terms of ethylene tolerance on day 3 than the WT, but not to the same level as ORF14-3. Additionally, *rol*B2 showed similar ethylene tolerance as the WT on day 3. However, ΔORF13a-2 exhibited decreased ethylene tolerance, indicating specific *rol* genes/ORFs effects and highlighting the importance of ethylene tolerance studies as an attractive trait for *Kalanchoë* breeders. Petal blackening and complete flower closure were the criteria for labeling flower senescence. In ORF14-3, an increased postharvest quality duration with <20% senescent flowers until day 4 after ethylene exposure was observed (**Figure 5C**). In contrast, more than 50% of the flowers senesced in all other overexpressing lines and WT on day 4.

rolC and ΔORF13a Are Soluble Proteins and Localize to the Cytoplasm

Knowing the subcellular localization of a protein encoded by a gene may be useful when trying to elucidate the functional role of a gene. Thus, in order to assess the subcellular localization of *rol*C and ΔORF13a, constructs of their nucleotide sequence fused to eGFP at either the N or C terminus were prepared. Coexpression of the constructs with soluble mRFP1 as a control was performed in *Nicotiana benthamiana* to reveal the subcellular localization of the encoded proteins. Confocal images of ΔORF13a constructs tagged at both C and N termini showed that ΔORF13a is soluble and localizes in the cytoplasm, filling the space around the cortical endoplasmic reticulum (ER) as well as entering the nucleus (**Figures 6A–I**). The addition of the tag at either the N or C terminus did not influence the observed localization of ΔORF13a. In contrast, rolC tagged at the C terminus localized to the cytoplasm and entered the nucleus (**Figures 7A–F**). When rolC was tagged with eGFP at the N terminus, rolC appeared to be in the cytoplasm, but fluorescence was not detectable inside the nucleus, instead the fluorescence was only observed in the nuclear membrane (**Figures 7G–L**), suggesting that the eGFP tag interferes with the localization of the rolC protein. Therefore, to thoroughly assess the localization of rolC and possible effects of the eGFP tag, the localization experiments in *N. benthamina* were repeated coexpressing the *eGFP-rol*C construct with the construct of *SbCYP89A1* fused to *mRFP1* (as a control of a protein which localizes to ER and nuclear membrane). The confocal images only revealed overlay of the eGFP-rolC and SbCYP89A1-mRFP1 in the nuclear membrane, but not in the ER membrane network; eGFP-rolC remained a soluble protein localized to the cytoplasm, but was no longer detected inside the nucleus and remained at the nuclear membrane (**Figures 8A–F**).

DISCUSSION

In the current study, multiple transformation events generated independent transgenic lines of *rol*B, *rol*C, ΔORF13a, and ORF14 exhibiting clear morphological alterations. *De novo* organogenesis of *K. blossfeldiana* 'Molly' transgenic lines differed in efficiency between the investigated overexpression constructs, i.e., *rol*B, *rol*C, ΔORF13a, and ORF14, and the highest transformation rate was observed for ORF14 (2.9%) and lowest for *rol*C (0.5%). In this study, the transformation rate was lower than in earlier studies (Zia et al., 2010; Wang et al., 2019) and it followed previous transformation protocols optimized for *R. rhizogenes*-mediated transformation that included high concentration of cytokinin to promote the *de novo* organogenesis of shoots (Christensen et al., 2008; Hegelund et al., 2017). *Agrobacterium*-mediated transformation of multiple species of the *Kalanchoë* genus has been reported. For example, *K. laxiflora* transformed with either pCambia1305 or pCambia2305 in multiple *A. tumefaciens* strains revealed 4–21% positive transformation events *via* transient GUS activity assays (Wang et al., 2019). A compact habit and reduced plant growth was observed in all the transgenic lines when the overexpressing

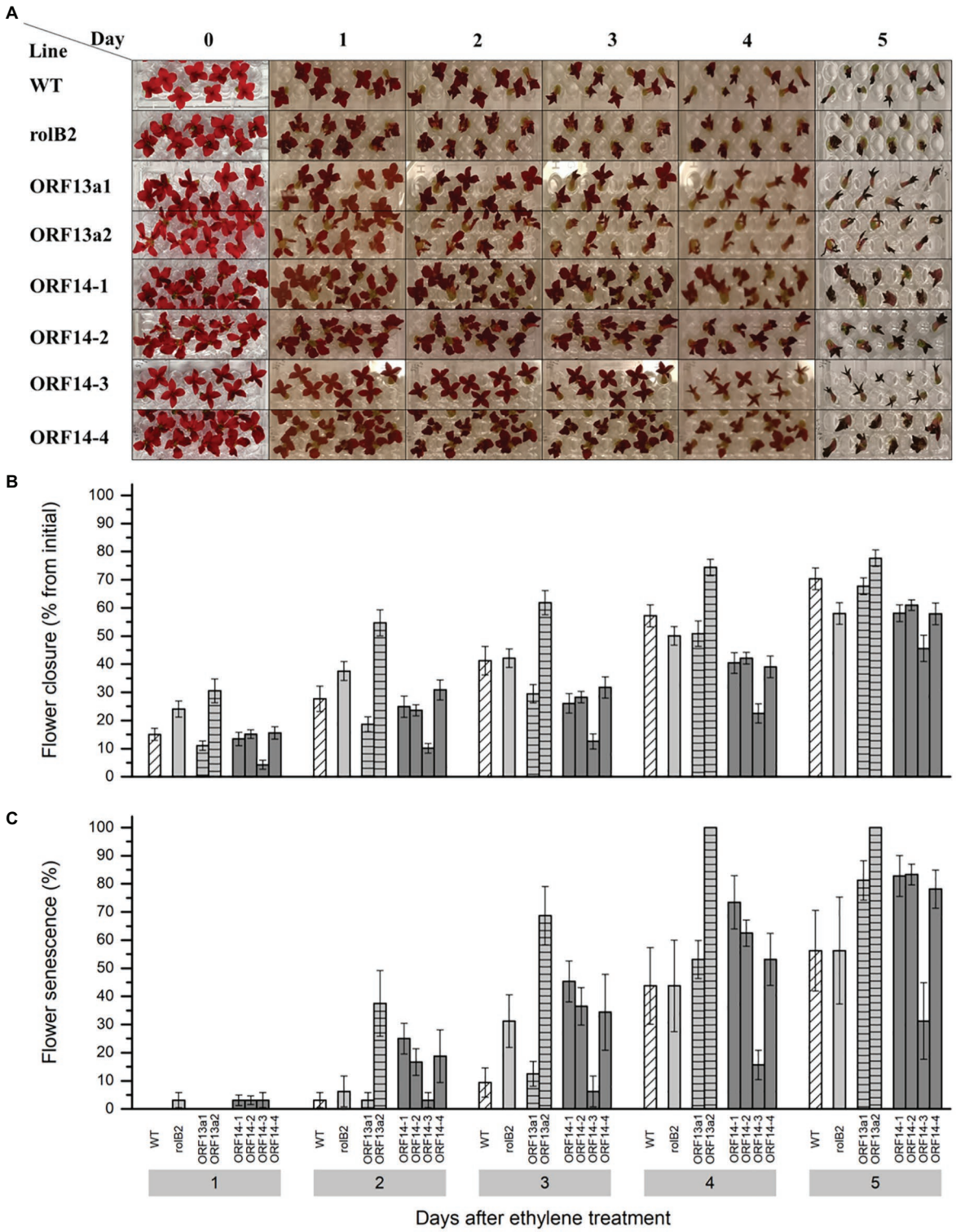

FIGURE 5 | Ethylene sensitivity among the *rol* genes/ORFs overexpressing lines. **(A)** Exogenous ethylene (0.5 μl L^{-1}) applied to detached *K. blossfeldiana* 'Molly' flowers of WT and overexpressing lines (*rol*B2, ΔORF13a-1, ΔORF13a-2, ORF14-1, ORF14-2, ORF14-3, and ORF14-4) placed in micro titer plates with water inside a hermetic sealed glass tank. A control group of the same genotype consisted of the same setting without the addition of ethylene. **(B)** Flower diameter was collected daily for 5 days after sealing the glass tanks and the flower closure is presented as percentage from the initial diameter of ethylene exposed flowers. **(C)** Senescent detached flower percentage on each evaluation day. Data columns represent the difference average ± SE (n = 8–10) and different lower case letters represent statistical significance using Scott-Knot test ($p \leq 0.05$) within the time point.

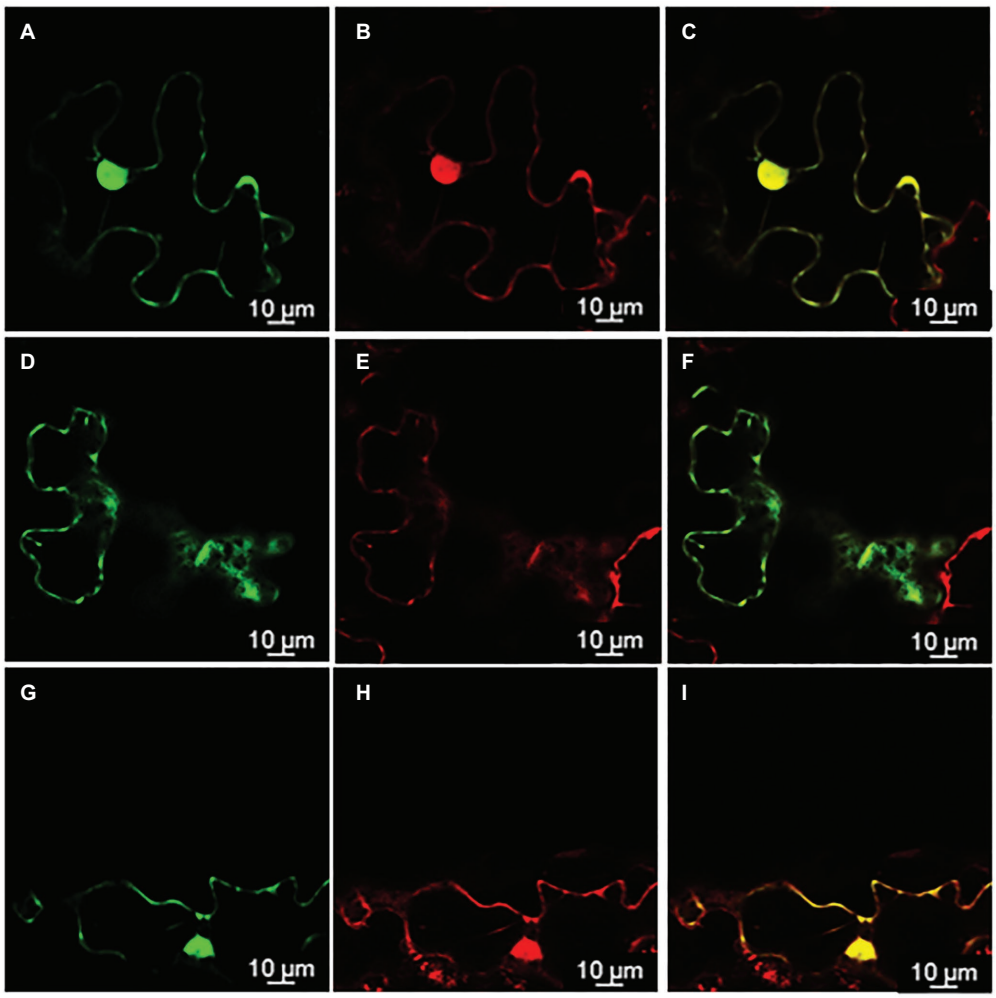

FIGURE 6 | ΔORF13a localization in the cytoplasm visualized by confocal microscopy of *Nicotiana benthamiana* epidermal leaves. **(A)** ΔORF13a fused to enhanced Green Fluorescent Protein (eGFP) on its C-terminal end permeates through the nuclear pores and can be found inside the nucleus **(B)** as confirmed by soluble monomeric Red Fluorescent Protein1 (mRFP1) control, panel **(C)** is an overlay of signals from ΔORF13a-eGFP and mRFP1 demonstrating complete co-localization of both proteins. **(D)** Soluble proteins fill out the cytoplasm around the cortical endoplasmic reticulum (ER) as observed for ΔORF13a-eGFP and **(E)** mRFP1, panel **(F)** is an overlay of signals from ΔORF13a-eGFP and mRFP1 demonstrating complete co-localization of both proteins. **(G–I)** Fusion of eGFP to the N-terminal end of ΔORF13a did not affect the localization of ΔORF13a.

single gene assessment approach was utilized (**Figures 2A,B**). This is in accordance with other previous studies that targeted transformation with either WT *R. rhizogenes* (Christensen et al., 2008), single genes with endogenous promoters (Zhu et al., 2001; Bettini et al., 2003; Kubo et al., 2006), or with *35S* driven expression (Schmülling et al., 1988; Faiss et al., 1996; Koshita et al., 2002; Kodahl et al., 2016).

The transgenic lines of all investigated constructs displayed statistically significant ($p \leq 0.05$) reduced plant height, diameter, number of branches, number of leaves, leaf area, fresh, and dry weight compared to WT (**Figures 3A–G**). In general, vegetative growth among the transformed plants changed greatly, this was the case for *rol*B1 and *rol*B2, which correlates to the observations in *A. thaliana* (Kodahl et al., 2016). In the present study, the *rol*B1 line was categorized as having a relative low copy number while *rol*B2 was estimated as a single copy line, and the expression levels in the latter had a 5-fold increase compared to *rol*B1. Therefore, a higher copy number indicated a lower expression of *rol*B. Similarly, Komarovská et al. (2010) observed that higher *rol* gene copy number integration was associated with weaker transgenic expression as well as a lesser aberrant phenotype in *Hypericum perforatum*. A stepwise reduction in plant height and diameter, leaf number, and area was observed for fresh and dry weight as well in decreasing order for WT > *rol*B1 > *rol*B2. Moreover, it seemed that in the *rol*B lines, a single copy event (**Table 2**) led to very high expression levels (**Table 3**), which in turn decreased all other phenotype parameters observed in this study (**Figures 2A–G**). This support the well-established paradigm of strong association of *rol*B to stunted growth and this has also been reported in *A. thaliana* (Dehio and Schell, 1994; Kodahl et al., 2016), *N. tabacum* (Schmülling et al., 1988), and *Lycopersicum esculentum*

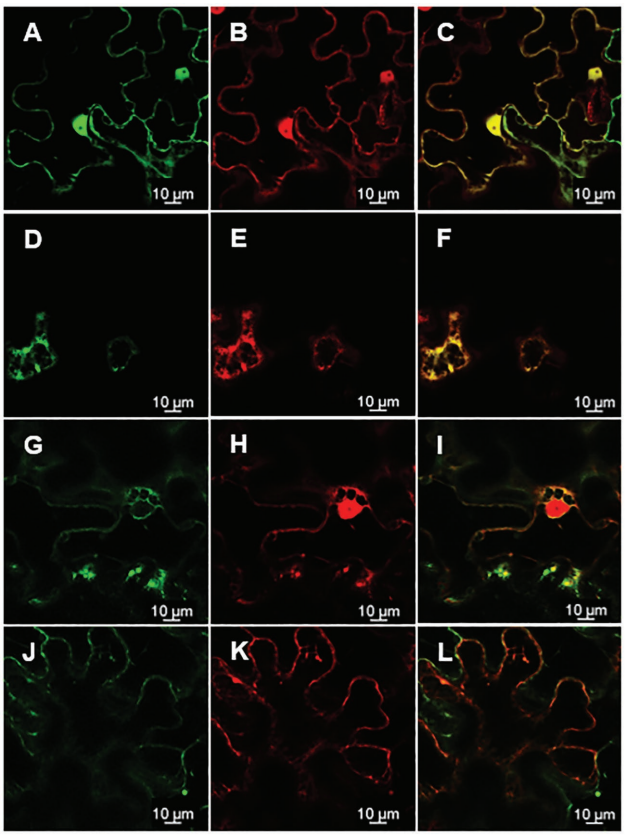

FIGURE 7 | Position of the eGFP tag on rolC affects its subcellular localization as visualized by confocal microscopy of *N. benthamiana* epidermal leaves. **(A)** rolC fused to eGFP on its C-terminal end permeates through the nuclear pores and can be found inside the nucleus **(B)** as confirmed by soluble mRFP1 control, panel **(C)** is an overlay of signals from rolC-eGFP and mRFP1 demonstrating complete co-localization of both proteins. **(D)** Soluble proteins fill out the cytoplasm around the cortical ER as observed for rolC-eGFP and **(E)** mRFP1, panel **(F)** is an overlay of signals from rolC-eGFP and mRFP1 demonstrating complete co-localization of both proteins. **(G)** rolC fused to eGFP on its N-terminal end observed on the nuclear membrane. **(H)** Soluble mRFP1 permeates into the nucleus. Panel **(I)** shows incomplete co-localization of eGFP-rolC and mRFP1. **(J)** rolC fused to eGFP on its N-terminal end. **(K)** Soluble mRFP1. **(L)** Overlay of signals from eGFP-rolC and mRFP1.

(Arshad et al., 2014). Similarly, growth inhibition by increasing expression levels of *rol*B was observed in *Rubia cordifolia* callus. Other growth inhibition effects, like early leaf necrosis in *rol*B transgenic plants were previously reported in *N. tabacum* and *A. thaliana* (Schmülling et al., 1988; Nilsson et al., 1993a; Dehio and Schell, 1994; Kodahl et al., 2016), but in this study, leaf necrosis was not observed in any of the overexpressing *rol*B lines of *K. blossfeldiana*. The absence of necrosis could be attributed to the ability to suppress reactive oxygen species (ROS) observed in light induced stress in *rol*B transformed *R. cordifolia* callus (Bulgakov et al., 2012), potentially due to *rol*B regulation of NADPH oxidase isoforms (Veremeichik et al., 2016). In addition, there is evidence that the fresh and dry weight of *rolB* lines is significantly lower than that of WT in *A. thaliana* (Kodahl et al., 2016). It has been documented that the effect of *rol* genes vary in response among different species (Welander and Zhu, 2010; Grishchenko et al., 2016; Kodahl et al., 2016; Bulgakov et al., 2018). In terms of chlorophyll content, the *rol*B lines, in the current study, did not differ but had lower content compared to WT, thus not influenced by the differential copy number and expression levels observed. Moreover, Kodahl et al. (2016) suggested that the light green color of *A. thaliana* transformed with *rol*B probably was caused by the decrease of chlorophyll content. However, these results contradict the findings obtained in *rol*B under its native promoter in *Solanum lycopersicum*, where chlorophyll a/b content and non-photochemical quenching were significantly increased as well as the upregulation of five genes involved in chloroplast function (Bettini et al., 2016a). Moreover, some studies suggested that there was no difference in chlorophyll content of *S. lycopersium* transformed with *rol*B (van Altvorst et al., 1992; Arshad et al., 2014). Additionally, there has been multiple indications that *rol*B has an impact on environmental adaptive response in plants, e.g., lower accumulation of ROS under stress by ROS scavenging enzymes (Bulgakov et al., 2012), increased peroxidases activity (Veremeichik et al., 2012) and its class III production (Shkryl et al., 2013), modulation of photosynthetic activity under far-red light (Bettini et al., 2020), resistance to light stress (Bulgakov et al., 2013), as well as pathogen infection (Arshad et al., 2014).

The dwarfism and compact habit correlated with *rol*C presence have been reported in *N. tabacum* (Schmülling et al., 1988), *Chrysanthemum morifolium* (Mitiouchkina and Dolgov, 2000), *Salpignosis siniata* (Lee et al., 1996), *Petunia* (Winefield et al., 1999), and *Pelargonium* × *domenicum* (Boase et al., 2004). Here, we showed that an extreme compact habit and reduced plant growth were present *rol*C1 showing reductions of >85% for all traits. A super-dwarfed pelargonium *35S::rol*C was also found and the extreme phenotype was attributed to the insertion of a single transgene copy (Boase et al., 2004). However, despite a consistently compact habit phenotype observed in *rol*C1 and the respective gene presence supported by sequencing, it was not possible to neither determine number of transgene insertions nor obtain consistent gene expression data for *rol*C1 due to inconsistencies in detecting its presence. Taken these together, this point to a probable chimeric line that displayed the ability to survive through multiple sub-culturing rounds on kanamycin-supplemented media and showed a consistent phenotype during the flower induction experiment. The gene expression in transgenic lines driven by the *35S* promoter is known to be unstable due to various causes, e.g., silencing, post-transcriptional modifications, but mostly because the cells are a mixture of WT and transgenic cells to different proportions across tissues (Schmülling and Schell, 1993; Komarovská et al., 2010; Marenkova et al., 2012). Moreover, multiple transformation events could potentially have generated different number of insertions into the genome as well as yielding chimeric transformants. Different tissue culture techniques, e.g., second round of shoot *de novo* organogenesis, could be implemented to avoid such scenarios (Ding et al., 2020; Malabarba et al., 2020). In terms of the number of leaves, the *rol*C1 line in our study had a reduction

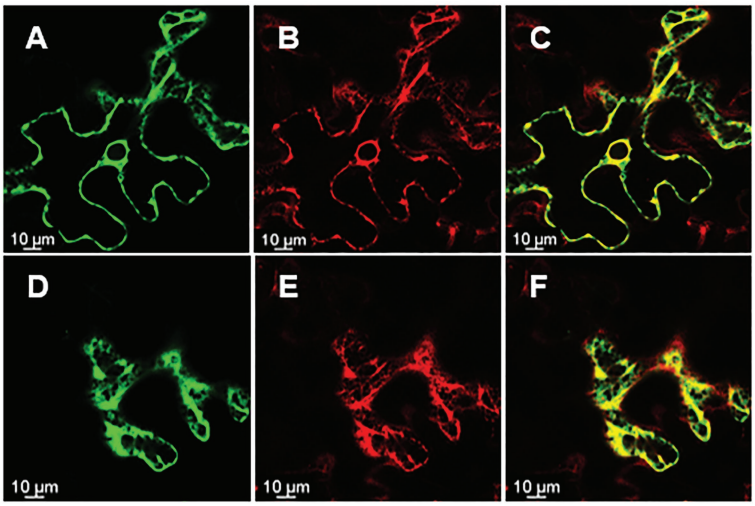

FIGURE 8 | rolC with N-terminus eGFP tag visualized by confocal microscopy of *N. benthamiana* epidermal leaves. **(A)** rolC with eGFP tag on its N-terminal end localizes to the nuclear membrane **(B)** mRFP1 fused to SbCYP89A1. **(C)** Overlay of signals from eGFP-rolC and SbCYP89A1-mRFP1 demonstrating co-localization of both proteins on the nuclear membrane. **(D)** eGFP-rolC appears soluble filling the cytoplasm **(E)** Sb-CYP89A1-mRFP1 localizes to the ER membrane network; **(F)** is an overlay of signals from eGFP-rolC and SbCYP89A1-mRFP1 showing differential localization of both proteins.

relative to WT. On the contrary, the number of leaves of *Petunia* transformed with *rol*C was increased (Winefield et al., 1999). Compared with WT, the leaf area of the *rol*C1 line was greatly reduced. In the study of *Petunia* (Winefield et al., 1999), the leaf area of plants transformed with *rol*C was also decreased. Additionally, the *rol*C1 exhibited the lowest chlorophyll index. Conversely, the impaired chlorophyll content seemed to directly affect plant growth. The proposed effect of rolC as a β-glucosidase is known for releasing cytokinin from its N-glucosides (Estruch et al., 1991a), but other studies have shown lower amounts of cytokinin in overexpressing *rol*C transgenic tobacco (Nilsson et al., 1993b). Therefore, the *rol*C known effect in cytokinin release appears not to be directly linked to higher cytokinin levels. It remains unclear why the expected positive effects of the *rol*C presence *in planta*, e.g., reduced senescence, was not observed in the obtained transgenic line.

The role and effects of ORF13a remain elusive in the literature. The presence of ORF13a has been detected in *Nicotiana* species, first in the genome of wild *N. glauca* (Suzuki et al., 2002), and later transcriptomic studies of *N. noctiflora* reported an ORF13a transcript being expressed in this species (Long et al., 2016), suggesting this was the result of an ancient horizontal gene transfer event in an ancestor of these species. More recently, the presence of an intact copy of ORF13a in cT-DNA of *Linaria vulgaris* was observed (Vladimirov et al., 2019). However, the function of ORF13a in those studies was not investigated in detail. When Lemcke and Schmülling (1998) overexpressed ORF13a in *N. tabacum* plants, there was no observable difference between transformed plants and WT, therefore, the effect of ORF13a was not further investigated. Nevertheless, Hansen et al. (1994) first reported SPXX DNA-binding motifs at the C terminus of the ORF13a protein sequence, suggesting a potential regulatory role. In this study, we overexpressed a truncated version of ORF13a, which excluded the SPXX-DNA binding motifs from an agropine *R. rhizogenes* strain and detected an observable difference in transformed plants compared to WT. The relative number of insertions of both ΔORF13a lines were characterized as low copy and the transcript levels were ca. 2-fold higher in ΔORF13a-2 (**Tables 2, 3**). In a similar fashion, ΔORF13a-1 and ΔORF13a-2 showed analogous patterns of gene expression and values in biometrical parameters as the *rol*B1 and 2, in general supporting the higher copy number connection to a weaker gene expression, thus less aberrant phenotype (Komarovská Aet al., 2010). Therefore, the plant height and diameter, number of branches and leaves, leaf area, and fresh and dry weight were higher in WT followed by ΔORF13a-1 and then ΔORF13a-2 (**Figures 3A–G**). As mentioned before, a higher expression level led to a more compact habit and reduced plant growth in ΔORF13a. It is still uncertain if the effects observed in this study compared to previous reports are due to the omission of the SPXX-DNA binding motif, the use of *K. blossfeldiana* or to the position where the T-DNA was integrated. However, the reproducible phenotype in both ΔORF13a lines of the same species suggests that the SPXX-DNA binding motif influences the function of ORF13a. Further studies in different plants would be required to elucidate the functional mechanism of the SPXX-motif in ORF13a.

Overexpression of ORF14 was confirmed by RT-qPCR and the expression levels were relatively low, ca. 1-fold after *KlActin* and WT standardization, with an increase in ORF14-2 with approximately 1.5-fold. Moreover, ORF14 lines relative copy number was low copy range, which is contrasting to *rol*B and ΔORF13a lines where a lower copy number was associated with high transcript accumulation. The use of ORF14 in an overexpressing cassette was reported to have no changes in the

morphology of transgenic plants (Lemcke and Schmülling, 1998). Interestingly, in this study, the effect of overexpressing ORF14 was a compact habit and reduced plant growth in comparison to WT. Additionally, ORF14-1 and 2 had a compactness level to the same extent as the most compact habit lines of *rol*B and ΔORF13a despite the display of increase in the respective gene expression. This fact opens up to more intriguing questions, e.g. ORF14 could potentially be as strong compactness denominator as *rol*B, as more light is shed on the less explored ORFs. It is important to highlight that the crescent number of leaves observed in ORF14-1 and ORF14-3 only resulted in statistically significant larger leaf area for ORF14-3, which indicates that ORF14-2 had more, but smaller leaves compared to ORF14-1. As mentioned previously, Lemcke and Schmülling (1998) did not observe a distinct phenotype for overexpressing neither ORF14 nor ORF13a. In general, it has been hypothesized that both ORF13 and ORF14 have a synergistic effect to the *rol* genes (Aoki and Syono, 1999b).

The number of flowers was reduced in the overexpressing lines compared to WT, which was expected since stunted vegetative growth is usually followed by a decrease in flower number (Christensen et al., 2008). The decrease in total flower numbers of approximately 50% in relation to WT for *rol*B1, ΔORF13a-1, and ORF14-3 is in accordance with data from Christensen et al. (2008) on *Kalanchoë* transformed with WT *R. rhizogenes*. However, *rol*B2, ΔORF13a-1, ORF14-1, and ORF14-2 showed approximately 85% less flowers in relation to WT, while *rol*C1 showed 99% reduction. However, in contrast, a large number of flowers were observed in chrysanthemum transformed with *rol*C (Mitiouchkina and Dolgov, 2000). Despite the lower number of flowers, a decrease in ornamental value was not observed for the *rol*B1, ΔORF13a-1, and ORF14-3 since these lines had flower numbers proportionally reduced according to the overall vegetative growth decrease. The number of flowers in tomato plants transformed with *rol*A and *rol*B was influenced by the cultivar ploidy levels, where 4x plants exhibited low flower production, i.e., 0–50 flowers, while diploid showed 100 to over 400 flowers (van Altvorst et al., 1992). In *A. thaliana*, the number of inflorescences did not differ between *rol*B and WT; however, the ratio inflorescence:leaf area revealed that *rol*B had a larger number of inflorescences per rosette area (Kodahl et al., 2016). The altered phenotype in *rol*A, *rol*B, and *rol*C transgenic *Glycine max* plants induced earlier flowering with fewer flowers than control plants (Zia et al., 2010). In natural transformation with *R. rhizogenes*, delayed flowering is an often observed significant drawback. Early or unaltered anthesis is an important factor for commercial production of ornamental plants, as delayed flowering implies in longer production span, hence higher costs. In the present study, WT had its first open flower after 68.9 ± 0.9 days and there was no alteration in flowering time for *rol*B1, *rol*B2, ΔORF13a-1, and ORF14-3. However, 12 days anthesis delay was observed for ΔORF13a-2, ORF14-1, and ORF14-2 and ultimately a 24 days postponement was observed for *rol*C1 (**Figure 4C**). On the contrary, other *rol*C transformed species, such as *Solanum tuberosum* (Fladung, 1990; Schmülling et al., 1993), *Atropa belladonna* (Kurioka et al., 1992), and *Osteospermum* (Giovannini et al., 1999; Allavena et al., 2000), had the characteristics of early flowering. The presence of *rol* genes/ORFs revealed substantial variation in flowering time, i.e., early, non-altered, or late flowering have been reported. The 'Molly' cultivar transformed with unmodified *R. rhizogenes* showed that most F1 and F2 progeny obtained by selfing displayed either later or unmodified anthesis onset, the exception was 2,202 lines that had earlier flowering than WT (Lütken et al., 2012b). The above indicated that, in regard to anthesis, the presence of the complete T-DNA can be compensated by a single *rol* gene/ORF in an overexpressing setup. The flowering period was either equal or decreased for the transformed lines compared to WT (**Figure 4D**). In contrast, *K. blossfeldiana* 'Molly' carrying the complete T-DNA, in self-crossed F1 and F2 populations, displayed a number of lines with early flowering (Lütken et al., 2012b). The *35S* promoter effect in the current study seemed to reduce the potential early anthesis effect observed by Lütken et al. (2012b). The *K. blossfeldiana* 'Molly' flower diameter remained unchanged despite the presence of overexpressing *rol* genes/ORFs (**Figure 4E**). Conversely, the same species naturally transformed with *R. rhizogenes* showed reduced flower diameter in both F1 and F2 progenies to a partial extent of the obtained crossings (Lütken et al., 2012b). Furthermore, it has been reported that pelargonium transformed with *rol*C exhibited characteristics of reduced petal area and flower diameter (Boase et al., 2004). To our knowledge, an alteration in the usual *Kalanchoë* 4-petal configuration was observed for the first time in the *rol*C1 line, although not significant due to the low number of flowers observed in this line (**Figure 4F**). Interestingly, it was found that the flower shape of the *rol*C line of chrysanthemum changed and the petals became wider (Mitiouchkina and Dolgov, 2000). Other studies have shown reduction in flower diameter (Lütken et al., 2012b; Kodahl et al., 2016) as well as alteration in pistil morphology, e.g., hyperstyly (Sinkar et al., 1988; van Altvorst et al., 1992).

Flower longevity and ethylene tolerance of flowers are important quality indexes of potted flowering plants. Ethylene tolerance or at least low ethylene sensitivity is necessary, especially for *K. blossfeldiana*, which is known for its sensitivity to ethylene (Woltering, 1987; Müller et al., 1998; Serek and Reid, 2000). Interestingly, in the present study, detached flowers of ORF14-3 showed increased tolerance to exogenous ethylene compared to WT and all other overexpressing lines. Additionally, other ORF14 lines, i.e., 1, 2, and 4, as well as ΔORF13a-1 showed less prominent but still improved ethylene tolerance compared to WT. Increased tolerance to ethylene was also detected in detached flowers of *K. blossfeldiana* transformed with unmodified *R. rhizogenes*, therefore carrying the full T-DNA containing all *rol* genes and ORFs (Christensen and Müller, 2009). The investigation of ethylene tolerance in Ri flowers has been previously discussed in terms of the presence of the *rol*C gene and a lower production of ethylene in these plants (Martin-Tanguy et al., 1993) as well as its cytokinin-like effect in plants (Schmülling et al., 1988; Zuker et al., 2001; Casanova et al., 2003). Moreover, there is the

known alteration in source-sink relationship that led to higher glucose and sucrose levels in *rol*C and *ipt* transformed plants (Hall, 1992; Yokoyama et al., 1994; Veena and Taylor, 2007; Mohajjel-Shoja et al., 2011). Collectively, it indicated a strong connection to increased flower longevity due to a potentially higher sucrose flower content linked to a higher ethylene tolerance found in other ornamentals, e.g., cut (Kazuo et al., 2015) and potted (Monteiro et al., 2002) roses, as well as the downregulation of petal senescence associated genes (Hoeberichts et al., 2007). The present study was not able to investigate the ethylene and overexpression of *rol*C relation due to the extremely low flower production in this line (**Figure 4A**). Interestingly, the most relevant tolerance to ethylene was found in overexpressing ORF14 lines. This is new data as to the best of our knowledge as the ORF14 literature only describes its role as an accessory sequence that mildly mediated rooting in synergy with *rol*B (Aoki and Syono, 1999b).

The subcellular localization of a protein is physiologically important and can provide insights for future functional characterization. In this study, we conducted transient expression in *N. benthamiana* and show the subcellular localization of two proteins causing significant phenotype alterations in *K. blossfeldiana*: ΔORF13a and rolC. We present that ΔORF13a is a soluble protein that fills the cytoplasm and can permeate into the nucleus. There are according to our knowledge no studies on the subcellular localization of ORF13a to compare our results with. It is therefore unknown if the SPXX-motif repeats in ORF13a would influence localization since these motifs have DNA-binding properties, hence further investigation is needed. We observed that rolC is also a soluble protein that fills the cytoplasm able to permeate into the nucleus. Immunolocalization performed by Estruch et al. (1991b) also reported rolC as a soluble protein in the cytoplasm. Lalonde et al. (2003) reported the same, by tagging rolC with eGFP on its C-terminal end; however, they did not construct an eGFP fusion in the N-terminal end of rolC. We showed that when the position of the eGFP tag on rolC was moved from the C-terminal to the N-terminal end, rolC remained a soluble protein, but was no longer detected inside the nucleus and was found in the nuclear membrane. Proteins localized to the nuclear membrane typically display localization to the ER membrane network as well, but our experiments with co-expression of an ER/nuclear membrane control (SbCYP89A1-mRFP1) and eGFP-rolC in *N. benthamiana* leaves showed that rolC is indeed soluble and eGFP does not interfere with a localization signal to the ER membrane network. Given the size of rolC (~20KD) and of eGFP (~37KD), the fusion of these proteins could passively diffuse through the nuclear pore complex (Timney et al., 2016), therefore, it is likely that the eGFP fusion at the C-terminal end of rolC affects either a nuclear export signal or a protein-protein interaction domain of rolC with a protein in the nuclear membrane (Weill et al., 2019). These results can hopefully provide the basis for greater insights through further investigations on the functional characterization of *rol* genes and other ORFs derived proteins.

CONCLUSION

We have found distinct phenotypes when individual *rol* genes and other ORFs were transformed into *Kalanchoë*, contributing to substantial changes in ethylene tolerance. The ORF14 was consistently more tolerant to this hormone and presents a new target toward ethylene tolerance studies in both Ri and overexpressing *rol* gene/ORF lines. A higher expression level combined with a single or lower number of gene copy insertions resulted in a more compact habit and reduced plant growth phenotype in *rol*B, ΔORF13a, and ORF14 lines. Additionally, novel protein data document that ΔORF13a is a soluble protein that permeates to the nucleus, while rolC-eGFP tag in the N-terminal end aborts its localization to the nuclear membrane. The increased knowledge about the differential effect of selected individual *rol* genes and previously unknown ORFs contributes to further development of *R. rhizogenes*-based transformation as a breeding tool in horticulture and agriculture. Collectively, a strong modulation of the compacted habit phenotype in terms of the distinguished effects each individual *rol* gene and selected ORFs display was found. This affected flower number and size, plant compactness as well as timing of anthesis, flower longevity, and ethylene tolerance.

DATA AVAILABILITY STATEMENT

The datasets presented in this study can be found in online repositories. The names of the repository/repositories and accession number(s) can be found in the article/**Supplementary Material**.

AUTHOR CONTRIBUTIONS

BF, AA, and HL conceptualized the present idea, planned the experiments, and contributed to the interpretation of results. BF, YT, YL, HH, NS, JX, and AA performed the experimental work and data processing. YT, YL, HH, NS, and JX documented the images presented. BF and AA wrote the original manuscript and organized the figures and tables. BF, JH, RM, AA, and HL provided critical feedback to the original manuscript editing. All authors contributed to the article and approved the submitted version.

FUNDING

The Danish Council for Independent Research supported this research (grant no. DFF-7017-00197). The Chinese Scholarship Council provided scholarships to YT (MSc grant no. 201806300008) and JH (PhD grant no. 201906760024).

SUPPLEMENTARY MATERIAL

The Supplementary Material for this article can be found online at: https://www.frontiersin.org/articles/10.3389/fpls.2021.672023/full#supplementary-material

REFERENCES

Allavena, A., Giovannini, A., Berio, T., Spena, A., Zottini, M., Accotto, G. P., et al. (2000). Genetic engineering of *Osteospermum* spp. a case story. *Acta Hortic.* 508, 129–134. doi: 10.17660/actahortic.2000.508.16

Aoki, S., and Syono, K. (1999a). Horizontal gene transfer and mutation: ngrol genes in the genome of *Nicotiana glauca*. *Proc. Natl. Acad. Sci. U. S. A.* 96, 13229–13234. doi: 10.1073/pnas.96.23.13229

Aoki, S., and Syono, K. (1999b). Synergistic function of rolB, rolC, ORF13 and ORF14 of TL-DNA of *Agrobacterium rhizogenes* in hairy root induction in *Nicotiana tabacum*. *Plant Cell Physiol.* 40, 252–256. doi: 10.1093/oxfordjournals.pcp.a029535

Aranda, P. S., LaJoie, D. M., and Jorcyk, C. L. (2012). Bleach gel: a simple agarose gel for analyzing RNA quality. *Electrophoresis* 33, 366–369. doi: 10.1002/elps.201100335

Arshad, W., Haq, I. U., Waheed, M. T., Mysore, K. S., and Mirza, B. (2014). Agrobacterium-mediated transformation of tomato with rolB gene results in enhancement of fruit quality and foliar resistance against fungal pathogens. *PLoS One* 9:e96979. doi: 10.1371/journal.pone.0096979

Bartlett, J. G., Alves, S. C., Smedley, M., Snape, J. W., and Harwood, W. A. (2008). High-throughput *Agrobacterium*-mediated barley transformation. *Plant Methods* 4:22. doi: 10.1186/1746-4811-4-22

Bergstrand, K. J. I. (2017). Methods for growth regulation of greenhouse produced ornamental pot- and bedding plants—a current review. *Folia Hortic.* 29, 63–74. doi: 10.1515/fhort-2017-0007

Bettini, P. P., Lazzara, L., Massi, L., Fani, F., and Mauro, M. L. (2020). Effect of far-red light exposure on photosynthesis and photoprotection in tomato plants transgenic for the *Agrobacterium rhizogenes* rolB gene. *J. Plant Physiol.* 245:153095. doi: 10.1016/j.jplph.2019.153095

Bettini, P. P., Marvasi, M., Fani, F., Lazzara, L., Cosi, E., Melani, L., et al. (2016a). *Agrobacterium rhizogenes* rolB gene affects photosynthesis and chlorophyll content in transgenic tomato (*Solanum lycopersicum* L.) plants. J. *Plant Physiol.* 204, 27–35. doi: 10.1016/j.jplph.2016.07.010

Bettini, P., Michelotti, S., Bindi, D., Giannini, R., Capuana, M., and Buiatti, M. (2003). Pleiotropic effect of the insertion of the *Agrobacterium rhizogenes* rolD gene in tomato (*Lycopersicon esculentum* mill.). *Theor. Appl. Genet.* 107, 831–836. doi: 10.1007/s00122-003-1322-0

Bettini, P. P., Santangelo, E., Baraldi, R., Rapparini, F., Mosconi, P., Crinò, P., et al. (2016b). *Agrobacterium rhizogenes* rolA gene promotes tolerance to *Fusarium oxysporum* f. sp. lycopersici in transgenic tomato plants (*Solanum lycopersicum* L.). *J. Plant Biochem. Biotechnol.* 25, 225–233. doi: 10.1007/s13562-015-0328-4

Boase, M. R., Winefield, C. S., and Lill, T. A. (2004). Transgenic regal pelargoniums that express the rol c gene from *Agrobacterium rhizogenes* exhibit a dwarf floral and vegetative phenotype. *In Vitro Cell. Dev. Biol. Plant* 40, 46–50. doi: 10.1079/IVP2003476

Bouchez, D., and Camilleri, C. (1990). Identification of a putative rol B gene on the TR-DNA of the *Agrobacterium rhizogenes* A4 Ri plasmid. *Plant Mol. Biol.* 14, 617–619. doi: 10.1007/BF00027507

Bulgakov, V. P., Gorpenchenko, T. Y., Veremeichik, G. N., Shkryl, Y. N., Tchernoded, G. K., Bulgakov, D. V., et al. (2012). The rolB gene suppresses reactive oxygen species in transformed plant cells through the sustained activation of antioxidant defense. *Plant Physiol.* 158, 1371–1381. doi: 10.1104/pp.111.191494

Bulgakov, V. P., Shkryl, Y. N., Veremeichik, G. N., Gorpenchenko, T. Y., and Vereshchagina, Y. V. (2013). Recent advances in the understanding of *Agrobacterium rhizogenes*-derived genes and their effects on stress resistance and plant metabolism. *Adv. Biochem. Eng. Biotechnol.* 134, 1–22. doi: 10.1007/10_2013_179

Bulgakov, V. P., Vereshchagina, Y. V., Bulgakov, D. V., Veremeichik, G. N., and Shkryl, Y. N. (2018). The rolB plant oncogene affects multiple signaling protein modules related to hormone signaling and plant defense. *Sci. Rep.* 8:2285. doi: 10.1038/s41598-018-20694-6

Camilleri, C., and Jouanin, L. (1991). The TR-DNA region carrying the auxin synthesis genes of the *Agrobacterium rhizogenes* agropine-type plasmid pRiA4: nucleotide sequence analysis and introduction into tobacco plants. *Mol. Plant-Microbe Interact.* 4, 155–162. doi: 10.1094/MPMI-4-155

Capone, I., Cardarelli, M., Trovato, M., and Costantino, P. (1989). Upstream non-coding region which confers polar expression to Ri plasmid root inducing gene rolB. *Mol. Gen. Genet.* 216, 239–244. doi: 10.1007/BF00334362

Cardarelli, M., Mariotti, D., Pomponi, M., Spanò, L., Capone, I., and Costantino, P. (1987). *Agrobacterium rhizogenes* T-DNA genes capable of inducing hairy root phenotype. *Mol. Gen. Genet.* 209, 475–480. doi: 10.1007/BF00331152

Casanova, E., Trillas, M. I., Moysset, L., and Vainstein, A. (2005). Influence of rol genes in floriculture. *Biotechnol. Adv.* 23, 3–39. doi: 10.1016/j.biotechadv.2004.06.002

Casanova, E., Zuker, A., Trillas, M. I., Moysset, L., and Vainstein, A. (2003). The rolC gene in carnation exhibits cytokinin- and auxin-like activities. *Sci. Hortic.* 97, 321–331. doi: 10.1016/S0304-4238(02)00155-3

Chilton, M.-D., Tepfer, D. A., Petit, A., David, C., Casse-Delbart, F., and Tempé, J. (1982). *Agrobacterium rhizogenes* inserts T-DNA into the genomes of the host plant root cells. *Nature* 295, 432–434. doi: 10.1038/295432a0

Christensen, B., and Müller, R. (2009). *Kalanchoë blossfeldiana* transformed with rol genes exhibits improved postharvest performance and increased ethylene tolerance. *Postharvest Biol. Technol.* 51, 399–406. doi: 10.1016/j.postharvbio.2008.08.010

Christensen, B., Sriskandarajah, S., Jensen, E. B., Lütken, H., and Müller, R. (2010). Transformation with rol genes from *Agrobacterium rhizogenes* as a strategy to breed compact ornamental plants with improved postharvest quality. *Acta Hortic.* 855, 69–76. doi: 10.17660/ActaHortic.2010.855.8

Christensen, B., Sriskandarajah, S., Serek, M., and Müller, R. (2008). Transformation of *Kalanchoë blossfeldiana* with rol-genes is useful in molecular breeding towards compact growth. *Plant Cell Rep.* 27, 1485–1495. doi: 10.1007/s00299-008-0575-0

Clifford, S. C., Runkle, E. S., Langton, F. A., Mead, A., Foster, S. A., Pearson, S., et al. (2004). Height control of poinsettia using photoselective filters. *HortScience* 39, 383–387. doi: 10.21273/HORTSCI.39.2.383

De Castro, V. L., Goes, K. P., and Chiorato, S. H. (2004). Developmental toxicity potential of paclobutrazol in the rat. *Int. J. Environ. Health Res.* 14, 371–380. doi: 10.1080/09603120400004055

Dehio, C., and Schell, J. (1994). Identification of plant genetic loci involved in a posttranscriptional mechanism for meiotically reversible transgene silencing. *Proc. Natl. Acad. Sci.* 91, 5538–5542. doi: 10.1073/pnas.91.12.5538

De Paolis, A., Frugis, G., Giannino, D., Iannelli, M. A., Mele, G., Rugini, E., et al. (2019). Plant cellular and molecular biotechnology: following Mariotti's steps. *Plan. Theory* 8, 1–27. doi: 10.3390/plants8010018

Desmet, S., De Keyser, E., Van Vaerenbergh, J., Baeyen, S., Van Huylenbroeck, J., Geelen, D., et al. (2019). Differential efficiency of wild type rhizogenic strains for rol gene transformation of plants. *Appl. Microbiol. Biotechnol.* 103, 6657–6672. doi: 10.1007/s00253-019-10003-0

Ding, L., Chen, Y., Ma, Y., Wang, H., and Wei, J. (2020). Effective reduction in chimeric mutants of poplar trees produced by CRISPR/Cas9 through a second round of shoot regeneration. *Plant Biotechnol. Rep.* 14, 549–558. doi: 10.1007/s11816-020-00629-2

Estruch, J. J., Chriqui, D., Grossmann, K., Schell, J., and Spena, A. (1991a). The plant oncogene rolC is responsible for the release of cytokinins from glucoside conjugates. *EMBO J.* 10, 2889–2895.

Estruch, J. J., Parets-Soler, A., Schmülling, T., and Spena, A. (1991b). Cytosolic localization in transgenic plants of the rolC peptide from *Agrobacterium rhizogenes*. *Plant Mol. Biol.* 17, 547–550. doi: 10.1007/BF00040654

European Union (2001). Directive 2001/18/EC of the European Parliament and of the Council on the Deliberate Release Into the Environment of Genetically Modified Organisms. Brussels: DIRECTIVE 2001/18/EC. Available at: https://eur-lex.europa.eu/legal-content/EN/TXT/?uri=celex:32001L0018 (Accessed February 20, 2021).

Faiss, M., Strnad, M., Redig, P., Dolezal, K., Hanus, J., Van Onckelen, H., et al. (1996). Chemically induced expression of the rolC-encoded beta-glucosidase in transgenic tobacco plants and analysis of cytokinin metabolism: rolC does not hydrolyze endogenous cytokinin glucosides in planta. *Plant J.* 10, 33–46. doi: 10.1046/j.1365-313X.1996.10010033.x

Ferreira, D. F. (2011). Sisvar: a computer statistical analysis system. *Ciência e Agrotecnologia* 35, 1039–1042. doi: 10.1590/S1413-70542011000600001

Fladung, M. (1990). Transformation of diploid and tetraploid potato clones with the rol C gene of *Agrobacterium rhizogenes* and characterization of transgenic plants. *Plant Breed.* 104, 295–304. doi: 10.1111/j.1439-0523.1990.tb00439.x

Gargul, J. M., Mibus, H., and Serek, M. (2013). Constitutive overexpression of nicotiana GA2ox leads to compact phenotypes and delayed flowering in *Kalanchoë blossfeldiana* and *Petunia hybrida*. *Plant Cell Tissue Organ Cult.* 115, 407–418. doi: 10.1007/s11240-013-0372-5

Gennarelli, M. C., Hagiwara, J. C., Tosto, D., Álvarez, M. A., Borja, M., and Escandón, A. S. (2009). Genetic transformation of calibrachoa excellens via

Agrobacterium rhizogenes: changing morphological traits. *J. Hortic. Sci. Biotechnol.* 84, 305–311. doi: 10.1080/14620316.2009.11512522

Geu-flores, F., Nour-eldin, H. H., Nielsen, M. T., and Halkier, B. A. (2007). USER fusion: a rapid and efficient method for simultaneous fusion and cloning of multiple PCR products. *Nucleic Acids Res.* 35:e55. doi: 10.1093/nar/gkm106

Giovannini, A., Zothni, M., Morreale, G., Spena, A., Allavena, A., Im, S., et al. (1999). Ornamental traits modification by Rol genes in *Osteospermum ecklonis* transformed with *Agrobacterium tumefaciens*. *In Vitro Cell. Dev. Biol. Plant* 35, 70–75. doi: 10.1007/s11627-999-0012-2

Grishchenko, O. V., Kiselev, K. V., Tchernoded, G. K., Fedoreyev, S. A., Veselova, M. V., Bulgakov, V. P., et al. (2016). RolB gene-induced production of isoflavonoids in transformed *Maackia amurensis* cells. *Appl. Microbiol. Biotechnol.* 100, 7479–7489. doi: 10.1007/s00253-016-7483-y

Hall, S. (1992). Altered morphology in transgenic tobacco plants that overproduce cytokinins in specific tissues and organs. *Dev. Biol.* 395, 386–395. doi: 10.1016/0012-1606(92)90123-x

Hansen, G., Larribe, M., Vaubert, D., Tempo, J., Biermann, B. J., Montoya, A. L., et al. (1991). *Agrobacterium rhizogenes* pRi8196 T-DNA: mapping and DNA sequence of functions involved in mannopine synthesis and hairy root differentiation. *Proc. Natl. Acad. Sci. U. S. A.* 88, 7763–7767. doi: 10.1073/pnas.88.17.7763

Hansen, G., Vaubert, D., Clérot, D., Tempé, J., and Brevet, J. (1994). A new open reading frame, encoding a putative regulatory protein, in *Agrobacterium rhizogenes* T-DNA. *C. R. Acad. Sci.* 317, 49–53.

Hegelund, J. N., Lauridsen, U. B., Wallström, S. V., Müller, R., and Lütken, H. (2017). Transformation of campanula by wild type *Agrobacterium rhizogenes*. *Euphytica* 213, 1–9. doi: 10.1007/s10681-017-1845-0

Hoeberichts, F. A., Van Doorn, W. G., Vorst, O., Hall, R. D., and Van Wordragen, M. F. (2007). Sucrose prevents up-regulation of senescence-associated genes in carnation petals. *J. Exp. Bot.* 58, 2873–2885. doi: 10.1093/jxb/erm076.

Islam, M. A., Lütken, H., Haugslien, S., Blystad, D.-R., Torre, S., Rolcik, J., et al. (2013). Overexpression of the AtSHI gene in poinsettia, *Euphorbia pulcherrima*, results in compact plants. *PLoS One* 8:e53377. doi: 10.1371/annotation/010f6c7f-9745-4810-a370-c96fb1f583e9

Karimi, M., Inzé, D., and Depicker, A. (2002). GATEWAY™ vectors for agrobacterium-mediated plant transformation. *Trends Plant Sci.* 7, 193–195. doi: 10.1016/S1360-1385(02)02251-3

Kazuo, I., Masayuki, K., Ryo, N., Yoshihiko, K., and Kunio, Y. (2015). Soluble carbohydrates and variation in vase-life of soluble carbohydrates and variation in vase-life of cut rose cultivars. *J. Hortic. Sci. Biotechnol.* 80, 280–286. doi: 10.1080/14620316.2005.11511930

Kodahl, N., Müller, R., and Lütken, H. (2016). The *Agrobacterium rhizogenes* oncogenes rolB and ORF13 increase formation of generative shoots and induce dwarfism in *Arabidopsis thaliana* (L.) Heynh. *Plant Sci.* 252, 22–29. doi: 10.1016/j.plantsci.2016.06.020

Komarovská, H., Košuth, J., Giovannini, A., Smelcerovic, A., Zuehlke, S., and Čellárová, E. (2010). Effect of the number of rol genes integrations on phenotypic variation in hairy root-derived *Hypericum perforatum* L. plants. *Z. Naturforsch. C* 65, 701–712. doi: 10.1515/znc-2010-11-1211

Koshita, Y., Nakamura, Y., Kobayashi, S., and Morinaga, K. (2002). Introduction of the rolC gene into the genome of the japanese persimmon causes dwarfism. *J. Japanese Soc. Hortic. Sci.* 71, 529–531. doi: 10.2503/jjshs.71.529

Kubo, T., Tsuro, M., Tsukimori, A., Shizukawa, Y., Takemoto, T., Inaba, K., et al. (2006). Morphological and physiological changes in transgenic *Chrysanthemum morifolium* ramat. 'Ogura-nishiki' with rolC. *J. Japanese Soc. Hortic. Sci.* 75, 312–317. doi: 10.2503/jjshs.75.312

Kurioka, Y., Suzuki, Y., Kamada, H., and Harada, H. (1992). Promotion of flowering and morphological alterations in *Atropa belladonna* transformed with a CaMV 35S-rolC chimeric gene of the Ri plasmid. *Plant Cell Rep.* 12, 1–6. doi: 10.1007/BF00232412

Lakatos, L., Szittya, G., Silhavy, D., and Burgyan, J. (2004). Molecular mechanism of RNA silencing suppression mediated by p19 protein. *EMBO J.* 23, 876–884. doi: 10.1038/sj.emboj.7600096

Lalonde, S., Weise, A., Walsh, R. P., Ward, J. M., and Frommer, W. B. (2003). Fusion to GFP blocks intercellular trafficking of the sucrose transporter SUT1 leading to accumulation in companion cells. *BMC Plant Biol.* 3:8. doi: 10.1186/1471-2229-3-8

Laursen, T., Borch, J., Knudsen, C., Bavishi, K., Torta, F., Martens, H. J., et al. (2016). Characterization of a dynamic metabolon producing the defense compound dhurrin in sorghum. *Science* 354, 890–893. doi: 10.1126/science.aag2347

Lee, C. W., Wang, L., Ke, S., Qin, M., and Cheng, Z.-M. (1996). Expression of the rolC gene in transgenic plants of *Salpiglossis sinuata* L. *HortScience* 31:571. doi: 10.21273/hortsci.31.4.571e

Lemcke, K., and Schmülling, T. (1998). Gain of function assays identify non-rol genes from *Agrobacterium rhizogenes* TL-DNA that alter plant morphogenesis or hormone sensitivity. *Plant J.* 15, 423–433. doi: 10.1046/j.1365-313X.1998.00223.x

Liu, N., Shang, W., Li, C., Jia, L., Wang, X., and Xing, G. (2018). Evolution of the SPX gene family in plants and its role in the response mechanism to phosphorus stress. *Open Biol.* 8:170231. doi: 10.1098/rsob.170231

Long, N., Ren, X., Xiang, Z., Wan, W., and Dong, Y. (2016). Sequencing and characterization of leaf transcriptomes of six diploid *Nicotiana* species. *J. Biol. Res.* 23, 1–12. doi: 10.1186/s40709-016-0048-5

Lütken, H., Clarke, J. L., and Müller, R. (2012a). Genetic engineering and sustainable production of ornamentals: current status and future directions. *Plant Cell Rep.* 31, 1141–1157. doi: 10.1007/s00299-012-1265-5

Lütken, H., Jensen, L. S., Topp, S. H., Mibus, H., Müller, R., and Rasmussen, S. K. (2010). Production of compact plants by overexpression of AtSHI in the ornamental *Kalanchoë*. *Plant Biotechnol. J.* 8, 211–222. doi: 10.1111/j.1467-7652.2009.00478.x

Lütken, H., Laura, M., Borghi, C., Ørgaard, M., Allavena, A., and Rasmussen, S. K. (2011). Expression of KxhKN4 and KxhKN5 genes in *Kalanchoë blossfeldiana* 'Molly' results in novel compact plant phenotypes: towards a cisgenesis alternative to growth retardants. *Plant Cell Rep.* 30, 2267–2279. doi: 10.1007/s00299-011-1132-9

Lütken, H., Wallström, S. V., Jensen, E. B., Christensen, B., and Müller, R. (2012b). Inheritance of rol-genes from *Agrobacterium rhizogenes* through two generations in *Kalanchoë*. *Euphytica* 188, 397–407. doi: 10.1007/s10681-012-0701-5

Malabarba, J., Chevreau, E., Dousset, N., Veillet, F., Moizan, J., and Vergne, E. (2020). New strategies to overcome present CRISPR/Cas9 limitations in apple and pear: efficient dechimerization and base editing. *Int. J. Mol. Sci.* 22:319. doi: 10.3390/ijms22010319

Mandal, D., Srivastava, D., and Sinharoy, S. (2020). "Optimization of hairy root transformation for the functional genomics in chickpea: a platform for nodule developmental studies," in *Legume Genomics*. eds. M. Jain and R. Garg (New York, NY: Humana), 335–348.

Marenkova, T. V., Loginova, D. B., and Deineko, E. V. (2012). Mosaic patterns of transgene expression in plants. *Russ. J. Genet.* 48, 249–260. doi: 10.1134/S1022795412030088

Martin-Tanguy, J., Corbineau, F., Burtin, D., Gozal, B.-H., and Tepfer, D. (1993). Genetic transformation with a derivative of rolC from *Agrobacterium rhizogenes* and treatment with α-aminoisobutyric acid produce similar phenotypes and reduce ethylene production and the accumulation of water-insoluble polyamine-hydroxycinnamic acid conju. *Plant Sci.* 93, 63–76. doi: 10.1016/0168-9452(93)90035-X

Mashiguchi, K., Hisano, H., Takeda-Kamiya, N., Takebayashi, Y., Ariizumi, T., Gao, Y., et al. (2019). *Agrobacterium tumefaciens* enhances biosynthesis of two distinct auxins in the formation of crown galls. *Plant Cell Physiol.* 60, 29–37. doi: 10.1093/pcp/pcy182

McMahon, M. (1999). Development of chrysanthemum meristems grown under far-red absorbing filters and long or short photoperiods. *J. Am. Soc. Hortic. Sci.* 124, 483–487. doi: 10.21273/JASHS.124.5.483

Mishiba, K. I., Nishihara, M., Abe, Y., Nakatsuka, T., Kawamura, H., Kodama, K., et al. (2006). Production of dwarf potted gentian using wild-type *Agrobacterium rhizogenes*. *Plant Biotechnol.* 23, 33–38. doi: 10.5511/plantbiotechnology.23.33

Mitiouchkina, T. Y., and Dolgov, S. V. (2000). Modification of chrysanthemum plant and flower architecture by RolC gene from agrobacterium rhizogches introduction. *Acta Hortic.* 508, 163–172. doi: 10.17660/ActaHortic.2000.508.21

Mohajjel-Shoja, H., Clément, B., Perot, J., Alioua, M., and Otten, L. (2011). Biological activity of the *Agrobacterium rhizogenes*—derived *trolC* gene of *Nicotiana tabacum* and its functional relation to other *plast* genes. *Mol. Plant-Microbe Interact.* 24, 44–53. doi: 10.1094/MPMI-06-10-0139

Monteiro, A., Nell, T. A., and Barrett, J. E. (2002). Effects of exogenous sucrose on carbohydrate levels, flower respiration and longevity of potted miniature rose (*Rosa hybrida*) flowers during postproduction. *Postharvest Biol. Technol.* 26, 221–229. doi: 10.1016/S0925-5214(02)00010-8

Müller, R., Andersen, A. S., and Serek, M. (1998). Differences in display life of miniature potted roses (*Rosa hybrida* L.). *Sci. Hortic.* 76, 59–71. doi: 10.1016/S0304-4238(98)00132-0

Neumann, M., Prahl, S., Caputi, L., Hill, L., Kular, B., Walter, A., et al. (2020). Hairy root transformation of *Brassica rapa* with bacterial halogenase genes and regeneration to adult plants to modify production of indolic compounds. *Phytochemistry* 175:112371. doi: 10.1016/j.phytochem.2020.112371

Nilsson, O., Crozier, A., Schmülling, T., Sandberg, G., and Olsson, O. (1993a). Indole-3-acetic acid homeostasis in transgenic tobacco plants expressing the *Agrobacterium rhizogenes rolB* gene. *Plant J.* 3, 681–689. doi: 10.1111/j.1365-313X.1993.00681.x

Nilsson, O., Moritz, T., Imbault, N., Sandberg, G., and Olsson, O. (1993b). Hormonal characterization of transgenic tobacco plants expressing the rolC gene of *Agrobacterium rhizogenes* TL-DNA. *Plant Physiol.* 102, 363–371. doi: 10.1104/pp.102.2.363

Pérez de la Torre, M. C., Fernández, P., Greppi, J. A., Coviella, M. A., Fernández, M. N., Astigueta, F., et al. (2018). Transformation of mecardonia (plantaginaceae) with wild-type *Agrobacterium rhizogenes* efficiently improves compact growth, branching and flower related ornamental traits. *Sci. Hortic.* 234, 300–311. doi: 10.1016/j.scienta.2018.02.047

Rademacher, W. (2000). Growth retardants: effects on gibberellin biosynthesis and other metabolic pathways. *Annu. Rev. Plant Physiol. Plant Mol. Biol.* 51, 501–531. doi: 10.1146/annurev.arplant.51.1.501

Rademacher, W. (2016). Chemical regulators of gibberellin status and their application in plant production. *Annu. Plant Rev.* 49, 359–404. doi: 10.1002/9781119210436.ch12

Rangslang, R. K., Liu, Z., Lütken, H., and Favero, B. T. (2018). Agrobacterium spp. genes and ORFs: mechanisms and applications in plant science. *Ciência e Agrotecnologia* 42, 453–463. doi: 10.1590/1413-70542018425000118

Rueden, C. T., Schindelin, J., Hiner, M. C., Dezonia, B. E., Walter, A. E., Arena, E. T., et al. (2017). ImageJ2: imagej for the next generation of scientific image data. *BMC Bioinform.* 18:529. doi: 10.1186/s12859-017-1934-z

Schmülling, T., Fladung, M., Grossmann, K., and Schell, J. (1993). Hormonal content and sensitivity of transgenic tobacco and potato plants expressing single rol genes of *Agrobacterium rhizogenes* T-DNA. *Plant J.* 3, 371–382. doi: 10.1046/j.1365-313X.1993.t01-20-00999.x

Schmülling, T., and Schell, J. (1993). Transgenic tobacco plants regenerated from leaf disks can be periclinal chimeras. *Plant Mol. Biol.* 21, 705–708. doi: 10.1007/BF00014554

Schmülling, T., Schell, J., and Spena, A. (1988). Single genes from *Agrobacterium rhizogenes* influence plant development. *EMBO J.* 7, 2621–2629. doi: 10.1002/j.1460-2075.1988.tb03114.x

Schmulling, T., Schell, J., and Spena, A. (1989). Promoters of the rolA, B, and C genes of *Agrobacterium rhizogenes* are differentially regulated in transgenic plants. *Plant Cell* 1:665. doi: 10.1105/tpc.1.7.665

Serek, M., and Reid, M. S. (2000). Ethylene and postharvest performance of potted *Kalanchoë*. *Postharvest Biol. Technol.* 18, 43–48. doi: 10.1016/S0925-5214(99)00055-1

Shkryl, Y. N., Veremeichik, G. N., Bulgakov, V. P., Avramenko, T. V., Günter, E. A., Ovodov, Y. S., et al. (2013). The production of class III plant peroxidases in transgenic callus cultures transformed with the rolB gene of *Agrobacterium rhizogenes*. *J. Biotechnol.* 168, 64–70. doi: 10.1016/j.jbiotec.2013.08.014

Sinkar, V. P., Pythoud, F., White, F. F., Nester, E. W., and Gordon, M. P. (1988). rolA locus of the Ri plasmid directs developmental abnormalities in transgenic tobacco plants. *Genes Dev.* 2, 688–697. doi: 10.1101/gad.2.6.688

Slightom, J. L., Durand-Tardif, M., Jouanin, L., and Tepfer, D. (1986). Nucleotide sequence analysis of TL-DNA of *Agrobacterium rhizogenes* agropine type plasmid. Identification of open reading frames. *J. Biol. Chem.* 261, 108–121. doi: 10.1016/S0021-9258(17)42439-2

Solovyev, V., Kosarev, P., Seledsov, I., and Vorobyev, D. (2006). Automatic annotation of eukaryotic genes, pseudogenes and promoters. *Genome Biol.* 7 (Suppl. 1), 1–12. doi: 10.1186/gb-2006-7-s1-s10

Student, G. (1908). The probable error of a mean. *Biometrika* 6:1. doi: 10.2307/2331554

Suzuki, K., Yamashita, I., and Nobukazu, T. (2002). Tobacco plants were transformed by *Agrobacterium rhizogenes* infection during their evolution. *Plant J.* 32, 775–787. doi: 10.1046/j.1365-313X.2002.01468.x

Tepfer, D. (1990). Genetic transformation using *Agrobacterium rhizogenes*. *Physiol. Plant.* 79, 140–146. doi: 10.1111/j.1399-3054.1990.tb05876.x

Timney, B. L., Raveh, B., Mironska, R., Trivedi, J. M., Kim, S. J., Russel, D., et al. (2016). Simple rules for passive diffusion through the nuclear pore complex. *J. Cell Biol.* 215, 57–76. doi: 10.1083/jcb.201601004

Topp, S. H., Rasmussen, S. K., and Sander, L. (2008). Alcohol induced silencing of gibberellin 20-oxidases in *Kalanchoë blossfeldiana*. *Plant Cell Tissue Organ Cult.* 93, 241–248. doi: 10.1007/s11240-008-9368-y

Trovato, M., Maras, B., Linhares, F., and Costantino, P. (2001). The plant oncogene rolD encodes a functional ornithine cyclodeaminase. *Proc. Natl. Acad. Sci. U. S. A.* 98, 13449–13453. doi: 10.1073/pnas.231320398

van Altvorst, A. C., Bino, R. J., van Dijk, A. J., Lamers, A. M. J., Lindhout, W. H., van der Mark, F., et al. (1992). Effects of the introduction of *Agrobacterium rhizogenes* rol genes on tomato plant and flower development. *Plant Sci.* 83, 77–85. doi: 10.1016/0168-9452(92)90064-S

Veena, V., and Taylor, C. G. (2007). *Agrobacterium rhizogenes*: recent developments and promising applications. *In Vitro Cell. Dev. Biol. Plant* 43, 383–403. doi: 10.1007/s11627-007-9096-8

Veremeichik, G., Bulgakov, V., and Shkryl, Y. (2016). Modulation of NADPH-oxidase gene expression in rolB-transformed calli of *Arabidopsis thaliana* and *Rubia cordifolia*. *Plant Physiol. Biochem.* 105, 282–289. doi: 10.1016/j.plaphy.2016.05.014

Veremeichik, G. N., Shkryl, Y. N., Bulgakov, V. P., Avramenko, T. V., and Zhuravlev, Y. N. (2012). Molecular cloning and characterization of seven class III peroxidases induced by overexpression of the agrobacterial rolB gene in *Rubia cordifolia* transgenic callus cultures. *Plant Cell Rep.* 31, 1009–1019. doi: 10.1007/s00299-011-1219-3

Vladimirov, I. A., Pavlova, O. A., Polev, D. E., and Bogomaz, D. I. (2019). cT-DNA in *Linaria vulgaris* L. is multicopy, inverted and homogenized. bioRxiv [Preprint]. 1–13. doi: 10.1101/615328.

Wang, X., Chen, X., Cheng, Q., Zhu, K., Yang, X., and Cheng, Z. (2019). Agrobacterium–mediated transformation of *Kalanchoë laxiflora*. *Hortic. Plant J.* 5, 221–228. doi: 10.1016/j.hpj.2019.07.001

Weill, U., Krieger, G., Avihou, Z., Milo, R., Schuldiner, M., and Davidi, D. (2019). Assessment of GFP tag position on protein localization and growth fitness in yeast. *J. Mol. Biol.* 431, 636–641. doi: 10.1016/j.jmb.2018.12.004

Welander, M., and Zhu, L. H. (2010). Rol genes: molecular biology, physiology, morphology, breeding uses. *Plant Breed. Rev.* 26, 79–103. doi: 10.1002/9780470650325.ch3

White, F. F., Taylor, B. H., Huffman, G. A., Gordon, M. P., and Nester, E. W. (1985). Molecular and genetic analysis of the transferred DNA regions of the root-inducing plasmid of *Agrobacterium rhizogenes*. *J. Bacteriol.* 164, 33–44. doi: 10.1128/JB.164.1.33-44.1985

Winefield, C., Lewis, D., Arathoon, S., and Deroles, S. (1999). Alteration of petunia plant form through the introduction of the rolC gene from *Agrobacterium rhizogenes*. *Mol. Breed.* 5, 543–551. doi: 10.1023/A:1009638401275

Woltering, E. J. (1987). Effects of ethylene on ornamental pot plants: a classification. *Sci. Hortic.* 31, 283–294. doi: 10.1016/0304-4238(87)90054-9

Yokoyama, R., Hirose, T., Fujii, N., Aspuria, E. T., Kato, A., and Uchimiya, H. (1994). The role promoter of *Agrobacterium rhizogenes* Ri plasmid is activated by sucrose in transgenic tobacco plants. *Mol. Gen. Genet.* 244, 15–22. doi: 10.1007/BF00280182

Zhu, L., Holefors, A., Ahlman, A., Xue, Z., and Welander, M. (2001). Transformation of the apple rootstock M. 9/29 with the rol B gene and its influence on rooting and growth. *Plant Sci.* 160, 433–439. doi: 10.1016/S0168-9452(00)00401-5

Zia, M., Mirza, B., Malik, S. A., and Chaudhary, M. F. (2010). Expression of rol genes in transgenic soybean (*Glycine max* L.) leads to changes in plant phenotype, leaf morphology, and flowering time. *Plant Cell Tissue Organ Cult.* 103, 227–236. doi: 10.1007/s11240-010-9771-z

Zuker, A., Tzfira, T., Scovel, G., Ovadis, M., Shklarman, E., Itzhaki, H., et al. (2001). RolC-transgenic carnation with improved horticultural traits: quantitative and qualitative analyses of greenhouse-grown plants. *J. Am. Soc. Hortic. Sci.* 126, 13–18. doi: 10.21273/JASHS.126.1.13

Conflict of Interest: The authors declare that the research was conducted in the absence of any commercial or financial relationships that could be construed as a potential conflict of interest.

frontiers in Plant Science

ORIGINAL RESEARCH
published: 14 June 2021
doi: 10.3389/fpls.2021.640608

Petunia Performance Under Application of Animal-Based Protein Hydrolysates: Effects on Visual Quality, Biomass, Nutrient Content, Root Morphology, and Gas Exchange

Giuseppe Cristiano and Barbara De Lucia*

Department of Agricultural and Environmental Sciences, University of Bari Aldo Moro, Bari, Italy

Sustainable plant production practices have been implemented to reduce the use of synthetic fertilizers and other agrochemicals. One way to reduce fertilizer use without negatively impacting plant nutrition is to enhance crop uptake of nutrients with biostimulants. As the effectiveness of a biostimulant can depend on the origin, species, dose, and application method, the aim of this research was to evaluate the effect of a commercial animal-based protein hydrolysate (PH) biostimulant on the visual quality, biomass, macronutrient content, root morphology, and leaf gas exchange of a petunia (*Petunia* × *hybrida* Hort. "red") under preharvest conditions. Two treatments were compared: (a) three doses of an animal-based PH biostimulant: 0 (D0 = control), 0.1 (D0.1 = normal), and 0.2 g L^{-1} (D0.2 = high); (b) two biostimulant application methods: foliar spray and root drenching. The dose × method interaction effect of PH biostimulant on the plants was significant in terms of quality grade and fresh and dry biomass. The high dose applied as foliar spray produced petunias with extra-grade visual quality (number of flowers per plant 161, number of leaves per plant 450, and leaf area per plant 1,487 cm^2) and a total aboveground dry weight of 35 g, shoots (+91%), flowers (+230%), and leaf fresh weight (+71%). P and K contents were higher than in untreated petunias, when plants were grown with D0.2 and foliar spray. With foliar spray at the two doses, SPAD showed a linear increase (+21.6 and +41.0%) with respect to untreated plants. The dose × method interaction effect of biostimulant application was significant for root length, projected and total root surface area, and number of root tips, forks, and crossings. Concerning leaf gas exchange parameters, applying the biostimulant at both doses as foliar spray resulted in a significant improvement in net photosynthesis (D0.1: 22.9 μmol CO_2 m^{-2} s^{-1} and D0.2: 22.4 μmol CO_2 m^{-2} s^{-1}) and stomatal conductance (D0.1: 0.42 mmol H_2O m^{-2} s^{-1} and D0.2: 0.39 mmol H_2O m^{-2} s^{-1}) compared to control. These results indicate that application of PH biostimulant at 0.2 g L^{-1} as foliar spray helped to achieve extra-grade plants and that this practice can be exploited in sustainable greenhouse conditions for commercial production of petunia.

Keywords: biostimulant, environmentally friendly ornamentals, foliar spray, marketable extra grade, pot plant

OPEN ACCESS

Edited by:
Antonio Ferrante, University of Milan, Italy

Reviewed by:
Pradeep Kumar, Central Arid Zone Research Institute (ICAR), India
Sergio Mugnai, Erasmus University Rotterdam, Netherlands

****Correspondence:***
Giuseppe Cristiano
giuseppe.cristiano@uniba.it

Specialty section:
This article was submitted to Crop and Product Physiology, a section of the journal Frontiers in Plant Science

Received: *11 December 2020*
Accepted: *21 April 2021*
Published: *14 June 2021*

Citation:
Cristiano G and De Lucia B (2021) Petunia Performance Under Application of Animal-Based Protein Hydrolysates: Effects on Visual Quality, Biomass, Nutrient Content, Root Morphology, and Gas Exchange. Front. Plant Sci. 12:640608. doi: 10.3389/fpls.2021.640608

INTRODUCTION

The use of chemicals, water, energy, and plastic has exposed greenhouse horticulture to criticism for its environmental impact (Wandl and Haberl, 2017; Gruda et al., 2019). The marketability of greenhouse bedding plants is greatly influenced by the intensive conditions of their production, aimed at avoiding aesthetic defects due to nutritional imbalances and biotic and abiotic stresses.

Petunia (*Petunia* × *hybrida* Hort.) is a leading cultivated bedding plant used in private and public parks and gardens (Arancon et al., 2008); vegetatively vigorous petunias, such as Potunia®, with round habit and large flowers have revolutionized the genus. Nurserymen grow petunias in limited pot volumes that require frequent irrigation and high fertilization rates (James and van Lersel, 2001), ranging from 200 to 500 mg L^{-1} N (Chavez et al., 2008; Fain et al., 2008), which can cause contamination of ground and surface water (Lang and Pannuk, 1998; Hansen et al., 2017; Shu et al., 2019) and climate change (Bouwman et al., 2013; Zhang et al., 2015). Today, it is necessary to consider the sustainability of nursery production (Isaak and Lentz, 2020). Sustainable plant production practices have been studied to reduce the use of synthetic fertilizers and other agrochemicals. One way in which fertilizer use can be reduced without negatively impacting plant nutrition is to enhance crop uptake of nutrients with biostimulants (Kunicki et al., 2010; Baglieri et al., 2014; Halpern et al., 2015; De Pascale et al., 2017; Toscano et al., 2018; Parađiković et al., 2019; De Pascale et al., 2020). "A plant biostimulant shall be an EU fertilizing product, the function of which is to stimulate plant nutrition processes independently of the product's nutrient content with the sole aim of improving one or more of the following characteristics of the plant or the plant rhizosphere: (i) nutrient use efficiency, (ii) tolerance to abiotic stress, (iii) quality traits, or (iv) availability of confined nutrients in the soil or rhizosphere" (The European Parliament and the Council of the European Union, 2019).

Protein hydrolysates (PHs) consisting mainly of signaling peptides and free amino acids, "manufactured from protein sources by partial hydrolysis" (Schaafsma, 2009), have gained prominence as non-microbial biostimulants because of their potential to enhance plant growth, yield, and quality (Ertani et al., 2009; Calvo et al., 2014; Colla et al., 2014, 2017a,b; Nardi et al., 2016; Carillo et al., 2019; Rouphael and Colla, 2020). Venugopal (2016) found that enzymatic hydrolysis of plant or animal sources ensures biostimulant products of higher quality than does chemical hydrolysis. Animal-based PH biostimulants have a higher N content (9–16% d.m.) than plant-based biostimulants (Colla et al., 2015).

Vegetables, such as tomato (Polo and Mata, 2018; Sestili et al., 2018; Casadesús et al., 2019), rocket (Caruso et al., 2019), celery (Consentino et al., 2020), lettuce (Polo et al., 2006; Xu and Mou, 2017), basil (Rouphael et al., 2021), and spinach (Kunicki et al., 2010), and tree crops, such as kiwifruit (Quartieri et al., 2002), papaya (Morales-Pajan and Stall, 2003), and passion fruit (Morales-Pajan and Stall, 2004), have been tested with animal-based PHs, with the aim of improving plant performance and abiotic stress resistance. Less attention to the use of animal-based PH biostimulants has been paid for ornamental species, especially bedding plants. In a globalized world, consumer demand for quality and novelty guides the global market of ornamental bedding plants (Lütken et al., 2010). Regarding consumers, a study carried out by Sánchez-Bravo et al. (2021) showed that a sustainable product has better quality. Sustainability is achieved via critical adjustments on cultivation by minimizing fuel and electricity use, adopting integrated nutrient management and integrated pest and disease management, and using recyclable materials and peat-alternative growing compounds (European Biostimulants Industry Council (EBIC), 2013; Darras, 2020). Sustainability assessment of potted plant focused mainly on environmental aspects such as carbon footprint (Soode et al., 2013; Ingram et al., 2019; Havardi-Burger et al., 2020).

If we apply the concept of quality of vegetable seedlings (Gruda, 2005) to ornamental plants, we can say that quality is not fixed but is a complex prerequisite. Quality has various extrinsic, or visual, and intrinsic, such as environmental and social, components. Consumers choose flowering plants with high aesthetic quality: compact, branched, with many flowers and leaves, a good balance between plant and pot size, and dark green leaves without blemishes or signs of stress (Kader, 2000; Ferrante et al., 2015; Bergstrand, 2017). Flower grading means dividing flowers into several grades according to the quality based on the appearance (Sun et al., 2017). For marketing purposes, ornamental potted plant quality is classified into four grades according to appearance: extra (extra-large) > 1st (large) > 2nd (medium) > 3rd (small)[1].

Unfortunately, for bedding plants, few growers and traders pay attention to quality grading.

The visual quality of ornamental plants is necessarily linked to an adequate content of nutrients, in order to achieve the standards of commercialization and consumption (Marschner, 2011). Nitrogen (N) is the chief among minerals in plant nutrition, and its deficiency is considered as one of the limiting factors for quality: Nordstedt et al. (2020) showed that the visual symptoms of leaf yellowing in control plants compared to biostimulant-treated plants (*Pseudomonas* strains) were less severe in *P.* × *hybrida*, increasing the quality of ornamental potted plants grown under low-nutrient regimens.

Leaf gas exchanges can be used for evaluating the efficacy of biostimulant treatments: Bulgari et al. (2019) on lettuce reported that the biostimulant Retrosal® could stimulate crop performance and quality by keeping open stomata, maintaining photosynthesis, source-sink relations (growth), and thus protecting from possible photoinhibition/photo-oxidation effects.

Therefore, a comprehensive study is needed to improving quality and sustainability in potted petunia cultivation.

As the effectiveness of a biostimulant can depend on origin, species, dose, and application method, the aim of this research was to evaluate the effect of a commercial animal-based PH biostimulant on the quality, biomass, macronutrient content,

[1]https://www.flowerscanadagrowers.com/home

root morphology, and leaf gas exchange of petunia under preharvest conditions.

MATERIALS AND METHODS

Treatments and Experimental Design

Two treatments were compared: (a) three doses of an animal-based PH biostimulant (D): 0 (D0 = control), 0.1 (D0.1 = normal), and 0.2 g L^{-1} (D0.2 = high); and (b) two biostimulant application methods (M): foliar spray (Fo) and root drenching (Dr).

The biostimulant was applied to the leaves of petunias, using a manual sprayer at a volume of 150 mL $plant^{-1}$. Root drenching was performed applying the same volume directly to the growing medium. The same volume of distilled water was applied to the control as foliar spray or root drenching.

The treatments were performed in randomized complete block design and 18 experimental units (three doses × two biostimulant application methods × three replicates). Each experimental unit consisted of 10 plants (n = 180 plants in total).

The experiment was conducted from November 2016 to March 2017 in the heated greenhouse at the University Campus in Bari (Italy) (41 07′33.79″ N; 16°52′09.44″ E; altitude 3.35 m); average air temperature was 20°C/13°C day/night, and relative humidity range was 40–65%. Rooted plants of *Petunia* × *hybrida* Hort., Potunia® series, and red (Dunnen®) cultivar were used for the study. The Potunia® series of petunias features vigorous, rounded, compact, well-branched plants with an abundance of flowers.

On November 10, 2016, single petunia plants were transplanted into 1.2-L pots that were arranged at a density of 15 plants m^{-2}. The substrate was a mixture of peat (Plantaflor®, Germany) and perlite (Perlitech, Italy) 80:20 (vol/vol).

Hydrostim® (Hydrofert, Italy), a completely soluble commercial animal-derived powdered PH product, authorized in organic farming, was used to treat the plants. It is obtained by enzymatic hydrolysis of proteins from erythrocytes (red blood cells) and contains 38% organic matter, 10.2% total N, and 52% amino acids (**Table 1**). The recommended dose is 10–12 g 100 L^{-1} for vegetables and trees and 15 g 100 L^{-1} for citrus trees.

Biostimulant treatments began 4 weeks after transplant and were applied weekly eight times, until flower bud differentiation. The plants were fertigated with a nutrient solution used in the standard cultivation technique, containing (in mg L^{-1}) 40 N, 8 phosphorus (P), 60 potassium (K), 44 calcium, and 8 magnesium, plus microelements (3 iron, 2 manganese, 0.1 copper, and 0.5 boron), E.C. 1.2 dS m^{-1}, pH 5.8.

Growth Measurements: Ornamental Visual Characteristics and Biomass

At harvest, 150 days after transplant, the plants were graded for visual quality and plant biomass. Leaf macronutrient content, root morphology, and gas exchange were also evaluated.

To determine visual quality and fresh and dry biomass, the plants were divided into four grades according to UE market rules: extra (extra-large) > 1st (large) > 2nd (medium) > 3rd (small) as reported in **Table 2**. All grades of Petunia plants are required to have the following characteristics, under penalty of rejection: symmetrical shape, optimum floral display, uniformly distributed flower buds, strong stems, verdant foliage, no evidence of nutritional deficiency, disease, insect damage or mechanical injury, and well-developed root system.

To determine agronomic characteristics, the plants were separated from the growing medium and divided into shoots, leaves, and flowers. These were oven-dried to constant weight at 70°C. For each treatment, six plants were used to determine the number of shoots, leaves, and flowers per plant. Total leaf area per plant was measured with a leaf area meter (Delta-T; Decagon Devices, Pullman, WA, United States). Chlorophyll SPAD index (Minolta Chlorophyll Meter SPAD-502) and total aboveground (shoot + leaves + flowers) fresh and dry weight were also measured.

Root Morphology

Root morphology was assessed on the basis of root length, projected and total surface area, and number of tips, forks, and crossings on six plants for each treatment. The root system was separated from the aerial part and substrate. It was washed and scanned at 400 dpi (Epson Expression© 10000 XL scanner; Japan). The images were then processed using image analysis software (WinRHIZO v. 2005b©; Regent Instruments Inc., QC, Canada).

Leaf Nutritional Status

Nutrient concentrations were determined in leaf samples. N was analyzed by the Kjeldahl method; total P and K contents were quantified according to EN 13650 (2001) by ICP-OES (inductively coupled plasma–optical emission spectrometry). The results are expressed as percentage of macronutrients. Six plants were used for each treatment.

Gas Exchange and Chlorophyll Fluorescence Measurements

At the phenological stage of full bloom, leaf gas exchange was measured using an IRGA LI-6400XT portable gas exchange system (Li-COR, Lincoln, NE, United States), equipped with a

TABLE 1 | Amino acid content of the commercial animal-based PH biostimulant (Hydrostim) used on petunia plants.

Amino acid	Content (mg L^{-1})	Amino acid	Content (mg L^{-1})
Valine	0.15	Betaine	2.02
Threonine	0.34	Leucine	2.21
Tyrosine	0.34	Arginine	2.98
Methionine	0.38	Aspartic acid	3.45
Cysteine + cystine	0.46	Alanine	4.94
Isoleucine	0.86	Hydroxyproline	5.28
Phenylalanine	1.24	Proline	6.50
Lysine	1.85	Glutamic acid	6.52
Serine	1.62	Glycine	10.9
Histidine	<LQ	Tryptophan	<DL

DL, detection limit.

TABLE 2 | Parameters and ranges of the four quality visual grades for petunia plants according to https://www.flowerscanadagrowers.com/uploads/2016/11/grades%20&%20standards%20for%20foliage%20plants1.pdf.

Quality visual grades	Flower/plant (no.)	Leaves/plant (no.)	Leaf area/plant (cm^2)	Shoots fresh weight/plant (g)	Flowers fresh weight/plant (g)	Leaves fresh weight/plant (g)	Aboveground dry weight/plant (g)
Extra	143–165	417–451	1,345–1,489	167–193	37–44	75–84	32–37
First	120–142	382–416	1,199–1,344	140–166	29–36	66–75	27–31
Second	97–141	347–381	1,053–1,198	113–139	21–28	56–65	21–26
Third	74–96	312–346	907–1,052	86–112	13–20	46–55	15–20

2 cm^2 leaf chamber with a built-in fluorescence system (LI-6400-40; Li-COR).

Input airflow and CO_2 concentration were set at 300 μmol s^{-1}, and CO_2 concentration was fixed at 400 ppm, respectively. Measurements were performed at the same time of the day (9–11 am and 1–3 pm CET) to minimize physiological changes due to environmental effects on fully expanded mature leaves of the same age. The fluorescence measurements were performed on the plants using a different order each day. No shift in parameters was noted during the day as we avoided the early and late hours. The plants were never under water stress.

Leaves were exposed to a saturating photosynthetic photon flux density of 1,000 μmol m^{-2} s^{-1} at a temperature of 25°C and with relative humidity in the leaf cuvette in the range of 40–60%. The parameters were recorded when the leaves inside the chamber reached steady state. The instrument provides a continuous display of gas exchange parameters. Steady state was reached when the first decimal of photosynthesis was stable (and therefore the other parameters). This usually happened after 2–3 min, as the air flow of 0.44 L min^{-1} was sufficient to produce fast air turnover inside the small fluorescence chamber.

Photosynthesis (A) and stomatal conductance (gs) was calculated by Li-COR software. The maximum quantum efficiency of PSII (Fv/Fm) and the actual quantum yield of PSII in illuminated leaves (F′v/F′m) were measured following a saturating pulse of light (10,000 μmol m^{-2} s^{-1}). The gas exchange and fluorescence data are means of at least eight leaves per replication. Fv/Fm determinations were performed after adapting the leaves to the dark for 30 min. Shading clips were used on measured leaves, and the plant to be measured was also placed in a dark room.

Statistical Analysis

The data were analyzed by two-way analysis of variance using Co-Stat statistics software. Treatment means were separated by Duncan multiple-range test ($P \leq 0.05$).

RESULTS

Visual Quality Characteristics and Plant Biomass

The dose × method (D × M) interaction effect of PH biostimulant and the plants was significant in terms of quality grade and dry biomass (**Figure 1**). Application of PHs to the plants at both doses (D0.1 and D0.2) increased quality grade with respect to untreated plants.

The high dose (D0.2) applied as foliar spray produced petunias with extra-grade visual quality (number of flowers per plant 161; number of leaves per plant 450; and leaf area per plant 1,487 cm^2) and a total aboveground dry weight of 35 g.

Regarding the D × M interaction of biostimulant application, increasing PH concentration of foliar spray from D0.1 to D0.2 resulted in the best quality grade: 3rd grade (control) < 1st grade (D0.1) < extra grade (D0.2) for leaf area and aboveground dry biomass (**Figure 1**). Plants treated by root drenching at D0.1 achieved 1st grade, whereas controls achieved 3rd grade; application of biostimulant at D0.2 did not result in any significant improvement in quality grade.

Figure 2 shows that plants treated with increasing concentrations of foliar spray from 0 to 0.1 and 0.2 g L^{-1} increased in quality grade: 3rd grade (control) < 1st grade (D0.1 g L^{-1}) < extra grade (D0.2) in terms of shoots (+91%), flowers (+230%), and leaf fresh weight (+71%). With root drenching at D0.1 or D0.2, plants achieved 1st grade.

Root Morphology

Application of the animal-derived PH biostimulant Hydrostim to the plants at doses of 0.1 and 0.2 g L^{-1}, whether by foliar spray or root drenching, positively influenced root morphology with respect to untreated plants (**Tables 3**, **4**). The D × M interaction effect of biostimulant application (D × M) was significant for root length, projected and total root surface area (**Table 3**), and number of root tips, forks, and crossings (**Table 4**).

Regarding root length and projected and total root surface area, plants treated by foliar spray at a dose of 0.2 g L^{-1} achieved higher values than plants treated differently: 3.15 m × 10^3 $plant^{-1}$, 146.5 cm^2 $plant^{-1}$, and 435.0 cm^2 $plant^{-1}$, respectively (**Table 3**). The same significant trend was recorded in plants treated with 0.2 g L^{-1} as foliar spray (**Table 4**) for number of root tips (24.3 × 10^3 $plant^{-1}$), forks (20.4 × 10^3 $plant^{-1}$), and crossings (330.6 × 10^3 $plant^{-1}$).

Leaf Nutritional Status

The D × M interaction of biostimulant application was found to be significant for leaf content of macronutrients N, P, and K (**Table 5**). Doses D0.1 and D0.2 as a foliar spray both increased total N (+54 and +65%, respectively), whereas when the biostimulant was applied as root drench, N content increased by 43%. P and K content achieved higher values than untreated petunias, when plants were treated

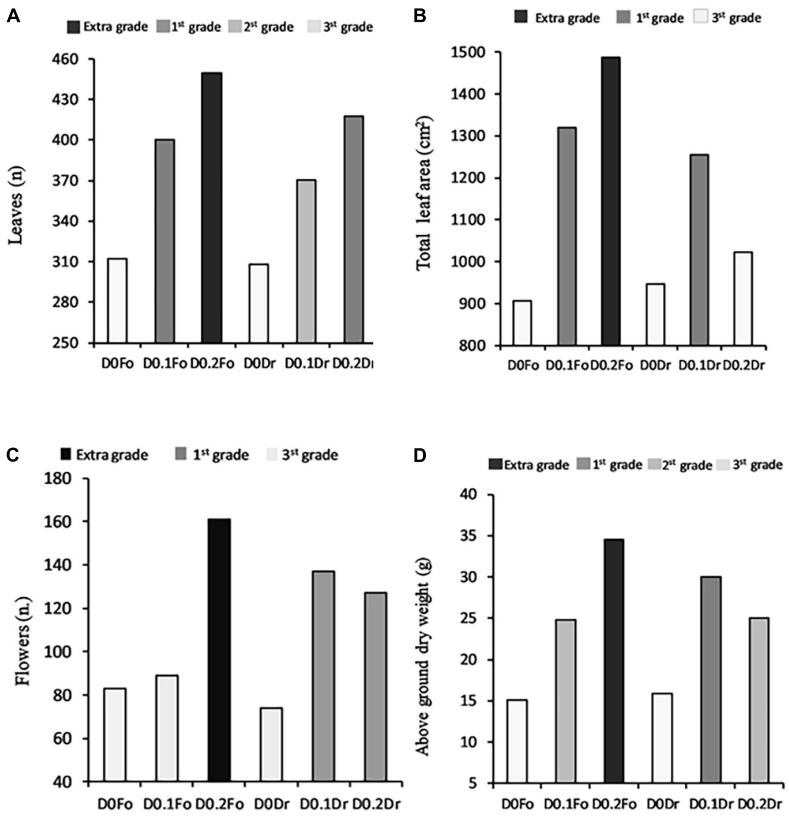

FIGURE 1 | Interaction effects of biostimulant dose (D0, D0.1, and D0.2) × application method (Fo = foliar spray and Rd = root drenching) on petunia plant grade [leaf number **(A)**, total leaf area **(B)**, flower number **(C)**, and dry weight of aboveground parts **(D)**].

with D0.2 as foliar spray, increasing by +0.33 and +38%, respectively. The only significantly different leaf content of K was recorded with root drenching at D0.1: +3.08% with respect to control.

SPAD, Leaf Gas Exchange, and Chlorophyll Fluorescent Measurements

Animal-based PH biostimulant had a positive influence on parameters related to SPAD, leaf gas exchange, and chlorophyll fluorescence (**Table 6**). The D × M interaction effect of biostimulant application (D × M) was significant for SPAD: using foliar spray at doses D0.1 and D0.2, SPAD showed a linear increase (+21.6 and +41.0%) with respect to untreated plants. Conversely, using root drenching, D0.1 produced an increase (+13%) with respect to control.

Concerning leaf gas exchange parameters, application of biostimulant as foliar spray at both doses led to a significant improvement in net photosynthesis (D0.1: 22.9 μmol CO_2 m^{-2} s^{-1}; D0.2: 22.4 μmol CO_2 m^{-2} s^{-1}) and stomatal conductance (D0.1: 0.42 mmol H_2O m^{-2} s^{-1} and D0.2: 0.39 mmol H_2O m^{-2} s^{-1}) with respect to control plants.

A significant D × M interaction was found for chlorophyll fluorescence: application of biostimulant as foliar spray at D0.1 was associated with the highest value (**Table 6**).

DISCUSSION

In this article, potted petunia plants were treated at two doses (D0.1 = normal and D0.2 = high) or not treated (D0) with an animal-based PH biostimulant, Hydrostim, applied by foliar spray or root drenching. The first dose of biostimulant D0.1 was that recommended by the manufacturer; the second D0.2 was double that amount.

Ertani et al. (2013) found that application of low doses (0.01 and 0.1 mL L^{-1}) of an animal-derived PH, rich in amino acids, promoted maize seedling growth. In their experiments, other authors have applied the recommended dose: Casadesús et al. (2020) applied an animal PH biostimulant (Pepton) at a recommended dose of 4 kg ha^{-1} to tomato plants; Cristiano et al. (2018) treated snapdragon plants at a recommended dose of 0.1 g L^{-1}. The effectiveness of the application method (foliar spray or soil drench) appears to be species-dependent: Sestili et al. (2018) showed that drench applications of PH were more effective in improving plant growth and total N uptake than foliar sprays in tomato.

In the present study, an animal-derived PH biostimulant (Hydrostim), rich in amino acids (52%), was applied to petunias and was found to improve visual quality traits (**Figure 1**), plant biomass (**Figure 2**), leaf nutrient content (**Table 3**), root morphology (**Tables 4**, **5**), and leaf gas

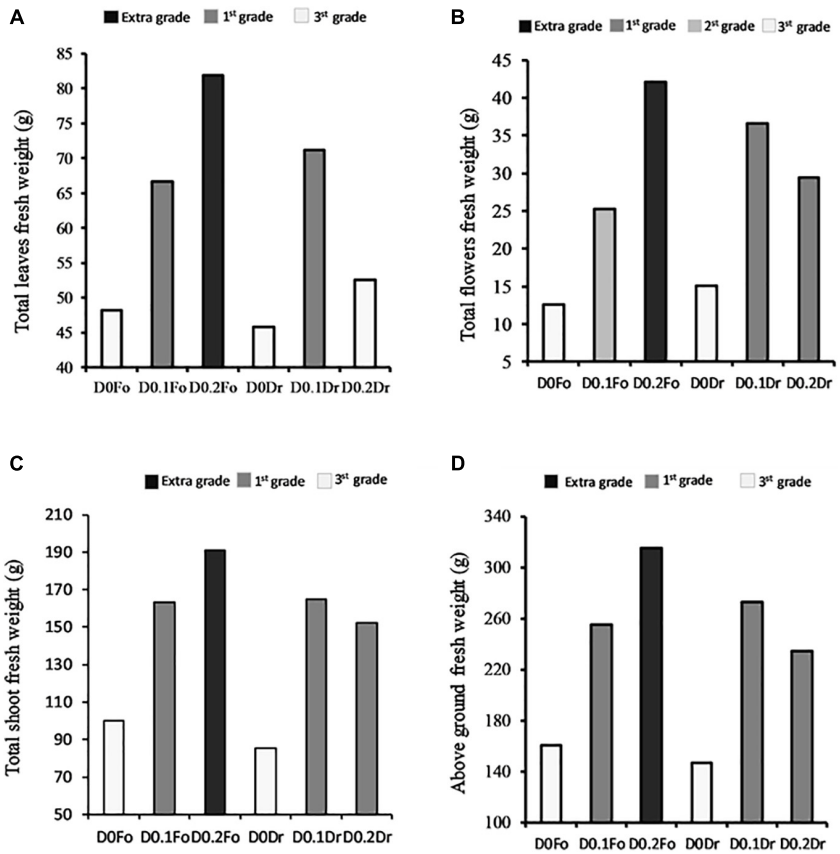

FIGURE 2 | Interaction effects of biostimulant dose (D0, D0.1, and D0.2) × application method (Fo = foliar spray and Rd = root drenching) on petunia plant grade [total fresh weight of leaves **(A)**, total fresh weight of flowers **(B)**, total fresh weight of shoots **(C)**, and aboveground fresh weight **(D)**].

TABLE 3 | Dose × method interaction of animal-derived PH biostimulant on root length (m × 10^3/plant), projected area (cm^2/plant), total surface area (cm^2/plant) in petunia plants for doses D0, D0.1, and D0.2, and foliar spray and root drench application methods.

Root parameters	Dose (g L^{-1}) (D)					
	0		0.1		0.2	
	Application method					
	Foliar spray	Root drenching	Foliar spray	Root drenching	Foliar spray	Root drenching
Length	1.25d	1.33d	2.14c	2.66b	3.15a	2.74b
Projected area	66.6c	70.6c	91.2bc	111.1b	146.5a	138.4a
Total surface area	202.2d	220.1d	272.9cd	347.9bc	435.0a	414.7ab

Different letters in a given row indicate significant differences according to Duncan multiple-range test ($P \leq 0.05$) ($n = 3$).

exchange (**Table 6**). Our findings show that the most promising treatment for petunia plants was foliar spray at 0.2 g L^{-1}. On the contrary, Cerdán et al. (2008, 2013) observed growth inhibition in tomato plants treated with an animal-derived PH, and Lisiecka et al. (2011) found no improvement in strawberry plants. These different results could be due to the different commercial PHs, plant species, concentrations, and growth conditions.

Our visual quality trait results (**Figure 1**) agree with the findings of other researchers; for example, Zulfiqar et al. (2019) demonstrated that the biostimulant *Moringa oleifera* leaf extract (MOLE) improved preharvest quality of sword lily: corms soaked in MOLE + salicylic acid + gibberellic acid showed enhanced growth and development: longer floral stems, more leaves and larger leaf area. Parrado et al. (2008) demonstrated that application of an animal-derived PH (Siapton) to tomato plants elicited a significant increase in various plant growth parameters and number of flowers per plant. Ertani et al. (2013) obtained 4 and 8% increases in leaf dry weight of maize at meat-hydrolysate doses of 0.01 and at 0.1 mL L^{-1}, respectively.

TABLE 4 | Dose × method interaction of animal-derived PH biostimulant on root tips (n 10^3/plant), forks (n 10^3/plant), and crossings (n 10^3/plant) in petunia plants for doses D0, D0.1, and D0.2 and foliar spray and root drench application methods.

Root parameters	Dose (g L^{-1}) (D)					
	0		0.1		0.2	
	Application method					
	Foliar spray	Root drenching	Foliar spray	Root drenching	Foliar spray	Root drenching
Tips	8.4d	9.0d	18.4b	15.2c	24.3a	18.0b
Forks	7.1d	7.5d	15.5b	12.8c	20.4a	15.2b
Crossings	153.7c	167.3c	207.4bc	264.4ab	330.6a	314.5a

Different letters in a given row indicate significant differences according to Duncan multiple-range test ($P \leq 0.05$) (n = 3).

TABLE 5 | Dose × method interaction of animal-derived PH biostimulant on N, P, and K leaf total content in petunia plants for doses D0, D0.1, and D0.2 and foliar spray and root drench application methods.

Leaf mineral content (%)	Dose (g L^{-1}) (D)					
	0		0.1		0.2	
	Application method					
	Foliar spray	Root drenching	Foliar spray	Root drenching	Foliar spray	Root drenching
N	2.02c	2.10c	3.11ab	2.91b	3.34a	2.89b
P	0.12c	0.15c	0.23b	0.22b	0.32a	0.21b
K	2.36c	2.38c	2.97a	2.52b	3.27a	2.45b

Different letters in a given row indicate significant differences according to Duncan multiple-range test ($P \leq 0.05$) (n = 3).

TABLE 6 | Dose × method interaction of animal-derived PH biostimulant on chlorophyll index (SPAD), net photosynthesis (μmol CO_2 m^{-2} s^{-1}), stomatal conductance (mmol H_2O m^{-2} s^{-1}), and chlorophylls fluorescence (Fv/Fm) in petunia plants for doses D0, D0.1, and D0.2 and foliar spray and root drench application methods.

Physiological parameters	Dose (g L^{-1}) (D)					
	0		0.1		0.2	
	Application method					
	Foliar spray	Root drenching	Foliar spray	Root drenching	Foliar spray	Root drenching
Chlorophyll Index	37.5c	37.7c	45.6b	42.6bc	52.9a	39.8c
Net photosynthesis	14.9c	17.2c	22.9a	21.5a	22.4a	19.6b
Stomatal conductance	0.25c	0.26c	0.39ab	0.37ab	0.42a	0.33b
Chlorophyll fluorescence	0.83c	0.82c	0.95a	0.91b	0.90b	0.89b

Different letters in a given row indicate significant differences according to Duncan multiple-range test ($P \leq 0.05$) (n = 3).

Regarding ornamental flower crops, the present study is in line with reports by De Lucia and Vecchietti (2012), who investigated the effects of three different agricultural biostimulants on lily hybrids grown in a soilless system: animal-derived PH biostimulant increased leaf area and flower bud number with respect to untreated controls. It is thought that signaling molecules in the biostimulant, such as free amino acids, promote endogenous phytohormonal biosynthesis, thus stimulating growth (Rouphael et al., 2017b).

Bulgari et al. (2015) found that bedding plant quality depended on visual appearance, as well as flower number and plant biomass. Cirillo et al. (2018) found that the effects on growth, ornamental quality, leaf gas exchanges, and mineral composition of spraying three different species of bedding plant (*Begonia tuberhybrida*, *Pelargonium peltatum*, and *Viola cornuta*) with increasing concentrations of a commercial legume-derived PH (Trainer) (0, 1, 3, and 5 mL L^{-1}) were species-dependent. In particular, the normal concentration (1 mL L^{-1}) enhanced several growth and quality parameters (plant height, canopy volume, leaf area, and number of flowers per plant) of *P. peltatum*, whereas positive effects of biostimulant application to *B. tuberhybrida* and *V. cornuta* were only observed at higher concentrations.

The results of our experiment demonstrate that Hydrostim, containing organic N and amino acids, has multifaceted action that may ensure achievement of extra-grade quality in Petunia

(**Figures 1**, **2**). Lucini et al. (2018) showed that substrate drench with a biostimulant containing lateral root–promoting peptides and lignosulfonates increased biomass production in melon. Cristiano et al. (2018) showed that aboveground plant biomass was not differentially affected by the method of application of biostimulant in two F1 *Antirrhinum majus* L. hybrids ("yellow floral showers" and "red sonnet"). By contrast, our results (**Figures 1**, **2**), suggest that PH biostimulant applied to petunia as foliar spray increased fresh and dry biomass production more than drenching (**Figure 2**), mainly through slightly higher leaf area (larger surface for light assimilation, **Figure 1**) and SPAD and significantly higher net photosynthesis rate (**Table 6**). According to Rouphael et al. (2017a), increasing crop effectiveness is due to greater absorption of nutrients.

Our findings show that N content increased with application of PH biostimulant as foliar spray (**Table 5**). N content is also important regarding visual quality assessment of the leaves: discoloration such as yellowing appears in the older leaves and a size reduction of younger leaves due to N deficiencies too (Gibson et al., 2007; Barker and Pilbeam, 2007; Datnoff and Elmer, 2016). Flowering is in general delayed and reduced in number and size. Our hypothesis, based on the recent literature, is that higher N content could be related to increased gene expression. Wilson et al. (2018) reported that gelatin hydrolysate treatment increased the expression of genes coding for amino acid permeases (*AAP3* and *AAP6*) and transporters of amino acids and N. They concluded that gelatin hydrolysate provided a sustained source of N and acted as a biostimulant.

P and K are also important elements for plant growth, as well as visual and overall quality. P plays a significant role in energy storage, energy transfer, photosynthesis, cell division, and cell enlargement. Niedziela et al. (2008) showed that shorter stem length was due to P deficiency in *Lilium longiflorum*. Adequate P is needed for the promotion of early root formation and growth. K deficiency has been associated with fewer flowers (Dufault et al., 1990). In photosynthesis, K regulates the opening and closing of stomata and therefore CO_2 uptake (Wang et al., 2013). It plays a major role in water regulation in plants (osmoregulation) and is essential at almost every step of protein synthesis. Colla et al. (2017a) showed that four foliar applications of a legume-derived PH at a concentration of 3 mL L^{-1} during the growing cycle increased K content of greenhouse tomatoes. Recent studies have shown yield and nutrient uptake enhancement with PH biostimulant (Calvo et al., 2014).

In our experiment, the better agronomic responses of PH-treated petunia may be associated with enhanced root morphology (**Tables 4**, **5**) that could facilitate N uptake and leaf N content. In maize treated hydroponically with 0.01 and 0.1 mL L^{-1} of a meat-hydrolysate biostimulant, Ertani et al. (2013) found that root dry weight increased by +30 and +24%, respectively, compared to untreated controls. Casadesús et al. (2020) assessed the effect of Pepton (an animal-based PH biostimulant) on tomato plants cultivated under suboptimal conditions. They found that Pepton had a positive effect on primary and lateral root growth through a direct influence of amino acid availability and through salicylic acid accumulation in response to stressful conditions.

Our results agree with those of other studies that have shown that applications of plant- and animal-based PH biostimulants are able to optimize plant photosynthesis (Kang and van Lersel, 2004; Rouphael and Colla, 2020). The enhanced photosynthetic capacity observed in our petunias treated with Hydrostim as foliar spray increased biomass accumulation (**Figure 2** and **Table 3**). Leaf chlorophyll content (SPAD index) was consistent with the results observed for photosynthetic activity. Loh et al. (2002) showed that SPAD is useful for assessing the quality of ornamentals, as it is correlated with good general condition and leaf greenness.

CONCLUSION

In this article, we compared three doses (0, 0.1, and 0.2 g L^{-1}) and two application methods (foliar spray and root drenching) to assess the effect of a commercial biostimulant (Hydrostim: animal-based PHs) on visual quality, biomass, macronutrient content, root morphology, and leaf gas exchange in potted Petunia cultivation. We found that application as foliar spray at a dose of 0.2 g L^{-1} helped to achieve extra-grade plants; the high dose (D0.2) also had the strongest effect on dry biomass; leaf N, P, and K content; and root morphology.

In the last 10 years, much attention has been focused on the use of biowaste-sourced products, such as animal-based PHs, in ecofriendly sustainable agriculture, due also to the contribution of these products to the problem of waste disposal. Our results suggest that application of animal-based PHs can be exploited under sustainable greenhouse conditions in the commercial production of petunia.

DATA AVAILABILITY STATEMENT

The raw data supporting the conclusions of this article will be made available by the authors, without undue reservation.

AUTHOR CONTRIBUTIONS

GC and BD conceived and designed the research, performed the experiments, prepared the materials, analyzed the data, and wrote the manuscript. Both authors revised the manuscript, read, and approved the final manuscript.

FUNDING

This work was supported by the Apulia Region Special Grant "PIF Florovivaismo" (2015–2016).

SUPPLEMENTARY MATERIAL

The Supplementary Material for this article can be found online at: https://www.frontiersin.org/articles/10.3389/fpls.2021.640608/full#supplementary-material

REFERENCES

Arancon, N. Q., Edwards, C. A., Babenko, A., Cannon, J., Galvis, P., and Metzger, J. D. (2008). Influences of vermicomposts, produced by earthworms and microorganisms from cattle manure, food waste and paper waste, on the germination, growth and flowering of petunias in the greenhouse. *Appl. Soil Ecol.* 39, 91–99. doi: 10.1016/j.apsoil.2007.11.010

Baglieri, A., Cadili, V., Mozzetti Monterumici, C., Gennari, M., Tabasso, S., Montoneri, E., et al. (2014). Fertilization of bean plants with tomato plants hydrolysates. Effect on biomass production, chlorophyll content and N assimilation. *Sci. Hortic.* 176, 194–199. doi: 10.1016/j.scienta.2014.07.002

Barker, A. V., and Pilbeam, D. J. (2007). *Handbook of Plant Nutrition*. Boca Raton, FL: Taylor and Francis.

Bergstrand, K. J. I. (2017). Methods for growth regulation of greenhouse produced ornamental pot-and bedding plants–a current review. *Folia Hortic.* 29, 63–74. doi: 10.1515/fhort-2017-0007

Bouwman, L., Goldewijk, K. K., Van Der Hoek, K. W., Beusen, A. H. W., Van Vuuren, D. P., Willems, J., et al. (2013). Exploring global changes in nitrogen and phosphorus cycles in agriculture induced by livestock production over the 1900-2050 period. *Proc. Nat. Acad. Sci. U. S. A.* 110, 20882–20887. doi: 10.1073/pnas.1012878108

Bulgari, R., Cocetta, G., Trivellini, A., Vernieri, P., and Ferrante, A. (2015). Biostimulants and crop responses: a review. *Biol. Agric. Hortic.* 31, 1–17. doi: 10.1080/01448765.2014.964649

Bulgari, R., Trivellini, A., and Ferrante, A. (2019). Effects of two doses of organic extract-based biostimulant on greenhouse lettuce grown under increasing NaCl concentrations. *Front. Plant Sci.* 9:1870. doi: 10.3389/fpls.2018.01870

Calvo, P., Nelson, L., and Kloepper, J. W. (2014). Agricultural uses of plant biostimulants. *Plant Soil* 383, 3–41. doi: 10.1007/s11104-014-2131-8

Carillo, P., Colla, G., Fusco, G. M., Dell'Aversana, E., El-Nakhel, C., Giordano, M., et al. (2019). Morphological and physiological responses induced by protein hydrolysate-based biostimulant and nitrogen rates in greenhouse spinach. *Agronomy* 9:450. doi: 10.3390/agronomy9080450

Caruso, G., De Pascale, S., Cozzolino, E., Cuciniello, A., Cenvinzo, V., Bonini, P., et al. (2019). Yield and nutritional quality of Vesuvian Piennolo tomato PDO as affected by farming system and biostimulant application. *Agronomy* 9:505. doi: 10.3390/agronomy9090505

Casadesús, A., Pérez-Llorca, M., Munné-Bosch, S., and Polo, J. (2020). An enzymatically hydrolyzed animal protein-based biostimulant (pepton) increases salicylic acid and promotes growth of tomato roots under temperature and nutrient stress. *Front. Plant Sci.* 11:953. doi: 10.3389/fpls.2020.00953

Casadesús, A., Polo, J., and Munné-Bosch, S. (2019). Hormonal effects of an enzymatically hydrolyzed animal protein-based biostimulant (Pepton) in water-stressed tomato plants. *Front. Plant Sci.* 10:758. doi: 10.3389/fpls.2019.00758

Cerdán, M., Sánchez-Sánchez, A., Oliver, M., Juárez, M., and Sánchez-Andreu, J. J. (2008). Effect of foliar and root applications of amino acids on iron uptake by tomato plants. *Acta Hortic.* 830, 481–488. doi: 10.17660/ActaHortic.2009.830.68

Cerdán, M., Sánchez-Sánchez, A., Jordá, J. D., Juárez, M., and Sánchez-Andreu, J. (2013). Effect of commercial amino acids on iron nutrition of tomato plants grown under lime-induced iron deficiency. *J. Plant Nutr. Soil Sci.* 176, 859–866. doi: 10.1002/jpln.201200525

Chavez, W., Di Benedetto, A., Civeira, G., and Lavado, R. (2008). Alternative soilless media for growing Petunia × hybrida and Impatiens wallerana: physical behavior, effect of fertilization and nitrate losses. *Biores. Tech.* 99, 8082–8087. doi: 10.1016/j.biortech.2008.03.063

Cirillo, C., Rouphael, Y., Pannico, A., El-Nakhel, C., Colla, G., and De Pascale, S. (2018). Application of protein hydrolysate-based biostimulant as new approach to improve performance of bedding plants. *Acta Hortic.* 1215, 443–448. doi: 10.17660/ActaHortic.2018.1215.80

Colla, G., Cardarelli, M., Bonini, P., and Rouphael, Y. (2017a). Foliar applications of protein hydrolysate, plant and seaweed extracts increase yield but differentially modulate fruit quality of greenhouse tomato. *HortScience* 52, 1214–1220. doi: 10.21273/HORTSCI12200-17

Colla, G., Hoagland, L., Ruzzi, M., Cardarelli, M., Bonini, P., Canaguier, R., et al. (2017b). Biostimulant action of protein hydrolysates: unraveling their effects on plant physiology and microbiome. *Front. Plant Sci.* 8:2202. doi: 10.3389/fpls.2017.02202

Colla, G., Nardi, S., Cardarelli, M., Ertani, A., Lucini, L., Canaguier, R., et al. (2015). Protein hydrolysates as biostimulants in horticulture. *Sci. Hortic.* 196, 28–38. doi: 10.1016/j.scienta.2015.08.037

Colla, G., Rouphael, Y., Canaguier, R., Svecova, E., and Cardarelli, M. (2014). Biostimulant action of a plant-derived protein hydrolysate produced through enzymatic hydrolysis. *Front. Plant Sci.* 5:448. doi: 10.3389/fpls.2014.00448

Consentino, B. B., Virga, G., La Placa, G. G., Sabatino, L., Rouphael, Y., Ntatsi, G., et al. (2020). Celery (Apium graveolens L.) performances as subjected to different sources of protein hydrolysates. *Plants* 9, 12–1633. doi: 10.3390/plants9121633

Cristiano, G., Pallozzi, E., Conversa, G., Tufarelli, V., and De Lucia, B. (2018). Effects of an animal-derived biostimulant on the growth and physiological parameters of potted snapdragon (Antirrhinum majus L.). *Front. Plant Sci.* 9:861. doi: 10.3389/fpls.2018.00861

Darras, A. I. (2020). Implementation of sustainable practices to ornamental plant cultivation worldwide: a critical review. *Agronomy* 10:1570. doi: 10.3390/agronomy10101570

Datnoff, L. E., and Elmer, W. H. (2016). "Mineral nutrition and florists' crops diseases," in *Handbook of Florists' Crops Diseases. Handbook of Plant Disease Management*, eds R. McGovern and W. Elmer (Cham: Springer).

De Lucia, B., and Vecchietti, L. (2012). Type of biostimulant and application method effects on stem quality and root system growth in LA Lily. *Eur. J. Hortic. Sci.* 77, 1–10.

De Pascale, S., Rouphael, Y., Cirillo, C., and Colla, G. (2020). Plant biostimulants in greenhouse horticulture: recent advances and challenges ahead. *Acta Hortic.* 1271, 327–334. doi: 10.17660/ActaHortic.2020.1271.45

De Pascale, S., Rouphael, Y., and Colla, G. (2017). Plant biostimulants: innovative tool for enhancing plant nutrition in organic farming. *Eur. J. Hortic. Sci.* 82, 277–285. doi: 10.17660/eJHS.2017/82.6.2

Dufault, R. J., Phillip, T. L., and Kelly, J. W. (1990). Nitrogen and potassium fertility and plant populations influence field production of gerbera. *HortScience* 25, 1599–1602. doi: 10.21273/HORTSCI.25.12.1599

EN 13650 (2001). Soil Improvers and Growing Media-Extraction of Aqua Regia Soluble Elements.

Ertani, A., Cavani, L., Pizzeghello, D., Brandellero, E., Altissimo, A., Ciavatta, C., et al. (2009). Biostimulant activity of two protein hydrolyzates in the growth and nitrogen metabolism of maize seedlings. *J. Plant Nutr. Soil Sci.* 172, 237–244. doi: 10.1002/jpln.200800174

Ertani, A., Schiavon, M., Muscolo, A., and Nardi, S. (2013). Alfalfa plant-derived biostimulant stimulate short-term growth of salt stressed Zea mays L. plants. *Plant Soil* 364, 145–158. doi: 10.1007/s11104-012-1335-z

European Biostimulants Industry Council [EBI] (2013). *Promoting the Biostimulant Industry and the Role of Plant Biostimulants in Making Agriculture More Sustainable*. Antwerp: European Biostimulants Industry Council.

Fain, G. B., Gilliam, C. H., Sibley, J. L., Boyer, C. R., and Witcher, A. L. (2008). Wholetree substrate and fertilizer rate in production of greenhouse-grown petunia (Petunia× hybrida Vilm.) and marigold (Tagetes patula L.). *HortScience* 43, 700–705. doi: 10.21273/hortsci.43.3.700

Ferrante, A., Trivellini, A., Scuderi, D., Romano, D., and Vernieri, P. (2015). Post-production physiology and handling of ornamental potted plants. *Postharvest Biol. Tec.* 100, 99–108. doi: 10.1016/j.postharvbio.2014.09.005

Gibson, J. L., Pitchay, D. S., Williams-Rhodes, A. L., Whipker, B. E., Nelson, P. V., and Dole, J. M. (2007). *Nutrient Deficiencies in Bedding Plants: A Pictorial Guide for Identification and Correction*. Batavia: Ball Publishing, 1–369.

Gruda, N. (2005). Impact of environmental factors on product quality of greenhouse vegetables for fresh consumption. *Crit. Rev. Plant Sci.* 24, 227–247. doi: 10.1080/07352680591008628

Gruda, N., Bisbis, M., and Tanny, J. (2019). Influence of climate change on protected cultivation: impacts and sustainable adaptation strategies–a review. *J. Clean. Prod.* 225, 481–495. doi: 10.1016/j.jclepro.2019.03.210

Halpern, M., Bar-Tal, A., Ofek, M., Minz, D., Muller, T., and Yermiyahu, U. (2015). The use of biostimulants for enhancing nutrient uptake. *Adv. Agron.* 130, 141–174. doi: 10.1016/bs.agron.2014.10.001

Hansen, B., Thorling, L., Schullehner, J., Termansen, M., and Dalgaard, T. (2017). Groundwater nitrate response to sustainable nitrogen management. *Sci. Rep.* 7:8566. doi: 10.1038/s41598-017-07147-2

Havardi-Burger, N., Mempel, H., and Bitsch, V. (2020). Sustainability challenges and innovations in the value chain of flowering potted plants for the german market. *Sustainability.* 12:1905. doi: 10.3390/su12051905

Ingram, D. L., Hall, C. R., and Knight, J. (2019). Understanding carbon footprint in production and use of landscape plants. *HortTechnology* 29, 6–10. doi: 10.21273/HORTTECH04220-18

Isaak, M., and Lentz, W. (2020). Consumer preferences for sustainability in food and non-food horticulture production. *Sustainability* 12:7004. doi: 10.3390/su12177004

James, E. C., and van Lersel, M. W. (2001). Fertilizer concentration affects growth and flowering of subirrigated petunias and begonias. *HortScience* 36, 40–44. doi: 10.21273/hortsci.36.1.40

Kader, A. A. (2000). Quality of horticultural products. *Acta Hortic.* 517, 17–18. doi: 10.17660/actahortic.2000.517.1

Kang, J. G., and van Lersel, M. W. (2004). Nutrient solution concentration affects shoot: root ratio, leaf area ratio, and growth of subirrigated salvia (Salvia splendens). *HortScience* 39, 49–54. doi: 10.21273/hortsci.39.1.49

Kunicki, E., Grabowska, A., Sêkara, A., and Wojciechowska, R. (2010). The effect of cultivar type, time of cultivation, and biostimulant treatment on the yield of spinach (Spinacia oleracea L.). *Folia Hortic.* 22, 9–13. doi: 10.2478/fhort-2013-0153

Lang, H. J., and Pannuk, T. R. (1998). Effects of fertilizer concentration and minimum-leach drip irrigation on the growth of New Guinea impatiens. *HortScience* 33, 83–688. doi: 10.21273/hortsci.33.4.683

Lisiecka, J., Knaflewski, M., Spizewski, T., Fraszczak, B., Kaluzewicz, A., and Krzesinski, W. (2011). The effect of animal protein hydrolysate on quantity and quality of strawberry daughter plants cv 'Elsanta'. *Acta Sci. Pol. Hortorum Cultus.* 10, 31–40.

Loh, F. C., Grabosky, J. C., and Bassuk, N. L. (2002). Using the SPAD 502 meter to assess chlorophyll and nitrogen content of benjamin fig and cottonwood leaves. *HortTechnology* 12, 682–686. doi: 10.21273/horttech.12.4.682

Lucini, L., Rouphael, Y., Cardarelli, M., Bonini, P., Baffi, C., and Colla, G. (2018). A vegetal biopolymer-based biostimulant promoted root growth in melon while triggering brassinosteroids and stress-related compounds. *Front. Plant Sci.* 9:472. doi: 10.3389/fpls.2018.00472

Lütken, H., Jensen, L. S., Topp, S. H., Mibus, H., Muller, R., and Rasmussen, S. K. (2010). Production of compact plants by overexpression of AtSHI in the ornamental Kalanchoe. *Plant Biotechnol. J.* 8, 211–222. doi: 10.1111/j.1467-7652.2009.00478.x

Marschner, H. (2011). *Marschner's Mineral Nutrition of Higher Plants*. Cambridge, MA: Academic press.

Morales-Pajan, J. P., and Stall, W. (2004). Passion fruit (*Passiflora edulis*) transplant production i affected by selected biostimulants. *Proc. Fla. State Hortic. Soc.* 117, 224–227.

Morales-Pajan, J. P., and Stall, W. M. (2003). Papaya (Carica papaya) response to foliar treatments with organic complexes of peptides and amino acids. *Proc. Fla. State Hortic. Soc.* 116, 30–32.

Nardi, S., Pizzeghello, D., Schiavon, M., and Ertani, A. (2016). Plant biostimulants: physiological responses induced by protein hydrolyzed-based products and humic substances in plant metabolism. *Sci. Agr.* 73, 18–23. doi: 10.1590/0103-9016-2015-0006

Niedziela, C. E. Jr., Kim, S. H., Nelson, P. V., and De Hertogh, A. A. (2008). Effects of N–P–K deficiency and temperature regime on the growth and development of Lilium longiflorum 'Nellie White'during bulb production under phytotron conditions. *Sci. Hortic.* 116, 430–436. doi: 10.1016/j.scienta.2008.02.015

Nordstedt, N. P., Chapin, L. J., Taylor, C. G., and Jones, M. L. (2020). Identification of *Pseudomonas* Spp. that increase ornamental crop quality during abiotic stress. *Front. Plant Sci.* 10:1754. doi: 10.3389/fpls.2019.01754

Parađiković, N., Teklić, T., Zeljković, S., Lisjak, M., and Špoljarević, M. (2019). Biostimulants research in some horticultural plant species—a review. *Food Energy Secur.* 8:e00162. doi: 10.1002/fes3.162

Parrado, J., Bautista, J., Romero, E. J., García-Martínez, A. M., Friaza, V., and Tejada, M. (2008). Production of a carob enzymatic extract: potential use as a biofertilizer. *Bioresour. Technol.* 99, 2312–2318. doi: 10.1016/j.biortech.2007.05.029

Polo, J., Barroso, R., Ródenas, J., Azcón-Bieto, J., Cáceres, R., and Marfà, O. (2006). Porcine hemoglobin hydrolysate as a biostimulant for lettuce plants subjected to conditions of thermal stress. *HortTechnology* 16, 483–487. doi: 10.21273/horttech.16.3.0483

Polo, J., and Mata, P. (2018). Evaluation of a biostimulant (pepton) based in enzymatic hydrolyzed animal protein in comparison to seaweed on root development extracts, vegetative growth, flowering, and yield of gold cherry tomatoes stress ambient grown under low field conditions. *Front. Plant Sci.*:8–2261. doi: 10.3389/fpls.2017.02261

Quartieri, M., Cavani, L., Lucchi, A., Marangoni, B., and Tagliavini, M. (2002). Effects of the rate of protein hydrolysis spray concentration on growth of potted kiwifruit (*Actinidia deliciosa*) plants. *Acta Hortic.* 594, 341–347. doi: 10.17660/ActaHortic.2002.594.42

Rouphael, Y., Cardarelli, M., Bonini, P., and Colla, G. (2017a). Synergistic action of a microbial-based biostimulant and a plant derived-protein hydrolysate enhances lettuce tolerance to alkalinity and salinity. *Front. Plant Sci.* 8:131. doi: 10.3389/fpls.2017.00131

Rouphael, Y., Carillo, P., Cristofano, F., Cardarelli, M., and Colla, G. (2021). Effects of vegetal-versus animal-derived protein hydrolysate on sweet basil morpho-physiological and metabolic traits. *Sci. Hortic.* 284:110123. doi: 10.1016/j.scienta.2021.110123

Rouphael, Y., and Colla, G. (2020). Editorial: biostimulants in agriculture. *Front. Plant Sci.* 11:40. doi: 10.3389/fpls.2020.00040

Rouphael, Y., Colla, G., Giordano, M., El-Nakhel, C., Kyriacou, M. C., and De Pascale, S. (2017b). Foliar applications of a legume-derived protein hydrolysate elicit dose dependent increases of growth, leaf mineral composition, yield and fruit quality in two greenhouse tomato cultivars. *Sci. Hortic.* 22, 353–360. doi: 10.1016/j.scienta.2017.09.007

Sánchez-Bravo, P., Chambers, E., Noguera-Artiaga, L., Sendra, E., Chambers, E., and Carbonell-Barrachina, ÁA. (2021). Consumer understanding of sustainability concept in agricultural products. *Food Qual. Prefer.* 89:104136. doi: 10.1016/j.foodqual.2020.104136

Schaafsma, G. (2009). Safety of protein hydrolysates, fractions thereof and bioactive peptides in human nutrition. *Eur. J. Clin. Nutr.* 63, 1161–1168. doi: 10.1038/ejcn.2009.56

Sestili, F., Rouphael, Y., Cardarelli, M., Pucci, A., Bonini, P., Canaguier, R., et al. (2018). Protein hydrolysate stimulates growth in tomato coupled with N-dependent gene expression involved in N assimilation. *Front. Plant Sci.* 9:1233. doi: 10.3389/fpls.2018.01233

Shu, J., Wu, H., Chen, M., Wei, L., Wang, B., Li, B., et al. (2019). Simultaneous optimizing removal of manganese and ammonia nitrogen from electrolytic metal manganese residue leachate using chemical equilibrium model. *Ecotoxicol. Environ. Saf.* 172, 273–280.

Soode, E., Weber-Blaschke, G., and Richter, K. (2013). Comparison of product carbon footprint standards with a case study on poinsettia (Euphorbia pulcherrima). *Int. J. Life Cycle Assess.* 18, 1280–1290.

Sun, Y., Zhu, L., Wang, G., and Zhao, F. (2017). Multi-Input Convolutional Neural Network for Flower Grading. *J. Electr. Comput. Eng.* 2017, 1–8. doi: 10.1155/2017/9240407

The European Parliament and the Council of the European Union (2019). *Regulation (EU) 2019/1009 of the European Parliament and the Council of 5 June 2019 Laying Down Rules on the Making Available on the Market of EU Fertilising Products and Amending Regulations (EC) No 1069/2009 and (EC) No 1107/2009 and Repealing Regulation (EC) No 2003/2003; OJ L 170, 25.6.2019*, 1–114.

Toscano, S., Romano, D., Massa, D., Bulgari, R., Franzoni, G., and Ferrante, A. (2018). Biostimulant applications in low input horticultural cultivation systems. *Italus Hortus.* 25, 27–36. doi: 10.26353/j.itahort/2018.1.2736

Venugopal, V. (2016). Enzymes from seafood processing waste and their applications in seafood processing. *Adv. Food Nutr. Res.* 78, 47–69. doi: 10.1016/bs.afnr.2016.06.004

Wandl, M. T., and Haberl, H. (2017). Greenhouse gas emissions of small scale ornamental plant production in Austria—a case study. *J. Clean. Prod.* 141, 1123–1133. doi: 10.1016/j.jclepro.2016.09.093

Wang, M., Zheng, Q., Shen, Q., and Guo, S. (2013). The critical role of potassium in plant stress response. *Int. J. Mol. Sci.* 14, 7370–7390. doi: 10.3390/ijms14047370

Wilson, H. T., Amirkhani, M., and Taylor, A. G. (2018). Evaluation of gelatin as a biostimulant seed treatment to improve plant performance. *Front. Plant Sci.* 9:1006. doi: 10.3389/fpls.2018.01006

Xu, C., and Mou, B. (2017). Drench application of fish-derived protein hydrolysates affects lettuce growth, chlorophyll content, and gas exchange. *Hort Tech.* 27, 539–543. doi: 10.21273/HORTTECH03723-17

Zhang, X., Davidson, E. A., Mauzerall, D. L., Searchinger, T. D., Dumas, P., and Shen, Y. (2015). Managing nitrogen for sustainable development. *Nature* 528, 51–59. doi: 10.1038/nature15743

Zulfiqar, F., Navarro, M., Ashraf, M., Akram, N. A., and Munné-Bosch, S. (2019). Nanofertilizer use for sustainable agriculture: advantages and limitations. *Plant Sci.* 289:110270. doi: 10.1016/j.plantsci.2019.110270

Conflict of Interest: The authors declare that the research was conducted in the absence of any commercial or financial relationships that could be construed as a potential conflict of interest.

frontiers in Plant Science

ORIGINAL RESEARCH
published: 15 July 2021
doi: 10.3389/fpls.2021.639717

A Cytokinin Analog Thidiazuron Suppresses Shoot Growth in Potted Rose Plants via the Gibberellic Acid Pathway

Fisun G. Çelikel[1,2], Qingchun Zhang[1,3], Yanlong Zhang[3], Michael S. Reid[1] and Cai-Zhong Jiang[1,4]**

[1] Department of Plant Sciences, University of California, Davis, Davis, CA, United States, [2] Department of Horticulture, Ondokuz Mayıs University, Samsun, Turkey, [3] College of Landscape Architecture and Arts, Northwest A&F University, Xianyang, China, [4] Crops Pathology and Genetics Research Unit, USDA-ARS, Davis, CA, United States

OPEN ACCESS

Edited by:
Antonio Ferrante, University of Milan, Italy

Reviewed by:
Daqi Fu, China Agricultural University, China
Samir Debnath, St. John's Research and Development Centre, Agriculture and Agri-Food Canada, Canada

***Correspondence:**
Michael S. Reid
msreid@ucdavis.edu
Cai-Zhong Jiang
cjiang@ucdavis.edu

Specialty section:
This article was submitted to Crop and Product Physiology, a section of the journal Frontiers in Plant Science

Received: *09 December 2020*
Accepted: *15 June 2021*
Published: *15 July 2021*

Citation:
Çelikel FG, Zhang Q, Zhang Y, Reid MS and Jiang C-Z (2021) A Cytokinin Analog Thidiazuron Suppresses Shoot Growth in Potted Rose Plants via the Gibberellic Acid Pathway. Front. Plant Sci. 12:639717. doi: 10.3389/fpls.2021.639717

Application of thidiazuron (*N*-phenyl-*N*′-1,2,3-thiadiazol-5-ylurea, TDZ), a cytokinin analog, to inhibit the leaf yellowing that occurs after pinching potted rose plants, resulted in compact plants with shorter shoots and thicker internodes. Two weeks after treatment with 100 μM of TDZ, new shoots were half as long as those in control plants, and stem diameters were about 40% greater. This effect of TDZ is associated with changes in cell architecture. Although TDZ treatment stimulated ethylene production by the plants, inhibitors of ethylene biosynthesis (2-aminoethoxyvinyl glycine) or action (silver thiosulfate) did not affect the response of plants to TDZ. We found that TDZ treatment significantly suppressed the expression of bioactive gibberellic acid (GA) biosynthesis genes encoding GA3 and GA20 oxidases and slightly increased the expression of GA catabolism genes encoding GA2 oxidase. Application of GA_3 and TDZ together resulted in normal elongation growth, although stem diameters were still somewhat thicker. Our results suggest that TDZ regulates shoot elongation and stem enlargement in potted rose plants through the modulation of bioactive GA biosynthesis.

Keywords: ethylene, GA oxidase enzymes, gene expression, internode length and thickness, microscopy, miniature rose, plant height, thidiazuron

INTRODUCTION

Potted miniature roses (*Rosa hybrida* L.) are popular year-round potted plants, with an increase in production for special days such as Mother's Day and Easter in the United States. However, the leaves of potted roses turn yellow and abscise after pinching (a technique that intends to stimulate branching), as well as under low light conditions after production (Zieslin et al., 1976; Tjosvold et al., 1994). In a previous studies, we used the cytokinin analog thidiazuron (TDZ) as a tool for

extending the life of potted plants (Jiang et al., 2009) and preventing leaf yellowing after pinching potted miniature roses (Çelikel et al., 2019). In addition to effective prevention of leaf yellowing, we found that concentrations of TDZ higher than 80 μM inhibited shoot growth, resulting in plants with shorter and thicker stems.

Plant height control is important in maintaining the compactness and quality of potted plants during and after production (Miller, 2012). The lower light conditions in homes and offices could result in an increase in plant height and a reduction of postharvest quality. To provide compact plants, growers apply plant growth regulators, such as ethylene (released from ethephon) (Çelikel and Demir, 2019), or more commonly, inhibitors of gibberellin biosynthesis (such as flurprimidol, ancymidol, and paclobutrazol) (Miller, 2012; Demir and Çelikel, 2019), to suppress extension growth after production. Our findings that the anti-yellowing effect of TDZ was accompanied by a marked reduction of elongation growth are therefore of considerable practical interest.

The main commercial use of TDZ is as a defoliant in cotton, an activity that results from stimulation of ethylene production and accelerated abscission when the plants are sprayed with relatively low concentrations of the regulator (Suttle, 1985, 1986). Ethylene is known to reduce extension growth in many species, and thus we hypothesized that the reduction in elongation growth in miniature rose plants is due to TDZ-induced ethylene production.

MATERIALS AND METHODS

Plant Material and Measurements

Potted miniature roses (*R. hybrida* L. cv.; Parade® Rose-Apollo®), grown using the standard commercial procedure in 4-inch pots, were obtained from a private farm (Rocket Farms, previously Nurserymen's Exchange Inc.) in Half Moon Bay, CA, United States during the summer months. The potted roses were pinched 5 days before shipping to University of California, Davis, CA, United States. After treatment with plant growth regulators or inhibitors of ethylene, plants were placed in a greenhouse at 21°C day/16°C night mean temperatures and natural photoperiods. Plant growth was monitored by measuring the length of the longest shoot. The length and diameter of the third and fourth internodes were measured using a digital caliper at 5, 7, 15, 21, and 25 days after treatment.

Treatments With Plant Growth Regulators

Thidiazuron

The stock solution with 10 mM of TDZ was prepared by dissolving pure TDZ (Sigma, St. Louis, MO, United States) in 1 M NaOH and diluted to a proper concentration for treatments (Ferrante et al., 2002). The same diluted concentration of NaOH was used in preparing the control treatment. Potted roses were sprayed with 0 (control), 10, 20, 40, 80, and 100 μM TDZ. The highest concentration of 100 μM TDZ was used for combined treatments with ethylene inhibitors and gibberellic acid (GA_3).

2-Aminoethoxyvinyl Glycine

One day before treatment with 100 μM TDZ, potted roses were sprayed with a 0.5 mM solution of 2-aminoethoxyvinyl glycine (AVG; Sigma) to inhibit ethylene production (Saltveit, 2005). Plants were allowed to dry for 8 h before being sprayed with 100 μM TDZ.

Silver Thiosulfate

Silver thiosulfate (STS) concentrate was prepared as described by Reid et al. (1980). Potted rose plants were sprayed with 0.2 mM STS to inhibit ethylene action (Serek and Reid, 1993) and allowed to dry for 8 h before being sprayed with 100 μM TDZ.

Gibberellic Acid

Plants were sprayed with 100 μM GA_3 (Merck) solution as described by De La Guardia and Benlloch (1980). Some plants were then transferred to the greenhouse for evaluation; replicate plants were allowed to dry for 8 h before being sprayed with TDZ.

Microscopy

Hand-cut transverse and longitudinal sections were prepared at the middle of the third internode at 15 days after treatment with 0 (control) and 100 μM TDZ. Cell sizes (i.e., length and width) were determined from images photographed using a binocular microscope.

Ethylene Production

The effects of different treatments on rates of ethylene production by branches excised from the plants were determined by placing them in 20 ml airtight vials containing 2 ml H_2O. The vials were flushed with compressed air that had been passed through a column filled with Ethysorb (aluminum oxide coated with $KMnO_4$, Stay Fresh Ltd., London, United Kingdom) to remove hydrocarbons. The vials were sealed for 2 h and held at 25°C, and then 3 ml of the headspace gas was injected into a Shimadzu model GC-8A gas chromatograph fitted with an aluminum oxide column and a flame ionization detector (Yin et al., 2019). The detection limit for ethylene was 5 nl/l. Ethylene production was determined in six replicate samples from each treatment.

Semiquantitative PCR Analyses

Samples were taken from the third and fourth internodes at 7 and 15 days after spraying with 0 (control) or 100 μM TDZ. Total RNA was extracted using TRIzol Reagent (Invitrogen, Carlsbad, CA, United States) and treated with RNase-free DNase (Promega, Madison, WI, United States) to remove any contaminating genomic DNA. The first-strand cDNA was synthesized using 2 μg of total RNA, oligo d(T) primers, random hexamers, and SuperScript reverse transcriptase (Invitrogen). This cDNA was used for semiquantitative PCR analysis (Chen et al., 2004) to determine the abundance of transcripts encoding enzymes involved in GA biosynthesis and catabolism. The amplification primers for the different target genes related to bioactive GA biosynthesis and catabolism (e.g., *GA2ox*, *GA20ox-1*, *GA20ox-2*,

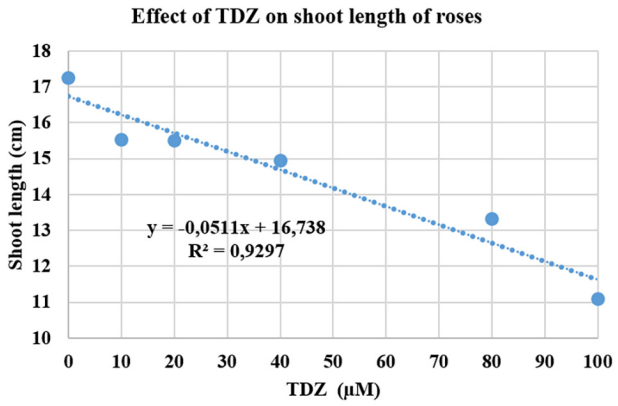

FIGURE 1 | Effects of thidiazuron (TDZ) concentrations on the length of the primary shoot in miniature rose plants. Potted plants were sprayed with different concentrations of TDZ and then placed in the greenhouse for 2 weeks.

and *GA3ox*) and for the 26 rRNA used as an internal control are shown in **Supplementary Table 1**.

Statistical Analysis

The data were analyzed using one-way ANOVA with the generalized linear model procedure of JMP 10.0 software (Cary, NC, United States). Differences among treatments were analyzed using the Student's *t*-test ($P < 0.05$). For all treatments, we used 16 replicate plants; ethylene measurements were conducted on six replicate branches per treatment. Experiments were repeated at least three times.

RESULTS

Effects of TDZ Concentrations on Shoot Length in Miniature Rose Plants

The effect of different concentrations of TDZ on the length of the primary shoot of pinched miniature roses after 2 weeks in the greenhouse is shown in **Figure 1**. The main shoot length was measured 2 weeks after TDZ application. The results showed a significant negative linear relationship between the length of the primary (longest) shoot and TDZ treatment concentration (**Figure 1**).

The substantial improvement in compactness in plants treated with 100 μM TDZ, whose height was essentially unchanged after 2 weeks (**Figure 2**), was not accompanied by any negative effects on the plants. Therefore, we used 100 μM TDZ as the treatment in subsequent experiments.

Effects of TDZ on Shoot Length and Thickness in Miniature Rose Plants

The application of 100 μM TDZ essentially prevented extension growth in potted miniature rose plants (**Figure 3A**). The difference from the controls was significant after 1 week, and by 2 weeks shoots on the controls were more than two times longer than those on the treated plants (**Figure 3A**). The internodes of the treated plants were substantially shorter and thicker than those of the control plants (**Figure 3B**).

Effects of TDZ on Cell Sizes of Miniature Rose Plants

Hand-cut transverse sections from the third internode were used to determine the effect of 100 μM TDZ on the diameter of cells in the cortex and the pith (**Figure 4**). The size of pith cells in the third internode after 15 days of treatment is shown in **Figure 4B**. The wider cortex and pith in the TDZ-treated plants (**Figure 4A**) were associated with a 25% increase in pith cell size and a 100% increase in diameter of the cortical cells (**Figure 4B**). Hand-cut longitudinal sections of the third internode at 15 days after treatment with 100 μM TDZ (**Figure 5**) showed approximately 100% radial increase in the size of the pith cells, but little change in their height (**Figure 5B**).

Effects of TDZ and AVG Treatments on Ethylene Production

Treatment with 100 μM TDZ significantly increased ethylene production of cut miniature rose shoots by 12 h (**Figure 6**) and production continued to increase by 96 h. This increase was suppressed by pretreatment with 0.5 mM AVG, an ethylene synthesis inhibitor (**Figure 6**).

Effects of Ethylene Inhibitors and TDZ on Shoot Growth of Potted Rose Plants

We used ethylene inhibitors to investigate the role of increased ethylene production in TDZ-treated plants on the growth response to TDZ. Pretreatment with AVG had no effect on the inhibition of shoot elongation in response to TDZ treatment (**Figure 7A**). Curiously, the AVG treatment alone also had a significant inhibitory effect on shoot elongation, although not as pronounced as that resulting from treatment with TDZ. These effects were mirrored in the length of the third internode (**Figure 7B**), but the reduction in elongation resulting from AVG treatment was not associated with increased stem diameter.

The ethylene action inhibitor STS had no effect on shoot elongation as seen in the main shoot length (**Figure 8A**) and third internode length (**Figure 8B**) in miniature rose plants. TDZ significantly inhibited shoot elongation and combined treatment with STS did not change the effect of TDZ (**Figure 8**), although the thickness of stems with the combined treatment was slightly less than that of stems treated along with TDZ (**Figure 8B**).

Effects of TDZ on the Expression of Genes Encoding GA Oxidase Enzymes

To test the effect of TDZ on GA biosynthesis in potted rose plants, we examined the effect of TDZ on the expression of genes encoding GA catabolism GA2-oxidase (*GA2ox*), which deactivates GAs, and those of some enzymes involved in bioactive GA biosynthesis (i.e., *GA3ox*, *GA20ox-1*, and *GA20ox-2*). Semiquantitative RT-PCR analysis revealed that the expression of *GA2ox* was promoted slightly by TDZ in both the third and

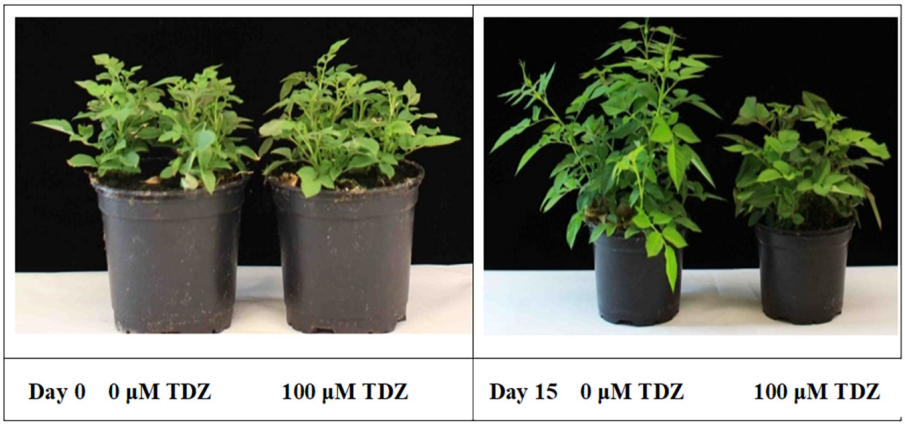

FIGURE 2 | Effects of TDZ application on shoot growth of potted rose plants. Plants on the day of TDZ treatment **(left)** and 2 weeks after spraying with 0 (control) and 100 µM TDZ **(right)**.

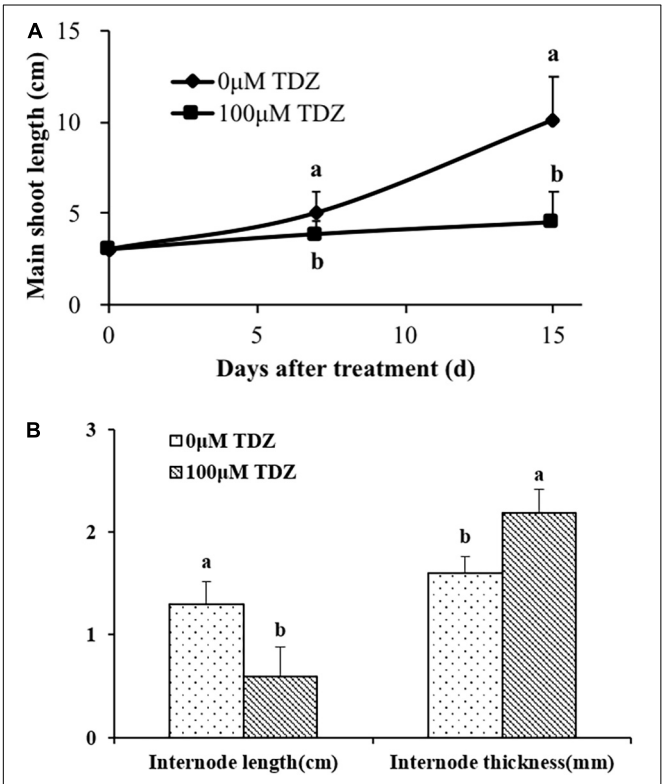

FIGURE 3 | Effects of application of 100 µM TDZ on shoot length **(A)** and the third internode length and thickness **(B)** of miniature rose plants 2 weeks after treatment. Means (±SE, n = 16) with different letters are significantly different at $P \leq 0.05$.

fourth internodes (**Figure 9**). The expression of *GA20ox-2* was obviously suppressed by TDZ, especially in the fourth internode (**Figure 9**). Fifteen days after TDZ treatment, the abundance of transcripts of *GA3ox* and *GA20ox-1* was much lower, particularly in the third internode.

The Interaction Between GA3 and TDZ on Shoot Growth of Potted Rose Plants

Treatment of rose plants with 100 µM GA_3 significantly increased extension growth in miniature rose plants (**Figure 10**). The inhibition of extension growth by TDZ was only modestly (although significantly) reversed by a combined treatment with the two regulators.

Gibberellic acid (GA_3) treatment substantially increased the lengths of both the third and fourth internodes (**Figure 11**). In contrast to the effects of the combined treatment on the total shoot length (**Figure 10**), GA_3 overcame the inhibition of elongation in the third and fourth internodes resulting from TDZ treatment. The increase in the thickness of the internodes resulting from TDZ treatment was not affected by the treatment with GA_3 (**Figure 11**).

DISCUSSION

Controlling the plant height is important for the production and postharvest quality of potted plants (Miller, 2012). Postharvest elongation in the low light conditions of many homes and offices results in loss of compactness and visual quality. In an earlier study, we showed that TDZ reduced the leaf yellowing and abscission in potted miniature roses (Çelikel et al., 2019), an effect of this cytokinin analog that has also been shown in cut *Matthiola* (Mok et al., 1982; Ferrante et al., 2009), *Alstroemeria* (Ferrante et al., 2002), *Tulipa* and *Chrysanthemum* (Ferrante et al., 2003), and *Lupinus densiflorus* (Sankhla et al., 2005). Effects of cytokinins on leaf senescence (Wingler et al., 1998), meristem activity, and branching (e.g., Werner et al., 2001; Kyozuka, 2007; Nieminen et al., 2008) are well known. The inhibition of shoot elongation and increased stem diameter that we reported in this study is not commonly associated with cytokinin effects, although Mundhara and Rashid (2005) reported that *Linum* seedlings tissue-cultured in a medium containing 0.1 µM TDZ showed inhibition of root, hypocotyl elongation, and swelling

and tightening of the cotyledons. In this study, we found a significant linear decrease in the length of the shoots of miniature rose plants as the concentration of TDZ increased up to 100 μM (**Figure 1**). Therefore, we used 100 μM TDZ in further experiments investigating the basis for its inhibitory effect on shoot growth in miniature rose plants, an effect with obvious commercial implications.

Plant extension growth is regulated by environmental and physiological factors, mediated by the gibberellins and ethylene. Commercially, TDZ is used to defoliate cotton leaves, a response that was shown to be the result of local stimulation of ethylene production (Suttle, 1985, 1986). Suttle (1986) concluded that the enhanced ethylene production in cotton leaves following TDZ treatment was the consequence of an increase in the formation and oxidation of the ethylene precursor 1-aminocyclopropane-1-carboxylic acid. Ethylene is known to inhibit extension growth, for example, in *Pinus sylvestris* and *Picea slauca* shoots (Little and Macdonald, 2003), sunflower hypocotyls (Pearce et al.,

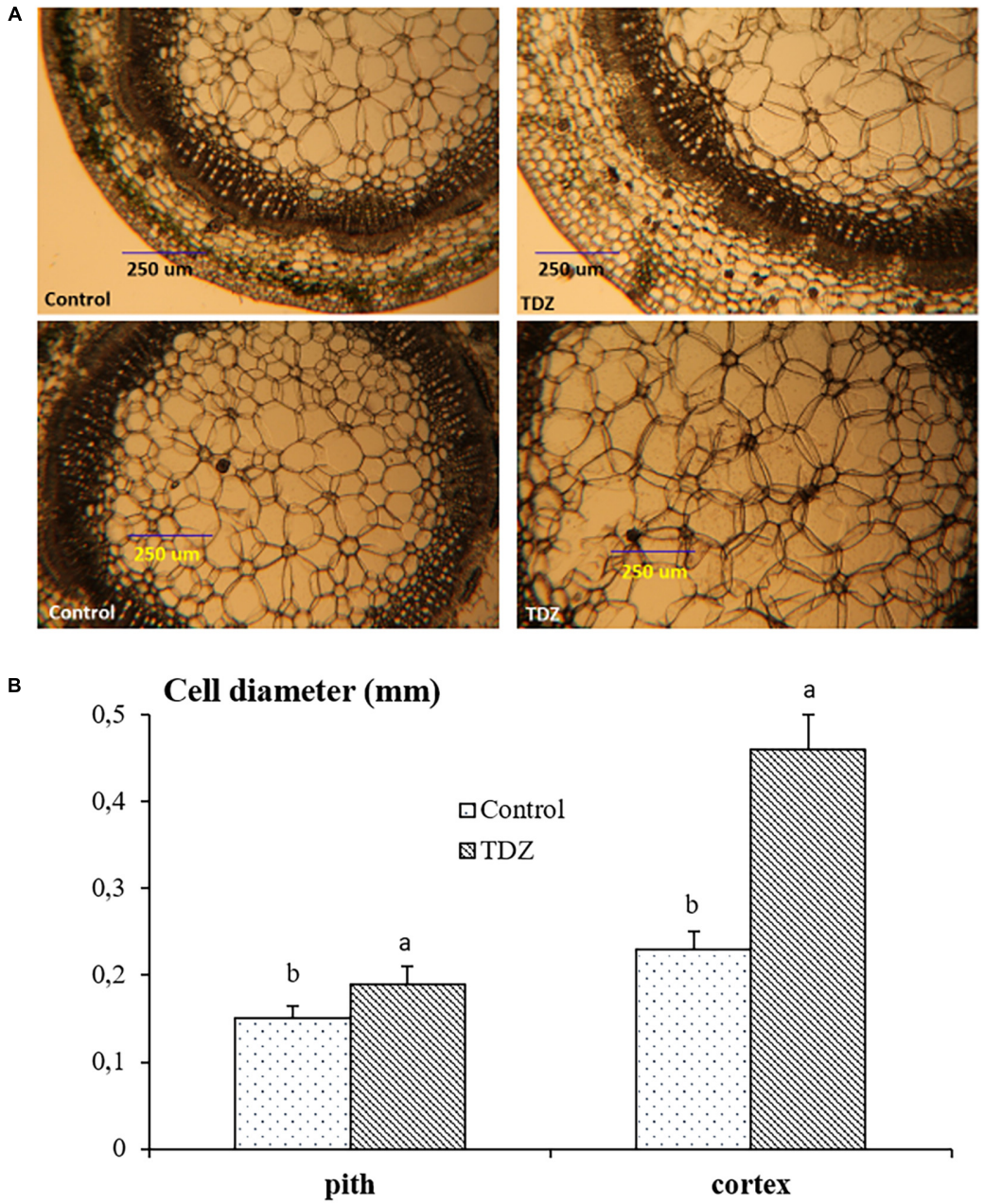

FIGURE 4 | Representative hand-cut transverse sections **(A)** and mean diameters of pith and cortex cells **(B)** of third internode after 15 days of treatment with 100 μM TDZ. The data were taken around the middle sections randomly. Scale bar = 0.25 mm. Means (±SE, n = 16) with different letters are significantly different at $P \leq 0.05$.

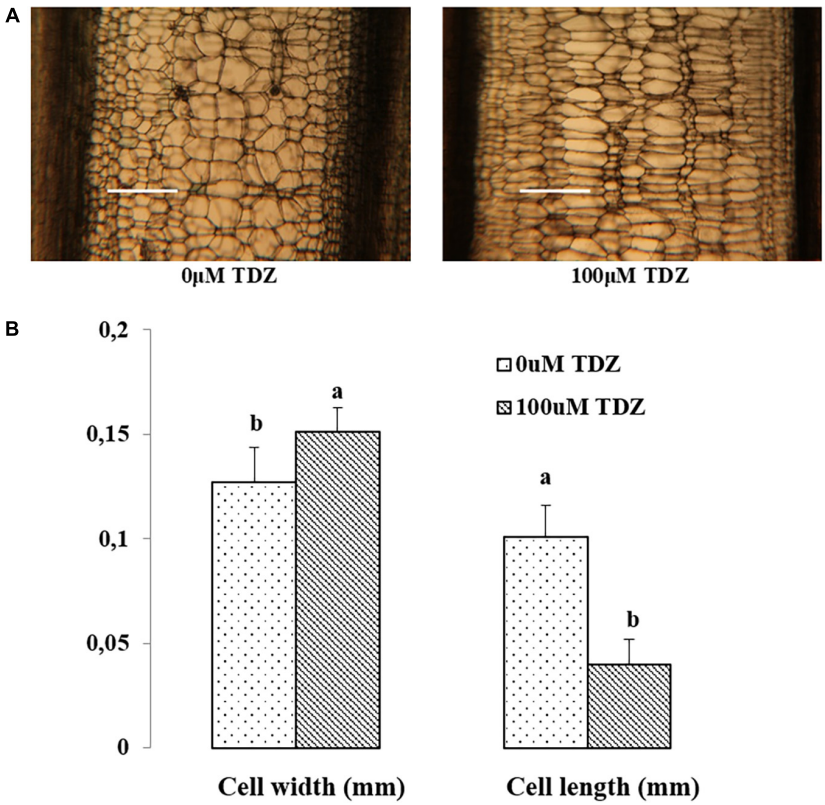

FIGURE 5 | Representative hand-cut longitudinal sections **(A)** and pith cell width (mm) and length (mm) **(B)** of third internodes after 15 days of TDZ treatment. Scale bar = 0.25 mm. The data (means ± SE, n = 16) followed by different letters are significantly different at $P \leq 0.05$.

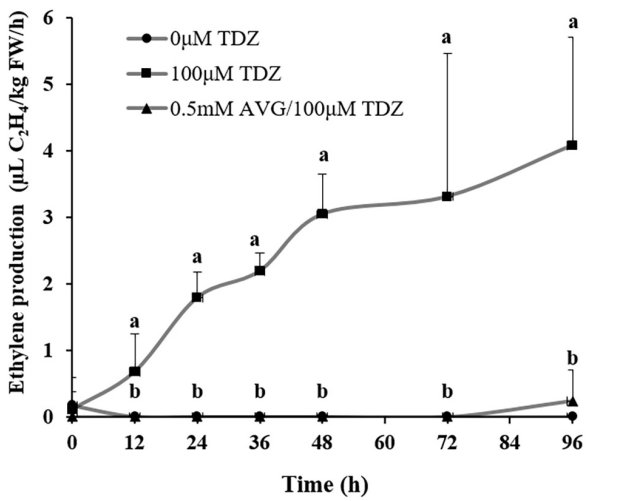

FIGURE 6 | The effect of TDZ on the time course of ethylene production in shoots from control and AVG pretreated miniature rose plants. Means (±SE, n = 6) within days with different letters are significantly different at $P \leq 0.05$.

1991; Johnston et al., 1996), maize roots (Alarcon et al., 2009), and iris pedicels (Çelikel and van Doorn, 2015). Since TDZ treatment dramatically increased ethylene production in rose shoots (**Figure 6**), we hypothesized that the inhibition of extension growth in the shoots might be an effect of ethylene.

Application of AVG, which almost totally inhibited the TDZ-stimulated increase in ethylene production, did not, however, prevent the inhibition of stem growth by TDZ (**Figure 7**). Since AVG alone partially inhibited extension growth (suggesting a positive role for endogenous ethylene in normal growth), we tested the effect of STS, which inhibits ethylene action. STS treatment alone had no effect on the growth of the shoots (**Figure 8**), and the inhibitor affected neither the growth response of plants to TDZ nor the TDZ-stimulated modifications of internode architecture (**Figure 8B**). These data indicate that ethylene is not directly involved in the inhibitory effect of TDZ on shoot growth in miniature rose plants.

Gibberellins are important regulators of extension growth in plants, stimulating cell elongation along the longitudinal axis (Shibaoka, 1994). Stem elongation was inhibited in gibberellin-deficient *Arabidopsis* mutants (Sun and Kamiya, 1994; Chiang et al., 1995), and the gibberellin inhibitor paclobutrazol suppresses growth in a wide range of plant species by decreasing the concentrations of endogenous gibberellins (Tsegaw et al., 2005). Gibberellin inhibitors have been used during production to control the plant height after harvest (Miller, 2012) and in the production of potted bulbous flowers (Demir and Çelikel, 2019). Since the inhibition

of extension growth in TDZ-treated roses did not appear to be the result of stimulated ethylene production, we investigated the effects of TDZ on expressions of genes encoding enzymes involved in gibberellin biosynthesis and degradation (catabolism). Semiquantitative RT-PCR results showed that TDZ application inhibited the expression of genes encoding the bioactive GA biosynthetic enzymes, GA20 oxidase-1, GA3 oxidase, and GA20 oxidase-2 (**Figure 9**). TDZ also increased the expression of genes encoding GA2 oxidase, an enzyme that inactivates endogenous bioactive GAs. Our results in miniature rose plants confirm previous data from *Arabidopsis* seedlings that cytokinin application inhibits the expression of

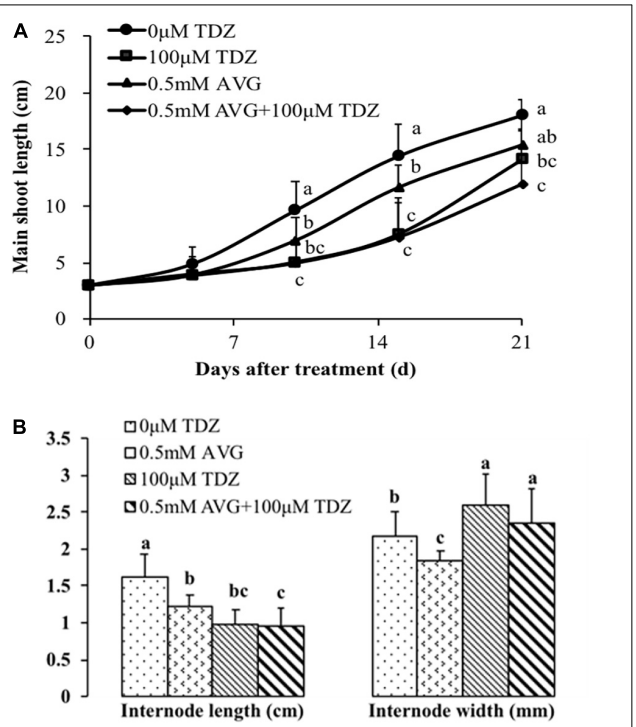

FIGURE 7 | Effects of the ethylene biosynthesis inhibitor AVG at 0.5 mM and 100 μM TDZ applications alone and together on the main shoot length **(A)** and third internode length and thickness **(B)** of potted miniature rose plants. The main shoot length was measured on 5, 10, 15, and 21 days, while the data on the third internode length and thickness were taken after 3 weeks. Means (±SE, n = 16) within days **(A)** and length or thickness **(B)** with different letters are significantly different at $P \leq 0.05$.

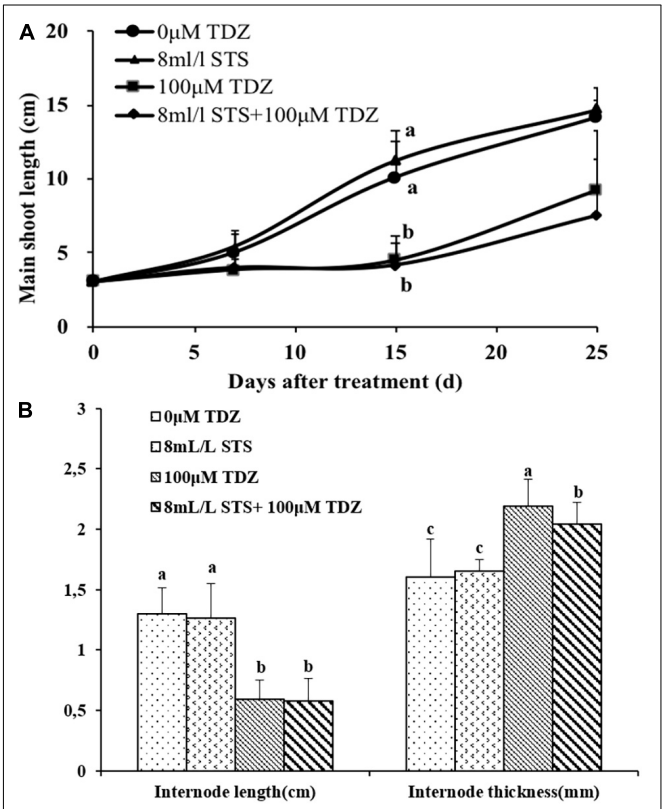

FIGURE 8 | Effects of ethylene action inhibitor STS and TDZ applications alone and together on the main shoot length measured on 1, 2, and 3 weeks **(A)**, and third internode length and thickness (width) measured after 2 weeks **(B)** of potted miniature rose plants. Means (±SE, n = 16) within days **(A)** and length or thickness **(B)** with different letters are significantly different at $P \leq 0.05$.

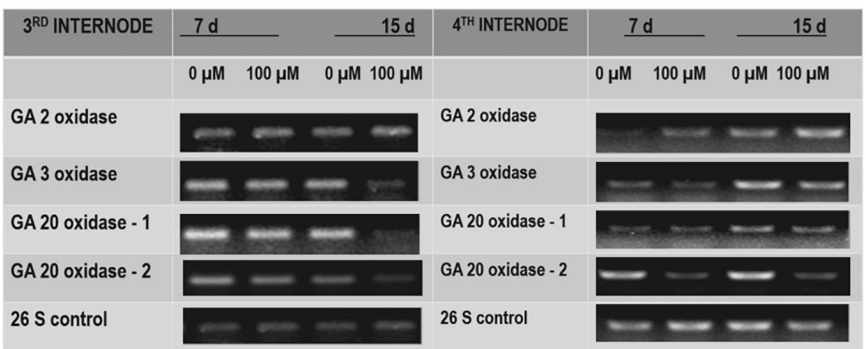

FIGURE 9 | The effects of TDZ on the abundance of transcripts for gibberellic acid (GA) 2 oxidase, GA3 oxidase, and GA20 oxidase. The third and fourth internodes from the base were harvested at 7 and 15 days after TDZ treatment for RNA extraction and semiquantitative PCR analyses.

genes encoding GA20 and GA_3 oxidases (Brenner et al., 2005). Changes in GA20 oxidase gene expression strongly affected the stem length in potato plants (Carrera et al., 2000), and GA3-oxidase gene expression influenced GA biosynthesis and growth and development in pea (Reinecke et al., 2013). Therefore, we hypothesized that TDZ application to miniature rose plants inhibited shoot elongation by reducing the endogenous GA concentration.

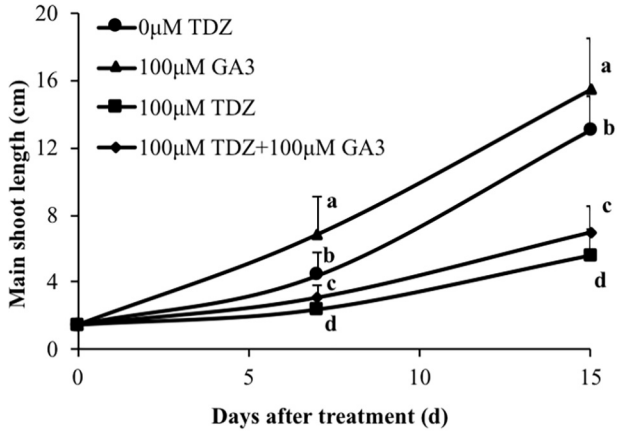

FIGURE 10 | Effects of 100 μM TDZ and GA_3 spray treatments on the main shoot length of potted miniature rose plants after 1 and 2 weeks. Means (±SE, n = 16) within days with different letters are significantly different at $P \leq 0.05$.

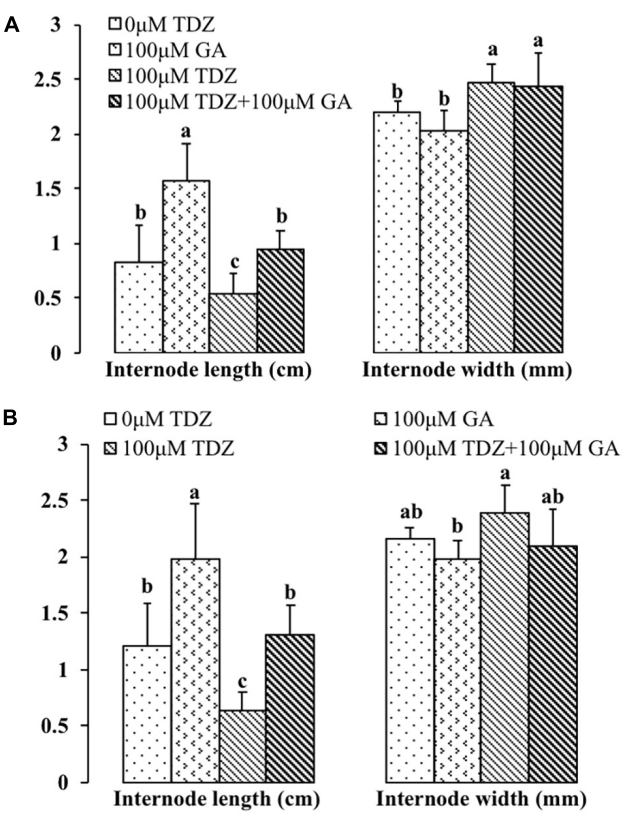

FIGURE 11 | Effects of 100 μM TDZ and GA_3 spray treatments alone and together on the third **(A)** and fourth **(B)** internode length and thickness (width) of potted miniature rose plants for 2 weeks after the treatments. Means (±SE, n = 16) within length or thickness with different letters are significantly different at $P \leq 0.05$.

We tested this hypothesis by applying GA_3 to the control and TDZ-treated rose plants. In contrast to the effects of ethylene inhibitors, exogenous GA_3 application combined with TDZ prevented the TDZ-mediated inhibition of shoot growth in the third and fourth internodes (**Figure 11**).

Cytokinins and gibberellins play important roles in the regulation of plant growth. They have antagonistic effects on shoot and root elongation, cell differentiation, and meristem activity and interact at the synthesis, catabolism, and signaling levels in the model plant *Arabidopsis* (Weiss and Ori, 2007). In the shoot apical meristem, cytokinin appears to induce the expression of *GA2ox* and promote GA deactivation for controlling the balance between cytokinin and GA (Jasinski et al., 2005). However, in the later stage of cell maturation and elongation, GA appears to play a reverse antagonistic role by inhibiting cytokinin responses for maintaining low cytokinin and high GA signals in *Arabidopsis* (Greenboim-Wainberg et al., 2005). Our results provide another example of such an antagonistic effect between cytokinin-like TDZ and GA in the control of stem maturation and elongation of a horticultural crop. The findings in this study provide an alternative approach for plant height control in maintaining the compactness and quality of horticultural plants during and after production.

The inhibition of shoot elongation by TDZ was accompanied by an increase in the stem thickness (**Figure 8**), and this was associated with marked changes in the cell size. The diameter of cells in the cortex doubled, and pith cell diameters increased by 25% (**Figure 4B**). Longitudinal sections revealed a dramatic change in the shape of the pith cells, from typically isodiametric in the controls to a flattened discoid in the TDZ-treated internodes, reflecting the inhibition of axial growth and some reallocation to radial growth (**Figure 5B**). Cytokinins are known to induce radial cell expansion (Shibaoka, 1994), and thus, this change is consistent with the cytokinin activity of TDZ (Nisler, 2018).

DATA AVAILABILITY STATEMENT

The original contributions presented in the study are included in the article/**Supplementary Material**, further inquiries can be directed to the corresponding authors.

AUTHOR CONTRIBUTIONS

All authors listed have made a substantial, direct and intellectual contribution to the work, and approved it for publication.

FUNDING

FÇ received a grant from the Council of Higher Education in Turkey for the research program at University of California, Davis, CA, United States.

ACKNOWLEDGMENTS

We are grateful to Linda Donnelly, Chao Ma, and Sevim Demir for their kind technical assistance in experiments. We acknowledged Junping Gao for providing the sequences of GA2 oxidase, GA3 oxidase, and GA20 oxidase. Plant materials were provided by a private farm (Rocket Farms, previously Nurserymen's Exchange Inc.) in Half Moon Bay, CA, United States.

SUPPLEMENTARY MATERIAL

The Supplementary Material for this article can be found online at: https://www.frontiersin.org/articles/10.3389/fpls.2021.639717/full#supplementary-material

Supplementary Table 1 | Amplification primers for the different target genes (*GA2ox*, *GA20ox-1*, *GA20ox-2*, and *GA3ox*) and for the 26 rRNA used as an internal control.

REFERENCES

Alarcon, M. V., Lloret-Salamanca, A., Lloret, P. G., Iglesias, D. J., Talon, M., and Salguero, J. (2009). Effects of antagonists and inhibitors of ethylene biosynthesis on maize root elongation. *Plant Signal. Behav.* 4, 1154–1156. doi: 10.4161/psb.4.12.9948

Brenner, W. G., Romanov, G. A., Kollmer, I., Burkle, L., and Schmulling, T. (2005). Immediate-early and delayed cytokinin response genes of Arabidopsis thaliana identified by genome-wide expression profiling reveal novel cytokinin-sensitive processes and suggest cytokinin action through transcriptional cascades. *Plant J.* 44, 314–333. doi: 10.1111/j.1365-313x.2005.02530.x

Carrera, E., Bou, J., García-Martínez, J. L., and Prat, S. (2000). Changes in GA 20-oxidase gene expression strongly affect stem length, tuber induction and tuber yield of potato plants. *Plant J.* 22, 247–256. doi: 10.1046/j.1365-313x.2000.00736.x

Çelikel, F. G., and Demir, S. (2019). Effects of ethephon spray on plant quality and growth parameters of potted Narcissus tazetta. *Acta Hortic.* 1263, 439–447. doi: 10.17660/actahortic.2019.1263.57

Çelikel, F. G., and van Doorn, W. G. (2015). *Hormonal Regulation of Flower Opening in Iris, 1060 ed*. Leuven: International Society for Horticultural Science (ISHS), 47–53.

Çelikel, F. G., Zhang, Q. C., Reid, M. S., and Jiang, C. Z. (2019). Thidiazuron maintains quality of miniature rose plants in pots. *Acta Hortic.* 1263, 343–349. doi: 10.17660/actahortic.2019.1263.45

Chen, J.-C., Jiang, C.-Z., Gookin, T. E., Hunter, D. A., Clark, D. G., and Reid, M. S. (2004). Chalcone synthase as a reporter in virus-induced gene silencing studies of flower senescence. *Plant Mol. Biol.* 55, 521–530. doi: 10.1007/s11103-004-0590-7

Chiang, H.-H., Hwang, I., and Goodman, H. M. (1995). Isolation of the Arabidopsis GA4 locus. *Plant Cell* 7, 195–201. doi: 10.2307/3869995

De La Guardia, M. D., and Benlloch, M. (1980). Effects of potassium and gibberellic acid on stem growth of whole sunflower plants. *Physiol. Plant.* 49, 443–448. doi: 10.1111/j.1399-3054.1980.tb03332.x

Demir, S., and Çelikel, F. G. (2019). Effects of plant growth regulators on plant height and quantitative properties of Narcissus tazetta. *Turk. J. Agric. For.* 43, 105–114. doi: 10.3906/tar-1802-106

Ferrante, A., Hunter, D. A., Hackett, W. P., and Reid, M. S. (2002). Thidiazuron—a potent inhibitor of leaf senescence in Alstroemeria. *Postharvest Biol. Technol.* 25, 333–338. doi: 10.1016/s0925-5214(01)00195-8

Ferrante, A., Mensuali-Sodi, A., and Serra, G. (2009). Effect of thidiazuron and gibberellic acid on leaf yellowing of cut stock flowers. *Cent. Eur. J. Biol.* 4, 461–468. doi: 10.2478/s11535-009-0039-8

Ferrante, A., Tognoni, F., Mensuali-Sodi, A., and Serra, G. (2003). Treatment wit thidiazuron for preventing leaf yellowing in cut tulips and chrysanthemum. *Acta Hortic.* 624, 357–363. doi: 10.17660/actahortic.2003.624.49

Greenboim-Wainberg, Y., Maymon, I., Borochov, R., Alvarez, J., Olszewski, N., Ori, N., et al. (2005). Cross talk between gibberellin and cytokinin: the Arabidopsis GA-response inhibitor SPINDLY plays a positive role in cytokinin signaling. *Plant Cell* 17, 92–102. doi: 10.1105/tpc.104.028472

Jasinski, S., Piazza, P., Craft, J., Hay, A., Woolley, L., Rieu, I., et al. (2005). KNOX action in Arabidopsis is mediated by coordinate regulation of cytokinin and gibberellin activities. *Curr. Biol.* 15, 1560–1565. doi: 10.1016/j.cub.2005.07.023

Jiang, C. Z., Wu, L., Macnish, A. J., King, A., Yi, M., and Reid, M. S. (2009). "Thidiazuron, a non-metabolized cytokinin, shows promise in extending the life of potted plants," in *Proceedings of the Ix International Symposium on Postharvest Quality of Ornamental Plants*, eds C. O. Ottosen, B. Grout, and R. Mueller (Leuven: International Society for Horticultural Science)59–65. doi: 10.17660/actahortic.2009.847.6

Johnston, W. J., Golob, C. T., Sitton, J. W., and Schultz, T. R. (1996). Effect of temperature and postharvest field burning of Kentucky bluegrass on germination of sclerotia of Claviceps purpurea. *Plant Dis.* 80, 766–768. doi: 10.1094/pd-80-0766

Kyozuka, J. (2007). Control of shoot and root meristem function by cytokinin. *Curr. Opin. Plant Biol.* 10, 442–446. doi: 10.1016/j.pbi.2007.08.010

Little, C. H. A., and Macdonald, J. E. (2003). Effects of exogenous gibberellin and auxin on shoot elongation and vegetative bud development of Pinus sylvestris and Picea slauca. *Tree Physiol.* 23, 73–83. doi: 10.1093/treephys/23.2.73

Miller, W. B. (2012). Current status of growth regulator usage in flower bulb forcing in north america. *Floric. Ornament. Biotechnol.* 6, 35–44.

Mok, M. C., Mok, D. W. S., Armstrong, D. J., Shudo, K., Isogai, Y., and Okamoto, T. (1982). Cytokinin activity of N-phenyl-N′ -1,2,3,-thiadiazol-5-ylurea (thidiazuron). *Phytochemistry* 21, 1509–1511. doi: 10.1016/s0031-9422(82)85007-3

Mundhara, R., and Rashid, A. (2005). TDZ-induced triple-response and shoot formation on intact seedling of Linum, putative role of ethylene in regeneration. *Plant Sci.* 170, 185–190. doi: 10.1016/j.plantsci.2005.06.015

Nieminen, K., Immanen, J., Laxell, M., Kauppinen, L., Tarkowski, P., Dolezal, K., et al. (2008). Cytokinin signaling regulates cambial development in poplar. *Proc. Natl. Acad. Sci. U. S. A.* 105, 20032–20037. doi: 10.1073/pnas.0805617106

Nisler, J. (2018). "TDZ: mode of action, use and potential in agriculture," in *Thidiazuron: From Urea Derivative to Plant Growth Regulator*, eds N. Ahmad and M. Faisal (Singapore: Springer). First Online 24 March 2018.

Pearce, D. W., Reid, D. M., and Pharis, R. P. (1991). Ethylene-mediated regulation of gibberellin content and growth in Helianthus-Annuus L. *Plant Physiol.* 95, 1197–1202. doi: 10.1104/pp.95.4.1197

Reid, M., Paul, J., Farhoom, M., Kofranek, A., and Staby, G. (1980). Pulse treatments with the silver thiosulfate complex extends the vase life of cut carnations. *J. Am. Soc. Hortic. Sci.* 105, 25–27.

Reinecke, D. M., Wickramarathna, A. D., Ozga, J. A., Kurepin, L. V., Jin, A. L., Good, A. G., et al. (2013). Gibberellin 3-oxidase gene expression patterns influence gibberellin biosynthesis, growth, and development in pea. *Plant Physiol.* 163, 929–945. doi: 10.1104/pp.113.225987

Saltveit, M. E. (2005). Aminoethoxyvinylglycine (AVG) reduces ethylene and protein biosynthesis in excised discs of mature-green tomato pericarp tissue. *Postharvest Biol. Technol.* 35, 183–190. doi: 10.1016/j.postharvbio.2004.07.002

Sankhla, N., Mackay, W. A., and Davis, T. D. (2005). "Effect of thidiazuron on senescence of flowers in cut inflorescences of Lupinus densiflorus Benth," in *Proceedings of the VIIIth International Symposium on Postharvest Physiology of*

Ornamental Plants, eds N. Marissen, W. G. VanDoorn, and U. VanMeeteren (Leuven: International Society for Horticultural Science), 239–243. doi: 10.17660/actahortic.2005.669.31

Serek, M., and Reid, M. S. (1993). Anti-ethylene treatments for potted christmas cactus-efficacy of inhibitors of ethylene action and biosynthesis. *HortScience* 28, 1180–1181. doi: 10.21273/hortsci.28.12.1180

Shibaoka, H. (1994). Plant hormone-induced changes in the orientation of cortical microtubules: alterations in the cross-linking between microtubules and the plasma membrane. *Annu. Rev. Plant Physiol. Plant Mol. Biol.* 45, 527–544. doi: 10.1146/annurev.pp.45.060194.002523

Sun, T.-P., and Kamiya, Y. (1994). The Arabidopsis GA1 locus encodes the cyclase ent-kaurene synthetase A of gibberellin biosynthesis. *Plant Cell* 6, 1509–1518. doi: 10.2307/3869986

Suttle, J. C. (1985). Involvement of Ethylene in the Action of the Cotton Defoliant Thidiazuron. *Plant Physiol.* 78, 272–276. doi: 10.1104/pp.78.2.272

Suttle, J. C. (1986). Cytokinin-induced ethylene biosynthesis in nonsenescing cotton leaves. *Plant Physiol.* 82, 930–935. doi: 10.1104/pp.82.4.930

Tjosvold, S. A., Wu, M.-J., and Reid, M. S. (1994). Reduction of postproduction quality loss in potted miniature roses. *HortScience* 29, 293–294. doi: 10.21273/hortsci.29.4.293

Tsegaw, T., Hammes, S., and Robbertse, J. (2005). Paclobutrazol-induced leaf, stem, and root anatomical modifications in potato. *HortScience* 40, 1343–1346. doi: 10.21273/hortsci.40.5.1343

Weiss, D., and Ori, N. (2007). Mechanisms of cross talk between gibberellin and other hormones. *Plant Physiol.* 144, 1240–1246. doi: 10.1104/pp.107.100370

Werner, T., Motyka, V., Strnad, M., and Schmulling, T. (2001). Regulation of plant growth by cytokinin. *Proc. Natl. Acad. Sci. U. S. A.* 98, 10487–10492.

Wingler, A., von Schaewen, A., Leegood, R. C., Lea, P. J., and Quick, W. P. (1998). Regulation of leaf senescence by cytokinin, sugars, and light – effects on NADH-dependent hydroxypyruvate reductase. *Plant Physiol.* 116, 329–335. doi: 10.1104/pp.116.1.329

Yin, D., Sun, D., Han, Z., Ni, D., Norris, A., and Jiang, C.-Z. (2019). PhERF2, an ethylene-responsive element binding factor, plays an essential role in waterlogging tolerance of petunia. *Hortic. Res.* 6:83. doi: 10.1038/s41438-019-0165-z

Zieslin, N., Mor, Y., Bachrach, A., Haaze, H., and Kofranek, A. M. (1976). Controlling the growth and development of rose plants after planting. *Sci. Hortic.* 4, 63–72. doi: 10.1016/0304-4238(76)90066-2

Conflict of Interest: The authors declare that the research was conducted in the absence of any commercial or financial relationships that could be construed as a potential conflict of interest.

Advantages of publishing in Frontiers

OPEN ACCESS
Articles are free to read for greatest visibility and readership

FAST PUBLICATION
Around 90 days from submission to decision

HIGH QUALITY PEER-REVIEW
Rigorous, collaborative, and constructive peer-review

TRANSPARENT PEER-REVIEW
Editors and reviewers acknowledged by name on published articles

Frontiers
Avenue du Tribunal-Fédéral 34
1005 Lausanne | Switzerland

Visit us: www.frontiersin.org
Contact us: frontiersin.org/about/contact

REPRODUCIBILITY OF RESEARCH
Support open data and methods to enhance research reproducibility

DIGITAL PUBLISHING
Articles designed for optimal readership across devices

FOLLOW US
@frontiersin

IMPACT METRICS
Advanced article metrics track visibility across digital media

EXTENSIVE PROMOTION
Marketing and promotion of impactful research

LOOP RESEARCH NETWORK
Our network increases your article's readership